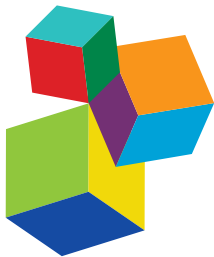


VESTIBULAR CONTRIBUTIONS TO HEALTH AND DISEASE

EDITED BY: Bernard Cohen, Richard Lewis and Jose Antonio Lopez-Escamez
PUBLISHED IN: Frontiers in Neurology





Frontiers Copyright Statement

© Copyright 2007-2018 Frontiers Media SA. All rights reserved.

All content included on this site, such as text, graphics, logos, button icons, images, video/audio clips, downloads, data compilations and software, is the property of or is licensed to Frontiers Media SA ("Frontiers") or its licensees and/or subcontractors. The copyright in the text of individual articles is the property of their respective authors, subject to a license granted to Frontiers.

The compilation of articles constituting this e-book, wherever published, as well as the compilation of all other content on this site, is the exclusive property of Frontiers. For the conditions for downloading and copying of e-books from Frontiers' website, please see the Terms for Website Use. If purchasing Frontiers e-books from other websites or sources, the conditions of the website concerned apply.

Images and graphics not forming part of user-contributed materials may not be downloaded or copied without permission.

Individual articles may be downloaded and reproduced in accordance with the principles of the CC-BY licence subject to any copyright or other notices. They may not be re-sold as an e-book.

As author or other contributor you grant a CC-BY licence to others to reproduce your articles, including any graphics and third-party materials supplied by you, in accordance with the Conditions for Website Use and subject to any copyright notices which you include in connection with your articles and materials.

All copyright, and all rights therein, are protected by national and international copyright laws.

The above represents a summary only. For the full conditions see the Conditions for Authors and the Conditions for Website Use.

ISSN 1664-8714
ISBN 978-2-88945-520-1
DOI 10.3389/978-2-88945-520-1

About Frontiers

Frontiers is more than just an open-access publisher of scholarly articles: it is a pioneering approach to the world of academia, radically improving the way scholarly research is managed. The grand vision of Frontiers is a world where all people have an equal opportunity to seek, share and generate knowledge. Frontiers provides immediate and permanent online open access to all its publications, but this alone is not enough to realize our grand goals.

Frontiers Journal Series

The Frontiers Journal Series is a multi-tier and interdisciplinary set of open-access, online journals, promising a paradigm shift from the current review, selection and dissemination processes in academic publishing. All Frontiers journals are driven by researchers for researchers; therefore, they constitute a service to the scholarly community. At the same time, the Frontiers Journal Series operates on a revolutionary invention, the tiered publishing system, initially addressing specific communities of scholars, and gradually climbing up to broader public understanding, thus serving the interests of the lay society, too.

Dedication to quality

Each Frontiers article is a landmark of the highest quality, thanks to genuinely collaborative interactions between authors and review editors, who include some of the world's best academicians. Research must be certified by peers before entering a stream of knowledge that may eventually reach the public - and shape society; therefore, Frontiers only applies the most rigorous and unbiased reviews.

Frontiers revolutionizes research publishing by freely delivering the most outstanding research, evaluated with no bias from both the academic and social point of view. By applying the most advanced information technologies, Frontiers is catapulting scholarly publishing into a new generation.

What are Frontiers Research Topics?

Frontiers Research Topics are very popular trademarks of the Frontiers Journals Series: they are collections of at least ten articles, all centered on a particular subject. With their unique mix of varied contributions from Original Research to Review Articles, Frontiers Research Topics unify the most influential researchers, the latest key findings and historical advances in a hot research area! Find out more on how to host your own Frontiers Research Topic or contribute to one as an author by contacting the Frontiers Editorial Office: researchtopics@frontiersin.org

VESTIBULAR CONTRIBUTIONS TO HEALTH AND DISEASE

Topic Editors:

Bernard Cohen, Icahn School of Medicine at Mount Sinai, United States

Richard Lewis, Harvard University Cambridge, United States

Jose Antonio Lopez-Escamez, Junta de Andalucía de Genómica e Investigación Oncológica (GENYO), Spain



The cover photograph was kindly supplied by Dr. Ian Curthoys and shows the human temporal bone, dissected to expose the three bony semicircular canals. The diameter of each semicircle is about 6mm. The bony wall of the external ear canal can also be seen. This photograph is reprinted from "Planar relationships of the semicircular canals in man," by Blanks, Curthoys and Markham, Acta Oto-Laryngologica, 1975, with the permission of Taylor & Francis Ltd, <http://www.tandfonline.com>.

This eBook reviews recent developments in vestibular physiology and pathophysiology and covers a range of topics, including diagnostic tests, treatment approaches, central and peripheral vestibular mechanisms, and vestibulo-autonomic interactions.

Citation: Cohen, B., Lewis, R., Lopez-Escamez, J. A., eds. (2018). Vestibular Contributions to Health and Disease. Lausanne: Frontiers Media. doi: 10.3389/978-2-88945-520-1

Table of Contents

- 05 Editorial: Vestibular Contributions to Health and Disease**
Bernard Cohen and Richard Lewis

VESTIBULAR PHYSIOLOGY: BASIC SCIENCE

- 08 Magnetic Vestibular Stimulation (MVS) As a Technique for Understanding the Normal and Diseased Labyrinth**
Bryan K. Ward, Jorge Otero-Millan, Prem Jareonsettasin, Michael C. Schubert, Dale C. Roberts and David S. Zee
- 16 Sustained and Transient Vestibular Systems: A Physiological Basis for Interpreting Vestibular Function**
Ian S. Curthoys, Hamish G. MacDougall, Pierre-Paul Vidal and Catherine de Waele
- 31 Descending Influences on Vestibulospinal and Vestibulosympathetic Reflexes**
Andrew A. McCall, Derek M. Miller and Bill J. Yates
- 46 Coding of Velocity Storage in the Vestibular Nuclei**
Sergei B. Yakushin, Theodore Raphan and Bernard Cohen

VESTIBULAR PATHOPHYSIOLOGY: UNDERSTANDING, DIAGNOSING, AND TREATING VESTIBULAR DISORDERS

- 65 Vestibulo-Ocular Reflex Stabilization after Vestibular Schwannoma Surgery: A Story Told by Saccades**
Angel Batuecas-Caletrio, Jorge Rey-Martinez, Gabriel Trinidad-Ruiz, Eusebi Matiño-Soler, Santiago Santa Cruz-Ruiz, Angel Muñoz-Herrera and Nicolas Perez-Fernandez
- 73 Clinical Subgroups in Bilateral Meniere Disease**
Lidia Frejo, Andres Soto-Varela, Sofía Santos-Perez, Ismael Aran, Angel Batuecas-Caletrio, Vanesa Perez-Guillen, Herminio Perez-Garrigues, Jesus Fraile, Eduardo Martin-Sanz, Maria C. Tapia, Gabriel Trinidad, Ana María García-Arumí, Rocío González-Aguado, Juan M. Espinosa-Sánchez, Pedro Marques, Paz Perez, Jesus Benitez and Jose A. Lopez-Escamez On Behalf of the Meniere's Disease Consortium (MeDiC)
- 83 An Exploratory Study to Detect Ménière's Disease in Conventional MRI Scans Using Radiomics**
E. L. van den Burg, M. van Hoof, A. A. Postma, A. M. L. Janssen, R. J. Stokroos, H. Kingma and R. van de Berg
- 92 The Skull Vibration-Induced Nystagmus Test of Vestibular Function—A Review**
Georges Dumas, Ian S. Curthoys, Alexis Lion, Philippe Perrin and Sébastien Schmerber
- 110 The Video Head Impulse Test**
G. M. Halmagyi, Luke Chen, Hamish G. MacDougall, Konrad P. Weber, Leigh A. McGarvie and Ian S. Curthoys

- 133 Superior Canal Dehiscence Syndrome: Lessons from the First 20 Years**
Bryan K. Ward, John P. Carey and Lloyd B. Minor
- 143 Balance Screening of Vestibular Function in Subjects Aged 4 Years and Older: A Living Laboratory Experience**
María Carolina Bermúdez Rey, Torin K. Clark and Daniel M. Merfeld
- 152 Multivariate Analyses of Balance Test Performance, Vestibular Thresholds, and Age**
Faisal Karmali, María Carolina Bermúdez Rey, Torin K. Clark, Wei Wang and Daniel M. Merfeld
- 168 Treatment of the Mal de Débarquement Syndrome: A 1-Year Follow-up**
Mingjia Dai, Bernard Cohen, Catherine Cho, Susan Shin and Sergei B. Yakushin
- 178 Hypothesis: The Vestibular and Cerebellar Basis of the Mal de Débarquement Syndrome**
Bernard Cohen, Sergei B. Yakushin and Catherine Cho

VESTIBULO-SYMPATHETIC INTERACTIONS

- 189 Vestibular Modulation of Sympathetic Nerve Activity to Muscle and Skin in Humans**
Elie Hammam and Vaughan G. Macefield
- 203 Vestibular Activation Habituates the Vasovagal Response in the Rat**
Bernard Cohen, Giorgio P. Martinelli, Yongqing Xiang, Theodore Raphan and Sergei B. Yakushin
- 219 A Historical View of Motion Sickness—A Plague at Sea and on Land, Also with Military Impact**
Doreen Huppert, Judy Benson and Thomas Brandt
- 234 Determinants of Motion Sickness in Tilting Trains: Coriolis/Cross-Coupling Stimuli and Tilt Delay**
Giovanni Bertolini, Meek Angela Durmaz, Kim Ferrari, Alexander Küffer, Charlotte Lambert and Dominik Straumann



Editorial: Vestibular Contributions to Health and Disease

Bernard Cohen¹ and Richard Lewis^{2,3*}

¹ Department of Neurology, Mount Sinai School of Medicine, New York, NY, United States, ² Department of Otolaryngology, Harvard Medical School, Boston, MA, United States, ³ Department of Neurology, Harvard Medical School, Boston, MA, United States

Keywords: vestibular, physiology, pathophysiology, labyrinth, disease

Editorial on the Research Topic

Vestibular Contributions to Health and Disease

INTRODUCTION

The inter-related functions of several systems that evolved hundreds of millions of years ago, the vestibular, sympathetic, and cardiovascular systems, have important clinical implications in modern neurology and neuro-otology. Operating largely out of consciousness, the vestibular system responds to head and body movement in any direction, stabilizes the head and body with regard to gravity in three-dimensional space, and maintains vital bodily functions through an interaction of vestibular-related components of the brainstem and cerebellum with the cardiovascular and sympathetic systems.

We conceived this volume as an opportunity to highlight some of the basic science and clinical findings that have arisen over the first years of the twenty-first century with regard to these systems. Our concept was to have several broad topics: 1. fundamental vestibular, brainstem, and cerebellar science; 2. new approaches to vestibular diagnosis, pathology, and treatment; and 3. investigations of the vestibular impact on the cardiovascular and sympathetic systems. Topics include the function of the otolith organs, evaluation of the vestibulo-ocular reflex (VOR) in pathologic conditions, and the vestibular input to sympathetic functions such as the vestibulo-sympathetic reflex (VSR). Motion sickness, a vestibulo-sympathetic interaction, is considered both historically and in terms of its typical clinical presentation. Also included are summaries of a little known receptor system, the skin sympathetic nerve activity (SSNA), which forms an important part of the sympathetic “fight or flight” response, and a new hypothesis about the neural basis for the Mal de Debarquement syndrome (MdDS).

OPEN ACCESS

Edited and Reviewed by:

Michael Strupp,
Ludwig-Maximilians-Universität
München, Germany

*Correspondence:

Richard Lewis
richard_lewis@meei.harvard.edu

Specialty section:

This article was submitted
to Neuro-Otology,
a section of the journal
Frontiers in Neurology

Received: 06 February 2018

Accepted: 19 February 2018

Published: 19 March 2018

Citation:

Cohen B and Lewis R (2018)
Editorial: Vestibular Contributions
to Health and Disease.
Front. Neurol. 9:117.
doi: 10.3389/fneur.2018.00117

VESTIBULAR PHYSIOLOGY—BASIC SCIENCE

Ward et al. demonstrate that large *Tesla* magnets used in MRI scanners activate the peripheral end organ in a manner that replicates a constant angular acceleration. Thus, the MRI magnet allows one to study adaptation to this type of stimulus and simultaneously provides a way to identify, modify, or remove the vestibular activation that contaminates “resting” functional MRI scans.

Curthoys et al. demonstrate that otolith activity can be functionally segregated into static or sustained responses and transient responses, with the latter transduced primarily by type I hair cells. They show how this static-dynamic dichotomy could be clinically relevant, with particular reference to vestibular responses measured in the extra-ocular muscles and evoked with skull vibration (ocular vestibular-evoked myogenic potential).

McCall et al. provide an extensive review of the inputs and outputs of the vestibular system, particularly directed toward vestibulospinal and reticulospinal contributions. A large literature demonstrates significant differences in the functional characteristics of vestibulospinal and reticulospinal projections in alert and anesthetized cats and non-human primates and emphasizes the complexity of the terminations in neural groups adjacent to the motor neurons.

Yakushin et al. (1) found that vestibular only (VO) neurons in the vestibular nuclei are responsible for the shift of the axis of eye rotation toward gravity. The VO neurons did not modulate with head position and most likely underlie the direct pathway linking the vestibular end organ with the ocular motor nuclei. When tested in three dimensions, the VO neurons on either side of the brainstem responded differently to ipsilateral and contralateral rotations and were insensitive to drowsiness, in contrast to oculomotor-related vestibular neurons.

VESTIBULAR PATHOPHYSIOLOGY— UNDERSTANDING, DIAGNOSING, AND TREATING VESTIBULAR DISORDERS

The pathophysiology of vestibular compensation is considered in a paper by Batuecas-Caletro et al. They studied outcomes in patients undergoing surgical resection of vestibular nerve schwannomas and observed that the characteristics of re-fixation saccades correlated with compensation.

Frejo et al. address the pathophysiology of Meniere's disease, classifying patients with bilateral disease based on co-morbidities such as migraine or autoimmune disease. They propose that this form of phenotyping may help segregate the different mechanisms that result in the Meniere's syndrome and could eventually be linked to specific genetic syndromic diagnoses.

van den Burg et al. demonstrated an exciting new development in the diagnosis of Meniere's disease, namely imaging that identified anatomic abnormalities in this illness. Specifically, enlargement of the semicircular canals was observed, a finding that mirrors the earlier results of Hallpike 80 years ago (2).

Dumas et al. show that vibration can elicit evidence of vestibular asymmetry in patients with peripheral deficits, even when they are fully compensated. The underlying physiology is not certain, but the authors argue that both canal and otolith afferents are activated by skull vibration. This technique could offer a quick new way to estimate the presence of semicircular canal lesions without rotational apparatus or caloric stimulation.

Halmagyi et al. review their technique for characterizing canal function and analyzing lesions of individual semicircular canals using the video head impulse test. Rapid head movement and observation of the evoked eye movements are much closer to the natural function of the VOR. As a result, head impulse testing using video goggles to measure eye movement responses has become relatively omnipresent in vestibular clinical laboratories. This paper reviews the experience to date with this method including its shortcomings and potential new uses.

The history of the superior canal dehiscence syndrome (SCD), which is now approaching two decades after its initial description by Lloyd Minor, is reviewed by Ward et al. This paper summarizes the clinical presentation, diagnosis, and therapeutic options for SCD. Because it can be treated surgically by inactivating the abnormal canal or closing the defect in its roof, it is essential that this diagnosis be considered when the clinical signs suggest its presence.

Karmali et al. examine how self-motion perceptual thresholds relate to age and fall risk, and find that while all of the tested angular, linear, and tilt thresholds that were measured increase with age, only roll tilt thresholds have a meaningful correlation with fall risk.

Dai et al. review the results of treatment of the MdDS in 141 patients. Their discovery of the first successful treatment for the MdDS, reported in 2014, has led to extensive experience treating this disorder which they report here. They found that the treatment was initially successful in 75% of patients, although efforts still must be made to stabilize the patients better in the time after treatment (Dai et al.).

The neural mechanism underlying the MdDS is considered by Cohen et al. They posit that MdDS had arises after prolonged exposure to roll tilts causes a lateral shift of the pitch orientation vector in the cerebellar nodulus. This activates VO neurons in the vestibular nuclei and causes them to oscillate at 0.2 Hz, resulting in the continuous sensation of rocking, swaying, and/or bobbing, which are characteristic of MdDS.

VESTIBULO-SYMPATHETIC INTERACTIONS

A major theme of vestibular research in the twenty-first century has been expanding the realm of studies to include the frequently overlooked vestibular effects on the sympathetic nervous system, which helps control blood pressure, heart rate, sweating, and other basic behaviors. There are *two distinctly different components* to the VSR. One component, using glutamatergic transmission, involves the otolith system and the vertical semicircular canals [Holstein et al.; (3); Yakushin et al.; (4)]. Vestibular stimulation, i.e., upward, linear acceleration of the head and body produced by standing causes constriction of peripheral blood vessels in the legs by activating muscle sympathetic nerve activity (MSNA) (5–8).

Studying the effect of sinusoidal galvanic vestibular stimulation (sGVS) on anesthetized rats, Cohen and colleagues found that such stimulation initially caused a drop in BP and HR, a vasovagal response that is the precursor of neurogenic syncope (9). Interestingly, the vasovagal response disappeared with continued bouts of stimulation with sGVS, which was associated with a change in the response of BP and HR. The authors raise the possibility that such vestibular stimulation potentially could be used to thwart the occurrence of neurogenic syncope.

A second VSR system originates largely in the lateral and vertical semicircular canals and the otolith organs and projects into other aspects of the sympathetic system, using serotonin as the transmitter to initiate anxiety, sweating, and fear (10–14).

Hammam and Macefield studied SSNA, a little known set of receptors activated by vestibular input that are critical for generating phenomena associated with motion sickness. Activated by weak linear acceleration along the horizontal plane, the SSNA is responsible for pallor and sweating. In comparison with the MSNA, which activates BP upon standing, the SSNA is also activated by linear acceleration, but the strength of the activation is orders of magnitude weaker than that elicited by MSNA. A striking finding was that SSNA is associated with the symptoms of motion sickness, namely nausea and vomiting, as well as with skin pallor and sweating.

Motion sickness, produced by activation of this system, has been an accompanying feature of travel for centuries. Huppert et al. provide a comprehensive review of motion sickness in their historical context. It is clear that the ancient Chinese and Greeks were well aware that body motion was responsible for “cart” sickness and seasickness, but the actual provocative motions were still a mystery. The authors review the incidents of both Chinese and European history when such seasickness proved to be a vital force that helped decide the course of battles and the fates of various nations.

Recent experiments have come closer to understanding the nature of the provocative motions responsible for producing nausea and motion sickness. The causes of motion sickness on tilting trains (15) were revisited, with refined apparatus by Bertolini et al. who argue that specific motion patterns, namely

those that elicit Coriolis forces (which are generated when one moves within a moving reference frame), are particularly likely to elicit symptoms of motion sickness. An earlier study on tilting trains (15) concluded that motion sickness in the passengers came when the roll tilt of the cars was initiated after the train had entered into the curve. This implicated roll as the exciting source of the motion sickness, confirming the findings of Griffin and colleagues (16, 17). Bertolini et al. were able to show that motion sickness was dependent on starting the roll after the rotation had begun, as in the earlier study (15), showing that it was a combination of linear acceleration and roll that had caused the motion sickness.

CONCLUSION

This collection of papers provides insight into the current state of vestibular research at levels ranging from basic physiology to clinical treatment. In particular, we feel that vestibular-autonomic interactions, which have been relatively neglected by much of the vestibular community, will ultimately prove to be an area of much significance for both the normal and pathologic influences of the vestibular system on behavior.

AUTHOR CONTRIBUTIONS

BC and RL contributed equally to this manuscript.

REFERENCES

- Raphan T, Cohen B. The vestibulo-ocular reflex in three dimensions. *Exp Brain Res* (2002) 145:1–27. doi:10.1007/s00221-002-1067-z
- Hallpike CS, Wright AJ. On the histological changes in the temporal bones of a case of Meniere's disease: (section of otology and section of laryngology). *Proc R Soc Med* (1939) 12:1646–56.
- Holstein GR, Friedrich VLJ, Martinelli GP. Projection neurons of the vestibulo-sympathetic reflex pathway. *J Comp Neurol* (2014) 522:2053–74. doi:10.1002/cne.23517
- Lee TK, Lois JH, Troupé JH, Wilson TD, Yates BJ. Transneuronal tracing of neural pathways that regulate hindlimb muscle blood flow. *Am J Physiol Regul Integr Comp Physiol* (2007) 292:R1532–41. doi:10.1152/ajpregu.00633.2006
- Wallin BG, Sundlöf G. Sympathetic outflow to muscles during vasovagal syncope. *J Auton Nerv Syst* (1982) 6:287–91. doi:10.1016/0165-1838(82)90001-7
- Macefield VG, Wallin BG. Effects of static lung inflation on sympathetic activity in human muscle nerves at rest and during asphyxia. *J Auton Nerv Syst* (1995) 53:148–56. doi:10.1016/0165-1838(94)00174-1
- Macefield VG, Gandevia SC, Henderson LA. Neural sites involved in the sustained increase in muscle sympathetic nerve activity induced by inspiratory capacity apnea: a fMRI study. *J Appl Physiol* (2006) 100:266–73. doi:10.1152/japplphysiol.00588.2005
- Yates BJ, Bolton PS, Macefield VG. Vestibulo-sympathetic responses. *Compr Physiol* (2014) 4:851–87. doi:10.1002/cphy.c130041
- Cohen B, Martinelli GP, Ogorodnikov D, Xiang Y, Raphan T, Holstein GR, et al. Vestibular activation habituates the vasovagal response in the rat. *Exp Brain Res* (2011) 1:45–55. doi:10.3389/fnneur.2017.00083
- Guyenet PG. The sympathetic control of blood pressure. *Nat Rev Neurosci* (2006) 7:335–46. doi:10.1038/nrn1902
- Balaban CD. Vestibular nucleus projections to the parabrachial nucleus in rabbits: implications for vestibular influences on the autonomic nervous system. *Exp Brain Res* (1996) 108:367–81. doi:10.1007/BF00227260
- Balaban CD. Projections from the parabrachial nucleus to the vestibular nuclei: potential substrates for autonomic and limbic influences on vestibular responses. *Brain Res* (2004) 996:126–37. doi:10.1016/j.brainres.2003.10.026
- McCandless CH, Balaban CD. Parabrachial nucleus neuronal responses to off-vertical axis rotation in macaques. *Exp Brain Res* (2010) 202:271–90. doi:10.1007/s00221-009-2130-9
- Balaban CD, Ogburn SW, Warshafsky SG, Ahmed A, Yates BJ. Identification of neural networks that contribute to motion sickness through principal components analysis of Fos labeling induced by galvanic vestibular stimulation. *PLoS One* (2014) 9:e86730. doi:10.1371/journal.pone.0086730
- Cohen B, Dai M, Ogorodnikov D, Laurens J, Raphan T, Muller P, et al. Motion sickness on tilting trains. *FASEB J* (2011) 25:3765–74. doi:10.1096/fj.11-184887
- Joseph JA, Griffin MJ. Motion sickness from combined lateral and roll oscillation: effect of varying phase relationships. *Aviat Space Environ Med* (2007) 78:944–50. doi:10.3357/ASEM.2043.2007
- Donohew BE, Griffin MJ. Motion sickness: effect of the frequency of lateral oscillation. *Aviat Space Environ Med* (2004) 75:649–56.

Conflict of Interest Statement: The authors declare that the research was conducted in the absence of any commercial or financial relationships that could be construed as a potential conflict of interest.

Copyright © 2018 Cohen and Lewis. This is an open-access article distributed under the terms of the Creative Commons Attribution License (CC BY). The use, distribution or reproduction in other forums is permitted, provided the original author(s) and the copyright owner are credited and that the original publication in this journal is cited, in accordance with accepted academic practice. No use, distribution or reproduction is permitted which does not comply with these terms.



Magnetic Vestibular Stimulation (MVS) As a Technique for Understanding the Normal and Diseased Labyrinth

Bryan K. Ward^{1*}, Jorge Otero-Millan², Prem Jareonsettasin³, Michael C. Schubert^{3,4}, Dale C. Roberts^{1,2} and David S. Zee^{1,2,5,6}

¹Department of Otolaryngology-Head and Neck Surgery, The Johns Hopkins University, Baltimore, MD, USA, ²Department of Neurology, The Johns Hopkins University, Baltimore, MD, USA, ³Department of Neuroscience, Exeter College, University of Oxford, Oxford, UK, ⁴Department of Physical Medicine and Rehabilitation, The Johns Hopkins University, Baltimore, MD, USA, ⁵Department of Neuroscience, The Johns Hopkins University, Baltimore, MD, USA, ⁶Department of Ophthalmology, The Johns Hopkins University, Baltimore, MD, USA

OPEN ACCESS

Edited by:

Jose Antonio Lopez-Escamez,
Center for Genomic and Oncology
Research (Genyo), Spain

Reviewed by:

Angel Batuecas-Caletro,
Complejo Hospitalario de Salamanca,
Spain
Pierre-Paul Vidal,
Université Paris Descartes, France

*Correspondence:

Bryan K. Ward
bward15@jhmi.edu

Specialty section:

This article was submitted
to Neuro-otology,
a section of the journal
Frontiers in Neurology

Received: 04 February 2017

Accepted: 15 March 2017

Published: 05 April 2017

Citation:

Ward BK, Otero-Millan J, Jareonsettasin P, Schubert MC, Roberts DC and Zee DS (2017) Magnetic Vestibular Stimulation (MVS) As a Technique for Understanding the Normal and Diseased Labyrinth. *Front. Neurol.* 8:122.
doi: 10.3389/fneur.2017.00122

Humans often experience dizziness and vertigo around strong static magnetic fields such as those present in an MRI scanner. Recent evidence supports the idea that this effect is the result of inner ear vestibular stimulation and that the mechanism is a magnetohydrodynamic force (Lorentz force) that is generated by the interactions between normal ionic currents in the inner ear endolymph and the strong static magnetic field of MRI machines. While in the MRI, the Lorentz force displaces the cupula of the lateral and anterior semicircular canals, as if the head was rotating with a constant acceleration. If a human subject's eye movements are recorded when they are in darkness in an MRI machine (i.e., without fixation), there is a persistent nystagmus that diminishes but does not completely disappear over time. When the person exits the magnetic field, there is a transient aftereffect (nystagmus beating in the opposite direction) that reflects adaptation that occurred in the MRI. This magnetic vestibular stimulation (MVS) is a useful technique for exploring set-point adaptation, the process by which the brain adapts to a change in its environment, which in this case is vestibular imbalance. Here, we review the mechanism of MVS, how MVS produces a unique stimulus to the labyrinth that allows us to explore set-point adaptation, and how this technique might apply to the understanding and treatment of vestibular and other neurological disorders.

Keywords: vestibular diseases, dizziness, magnetic resonance imaging, labyrinthine fluids, magnetic vestibular stimulation, biophysics

In 2009, Marcelli et al. were studying the effects of a caloric (cold water) vestibular stimulus on the brain using functional MRI (fMRI) when they observed a slow drift of the eyes in some of their subjects while they lay in darkness inside the 1.5 T magnetic field, before irrigating the ear or taking any images (1). Recall that, in an MRI machine, the large static magnetic field is always active, whereas high frequency oscillations in the magnetic field are only present when obtaining images. Marcelli et al. speculated that this unexpected nystagmus in the MRI machine was due to effects of the strong static magnetic fields on the labyrinth itself. Key to making this observation was the elimination of the visual fixation mechanisms that normally suppress unwanted nystagmus induced from an imbalance in labyrinthine inputs. Bringing out or increasing the intensity of a nystagmus by removal of visual fixation is a classical technique in the examination of patients with vestibular

disorders. It helps one to decide if the lesion might be in central pathways in the brain, in which case fixation often has no effect on the intensity of nystagmus. This maneuver is the equivalent in the vestibulo-ocular system of the Romberg sign of classical neurology in which eliminating vision causes patients to lose balance if the contributions of their vestibular or somatosensory systems to postural stability are deficient. By eliminating visual fixation and relying on principles of the physical examination, Marcelli et al. had observed a direct effect of strong magnetic fields on the human vestibular system.

MAGNETIC VESTIBULAR STIMULATION (MVS)—DISCOVERING THE MECHANISM

While it had been known for decades that human subjects exposed to high-strength magnetic fields often feel off balance or dizzy (2–6), the observation by Marcelli et al. was the first objective sign of a vestibular imbalance in human subjects that were inside high-strength MRI machines. Prior animal experiments, in which the effects of strong magnetic fields on posture were studied (7–10), suggested that stimulation of the labyrinth might be the culprit but not enough evidence had been marshaled to develop a convincing explanation of the actual mechanism.

Working with Marcelli, we investigated this phenomenon further by recording eye movements in normal humans exposed to a strong (7 T) static magnetic field (11). No images were taken so that the effect could be attributed entirely to the constant magnetic field of the MRI machine. With elimination of visual fixation and recording eye movements with infrared video techniques, we found that (1) all normal human subjects tested had horizontal nystagmus while lying in the MRI bore (Figure 1); (2) the direction of nystagmus reversed with extreme head pitch, i.e., there was a null position in which there was no nystagmus; (3) the direction of nystagmus reversed with direction of entry (feet first versus head first into the front of the bore or head first into the front of the bore versus head first into the back of the bore); (4) the effect showed some decay while the subject was in the bore, but nystagmus was still present at 90 min of stimulation, the longest time tested; (5) the effect did not depend on rate of motion into or out of the bore; (6) the intensity of the nystagmus scaled roughly linearly with the strength of the magnetic field (comparing responses in a 7- and 3-T magnet); and (7) no nystagmus was observed in patients with bilateral peripheral vestibular loss, who were tested in several head positions to make sure being in a null orientation was not the reason for the absence of nystagmus (11).

Based on these compelling empirical observations and knowledge of magnetic field properties, we were able to rule out several candidate theories and hypothesize that the nystagmus arose because of a sustained pressure, transmitted *via* the endolymph fluid of the lateral semicircular canals, onto the cupula of the lateral semicircular canal. With this hypothesis, we presume that the pressure is generated by magnetohydrodynamic forces known as Lorentz forces arising from the interaction between the static magnetic field of the MRI machine and the constant mechano-electrical transduction currents in the ion-rich endolymphatic

fluid. These ionic currents normally flow through the transduction channels of utricular hair cells and support their resting discharge rate. The Lorentz force, which is perpendicular to both the magnetic field and electrical current directions (Figure 2), can then generate a fluid pressure across the utricle and through the canal, producing a sustained displacement of the cupula, such as that which happens during a natural rotation of the head at a *constant acceleration*. The intensity of the nystagmus produced in the 7 T MRI machine was compatible with the known number of hair cells and the strength of their respective ion currents as well as the amount of fluid pressure and cupula displacement needed to produce a nystagmus of that intensity (11). Because one lateral canal is excited and the other is inhibited, the pattern of horizontal nystagmus is similar to that elicited by a natural rotation around the earth-vertical axis, with the exception of an additional torsional component in the MRI machine (see below). We emphasize here that the endolymph serves a dual purpose: it transmits ionic current into hair cells in the utricle to sustain their resting discharge, and it is the conduit by which the Lorentz force is transmitted as a pressure onto the cupula, pushing it to a persistently deviated position, producing a sustained nystagmus.

Further evidence from human patients with loss of function in one labyrinth indicates that there is also activation of the nearby anterior semicircular canals in the MRI machine, which in an intact subject would be excitation of one canal and inhibition of the other (12). Based on the classical studies of the nineteenth century giants of vestibular physiology—Ewald, Flourens, and Breuer—we predicted that, in intact subjects, any vertical components to the nystagmus from activation of the anterior semicircular canals would subtract, but any torsional components (because they are oppositely directed) would add. Recall Ewald's laws, (1) activation of an individual canal induces eye (or head) motion in a plane parallel to that of the activated semicircular canal, (2) the lateral SCC have a brisker response to ampullopetal (excitation) than ampullofugal (inhibition) fluid flow, and (3) the vertical SCC have a brisker response to ampullofugal (excitation) than ampullopetal (inhibition) fluid flow. When only one labyrinth is functioning, there will still be a horizontal component of the nystagmus (either from excitation or inhibition of the remaining lateral SCC) but also a vertical component, the direction depending on which anterior canal remains intact. Considering how the magnetic field is oriented in our scanner (field pointing head to toe), most normal subjects develop a horizontal nystagmus with slow phases to the left because the right lateral canal is being excited and the left inhibited. In patients with a loss of labyrinthine function on the left side, the unbalanced anterior canal inputs lead to an upward beating component to their nystagmus while patients with loss on the right side develop a downward beating component to their nystagmus (12). Since activation of an anterior semicircular canal also induces torsion, in intact human subjects not only should the vertical components cancel but the torsional components (which are in opposite directions in the two labyrinths) should sum since one side is being inhibited and the other excited. This produces a torsional component that adds to the horizontal component. This indeed is the case so that normal human subjects show a mixed horizontal-torsional nystagmus in the MRI machine (see Video S1 in Supplementary Material). The pattern is unusual,

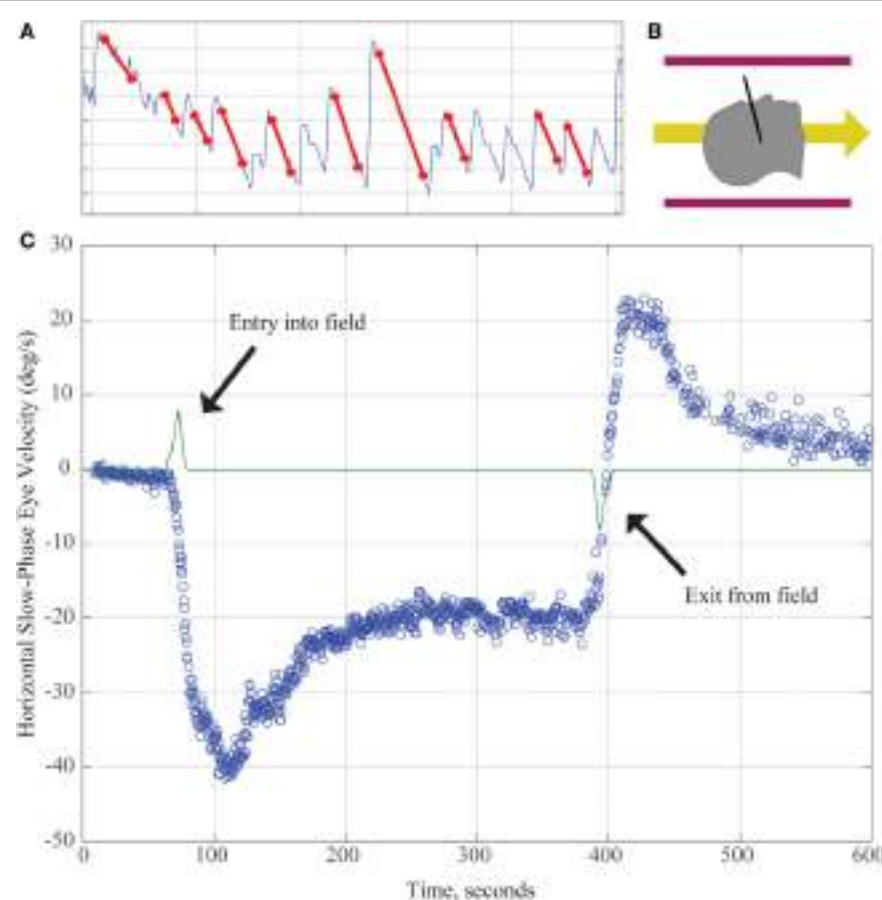


FIGURE 1 | (A) Horizontal position of the eye as a function of time demonstrating slow and quick phases of nystagmus over about 8 s. The slope of the slow component (marked with red lines) is used to calculate the slow-phase velocity (SPV) in panel **(C)**. **(B)** Subjects enter the magnetic field head-first (magnetic field vector shown by yellow arrow). Black line demonstrates approximate location of Reid's plane. **(C)** SPV versus time. The green line represents electromagnetic induction due to motion through the magnetic field gradient, with peaks marking time of entry/exit from the magnetic field. Each blue dot represents SPV of a beat of nystagmus. SPV increases to a peak shortly after entry before partially adapting. After exiting the magnet, an aftereffect appears with nystagmus in the opposite direction. Its rate of decay reflects the dissipation of the adaptation that had taken place inside the MRI.

however, in that the top poles of the eyes rotate in a slow phase *away* from the ear toward which the horizontal component of the slow phase is directed. In contrast, in the more common pattern of a mixed horizontal-torsional nystagmus, for example, as seen after a unilateral loss of labyrinthine function, the top poles of the eyes rotate in a slow phase *toward* the same ear as the horizontal component of the slow phase is directed (13). We emphasize here that these seemingly complicated patterns of nystagmus are easily derived from the laws of Ewald and Flourens, known for nearly 150 years.

One other issue that was raised in our initial study was why there was so much variability in the null position among subjects (range up to 50°) (11). We can only speculate, but we attribute some portion to the inherent variability of the orientation of the bony labyrinth in the skull and the rest to other natural physiological and geometric variation of the labyrinth. The implications of a null are important since fMRI studies of all types, including resting-state connectivity become susceptible to artifacts from stimulation of the labyrinth by the magnetic field, and in turn, the brain. Whether fixation is prevented (the eyes are closed or

the subject is in darkness), or the eyes are open, allowing fixation suppression of the induced nystagmus, the brain will be activated in many regions. Note there are wide spread projections of vestibular sensory information to almost every area of the brain (14, 15). This vestibular activation can introduce a confound when trying to relate behaviors to changes in the metabolic activity in the brain. Of course, this problem goes away if the head of the subject is positioned in the scanner in the null position where no nystagmus is produced.

MVS: AN EXPERIMENTAL PARADIGM FOR “SET-POINT ADAPTATION”

How Does the Brain Keep Central Tone Balanced?

Recognized by Sherrington as a key principle of postural control, tone (set point) is optimally achieved *via* sustained balance level of opposing tonic neural activity in a push-pull fashion (16, 17). Semicircular canals work in coplanar pairs that are reciprocally

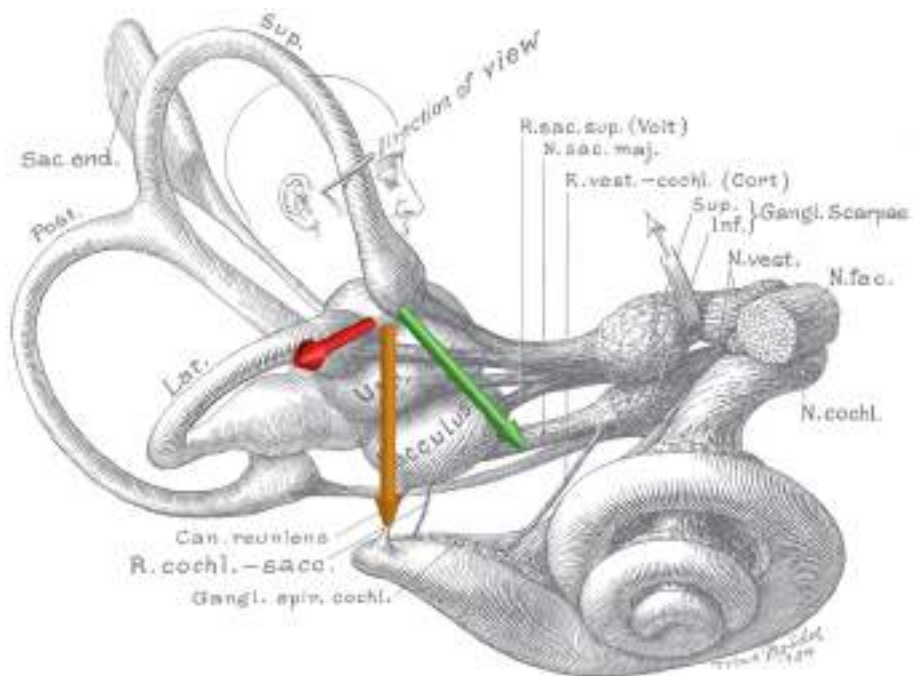


FIGURE 2 | Schematic of the inner ear with approximate locations of magnetic field, net ionic current, and Lorentz force vectors. Note the anatomic relationship between the utricle and ampulla of the lateral and anterior semicircular canals. The green arrow represents the net ionic current of the utricle. The orange arrow represents the direction of the magnetic field vector (head to toe), when a person is lying in the strong static magnetic field of an MRI. The red arrow represents the resultant net Lorentz force from the cross product of the current and magnetic field vectors. Original illustration #933 in the Walters Collection of the Max Brödel Archives, Department of Art as Applied to Medicine, The Johns Hopkins University School of Medicine, Baltimore.

excited and inhibited as they transduce head rotations, therefore, serve as a prototypical model for the study of set-point adaptation.

Consider the archetypical clinical challenge when a human suddenly loses function of one labyrinth: a strong spontaneous nystagmus initially appears due to the central tone imbalance that is created by the asymmetry in afferent activity from the labyrinths. The nystagmus eventually subsides as central balance is restored, but usually takes days to weeks to completely resolve (18). Furthermore, should a patient who has recovered from a previous loss of function in one labyrinth suddenly lose function in the remaining labyrinth, the patient shows a strong spontaneous nystagmus similar to but oppositely directed from that brought on by the original loss of function on one side (19). This “Bechterew’s phenomenon” occurs even when neither labyrinth is active as shown by absent caloric responses. The reason, of course, is that activity within the vestibular nuclei had been rebalanced after the initial loss of function in one labyrinth. When activity from the remaining labyrinth is subsequently lost, a new imbalance is created centrally just as if the function of a single labyrinth was removed again. This sequence of events simply reflects the ability of the brain to rebalance activity centrally in spite of a persistent asymmetry in peripheral activity.

Without adaptation (or what some call vestibular compensation), persistent nystagmus impairs vision, thus the brain must have mechanisms to rid itself of nystagmus. How does this happen?

Early Studies of Set-Point Adaptation

Nearly 50 years ago, seminal studies were performed almost simultaneously by two groups addressing the mechanisms by which nystagmus is removed when there is a sustained vestibular imbalance (18, 20). Normal human subjects rotated in a chair at a constant acceleration develop a nystagmus that is sustained because of the mechanical properties of the cupula-semicircular canal and endolymph. Any relatively constant sustained nystagmus is a low-frequency stimulus and is presumably interpreted by the brain as resulting from disease since sustained nystagmus almost never occurs naturally unless there is a lesion producing a persistent tone imbalance. Of course, this experimental paradigm using sustained rotation of the head, while producing a sustained nystagmus, does not perfectly mimic a naturally occurring lesion in one labyrinth because in normal subjects there is a tonic level of activity coming from both labyrinths and one side is excited and the other inhibited. Nevertheless, by using a constant acceleration stimulus, important information was gleaned about the immediate response of the brain to a vestibular imbalance. By its nature, however, a constantly accelerating head rotation can only be imposed so long before the speed of rotation exceeds values that are feasible or safe. Consequently, during rotation, a sustained nystagmus could only be maintained for a few minutes so that any adaptation was incomplete and relatively short-lived with decay time constants on the order of few minutes. Nevertheless, quantitative models were developed that nicely mimicked the real data, though nothing could be inferred about adaptation

taking place beyond the first few minutes of a sustained vestibular imbalance.

A sustained nystagmus can also be elicited with prolonged caloric irrigation of the ear canal. Several groups observed that a long-duration caloric irrigation appeared to reach a steady state (up to 60 min), as the nystagmus did not decay to 0 (21, 22). Prolonged caloric stimulation, however, is uncomfortable and also variable among individuals depending upon the thermal conductivity and anatomical configuration of the bony labyrinth in the skull. While the main effect of caloric stimulation is changing the density of the fluid within the semicircular canal, it also has a direct thermal effect on nervous tissue. Even so, the persistent nystagmus from a caloric irrigation appears to be independent of any direct thermal effect on activity in the hair cells and the vestibular nerve (22). In spite of these limitations, a caloric stimulus has one advantage over MVS since it is unilateral and, in this way, better mimics a lesion of one lateral semicircular canal. MVS, while producing a sustained nystagmus, excites one lateral semicircular canal and inhibits the other.

MVS to Elicit “Set-Point Adaptation”

Recently, we used MVS to extend our knowledge of the time courses of rebalancing tone within the vestibular nuclei, as a model of set-point adaptation. Magnetic vestibular stimulation (MVS) is a simple, safe, and comfortable way to induce a sustained nystagmus and is uniquely suited to study how the brain adapts to a sustained vestibular imbalance. We placed subjects in a 7 T MRI for up to 90 min, during which they showed a persistent nystagmus (23). During this period of sustained MVS, however, slow-phase velocity, after rising relatively quickly to its maximum value, slowly began to decay. We assume that if the MVS could have been sustained for even longer periods, the nystagmus would have eventually disappeared, as occurs over days following an actual loss of function, e.g., after a vestibular nerve section. This gradual fading of the MVS nystagmus represents the action of adaptive processes that monitor and adjust set points. When the adaptive stimulus is abruptly removed, as when the subject exits the MRI bore, an aftereffect appears, revealing the prior adaptation, with oppositely directed slow phases that slowly dissipate at a rate commensurate with how long the initial nystagmus was sustained in the magnet.

A typical example of MVS-induced nystagmus and the attempt of an adaptive mechanism to rid itself of it is shown in **Figure 3** (data points) for a 90-min period of stimulation. Our observations suggest a process that occurs over multiple time courses, and we developed an analytical model that incorporated three integrators of varying dynamic properties (progressively longer time constants) to simulate our data (23). Slower dynamic properties shift the system in stages toward a new 0 set point by gradually eliminating the unwanted bias.

Error Signals and the Implementation of the Adaptive Response

What are the error signals responsible for driving set-point adaptation of the vestibulo-ocular reflex (VOR)? Although

vision and retinal slip are critical signals for adaptation of the dynamic components of the VOR, i.e., the gain of the VOR during head movement, they appear to be unnecessary or at least have only a minimal impact upon VOR set-point adaptation. As a consequence of spontaneous nystagmus, retinal slip is an obvious error signal to drive set-point adaptation. We found, however, that the rate of the early components of adaptation in the MRI scanner, and their aftereffect (reflecting the adaptive rebalancing that had occurred while in the MRI scanner) were nearly superimposable regardless of whether the eyes were fixing on a target or the subject was in darkness in the MRI machine (**Figure 4**). Whether or not vision influences the later components of set-point adaptation is unknown, but after acute unilateral labyrinthectomy in the monkey, an absence of vision does not prevent the disappearance of the spontaneous nystagmus (24).

Where in the brain do these processes of vestibular adaptation take place? For dynamic adaptation of the gain of an inappropriate VOR, signals of unwanted retinal image motion during head movements are thought to be received by the cerebellum that, in turn, recalibrates the eye movement response. For static, set-point adaptation of the VOR, there must exist a mechanism that monitors the spontaneous neural discharge occurring at the vestibular nuclei in order to rebalance the activity between the two sides. The commissural system between the vestibular nuclei may mediate the rebalancing of activity (25, 26). Whether the cerebellum is involved in this process is uncertain (27), but there is evidence from other learning paradigms that the cerebellum participates in set-point adaptation. Examples included control of posture, pointing, and alignment of the eyes (28–30). Furthermore, it is unknown how the brain implements set-point adaptation with multiple time constants, but as in vestibular compensation, this is likely to occur at multiple biological levels—changes in gene expression, neurotransmitter levels, inflammatory responses, synaptic activity, neurogenesis, and other unidentified changes at cellular, network, and cognitive levels (31). Future knowledge on the substrates of adaptation may lead to ways to alter the time constants favorably, allowing new treatments for human disease.

FURTHER IMPLICATIONS AND FUTURE DIRECTIONS OF MVS

Although our interest in MVS began as a curiosity—why were people experiencing dizziness in a strong MRI?—an understanding of the mechanism has greatly expanded its applicability. MVS has helped us to understand how the brain restores equilibrium in response to a sustained vestibular imbalance, such as which occurs in the more natural circumstance when one labyrinth is impaired. These studies have implications for how the brain adapts to any environmental perturbation or unwanted internal change that requires a change in set point to maintain equilibrium and balanced tone and may offer clues to the pathophysiology of set-point disorders such as ocular motor integrator defects producing nystagmus and cervical dystonia producing wry neck. In the vestibular system, we can

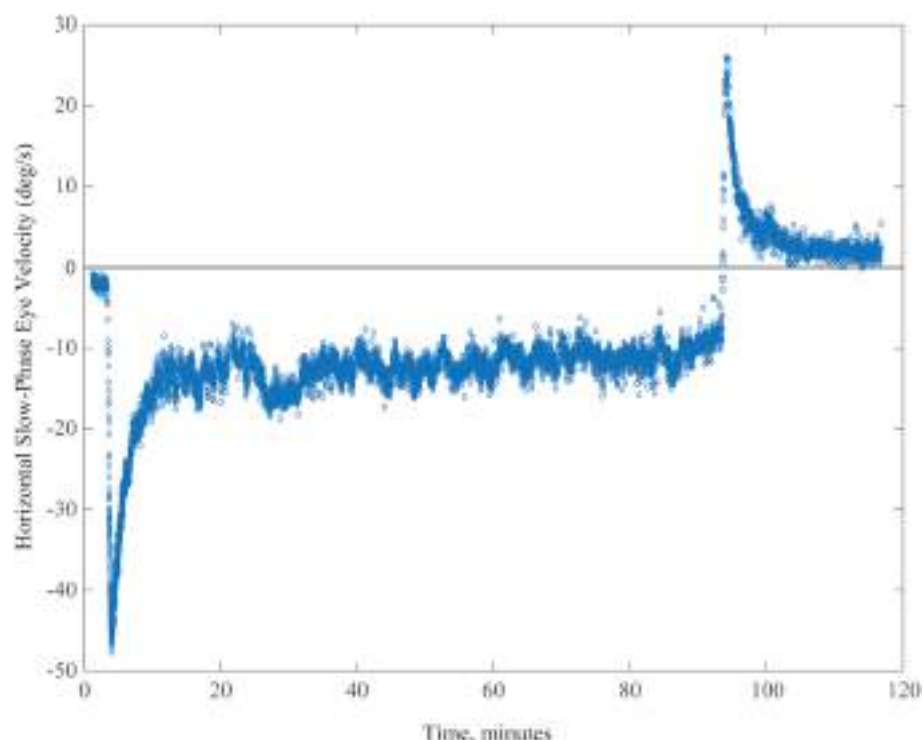


FIGURE 3 | Example of spontaneous nystagmus for up to 90 min in an MRI machine. Graph shows horizontal slow-phase eye velocity of a single subject with negative representing left and positive right. The nystagmus incompletely adapts, and the aftereffect exceeds 30 min, reflecting the relatively long duration of being in the MRI machine.

now explore which parts of the brain are involved in the various time courses of adaptation.

There are implications too for studies of functional and resting-state MRI. On the caveat side, any induced nystagmus, whether or not it is suppressed by fixation, will be accompanied by dramatic changes in activity in many parts of the brain due to the widespread projections of information emanating from the labyrinth. Such metabolic activity could be an important confound in interpreting fMRI studies (32, 33) as well as the fact that vestibular activation of MVS is subject to adaptive mechanisms that try and eliminate it. Positioning the head in the null position might eliminate the MVS effect. On the other hand, MVS-induced nystagmus and the corresponding changes in metabolic activity in the brain can be used to map out the central projections of vestibular afferent activity [e.g., Hitier et al. (34)] [as Marcelli et al., tried to do with his original studies using caloric stimuli when MVS was discovered (1)] as well as changes in activity in different locations that reflect vestibular adaptation over the different time courses that we have discovered.

We also foresee applications to clinical problems. By studying patients with vestibular disorders, we may learn how and in which structures the brain has adapted to a prior lesion, and how it might adapt to a new vestibular imbalance, be it static (involving resting tone) or dynamic (involving compensatory movements in response to head rotations). One wonders if persistent MVS

might be a form of vestibular therapy itself, prodding the brain to adapt better to previous vestibular disorders. Furthermore, in a stationary, supine subject, MVS creates an unnatural pattern of labyrinthine activation. The semicircular canal activation signals the head is rotating but the otoliths signals do not since the head is stationary and the gravity vector is unchanging. Recall when a subject is rotating around an Earth-horizontal axis while lying parallel to the ground (barbecue rotation), there will be a changing gravity vector that activates the otoliths that also signals (like the accompanying canal activation) that the head is rotating. Thus, the “unnatural” pattern of activation in the MRI machine may be used to explore the pathophysiology of the disordered and often disabling perceptions in patients in whom the problem seems to be an inability to resolve conflicts among visual, proprioceptive, and vestibular information. Even higher-level cognitive disorders, e.g., hemi-spatial neglect, might be helped by MVS. Such disorders have been shown previously to be temporarily ameliorated using caloric or galvanic stimulation (35, 36), but these are cruder and less easily tolerated forms of labyrinthine activation.

To epitomize, MVS is a relatively simple, safe, and novel way of stimulating the labyrinth. Much as did caloric, galvanic, and artificial rotational stimulation, we expect that MVS will bring important scientific and clinical advances to our understanding of how the vestibular system works and how it repairs itself when faced with disease or trauma.

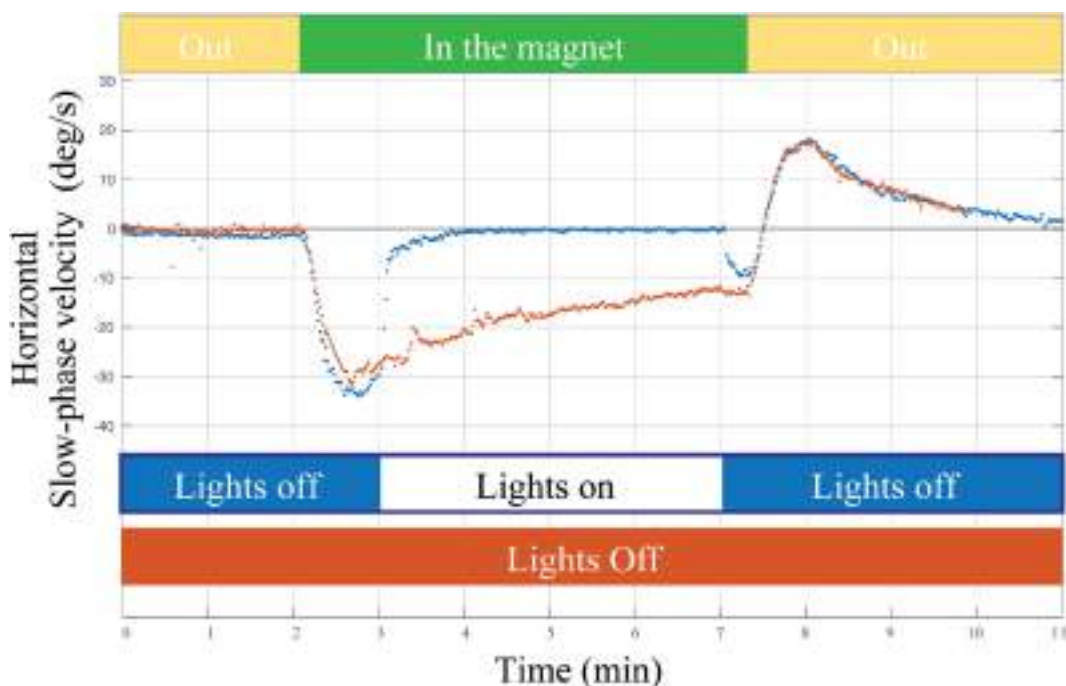


FIGURE 4 | Example of a single subject entering the MRI head first supine position in two conditions: (1) lights off for 2 min outside the magnet, 5 min inside the magnet, and 2 min outside the magnet (orange trace) and (2) lights turned on for approximately 4 min of fixation inside the magnet (blue trace). Visual fixation had negligible impact on the rate of adaptation or on the aftereffect (reflecting adaptation in the MRI regardless of whether the lights were on or off).

AUTHOR CONTRIBUTIONS

DZ and BW performed the initial drafts of the manuscript. DR created the initial draft of **Figure 1**. BW created **Figure 2**. JO-M created the initial versions of **Figures 3** and **4**. All authors were involved in data collection and editing and approval of the final version of the manuscript.

FUNDING

This study was funded by the Fight for Sight and Leon Levy Foundations, The Johns Hopkins Medicine Discovery Fund, and the Cinquegrana, Lott, and Schwerin families.

REFERENCES

1. Marcelli V, Esposito F, Aragri A, Furia T, Riccardi P, Tosetti M, et al. Spatio-temporal pattern of vestibular information processing after brief caloric stimulation. *Eur J Radiol* (2009) 70:312–6. doi:10.1016/j.ejrad.2008.01.042
2. Schenck JF, Dumoulin CL, Redington RW, Kressel HY, Elliott RT, McDougall IL. Human exposure to 4.0-Tesla magnetic fields in a whole-body scanner. *Med Phys* (1992) 19:1089–98. doi:10.1118/1.596827
3. Kangarlu A, Burgess RE, Zhu H, Nakayama T, Hamlin RL, Abduljalil AM, et al. Cognitive, cardiac, and physiological safety studies in ultra high field magnetic resonance imaging. *Magn Reson Imaging* (1999) 17:1407–16. doi:10.1016/S0730-725X(99)00086-7
4. de Vocht F, van Droege H, Engels H, Kromhout H. Exposure, health complaints and cognitive performance among employees of an MRI scanners manufacturing department. *J Magn Reson Imaging* (2006) 23:197–204. doi:10.1002/jmri.20485
5. Schaap K, Christopher-de Vries Y, Mason CK, de Vocht F, Portengen L, Kromhout H. Occupational exposure of healthcare and research staff to static magnetic stray fields from 1.5–7 Tesla MRI scanners is associated with reporting of transient symptoms. *Occup Environ Med* (2014) 71:423–9. doi:10.1136/oemed-2013-101890
6. Schenck JF. Health and physiological effects of human exposure to whole-body four-Tesla magnetic fields during MRI. *Ann N Y Acad Sci* (1992) 649:285–301. doi:10.1111/j.1749-6632.1992.tb49617.x

SUPPLEMENTARY MATERIAL

The Supplementary Material for this article can be found online at <http://journal.frontiersin.org/article/10.3389/fneur.2017.00122/full#supplementary-material>.

VIDEO S1 | A mixed horizontal-torsional eye movement in a healthy adult lying supine in the bore of a 7-T MRI machine. This unusual nystagmus pattern has a torsional component in which the top poles of the eyes rotate in a slow phase pattern of nystagmus away from the ear toward which the horizontal component of the slow phase is directed. This is in contrast to the more common pattern of a mixed horizontal-torsional nystagmus, for example, as seen after a unilateral loss of labyrinthine function, where the top poles of the eyes rotate in a slow phase toward the same ear as the horizontal component of the slow phase is directed. This reflects the unusual combined stimulation pattern of the anterior and lateral semicircular canals.

7. Houpt TA, Pittman DW, Barranco JM, Brooks EH, Smith JC. Behavioral effects of high-strength static magnetic fields on rats. *J Neurosci* (2003) 23: 1498–505.
8. Houpt TA, Cassell JA, Riccardi C, DenBleyker MD, Hood A, Smith JC. Rats avoid high magnetic fields: dependence on an intact vestibular system. *Physiol Behav* (2007) 92:741–7. doi:10.1016/j.physbeh.2007.05.062
9. Snyder DJ, Jahng JW, Smith JC, Houpt TA. c-Fos induction in visceral and vestibular nuclei of the rat brain stem by a 9.4 T magnetic field. *Neuroreport* (2000) 11:2681–5. doi:10.1097/00001756-200008210-00015
10. Houpt TA, Pittman DW, Riccardi C, Cassell JA, Lockwood DR, Barranco JM, et al. Behavioral effects on rats of high strength magnetic fields generated by a resistive electromagnet. *Physiol Behav* (2005) 86:379–89. doi:10.1016/j.physbeh.2005.08.008
11. Roberts DC, Marcelli V, Gillen JS, Carey JP, Della Santina CC, Zee DS. MRI magnetic field stimulates rotational sensors of the brain. *Curr Biol* (2011) 21:1635–40. doi:10.1016/j.cub.2011.08.029
12. Ward BK, Roberts DC, Della Santina CC, Carey JP, Zee DS. Magnetic vestibular stimulation in subjects with unilateral labyrinthine disorders. *Front Neurol* (2014) 5:28. doi:10.3389/fnneur.2014.00028
13. Otero-Millan J, Zee DS, Schubert MC, Roberts DC, Ward BK. Three-dimensional eye movement recordings during magnetic vestibular stimulation. *J Neurol* (2017). doi:10.1007/s00415-017-8420-4
14. Kirsch V, Keeser D, Hergenroeder T, Ertl O, Ertl-Wagner B, Brandt T, et al. Structural and functional connectivity mapping of the vestibular circuitry from human brainstem to cortex. *Brain Struct Funct* (2016) 221:1291–308. doi:10.1007/s00429-014-0971-x
15. de Waele C, Baudouinère PM, Lepecq JC, Tran Ba Huy P, Vidal PP. Vestibular projections in the human cortex. *Exp Brain Res* (2001) 141:541–51. doi:10.1007/s00221-001-0894-7
16. Zee DS, Jareonsettasin P, Leigh RJ. Ocular stability and set-point adaptation. *Philos Trans R Soc Lond B Biol Sci* (2017) 372:20160199. doi:10.1098/rstb.2016.0199
17. Sherrington C. Postural activity of muscle and nerve. *Brain* (1915) 38:191–234. doi:10.1093/brain/38.3.191
18. Malcolm R, Jones GM. A quantitative study of vestibular adaptation in humans. *Acta Otolaryngol* (1970) 70:126–35. doi:10.3109/00016487009181867
19. Zee DS, Preziosi TJ, Proctor LR. Bechterew's phenomenon in a human patient. *Ann Neurol* (1982) 12:495–6. doi:10.1002/ana.410120519
20. Young LR, Oman CM. Model for vestibular adaptation to horizontal rotation. *Aerospace Med* (1969) 40:1076–80.
21. Baertschi AJ, Johnson RN, Hanna GR. A theoretical and experimental determination of vestibular dynamics in caloric stimulation. *Biol Cybern* (1975) 20:175–86. doi:10.1007/BF00342638
22. Bock O, von Koschitzky H, Zangemeister WH. Vestibular adaptation to long-term stimuli. *Biol Cybern* (1979) 33:77–9. doi:10.1007/BF00355256
23. Jareonsettasin P, Otero-Millan J, Ward BK, Roberts DC, Schubert MC, Zee DS. Multiple time courses of vestibular set-point adaptation revealed by sustained magnetic field stimulation of the labyrinth. *Curr Biol* (2016) 26:1359–66. doi:10.1016/j.cub.2016.03.066
24. Fetter M, Zee DS, Proctor LR. Effect of lack of vision and of occipital lobectomy upon recovery from unilateral labyrinthectomy in rhesus monkey. *J Neurophysiol* (1988) 59:394–407.
25. Fetter M, Zee DS. Recovery from unilateral labyrinthectomy in rhesus monkey. *J Neurophysiol* (1988) 59:370–93.
26. Galiana HL, Flohr H, Jones GM. A reevaluation of intervestibular nuclear coupling: its role in vestibular compensation. *J Neurophysiol* (1984) 51(2): 242–59.
27. Haddad GM, Friendlich AR, Robinson DA. Compensation of nystagmus after VIIth nerve lesions in vestibulo-cerebellatectomized cats. *Brain Res* (1977) 135:192–6. doi:10.1016/0006-8993(77)91066-6
28. Lewis RF, Tamargo RJ. Cerebellar lesions impair context-dependent adaptation of reaching movements in primates. *Exp Brain Res* (2001) 138:263–7. doi:10.1007/s002210100719
29. Takakusaki K. Functional neuroanatomy for posture and gait control. *J Mov Disord* (2017) 10:1–17. doi:10.14802/jmd.16062
30. Patel VR, Zee DS. The cerebellum in eye movement control: nystagmus, coordinate frames and disconjugacy. *Eye (Lond)* (2015) 29:191–5. doi:10.1038/eye.2014.271
31. Lacour M, Helmchen C, Vidal P-P. Vestibular compensation: the neuro-otologist's best friend. *J Neurol* (2016) 263:54–64. doi:10.1007/s00415-015-7903-4
32. Boegle R, Stephan T, Ertl M, Glasauer S, Dieterich M. Magnetic vestibular stimulation modulates default mode network fluctuations. *Neuroimage* (2016) 127:409–21. doi:10.1016/j.neuroimage.2015.11.065
33. Boegle R, Ertl M, Stephan T, Dieterich M. Magnetic vestibular stimulation influences resting-state fluctuations and induces visual-vestibular biases. *J Neurol* (2017). doi:10.1007/s00415-017-8447-6
34. Hitier M, Besnard S, Smith PF. Vestibular pathways involved in cognition. *Front Integr Neurosci* (2014) 8:59. doi:10.3389/fnint.2014.00059
35. Moon S, Lee B, Na D. Therapeutic effects of caloric stimulation and optokinetic stimulation on hemispatial neglect. *J Clin Neurol* (2006) 2:12–28. doi:10.3988/jcn.2006.2.1.12
36. Wilkinson D, Zubko O, Sakel M, Coulton S, Higgins T, Pullicino P. Galvanic vestibular stimulation in hemi-spatial neglect. *Front Integr Neurosci* (2014) 8:4. doi:10.3389/fnint.2014.00004

Conflict of Interest Statement: The authors declare that the research was conducted in the absence of any commercial or financial relationships that could be construed as a potential conflict of interest.

Copyright © 2017 Ward, Otero-Millan, Jareonsettasin, Schubert, Roberts and Zee. This is an open-access article distributed under the terms of the Creative Commons Attribution License (CC BY). The use, distribution or reproduction in other forums is permitted, provided the original author(s) or licensor are credited and that the original publication in this journal is cited, in accordance with accepted academic practice. No use, distribution or reproduction is permitted which does not comply with these terms.



Sustained and Transient Vestibular Systems: A Physiological Basis for Interpreting Vestibular Function

Ian S. Curthoys^{1*}, Hamish G. MacDougall¹, Pierre-Paul Vidal² and Catherine de Waele³

¹Vestibular Research Laboratory, School of Psychology, The University of Sydney, Sydney, NSW, Australia, ²Cognition and Action Group, CNRS UMR8257, Centre Universitaire des Saints-Pères, University Paris Descartes, Paris, France, ³ENT Department, Salpêtrière Hospital, Paris, France

OPEN ACCESS

Edited by:

Bernard Cohen,
Icahn School of Medicine at
Mount Sinai, USA

Reviewed by:

Shinichi Iwasaki,
University of Tokyo, Japan
Richard D. Rabbitt,
University of Utah, USA
Hans VanDerSteen,
Erasmus University Rotterdam,
Netherlands

*Correspondence:

Ian S. Curthoys
ian.curthoys@sydney.edu.au

Specialty section:

This article was submitted to
Neuro-otology,
a section of the journal
Frontiers in Neurology

Received: 16 January 2017

Accepted: 14 March 2017

Published: 30 March 2017

Citation:

Curthoys IS, MacDougall HG, Vidal P-P and de Waele C (2017) Sustained and Transient Vestibular Systems: A Physiological Basis for Interpreting Vestibular Function. *Front. Neurol.* 8:117.
doi: 10.3389/fneur.2017.00117

Otolithic afferents with regular resting discharge respond to gravity or low-frequency linear accelerations, and we term these the static or sustained otolithic system. However, in the otolithic sense organs, there is anatomical differentiation across the maculae and corresponding physiological differentiation. A specialized band of receptors called the striola consists of mainly type I receptors whose hair bundles are weakly tethered to the overlying otolithic membrane. The afferent neurons, which form calyx synapses on type I striolar receptors, have irregular resting discharge and have low thresholds to high frequency (e.g., 500 Hz) bone-conducted vibration and air-conducted sound. High-frequency sound and vibration likely causes fluid displacement which deflects the weakly tethered hair bundles of the very fast type I receptors. Irregular vestibular afferents show phase locking, similar to cochlear afferents, up to stimulus frequencies of kilohertz. We term these irregular afferents the transient system signaling dynamic otolithic stimulation. A 500-Hz vibration preferentially activates the otolith irregular afferents, since regular afferents are not activated at intensities used in clinical testing, whereas irregular afferents have low thresholds. We show how this sustained and transient distinction applies at the vestibular nuclei. The two systems have differential responses to vibration and sound, to ototoxic antibiotics, to galvanic stimulation, and to natural linear acceleration, and such differential sensitivity allows probing of the two systems. A 500-Hz vibration that selectively activates irregular otolithic afferents results in stimulus-locked eye movements in animals and humans. The preparatory myogenic potentials for these eye movements are measured in the new clinical test of otolith function—ocular vestibular-evoked myogenic potentials. We suggest 500-Hz vibration may identify the contribution of the transient system to vestibular controlled responses, such as vestibulo-ocular, vestibulo-spinal, and vestibulo-sympathetic responses. The prospect of particular treatments targeting one or the other of the transient or sustained systems is now being realized in the clinic by the use of intratympanic gentamicin which preferentially attacks type I receptors.

Abbreviations: ABR, auditory brainstem response; ACS, air-conducted sound; BCV, bone-conducted vibration; Fz, the midline of forehead at the hairline; GVS, galvanic vestibular stimulation; IO, inferior oblique eye muscle; ITG, intratympanic gentamicin; MSNA, muscle sympathetic nerve activity; VEMP, vestibular-evoked myogenic potential; CVEMEP, cervical vestibular-evoked myogenic potential; oVEMP, ocular vestibular-evoked myogenic potential; OCR, ocular counterrolling; PID, proportional–integral–derivative; SCD, semicircular canal dehiscence; n10, the initial negative potential of the oVEMP at about 10 ms latency; SCM, sternocleidomastoid muscle; VIN, vibration-induced nystagmus; VsEP, vestibular-evoked potential.

We suggest that it is valuable to view vestibular responses by this sustained-transient distinction.

Keywords: **vestibular, utricular, sound, vibration, otolith, vestibular-evoked myogenic potential, vestibulo-ocular reflex, vestibular-evoked myogenic potentials**

KEY CONCEPTS

Vestibular afferents with regular resting discharge constitute a system for signaling sustained vestibular stimuli, such as maintained head tilts.

Vestibular afferents with irregular resting activity constitute a system for signaling transient vestibular stimuli.

Otolith irregular afferents originate from a specialized region of the otolithic maculae called the striola and form calyx synapses on type I receptors which have fast membrane dynamics.

Otolith irregular afferents are selectively activated by high-frequency (~500 Hz) low-intensity BCV and ACS. Regular otolithic afferents do not respond to these stimuli at comparable levels.

Ototoxic antibiotics selectively affect type I receptors and thus the transient system.

The 500-Hz vibration causes eye movements in humans, and the preparatory myogenic potentials for these movements are the ocular VEMPs which index the activity of the transient system.

Vestibular nucleus neurons exhibit transient or sustained responses, as in the periphery.

INTRODUCTION

The early recordings of the response of cat single vestibular nucleus neurons to angular acceleration established that different neurons had very different response patterns to identical angular acceleration stimuli (1–3). Some neurons showed a sustained response to maintained stimuli (termed tonic neurons), whereas others showed a transient response to the same stimulus (termed kinetic neurons). These results were confirmed and extended in later research which also showed a similar distinction applied to primary semicircular canal (4–6) and otolithic neurons (7–9). That research and later work showed how these characteristics were associated with the regularity of resting discharge of primary afferent neurons—neurons with regular resting discharge showing sustained (tonic) responses to maintained stimuli, whereas neurons with irregular resting discharge showed transient (kinetic or phasic) responses to the same stimuli (10). There is a continuum of regularity, and we will use the terms sustained and transient for convenience to refer to the ends of this continuum.

This review shows how recent evidence about otolithic responses to sound and vibration demonstrates the value of applying this distinction of sustained and transient from the receptors to the behavioral responses. We suggest it is a valuable principle for interpreting the results of vestibular functional tests—focusing attention on different aspects of the response rather than just treating the whole response as uniform. This is especially clear with the otoliths, but even with the canals it is useful to distinguish between responses to the onset of an

acceleration, as opposed to responses during maintained accelerations. The paper will not cover particular areas in great detail since it has already been done in many other reviews to which the reader is referred. Instead, we aim to bring together evidence from physiology to highlight the relevance of this evidence for understanding vestibular function testing as used clinically. The first part of this review covers physiological evidence and the second part covers the application of the sustained-transient principle to vestibular responses.

PHYSIOLOGICAL DATA

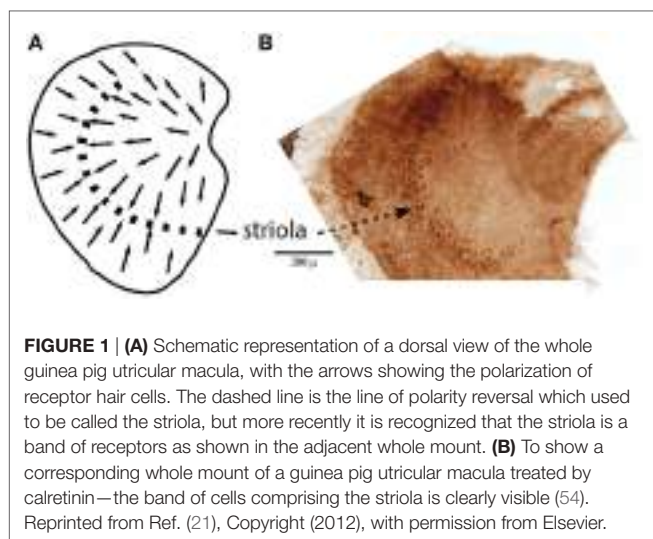
Peripheral Vestibular Physiology

The regularity of resting discharge of vestibular primary afferents is associated with a range of characteristics, such as conduction velocity, axon thickness, and a range of response dimensions, such as gain to acceleration, sensitivity to electrical vestibular stimulation [including so-called galvanic vestibular stimulation (GVS)—DC or low-frequency electrical stimulation of the sense organs]. While afferents from all vestibular sense organs are activated by GVS at approximately equal thresholds (11) irregular afferents from each sense organ have a significantly lower threshold for GVS activation than regular neurons.

Angular and linear acceleration of the whole animal have been the usual stimuli in studies of vestibular physiology, and it has been shown in a number of species that regular and irregular neurons have different frequency responses—with irregular afferents (both canal and otolithic) typically having an increased gain and increasing phase lead with increasing frequency—interpreted as showing that irregular afferents are responsive to both acceleration and change in acceleration (jerk). The characteristics of regular and irregular neurons have been summarized by Goldberg's definitive review of vestibular afferent diversity (10).

In summary, first-order vestibular neurons with regular resting discharge comprised bouton and dimorphic neurons which synapse on the barrel-shaped type II receptors mainly in the peripheral zone of the cristae and in the extrastriolar zone of the otolithic maculae. They are characterized by thin or medium-sized, slow conducting axons and with a low sensitivity to head rotation and relatively low sensitivity to GVS. Irregular first-order vestibular neurons comprised calyx and dimorphic neurons, which innervate the central cristae and the striolar zones of the otolithic maculae, synapsing predominantly on the amphora-shaped type I receptors (**Figure 1**). They are characterized by large- or medium-sized fast conducting axons. Their sensitivity to GVS is on average six times higher than that of the regular afferents (11, 12).

In addition, some vestibular afferents show a sensitive response to sound and vibration (13–15). Recent research has extended this account (16–21). The major result is that the otolith irregular neurons originating from a special band of receptors



on the otolithic macula called the striola (**Figure 2**) respond to both air-conducted sound (ACS) and bone-conducted vibration (BCV) up to very high frequencies (>1,000 Hz), while regular neurons—mainly from extrastriolar areas—show modest or absent responses to such stimuli (see **Figure 2**).

Detailed analysis of the timing of the action potentials of irregular afferents evoked by sound or vibration show they are phase locked to individual cycles of the ACS (up to 3,000 Hz) or BCV stimulus (up to 2,000 Hz) (**Figure 3**) (20). Phase locking means that the exact timing of the action potential is locked to a particular phase angle (or a narrow band of phase angles) of the stimulus waveform at that frequency (**Figure 3**). It does not mean the cell generates an action potential once per cycle up to thousands of Hertz, but that the moment when the cell fires is locked to the particular narrow band of phase angles of the stimulus waveform at that frequency. A vestibular afferent may miss many cycles, but when it does fire it is locked to the phase angle of the stimulus waveform. The phase locking of vestibular afferents is similar to the well-documented phase locking of cochlear afferents to ACS, known since the study of Rose et al. (22).

In stark contrast, regular neurons (canal or otolith) are not activated by ACS or BCV stimuli—at least in response to stimulus levels used in clinical studies of human otolithic function (see **Figure 2B**)—and so do not show phase locking. As the example in **Figure 2** shows, regular neurons simply continue to fire at their resting rate during stimuli which are much more intense than those which cause activation of irregular neurons. Irregular afferents have very low thresholds to BCV—at or below the levels needed for auditory brainstem response threshold. McCue and Guinan (13, 23, 24) showed that irregular saccular afferents were activated by ACS, and Murofushi et al. (14, 25, 26) reported that saccular afferents could be activated by high intensity ACS click stimuli. These results have been confirmed years later (17, 20). Curthoys et al. (18) tested the specific, sensitive response of irregular utricular neurons to 500 Hz BCV in guinea pig and found that very few utricular regular afferents were activated by high intensity ACS or BCV stimulation. That has also been

confirmed in rat: where few regular afferents are activated even by intense ACS, although ACS is an effective stimulus for irregular neurons (27, 28). It has been shown that both saccular and utricular irregular afferents are activated by both 500 Hz ACS and BCV (21).

This clear phase locking of irregular vestibular afferents to such high frequencies of ACS and BCV stimulation has posed questions about how vestibular hair cell transduction mechanisms operate at such high frequencies. Vestibular responses are usually thought of as being for stimuli to a few tens of Hertz, not to stimuli of over 1,000 Hz. Furthermore, the fact that irregular and regular afferents have such very different responses to sound and vibration raises the possibility of the use of sound and vibration to probe the relative contribution of irregular (transient) and regular (sustained) otolithic afferents to various physiological and even behavioral responses, and thus the likely functional roles of these classes of afferents. One other question is of the mechanisms responsible for the regularity of resting discharge, which is now clearly established as being due to membrane characteristics of the afferent neurons (29–31).

In these studies, the usual result is that in animals with intact bony labyrinths, afferent neurons (either regular or irregular) from semicircular canals are not activated or only weakly activated by very intense stimulus levels of 500 Hz BCV and ACS (18, 27, 28). However, there are drastic changes in neural response after a small hole is made in the bony wall of the semicircular canal (even just 0.1 mm diameter in the case of the guinea pig). This opening, called a dehiscence or a semicircular canal dehiscence (SCD) results in a previously unresponsive irregular canal afferent being activated by sound and vibration at low stimulus levels (32, 33). The evidence is that the SCD decreases the impedance of the labyrinth and so, it is argued, acts to increase the fluid displacement sufficiently to deflect the receptors.

More recently, it has been found that even in animals with intact bony labyrinths, irregular canal afferents can be activated by very low-frequency BCV and indeed phase lock to 100 Hz BCV (17). However, the response of these irregular canal afferents declines with increasing BCV frequency, and so these irregular canal afferents are not activated at 500 Hz BCV even at high stimulus levels (17, 34, 35). In light of this evidence, we conclude 500 Hz BCV is a selective stimulus for irregular otolithic neurons. It is probable that this activation of canal afferents by such low-frequency BCV is the neural mechanism responsible for the clinical test of vestibular function—skull vibration-induced nystagmus (35, 36).

Mechanism

How can vestibular receptors and irregular otolithic afferents respond to such very high frequencies? Textbook schematic diagrams of the cristae and otolithic maculae give the impression that each vestibular sense organ is a uniform structure with receptor hair cells of similar height. It is now clear that is the very opposite of what is the case. Each macula and each crista shows complex anatomical differentiation across the surface. The receptor types are differentially distributed with predominantly type I receptors at the striola (37). The extrastriolar receptors appear to be more tightly tethered to the otoconial membrane (38) than are

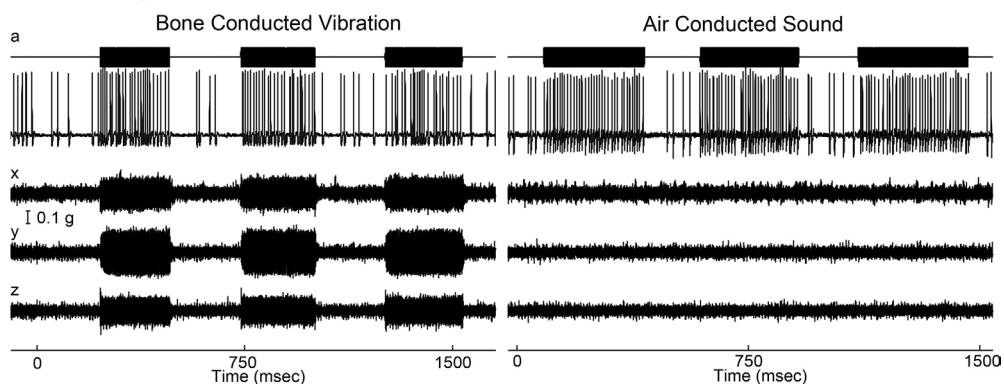
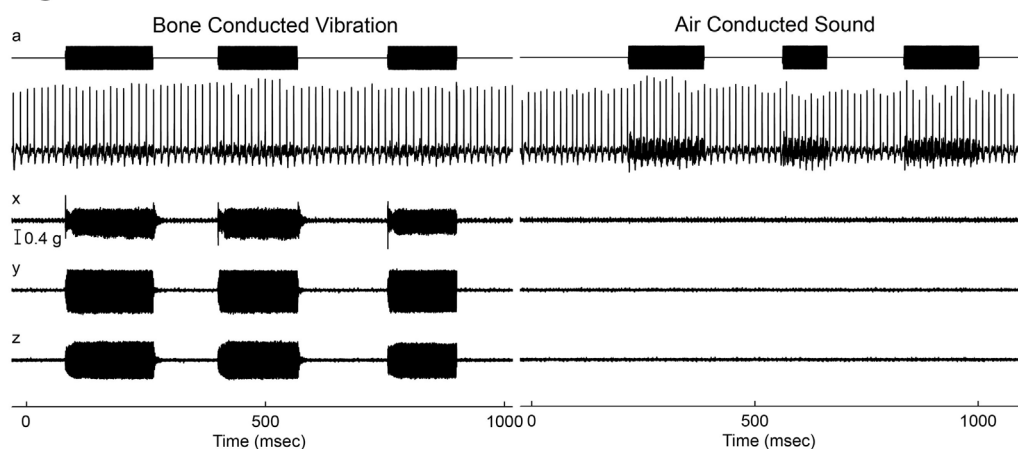
A Utricular irregular afferent**B Regular afferent**

FIGURE 2 | Resting discharge pattern and response to stimulation of an irregular and a regular afferent. **(A)** Time series of an irregular otolith neuron during stimulation by 500 Hz bone-conducted vibration (BCV) and air-conducted sound (ACS). The top trace (a) shows the command voltage, indicating when the stimulus is on. The second trace shows the action potentials by extracellular recording. The three bottom traces (x, y, z) show the triaxial accelerometer recording of the stimulus. The left panel is an example of response to BCV stimulation and the right of the response to ACS stimulation of the same neuron, showing it is clearly activated by both stimulus types. Note the scale of stimulus intensity in g at the left margin between traces x and y. The irregular resting discharge is seen before stimulus onset, followed by a large increase in firing during both BCV and ACS. **(B)** Time series of a regular semicircular canal neuron during stimulation by BCV and ACS as above. The regular discharge is seen before the stimulus onset. The stimuli are far stronger than in panel **(A)**, but there is no evidence of activation of this regular neuron by these strong stimuli. From Ref. (19), Curthoys and Vulovic, © Springer-Verlag, 2010, reproduced with permission of Springer.

the striolar receptors. Receptors across the maculae (and cristae) are not of uniform height: at the striola of the maculae and at the crest of the cristae, the receptor hair bundles are shorter (and stiffer) than in the extrastriolar areas. Remarkably, this height difference can even be seen in Hunter-Duvar's scanning electron micrograph of the whole utricular macula of the chinchilla (39). Morphological evidence shows apparently looser tethering of the hair bundles of striolar receptors to the overlying otolithic membrane in comparison with comparable receptors in the periphery of the macula (extrastriolar receptors) (38–44).

Most models of otolithic stimulation model displacement of the gelatinous otoconial membrane with otoconia adherent to its upper surface in response to linear acceleration stimulation, e.g., Ref. (45, 46). In such models, frequencies in the kilohertz range are beyond the upper mechanical cutoff of the system. Nevertheless, it is clear from the neural recordings that action

potentials in individual neurons do respond and are phase locked to a narrow band of phases for stimulus frequencies even as high as 3,000 Hz (Figure 3). Phase locking of irregular vestibular afferents shows that every single cycle of the stimulus waveform is the adequate stimulus for the receptor–afferent complex. For this to happen at kilohertz frequencies, the receptor membrane and calyx membrane must have extremely fast dynamics, and indeed, the very fast dynamics of vestibular type I receptors and calyx membranes have been shown beautifully by the studies of Songer and Eatock (47). They used intracellular recording of receptor and calyx potentials in response to mechanical displacement of the hair bundle at very high frequencies and demonstrated the very fast membrane and synaptic dynamics of type I vestibular receptors and calyx afferents.

In light of this phase locking up to such high frequencies, we have suggested that the hair bundles of the striolar otolithic

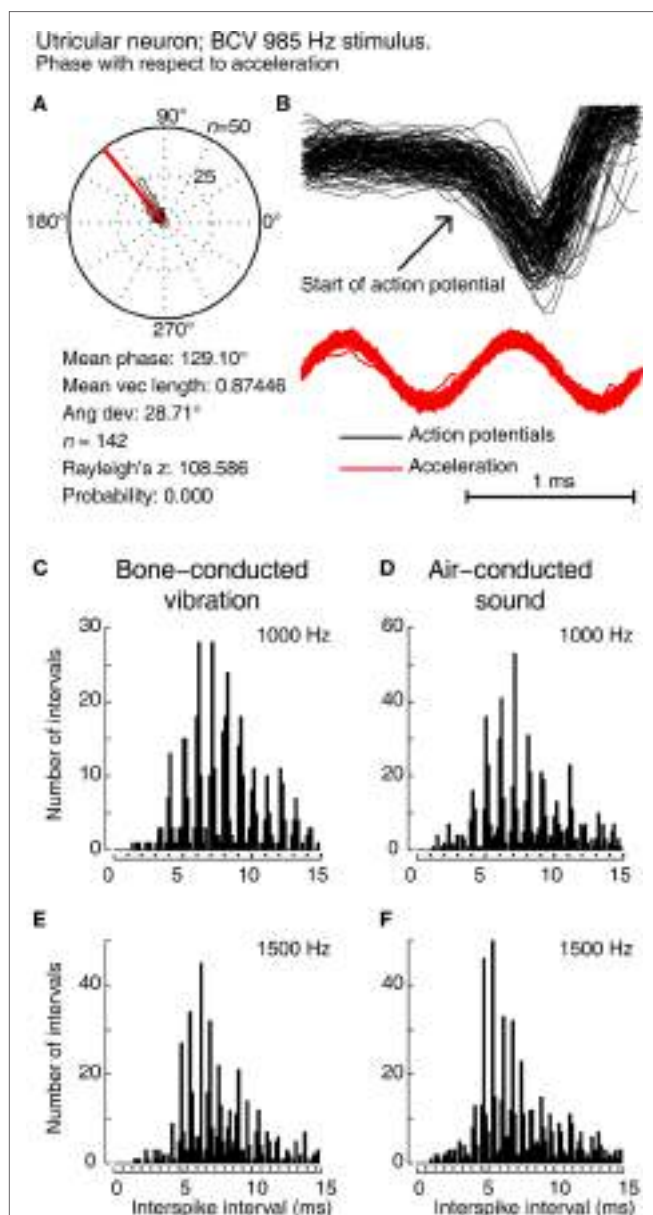


FIGURE 3 | Showing phase locking of a single utricular neuron. (A,B) Time series of successive action potentials of the neuron to bone-conducted vibration (BCV) at 985 Hz. Panel (B) shows 142 action potentials superimposed and the onset of the action potential is shown by the arrow. The red trace shows the x channel of the 3D linear accelerometer. Panel (A) shows the circular histogram of the phases of the action potentials clustered around a mean of 129.1°, with angular deviation 28.7°. The test of circular uniformity, Rayleigh's z , is highly significant showing the probability of a uniform phase distribution is <0.001 . The neuron misses some cycles, but when it fires is locked to the stimulus waveform. (C–F) Histograms of interspike intervals to show phase locking in the same utricular afferent neuron in guinea pig at two high frequencies of BCV (C,E) and air-conducted sound (ACS) stimuli (D,F). The bin width is 0.16 ms. The dots below each histogram show integral multiples of the period for the given stimulus frequency. The clustering around these integral multiples demonstrates phase locking at both frequencies. This figure is a replotted version of the histograms of the response of neuron 151011, which has been published as Figure 10 of Curthoys et al. (20). Reprinted from Ref. (20), © 2016, with permission of Elsevier.

receptors are deflected by each cycle of fluid displacement caused by the stapes pumping into the fluid-filled inner ear (33). This fluid displacement is small but vestibular receptors have great sensitivity: the maximum sensitivity of the hair bundles of vestibular receptors is around 0.40° of cilia deflection, similar to the value for cochlear receptors (0.39°) (48), caused by just a few nanometers of fluid displacement.

We (33) have put forward the following account. Striola receptors are predominantly amphora-shaped type I receptors (37) and have short stiff hair bundles (44, 49), apparently loosely attached to the overlying otolithic membrane (38). This fluid motion within the fluid-filled hole in the gel-filament layer of the otolithic membrane produces a drag force on the hair bundle, causing it to deflect. The fluid environment is so viscously dominated (Reynold's Numbers of 10^{-3} to 10^{-2}) that bundles move instantaneously with any fluid movement. In other words, this coupling of fluid motion to hair bundle is so strong that the hair bundle displacement follows the fluid displacement almost exactly (17). Thus, fluid displacement is synonymous with hair bundle displacement.

Complementing that anatomical evidence is physiological evidence from recordings of primary otolithic afferent neurons originating from striola type I receptors as shown by neurobiotin labeling (21) (Figure 4A), these afferents have irregular resting discharge and are activated by ACS and BCV up to very high frequencies. There is evidence that it is the striolar receptor hair cells (probably mainly type I receptors) which respond to frequencies far higher than modeling of canal or otolith mechanics indicates. This account is indirectly confirmed by the effect of SCD on the response of irregular canal afferents from the crest of the crista (17). Prior to the SCD, these neurons do not respond to ACS or BCV at the levels used in human clinical testing, whereas after the SCD [which acts to increase fluid displacement (50, 51)] these same irregular afferents show strong phase-locked activation to the same stimulus (33) (Figure 4B).

Why is it that regular afferents are not responsive to vibration and sound at such high frequencies? One possible reason is that regular neurons synapse on few type I receptors mainly in extrastriolar areas, whereas their largest number of synapses are usually on multiple extrastriolar type II receptors with long cilia apparently more tightly tethered to the overlying gel-filament layer (38). In this way, fluid displacement would be less likely to activate type II receptors because, instead of projecting into holes in the overlying membrane, the hair bundles project into the gel-filament layer or cupula, which limits the deflection of the receptors.

Mechanism—Summary

There are two issues: (1) the regularity of resting discharge and (2) the response to sound and vibration determined by receptor mechanisms. These are two different aspects of the afferent response, and the evidence is that they are determined by different factors.

- (1) Recent evidence shows that regularity of vestibular afferent resting discharge is due to membrane characteristics (29–31). That has been most convincingly shown by recent

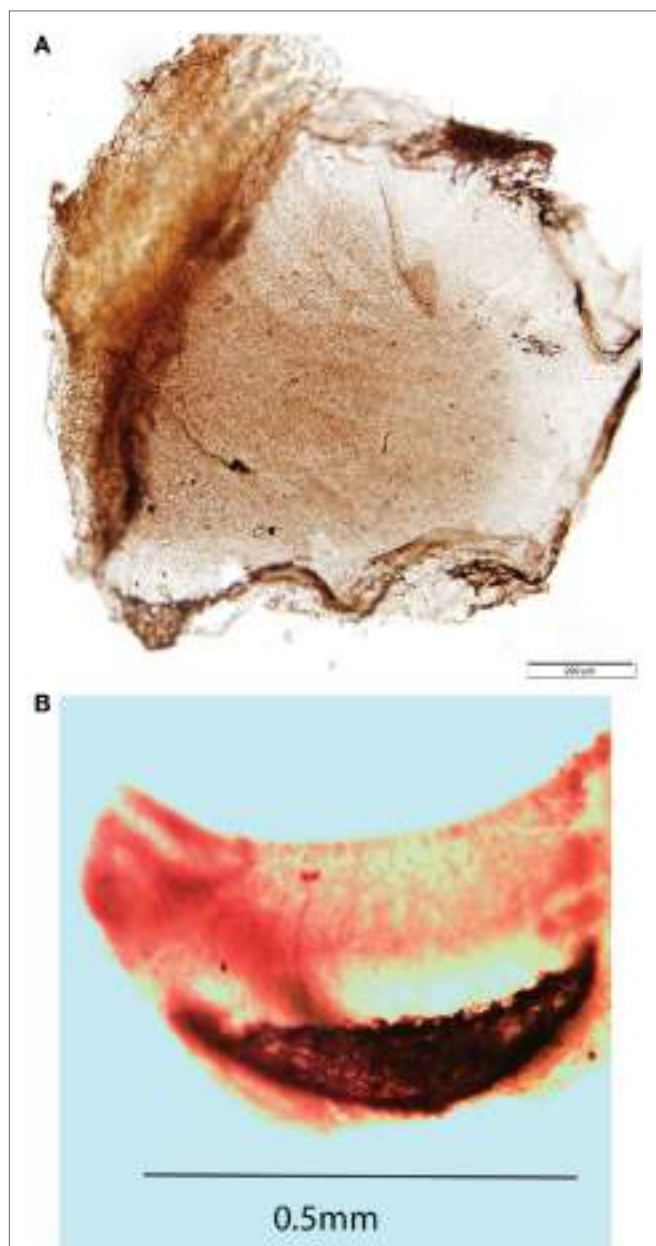


FIGURE 4 | (A) Direct dorsal view of a whole mount of a guinea pig utricular macula showing one neuron labeled by neurobiotin activated by both 500 Hz bone-conducted vibration (BCV) and air-conducted sound (ACS). The labeled axon terminates on three calyx endings which envelop the whole type I receptor(s), but in addition there are small bouton endings, so this axon is strictly a dimorphic afferent. The calyx receptors are in or close to the striolar area of the utricular macula. The scale bar is 200 μ m. Reprinted from Ref. (21), Copyright (2012), with permission from Elsevier. **(B)** Whole mount of the crista of the anterior canal of a guinea pig showing an afferent fiber labeled by neurobiotin which forms two calyx endings enveloping two type I receptors at the crest of the crista. This neuron was unresponsive to ACS prior to a semicircular canal dehiscence, but showed activation and phase locking to 985 Hz ACS after dehiscence.

experiments blocking specific membrane channels. This is the empirical evidence—the regularity of afferent discharge is due to channels of the afferent membrane and not the

receptors. Neurobiotin labeling has shown that the irregular afferents which respond to these stimuli form calyx synapses on striolar type 1 receptor cells, not on type I extrastriolar receptors (20, 21). However, the receptor type does not determine the regularity of resting discharge: fish only have type II receptors but they have both regular and irregular afferents (52).

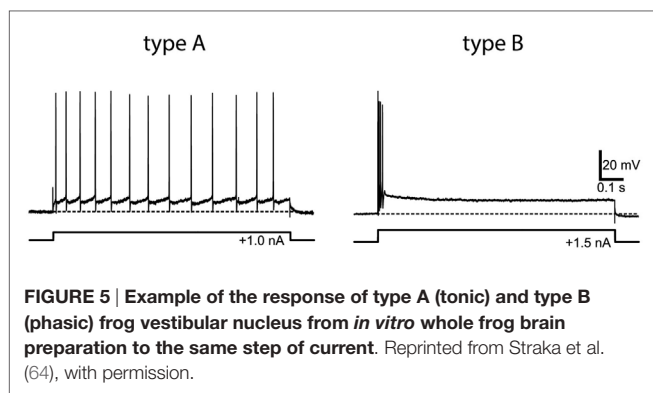
- (2) We (33) have put forward the hypothesis that the short stiff hair bundles of these striolar receptors are deflected by fluid displacement once per stimulus cycle so the calyx-bearing afferents of striolar irregular afferents are activated once per cycle, resulting in phase-locked action potentials up to such high frequencies. Hair cell height and stiffness have been demonstrated to vary across the macula surface (39, 49, 53–55). The cells which do show high-frequency phase locking are from calyx-bearing afferents originating from the striola (21) with shorter stiffer receptor hair cells. Afferents from extrastriolar areas do not show high-frequency phase locking. With only type II receptors, fish also show phase locking, but to much lower frequencies (~400 Hz), and it may be that the type I receptor calyx combination allows the very high-frequency phase locking found in guinea pigs.

Central

The sustained–transient distinction is clear at the level of the primary afferent, whereas these complementary afferent systems would appear to be lost centrally (10, 56–58). In those studies, it was found that regular and irregular afferents projected to second-order vestibular neurons and showed overlapping projections—such that many second-order neurons received input from both regular and irregular afferents. Different vestibular nucleus neurons showed different strengths of irregular and regular projections. It appeared that the sustained and transient systems from the periphery were not established centrally (57, 58).

However, *in vitro* physiological studies, recording from vestibular nucleus neurons in slice preparations, have shown that at the vestibular nucleus there is clear evidence of different neurons with very different temporal responses to identical stimuli (injected current in these cases, rather than angular or linear acceleration), and that these neurons can be characterized by the same sustained–transient distinction as for primary afferents. Type A neurons show tonic characteristics—maintained firing to a step of injected current—whereas type B neurons show a brief high-frequency burst of spikes at stimulus onset (see Figure 5). These patterns have been established in frog and in mammals and echo the phasic-tonic distinction of Shimazu and Precht (2) in cat vestibular nucleus neurons. In frog, there are two well-defined populations of neurons with very different membrane properties and response patterns, and these correspond well to the transient and sustained classes. One approach has been to consider these matters from the point of view of filter characteristics, which is just another way of schematizing sustained (low-pass filter) and transient (high-pass filter) systems.

These results from *in vitro* studies (59) and from frogs (60–66) have been shown to apply also in mammalian vestibular system. Type A and B neurons previously found in brainstem slices



were identified in the guinea pig whole-brain preparation, and these neurons receive direct inputs from the vestibular nerve. Type A and B vestibular nucleus neurons differ in their intrinsic membrane properties which are responsible for the very different response patterns shown in Figure 5 (62, 67) and for the different filtering properties (61, 68).

SUSTAINED AND TRANSIENT ASPECTS OF VESTIBULAR RESPONSES

Tools for Probing the Functional State of the Sustained and Transient Systems

The evidence from physiology reviewed above establishes the sustained and transient categories of vestibular neural responses and provides tools for exploring the sustained and transient aspects of vestibular responses and how pathology may affect them. Using these tools, it is possible to identify sustained and transient aspects of behavioral responses. However, is this quest valuable for evaluating vestibular responses? We consider it is, because whereas some disorders affect all afferents it is likely that different treatments (e.g., gentamicin) and disorders will differentially affect the sustained and transient systems.

Acceleration Frequency

The frequency of the acceleration stimulus is one such tool. Sustained and transient systems have different frequency responses to acceleration stimulation (10)—the irregular neurons of both canals and otoliths showing a high-frequency preference, which has been interpreted as jerk sensitivity.

Galvanic

Galvanic stimulation *via* surface electrodes on the mastoids has been used in a very large number of studies of human vestibular responses. GVS is a complex stimulus which acts on all vestibular sense organs (11). It had been argued that GVS acts only on the afferent axon at the “spike trigger zone,” but the careful experiments of Gensberger et al. (69) show that GVS acts on both receptors and the axon. While irregular afferents do have a lower threshold for galvanic stimulation compared to regular neurons (11, 12), the numerical difference is not large and the variability between neurons is considerable. In principle, low-current, short-duration galvanic stimulation should preferentially activate irregular

axons, and indeed, this stimulus is effective for evoking a myogenic response which, in light of the above evidence, we consider is a transient vestibular response—vestibular-evoked myogenic potentials (VEMPs)—discussed below (70, 71).

Vibration

The very different otolithic afferent responses to vibration mean that vibration is a particularly powerful tool in differentiating sustained and transient responses. Otolithic irregular afferent neurons are activated by high frequencies of vibration, whereas otolithic regular neurons are not activated at intensities used in usual clinical practice. Some caution is needed since recent results have shown that low-frequency BCV is not selective for otoliths: even in animals with intact bony labyrinths, 100-Hz BCV activates canal afferents (17). But the response of these canal neurons to BCV declines as the BCV frequency is increased, so that at 500 Hz there is no detectable activation at intensities which are used clinically. In light of this, we consider it reasonable to conclude that if high-frequency vibration (e.g., 500 Hz) elicits a response, then it is due to the action of the irregular otolithic afferents—the otolithic transient system, originating predominantly from type I receptors at the striola.

Vestibular-Evoked Potentials (VsEP)

Brief pulses of linear acceleration cause a short latency-evoked potential (called a VsEP) recorded in a variety of species with a variety of recording montages (72–76). Control experiments after cochlea ablation have shown that the VsEP is not due to the cochlea, but is a neural response to otolithic activation (77). The VsEP would appear to be due to the otolithic transient system, since it is change in linear acceleration (jerk) which is the adequate stimulus for the VsEP (78).

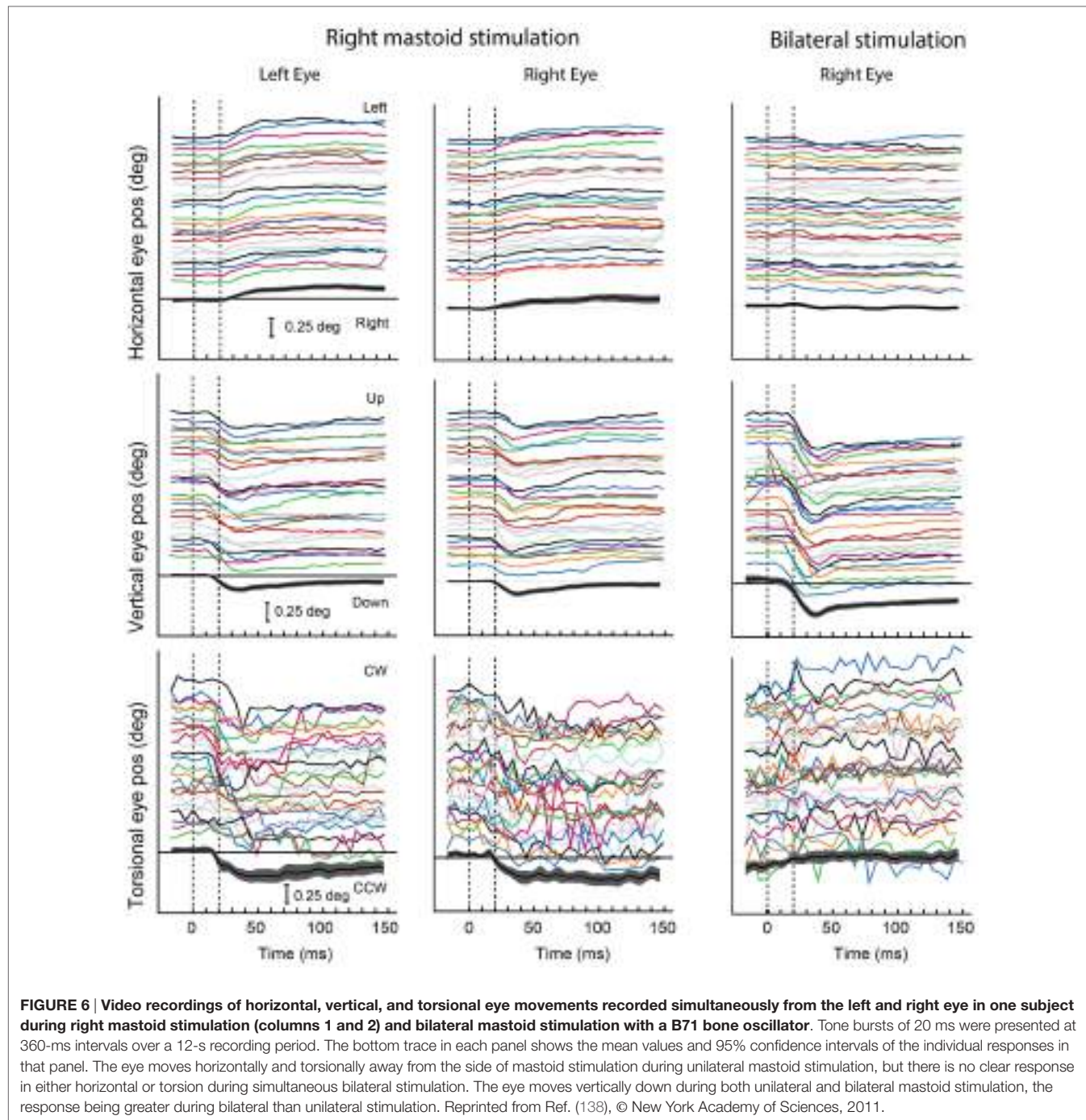
Gentamicin

Animal studies have shown that the type I receptors are more vulnerable to the effects of ototoxic antibiotics than are the type II receptors (79–81). In human patients, gentamicin is administered for therapeutic reasons either systemically or more commonly by intratympanic injection [intratympanic gentamicin (ITG)]. On the above account, it follows that gentamicin should affect the transient system and leave the sustained system relatively unaffected. As we show below, the responses to ITG are now identifying the differences between the sustained and transient systems.

SUSTAINED AND TRANSIENT ASPECTS OF BEHAVIORAL RESPONSES

Otolithic Responses

There are profound differences in otolith-mediated responses—even eye-movement responses—due to the characteristics of the otolithic stimuli. For example: on the one hand are maintained eye-movement responses to maintained otolithic stimuli, such as maintained roll-tilt. On the other hand, there are brief eye-movement responses to transient otolithic stimuli such as clicks or brief tone bursts (Figure 6). The otoliths transduce both of these very different stimulus aspects, and we suggest they do so by



means of the different receptor types and the different sustained and transient neural systems. We discuss these examples below.

A maintained rolled head position alters the linear acceleration stimulus to the otoliths and causes both eyes to adopt a rolled position in the orbit in the opposite direction to head tilt (82–84). This response is called ocular counterrolling (OCR). It is a maintained ocular response with very little adaptation, even over minutes, to the maintained otolithic stimulus (85). OCR would appear to be due to the action of regular afferents which show very little adaptation to maintained otolith stimulation

(7) in contrast to irregular afferents. These regular afferents are bouton or dimorphic afferents and receive input primarily from extrastriolar receptors, many of them being type II receptors (86), so we suggest that OCR reflects primarily the activity of the sustained system—regular otolithic afferents.

In contrast, brief bursts of 500-Hz BCV, which physiology has shown to selectively activate otolithic irregular afferents originating from striolar receptors, cause short-latency stimulus-locked eye movements in guinea pigs (87) and also in humans (see Figure 6) (88, 89). The pattern of these vibration-induced

eye movements is consistent with the pattern of cat eye movements to direct electrical stimulation of the utricular nerve (90). We suggest these small vibration-induced eye movements reflect the action of the transient system, since neurobiotin staining has shown that it is irregular afferents synapsing on striolar type I receptors which are differentially activated by the same 500-Hz vibration stimulus eliciting the eye movements. In confirmation is the fact that the analogous guinea pig eye-movement response to 500 Hz BCV is abolished by ITG at low concentration which does not affect auditory brainstem threshold response (87).

It has been argued that irregular neurons comprise the transient system. But how is it that their activation, for example, by sustained vibration, can result in maintained nystagmus? For example, maintained 100-Hz vibration stimulation of one mastoid in a patient with unilateral loss induces a nystagmus during the stimulation (vibration-induced nystagmus). It would appear that such a maintained nystagmus during a maintained vibration stimulus should be due to the sustained system (regular neurons), which the physiology shows, are not activated by vibration.

The answer lies in the fact that for irregular neurons every single cycle of the stimulus is the direct stimulus to the receptor/afferent neuron. So a maintained 100-Hz vibration will cause 100 repetitive activations, once per cycle, of irregular afferents. So the average firing rate of irregular neurons will increase, just as would occur during a sustained deflection of the cupula during an angular acceleration, and a sustained nystagmus will result.

There are three pieces of evidence in support of such an account:

1. stimulus onset and offset. Vibration-induced activation of irregular neurons starts on the first cycle of the stimulus and so one would expect any nystagmus to start at the very onset of the vibration. That is the observed result [summarized in Dumas et al. (35)].
2. Similarly, the vibration-induced neural activation ceases abruptly at vibration offset and so one expects the nystagmus to cease abruptly without any decay or overshoot. That is the observed result (35).
3. As vibration frequency is increased on successive trials from 30 to 100 Hz, the number of phase-locked spikes/s will increase and so one expects nystagmus velocity to increase in a corresponding fashion. That is the observed result (35). For these reasons, we consider that a repetitive activation of the transient system can produce a maintained eye movement, or nystagmus, just as can a maintained deflection of the cupula during a long-duration angular acceleration. The train of action potentials in the afferent fibers will be indistinguishable for these two stimuli.

These results are complemented by other evidence from the preparatory potentials of the muscles activated by BCV, called VEMPs. These are recorded in response to brief clicks or bursts of 500-Hz ACS or BCV, which the physiological evidence shows to selectively activate otolith irregular neurons. In response to stimuli which are specific for otolith irregular afferents, these VEMPs are small EMGs recorded by electrodes beneath the eyes [ocular vestibular-evoked myogenic potential

(oVEMPs)] or over the tensed sternocleidomastoid muscle [cervical vestibular-evoked myogenic potential (cVEMP)] (91–93) (Figure 7). The short latency potentials have been

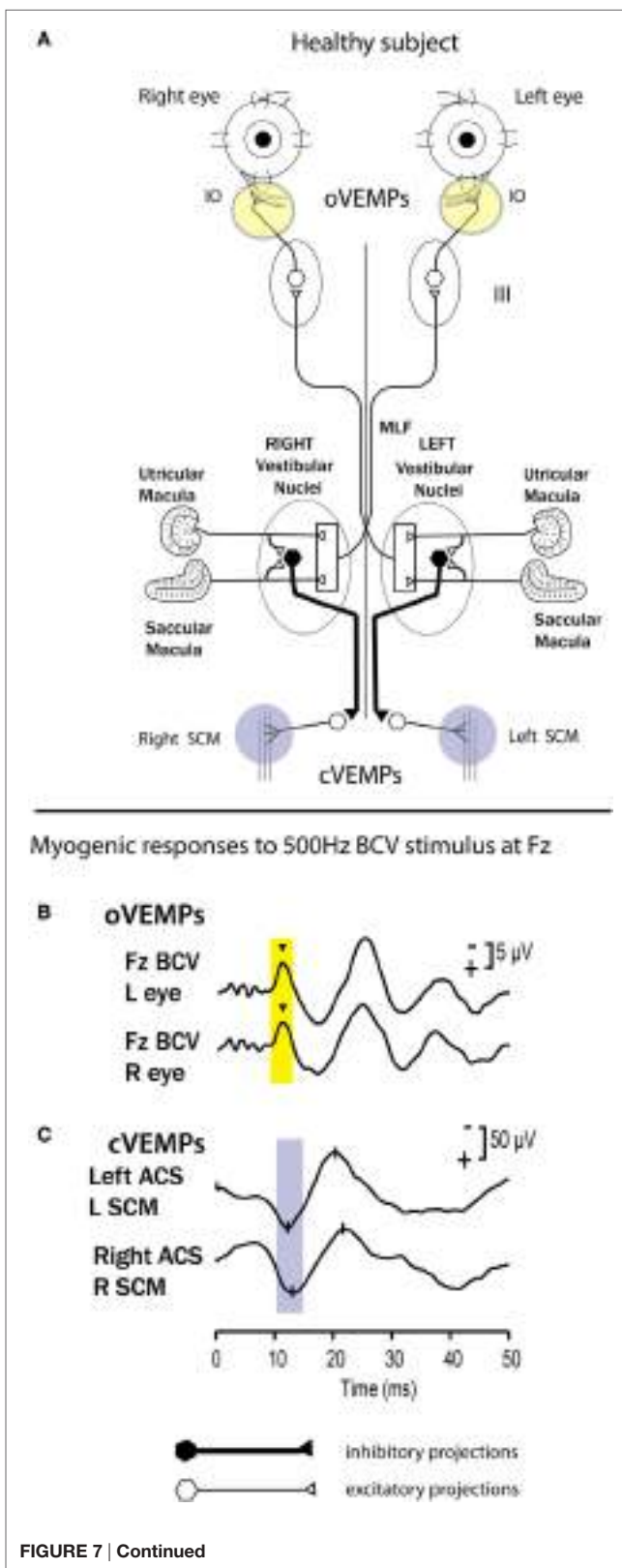


FIGURE 7 | Continued

FIGURE 7 | Continued

(A) A simplified schematic version of some of the known neural vestibulo-ocular and vestibulo-collic projections which underlie the ocular vestibular-evoked myogenic potential (oVEMP) and cervical vestibular-evoked myogenic potential (cVEMP) responses. It is based on known anatomical projections and physiological results from Suzuki et al. (90) that high-frequency electrical stimulation of the utricular nerve results in the activation of the contralateral inferior oblique (IO) and the ipsilateral superior oblique. Electrodes over the IO (circles) record the oVEMP. In human subjects, surface electrodes over the IO record the oVEMP, and the n10 component is shown by the inverted caret. **(B)**, Fz bone-conducted vibration (BCV) refers to the fact that the BCV stimulus was delivered to the midline of the forehead at the hairline, and this location is known as Fz. Afferents from the saccular and utricular macula project to the vestibular nuclei, but the exact termination of these afferents in the vestibular nuclei is not presently known, so this figure represents the present uncertainty as an open box. The otolithic projections to other eye muscles are not shown. The projections of the saccular macula in the inferior vestibular nerve, synapsing on an inhibitory neuron in the vestibular nucleus (black hexagon), projecting to spinal motoneurons controlling the sternocleidomastoid muscle (SCM), are established by Uchino and Kushiro (139). Electrodes over contracted SCM muscles record the cVEMP. **(B,C)** Examples of averaged EMG responses, oVEMP responses **(B)** and cVEMP responses **(C)** for a healthy subject. The yellow and blue vertical bands mark the time of healthy oVEMP n10 and cVEMP p13 responses, respectively. This healthy subject displays n10 responses of similar magnitude and symmetrical p13-n23 responses. Reprinted from Ref. (138), © New York Academy of Sciences, 2011.

demonstrated to be indicators of utricular function (oVEMP) and saccular function (cVEMP) (87, 94, 95). VEMPs are now widely used clinically (71, 95).

So, in our terms, ocular counter roll is a test of static (maintained) otolith function—how the otoliths respond to maintained roll-tilt stimulus—in contrast to VEMP responses, which are tests of otolith dynamic responses to transient otolithic stimulation mediated by otolith striolar type I receptors and otolith irregular afferents. Regular afferents are not activated by these transient sounds and vibrations, which are such effective stimuli in eliciting otolith dynamic responses.

What is the clinical value of making this distinction? Immediately after surgical unilateral vestibular loss, there is asymmetrical OCR (82), but over time the effect of unilateral loss on OCR is not consistent, so that the OCR test of sustained function does not clearly detect a unilateral vestibular loss acutely and chronically. Presumably, processes of vestibular compensation are acting to reduce any asymmetry. The data from studies of the OCR of patients after vestibular neuritis also show great variability, but here it is not known conclusively whether otolith function may have returned after the neuritis (96, 97). On the other hand, VEMPs do show a clear asymmetry after unilateral vestibular loss acutely and chronically after surgical unilateral loss (98, 99) and after neuritis (100). The asymmetrical VEMPs are preserved for many years and probably permanently after the vestibular loss (92, 101–103). The clinical value lies in realizing that one cannot rely on the results of one of the tests of otolith function: the test of static otolithic function—OCR—which may show symmetrical responses indicating normal otolithic function, whereas in the same patient, the VEMPs may show the loss of transient otolithic function and so identify the patient's problem (95, 104).

Semicircular Canal Responses

During normal head movements, the neural drives from the sustained and transient systems are combined to generate smooth compensatory responses. For example, in response to brief, passive unpredictable horizontal head angular accelerations (a head impulse), they combine to generate a smooth compensatory eye movement—the vestibulo-ocular reflex (VOR). One index of the adequacy of vestibular responses is VOR gain, typically defined as the ratio of the area under the eye velocity record to the corresponding area under the head velocity record during the head impulse. This clinical test is called the video head impulse test (vHIT) (105, 106). VOR gain measured in this way is a global measure of the whole response to a head turn, and as such, it cannot show the fine detail of the time series of the response which may reflect the way in which the sustained and transient systems are combined. Fortunately, an answer about how these systems work may be provided by the therapeutic treatment of patients with Meniere's disease by the use of intratympanic injections of gentamicin (ITG) (107–111).

As noted above, histological studies in animals have shown that gentamicin differentially attacks type I receptors, and so ITG presumably selectively attenuates the contribution of type I receptors to generate responses to transient stimuli (79–81). We have argued that this loss of type I receptors will differentially degrade the irregular (transient) afferent system. Consistent with this account is the evidence that the human transient eye-movement response to brief 100-ms square wave pulses of electrical stimulation is impaired after systemic gentamicin, to a greater extent than the tonic response (112). The new evidence showing that galvanic stimulation acts on receptors (69) would predict such a decrease in the GVS response if the gentamicin-vulnerable type I receptors were degraded.

Recently, this ITG procedure for the treatment of patients with Meniere's disease has been combined with sequential vHIT testing of semicircular canal function (106) as a monitor of the effect of ITG (110). In many patients, the pre-ITG treatment eye-movement response to impulsive head rotations may be normal, but after just a single dose, there is frequently a change in the exact time series of the eye-movement response. Most clinicians have been interested in the global VOR gain measure since it appears that even a small reduction in VOR gain after ITG is associated with a decrease in patient reports of vertigo (110). The small reduction in VOR gain is objective evidence that the ITG treatment has worked, and the ITG injections should stop in order to minimize risk of potential hearing loss. On the evidence presented here, we suggest the exact time series of the response should be examined in detail. From a physiological viewpoint, there is good reason for such a change in the response pattern because it is likely that the early response is dominated by the very fast dynamics of the type I receptors and irregular afferents for the semicircular canals (113, 114).

Sustained and Transient Systems in Blood Pressure Control and Vestibulo-Sympathetic Responses?

There is now strong evidence that otolithic inputs contribute to early transient adjustments to human blood pressure control and muscle sympathetic nerve activity (MSNA) (115–122). The

neural pathways for these functions are even being mapped (123–125). These responses are modulated by sinusoidal galvanic stimuli which preferentially activate irregular otolithic neurons, although regular neurons are activated by galvanic stimuli at high intensities (11). Given that BCV is such an effective stimulus for the transient system, it will be of interest to see if bursts of 500-Hz BCV also modulate blood pressure and MSNA since that would establish the transient circuit from otolithic striolar receptors to sympathetic responses.

Escape Movements

Recent evidence suggests that type I receptors may even have a role in triggering escape behavior in response to hypoxia, and by implication in sudden infant death syndrome. Under hypoxic conditions, healthy mice show marked escape movements, but following ITG (which most probably disables the transient system selectively)—mice in the same hypoxic conditions show little escape movement (126–128). The neural pathways by which the transient system triggers escape behavior is not at all clear, but the possible significance of these results demands replication.

Proportional–Integral–Derivative (PID) Control

The existence of these complementary transient and sustained systems seems to reflect a fundamental principle in the design of robotic control of limb movement. Designers of robotics have adopted a principle for initiation of movement of robots called a PID controller (129, 130). The principle is that movement controllers should be governed not by a single control signal, such as velocity, but by a combination of acceleration, velocity, and position signals (131). Controlling movement by just one signal (e.g., velocity) does not ensure dynamical stability.

There is a big advantage in such a combination especially at the onset of a movement, since the acceleration component initiates the responses rapidly. If there had only been a velocity signal at the onset, the early response would have been inadequate. The appropriate combination of acceleration and velocity provides a functionally effective way of dealing with response initiation. In an analogous fashion, we suggest these transient and sustained inputs are combined to yield dynamically stable oculomotor responses (and postural responses) analogous to PID control. Zhou et al. (132) have shown how a PID model can closely approximate oculomotor performance.

A Complementary View

A series of studies from Cullen's group has approached the regular–irregular distinction from the point of view of analyzing the neural coding of information about self motion. Their analysis of the responses of regular and irregular monkey single neurons to repetitions of various vestibular stimuli leads to the conclusion that it is irregular neurons that have distinct advantages in self motion coding, for example, great temporal precision. Regular afferents code information *via* changes in firing rate, whereas irregular afferents give information about self motion *via* precise spike timing (133–137). The evidence we have presented here, such as the phase locking of irregular neurons to very high vibration frequencies, is exactly consistent with such ideas.

SUMMARY

The old ideas of the otoliths being uniform structures functioning mainly to signal direction of gravity or low-frequency linear acceleration is just totally inadequate. It is now being replaced by evidence showing that there is complex anatomical differentiation of receptors and afferents in each macula and also in the cristae of the canals. This anatomical diversity is matched by afferent diversity of physiological response with different neurons signaling sustained aspects of the stimulus as opposed to other neurons signaling changes in stimulation (the transient system). There is corresponding differentiation of neural types and neural responses at the vestibular nuclei. These different systems—sustained and transient—are differentially susceptible to ototoxic antibiotics, have different frequency responses, different sensitivity to galvanic stimulation, and most interestingly differential sensitivity to high-frequency BCV (500 Hz) and ACS. These differential sensitivities are now allowing the differential contribution of sustained and transient systems to vestibular responses, such as eye movements, and possibly other vestibular-evoked responses—such as blood pressure—as well. The prospect of particular treatments targeting one or the other of the systems is now being realized in the clinic by therapeutic treatment of ITG preferentially attacking type I receptors with reported benefit to patients while retaining considerable vestibular function. This paper has highlighted parallels between the response characteristics of vestibular afferents and basic principles of robotic design.

The old terms “vestibular stimulation” or “otolith stimulation” are just too vague—we now know that afferent input with very different dynamics conveys a range of different information. The evidence reviewed in this paper has pointed to the value of regarding vestibular responses in terms of the transient and sustained characteristics.

DEDICATION

This review is dedicated to Bernard Cohen who has made so many pioneering contributions to understanding vestibular function.

AUTHOR CONTRIBUTIONS

IC wrote the paper. P-PV contributed the section about central vestibular responses, HM contributed to the section on PID, and CW contributed to the section about clinical testing. All authors reviewed the text and approved the final paper.

ACKNOWLEDGMENTS

We thank Wally Grant for his excellent help. We thank Ann Burgess for her help in preparing this paper and for her excellent help over so many years in the research reported here. Much of the work reported here has been supported by the Garnett Passe and Rodney Williams Memorial Foundation, and I am very grateful for their continued support and for that of the National Health and Medical Research Foundation of Australia.

FUNDING

HM is supported by a Senior/Principal Research Fellowship from the Garnett Passe and Rodney Williams Memorial Foundation.

REFERENCES

1. Precht W, Shimazu H. Functional connections of tonic and kinetic vestibular neurons with primary vestibular afferents. *J Neurophysiol* (1965) 28(6):1014–28.
2. Shimazu H, Precht W. Tonic and kinetic responses of cat's vestibular neurons to horizontal angular acceleration. *J Neurophysiol* (1965) 28(6):991–1013.
3. Shimazu H, Precht W. Inhibition of central vestibular neurons from contralateral labyrinth and its mediating pathway. *J Neurophysiol* (1966) 29(3):467–92.
4. Fernandez C, Goldberg JM. Physiology of peripheral neurons innervating semicircular canals of the squirrel monkey. II. Response to sinusoidal stimulation and dynamics of peripheral vestibular system. *J Neurophysiol* (1971) 34(4):661–75.
5. Goldberg JM, Fernandez C. Physiology of peripheral neurons innervating semicircular canals of the squirrel monkey. 3. Variations among units in their discharge properties. *J Neurophysiol* (1971) 34(4):676–84.
6. Goldberg JM, Fernandez C. Physiology of peripheral neurons innervating semicircular canals of the squirrel monkey. I. Resting discharge and response to constant angular accelerations. *J Neurophysiol* (1971) 34(4):635–60.
7. Fernandez C, Goldberg JM. Physiology of peripheral neurons innervating otolith organs of the squirrel monkey. I. Response to static tilts and to long-duration centrifugal force. *J Neurophysiol* (1976) 39(5):970–84.
8. Fernandez C, Goldberg JM. Physiology of peripheral neurons innervating otolith organs of the squirrel monkey. II. Directional selectivity and force-response relations. *J Neurophysiol* (1976) 39(5):985–95.
9. Fernandez C, Goldberg JM. Physiology of peripheral neurons innervating otolith organs of the squirrel monkey. III. Response dynamics. *J Neurophysiol* (1976) 39(5):996–1008.
10. Goldberg JM. Afferent diversity and the organization of central vestibular pathways. *Exp Brain Res* (2000) 130(3):277–97. doi:10.1007/s002210050033
11. Kim J, Curthoys IS. Responses of primary vestibular neurons to galvanic vestibular stimulation (GVS) in the anaesthetised guinea pig. *Brain Res Bull* (2004) 64(3):265–71. doi:10.1016/j.brainresbull.2004.07.008
12. Goldberg JM, Smith CE, Fernandez C. Relation between discharge regularity and responses to externally applied galvanic currents in vestibular nerve afferents of the squirrel monkey. *J Neurophysiol* (1984) 51(6):1236–56.
13. McCue MP, Guinan JJ Jr. Acoustically responsive fibers in the vestibular nerve of the cat. *J Neurosci* (1994) 14(10):6058–70.
14. Murofushi T, Curthoys IS, Topple AN, Colebatch JG, Halmagyi GM. Responses of guinea pig primary vestibular neurons to clicks. *Exp Brain Res* (1995) 103(1):174–8. doi:10.1007/BF00241975
15. Young ED, Fernandez C, Goldberg JM. Responses of squirrel monkey vestibular neurons to audio-frequency sound and head vibration. *Acta Otolaryngol* (1977) 84(5–6):352–60. doi:10.3109/00016487709123977
16. Curthoys IS. Peripheral vestibular responses to sound. *Neuroembryol Aging* (2004) 3(4):207–14. doi:10.1159/000096798
17. Curthoys IS. The new vestibular stimuli: sound and vibration. Anatomical, physiological and clinical evidence. *Exp Brain Res* (2017) 235(4):957–72. doi:10.1007/s00221-017-4874-y
18. Curthoys IS, Kim J, McPhedran SK, Camp AJ. Bone conducted vibration selectively activates irregular primary otolithic vestibular neurons in the guinea pig. *Exp Brain Res* (2006) 175(2):256–67. doi:10.1007/s00221-006-0544-1
19. Curthoys IS, Vulovic V. Vestibular primary afferent responses to sound and vibration in the guinea pig. *Exp Brain Res* (2011) 210(3–4):347–52. doi:10.1007/s00221-010-2499-5
20. Curthoys IS, Vulovic V, Burgess AM, Sokolic L, Goonetilleke SC. The response of guinea pig primary utricular and saccular irregular neurons to bone-conducted vibration (BCV) and air-conducted sound (ACS). *Hear Res* (2016) 331:131–43. doi:10.1016/j.heares.2015.10.019
- P-PV is supported by funding from Centre National d'Etudes Spatiales (CNES), Agence Nationale de la Recherche (ANR), and Institut pour la Recherche sur la Moelle épinière et l'Encéphale (IRME). CW received support from Grand Audition Paris.
21. Curthoys IS, Vulovic V, Sokolic L, Pogson J, Burgess AM. Irregular primary otolith afferents from the guinea pig utricular and saccular maculae respond to both bone conducted vibration and to air conducted sound. *Brain Res Bull* (2012) 89(1–2):16–21. doi:10.1016/j.brainresbull.2012.07.007
22. Rose JE, Brugge JF, Anderson DJ, Hind JE. Phase-locked response to low-frequency tones in single auditory nerve fibers of the squirrel monkey. *J Neurophysiol* (1967) 30(4):769–93.
23. McCue MP, Guinan JJ Jr. Spontaneous activity and frequency selectivity of acoustically responsive vestibular afferents in the cat. *J Neurophysiol* (1995) 74(4):1563–72.
24. McCue MP, Guinan JJ Jr. Sound-evoked activity in primary afferent neurons of a mammalian vestibular system. *Am J Otol* (1997) 18(3):355–60.
25. Murofushi T, Curthoys IS. Physiological and anatomical study of click-sensitive primary vestibular afferents in the guinea pig. *Acta Otolaryngol* (1997) 117(1):66–72. doi:10.3109/00016489709117994
26. Murofushi T, Curthoys IS, Gilchrist DP. Response of guinea pig vestibular nucleus neurons to clicks. *Exp Brain Res* (1996) 111(1):149–52. doi:10.1007/BF00229565
27. Zhu H, Tang X, Wei W, Maklad A, Mustain W, Rabbitt R, et al. Input-output functions of vestibular afferent responses to air-conducted clicks in rats. *J Assoc Res Otolaryngol* (2014) 15(1):73–86. doi:10.1007/s10162-013-0428-6
28. Zhu H, Tang X, Wei W, Mustain W, Xu Y, Zhou W. Click-evoked responses in vestibular afferents in rats. *J Neurophysiol* (2011) 106(2):754–63. doi:10.1152/jn.00003.2011
29. Iwasaki S, Chihara Y, Komuta Y, Ito K, Sahara Y. Low-voltage-activated potassium channels underlie the regulation of intrinsic firing properties of rat vestibular ganglion cells. *J Neurophysiol* (2008) 100(4):2192–204. doi:10.1152/jn.01240.2007
30. Kalluri R, Xue J, Eatock RA. Ion channels set spike timing regularity of mammalian vestibular afferent neurons. *J Neurophysiol* (2010) 104(4):2034–51. doi:10.1152/jn.00396.2010
31. Liu XP, Woolerton JRA, Gaboyard-Niay S, Yang FC, Lysakowski A, Eatock RA. Sodium channel diversity in the vestibular ganglion: Na(V)1.5, Na(V)1.8, and tetrodotoxin-sensitive currents. *J Neurophysiol* (2016) 115(5):2536–55. doi:10.1152/jn.00902.2015
32. Carey JP, Hirvonen TP, Hullar TE, Minor LB. Acoustic responses of vestibular afferents in a model of superior canal dehiscence. *Otol Neurotol* (2004) 25(3):345–52. doi:10.1097/00129492-200405000-00024
33. Curthoys IS, Grant JW. How does high-frequency sound or vibration activate vestibular receptors? *Exp Brain Res* (2015) 233(3):691–9. doi:10.1007/s00221-014-4192-6
34. Curthoys IS, Vulovic V, Pogson J, Sokolic L. *Responses of Guinea Pig Primary Vestibular Afferents to Low Frequency (50–100Hz) Bone Conducted Vibration (BCV) – The Neural Basis of Vibration Induced Nystagmus*. Program No 57406 2012 Neuroscience Meeting Planner. New Orleans, LA: Society for Neuroscience (2013).
35. Dumas G, Curthoys IS, Lion A, Perrin A, Schmerber S. The skull vibration induced nystagmus test (SVINT) of vestibular function – a review. *Front Neurol* (2017) 8:41. doi:10.3389/fneur.2017.00041
36. Dumas G, Perrin P, Schmerber S, Lavieille JP. Nystagmus and vibration test research of mechanisms, theoretical methods: on 52 cases of unilateral vestibular lesions. *Rev Laryngol Otol Rhinol* (2003) 124(2):75–83.
37. Watanuki K, Meyer A. Morphological study of sensory epithelium of vestibular organs. *Tohoku J Exp Med* (1971) 104(1):55–63. doi:10.1620/tjem.104.55
38. Lim DJ. Morphological and physiological correlates in cochlear and vestibular sensory epithelia. *Scan Electron Microsc* (1976) 2:269–76.
39. Hunter-Duvar IM. An electron-microscopic study of the vestibular sensory epithelium. *Acta Otolaryngol* (1983) 95(5–6):494–507. doi:10.3109/00016488309139434

40. Brichta AM, Peterson EH. Functional architecture of vestibular primary afferents from the posterior semicircular canal of a turtle, *Pseudemys (Trachemys) scripta elegans*. *J Comp Neurol* (1994) 344(4):481–507. doi:10.1002/cne.903440402
41. Kessel RG, Kardon RH. The shape, polarization, and innervation of sensory hair cells in the guinea pig crista ampullaris and macula utriculi. *Scan Electron Microsc* (1979) 3:962–74.
42. Lim DJ. Fine morphology of the otoconial membrane and its relationship to the sensory epithelium. *Scan Electron Microsc* (1979) 3:929–38.
43. Lindeman HH. Studies on the morphology of the sensory regions of the vestibular apparatus with 45 figures. *Ergeb Anat Entwicklungsgesch* (1969) 42(1):1–113.
44. Spoon C, Grant W. Biomechanics of hair cell kinocilia: experimental measurement of kinocilium shaft stiffness and base rotational stiffness with Euler-Bernoulli and Timoshenko beam analysis. *J Exp Biol* (2011) 214 (Pt 5):862–70. doi:10.1242/jeb.051151
45. Dunlap MD, Grant JW. Experimental measurement of utricle system dynamic response to inertial stimulus. *J Assoc Res Otolaryngol* (2014) 15(4):511–28. doi:10.1007/s10162-014-0456-x
46. Grant W, Best W. Otolith-organ mechanics – lumped parameter model and dynamic-response. *Aviat Space Environ Med* (1987) 58(10):970–6.
47. Songer JE, Eatock RA. Tuning and timing in mammalian type I hair cells and calyceal synapses. *J Neurosci* (2013) 33(8):3706–24. doi:10.1523/jneurosci.4067-12.2013
48. Geleoc GSG, Lennan GWT, Richardson GP, Kros CJ. A quantitative comparison of mechano-electrical transduction in vestibular and auditory hair cells of neonatal mice. *Proc Biol Sci* (1997) 264(1381):611–21. doi:10.1098/rspb.1997.0087
49. Spoon C, Moravec WJ, Rowe MH, Grant JW, Peterson EH. Steady-state stiffness of utricular hair cells depends on macular location and hair bundle structure. *J Neurophysiol* (2011) 106(6):2950–63. doi:10.1152/jn.00469.2011
50. Songer JE, Rosowski JJ. The effect of superior canal dehiscence on cochlear potential in response to air-conducted stimuli in chinchilla. *Hear Res* (2005) 210(1–2):53–62. doi:10.1016/j.heares.2005.07.003
51. Songer JE, Rosowski JJ. The effect of superior-canal opening on middle-ear input admittance and air-conducted stapes velocity in chinchilla. *J Acoust Soc Am* (2006) 120(1):258–69. doi:10.1121/1.2204356
52. Boyle R, Highstein SM. Resting discharge and response dynamics of horizontal semicircular canal afferents of the toadfish, opanus-tau. *J Neurosci* (1990) 10(5):1557–69.
53. Fontilla MF, Peterson EH. Kinocilia heights on utricular hair cells. *Hear Res* (2000) 145(1–2):8–16. doi:10.1016/S0378-5955(00)00068-X
54. Li A, Xue J, Peterson EH. Architecture of the mouse utricle: macular organization and hair bundle heights. *J Neurophysiol* (2008) 99(2):718–33. doi:10.1152/jn.00831.2007
55. Xue JB, Peterson EH. Hair bundle heights in the utricle: differences between macular locations and hair cell types. *J Neurophysiol* (2006) 95(1):171–86. doi:10.1152/jn.00800.2005
56. Boyle R, Goldberg JM, Highstein SM. Inputs from regularly and irregularly discharging vestibular nerve afferents to secondary neurons in squirrel monkey vestibular nuclei. III. Correlation with vestibulospinal and vestibuloocular output pathways. *J Neurophysiol* (1992) 68(2):471–84.
57. Chen-Huang C, McCrea RA, Goldberg JM. Contributions of regularly and irregularly discharging vestibular-nerve inputs to the discharge of central vestibular neurons in the alert squirrel monkey. *Exp Brain Res* (1997) 114(3):405–22. doi:10.1007/pl000005650
58. Highstein SM, Goldberg JM, Moschovakis AK, Fernandez C. Inputs from regularly and irregularly discharging vestibular nerve afferents to secondary neurons in the vestibular nuclei of the squirrel monkey. II. Correlation with output pathways of secondary neurons. *J Neurophysiol* (1987) 58(4):719–38.
59. Eugene D, Idoux E, Beraneck M, Moore LE, Vidal PP. Intrinsic membrane properties of central vestibular neurons in rodents. *Exp Brain Res* (2011) 210(3–4):423–36. doi:10.1007/s00221-011-2569-3
60. Beraneck M, Pfanzelt S, Vassias I, Rohrger M, Vibert N, Vidal PP, et al. Differential intrinsic response dynamics determine synaptic signal processing in frog vestibular neurons. *J Neurosci* (2007) 27(16):4283–96. doi:10.1523/jneurosci.5232-06.2007
61. Beraneck M, Straka H. Vestibular signal processing by separate sets of neuronal filters. *J Vestib Res* (2011) 21(1):5–19. doi:10.3233/ves-2011-0396
62. Pfanzelt S, Roessert C, Rohrger M, Glasauer S, Moore LE, Straka H. Differential dynamic processing of afferent signals in frog tonic and phasic second-order vestibular neurons. *J Neurosci* (2008) 28(41):10349–62. doi:10.1523/jneurosci.3368-08.2008
63. Rossert C, Straka H, Glasauer S, Moore LE. Frequency-domain analysis of intrinsic neuronal properties using high-resistant electrodes. *Front Neurosci* (2009) 3:64. doi:10.3389/neuro.17.002.2009
64. Straka H, Beraneck M, Rohrger M, Moore LE, Vidal PP, Vibert N. Second-order vestibular neurons form separate populations with different membrane and discharge properties. *J Neurophysiol* (2004) 92(2):845–61. doi:10.1152/jn.00107.2004
65. Straka H, Lambert FM, Pfanzelt S, Beraneck M. Vestibulo-ocular signal transformation in frequency-tuned channels. In: Strupp M, Buttner U, Cohen B, editors. *Basic and Clinical Aspects of Vertigo and Dizziness*. (Vol. 1164). New York: The New York Academy of Sciences (2009). p. 37–44.
66. Straka H, Vibert N, Vidal PP, Moore LE, Dutia MB. Intrinsic membrane properties of vertebrate vestibular neurons: function, development and plasticity. *Prog Neurobiol* (2005) 76(6):349–92. doi:10.1016/j.pneurobio.2005.10.002
67. Beraneck M, Cullen KE. Activity of vestibular nuclei neurons during vestibular and optokinetic stimulation in the alert mouse. *J Neurophysiol* (2007) 98(3):1549–65. doi:10.1152/jn.00590.2007
68. Babalian AL, Vidal PP. Floccular modulation of vestibuloocular pathways and cerebellum-related plasticity: an in vitro whole brain study. *J Neurophysiol* (2000) 84(5):2514–28.
69. Gensberger KD, Kaufmann AK, Dietrich H, Branone F, Banchi R, Chagnaud BP, et al. Galvanic vestibular stimulation: cellular substrates and response patterns of neurons in the vestibulo-ocular network. *J Neurosci* (2016) 36(35):9097–110. doi:10.1523/jneurosci.4239-15.2016
70. Rosengren SM, Jombik P, Halmagyi GM, Colebatch JG. Galvanic ocular vestibular evoked myogenic potentials provide new insight into vestibulo-ocular reflexes and unilateral vestibular loss. *Clin Neurophysiol* (2009) 120(3):569–80. doi:10.1016/j.clinph.2008.12.001
71. Weber KP, Rosengren SM. Clinical utility of ocular vestibular-evoked myogenic potentials (oVEMPs). *Curr Neurol Neurosci Rep* (2015) 15(5):22. doi:10.1007/s11910-015-0548-y
72. Brown D. Electrotvestibulography: a review of recording techniques, nomenclature, and new experimental findings. *Front Neurotol* (2017).
73. Jones SM, Erway LC, Bergstrom RA, Schimenti JC, Jones TA. Vestibular responses to linear acceleration are absent in otoconia-deficient C57BL/6JEi-het mice. *Hear Res* (1999) 135(1–2):56–60. doi:10.1016/s0378-5955(99)00090-8
74. Jones SM, Jones TA. Ontogeny of vestibular compound action potentials in the domestic chicken. *J Assoc Res Otolaryngol* (2000) 1(3):232–42. doi:10.1007/s101620010026
75. Jones SM, Jones TA, Shukla R. Short latency vestibular evoked potentials in the Japanese quail (*Coturnix coturnix japonica*). *J Comp Physiol A* (1997) 180(6):631–8. doi:10.1007/s003590050079
76. Jones TA, Jones SM. Short latency compound action potentials from mammalian gravity receptor organs. *Hear Res* (1999) 136(1–2):75–85. doi:10.1016/s0378-5955(99)00110-0
77. Chihera Y, Wang V, Brown DJ. Evidence for the utricular origin of the vestibular short-latency-evoked potential (VsEP) to bone-conducted vibration in guinea pig. *Exp Brain Res* (2013) 229(2):157–70. doi:10.1007/s00221-013-3602-5
78. Jones TA, Jones SM, Vijayakumar S, Brugeaud A, Bothwell M, Chabbert C. The adequate stimulus for mammalian linear vestibular evoked potentials (VsEPs). *Hear Res* (2011) 280(1–2):133–40. doi:10.1016/j.heares.2011.05.005
79. Hirvonen TP, Minor LB, Hullar TE, Carey JP. Effects of intratympanic gentamicin on vestibular afferents and hair cells in the chinchilla. *J Neurophysiol* (2005) 93(2):643–55. doi:10.1152/jn.00160.2004
80. Lue JH, Day AS, Cheng PW, Young YH. Vestibular evoked myogenic potentials are heavily dependent on type I hair cell activity of the saccular macula in guinea pigs. *Audiol Neurotol* (2009) 14(1):59–66. doi:10.1159/000156701
81. Lyford-Pike S, Vogelheim C, Chu E, Della Santina CC, Carey JP. Gentamicin is primarily localized in vestibular type I hair cells after intratympanic administration. *J Assoc Res Otolaryngol* (2007) 8(4):497–508. doi:10.1007/s10162-007-0093-8

82. Diamond SG, Markham CH. Binocular counterrolling in humans with unilateral labyrinthectomy and in normal controls. *Ann N Y Acad Sci* (1981) 374:69–79. doi:10.1111/j.1749-6632.1981.tb30861.x
83. Diamond SG, Markham CH. Ocular counterrolling as an indicator of vestibular otolith function. *Neurology* (1983) 33(11):1460–9. doi:10.1212/WNL.33.11.1460
84. Diamond SG, Markham CH, Simpson NE, Curthoys IS. Binocular counterrolling in humans during dynamic rotation. *Acta Otolaryngol* (1979) 87(5–6):490–8. doi:10.3109/00016487909126457
85. Moore ST, Curthoys IS, McCoy SG. VTM – an image-processing system for measuring ocular torsion. *Comput Methods Programs Biomed* (1991) 35(3):219–30. doi:10.1016/0169-2607(91)90124-C
86. Fernandez C, Goldberg JM, Baird RA. The vestibular nerve of the chinchilla. III. Peripheral innervation patterns in the utricular macula. *J Neurophysiol* (1990) 63(4):767–80.
87. Vulovic V, Curthoys IS. Bone conducted vibration activates the vestibulo-ocular reflex in the guinea pig. *Brain Res Bull* (2011) 86(1–2):74–81. doi:10.1016/j.brainresbull.2011.06.013
88. Cornell ED, Burgess AM, MacDougall HG, Curthoys IS. Vertical and horizontal eye movement responses to unilateral and bilateral bone conducted vibration to the mastoid. *J Vestib Res* (2009) 19(1–2):41–7. doi:10.3233/VES-2009-0338
89. Cornell ED, Burgess AM, MacDougall HG, Curthoys IS. Bone conducted vibration to the mastoid produces horizontal, vertical and torsional eye movements. *J Vestib Res* (2015) 25(2):91–6. doi:10.3233/ves-150550
90. Suzuki JI, Tokumasu K, Goto K. Eye movements from single utricular nerve stimulation in the cat. *Acta Otolaryngol* (1969) 68(4):350–62. doi:10.3109/00016486909121573
91. Colebatch JG, Halmagyi GM, Skuse NF. Myogenic potentials generated by a click-evoked vestibulocollic reflex. *J Neurol Neurosurg Psychiatry* (1994) 57(2):190–7. doi:10.1136/jnnp.57.2.190
92. Iwasaki S, McGarvie LA, Halmagyi GM, Burgess AM, Kim J, Colebatch JG, et al. Head taps evoke a crossed vestibulo-ocular reflex. *Neurology* (2007) 68(15):1227–9. doi:10.1212/01.wnl.0000259064.80564.21
93. Rosengren SM, Todd NPM, Colebatch JG. Vestibular-evoked extraocular potentials produced by stimulation with bone-conducted sound. *Clin Neurophysiol* (2005) 116(8):1938–48. doi:10.1016/j.clinph.2005.03.019
94. Curthoys IS. A critical review of the neurophysiological evidence underlying clinical vestibular testing using sound, vibration and galvanic stimuli. *Clin Neurophysiol* (2010) 121(2):132–44. doi:10.1016/j.clinph.2009.09.027
95. Curthoys IS. The interpretation of clinical tests of peripheral vestibular function. *Laryngoscope* (2012) 122(6):1342–52. doi:10.1002/lary.23258
96. Schmid-Priscoveanu A, Straumann D, Bohmer A, Obzina H. Vestibulo-ocular responses during static head roll and three-dimensional head impulses after vestibular neuritis. *Acta Otolaryngol* (1999) 119(7):750–7. doi:10.1080/00016489950180379
97. Schmid-Priscoveanu A, Straumann D, Bohmer A, Obzina H. Is static ocular counterroll asymmetric after vestibular neuritis? In: Claussen CF, Haid CT, Hofferberth B, editors. *Equilibrium Research, Clinical Equilibriometry and Modern Treatment*. (Vol. 1201). Amsterdam: Elsevier (2000). p. 442–442.
98. Chiaravano E, Zamith F, Vidal PP, de Waele C. Ocular and cervical VEMPs: a study of 74 patients suffering from peripheral vestibular disorders. *Clin Neurophysiol* (2011) 122(8):1650–9. doi:10.1016/j.clinph.2011.01.006
99. Kinoshita M, Iwasaki S, Fujimoto C, Inoue A, Egami N, Chihara Y, et al. Ocular vestibular evoked myogenic potentials in response to air-conducted sound and bone-conducted vibration in vestibular schwannoma. *Otol Neurotol* (2013) 34(7):1342–8. doi:10.1097/MAO.0b013e31828d6539
100. Manzari L, Burgess AM, MacDougall HG, Curthoys IS. Vestibular function after vestibular neuritis. *Int J Audiol* (2013) 52(10):713–8. doi:10.3109/14992027.2013.809485
101. Iwasaki S, Murofushi T, Chihara Y, Ushio M, Suzuki M, Curthoys IS, et al. Ocular vestibular evoked myogenic potentials to bone-conducted vibration in vestibular schwannomas. *Otol Neurotol* (2010) 31(1):147–52. doi:10.1097/MAO.0b013e3181c0e670
102. Iwasaki S, Smulders YE, Burgess AM, McGarvie LA, MacDougall HG, Halmagyi GM, et al. Ocular vestibular evoked myogenic potentials in response to bone-conducted vibration of the midline forehead at Fz. A new indicator of unilateral otolithic loss. *Audiol Neurotol* (2008) 13(6):396–404. doi:10.1159/000148203
103. Manzari L, Tedesco A, Burgess AM, Curthoys IS. Ocular vestibular-evoked myogenic potentials to bone-conducted vibration in superior vestibular neuritis show utricular function. *Otolaryngol Head Neck Surg* (2010) 143(2):274–80. doi:10.1016/j.otohns.2010.03.020
104. Chiaravano E, Darlington C, Vidal P-P, Lamas G, de Waele C. The role of cervical and ocular vestibular evoked myogenic potentials in the assessment of patients with vestibular schwannomas. *PLoS One* (2014) 9(8):e105026. doi:10.1371/journal.pone.0105026
105. MacDougall HG, McGarvie LA, Halmagyi GM, Curthoys IS, Weber KP. Application of the video head impulse test to detect vertical semicircular canal dysfunction. *Otol Neurotol* (2013) 34(6):974–9. doi:10.1097/MAO.0b013e31828d676d
106. MacDougall HG, Weber KP, McGarvie LA, Halmagyi GM, Curthoys IS. The video head impulse test: diagnostic accuracy in peripheral vestibulopathy. *Neurology* (2009) 73(14):1134–41. doi:10.1212/WNL.0b013e3181bacf85
107. Bremer HG, van Rooy I, Pullens B, Colijn C, Stegeman I, van der Zaag-Loonen HJ, et al. Intratympanic gentamicin treatment for Meniere's disease: a randomized, double-blind, placebo-controlled trial on dose efficacy – results of a prematurely ended study. *Trials* (2014) 15:328. doi:10.1186/1745-6215-15-328
108. Carey J. Intratympanic gentamicin for the treatment of Meniere's disease and other forms of peripheral vertigo. *Otolaryngol Clin North Am* (2004) 37(5):1075–90. doi:10.1016/j.otc.2004.06.002
109. Carey JP. Vestibulotoxicity and management of vestibular disorders. *Volta Rev* (2005) 105(3):251–76.
110. Marques P, Manrique-Huarte R, Perez-Fernandez N. Single intratympanic gentamicin injection in Meniere's disease: VOR change and prognostic usefulness. *Laryngoscope* (2015) 125(8):1915–20. doi:10.1002/lary.25156
111. Viana LM, Bahmad F, Rauch SD. Intratympanic gentamicin as a treatment for drop attacks in patients with Meniere's disease. *Laryngoscope* (2014) 124(9):2151–4. doi:10.1002/lary.24716
112. Aw ST, Todd MJ, Aw GE, Weber KP, Halmagyi GM. Gentamicin vestibulotoxicity impairs human electrically evoked vestibulo-ocular reflex. *Neurology* (2008) 71(22):1776–82. doi:10.1212/01.wnl.0000335971.43443.d9
113. Hullar TE, Della Santina CC, Hirvonen T, Lasker DM, Carey JP, Minor LB. Responses of irregularly discharging chinchilla semicircular canal vestibular-nerve afferents during high-frequency head rotations. *J Neurophysiol* (2005) 93(5):2777–86. doi:10.1152/jn.01002.2004
114. Kim KS, Minor LB, Della Santina CC, Lasker DM. Variation in response dynamics of regular and irregular vestibular-nerve afferents during sinusoidal head rotations and currents in the chinchilla. *Exp Brain Res* (2011) 210(3–4):643–9. doi:10.1007/s00221-011-2600-8
115. Hammam E, Bolton PS, Kwok K, Macefield VG. Vestibular modulation of muscle sympathetic nerve activity during sinusoidal linear acceleration in supine humans. *Front Neurosci* (2014) 8:316. doi:10.3389/fnins.2014.00316
116. Hammam E, Hau CLV, Wong KS, Kwok K, Macefield VG. Vestibular modulation of muscle sympathetic nerve activity by the utricle during sub-perceptual sinusoidal linear acceleration in humans. *Exp Brain Res* (2014) 232(4):1379–88. doi:10.1007/s00221-014-3856-6
117. Hammam E, Kwok K, Macefield VG. Modulation of muscle sympathetic nerve activity by low-frequency physiological activation of the vestibular utricle in awake humans. *Exp Brain Res* (2013) 230(1):137–42. doi:10.1007/s00221-013-3637-7
118. Kaufmann H, Biaggioni I, Voustianiouk A, Diedrich A, Costa F, Clarke R, et al. Vestibular control of sympathetic activity – an otolith-sympathetic reflex in humans. *Exp Brain Res* (2002) 143(4):463–9. doi:10.1007/s00221-002-1002-3
119. Raphan T, Cohen B, Xiang YQ, Yakushin SB. A model of blood pressure, heart rate, and vaso-vagal responses produced by vestibulo-sympathetic activation. *Front Neurosci* (2016) 10:96. doi:10.3389/fnins.2016.00096
120. Voustianiouk A, Kaufmann H, Diedrich A, Raphan T, Biaggioni I, MacDougall H, et al. Electrical activation of the human vestibulo-sympathetic reflex. *Exp Brain Res* (2006) 171(2):251–61. doi:10.1007/s00221-005-0266-9
121. Waternaugh DE, Cothron AV, Wasmund SL, Wasmund WL, Carter R, Muenter NK, et al. Do vestibular otolith organs participate in human

- orthostatic blood pressure control? *Auton Neurosci* (2002) 100(1–2):77–83. doi:10.1016/s1566-0702(02)00142-x
122. Yates BJ, Bolton PS, Macefield VG. Vestibulo-sympathetic responses. *Compr Physiol* (2014) 4(2):851–87. doi:10.1002/cphy.c130041
 123. Holstein GP, Friedrich VL, Martinelli GP. Glutamate and GABA in vestibulo-sympathetic pathway neurons. *Front Neuroanat* (2016) 10:7. doi:10.3389/fnana.2016.00007
 124. Holstein GR, Friedrich VL, Martinelli GP. Projection neurons of the vestibulo-sympathetic reflex pathway. *J Comp Neurol* (2014) 522(9):2053–74. doi:10.1002/cne.23517
 125. Holstein GR, Friedrich VL, Martinelli GP. Imidazoleacetic acid-ribotide in vestibulo-sympathetic pathway neurons. *Exp Brain Res* (2016) 234(10):2747–60. doi:10.1007/s00221-016-4725-2
 126. Allen T, Garcia AJ, Tang J, Ramirez JM, Rubens DD. Inner ear insult ablates the arousal response to hypoxia and hypercarbia. *Neuroscience* (2013) 253:283–91. doi:10.1016/j.neuroscience.2013.08.059
 127. Allen T, Juric-Sekhar G, Campbell S, Mussar KE, Seidel K, Tan J, et al. Inner ear insult suppresses the respiratory response to carbon dioxide. *Neuroscience* (2011) 175:262–72. doi:10.1016/j.neuroscience.2010.11.034
 128. Ramirez S, Allen T, Villagracia L, Chae Y, Ramirez JM, Rubens DD. Inner ear lesion and the differential roles of hypoxia and hypercarbia in triggering active movements: potential implication for the sudden infant death syndrome. *Neuroscience* (2016) 337:9–16. doi:10.1016/j.neuroscience.2016.08.054
 129. Arimoto S. Fundamental problems of robot control, Part I, Innovations in the realm of robot servo-loops. *Robotica* (1995) 13:19–27. doi:10.1017/S0263574700017446
 130. Su YX, Zheng CH. PID control for global finite-time regulation of robotic manipulators. *Int J Syst Sci* (2017) 48(3):547–58. doi:10.1080/00207721.2016.1193256
 131. Mergner T, Maurer C, Peterka RJ. A multisensory posture control model of human upright stance. *Prog Brain Res* (2003) 142:189–201. doi:10.1016/S0079-6123(03)42014-1
 132. Zhou Y, Luo J, Hu JQ, Li HY, Xie SR. Bionic eye system based on fuzzy adaptive PID control. In *IEEE Robotics and Automation Society, ROBIO 2012: 2012 IEEE International Conference on Robotics and Biomimetics*. Piscataway, NJ: IEEE (2012). p. 1268–72.
 133. Cullen KE. The neural encoding of self-motion. *Curr Opin Neurobiol* (2011) 21(4):587–95. doi:10.1016/j.conb.2011.05.022
 134. Cullen KE. The vestibular system: multimodal integration and encoding of self-motion for motor control. *Trends Neurosci* (2012) 35(3):185–96. doi:10.1016/j.tins.2011.12.001
 135. Jamali M, Chacron MJ, Cullen KE. Self-motion evokes precise spike timing in the primate vestibular system. *Nat Commun* (2016) 7:13229. doi:10.1038/ncomms13229
 136. Jamali M, Mitchell DE, Dale A, Carriot J, Sadeghi SG, Cullen KE. Neuronal detection thresholds during vestibular compensation: contributions of response variability and sensory substitution. *J Physiol* (2014) 592(7):1565–80. doi:10.1113/jphysiol.2013.267534
 137. Jamali M, Sadeghi SG, Cullen KE. Response of vestibular nerve afferents innervating utricle and saccule during passive and active translations. *J Neurophysiol* (2009) 101(1):141–9. doi:10.1152/jn.91066.2008
 138. Curthoys IS, Vulovic V, Burgess AM, Cornell ED, Mezey LF, MacDougall HG, et al. The basis for using bone-conducted vibration or air-conducted sound to test otolithic function. *Ann N Y Acad Sci* (2011) 1233:231–41. doi:10.1111/j.1749-6632.2011.06147.x
 139. Uchino Y, Kushiro K. Differences between otolith- and semicircular canal-activated neural circuitry in the vestibular system. *Neurosci Res* (2011) 71(4):315–27. doi:10.1016/j.neures.2011.09.001

Conflict of Interest Statement: IC and HM are unpaid consultants to GN Otometrics, Taastrup, Denmark, but have received support from GN Otometrics for travel and attendance at conferences and workshops. For all other authors, the research was conducted in the absence of any commercial or financial relationships that could be construed as a potential conflict of interest.

Copyright © 2017 Curthoys, MacDougall, Vidal and de Waele. This is an open-access article distributed under the terms of the Creative Commons Attribution License (CC BY). The use, distribution or reproduction in other forums is permitted, provided the original author(s) or licensor are credited and that the original publication in this journal is cited, in accordance with accepted academic practice. No use, distribution or reproduction is permitted which does not comply with these terms.



Descending Influences on Vestibulospinal and Vestibulosympathetic Reflexes

Andrew A. McCall, Derek M. Miller and Bill J. Yates*

Department of Otolaryngology, University of Pittsburgh School of Medicine, Pittsburgh, PA, USA

This review considers the integration of vestibular and other signals by the central nervous system pathways that participate in balance control and blood pressure regulation, with an emphasis on how this integration may modify posture-related responses in accordance with behavioral context. Two pathways convey vestibular signals to limb motoneurons: the lateral vestibulospinal tract and reticulospinal projections. Both pathways receive direct inputs from the cerebral cortex and cerebellum, and also integrate vestibular, spinal, and other inputs. Decerebration in animals or strokes that interrupt corticobulbar projections in humans alter the gain of vestibulospinal reflexes and the responses of vestibular nucleus neurons to particular stimuli. This evidence shows that supratentorial regions modify the activity of the vestibular system, but the functional importance of descending influences on vestibulospinal reflexes acting on the limbs is currently unknown. It is often overlooked that the vestibulospinal and reticulospinal systems mainly terminate on spinal interneurons, and not directly on motoneurons, yet little is known about the transformation of vestibular signals that occurs in the spinal cord. Unexpected changes in body position that elicit vestibulospinal reflexes can also produce vestibulosympathetic responses that serve to maintain stable blood pressure. Vestibulosympathetic reflexes are mediated, at least in part, through a specialized group of reticulospinal neurons in the rostral ventrolateral medulla that project to sympathetic preganglionic neurons in the spinal cord. However, other pathways may also contribute to these responses, including those that dually participate in motor control and regulation of sympathetic nervous system activity. Vestibulosympathetic reflexes differ in conscious and decerebrate animals, indicating that supratentorial regions alter these responses. However, as with vestibular reflexes acting on the limbs, little is known about the physiological significance of descending control of vestibulosympathetic pathways.

OPEN ACCESS

Edited by:

Bernard Cohen,
Icahn School of Medicine at
Mount Sinai, USA

Reviewed by:

William Michael King,
University of Michigan, USA
Richard Nichols,
Georgia Institute of Technology, USA

*Correspondence:

Bill J. Yates
byates@pitt.edu

Specialty section:

This article was submitted to
Neuro-otology,
a section of the journal
Frontiers in Neurology

Received: 16 January 2017

Accepted: 09 March 2017

Published: 27 March 2017

Citation:

McCall AA, Miller DM and Yates BJ
(2017) Descending Influences on
Vestibulospinal and
Vestibulosympathetic Reflexes.
Front. Neurol. 8:112.
doi: 10.3389/fneur.2017.00112

INTRODUCTION

Historically, vestibular-elicited reflexes were considered to be stereotyped responses to particular head movements (1–3). However, recent research has shown that vestibular nucleus neurons receive inputs from a variety of sources in addition to the inner ear, such that vestibular-elicited reflexes are shaped in accordance with ongoing movements and behaviors. For example, the work of

Cullen et al. showed that some vestibular nucleus neurons compare the planned head movement with feedback sensory signals, and discharge in accordance with deviations from the intended movement (4–6). However, most studies that considered the modification of vestibular responses in a behavioral context focused on the control of eye movements and gaze (4, 7, 8), but not vestibular reflexes acting on the limbs and vestibulosympathetic responses that regulate blood pressure.

This review considers the integration of vestibular and other signals by the central nervous system pathways that participate in balance control and blood pressure regulation, with an emphasis on how this integration may modify posture-related responses in accordance with behavioral context. It starts with an overview of the pathways that relay vestibular signals to limb motoneurons and sympathetic preganglionic neurons, and then considers the integration of signals that occurs in these pathways. Next, evidence is presented that descending signals modify vestibulospinal reflexes acting on the limbs as well as vestibulosympathetic reflexes, presumably to shape the responses in accordance with physiological challenges that are present or anticipated, as well as behaviors and movements that are planned or being implemented. Finally, directions for future research are discussed. In total, the review describes how perspectives on vestibulospinal and vestibulosympathetic responses have evolved, such that these responses are now considered to be components of a hierarchy of systems that are activated to achieve stable movements without disturbances in blood pressure.

ORGANIZATION OF VESTIBULOSPINAL AND VESTIBULOSYMPATHETIC PATHWAYS

Vestibulospinal Pathways Acting on the Limbs

Two pathways originating in the vestibular nuclei provide inputs to spinal cord segments containing limb motoneurons. The medial vestibulospinal tract (MVST) originates in the rostral portion of the descending vestibular nucleus as well as the bordering areas of the medial and lateral vestibular nuclei (9–11). The main influences of this pathway are on upper-body musculature, particularly neck musculature, although a small fraction of MVST projections provide inputs to segments containing forelimb motoneurons (10–12). The lateral vestibulospinal tract (LVST) originates mainly from the lateral vestibular nucleus, with some contribution from the descending nucleus (9–11). This tract extends the entire length of the spinal cord and provides extensive inputs to spinal cord segments containing motoneurons that innervate forelimb and hindlimb muscles (13, 14). Since the LVST provides much more extensive inputs to the spinal cord segments containing limb motoneurons than does the MVST (10–12), it likely plays a predominant role in controlling postural responses of the limbs. Thus, the LVST will be a focus of this article.

The LVST mainly terminates in Rexed's laminae VII and VIII in the forelimb and hindlimb segments of the spinal cord, which contain premotor interneurons, and not directly on motoneurons (13–16). Electrophysiological studies have confirmed that most

connections of LVST axons with limb α-motoneurons are polysynaptic, although some weak monosynaptic inputs may occur to hindlimb motoneurons (17, 18). These observations suggest that signals conveyed through the LVST are processed and likely modified by spinal interneurons prior to reaching motoneurons. The LVST mainly has excitatory effects on extensor motoneurons, with some inhibitory effects on flexor motoneurons (17, 18). At least in cats, approximately half of LVST axons that terminate in lower cervical and upper thoracic spinal segments (which contain forelimb motoneurons) also have a branch to the lumbar spinal cord, raising the prospect that some LVST neurons simultaneously control muscle activity in both the forelimbs and hindlimbs (19).

Neurons whose axons project to the spinal cord in the pontine and medullary reticulospinal tracts (RST) also receive extensive vestibular inputs (20–23). These vestibular inputs are polysynaptic, indicating that vestibular nucleus neurons and other pathways convey labyrinthine signals to RST neurons, but that RST neurons do not receive direct inputs from vestibular nerve fibers (20, 21). RST neurons have both excitatory and inhibitory effects on flexor and extensor forelimb and hindlimb motoneurons (24–28), as opposed to LVST neurons that tend to excite extensor motoneurons and inhibit flexor motoneurons (17, 18). However, LVST and RST (24, 25, 29) neurons are similar in that their effects on the excitability of limb motoneurons are mainly polysynaptic, *via* spinal interneurons, and that the axons of both RST (30) and LVST (19) neurons are highly branched. Thus, the two major pathways that convey vestibular signals to limb motoneurons have some similarities, as well as some major differences.

Vestibulosympathetic Pathways

The first key study demonstrating that the vestibular system contributes to cardiovascular regulation was published by Doba and Reis (31). As discussed in detail in a recent review (32), considerable evidence from experiments in both human and animal subjects has shown that the vestibular system participates in regulating sympathetic nervous system activity, to provide for adjustments in blood pressure during movement.

A column of reticulospinal neurons located near the ventral surface of the rostral medulla plays a predominant role in controlling sympathetic nerve activity and blood pressure (33–36). These neurons comprise the rostral ventrolateral medulla (RVLM). Lesions of the RVLM abolished vestibulosympathetic responses (37), suggesting that reticulospinal neurons with cell bodies in the RVLM constitute the major pathway through which vestibular signals are conveyed to sympathetic preganglionic neurons in the thoracic spinal cord. RVLM neurons are components of the baroreceptor reflex arc, which also includes neurons in nucleus tractus solitarius (NTS) that receive baroreceptor inputs, as well as inhibitory neurons in the caudal ventrolateral medulla (CVLM) (38–41). The RVLM receives direct inputs from the caudal aspects of the vestibular nucleus complex (42–47), as does the NTS (42, 48–51) and CVLM (42, 43, 45–47). The connections from the caudal portions of the vestibular nuclei to brainstem regions that regulate sympathetic nervous system activity are shown in **Figure 1**. In addition, neurons in other areas of the

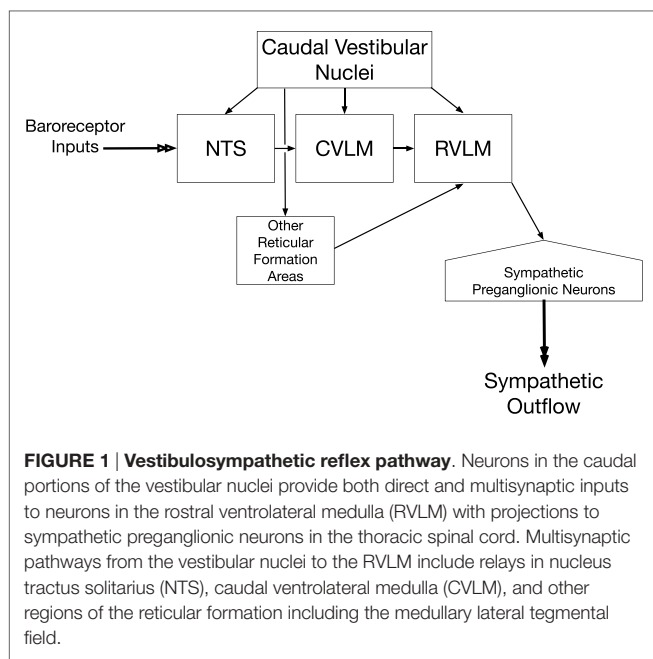


FIGURE 1 | Vestibulosympathetic reflex pathway. Neurons in the caudal portions of the vestibular nuclei provide both direct and multisynaptic inputs to neurons in the rostral ventrolateral medulla (RVLM) with projections to sympathetic preganglionic neurons in the thoracic spinal cord. Multisynaptic pathways from the vestibular nuclei to the RVLM include relays in nucleus tractus solitarius (NTS), caudal ventrolateral medulla (CVLM), and other regions of the reticular formation including the medullary lateral tegmental field.

reticular formation that project to the RVLM, including those in the lateral tegmental field, receive labyrinthine inputs (52). Thus, RVLM neurons that control sympathetic nervous system activity receive both direct and multisynaptic inputs from vestibular nucleus neurons.

Pathways for Dual Control of Sympathetic Outflow and Limb Muscle Activity

Although most studies have focused on pathways that independently regulate blood pressure and limb movements, transneuronal tracing studies demonstrated that neurons in the medial medullary reticular formation and adjacent raphe nuclei have collateralized projections to both sympathetic preganglionic neurons and limb motoneurons, as do some brainstem catecholaminergic neurons including those in locus coeruleus and nucleus subcoeruleus (53–56). As noted above, the activity of many medial medullary reticulospinal neurons is modulated by vestibular inputs (20–23). There is also evidence that medullary raphe spinal neurons (57, 58), as well as spinally projecting neurons in locus coeruleus (59–61), receive vestibular signals. However, it is not yet known whether the dual-control neurons mediate both vestibulosympathetic and vestibulospinal responses. Moreover, the physiological role of the dual-control pathways is currently unknown, but these pathways should not be ignored when considering vestibular control of motor and sympathetic nervous system activity.

INPUTS TO VESTIBULOSPINAL AND VESTIBULOSYMPATHETIC PATHWAYS

Inputs to the Vestibular Nuclei

The vestibular nucleus complex on each side of the brainstem receives a wide variety of inputs. These inputs include vestibular

signals from ipsilateral primary vestibular afferents and the contralateral vestibular nuclei, somatosensory inputs from the spinal cord, and modulatory signals from the cerebellum and higher-order brain centers. The convergence of widely dispersed inputs likely contributes, at least in part, to controlling the activity of vestibulospinal and vestibulosympathetic reflex pathways.

Vestibular Inputs

The central projections of vestibular afferents have been studied extensively and delineated in detail in prior reviews and chapters (8, 62), and thus will only be briefly described here. Vestibular afferents encode information about head tilt, translation, and rotations in space and project to the vestibular nuclear complex and to other areas of the nervous system that participate in balance control, such as the cerebellar nodulus and uvula (62–64). Vestibular afferents with peripheral processes innervating otolith and semicircular canal endorgans terminate ipsilaterally in all of the major vestibular nuclei, although projection patterns vary across species (62). Furthermore, the vestibular nuclei, excepting the lateral vestibular nucleus, are strongly interconnected by commissural projections from the contralateral side, and through ipsilateral intrinsic pathways (65, 66). Finally, inputs from multiple vestibular receptors, such as from otolith and semicircular canal inputs, converge onto single vestibular nucleus neurons, producing modulation of neural activity with varying spatial and temporal characteristics (termed spatiotemporal convergence) (67).

Spinal Inputs

Anatomic studies demonstrated that all levels of the spinal cord convey inputs to the vestibular nuclei (68–71). Cervical proprioceptive afferents send collaterals directly to the ipsilateral medial and inferior vestibular nuclei (68, 72, 73). Disynaptic pathways also carry afferent information from the cervical spinal cord to the medial, inferior, and lateral vestibular nuclei (74). Neurons within the lumbar enlargement send direct projections to the medial and inferior vestibular nuclei, and possibly the lateral vestibular nucleus (69, 70). Other indirect pathways, such as through the reticular formation and cerebellum, may also convey information from the spinal cord to the vestibular nuclei (70). Neurophysiologic studies conducted in a variety of species (mice, rat, cat, and cynomolgus monkey) and preparations confirmed that stimulation of somatosensory afferents from the neck and limbs modulates the activity of vestibular nucleus neurons (75–81).

Visual Inputs

Many neurons in the vestibular nuclei have activity that is related to eye position or eye movements [for reviews, see Ref. (4, 7, 8)]. Such neurons are not believed to contribute to vestibulospinal responses acting on the limbs and are largely absent from the caudal aspects of the vestibular nuclei that mediate vestibulosympathetic responses (82). Thus, these neurons will not be discussed further in this article. However, the activities of both neurons with eye-position sensitivity and “vestibular only” (VO) neurons that may contribute to vestibulospinal reflexes are modulated by movement of the visual field (optokinetic stimuli)

(83–87). It is well-established that visual inputs contribute to postural control (88–95), and there is evidence that visual signals modulate vestibulosympathetic responses (96). However, it is unknown whether visual contributions to these responses are mediated through optokinetic inputs to the vestibular nuclei, or via other pathways.

Cerebellar Inputs

Cerebellar outflow to the vestibular nuclei is largely through the deep cerebellar nuclei, which are comprised of the fastigial, interposed, and dentate nuclei. Purkinje neurons in the cerebellar cortex send inhibitory projections to the deep cerebellar nuclei (97), which subsequently project to a variety of targets in the brainstem. The fastigial nucleus has been shown in a number of studies to project heavily to the vestibular nuclear complex (98–102); a few studies have also demonstrated projections to the vestibular nuclei from the interposed (103, 104) and dentate nuclei (105).

Some cerebellar cortical Purkinje neurons, particularly those in the vestibulocerebellum, project directly to the vestibular nuclei. Immunostaining studies localizing protein kinase C (PKC), an enzyme found in Purkinje cells, demonstrated that cerebellar Purkinje cells project to the major vestibular nuclei (106, 107). Anterograde and retrograde tracing studies showed that flocculus Purkinje neurons terminate in all of the major vestibular nuclei as well as group y, a cytoarchitecturally distinct extension of the vestibular nuclei located dorsocaudal to the restiform body (108–110). Tracing data also demonstrated that Purkinje cells in the nodulus send axons to the medial, inferior, and superior vestibular nuclei and to group y (111–113). Purkinje cells in the uvula were also shown to project to the superior and medial vestibular nuclei (112). The delta-isoform of PKC, which heavily stains Purkinje cells in the folia of the uvula and nodulus as well as the posterior cerebellum, is found in the caudal vestibular nuclei (inferior and medial vestibular nuclei), indicative of a significant direct cerebellar projection to these regions (107, 114).

Cerebral Inputs

Direct corticovestibular projections have been demonstrated in a number of animal preparations and are best described in cats and non-human primates (115–120), as reviewed by Fukushima (121). In the cat, injection of retrograde tracers into the vestibular nuclei labeled neurons is widely dispersed in areas of cerebral cortex including areas 6, 2, and 3a (115, 117). Electrical stimulation of areas 2 and 3a resulted in excitatory and inhibitory responses of vestibular nucleus neurons (115). This study also showed that vestibular nucleus neurons with spinal projections were particularly likely to have their activity modulated by cortical stimulation (115). Similarly, electrical stimulation of cortical motor areas (pericruciate cortex) resulted in short-latency (possibly monosynaptic) and long-latency excitation and inhibition of vestibular nucleus neurons (116). Studies in a variety of non-human primate species showed that widely dispersed cortical areas, including parieto-insular vestibular cortex, area 3aV, temporal area T3, premotor area 6a, area 7ant in squirrel monkey (corresponding

to macaque area 2v), and the anterior cingulate cortex, project to the vestibular nuclei (119–122).

Inputs to Reticulospinal Neurons

As previously discussed, reticulospinal neurons in the pons and medulla [pontomedullary reticulospinal tract neurons (pmRSTn)] that contribute to postural control receive extensive inputs from the vestibular nuclei (20–23). Although all four vestibular nuclei provide inputs to pmRSTn, the distribution, and extent of the projections from each nucleus are not uniform (21). Electrical stimulation of the VIII cranial nerve evoked disynaptic and polysynaptic excitation as well as polysynaptic inhibition of neurons in the pontomedullary reticular formation, confirming anatomical evidence that these cells receive extensive labyrinthine inputs (21, 123). A study in decerebrate cats indicated that pmRSTn receive extensive inputs from the otolith organs, which supports the notion that the RST plays an important role in generating gravity-dependent postural reflexes (22). However, some pmRSTn did not respond to stimulation of the VIII nerve, showing that the function of the RST is not simply to transmit vestibular signals to the spinal cord (21).

Extensive spinoreticular projections convey spinal afferent inputs to the reticular formation (124–128). As noted above, vestibular nucleus neurons receive extensive spinal inputs, such that projections from the vestibular nuclei to the reticular formation are another potential route for transmitting signals from skin and muscle to pmRSTn. Cutaneous inputs to the reticular formation are prevalent (124, 125, 128–131). Drew and Colleagues (131) reported that the majority of medullary RST neurons responded to cutaneous inputs, usually with an excitatory response. There is less evidence that pmRSTn receive inputs from muscle afferents, although one study in decerebrate cats showed that vibration applied to the gastrocnemius–soleus muscle complex altered the firing in 27% of neurons located within the nucleus gigantocellularis (a region of the medullary reticular formation) (132).

Like vestibular nucleus neurons, pmRSTn receive direct inputs from cerebral cortex (133–140). Inputs to pmRSTn are mainly from motor and premotor cortex, whereas vestibular nucleus neurons receive inputs from widespread cortical areas, at least in non-human primates (121). RST neurons, like vestibulospinal neurons, also receive extensive inputs from the cerebellar fastigial nucleus (141–143). However, unlike vestibulospinal neurons, pmRSTn receive little direct input from cerebellar Purkinje cells. Thus, there is a possibility that RST neurons are subject to different cortical and cerebellar control than vestibulospinal neurons, although this notion has not been thoroughly examined experimentally.

As noted above, some of the inputs to pmRSTn resemble those to vestibulospinal neurons. In addition, some reticulospinal neurons receive inputs distinct from those to the vestibular nuclei. For example, a population of spinally projecting neurons in the ventral and caudal aspect of the pontine reticular formation mediates acoustic startle responses (144). Such responses entail the stiffening of the dorsal neck, body wall, and limbs to provide protection from predatory attack before a defensive action can

be engaged. The acoustic startle response entails monosynaptic inputs from the cochlear nuclei to reticulospinal neurons (145–148). Although vestibulospinal neurons may also mediate acoustic startle responses (149), the reticulospinal system appears to play a dominant role (150).

Shik et al. discovered in 1966 that electrical stimulation of a constrained region at the junction between the midbrain- and pons-elicited locomotion in animals (151). This area has subsequently been called the “mesencephalic locomotor region” (MLR) and has been identified across vertebrate species including man (152). The MLR does not project to the spinal cord, but provides inputs to pmRSTn (153, 154) that transmit locomotor signals to spinal premotor interneurons (155, 156). Hence, pmRSTn play a unique and pivotal role in controlling locomotion. There is no evidence that vestibulospinal neurons receive inputs from the MLR.

Although it is appreciated that a variety of inputs are conveyed to the reticular formation, little is known about the convergence of these inputs on single neurons (129). Moreover, only a few studies have entailed recordings from pmRSTn in conscious animals, or attempted to ascertain how the activity of these neurons changes during ongoing movements and across behavioral states.

Figure 2 summarizes the inputs to and connections of vestibulospinal and reticulospinal neurons.

Processing of Vestibulospinal and Reticulospinal Signals by Spinal Interneurons

As discussed above, few vestibulospinal and reticulospinal projections provide direct inputs to limb motoneurons, but instead mainly terminate on interneurons in Rexed's laminae

VII and VIII (24, 25, 29). A variety of identified types of spinal interneurons have been reported to receive labyrinthine inputs, including Renshaw cells (157, 158), Ia inhibitory interneurons (159, 160), propriospinal interneurons (161–163), and commissural interneurons (164–166). However, most experiments that characterized the responses of spinal interneurons to natural vestibular stimulation (whole-body rotations) did not identify the physiological role of those interneurons, or the convergent spinal and descending inputs they receive (167–169).

Considering the extensive projections of muscle spindle afferents to Rexed's lamina VII (170, 171), it seems likely that there is convergence and integration of vestibular and proprioceptive signals in the spinal cord. A variety of descending pathways from the brain terminate in Rexed's laminae VIII, including corticospinal, vestibulospinal, and reticulospinal projections [for review, see Ref. (172)]. A caveat is that the vestibulospinal system excites extensor motoneurons and inhibits flexor motoneurons (17, 18), while the reticulospinal system elicits both excitation and inhibition of flexor and extensor motoneurons (24–28). Thus, the spinal interneurons that receive inputs from the vestibulospinal and reticulospinal pathways must be at least partially distinct. Unfortunately, little is known about the convergence of signals from descending pathways in the spinal cord, and how the integration of the descending motor commands shapes ongoing and planned movements. Thus, the significance and physiological role of the processing of vestibular signals by spinal cord interneurons remain unclear. One role of the signal integration may be to adjust muscle activity when body orientation changes during locomotion, as while walking uphill (173–175).

It has also been suggested that the vestibulospinal and reticulospinal pathways provide inputs to gamma motoneurons, thereby affecting the gain of the myotatic reflex (176–178).

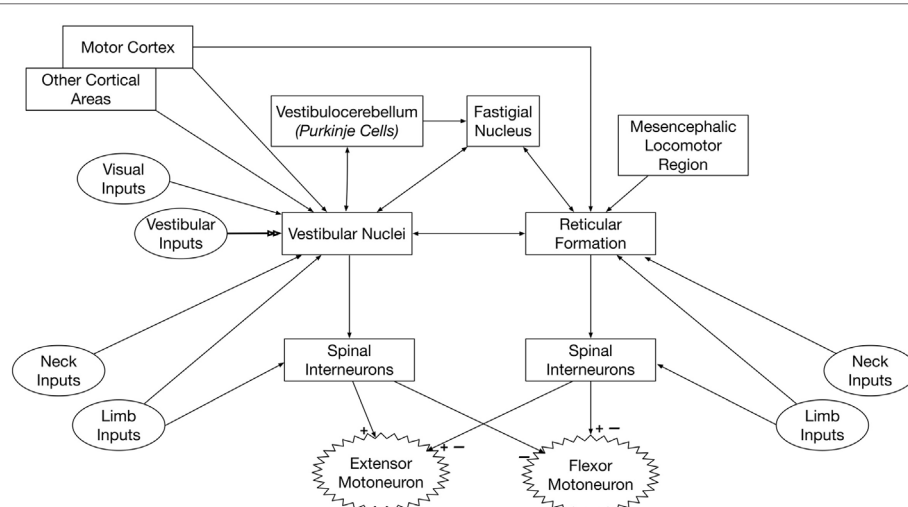


FIGURE 2 | Pathways that convey vestibular signals to limb motoneurons. Spinal premotor interneurons receive inputs from the vestibulospinal and reticulospinal pathways. The vestibulospinal system excites extensor motoneurons and inhibits flexor motoneurons, while the reticulospinal system elicits both excitation and inhibition of flexor and extensor motoneurons. Thus, the spinal interneurons that receive inputs from vestibulospinal and reticulospinal pathways must be at least partially distinct. The neurons of origin of reticulospinal and vestibulospinal projections integrate vestibular, neck, and limb inputs; this integration is modulated by signals from several brain regions, including the cerebral cortex and cerebellum.

However, some studies in animals (179), as well as recent experiments in humans (180, 181), indicated that vestibular signals do not affect the fusimotor system. Further experiments are needed to address the discrepancies in the conclusions of these studies.

Inputs to Vestibulosympathetic Neurons

Neurons in the RVLM that control sympathetic nervous system activity receive vestibular inputs through a variety of pathways (32), as illustrated in **Figure 1**. Since many of the relays from the vestibular nuclei to the RVLM are polysynaptic, it is difficult to identify “vestibulosympathetic neurons” during neurophysiologic experiments. Thus, much of what is known about convergence of signals in the vestibulosympathetic pathways was ascertained by determining inputs and behavioral states that modulate sympathetic nerve activity elicited by vestibular stimulation.

Baroreceptors provide a dominant input to sympathetic nervous system neurons that control blood pressure, such that an increase in blood pressure results in a decrease in the activity of RVLM neurons as well as the sympathetic preganglionic neurons they provide inputs to (38–41). It is thus not surprising that stimulation of baroreceptors by increasing blood pressure resulted in an attenuation of vestibulosympathetic responses (182). A number of studies demonstrated the convergence of vestibular and baroreceptor inputs onto RVLM neurons, including putative presympathetic neurons with projections to the thoracic spinal cord (183, 184).

Rostral ventrolateral medulla neurons receive inputs from a variety of brain regions, either directly or indirectly through connections in the baroreceptor reflex pathway. These brain regions include the periaqueductal gray (185), parabrachial nucleus (186–193), several hypothalamic nuclei (190, 194–215), the amygdala (195, 212, 216–219), and prefrontal and insular cortices (206, 212, 220–225). Thus, engagement of a wide variety of descending pathways could potentially modulate vestibulosympathetic responses.

TRANSFORMATION OF VESTIBULAR REFLEXES BY DESCENDING PATHWAYS

Transformation of Vestibulospinal and Reticulospinal Reflexes: Evidence from Animal Studies

The present body of knowledge regarding descending control of vestibulospinal reflexes largely stems from one of two experimental designs: comparing vestibular nucleus neuronal responses during active and passive movement in intact animals and comparing vestibular nucleus neural responses between decerebrate and intact preparations. While additional studies are clearly needed, in particular to discriminate which higher centers are responsible for modulating vestibulospinal reflexes, some insights can be gained from the present body of knowledge.

A subset of vestibular nucleus neurons identified in non-human primates, termed VO neurons, are thought to mediate vestibulospinal reflexes (226–229). The activity of VO neurons,

like other vestibular nucleus neurons and primary vestibular afferents, is modulated by passive (externally applied) head movement with respect to space. However, unlike other classes of vestibular nucleus neurons, the firing rate of VO neurons does not change during eye movements (230, 231). During active (self-generated) head movement, responses of VO neurons are dramatically attenuated (227, 231, 232). Furthermore, proprioceptive feedback must match that signaled by the active motor command (efference copy) to suppress VO neuronal activity during self-motion (233, 234). While the locations of the circuits that compare efference copy with proprioceptive feedback during a movement have not yet been fully elucidated, descending inputs from higher brain centers must play a key role since volitional movement is triggered from cerebral cortex. In addition, it is unknown whether VO neurons responsible for reflex posturing of the limbs respond differently to active and passive (unexpected) limb movements.

Decerebration results in a disconnection of brainstem centers, including the vestibular nuclei and reticular formation, from higher brain centers. In decerebrate animals, the neural circuitry of vestibulospinal pathways is simplified by removing descending cortical influences, permitting investigations in a reduced preparation. The interruption of supratentorial inputs to the lateral vestibular nucleus is thought to produce unsuppressed activation of extensor motoneurons by the LVST, resulting in decerebrate extensor posturing (235–237).

As previously discussed, there is widespread convergence of afferent inputs from multiple sources, including vestibular, somatosensory, and visual signals, in the vestibular nuclei. The effects of hindlimb somatosensory inputs on the activity of vestibular nucleus neurons have been studied in both decerebrate and conscious cats by the same investigators, using the same equipment and methodology during experiments in both preparations, thus permitting comparisons (75, 78, 238, 239). Comparisons in decerebrate and conscious cats of the effects of electrical stimulation of hindlimb nerves on vestibular nucleus neuronal activity revealed some similarities, as well as differences (238, 239). Similarities across preparations include the following: the majority of vestibular nucleus neurons received convergent limb inputs from multiple nerves; response latencies were ~20 ms suggesting that polysynaptic pathways conveyed limb inputs to vestibular nucleus neurons; most responses were excitatory; and the proportion of neurons activated by hindlimb nerve stimulation increased after bilateral labyrinthectomy (238, 239). By contrast, low-intensity stimuli [$<$ twice threshold (T) for eliciting a compound action potential in the stimulated nerve] elicited changes in activity of many vestibular nucleus neurons in decerebrate animals, but such low-intensity stimuli were ineffective in conscious animals. Only high-threshold stimuli ($\geq 3 T$) altered the activity of vestibular nucleus neurons in conscious animals. This finding suggests that supratentorial brain regions may suppress the transmission of inputs from large diameter hindlimb afferent fibers (i.e., group Ia and II afferents) to the vestibular nuclei in the conscious animal, or may block the responses of vestibular nucleus neurons to these signals.

Modulation of vestibular nucleus neuronal activity in response to hindlimb movement has also been compared

in decerebrate and conscious cats (75, 78). While vestibular nucleus neurons responded to hindlimb movement in both preparations, some important differences were notable (see **Figure 3**). In decerebrate cats, the majority of vestibular nucleus neurons whose activity was modulated by hindlimb movement encoded the direction of hindlimb movement, and most also encoded hindlimb position signals (78). By contrast, most vestibular nucleus neurons in conscious cats encoded limb movement irrespective of the direction of the movement and did not encode hindlimb position (75). These findings suggest an interesting parallel with that noted above for experiments that made use of electrical nerve stimulation. If large-fiber afferents, such as those from muscle spindles, are responsible for the directional and position-related responses noted in decerebrate animals, the near complete lack of such responses in conscious animals suggests that higher brain centers selectively suppress this afferent feedback.

Similar comparisons of responses to limb movement in decerebrate and conscious cats have been performed for reticular formation neurons (240). In both preparations, the majority of responsive reticular formation neurons encoded limb movement irrespective of the direction of the movement; few encoded limb position or the direction of limb movement. In other words, the responses of reticular formation neurons to limb movement in both decerebrate and conscious animals resembled those of vestibular nucleus neurons in conscious animals. No suppression of limb position signals to reticular formation neurons by supratentorial brain regions was observed (240), as noted for vestibular nucleus neurons (75). These findings raise the possibility that higher brain areas such as cerebral cortex play fundamentally different roles in regulating the activity of the vestibulospinal

and reticulospinal systems, although there is no experimental evidence to suggest the nature of the differences in regulation of the two systems.

Transformation of Vestibulospinal and Reticulospinal Reflexes: Evidence from Studies in Human Subjects

As discussed above, transecting the midbrain in animals produces unopposed activation of extensor motoneurons, resulting in decerebrate extensor posturing (235–237). In humans, strokes affecting the internal capsule, which damage corticobulbar projections, produce an analogous condition: muscle spasticity (241, 242). Spasticity manifests as a sharply lateralized increase in muscle tone with enhanced tendon jerks (243). Several studies suggested that spasticity in patients, like decerebrate rigidity in animals, results from increased activity of vestibulospinal pathways (244–246). This is in contrast to one study in cats, which provided evidence that spasticity and decerebrate rigidity are differentially mediated through vestibulospinal and reticulospinal projections (247). A recent study in hemispheric stroke subjects supports the notion that spasticity results from disinhibition of vestibulospinal projections. Responses of neck muscles to vestibular stimulation (cervical vestibular-evoked myogenic potentials) were compared on the intact and lesioned sides in stroke survivors with spasticity. The differences on the two sides were proportional to the severity of the spasticity (248); the responses on the lesioned side were amplified, as illustrated in **Figure 4**. In combination with data from animals discussed previously, these data support the notion that supratentorial regions of the brain regulate the excitability of vestibulospinal neurons.

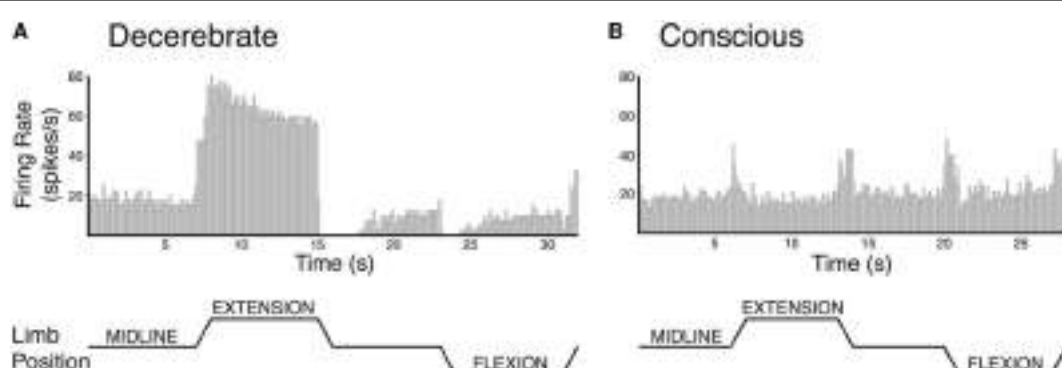


FIGURE 3 | Vestibular nucleus neurons responded to hindlimb movement in decerebrate (A) and conscious (B) cats, but the responses had different characteristics in the two preparations. Vestibular nucleus neuronal responses to hindlimb movement in the decerebrate cat typically included encoding the direction of hindlimb movement and encoding hindlimb position signals. For example, the firing rate of the vestibular nucleus neuron depicted in panel (A) increased with hindlimb movements toward extension and decreased with hindlimb movements toward flexion. Furthermore, when the hindlimb was held in extension, neuronal firing remained elevated. While neurons with such response characteristics were also present in conscious cats, they were much less common than in decerebrate cats. By contrast, the activities of most vestibular nucleus neurons in conscious cats with responses to hindlimb movement were modulated in a similar fashion during all tested directions of hindlimb movement. For example, the activity of the vestibular nucleus neuron depicted in panel (B) increased with each hindlimb movement (midline to extension; extension to midline; midline to flexion; and flexion to midline). In both panels (A,B), hindlimb movements were passively generated (externally applied) at 60°/s, lasted for a duration of 1 s, and were isolated to movements about the hip and knee joints. The hindlimb was held in each position for 7 s in panel (A) and 6 s in panel (B). Unit activity was binned in 0.1 s intervals and averaged over four repetitions in panel (A) and eight repetitions in panel (B). Panel (A) was adapted from Ref. (78); panel (B) was adapted from Ref. (75). Both panels were used with permission of the American Physiological Society.

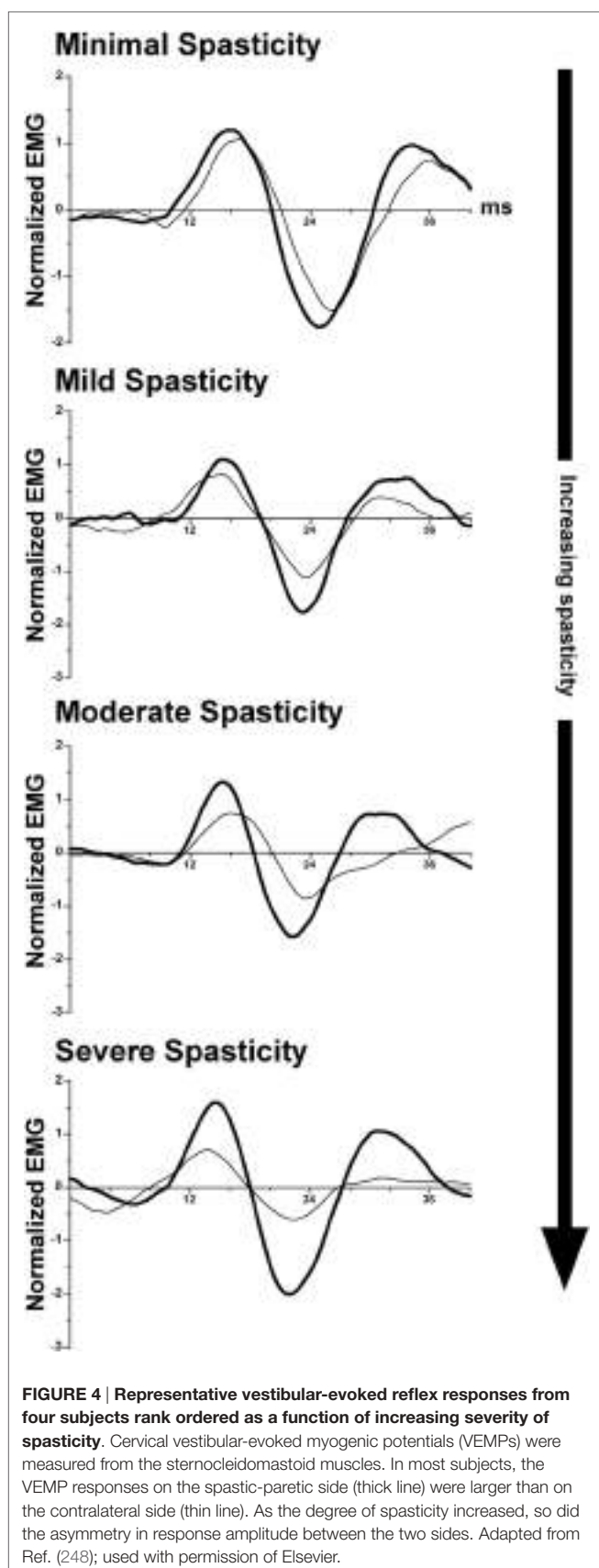


FIGURE 4 | Representative vestibular-evoked reflex responses from four subjects rank ordered as a function of increasing severity of spasticity. Cervical vestibular-evoked myogenic potentials (VEMPs) were measured from the sternocleidomastoid muscles. In most subjects, the VEMP responses on the spastic-paretic side (thick line) were larger than on the contralateral side (thin line). As the degree of spasticity increased, so did the asymmetry in response amplitude between the two sides. Adapted from Ref. (248); used with permission of Elsevier.

Transformation of Vestibulosympathetic Reflexes

Evidence that supratentorial brain regions affect the gain of vestibulosympathetic reflexes comes from a comparison of these responses in conscious and decerebrate animals (184). Whereas about half of RVLM neurons responded to 10–15° tilts in vertical planes in decerebrate felines, the activity of <1% of RVLM neurons was modulated by similar rotations in conscious cats (184). Large rotations are required to generate vestibulosympathetic responses in conscious animals, presumably because small-amplitude tilts (<40%) do not produce peripheral blood pooling that necessitates an increase in sympathetic nervous system activity (249, 250). It has been suggested that higher brain areas adjust the responsiveness of neurons in the vestibulosympathetic reflex pathway to vestibular inputs, so that the gain of the vestibulosympathetic reflex is appropriate for the ensuing movement or postural change (32). Recordings from conscious animals also provided evidence that following a bilateral labyrinthectomy, the gain of the baroreceptor reflex is adjusted by descending signals from supratentorial brain regions (251). As noted above, a number of supratentorial regions provide inputs to neurons that comprise the vestibulosympathetic reflex pathway, and it is unclear which of these regions participates in adjusting the response gain, and where along the pathway (vestibular nuclei, NTS, CVLM, RVLM) the gain adjustments occur.

The notion that sympathetic nerve activity is regulated by higher brain centers during movement is not new. In both animals and humans, adjustments in sympathetic nerve activity and alterations in the set point of the baroreceptor reflex are initiated when exercise begins (252, 253). The changes in the baroreceptor set point are needed to allow blood pressure to increase during exercise. The term “central command,” which was coined by Goodwin et al., refers to the parallel changes in autonomic nervous system activity that accompanies muscle contraction (254). Perhaps the best evidence for feedforward cardiovascular responses during movement comes from a study in paralyzed human subjects, who exhibited increases in blood pressure and heart rate that were graded to the intensity of imagined activity (255). In decerebrate or anesthetized cats, stimulation of regions of the lateral and caudal hypothalamus, fields of Forel, MLR, and midbrain ventral tegmental area elicit parallel changes in motor activity and cardiovascular responses (253, 256, 257). However, little is known about signal processing in these regions that leads to changes in sympathetic nerve activity and the baroreceptor reflex set point.

CONCLUSION AND DIRECTIONS FOR FUTURE RESEARCH

Although there is a considerable body of data regarding vestibular system contributions to maintenance of stable eye position, much less is known about vestibular reflexes that ensure postural stability and constant blood pressure during movement. This is likely because vestibulospinal pathways that act on the limbs and vestibulosympathetic pathways that affect the cardiovascular system are much more complicated than the three and four

neuron arcs that mediate vestibulo-ocular reflexes (3, 8). An often-overlooked aspect of vestibulospinal reflexes acting on the limbs is that they are mediated through premotor interneurons in the spinal cord (24, 25, 29), and not *via* direct connections of vestibulospinal and reticulospinal neurons with motoneurons. Virtually nothing is known about the convergence of descending motor signals with proprioceptive inputs in the spinal cord, and the role that spinal interneurons play in transforming the motor commands (11). Since there is a potential for spinal interneurons to integrate signals from a variety of descending motor pathways, the interneurons could potentially play an appreciable role in recovery of function if one of the pathways (or inputs to the pathways) is eliminated. Thus, a research focus is certainly warranted on the spinal interneurons that are components of vestibulospinal reflexes that act on the limbs.

Although it has been recognized for decades that both reticulospinal and vestibulospinal neurons convey vestibular signals to the spinal cord, and that these pathways receive somewhat different inputs, it is not yet clear if there is a distinct functional difference between the two pathways. As noted above, it is possible that signals conveyed through reticulospinal and vestibulospinal pathways converge on the same premotor spinal interneurons (11), although this is presently unknown. The reticulospinal pathway may be comprised of a number of parallel pathways with distinct functional roles such as mediating locomotion (153, 154), startle responses (144), and postural stability. Thus, it may be misleading to consider the reticulospinal pathway as a single functional pathway. Moreover, there is a paucity of data regarding the activity of vestibulospinal and reticulospinal neurons in awake, behaving animals, and the lack of this information complicates the determination of the physiologic roles of the pathways.

An experimental hurdle that complicates experiments in conscious animals on vestibulospinal and reticulospinal pathways is the difficulty in identifying neurons that are components of these pathways. Experiments entailing microstimulation in the spinal cord to ascertain the projections of vestibulospinal and reticulospinal neurons are tedious in paralyzed decerebrate or anesthetized animals (19), and even more complicated in conscious animals, since spinal stimulation can induce movement and extraneous inputs to the central nervous system. Consequently, there is a tendency to consider “VO neurons,” which are known to have a projection to the spinal cord, as a single class of neurons with uniform properties (227–230). Yet it is known from experiments in paralyzed animals that the branching pattern of individual vestibulospinal neurons can vary considerably (15, 16, 19). Vestibulospinal neurons that affect neck muscle activity may have

REFERENCES

1. Wilson VJ, Peterson BW. Peripheral and central substrates of vestibulospinal reflexes. *Physiol Rev* (1978) 58:80–105.
2. Wilson VJ, Peterson BW. Vestibulospinal and reticulospinal systems. In: Brookhart JM, Mountcastle VB, editors. *Handbook of Physiology. Section 1: The Nervous System, Volume II, Motor Control, Part 1*. Bethesda: American Physiological Society (1981). p. 667–702. doi:10.1002/cphy.cp010214
3. Goldberg JM, Fernandez C. Vestibular mechanisms. *Annu Rev Physiol* (1975) 37:129–62. doi:10.1146/annurev.ph.37.030175.001021
4. Cullen KE. Physiology of central pathways. *Handb Clin Neurol* (2016) 137:17–40. doi:10.1016/B978-0-444-63437-5.00002-9

dramatically different inputs and changes in activity across behavioral states than those that affect limb extensor activity. Thus, it is crucial to develop new methodology to ascertain the projection patterns of vestibulospinal neurons whose activity is monitored during neurophysiologic experiments, and to discontinue the practice of assuming that all vestibulospinal neurons must have the same properties. The same considerations should be applied to experiments on reticulospinal neurons.

Neurophysiologic experiments on neurons that constitute vestibulosympathetic pathways are in their infancy, and just two studies (184, 251) have monitored in conscious animals the activity of RVLM neurons that play a key role in regulating sympathetic nervous system activity. Little attention has been paid to the contributions of other pathways to vestibulosympathetic responses, including those originating in the medial reticular formation, raphe nuclei, and locus coeruleus that provide monosynaptic or polysynaptic inputs to both limb motoneurons and sympathetic preganglionic neurons (53–56). These pathways were identified in transneuronal tracing studies in rodents, and it is unclear whether they exist in other species, and what their role is in autonomic and motor control. In addition, it is critical that neurophysiologic studies on these neurons include an identification of their projection patterns, to ascertain which outputs they control.

In conclusion, it is now well-demonstrated that vestibulospinal and reticulospinal neurons that contribute to postural stability, and brainstem neurons that adjust blood pressure during postural alterations, receive converging inputs from a variety of sources, including cerebral cortex. Accordingly, the activity and responses to stimuli of the neurons can vary tremendously in conscious and “reduced” preparations, such as anesthetized and decerebrate animal models. In the ongoing efforts of the scientific community to foster the reproducibility of experiments and their translation to treatments for patients, the differences in responses between preparations must be fully considered.

AUTHOR CONTRIBUTIONS

All the authors co-wrote the manuscript and co-prepared the figures, and approved the final version of the manuscript.

FUNDING

The authors’ work related to this article is supported by the following grants from the National Institutes of Health of the United States: R01-DC013788 to BY, F32-DC015157 and T32-DC011499 to DM, and K08-DC013571 to AM.

5. Cullen KE. The vestibular system: multimodal integration and encoding of self-motion for motor control. *Trends Neurosci* (2012) 35:185–96. doi:10.1016/j.tins.2011.12.001
6. Cullen KE, Brooks JX, Jamali M, Carriot J, Massot C. Internal models of self-motion: computations that suppress vestibular reafference in early vestibular processing. *Exp Brain Res* (2011) 210:377–88. doi:10.1007/s00221-011-2555-9
7. Angelaki DE, Cullen KE. Vestibular system: the many facets of a multimodal sense. *Annu Rev Neurosci* (2008) 31:125–50. doi:10.1146/annurev.neuro.31.060407.125555
8. Goldberg JM, Wilson VJ, Cullen KE, Angelaki DE, Broussard DM, Buttner-Ennever J, et al. *The Vestibular System: A Sixth Sense*. New York: Oxford University Press (2012).

9. Akaike T. Comparison of neuronal composition of the vestibulospinal system between cat and rabbit. *Exp Brain Res* (1973) 18:429–32. doi:10.1007/BF00239110
10. Akaike T. Neuronal organization of the vestibulospinal system in the cat. *Brain Res* (1983) 259:217–27. doi:10.1016/0006-8993(83)91252-0
11. Shinoda Y, Sugiuchi Y, Izawa Y, Hata Y. Long descending motor tract axons and their control of neck and axial muscles. *Prog Brain Res* (2006) 151:527–63. doi:10.1016/S0079-6123(05)51017-3
12. Perlmutter SI, Iwamoto Y, Baker JF, Peterson BW. Interdependence of spatial properties and projection patterns of medial vestibulospinal tract neurons in the cat. *J Neurophysiol* (1998) 79:270–84.
13. Nyberg-Hansen R, Mascitti TA. Sites and mode of termination of fibers of the vestibulospinal tract in the cat. An experimental study with silver impregnation methods. *J Comp Neurol* (1964) 122:369–83. doi:10.1002/cne.901220307
14. Petras JM. Cortical, tectal and tegmental fiber connections in the spinal cord of the cat. *Brain Res* (1967) 6:275–324. doi:10.1016/0006-8993(67)90196-5
15. Kuze B, Matsuyama K, Matsui T, Miyata H, Mori S. Segment-specific branching patterns of single vestibulospinal tract axons arising from the lateral vestibular nucleus in the cat: a PHA-L tracing study. *J Comp Neurol* (1999) 414:80–96. doi:10.1002/(SICI)1096-9861(19991108)414:<80::AID-CNE7>3.3.CO;2-5
16. Shinoda Y, Ohgaki T, Futami T. The morphology of single lateral vestibulospinal tract axons in the lower cervical spinal cord of the cat. *J Comp Neurol* (1986) 249:226–41. doi:10.1002/cne.902490208
17. Grillner S, Hongo T, Lund S. The vestibulospinal tract. Effects on alpha-motoneurons in the lumbosacral spinal cord in the cat. *Exp Brain Res* (1970) 10:94–120. doi:10.1007/BF00340521
18. Wilson VJ, Yoshida M. Comparison of effects of stimulation of Deiters' nucleus and medial longitudinal fasciculus on neck, forelimb and hindlimb motoneurons. *J Neurophysiol* (1969) 32:743–58.
19. Abzug C, Maeda M, Peterson BW, Wilson VJ. Cervical branching of lumbar vestibulospinal axons. With an appendix by C.P. Bean. *J Physiol* (1974) 243:499–522. doi:10.1113/jphysiol.1974.sp010764
20. Peterson BW, Filion M, Felpel LP, Abzug C. Responses of medial reticular neurons to stimulation of the vestibular nerve. *Exp Brain Res* (1975) 22:335–50. doi:10.1007/BF00234670
21. Peterson BW, Abzug C. Properties of projections from vestibular nuclei to medial reticular formation in the cat. *J Neurophysiol* (1975) 38:1421–35.
22. Bolton PS, Goto T, Schor RH, Wilson VJ, Yamagata Y, Yates BJ. Response of pontomedullary reticulospinal neurons to vestibular stimuli in vertical planes. Role in vertical vestibulospinal reflexes of the decerebrate cat. *J Neurophysiol* (1992) 67:639–47.
23. Schor RH, Yates BJ. Horizontal rotation responses of medullary reticular neurons in the decerebrate cat. *J Vestib Res* (1995) 5:223–8. doi:10.1016/0957-4271(94)00034-Y
24. Engberg I, Lundberg A, Ryall RW. Reticulospinal inhibition of transmission in reflex pathways. *J Physiol* (1968) 194:201–23. doi:10.1113/jphysiol.1968.sp008402
25. Lloyd DPC. Activity in neurons of the bulbospinal correlation system. *J Neurophysiol* (1941) 4:115–34.
26. Magoun HW, Rhines R. An inhibitory mechanism in the bulbar reticular formation. *J Neurophysiol* (1946) 9:165–71.
27. Rhines R, Magoun HW. Brain stem facilitation of cortical motor response. *J Neurophysiol* (1946) 9:219–29.
28. Sprague JM, Chambers WW. Control of posture by reticular formation and cerebellum in the intact, anesthetized and unanesthetized and in the decerebrated cat. *Am J Physiol* (1954) 176:52–64.
29. Engberg I, Lundberg A, Ryall RW. Reticulospinal inhibition of transmission through interneurons of spinal reflex pathways. *Experientia* (1965) 21:612–3. doi:10.1007/BF02151565
30. Peterson BW, Maunz RA, Pitts NG, Mackel RG. Patterns of projections and branching of reticulospinal neurons. *Exp Brain Res* (1975) 23:333–51. doi:10.1007/BF00238019
31. Doba N, Reis DJ. Role of the cerebellum and vestibular apparatus in regulation of orthostatic reflexes in the cat. *Circ Res* (1974) 34:9–18. doi:10.1161/01.RES.34.1.9
32. Yates BJ, Bolton PS, Macefield VG. Vestibulo-sympathetic responses. *Compr Physiol* (2014) 4:851–87. doi:10.1002/cphy.c130041
33. Dampney RA, Goodchild AK, McAllen RM. Vasomotor control by subretrofacial neurones in the rostral ventrolateral medulla. *Can J Physiol Pharmacol* (1987) 65:1572–9. doi:10.1139/y87-247
34. Dampney RA. The subretrofacial nucleus: its pivotal role in cardiovascular regulation. *News Physiol Sci* (1990) 5:63–7.
35. Dampney RA. The subretrofacial vasomotor nucleus – anatomical, chemical and pharmacological properties and role in cardiovascular regulation. *Prog Neurobiol* (1994) 42:197–227. doi:10.1016/0301-0082(94)90064-7
36. Bourassa EA, Sved AF, Speth RC. Angiotensin modulation of rostral ventrolateral medulla (RVLM) in cardiovascular regulation. *Mol Cell Endocrinol* (2009) 302:167–75. doi:10.1016/j.mce.2008.10.039
37. Yates BJ, Siniaia MS, Miller AD. Descending pathways necessary for vestibular influences on sympathetic and inspiratory outflow. *Am J Physiol* (1995) 268:R1381–5.
38. Dampney RA. Functional organization of central pathways regulating the cardiovascular system. *Physiol Rev* (1994) 74:323–64.
39. Abboud FM, Thame MD. Interaction of cardiovascular reflexes in circulatory control. In: Shepherd JT, Abboud FM, editors. *Handbook of Physiology. Section 2: Circulation. Volume III: Peripheral Circulation and Organ Blood Flow, Part 2*. Bethesda, MD: American Physiological Society (1983). p. 497–555. doi:10.1002/cphy.cph020319
40. Gilbey MP, Spyer KM. Essential organization of the sympathetic nervous system. *Baillieres Clin Endocrinol Metab* (1993) 7:259–78. doi:10.1016/S0950-351X(05)80177-6
41. Spyer KM. Annual review prize lecture – central nervous mechanisms contributing to cardiovascular control. *J Physiol* (1994) 474:1–19. doi:10.1113/jphysiol.1994.sp019997
42. Porter JD, Balaban CD. Connections between the vestibular nuclei and brain stem regions that mediate autonomic function in the rat. *J Vestib Res* (1997) 7:63–76. doi:10.1016/S0957-4271(96)00138-3
43. Stocker SD, Steinbacher BC, Balaban CD, Yates BJ. Connections of the caudal ventrolateral medullary reticular formation in the cat brainstem. *Exp Brain Res* (1997) 116:270–82. doi:10.1007/PL00005755
44. Holstein GR, Friedrich VL Jr, Kang T, Kukielka E, Martinelli GP. Direct projections from the caudal vestibular nuclei to the ventrolateral medulla in the rat. *Neuroscience* (2011) 175:104–17. doi:10.1016/j.neuroscience.2010.12.011
45. Holstein GR, Friedrich VL Jr, Martinelli GP. Projection neurons of the vestibulo-sympathetic reflex pathway. *J Comp Neurol* (2014) 522:2053–74. doi:10.1002/cne.23517
46. Holstein GR, Friedrich VL Jr, Martinelli GP. Imidazoleacetic acid-ribotide in vestibulo-sympathetic pathway neurons. *Exp Brain Res* (2016) 234:2747–60. doi:10.1007/s00221-016-4725-2
47. Holstein GR, Friedrich VL Jr, Martinelli GP. Glutamate and GABA in vestibulo-sympathetic pathway neurons. *Front Neuroanat* (2016) 10:7. doi:10.3389/fnana.2016.00007
48. Balaban CD, Beryozkin G. Vestibular nucleus projections to nucleus tractus solitarius and the dorsal motor nucleus of the vagus nerve: potential substrates for vestibulo-autonomic interactions. *Exp Brain Res* (1994) 98:200–12. doi:10.1007/BF00228409
49. Yates BJ, Grelot L, Kerman IA, Balaban CD, Jakus J, Miller AD. Organization of vestibular inputs to nucleus tractus solitarius and adjacent structures in cat brain stem. *Am J Physiol* (1994) 267:R974–83.
50. Cai YL, Ma WL, Li M, Guo JS, Li YQ, Wang LG, et al. Glutamatergic vestibular neurons express Fos after vestibular stimulation and project to the NTS and the PBN in rats. *Neurosci Lett* (2007) 417:132–7. doi:10.1016/j.neulet.2007.01.079
51. Ruggiero DA, Mtui EP, Otake K, Anwar M. Vestibular afferents to the dorsal vagal complex: substrate for vestibular-autonomic interactions in the rat. *Brain Res* (1996) 743:294–302. doi:10.1016/S0006-8993(96)01099-2
52. Yates BJ, Balaban CD, Miller AD, Endo K, Yamaguchi Y. Vestibular inputs to the lateral tegmental field of the cat: potential role in autonomic control. *Brain Res* (1995) 689:197–206. doi:10.1016/0006-8993(95)00569-C
53. Kerman IA, Shabrang C, Taylor L, Akil H, Watson SJ. Relationship of presynaptic-premotor neurons to the serotonergic transmitter system in the rat brainstem. *J Comp Neurol* (2006) 499:882–96. doi:10.1002/cne.21129
54. Kerman IA. Organization of brain somatomotor-sympathetic circuits. *Exp Brain Res* (2008) 187:1–16. doi:10.1007/s00221-008-1337-5

55. Nam H, Kerman IA. Distribution of catecholaminergic presynaptic-pre-motor neurons in the rat lower brainstem. *Neuroscience* (2016) 324:430–45. doi:10.1016/j.neuroscience.2016.02.066
56. Kerman IA, Enquist LW, Watson SJ, Yates BJ. Brainstem substrates of sympathetic-motor circuitry identified using trans-synaptic tracing with pseudorabies virus recombinants. *J Neurosci* (2003) 23:4657–66.
57. Yates BJ, Goto T, Kerman I, Bolton PS. Responses of caudal medullary raphe neurons to natural vestibular stimulation. *J Neurophysiol* (1993) 70: 938–46.
58. Yates BJ, Goto T, Bolton PS. Responses of neurons in the caudal medullary raphe nuclei of the cat to stimulation of the vestibular nerve. *Exp Brain Res* (1992) 89:323–32. doi:10.1007/BF00228248
59. Pompeiano O. Relationship of noradrenergic locus coeruleus neurones to vestibulospinal reflexes. *Prog Brain Res* (1989) 80:329–43. doi:10.1016/S0079-6123(08)62228-1
60. Pompeiano O, Manzoni D, Barnes CD, Stampacchia G, d'Ascanio P. Responses of locus coeruleus and subcoeruleus neurons to sinusoidal stimulation of labyrinth receptors. *Neuroscience* (1990) 35:227–48. doi:10.1016/0306-4522(90)90078-I
61. Pompeiano O, Manzoni D, Barnes CD. Responses of locus coeruleus neurons to labyrinth and neck stimulation. *Prog Brain Res* (1991) 88:411–34. doi:10.1016/S0079-6123(08)63826-1
62. Newlands SD, Perachio AA. Central projections of the vestibular nerve: a review and single fiber study in the Mongolian gerbil. *Brain Res Bull* (2003) 60:475–95. doi:10.1016/S0361-9230(03)00051-0
63. Purcell IM, Perachio AA. Peripheral patterns of terminal innervation of vestibular primary afferent neurons projecting to the vestibulocerebellum in the gerbil. *J Comp Neurol* (2001) 433:48–61. doi:10.1002/cne.1124
64. Korte GE. The brainstem projection of the vestibular nerve in the cat. *J Comp Neurol* (1979) 184:279–92. doi:10.1002/cne.901840204
65. Epema AH, Gerrits NM, Voogd J. Commissural and intrinsic connections of the vestibular nuclei in the rabbit: a retrograde labeling study. *Exp Brain Res* (1988) 71:129–46. doi:10.1007/BF00247528
66. Carleton SC, Carpenter MB. Afferent and efferent connections of the medial, inferior and lateral vestibular nuclei in the cat and monkey. *Brain Res* (1983) 278:29–51. doi:10.1016/0006-8993(83)90223-8
67. Dickman JD, Angelaki DE. Vestibular convergence patterns in vestibular nuclei neurons of alert primates. *J Neurophysiol* (2002) 88:3518–33. doi:10.1152/jn.00518.2002
68. Neuhaber WL, Zenker W. Central distribution of cervical primary afferents in the rat, with emphasis on proprioceptive projections to vestibular, perihypoglossal, and upper thoracic spinal nuclei. *J Comp Neurol* (1989) 280:231–53. doi:10.1002/cne.902800206
69. McKelvey-Briggs DK, Saint-Cyr JA, Spence SJ, Partlow GD. A reinvestigation of the spinovestibular projection in the cat using axonal transport techniques. *Anat Embryol* (1989) 180:281–91. doi:10.1007/BF00315886
70. Pompeiano O. Spinovestibular relations: anatomical and physiological aspects. *Prog Brain Res* (1972) 37:263–96. doi:10.1016/S0079-6123(08)63907-2
71. Jian BJ, Acernece AW, Lorenzo J, Card JP, Yates BJ. Afferent pathways to the region of the vestibular nuclei that participates in cardiovascular and respiratory control. *Brain Res* (2005) 1044:241–50. doi:10.1016/j.brainres.2005.03.010
72. Prihoda M, Hiller M-S, Mayr R. Central projections of cervical primary afferent fibers in the guinea pig: an HRP and WGA/HRP tracer study. *J Comp Neurol* (1991) 308:418–31. doi:10.1002/cne.903080309
73. Bankoul S, Goto T, Yates B, Wilson VJ. Cervical primary afferent input to vestibulospinal neurons projecting to the cervical dorsal horn: an anterograde and retrograde tracing study in the cat. *J Comp Neurol* (1995) 353:529–38. doi:10.1002/cne.903530405
74. Sato H, Ohkawa T, Uchino Y, Wilson VJ. Excitatory connections between neurons of the central cervical nucleus and vestibular neurons in the cat. *Exp Brain Res* (1997) 115:381–6. doi:10.1007/PL00005708
75. McCall AA, Miller DM, DeMayo WM, Bourdages GH, Yates BJ. Vestibular nucleus neurons respond to hindlimb movement in the conscious cat. *J Neurophysiol* (2016) 116:1785–94. doi:10.1152/jn.00414.2016
76. Barresi M, Grasso C, Li Volsi G, Manzoni D. Effects of body to head rotation on the labyrinthine responses of rat vestibular neurons. *Neuroscience* (2013) 244:134–46. doi:10.1016/j.neuroscience.2013.04.010
77. Medrea I, Cullen KE. Multisensory integration in early vestibular processing in mice: the encoding of passive versus active motion. *J Neurophysiol* (2013) 110:2704–17. doi:10.1152/jn.01037.2012
78. Arshian MS, Hobson CE, Catanzaro MF, Miller DJ, Puterbaugh SR, Cotter LA, et al. Vestibular nucleus neurons respond to hindlimb movement in the decerebrate cat. *J Neurophysiol* (2014) 111:2423–32. doi:10.1152/jn.00855.2013
79. Kasper J, Schor RH, Wilson VJ. Response of vestibular neurons to head rotations in vertical planes. II. Response to neck stimulation and vestibular-neck interaction. *J Neurophysiol* (1988) 60:1765–78.
80. Sadeghi SG, Mitchell DE, Cullen KE. Different neural strategies for multimodal integration: comparison of two macaque monkey species. *Exp Brain Res* (2009) 195:45–57. doi:10.1007/s00221-009-1751-3
81. Gdowski GT, McCrea RA. Neck proprioceptive inputs to primate vestibular nucleus neurons. *Exp Brain Res* (2000) 135:511–26. doi:10.1007/s002210000542
82. Miller DM, Cotter LA, Gandhi NJ, Schor RH, Cass SP, Huff NO, et al. Responses of caudal vestibular nucleus neurons of conscious cats to rotations in vertical planes, before and after a bilateral vestibular neurectomy. *Exp Brain Res* (2008) 188:175–86. doi:10.1007/s00221-008-1359-z
83. Blazquez PM, Highstein SM. Visual-vestibular interaction in vertical vestibular only neurons. *Neuroreport* (2007) 18:1403–6. doi:10.1097/WNR.0b013e3282cdeed
84. Boyle R, Buttner U, Markert G. Vestibular nuclei activity and eye movements in the alert monkey during sinusoidal optokinetic stimulation. *Exp Brain Res* (1985) 57:362–9. doi:10.1007/BF00236542
85. Reisine H, Raphan T. Neural basis for eye velocity generation in the vestibular nuclei of alert monkeys during off-vertical axis rotation. *Exp Brain Res* (1992) 92:209–26. doi:10.1007/BF00227966
86. Bryan AS, Angelaki DE. Optokinetic and vestibular responsiveness in the macaque rostral vestibular and fastigial nuclei. *J Neurophysiol* (2009) 101:714–20. doi:10.1152/jn.90612.2008
87. Waespe W, Henn V. Neuronal activity in the vestibular nuclei of the alert monkey during vestibular and optokinetic stimulation. *Exp Brain Res* (1977) 27:523–38. doi:10.1007/BF00239041
88. Reynard F, Terrier P. Role of visual input in the control of dynamic balance: variability and instability of gait in treadmill walking while blindfolded. *Exp Brain Res* (2015) 233:1031–40. doi:10.1007/s00221-014-4177-5
89. Raffi M, Piras A, Persiani M, Squatrito S. Importance of optic flow for postural stability of male and female young adults. *Eur J Appl Physiol* (2014) 114:71–83. doi:10.1007/s00421-013-2750-4
90. Joseph Jilk D, Safavynia SA, Ting LH. Contribution of vision to postural behaviors during continuous support-surface translations. *Exp Brain Res* (2014) 232:169–80. doi:10.1007/s00221-013-3729-4
91. Bove M, Fenoglio C, Tacchino A, Pelosin E, Schieppati M. Interaction between vision and neck proprioception in the control of stance. *Neuroscience* (2009) 164:1601–8. doi:10.1016/j.neuroscience.2009.09.053
92. Palm HG, Strobel J, Achatz G, von Luebken F, Friemert B. The role and interaction of visual and auditory afferents in postural stability. *Gait Posture* (2009) 30:328–33. doi:10.1016/j.gaitpost.2009.05.023
93. Mahboobin A, Loughlin PJ, Redfern MS, Sparro PJ. Sensory re-weighting in human postural control during moving-scene perturbations. *Exp Brain Res* (2005) 167:260–7. doi:10.1007/s00221-005-0053-7
94. Bent LR, McFadyen BJ, Inglis JT. Visual-vestibular interactions in postural control during the execution of a dynamic task. *Exp Brain Res* (2002) 146:490–500. doi:10.1007/s00221-002-1204-8
95. Manchester D, Woollacott M, Zederbauer-Hylton N, Marin O. Visual, vestibular and somatosensory contributions to balance control in the older adult. *J Gerontol* (1989) 44:M118–27. doi:10.1093/geronj/44.4.M118
96. Jian BJ, Cotter LA, Emanuel BA, Cass SP, Yates BJ. Effects of bilateral vestibular lesions on orthostatic tolerance in awake cats. *J Appl Physiol* (1999) 86:1552–60.
97. Ito M, Yoshida M, Obata K, Kawai N, Udo M. Inhibitory control of intracerebellar nuclei by the Purkinje cell axons. *Exp Brain Res* (1970) 10:64–80. doi:10.1007/BF00340519
98. Noda H, Sugita S, Ikeda Y. Afferent and efferent connections of the oculomotor region of the fastigial nucleus in the macaque monkey. *J Comp Neurol* (1990) 302:330–48. doi:10.1002/cne.903020211

99. Homma Y, Nonaka S, Matsuyama K, Mori S. Fastigiofugal projection to the brainstem nuclei in the cat: an anterograde PHA-L tracing study. *Neurosci Res* (1995) 23:89–102. doi:10.1016/0168-0102(95)90019-5
100. Asanuma C, Thach WT, Jones EG. Brainstem and spinal projections of the deep cerebellar nuclei in the monkey, with observations on the brainstem projections of the dorsal column nuclei. *Brain Res* (1983) 286:299–322. doi:10.1016/0165-0173(83)90017-6
101. Batton RR, Jayaraman A, Ruggiero D, Carpenter MB. Fastigial efferent projections in the monkey: an autoradiographic study. *J Comp Neurol* (1977) 174:281–306. doi:10.1002/cne.901740206
102. Teune TM, van der Burg J, van der Moer J, Voogd J, Ruigrok TJ. Topography of cerebellar nuclear projections to the brain stem in the rat. *Prog Brain Res* (2000) 124:141–72. doi:10.1016/S0079-6123(00)24014-4
103. Compoint C, Buisseret-Delmas C, Diagne M, Buisseret P, Angaut P. Connections between the cerebellar nucleus interpositus and the vestibular nuclei: an anatomical study in the rat. *Neurosci Lett* (1997) 238:91–4. doi:10.1016/S0304-3940(97)00864-1
104. Gonzalo-Ruiz A, Leichnetz GR. Connections of the caudal cerebellar interpositus complex in a new world monkey (*Cebus apella*). *Brain Res Bull* (1990) 25:919–27. doi:10.1016/0361-9230(90)90189-7
105. Delfini C, Diagne M, Angaut P, Buisseret P, Buisseret-Delmas C. Dentatovestibular projections in the rat. *Exp Brain Res* (2000) 135:285–92. doi:10.1007/s002210000516
106. Barmack NH, Yakhnitsa V. Vestibularly evoked climbing-fiber responses modulate simple spikes in rabbit cerebellar Purkinje neurons. *Ann NY Acad Sci* (2002) 978:237–54. doi:10.1111/j.1749-6632.2002.tb07571.x
107. Barmack NH, Qian Z, Yoshimura J. Regional and cellular distribution of protein kinase C in rat cerebellar Purkinje cells. *J Comp Neurol* (2000) 427:235–54. doi:10.1002/1096-9861(20001113)427:2<235::AID-CNE6>3.0.CO;2-6
108. Umetani T. Efferent projections from the flocculus in the albino rat as revealed by an autoradiographic orthograde tracing method. *Brain Res* (1992) 586:91–103. doi:10.1016/0006-8993(92)91376-P
109. Balaban CD, Schuerger RJ, Porter JD. Zonal organization of flocculo-vestibular connections in rats. *Neuroscience* (2000) 99:669–82. doi:10.1016/S0306-4522(00)00232-3
110. Langer T, Fuchs AF, Chubb MC, Scudder CA, Lisberger SG. Floccular efferents in the rhesus macaque as revealed by autoradiography and horseradish peroxidase. *J Comp Neurol* (1985) 235:26–37. doi:10.1002/cne.902350103
111. Wylie DR, De Zeeuw CI, DiGiorgi PL, Simpson JI. Projections of individual Purkinje cells of identified zones in the ventral nodulus to the vestibular and cerebellar nuclei in the rabbit. *J Comp Neurol* (1994) 349:448–63. doi:10.1002/cne.903490309
112. Shojaku H, Sato Y, Ikarashi K, Kawasaki T. Topographical distribution of Purkinje cells in the uvula and the nodulus projecting to the vestibular nuclei in cats. *Brain Res* (1987) 416:100–12. doi:10.1016/0006-8993(87)91501-0
113. Walberg F, Dietrichs E. The interconnection between the vestibular nuclei and the nodulus: a study of reciprocity. *Brain Res* (1988) 449:47–53. doi:10.1016/0006-8993(88)91022-0
114. Barmack NH. Central vestibular system: vestibular nuclei and posterior cerebellum. *Brain Res Bull* (2003) 60:511–41. doi:10.1016/S0361-9230(03)00055-8
115. Wilson VJ, Zarzecki P, Schor RH, Isu N, Rose PK, Sato H, et al. Cortical influences on the vestibular nuclei of the cat. *Exp Brain Res* (1999) 125:1–13. doi:10.1007/s002210050651
116. Troiani D, Draicchio F, Bonci A, Zannoni B. Responses of vestibular neurons to stimulation of cortical sensorimotor areas in the cat. *Arch Ital Biol* (1993) 131:137–46.
117. Pogossian VI, Fanardjian VV. Organization of afferent projections to the ventral and dorsal regions of the cat lateral vestibular nucleus: an HRP study. *J Vestib Res* (1992) 2:107–22.
118. Nishiike S, Guldin WO, Baurle J. Corticofugal connections between the cerebral cortex and the vestibular nuclei in the rat. *J Comp Neurol* (2000) 420:363–72. doi:10.1002/(SICI)1096-9861(20000508)420:3<363::AID-CNE7>3.3.CO;2-O
119. Akbarian S, Grusser OJ, Guldin WO. Corticofugal projections to the vestibular nuclei in squirrel monkeys – further evidence of multiple cortical vestibular fields. *J Comp Neurol* (1993) 332:89–104. doi:10.1002/cne.903320107
120. Akbarian S, Grusser OJ, Guldin WO. Corticofugal connections between the cerebral cortex and brainstem vestibular nuclei in the macaque monkey. *J Comp Neurol* (1994) 339:421–37. doi:10.1002/cne.903390309
121. Fukushima K. Corticovestibular interactions: anatomy, electrophysiology, and functional considerations. *Exp Brain Res* (1997) 117:1–16. doi:10.1007/PL000005786
122. Guldin WO, Mirring S, Grusser OJ. Connections from the neocortex to the vestibular brain stem nuclei in the common marmoset. *Neuroreport* (1993) 5:113–6. doi:10.1097/00001756-199311180-00004
123. Abzug C, Peterson BW. Antidromic stimulation in the ponto-medullary reticular formation of local axon branches of contralateral vestibular neurons. *Brain Res* (1973) 64:407–13. doi:10.1016/0006-8993(73)90196-0
124. Fields HL, Clanton CH, Anderson SD. Somatosensory properties of spinoreticular neurons in the cat. *Brain Res* (1977) 120:49–66. doi:10.1016/0006-8993(77)90497-8
125. Maunz RA, Pitts NG, Peterson BW. Cat spinoreticular neurons: locations, responses and changes in responses during repetitive stimulation. *Brain Res* (1978) 148:365–79. doi:10.1016/0006-8993(78)90725-4
126. Kevetter GA, Haber LH, Yezierski RP, Chung JM, Martin RF, Willis WD. Cells of origin of the spinoreticular tract in the monkey. *J Comp Neurol* (1982) 207:61–74. doi:10.1002/cne.902070106
127. Chapman CD, Ammons WS, Foreman RD. Raphe magnus inhibition of feline T1-Tr spinoreticular tract cell responses to visceral and somatic inputs. *J Neurophysiol* (1985) 53:773–85.
128. Casey KL. Somatic stimuli, spinal pathways, and size of cutaneous fibers influencing unit activity in the medial medullary reticular formation. *Exp Neurol* (1969) 25:35–56. doi:10.1016/0014-4886(69)90070-3
129. Peterson BW, Anderson ME, Filion M. Responses of pontomedullary reticular neurons to cortical, tectal and cutaneous stimuli. *Exp Brain Res* (1974) 21:19–44. doi:10.1007/BF00234256
130. Peterson BW, Franck JL, Daunton NG. Changes in responses of medial pontomedullary reticular neurons during repetitive cutaneous, vestibular, cortical, and tectal stimulation. *J Neurophysiol* (1976) 39:564–81.
131. Drew T, Cabana T, Rossignol S. Responses of medullary reticulospinal neurons to stimulation of cutaneous limb nerves during locomotion in intact cats. *Exp Brain Res* (1996) 111:153–68. doi:10.1007/BF00227294
132. Pompeiano O, Barnes CD. Response of brain stem reticular neurons to muscle vibration in the decerebrate cat. *J Neurophysiol* (1971) 24:709–24.
133. Keizer K, Kuypers HG. Distribution of corticospinal neurons with collaterals to lower brain stem reticular formation in cat. *Exp Brain Res* (1984) 54:107–20. doi:10.1007/BF00235823
134. Keizer K, Kuypers HG. Distribution of corticospinal neurons with collaterals to the lower brain stem reticular formation in monkey (*Macaca fascicularis*). *Exp Brain Res* (1989) 74:311–8. doi:10.1007/BF00248864
135. Berrevoets CE, Kuypers HG. Pericruciate cortical neurons projecting to brain stem reticular formation, dorsal column nuclei and spinal cord in the cat. *Neurosci Lett* (1975) 1:257–62. doi:10.1016/0304-3940(75)90040-3
136. Matsuyama K, Drew T. Organization of the projections from the pericruciate cortex to the pontomedullary brainstem of the cat: a study using the anterograde tracer *Phaseolus vulgaris-leucoagglutinin*. *J Comp Neurol* (1997) 389:617–41. doi:10.1002/(SICI)1096-9861(19971229)389:4<617::AID-CNE6>3.0.CO;2-3
137. Rho MJ, Cabana T, Drew T. Organization of the projections from the pericruciate cortex to the pontomedullary reticular formation of the cat: a quantitative retrograde tracing study. *J Comp Neurol* (1997) 388:228–49. doi:10.1002/(SICI)1096-9861(19971117)388:2<228::AID-CNE4>3.0.CO;2-3
138. Kably B, Drew T. Corticoreticular pathways in the cat. I. Projection patterns and collateralization. *J Neurophysiol* (1998) 80:389–405.
139. Canedo A, Lamas JA. Pyramidal and corticospinal synaptic effects over reticulospinal neurones in the cat. *J Physiol* (1993) 463:475–89. doi:10.1113/jphysiol.1993.sp019606
140. Magni F, Willis WD. Cortical control of brain stem reticular neurons. *Arch Ital Biol* (1964) 102:418–33.
141. Eccles JC, Nicoll RA, Schwarz WF, Taborikova H, Willey TJ. Reticulospinal neurons with and without monosynaptic inputs from cerebellar nuclei. *J Neurophysiol* (1975) 38:513–30.
142. Takahashi M, Sugiuchi Y, Shinoda Y. Convergent synaptic inputs from the caudal fastigial nucleus and the superior colliculus onto pontine and

- pontomedullary reticulospinal neurons. *J Neurophysiol* (2014) 111:849–67. doi:10.1152/jn.00634.2013
143. Matsuyama K, Jankowska E. Coupling between feline cerebellum (fastigial neurons) and motoneurons innervating hindlimb muscles. *J Neurophysiol* (2004) 91:1183–92. doi:10.1152/jn.00896.2003
 144. Yeomans JS, Frankland PW. The acoustic startle reflex: neurons and connections. *Brain Res Brain Res Rev* (1995) 21:301–14. doi:10.1016/0165-0173(96)00004-5
 145. Lingenhohl K, Friauf E. Giant neurons in the rat reticular formation: a sensorimotor interface in the elementary acoustic startle circuit? *J Neurosci* (1994) 14:1176–94.
 146. Davis M, Gendelman DS, Tischler MD, Gendelman PM. A primary acoustic startle circuit: lesion and stimulation studies. *J Neurosci* (1982) 2:791–805.
 147. Lingenhohl K, Friauf E. Giant neurons in the caudal pontine reticular formation receive short latency acoustic input: an intracellular recording and HRP-study in the rat. *J Comp Neurol* (1992) 325:473–92. doi:10.1002/cne.903250403
 148. Nodal FR, Lopez DE. Direct input from cochlear root neurons to pontine reticulospinal neurons in albino rat. *J Comp Neurol* (2003) 460:80–93. doi:10.1002/cne.10656
 149. Li L, Steidl S, Yeomans JS. Contributions of the vestibular nucleus and vestibulospinal tract to the startle reflex. *Neuroscience* (2001) 106:811–21. doi:10.1016/S0306-4522(01)00324-4
 150. Steidl S, Faerman P, Li L, Yeomans JS. Kynurenone in the pontine reticular formation inhibits acoustic and trigeminal nucleus-evoked startle, but not vestibular nucleus-evoked startle. *Neuroscience* (2004) 126:127–36. doi:10.1016/j.neuroscience.2004.03.020
 151. Shik M, Severin F, Orlovskii G. [Control of walking and running by means of electric stimulation of the midbrain]. *Biofizika* (1966) 11:659–66.
 152. Ryczko D, Dubuc R. The multifunctional mesencephalic locomotor region. *Curr Pharm Des* (2013) 19:4448–70. doi:10.2174/1381612811319240011
 153. Orlovskii GN. [Work of reticulo-spinal neurons during locomotion]. *Biofizika* (1970) 15:728–37.
 154. Garcia-Rill E, Skinner RD. The mesencephalic locomotor region. II. Projections to reticulospinal neurons. *Brain Res* (1987) 411:13–20. doi:10.1016/0006-8993(87)90676-7
 155. Shefchyk SJ, Jordan LM. Excitatory and inhibitory postsynaptic potentials in alpha-motoneurons produced during fictive locomotion by stimulation of the mesencephalic locomotor region. *J Neurophysiol* (1985) 53: 1345–55.
 156. Noga BR, Kriellaars DJ, Brownstone RM, Jordan LM. Mechanism for activation of locomotor centers in the spinal cord by stimulation of the mesencephalic locomotor region. *J Neurophysiol* (2003) 90:1464–78. doi:10.1152/jn.00034.2003
 157. Pompeiano O, Wand P, Srivastava UC. Responses of Renshaw cells coupled with hindlimb extensor motoneurons to sinusoidal stimulation of labyrinth receptors in the decerebrate cat. *Pflugers Arch* (1985) 403:245–57. doi:10.1007/BF00583595
 158. Ross HG, Thewissen M. Inhibitory connections of ipsilateral semicircular canal afferents onto Renshaw cells in the lumbar spinal cord of the cat. *J Physiol* (1987) 388:83–99. doi:10.1113/jphysiol.1987.sp016603
 159. Jankowska E, Krutki P, Matsuyama K. Relative contribution of Ia inhibitory interneurones to inhibition of feline contralateral motoneurones evoked via commissural interneurones. *J Physiol* (2005) 568:617–28. doi:10.1113/jphysiol.2005.088351
 160. Hultborn H, Illert M, Santini M. Convergence on interneurones mediating the reciprocal Ia inhibition of motoneurones. III. Effects from supraspinal pathways. *Acta Physiol Scand* (1976) 96:368–91. doi:10.1111/j.1748-1716.1976.tb10188.x
 161. Anker AR, Sadacca BF, Yates BJ. Vestibular inputs to propriospinal interneurons in the feline C1-C2 spinal cord projecting to the C5-C6 ventral horn. *Exp Brain Res* (2006) 170:39–51. doi:10.1007/s00221-005-0186-8
 162. Alstermark B, Lundberg A, Pinter M, Sasaki S. Subpopulations and functions of long C3-C5 propriospinal neurones. *Brain Res* (1987) 404:395–400. doi:10.1016/0006-8993(87)91400-4
 163. Skinner RD, Remmel RS, Minor LB. Monosynaptic activation of long descending propriospinal neurons from the lateral vestibular nucleus and the medial longitudinal fasciculus. *Exp Neurol* (1984) 86:462–72. doi:10.1016/0014-4886(84)90081-5
 164. Bolton PS, Goto T, Wilson VJ. Commissural neurons in the cat upper cervical spinal cord. *Neuroreport* (1991) 2:743–6. doi:10.1097/00001756-199112000-00003
 165. Krutki P, Jankowska E, Edgley SA. Are crossed actions of reticulospinal and vestibulospinal neurons on feline motoneurons mediated by the same or separate commissural neurons? *J Neurosci* (2003) 23:8041–50.
 166. Kasumacic N, Lambert FM, Coulon P, Bras H, Vinay L, Perreault MC, et al. Segmental organization of vestibulospinal inputs to spinal interneurons mediating crossed activation of thoracolumbar motoneurons in the neonatal mouse. *J Neurosci* (2015) 35:8158–69. doi:10.1523/JNEUROSCI.5188-14.2015
 167. Wilson VJ. Convergence of neck and vestibular signals on spinal interneurons. *Prog Brain Res* (1988) 76:137–43. doi:10.1016/S0079-6123(08)64499-4
 168. Schor RH, Suzuki I, Timerick SJ, Wilson VJ. Responses of interneurons in the cat cervical cord to vestibular tilt stimulation. *J Neurophysiol* (1986) 56:1147–56.
 169. Suzuki I, Timerick SJ, Wilson VJ. Body position with respect to the head or body position in space is coded by lumbar interneurons. *J Neurophysiol* (1985) 54:123–33.
 170. Brown AG, Fyffe RE. The morphology of group Ia afferent fibre collaterals in the spinal cord of the cat. *J Physiol* (1978) 274:111–27. doi:10.1113/jphysiol.1978.sp012137
 171. Fyffe RE. The morphology of group II muscle afferent fibre collaterals. *J Physiol* (1979) 296:39–40.
 172. Kuypers HGJM. Anatomy of the descending pathways. In: Brookhart JM, Mountcastle VB, editors. *Handbook of Physiology. Section 1: The Nervous System, Volume II, Motor Control, Part 1*. Bethesda: American Physiological Society (1981). p. 597–666. doi:10.1002/cphy.cp010213
 173. Gottschall JS, Nichols TR. Head pitch affects muscle activity in the decerebrate cat hindlimb during walking. *Exp Brain Res* (2007) 182:131–5. doi:10.1007/s00221-007-1084-z
 174. Gottschall JS, Nichols TR. Neuromuscular strategies for the transitions between level and hill surfaces during walking. *Philos Trans R Soc Lond B Biol Sci* (2011) 366:1565–79. doi:10.1098/rstb.2010.0355
 175. Honeycutt CF, Gottschall JS, Nichols TR. Electromyographic responses from the hindlimb muscles of the decerebrate cat to horizontal support surface perturbations. *J Neurophysiol* (2009) 101:2751–61. doi:10.1152/jn.91040.2008
 176. Carli G, Dietsche-Spiff K, Pompeiano O. Responses of the muscle spindles and of the extrafusal fibres in an extensor muscle to stimulation of the lateral vestibular nucleus in the cat. *Arch Ital Biol* (1967) 105:209–42.
 177. Dietsche-Spiff K, Carli G, Pompeiano O. Comparison of the effects of stimulation of the 8th cranial nerve, the vestibular nuclei or the reticular formation on the gastrocnemius muscle and its spindles. *Arch Ital Biol* (1967) 105: 243–72.
 178. Pompeiano O, Dietsche-Spiff K, Carli G. Two pathways transmitting vestibulospinal influences from the lateral vestibular nucleus of Deiters to extensor fusimotor neurones. *Pflugers Arch Gesamte Physiol Menschen Tiere* (1967) 293:272–5. doi:10.1007/BF00417124
 179. Kasper J, Wilson VJ, Yamagata Y, Yates BJ. Neck muscle spindle activity in the decerebrate, unparalyzed cat: dynamics and influence of vestibular stimulation. *J Neurophysiol* (1989) 62:917–23.
 180. Bent LR, Bolton PS, Macefield VG. Vestibular inputs do not influence the fusimotor system in relaxed muscles of the human leg. *Exp Brain Res* (2007) 180:97–103. doi:10.1007/s00221-006-0836-5
 181. Knellwolf TP, Hammam E, Macefield VG. The vestibular system does not modulate fusimotor drive to muscle spindles in relaxed leg muscles of subjects in a near-vertical position. *J Neurophysiol* (2016) 115:2529–35. doi:10.1152/jn.01125.2015
 182. Kerman IA, Yates BJ. Regional and functional differences in the distribution of vestibulosympathetic reflexes. *Am J Physiol* (1998) 275:R824–35.
 183. Yates BJ, Yamagata Y, Bolton PS. The ventrolateral medulla of the cat mediates vestibulosympathetic reflexes. *Brain Res* (1991) 552:265–72. doi:10.1016/0006-8993(91)90091-9
 184. DeStefino VJ, Reighard DA, Sugiyama Y, Suzuki T, Cotter LA, Larson MG, et al. Responses of neurons in the rostral ventrolateral medulla to whole body rotations: comparisons in decerebrate and conscious cats. *J Appl Physiol* (2011) 110:1699–707. doi:10.1152/japplphysiol.00180.2011

185. Lovick TA. The periaqueductal gray-rostral medulla connection in the defence reaction: efferent pathways and descending control mechanisms. *Behav Brain Res* (1993) 58:19–25. doi:10.1016/0166-4328(93)90087-7
186. Felder RB, Mifflin SW. Modulation of carotid sinus afferent input to nucleus tractus solitarius by parabrachial nucleus stimulation. *Circ Res* (1988) 63:35–49. doi:10.1161/01.RES.63.1.35
187. Hamilton RB, Ellenberger H, Liskowsky D, Schneiderman N. Parabrachial area as mediator of bradycardia in rabbits. *J Auton Nerv Syst* (1981) 4:261–81. doi:10.1016/0165-1838(81)90049-7
188. Herbert H, Moga MM, Saper CB. Connections of the parabrachial nucleus with the nucleus of the solitary tract and the medullary reticular formation in the rat. *J Comp Neurol* (1990) 293:540–80. doi:10.1002/cne.902930404
189. Krukoff TL, Harris KH, Jhamandas JH. Efferent projections from the parabrachial nucleus demonstrated with the anterograde tracer *Phaseolus vulgaris* leucoagglutinin. *Brain Res Bull* (1993) 30:163–72. doi:10.1016/0361-9230(93)90054-F
190. Mifflin SW, Felder RB. Synaptic mechanisms regulating cardiovascular afferent inputs to solitary tract nucleus. *Am J Physiol* (1990) 259:H653–61.
191. Mraovitch S, Kumada M, Reis DJ. Role of the nucleus parabrachialis in cardiovascular regulation in cat. *Brain Res* (1982) 232:57–75. doi:10.1016/0006-8993(82)90610-2
192. Paton JF, Silva-Carvalho L, Thompson CS, Spyre KM. Nucleus tractus solitarius as mediator of evoked parabrachial cardiovascular responses in the decerebrate rabbit. *J Physiol* (1990) 428:693–705. doi:10.1113/jphysiol.1990.sp018235
193. Saper CB, Loewy AD. Efferent connections of the parabrachial nucleus in the rat. *Brain Res* (1980) 197:291–317. doi:10.1016/0006-8993(80)91117-8
194. Sapru HN. Role of the hypothalamic arcuate nucleus in cardiovascular regulation. *Auton Neurosci* (2013) 175:38–50. doi:10.1016/j.autneu.2012.10.016
195. Bowman BR, Kumar NN, Hassan SF, McMullan S, Goodchild AK. Brain sources of inhibitory input to the rat rostral ventrolateral medulla. *J Comp Neurol* (2013) 521:213–32. doi:10.1002/cne.23175
196. Kawabe T, Chitravanshi VC, Kawabe K, Sapru HN. Cardiovascular function of a glutamatergic projection from the hypothalamic paraventricular nucleus to the nucleus tractus solitarius in the rat. *Neuroscience* (2008) 153:605–17. doi:10.1016/j.neuroscience.2008.02.076
197. Horiuchi J, McDowall LM, Dampney RA. Differential control of cardiac and sympathetic vasomotor activity from the dorsomedial hypothalamus. *Clin Exp Pharmacol Physiol* (2006) 33:1265–8. doi:10.1111/j.1440-1681.2006.04522.x
198. Cravo SL, Possas OS, Ferreira-Neto ML. Rostral ventrolateral medulla: an integrative site for muscle vasodilation during defense-alerting reactions. *Cell Mol Neurobiol* (2003) 23:579–95. doi:10.1023/A:1025076130854
199. Fontes MA, Tagawa T, Polson JW, Cavanagh SJ, Dampney RA. Descending pathways mediating cardiovascular response from dorsomedial hypothalamic nucleus. *Am J Physiol Heart Circ Physiol* (2001) 280:H2891–901.
200. Coote JH, Yang Z, Pyner S, Deering J. Control of sympathetic outflows by the hypothalamic paraventricular nucleus. *Clin Exp Pharmacol Physiol* (1998) 25:461–3. doi:10.1111/j.1440-1681.1998.tb02235.x
201. Badoer E. Neurons in the hypothalamic paraventricular nucleus that project to the rostral ventrolateral medulla are not activated by hypotension. *Brain Res* (1998) 801:224–7. doi:10.1016/S0006-8993(98)00560-5
202. Kawano H, Masuko S. Substance P innervation of neurons projecting to the paraventricular hypothalamic nucleus in the rat nucleus tractus solitarius. *Brain Res* (1995) 689:136–40. doi:10.1016/0006-8993(95)00501-G
203. Martin DS, Haywood JR. Hemodynamic responses to paraventricular nucleus disinhibition with bicuculline in conscious rats. *Am J Physiol* (1993) 265:H1727–33.
204. Ebihara H, Kawasaki H, Nakamura S, Takasaki K, Wada A. Pressor response to microinjection of clonidine into the hypothalamic paraventricular nucleus in conscious rats. *Brain Res* (1993) 624:44–52. doi:10.1016/0006-8993(93)90058-U
205. Martin DS, Haywood JR. Sympathetic nervous system activation by glutamate injections into the paraventricular nucleus. *Brain Res* (1992) 577:261–7. doi:10.1016/0006-8993(92)90282-E
206. Cechetto DF, Chen SJ. Hypothalamic and cortical sympathetic responses relay in the medulla of the rat. *Am J Physiol* (1992) 263:R544–52.
207. Allen GV, Cechetto DF. Functional and anatomical organization of cardiovascular pressor and depressor sites in the lateral hypothalamic area: I. Descending projections. *J Comp Neurol* (1992) 315:313–32. doi:10.1002/cne.903150307
208. Markgraf CG, Winters RW, Liskowsky DR, McCabe PM, Green EJ, Schneiderman N. Hypothalamic, midbrain and bulbar areas involved in the defense reaction in rabbits. *Physiol Behav* (1991) 49:493–500. doi:10.1016/0031-9384(91)90270-X
209. Wible JH Jr, Luft FC, DiMicco JA. Hypothalamic GABA suppresses sympathetic outflow to the cardiovascular system. *Am J Physiol* (1988) 254:R680–7.
210. Mifflin SW, Spyre KM, Withington-Wray DJ. Baroreceptor inputs to the nucleus tractus solitarius in the cat: modulation by the hypothalamus. *J Physiol* (1988) 399:369–87. doi:10.1113/jphysiol.1988.sp017085
211. Jordan D, Mifflin SW, Spyre KM. Hypothalamic inhibition of neurones in the nucleus tractus solitarius of the cat is GABA mediated. *J Physiol* (1988) 399:389–404. doi:10.1113/jphysiol.1988.sp017087
212. van der Kooy D, Koda LY, McGinty JF, Gerfen CR, Bloom FE. The organization of projections from the cortex, amygdala, and hypothalamus to the nucleus of the solitary tract in rat. *J Comp Neurol* (1984) 224:1–24. doi:10.1002/cne.902240102
213. Kannan H, Yamashita H. Electrophysiological study of paraventricular nucleus neurons projecting to the dorsomedial medulla and their response to baroreceptor stimulation in rats. *Brain Res* (1983) 279:31–40. doi:10.1016/0006-8993(83)90160-9
214. Berk ML, Finkelstein JA. Efferent connections of the lateral hypothalamic area of the rat: an autoradiographic investigation. *Brain Res Bull* (1982) 8:511–26. doi:10.1016/0361-9230(82)90009-0
215. Ross CA, Ruggiero DA, Reis DJ. Afferent projections to cardiovascular portions of the nucleus of the tractus solitarius in the rat. *Brain Res* (1981) 223:402–8. doi:10.1016/0006-8993(81)91155-0
216. Saha S, Drinkhill MJ, Moore JP, Batten TF. Central nucleus of amygdala projections to rostral ventrolateral medulla neurones activated by decreased blood pressure. *Eur J Neurosci* (2005) 21:1921–30. doi:10.1111/j.1460-9568.2005.04023.x
217. Saha S. Role of the central nucleus of the amygdala in the control of blood pressure: descending pathways to medullary cardiovascular nuclei. *Clin Exp Pharmacol Physiol* (2005) 32:450–6. doi:10.1111/j.1440-1681.2005.04210.x
218. Schwaber JS, Kapp BS, Higgins GA, Rapp PR. Amygdaloid and basal forebrain direct connections with the nucleus of the solitary tract and the dorsal motor nucleus. *J Neurosci* (1982) 2:1424–38.
219. Kapp BS, Gallagher M, Underwood MD, McNall CL, Whitehorn D. Cardiovascular responses elicited by electrical stimulation of the amygdala central nucleus in the rabbit. *Brain Res* (1982) 234:251–62. doi:10.1016/0006-8993(82)90866-6
220. Verberne AJ, Owens NC. Cortical modulation of the cardiovascular system. *Prog Neurobiol* (1998) 54:149–68. doi:10.1016/S0301-0082(97)00056-7
221. Cechetto DF, Chen SJ. Subcortical sites mediating sympathetic responses from insular cortex in rats. *Am J Physiol* (1990) 258:R245–55.
222. Shipley MT. Insular cortex projection to the nucleus of the solitary tract and brainstem visceromotor regions in the mouse. *Brain Res Bull* (1982) 8:139–48. doi:10.1016/0361-9230(82)90040-5
223. Sevoz-Couche C, Comet MA, Bernard JF, Hamon M, Laguzzi R. Cardiac baroreflex facilitation evoked by hypothalamus and prefrontal cortex stimulation: role of the nucleus tractus solitarius 5-HT2A receptors. *Am J Physiol Regul Integr Comp Physiol* (2006) 291:R1007–15. doi:10.1152/ajpregu.00052.2006
224. Gabbott PL, Warner TA, Jays PR, Salway P, Busby SJ. Prefrontal cortex in the rat: projections to subcortical autonomic, motor, and limbic centers. *J Comp Neurol* (2005) 492:145–77. doi:10.1002/cne.20738
225. Owens NC, Verberne AJ. Medial prefrontal depressor response: involvement of the rostral and caudal ventrolateral medulla in the rat. *J Auton Nerv Syst* (2000) 78:86–93. doi:10.1016/S0165-1838(99)00062-4
226. Boyle R. Activity of medial vestibulospinal tract cells during rotation and ocular movement in the alert squirrel monkey. *J Neurophysiol* (1993) 70:2176–80.

227. Gdowski GT, McCrea RA. Integration of vestibular and head movement signals in the vestibular nuclei during whole-body rotation. *J Neurophysiol* (1999) 82:436–49.
228. Cullen KE, Roy JE. Signal processing in the vestibular system during active versus passive head movements. *J Neurophysiol* (2004) 91:1919–33. doi:10.1152/jn.00988.2003
229. McCrea RA, Gdowski GT, Boyle R, Belton T. Firing behavior of vestibular neurons during active and passive head movements: vestibulo-spinal and other non-eye-movement related neurons. *J Neurophysiol* (1999) 82: 416–28.
230. Cullen KE, Minor LB. Semicircular canal afferents similarly encode active and passive head-on-body rotations: implications for the role of vestibular efference. *J Neurosci* (2002) 22:RC226.
231. Roy JE, Cullen KE. Selective processing of vestibular reafference during self-generated head motion. *J Neurosci* (2001) 21:2131–42.
232. Roy JE, Cullen KE. Dissociating self-generated from passively applied head motion: neural mechanisms in the vestibular nuclei. *J Neurosci* (2004) 24:2102–11. doi:10.1523/JNEUROSCI.3988-03.2004
233. Brooks JX, Cullen KE. The primate cerebellum selectively encodes unexpected self-motion. *Curr Biol* (2013) 23:947–55. doi:10.1016/j.cub.2013.04.029
234. Brooks JX, Cullen KE. Early vestibular processing does not discriminate active from passive self-motion if there is a discrepancy between predicted and actual proprioceptive feedback. *J Neurophysiol* (2014) 111:2465–78. doi:10.1152/jn.00600.2013
235. Pompeiano O. The vestibulo-ocular and the vestibulospinal reflexes: noradrenergic influences on the plastic changes which affect the cerebellar cortex during vestibular adaptation. *Arch Ital Biol* (2006) 144:197–253.
236. Lund S, Pompeiano O. Monosynaptic excitation of alpha motoneurons from supraspinal structures in the cat. *Acta Physiol Scand* (1968) 73:1–21. doi:10.1111/j.1748-1716.1968.tb04075.x
237. Llinás R. Mechanisms of supraspinal actions upon spinal cord activities. differences between reticular and cerebellar inhibitory actions upon alpha extensor motoneurons. *J Neurophysiol* (1964) 27:1117–26.
238. McCall AA, Moy JD, Puterbaugh SR, DeMayo WM, Yates BJ. Responses of vestibular nucleus neurons to inputs from the hindlimb are enhanced following a bilateral labyrinthectomy. *J Appl Physiol* (2013) 114:742–51. doi:10.1152/japplphysiol.01389.2012
239. Jian BJ, Shintani T, Emanuel BA, Yates BJ. Convergence of limb, visceral, and vertical semicircular canal or otolith inputs onto vestibular nucleus neurons. *Exp Brain Res* (2002) 144:247–57. doi:10.1007/s00221-002-1042-8
240. Miller DM, DeMayo WM, Bourdages GH, Wittman S, Yates BJ, McCall AA. Neurons in the pontomedullary reticular formation receive converging inputs from the hindlimb and labyrinth. *Exp Brain Res* (2017) 235:1195–1207. doi:10.1007/s00221-017-4875-x
241. Wissel J, Manack A, Brainin M. Toward an epidemiology of poststroke spasticity. *Neurology* (2013) 80:S13–9. doi:10.1212/WNL.0b013e3182762448
242. Urban PP, Wolf T, Uebel M, Marx JJ, Vogt T, Stoeter P, et al. Occurrence and clinical predictors of spasticity after ischemic stroke. *Stroke* (2010) 41:2016–20. doi:10.1161/STROKEAHA.110.581991
243. Lance JW. Disordered muscle tone and movement. *Clin Exp Neurol* (1981) 18:27–35.
244. Katz RT, Rymer WZ. Spastic hypertonia: mechanisms and measurement. *Arch Phys Med Rehabil* (1989) 70:144–55.
245. Denny-Brown D. The nature of dystonia. *Bull N Y Acad Med* (1965) 41: 858–69.
246. Burke D. Spasticity as an adaptation to pyramidal tract injury. *Adv Neurol* (1988) 47:401–23.
247. Burke D, Knowles L, Andrews C, Ashby P. Spasticity, decerebrate rigidity and the clasp-knife phenomenon: an experimental study in the cat. *Brain* (1972) 95:31–48. doi:10.1093/brain/95.1.31
248. Miller DM, Klein CS, Suresh NL, Rymer WZ. Asymmetries in vestibular evoked myogenic potentials in chronic stroke survivors with spastic hypertonia: evidence for a vestibulospinal role. *Clin Neurophysiol* (2014) 125:2070–8. doi:10.1016/j.clinph.2014.01.035
249. Wilson TD, Cotter LA, Draper JA, Misra SP, Rice CD, Cass SP, et al. Vestibular inputs elicit patterned changes in limb blood flow in conscious cats. *J Physiol* (2006) 575:671–84. doi:10.1113/jphysiol.2006.112904
250. Yavorcik KJ, Reighard DA, Misra SP, Cotter LA, Cass SP, Wilson TD, et al. Effects of postural changes and removal of vestibular inputs on blood flow to and from the hindlimb of conscious felines. *Am J Physiol Regul Integr Comp Physiol* (2009) 297:R1777–84. doi:10.1152/ajpregu.00551.2009
251. Barman SM, Sugiyama Y, Suzuki T, Cotter LA, DeStefino VJ, Reighard DA, et al. Rhythmic activity of neurons in the rostral ventrolateral medulla of conscious cats: effect of removal of vestibular inputs. *Am J Physiol Regul Integr Comp Physiol* (2011) 301:R937–46. doi:10.1152/ajpregu.00265.2011
252. Fadel PJ, Raven PB. Human investigations into the arterial and cardiopulmonary baroreflexes during exercise. *Exp Physiol* (2012) 97:39–50. doi:10.1113/expphysiol.2011.057554
253. Waldrop TG, Eldridge FL, Iwamoto GA, Mitchell JH. Central neural control of respiration and circulation during exercise. In: Rowell LB, Shepherd JT, editors. *Handbook of Physiology, Section 12, Exercise: Regulation and Integration of Multiple Systems*. New York: Oxford University Press (1996). p. 333–80. doi:10.1002/cphy.cp120109
254. Goodwin GM, McCloskey DI, Mitchell JH. Cardiovascular and respiratory responses to changes in central command during isometric exercise at constant muscle tension. *J Physiol* (1972) 226:173–90. doi:10.1113/jphysiol.1972.sp009979
255. Gandevia SC, Killian K, McKenzie DK, Crawford M, Allen GM, Gorman RB, et al. Respiratory sensations, cardiovascular control, kinaesthesia and transcranial stimulation during paralysis in humans. *J Physiol* (1993) 470:85–107. doi:10.1113/jphysiol.1993.sp019849
256. Matsukawa K. Central command: control of cardiac sympathetic and vagal efferent nerve activity and the arterial baroreflex during spontaneous motor behaviour in animals. *Exp Physiol* (2012) 97:20–8. doi:10.1113/expphysiol.2011.057661
257. Nakamoto T, Matsukawa K, Liang N, Wakasugi R, Wilson LB, Horiuchi J. Coactivation of renal sympathetic neurons and somatic motor neurons by chemical stimulation of the midbrain ventral tegmental area. *J Appl Physiol* (2011) 110:1342–53. doi:10.1152/japplphysiol.01233.2010

Conflict of Interest Statement: The authors have no conflicts of interest to declare related to this manuscript. No third-party payments were received related to the contents, and the authors have no financial interests that influenced the writing of the article.

Copyright © 2017 McCall, Miller and Yates. This is an open-access article distributed under the terms of the Creative Commons Attribution License (CC BY). The use, distribution or reproduction in other forums is permitted, provided the original author(s) or licensor are credited and that the original publication in this journal is cited, in accordance with accepted academic practice. No use, distribution or reproduction is permitted which does not comply with these terms.



Coding of Velocity Storage in the Vestibular Nuclei

Sergei B. Yakushin^{1*}, Theodore Raphan² and Bernard Cohen¹

¹Department of Neurology, Icahn School of Medicine at Mount Sinai, New York, NY, United States, ²Department of Computer and Information Science, Brooklyn College (CUNY), Brooklyn, NY, United States

OPEN ACCESS

Edited by:

Stefano Ramat,
University of Pavia, Italy

Reviewed by:

Christopher Bockisch,
University of Zurich, Switzerland
Aasef G. Shaikh,
Case Western Reserve University,
United States
Suzanne A. E. Nooij,
Max Planck Society (MPG),
Germany

*Correspondence:

Sergei B. Yakushin
sergei.yakushin@mssm.edu

Specialty section:

This article was submitted
to Neuro-Otology,
a section of the journal
Frontiers in Neurology

Received: 02 March 2017

Accepted: 20 July 2017

Published: 16 August 2017

Citation:

Yakushin SB, Raphan T and Cohen B (2017) Coding of Velocity Storage in the Vestibular Nuclei. *Front. Neurol.* 8:386.
doi: 10.3389/fneur.2017.00386

Semicircular canal afferents sense angular acceleration and output angular velocity with a short time constant of ≈ 4.5 s. This output is prolonged by a central integrative network, velocity storage that lengthens the time constants of eye velocity. This mechanism utilizes canal, otolith, and visual (optokinetic) information to align the axis of eye velocity toward the spatial vertical when head orientation is off-vertical axis. Previous studies indicated that vestibular-only (VO) and vestibular-pause-saccade (VPS) neurons located in the medial and superior vestibular nucleus could code all aspects of velocity storage. A recently developed technique enabled prolonged recording while animals were rotated and received optokinetic stimulation about a spatial vertical axis while upright, side-down, prone, and supine. Firing rates of 33 VO and 8 VPS neurons were studied in alert cynomolgus monkeys. Majority VO neurons were closely correlated with the horizontal component of velocity storage in head coordinates, regardless of head orientation in space. Approximately, half of all tested neurons (46%) code horizontal component of velocity in head coordinates, while the other half (54%) changed their firing rates as the head was oriented relative to the spatial vertical, coding the horizontal component of eye velocity in spatial coordinates. Some VO neurons only coded the cross-coupled pitch or roll components that move the axis of eye rotation toward the spatial vertical. Sixty-five percent of these VO and VPS neurons were more sensitive to rotation in one direction (predominantly contralateral), providing directional orientation for the subset of VO neurons on either side of the brainstem. This indicates that the three-dimensional velocity storage integrator is composed of directional subsets of neurons that are likely to be the bases for the spatial characteristics of velocity storage. Most VPS neurons ceased firing during drowsiness, but the firing rates of VO neurons were unaffected by states of alertness and declined with the time constant of velocity storage. Thus, the VO neurons are the prime components of the mechanism of coding for velocity storage, whereas the VPS neurons are likely to provide the path from the vestibular to the oculomotor system for the VO neurons.

Keywords: monkey, vestibulo-ocular reflex, adaptation, gravity, velocity storage, spatial orientation, optokinetic after-nystagmus, vestibular-only neurons

Abbreviations: VOR, angular vestibulo-ocular reflex; MVN, medial vestibular nucleus; SVN, superior vestibular nucleus; VO, vestibular-only neuron in medial vestibular nucleus; VPS, vestibular-pause-saccade neuron in medial vestibular nucleus.

DEFINITIONS

Eigenvector, are orientation vectors associated with the velocity storage system matrix that are activated by stimulus velocity along a specific direction; velocity storage, integrative network of GABA_b sensitive neurons in the medial and superior vestibular nucleus (SVN). Type I neurons, neurons receiving convergent input from lateral, anterior, or posterior canals and increase their firing rate with rotation toward that canal located on ipsilateral side of the head. Type II vestibular-only (VO) neurons increase their firing rate with rotation toward the canal located on contralateral side of the head.

INTRODUCTION

When subjects are rotated, the hair cells in the semicircular canals respond to angular acceleration. Because of the elasticity of the cupula and the endolymph a signal related to head velocity is generated in the cupula afferents that decays with a time constant of 3–5 s (1). The sense of rotation, the neural activity in the vestibular nuclei, and the nystagmus generated by a step in head velocity rotation has a time constant of at least 15–25 s, indicating that there is central vestibular processing that lengthens the response time (2–4). The neural mechanism that converts the small time constant response at the canal afferents to the long time constant response found at the level of the vestibular nuclei, has been termed “a velocity storage integrator” (5–7). Full field rotation in light also activates velocity storage probably through the subcortical visual system (8–10). Rotation in light activates velocity storage from both of these modalities so that as the vestibular drive from the semicircular canals wanes, the visual system continues to drive velocity storage generating optokinetic nystagmus (OKN) (6, 8). Moreover, when the lights are extinguished, the optokinetic after-nystagmus (OKAN) has a time constant similar to that induced in darkness by rotation at the same velocity (6, 8, 10).

A key feature of velocity storage is that it is sensitive to the orientation of the head relative to gravity and can be associated with orientation vectors of the velocity storage system matrix that change as a function of head orientation (11–14). If the head is tilted side-down or in forward-back planes, the yaw velocity storage orientation vector shifts so that it tends to align with the spatial vertical (gravity), inducing corresponding pitch or roll slow phase eye velocities in head coordinates (11–14). This cross-coupling of the eye velocity occurs from yaw-to-pitch or roll based on otolith clues but not from roll-pitch to yaw [see Ref. (15, 16) for details].

Neurons that code the slow phase eye velocities of rotational nystagmus and OKN are located in the vestibular nuclei (4, 17, 18), and electric stimulation in this area elicits activation of the velocity storage mechanism (19). Midline sections of the commissural pathways at the level of the rostral medial vestibular nucleus (MVN) and SVN eliminate velocity storage (20, 21). This suggests that the network of neurons in the SVN and MVN and their commissural interconnections are critical for producing velocity storage. A critical finding was that following midline lesions, the degenerated neurons were located in the MVN and SVN and were GABA_b-ergic (22–24). This raised the possibility

that the neurons chiefly responsible for production of velocity storage were a GABA_b population. Support for this came from dosage-dependent suppression of velocity storage by intramuscular injection of a GABA_b antagonist, baclofen (25, 26).

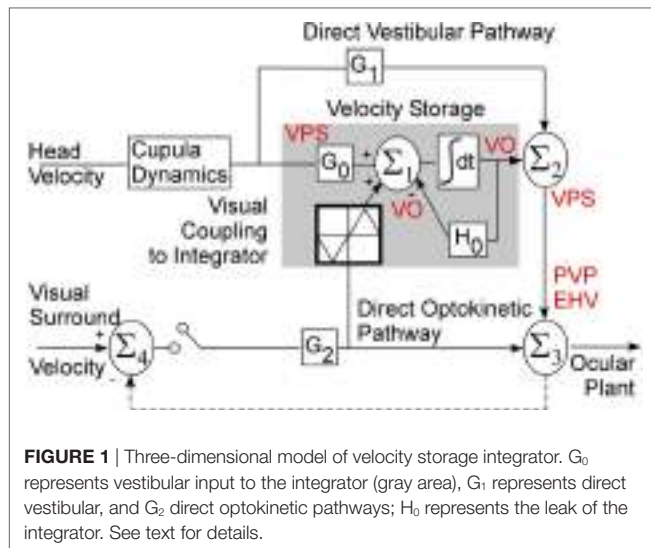
Using a wide range of stimuli that are known to activate velocity storage indicated that these neurons were VO and vestibular-pause-saccades (VPS) neurons (3). From this, it was hypothesized that the network of neurons in this area that implement velocity storage is presumably comprised of Type I and Type II VO neurons and VPS neurons are part of a later stage in the processing of vestibular signals, carrying the activity from the VPS neurons to the oculomotor system (3). Despite the progress in defining the behavioral properties of velocity storage, however, there has only been sparse information about its neuronal implementation in three dimensions, and those studies that have focused on the neuronal basis of velocity storage have been confined to one dimension, i.e., rotations about the spatial vertical axis (3, 27). These studies have shown that VO and VPS neurons code signals related to velocity storage, but due to the technical difficulties of recording neuronal firing rates stably in various head orientations for long periods of time, the role of the VO neurons in generating the three-dimensional spatial properties of velocity storage remains unexplored.

Novel techniques for long-term recording of neurons in the vestibular nuclei (28–32) have enabled the study of how VO and VPS neurons code the spatial properties of velocity storage in various head orientations. The importance of this is that it would identify the classes of VO and VPS neurons in the SVN and MVN that participate in the spatial orientation of eye velocity. This will fill a gap in our understanding of the importance of the role of VO and VPS neurons in vestibulo-oculomotor processing. Since the VO and VPS neurons are under control of the cerebellar nodulus (33), it should be possible to understand the circuitry in the central vestibular system that orients to the gravitational vertical and gives us a better idea of the underlying cause for the failure to do so.

Some of the data were previously published in abstract form (34). Convergent canal and otolith inputs for neurons in this study were previously published (32). Data on VOR time constant from one neuron in this study before and after baclofen injection were published elsewhere (25).

The Theoretical Basis of Velocity Storage

Velocity storage in one dimension was first modeled as a leaky integrator that can be activated by either vestibular or visual inputs. The lengthening of the time constant from that of the vestibular afferent time constant has generated different modeling approaches (6, 7) [see Ref. (5) for a comparison]. Essentially, the time constant is governed by a parameter h_0 in a feedback path whose inverse determines the time constant of the integrator. In three dimensions, the feedback becomes a system matrix, H_0 , whose eigenvalues determine the time constants of yaw, pitch, and roll and whose eigenvectors determine the orientation structure that characterize the orientation (14) (Figure 1). The off-diagonal terms in the system matrix are the cross-coupling parameters and code the spatial orientation aspects of velocity storage (14). This matrix has an upper triangular structure, which reflects the fact that cross-coupling only occurs from yaw-to-roll



and -pitch (14). The output signal from the integrator is then summated with the direct vestibular (Σ_1) and visual (Σ_2) signals before being processed by the oculomotor system, which includes the velocity-position integrator and plant (35) (Figure 1). Thus, the system matrix determines and predicts both the orientation and temporal properties of response to rotations in tilted head positions and predicts a wide range of experimental outcomes (11–14).

Relationship of the Model to Central Vestibular Neurons

The Raphan model views the VOR and visual–vestibular interaction as having direct and indirect pathways (Figure 1). Velocity storage is part of the indirect pathway and can be represented as a three-dimensional integrator, characterized by a system matrix (14). In accordance with this model, primary afferents project through a direct vestibular pathway to pre-oculomotor neurons with certain transduction gain level G_1 (Figure 1). This direct pathway may involve more than just the three-neuron arc (16). The target neurons for this pathway could be position-vestibular-pause (PVP) and/or eye-head-velocity (EHV) neurons (36, 37) or some neurons that directly projects to them as is shown on a schema (Figure 1). The same vestibular afferent activity projects to different central neurons with different transduction gain level G_0 . This signal is summed on neurons that realize the velocity storage network. The velocity storage integrator could be also activated through visual coupling to the integrator (Figure 1). This is accomplished by subtracting eye velocity from velocity of the visual surround, which generates retinal slip and having a dark–light switch, which inactivates the pathway in darkness. During optokinetic following at low frequencies, this pathway mainly activates pre-oculomotor neurons in the vestibular nuclei with a transduction gain G_2 . In contrast to the vestibular input, segregation between direct and indirect optokinetic inputs occurs at the frequency domain of the stimulus. That is, during sinusoidal oscillation of the visual surround at low frequency or during

rotation of visual surround at constant velocity this pathway also activates velocity storage (Figure 1). When the light is turned off (open switch) following a period of OKN stimulation, the activity stored in the integrator generates OKAN. In this study, we will relate the recorded neurons to the structure of this three-dimensional model.

MATERIALS AND METHODS

The activity of 33 VO and 8 vestibular-pause-saccade (VPS) neurons was recorded in the rostral medial and SVN in three cynomolgus monkeys (*Macaca fascicularis*). First, a head mount was implanted on the skull to provide painless head fixation in stereotaxic coordinates during testing (30, 38). At a second surgery, two three-turn coils were implanted on the left eye. The frontal coil measured the horizontal and vertical components of eye position (39, 40). Another coil, placed on the top of the eye, approximately orthogonal to the frontal coil (41), was used to measure the torsional component of eye position. The surgical procedures were performed under anesthesia in sterile conditions. The surgical procedures and experimental protocol conformed to the Guide for the Care and Use of Laboratory Animals and were approved by the Institutional Animal Care and Use Committee.

Data Collection and Processing

The animals were tested in a multi-axis vestibular stimulator (3), which has three gimballed axes for rotation: a horizontal axis parallel to the spatial horizontal, a nested yaw axis, and a doubly nested, inner pitch/roll axis. The yaw and pitch/roll axes were enclosed in a light-tight optokinetic cylinder, 91 cm in diameter, with 10° vertical black and white stripes equally distributed over the visual field. The axis of the cylinder was collinear with the yaw axis. Each axis went through the center of rotation of the head. The animals' heads were rigidly fixed in the stereotaxic plane.

Voltages related to eye position and to chair rotation about each axis were recorded with amplifiers with a bandpass of DC to 40 Hz, digitized at 500 Hz per channel with a 12-bit resolution, and stored for later analysis. Eye position voltages were smoothed and digitally differentiated by finding the slope of the least squares linear fit, corresponding to a filter with a 3-dB cutoff above 40 Hz, the cutoff frequency of the filters used for data acquisition. Unit activity was converted into pulses (BAK Electronics Inc.) of standard amplitude (5 V) and duration (0.5 ms). Pulses were delayed relative to action potentials by 0.5 ms. The time of the spike occurrence was stored relative to the nearest sampling time with the assumption that only one spike could occur within each sampling period (1.67 ms) or a frequency of 600 Hz (3). Eye movements were calibrated by rotating the animals in light at 30°/s about the pitch, roll, and yaw axes. It was assumed that horizontal and vertical gains were unity and roll gain was ≈0.6 in this condition [see Ref. (42), for details].

Random noise was used to keep animals alert. In some experiments, random noise was not used. Then responses to the same test when animal was and was not drowsy were compared.

Coordinate Frames

The head coordinate frame was defined by three axes: x (nasooroccipital, positive direction, back-to-front), y (interaural, positive, from the left ear), and z (body axis, positive, up). Positive directions for eye movements were defined by the right-hand rule: torsion toward the right ear [clockwise (CW) from the animal's point of view], vertical down, and left horizontal. Eye movements were defined by the direction of the slow phases of nystagmus, with slow phases to the animal's right as CW, and *vice versa*, i.e., slow phases to the left as counterclockwise (CCW).

Unit Recording

Details of the unit recording technique are provided elsewhere (29, 32, 38, 43). Briefly, the abducens nucleus was identified first (44) and VO and VPS neurons in the MVN and SVN were located about 1–2 mm caudal and 0–2 mm lateral from the center of the abducens nucleus (3, 29, 32). Special care was taken to ensure that the same neuron was recorded during the experiment, similar to our previous studies (28, 29, 32, 45). That is, we compared the shape of the recorded action potentials during the entire experiment. Canal convergent inputs or tests of other characteristics that were specific for the particular neuron were repeated at different times and compared during off-line analyses. Firing rates of each neuron with the animal in the upright position for 20 s at the onset of each test were recorded to monitor the stability of the resting firing rates. The resting firing rate was computed and plotted as a function of time off-line. We assumed that the unit recording was stable during the experiment if the SD about the mean value did not dramatically change (Figure 2). The units had differing spontaneous firing rates (FR), which in some cases were gradually modified during the experiments (Figures 2A,B).

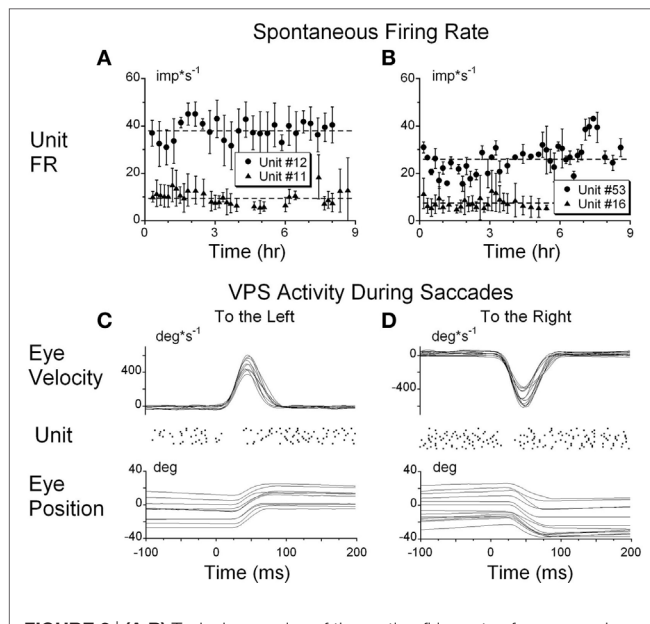


FIGURE 2 | (A,B) Typical examples of the resting firing rates from several neurons during the experiments. **(C,D)** Raster's of firing rate of the position-vestibular-pause (PVP) neuron during spontaneous saccades to the left **(C)** and to the right **(D)**. This PVP neuron paused its firing at the beginning of each saccade.

Unit #11 (Figure 2A) had only minor variations in the average firing rate, but the firing rate variations substantially increased after 7.5 h of recording. Unit #52 (Figure 2B, circles) had some variation of the average firing rate, which dramatically increased from 28.9 ± 3.3 to 38.5 ± 4.5 imp/s ($p < 0.01$) after ≈ 7.5 h of testing. Changes in firing rate of both neurons indicated that data obtained later than 7.5 h from the onset of the experiment could not be used for analyses.

Experimental Protocol

Vestibular-only and VPS neurons were identified during oscillation of the monkeys by hand about a spatial vertical axis. An audio monitor and an oscilloscope were used to select neurons whose firing rates were associated only with vestibularly induced eye and head velocity and had no obvious relation to eye position or ocular pursuit (3, 29, 46, 47). Thus, modulation of the firing rate of VO and VPS neurons was about the same regardless of whether the VOR was tested in darkness, in light, or suppressed or canceled by oscillation of the animal in phase with the visual surround. To determine that there was no relation to eye position, visually driven eye velocity, ocular pursuit, or spontaneous eye movements, the neuron was further examined off-line by color coding the firing rate on an x - y plot to determine its eye position and eye velocity sensitivity. This method was utilized to exclude all neurons whose eye position sensitivity was >0.05 imp/deg (32).

To identify whether the neurons were VPS cells, unit activity was synchronized with the beginning of 10–50 saccades of approximately identical amplitudes ($25^\circ \pm 3^\circ$) in all directions. Unit firing rate during saccades was analyzed using raster diagrams and superimposed average algorithms (Figures 2C,D). The pauses in activity were approximately overlaid for each saccade and the onset of the pause slightly preceded saccade onset and ended when the saccade reached peak velocity. Some units had pauses only for saccades to the left or right, but not during vertical saccades. Other units had pauses associated with saccades in all directions. This test was essential because neurons that have pauses during saccades only in a particular direction or during a portion of the saccadic interval frequently could not be detected on-line as VPS neurons using video or audio monitors (Figures 2C,D).

Tests to Determine Neuronal Sensitivities

Identification of canal and otolith-related inputs for all neurons were reported elsewhere (32). Each unit was also tested for convergent inputs from muscle proprioceptors by pressing on the muscles in the neck, arms, legs, and body and listening for changes in firing rate on an audio monitor or by noting changes in firing frequency on an oscilloscope. All units that had detectable convergent proprioceptive inputs were not studied further. This technique does not guarantee that all units with neck proprioceptive inputs were excluded from the analysis (48), but it eliminated a significant number of such neck-related neurons (32, 49). Therefore, the VO and VPS neurons tested in this study may represent a specific sub-group of units tested by others (50–52).

It was previously demonstrated that VO and VPS neurons have approximately the same sensitivity to sinusoidal oscillation at 0.2 Hz and above in darkness, in light and during suppression

of the VOR gain (46, 53). It was also demonstrated that visual following of an OKN stimulus at frequencies 0.05 Hz only are coded in such neurons (54). These studies concentrated only on one aspect of velocity storage and it is not clear whether only VO neurons were considered. To clarify, neurons in this study were tested during sinusoidal oscillation at 0.2 Hz in darkness, in light (OKN drum stationary in space while animal is oscillated in yaw), and during suppression of the VOR (OKN drum was linked to yaw axis and, therefore, animal and drum were oscillated in yaw in phase). Neurons were also tested by sinusoidal oscillation of OKN drum in yaw at frequencies from 0.01 to 0.5 Hz. When it was possible, rotational VOR tests were also performed at various frequencies.

To determine symmetry of neuronal responses for rotations in alternate directions the animals were rotated at 60°/s for 5 s and then stopped in light for 5 s to eliminate post-rotatory nystagmus and to determine the neuronal sensitivity to step rotation in ipsilateral and contralateral directions. The light was extinguished and after 2 s rotation was repeated in the alternate direction. Average neuronal firing rates over the first 2 s were computed from 10 rotations in each direction.

Tests to Determine the Relation of Neuronal Firing Rate to Velocity Storage in One Dimension

The animals were seated in a rotating chair with the head fixed in the stereotaxic position. The lights were extinguished and the animals were rotated about a yaw axis at a constant velocity 60°/s. The slow phase eye velocity was close to that of head velocity at the onset of rotation but gradually decayed to 0 over time. The rotation was stopped to induce post-rotatory nystagmus. The pre- and post-rotatory profiles were similar but opposite in polarity. After a brief 7-s period in light, similar rotation in the opposite direction induced oppositely directed per- and post-rotatory nystagmus. After a 10-min rest in light, the units were tested over a range of velocities from 30 to 180°/s in 30°/s increments, starting at 60°/s.

The monkeys were also rotated side-down about the spatial vertical axis to induce vertical (pitch) nystagmus, as described above. Additionally, some units were tested by tilting the animal right side down and then rotating it in the yaw 45° in CW and CCW directions to bring the left anterior-right posterior or right anterior-left posterior canal pair, respectively, to the plane of rotation. A short period in light for 4–5 s during post-rotatory nystagmus was used in some experiments (6, 8) to determine the neural activity during rapid time constant variations.

Tests to Determine the Relation of Neuronal Firing Rate to Velocity Storage in Three Dimensions

Optokinetic nystagmus was induced by rotation of the optokinetic drum about the animal's yaw axis with the axis of rotation coincident with the spatial vertical axis. The OKN drum was rotated at a constant velocity for 30 s and then OKAN was recorded in darkness while the animal was in the upright position. After a brief (5 s) exposure to light, OKN, and OKAN were recorded in the opposite direction. Typically, OKN was induced

at 60°/s, although some neurons were tested at velocities of 30, 90, and 120°/s. To test how neurons code spatial orientation of the velocity storage, OKN and OKAN were recorded with the animal tilted side down or prone-supine in 30° increments up to 90°. In these positions OKAN induced by rotation of the visual surround about the animal's yaw axis was initially only about the animal's head-yaw, but then cross-coupled to pitch or roll nystagmus, depending on the direction of the animal's tilt with regard to gravity.

It was previously shown that eye velocity declines along an eigenvector of velocity storage, which tends to shift toward the spatial vertical (12). Thus, correlation of the time constant of the unit firing rate with the time constant of the primary yaw eye velocity, which is dependent on tilt angle, indicated that the neuron was a VO or VPS neuron that coded only the yaw component of velocity storage. Then correlating the firing rate with the cross-coupled components would indicate that the unit coded the spatial properties of the velocity storage integrator.

Data Processing and Analyses

Eye positions were digitally differentiated to determine slow phase eye velocity after saccades had been identified (55), and marked off from further analyses. The accuracy of desaccading was visually verified, and in some cases (<5%) manually corrected.

The neuronal data were converted into an instantaneous frequency which is an inverse of the inter-spike interval (imp/s) to measure the dominant time constant of the firing rate during vestibular and OKN. The neuronal data were expressed as a histogram with a moving average. That is, the neuronal firing rate was binned in 25 ms intervals. Then values of the first five intervals were averaged and assigned to the middle (third) intervals. The first interval was then omitted and one more interval added to the average and the averaging procedure was repeated (3). Both methods of neuronal data presentation had similar values of average firing rate and sensitivity in response to sinusoidal oscillations at frequencies below 0.5 Hz, but substantially reduced data variation due to the moving average algorithm.

Vestibular per- and post-rotatory nystagmus induced in the upright were treated as dual time constant processes, where the first time constant of the cupula is known (4 s) and second time constant of the velocity storage integrator was determined. These algorithms of data fit were previously described (3, 6, 12). The decaying slow phase eye velocities and neuronal firing rate from the onset of OKAN till the time when they reached steady state level were fitted with a single time constant algorithm to measure the velocity storage of the OKAN induced in the upright position. OKAN induced when the animal was tilted side-down, forward, or backward were treated as dual time constant processes: the first, the time constant of the integrator and the second, the time constant of the cross-coupled component of eye velocity. The data were fit assuming that both time constants were unknown.

Statistical Analyses of the Data

The significance of the sinusoidal fit through the data was tested with an F-statistic, which is a reduced case of the general analysis

of variance (ANOVA) (42, 56). A standard two-tail *t*-test was used to compare two groups of data. An ANOVA was used to compare more than two groups of data. If the general ANOVA showed significant differences between data sets, then each between-group degree of freedom was analyzed separately by developing orthogonal contrasts. In this case, the results of the test were adjusted with a Scheffé approach (57).

RESULTS

Response of VO and VPS Neurons to Slow Phase Eye Velocity

The firing rates of 33 VO and 8 VPS neurons were studied during nystagmus induced by rotation at a constant velocity in darkness (38 units) or during OKAN (32 units) to determine their relationship to velocity storage. Fourteen additional neurons modulated their activity in relation to velocity storage but were only partially tested. Their neuronal activity was lost before a sufficient number of tests could be performed to determine their time constants as a function of head orientation or rotational velocity. Thus, after a neuron was selected for recording, there was a 75% chance that the neuron would survive over the entire testing period. Data from these 14 neurons were used in this study only to determine their sensitivity to step rotation.

Forty-one VO and VPS neurons formed the body of data that were extensively studied. These neurons were subjected to all tests to determine their relationship to velocity storage. One anterior canal-related neuron had no significant modulation. One posterior canal-related VPS cell was modulated significantly with each rotation, but its time constant was ≈ 4 s and was independent of the eye velocity response, which had the time constant of velocity storage (15–25 s). This suggests that a small population of VPS neurons is related to the direct vestibular pathway in support of

the model structure (**Figure 1**, G_1) and could provide input to the integrator (**Figure 1**, G_0).

Neuronal Firing Rates during VOR in Dark, in Light, and during Cancelation of the VOR with Sinusoidal OKN

The 22 VO and VPS neurons were recorded during steps of rotation in darkness (VOR dark), in light (VOR light), in a subject stationary visual surround (VOR cancellation), and during sinusoidal optokinetic stimulation (OKN). The average VOR gain was unity when tested in darkness or in light. The VOR gain decreased to 0.31 ± 0.25 during the cancellation paradigm ($p < 0.05$, ANOVA). The gain of the ocular following during sinusoidal OKN was 0.60 ± 0.15 , similar to the gains reported earlier (6, 8) and is consistent with the model (**Figure 1**).

The sensitivities of the firing rate of the VOR cancellation was not significantly different from that of VOR in dark (**Figures 3A,B**) or in light (not shown) for oscillation at 0.1 Hz and above ($p = 0.561$), but became progressively larger at 0.01 Hz, the frequency where velocity storage would play a significant role for rotation in darkness (**Figures 3A,B**).

Twenty of the 21 tested units did not respond to oscillation of the visual surround during OKN at 0.2 Hz. This reflected their insensitivity to cortically induced visual activity. However, the unit activity was modulated at lower frequencies of optokinetic stimulation (**Figure 3C**), indicating that the velocity storage integrator was sensitive to optokinetic stimulation at low frequencies (6). That is, the vestibular neurons were likely responding to activation through the subcortical pathway through the nucleus of the optic tract (NOT) (58, 59), not through the brainstem pathways to the oculomotor system through the flocculus. Regardless, **Figure 3C** supports the idea that VO and VPS neurons code velocity storage.

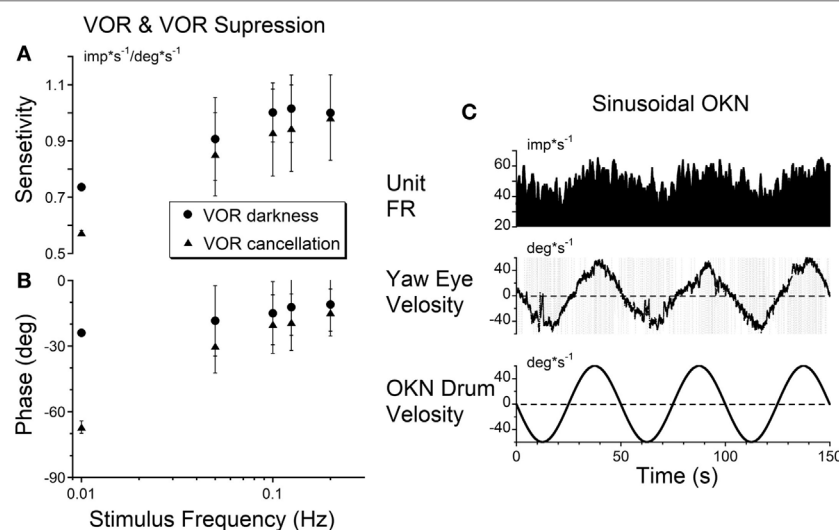


FIGURE 3 | (A,B) Gains (A) and phases (B) obtained from a typical vestibular-only neuron during sinusoidal oscillation in darkness (VOR darkness, filled circles) and oscillation in light with the subject-fixed visual surround (VOR cancellation, filled triangles). **(C)** Activity of the same neuron recorded during sinusoidal oscillation of optokinetic surround at 0.02 Hz [optokinetic nystagmus (OKN)].

One neuron, however, had a small but significant modulation of the firing rate during OKN stimulation at 0.2 Hz (0.101 $\text{imp} \cdot \text{s}^{-1} / \text{deg} \cdot \text{s}^{-1}$). Since the firing rate of this neuron was not related to eye position and velocity, this unit was identified as a VO neuron. Thus, a few VO neurons may have some access to the direct optokinetic input to velocity storage (Figure 1A, G₂).

Sensitivity to Angular Rotation in the CW and CCW Directions

Seventeen VO and six VPS neurons were sensitive to head rotation with the step of velocity in yaw (Figures 4A–C). One neuron in the left vestibular nuclei had a high sensitivity for rotation to the ipsilateral side (left, CCW, Type I, Figures 4D,E). Its firing rate ceased during rotation toward the contralateral side (right, CW) (Figure 4A). For such neurons, only the ipsilateral sensitivity could be computed (Table 1, dashes in values). There were three Type I and one Type II VO neurons that were sensitive to rotation only in one direction (17%, 4/23).

Another neuron, located in the right vestibular nuclei, had a comparable response to contralateral rotation (left, CCW, Type II), but a much smaller response to rotation toward the ipsilateral side (Figure 4B). The sensitivities of such neurons are shown in Table 1 (second block from the top) and are summarized in Figure 4F (gray symbols). All these neurons (48%, 11/23) were Type II neurons (9 VO and 2 VPS), and for all except one (Un #43; Table 1) the sensitivity to contralateral rotation was larger than the sensitivity to the ipsilateral side.

Thus, 65% of VO and VPS neurons in our study had an asymmetric response to rotation. There was no difference between VO and VPS neurons or whether the units received lateral canal, vertical canal, or an otolith input. Among 10 recorded neurons, seven received only vertical canal-related input (Table 1 (32)). Three other neurons received lateral canal-related input, two of which also had convergent vertical canal-related inputs. Thus, asymmetry in sensitivity did not correlate with whether neurons were VO or VPS cells or whether they received lateral canal,

vertical canal, or otolith inputs. A third neuron, located in the right vestibular nuclei, had comparable increases in firing rate during ipsilateral (CW, Type I) and decreases in firing rate during contralateral rotations (Figure 4C). The sensitivity of nine such neurons is shown on the bottom portion of Table 1.

Figure 4F summarizes responses of neurons with symmetrical (black circles) and asymmetrical (gray circles) sensitivities to rotations in both directions. By definition, neurons with symmetrical responses should lay along a diagonal line that goes from the unity sensitivity for rotation toward the ipsilateral and contralateral sides (gray dashed line). Neurons with asymmetrical sensitivity clustered in the upper left quadrant indicating that they all were Type 2. Four neurons with no sensitivity to rotation in one direction are not shown but they would lay along the ordinate 0 (dashed black horizontal line). Thus, we did not find any Type I neurons which responded to rotation in both directions asymmetrically.

Among nine neurons with symmetrical responses, four were Type I and five were Type II (Table 1, bottom two blocks). The relationship of the firing rate to the ipsilateral and contralateral rotations of these neurons is summarized in Figure 4F (black symbols). As expected, they are very close to the gray dashed symmetry line, i.e., their responses were approximately equal for CW and CCW rotations.

The Relation of the Neuronal Discharge to the Time Constant of the Yaw Angular Vestibulo-Ocular Reflex (VOR) Tested with Angular Rotations and OKN of Constant Velocities

A typical example of the changes in the neuronal firing rate of a VO neuron induced by head rotation at 60, 90, and 120°/s in darkness is shown in Figures 5A–C. During this test, the animal was extremely drowsy and slow phase eye velocity was frequently suppressed to 0. The unit firing rate decrease, however, was not

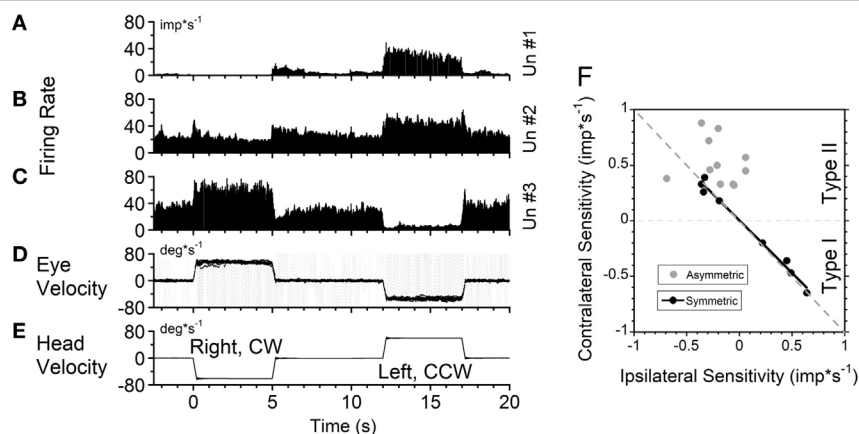


FIGURE 4 | Changes in neuronal firing rate of three vestibular-only neurons located in the left (A) and right (B,C) hemispheres in response to head rotation to the right ([E], negative velocity) and to the left (positive velocity) in darkness. (D) Superimposed eye velocities for 10 repeated rotations. Gray—original eye velocities. Black—slow phase eye velocities. See details in the text. (F) Relationship between average sensitivity to rotation toward ipsilateral (abscissa) and contralateral (ordinate) sides. Black symbols—neurons with identical sensitivities to rotation in both directions ($p < 0.05$). Gray symbols—neurons with asymmetrical sensitivities.

TABLE 1 | Neuronal sensitivity obtained by rotation with steps of velocity of 60°/s.

Monkey #	Unit #	Unit type	Sensitivity to rotation		p-Value	Canal input
			Ipsilateral	Contralateral		
M1	18	Vestibular-only (VO) 1	0.79 ± 0.26	–	<0.0001	LCi
M3	11	VO 1	1.01 ± 0.03	–	<0.0001	LCi and ACi
M3	16	VO 1	0.94 ± 0.26	–	<0.0001	LCi
M1	3	VO 2	0.06 ± 0.08	0.45 ± 0.08	<0.0001	ACi
M1	61	VO 2	–	0.76 ± 0.10	0.011	ACi
M1	64	VO 2	-0.06 ± 0.14	0.33 ± 0.11	<0.001	PCi
M1	66	VO 2	-0.21 ± 0.07	0.50 ± 0.13	<0.0001	ACi,c
M2	4	VO 2	-0.20 ± 0.09	0.83 ± 0.18	<0.0001	LCc and RAi
M3	12	VO 2	-0.28 ± 0.05	0.46 ± 0.14	0.003	LCc
M3	22	VO 2	-0.36 ± 0.12	0.88 ± 0.10	<0.0001	LCc
M3	29	VO 2	-0.05 ± 0.10	0.32 ± 0.10	<0.0001	PCc
M3	33	VO 2	0.06 ± 0.11	0.57 ± 0.16	<0.0001	ACi and PCi
M3	53	VO 2	-0.29 ± 0.07	0.72 ± 0.13	<0.0001	LCc and ACC
M3	23	VPS2	-0.18 ± 0.09	0.33 ± 0.06	<0.0001	PCi
M3	43	VPS2	-0.69 ± 0.41	0.38 ± 0.34	0.017	ACi
M1	58	VO 1	0.45 ± 0.12	-0.36 ± 0.15	0.218	LCi
M3	30	VO 1	0.49 ± 0.09	-0.47 ± 0.08	0.622	LCi and PCi
M3	45	VO 1	0.64 ± 0.12	-0.65 ± 0.11	0.948	LCi and ACi
M3	41	VPS1	0.22 ± 0.06	-0.20 ± 0.06	0.461	LCi
M1	67	VO 2	-0.33 ± 0.09	0.39 ± 0.14	0.285	PCi
M1	62	VPS2	-0.36 ± 0.25	0.33 ± 0.09	0.690	LCc
M3	58	VPS2	-0.34 ± 0.14	0.26 ± 0.09	0.174	ACi
M3	59	VPS2	-0.19 ± 0.07	0.18 ± 0.04	0.934	PCi

Canal inputs were determined in our previous study (32). LCi, ACi, and PCi are lateral, anterior, and posterior canals inputs from the ipsilateral side. LCc, ACC, and PCc, inputs the same canals from contralateral side. Ten rotations were performed in each direction.

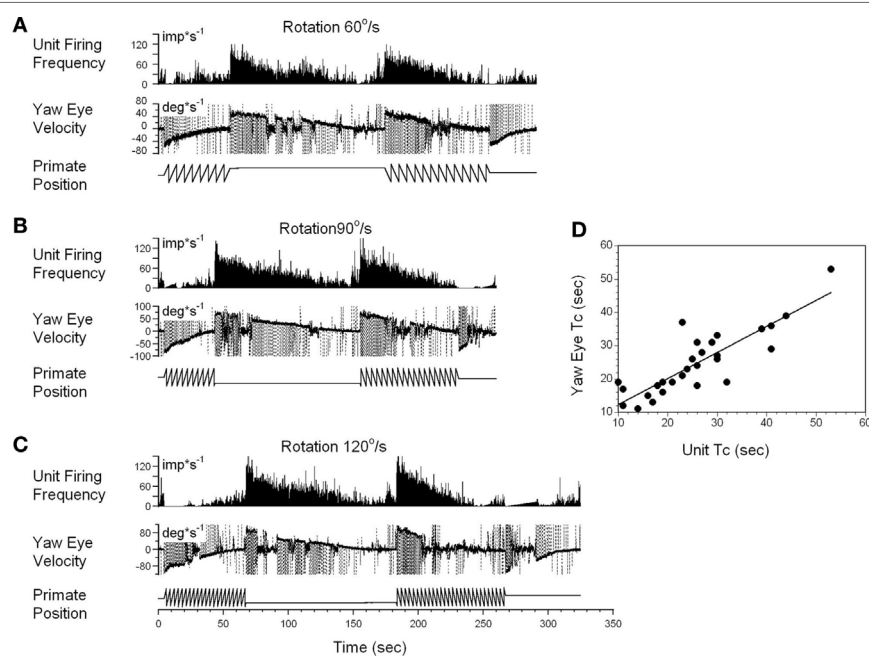


FIGURE 5 | Changes in the firing rate of a typical vestibular-only (VO) neuron that codes the yaw component of velocity storage during head rotation at 60°/s (**A**), 90°/s (**B**), and 120°/s (**C**). (**A–C**) In each section, after being in darkness for 5 s, the animal was rotated to the left (counter-clockwise) and then stopped while in darkness (primate position, tooth-like, and constant levels, respectively). Then rotation was repeated in the opposite (clockwise) direction. This sequence induces per-rotatory nystagmus to the right (Negative Eye Velocity) which gradually declined to 0. When rotation was stopped, it induces post-rotatory nystagmus in the opposite direction (positive eye velocity). This sequence of per- and post-rotatory nystagmus was repeated in the opposite directions. The experiment animal was extremely drowsy, and there was a sudden decline of slow phase eye velocities to 0. Drowsiness, however, did not affect firing rate of this VO neuron. (**D**) Relationship between the time constants of velocity storage determined from slow the phase eye velocity (ordinate) and from the neuronal firing rate (abscissa). Each data point on this graph represents a time constant measured for the oculomotor response and corresponding neuronal response. This is shown in the two responses in graphs (**A–C**). The black line is the linear regression of the data.

affected by this, and the gradual decrease to the bias level was the same as when the animal was alert (not shown). Periods of drowsiness were removed and time constant of slow phase eye velocity was compared to that of changes in neuronal firing rate (**Figure 5D**). Thus, the changes in the time constant of neuronal firing closely approximated the VOR time constant, which was the time constant of velocity storage. Additionally, drowsiness periods were occasionally observed during recording of almost every neuron, but drowsiness never affected the firing rate of the VO neurons.

Not every VO and VPS neuron had its firing rate related to velocity storage. Some neurons that had asymmetrical responses to CW and CCW rotations fell into this group, at least for the direction in which the sensitivity was lower (not shown). This supports the idea that the time constant of velocity storage for rotations in alternate directions is controlled by different neurons. This could also be the reason why the time constant for rotations in alternate directions are always slightly different, regardless of whether rotation was to the left or to the right.

Interestingly, while the firing rate of some neurons was altered by angular rotation, the time constant of the neuronal response was not correlated with the time constant of velocity storage as determined by the slow phase eye velocity. An example is shown in **Figure 6A**. This neuron increased its firing with leftward slow phase eye velocity (**Figure 6A**, yaw eye velocity upward) and decreased firing with rightward eye velocities (negative values). Once again small drowsiness intervals during the post-rotatory response to the left did not affect the neuronal firing rate. The time constants obtained from neuronal and oculomotor responses, however, were not correlated with any specific direction of head rotation (**Figure 6B**, $p > 0.05$). This neuron was significantly modulated during rotation at constant velocities, and the changes in its firing rate were not associated with the yaw component of velocity storage.

Vertical canal-related neurons typically did not respond to sinusoidal oscillation about the spatial vertical while upright (**Figure 7A**). Their modulation became significant when the animal was oscillated about the spatial vertical axis after being tilted left side down (**Figures 7B,E**). Furthermore, the modulation was even larger when the oscillation was in the plane of the left posterior canal that activated this neuron (**Figures 7C,F**). This

demonstrates that the firing rates of some neurons are specific to the canal plane that innervates these neurons. It suggests that the activity of the velocity storage in these neurons is actually coded in the canal rather than in the head coordinates. Since oculomotor responses are coded in the head coordinates (see Introduction), signals coding for the firing rates of this type of neuron should be converted from the canal into head coordinates.

Correlation of the time constants determined from neuronal and yaw oculomotor responses was significant for 15 VO neurons. **Figure 8** demonstrates the linear regression lines determined for these units (**Figure 8A**, black lines). The beginning and the end of each line indicates the range within which each neuron was tested. On average, the regression lines from VO neurons were clustered below the dashed line which indicates the 1:1 ratio of these parameters. An average slope was 0.593 ± 0.213 indicating that the time constant of velocity storage was longer in the activity of the VO neurons than in the oculomotor responses. There was only one VPS neuron, whose time constant was comparable to the accepted cupula time constant (≈ 4.5 s) and was independent of the time constant of VOR.

Drowsiness affectively changed the firing patterns of the VPS cells (not shown) (3, 60). Thus, the firing rates of VPS neurons are associated with oculomotor behavior, rather than with manifestations of velocity storage. Regardless, the activity of the five VPS neurons was significantly modulated by head rotation about the animal's yaw axis. When the time constant of the velocity storage obtained at different rotation velocities was plotted against the time constant of the neuronal firing rate, the two parameters were correlated (**Figure 8**, red lines). An average slope of the regression line for VPS was 0.307 ± 0.059 which is smaller than that for VO neurons ($p = 0.0092$).

Thirty two neurons were tested for the relationship of their firing rate to the time constant of OKAN. Among them were six vertical canal-related and one lateral canal-related neuron that did not respond to OKAN induced by drum rotation about the animal's yaw axis in the upright. Twelve neurons did respond to OKAN but causal relationship was not certain. Furthermore, there was not enough data to determine the relationship between the time constants of neuronal and oculomotor responses. The remaining 13 neurons were also related to yaw OKAN and were extensively tested. There was a significant correlation between

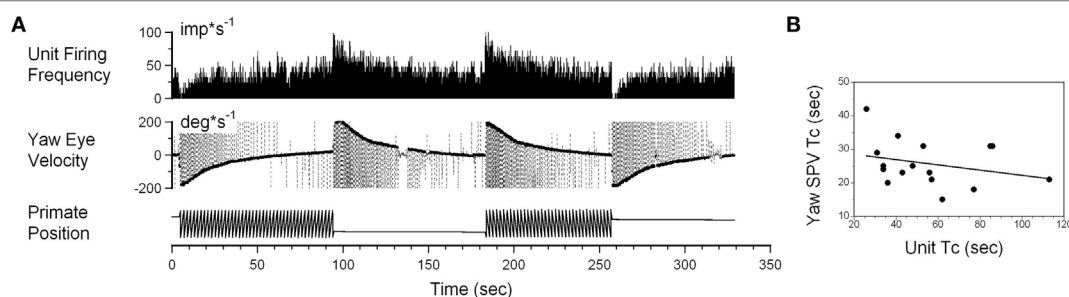


FIGURE 6 | (A) Changes in the neuronal firing rate induced by head rotation about a spatial vertical axis of vestibular-only neuron that does not code the yaw component of velocity storage. See also legend to **Figure 5** for details. **(B)** Changes in the time constant determined from yaw slow phase eye velocities (ordinate) did not correlate with changes determined from the neuronal firing rate (abscissa).

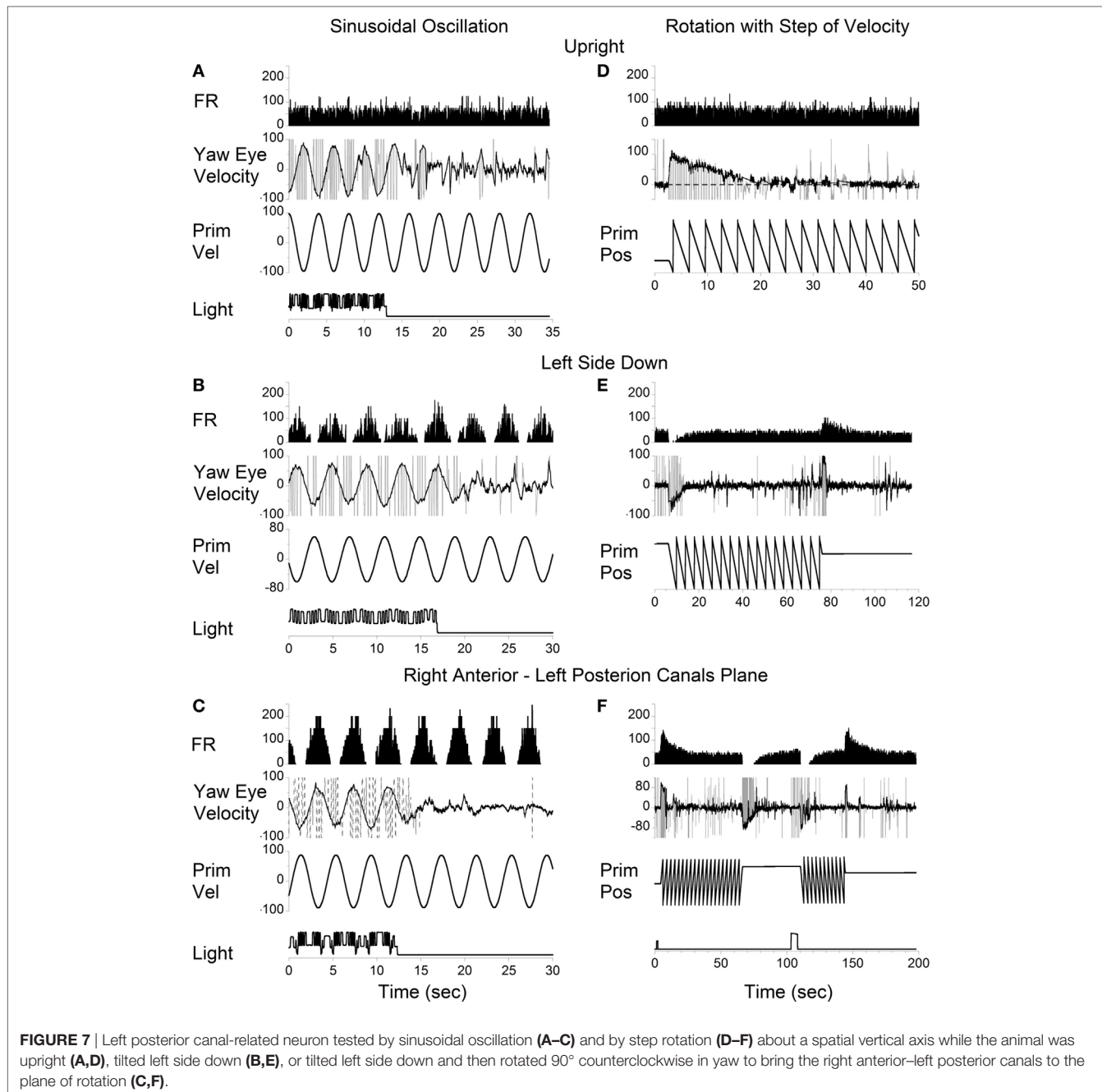


FIGURE 7 | Left posterior canal-related neuron tested by sinusoidal oscillation (**A–C**) and by step rotation (**D–F**) about a spatial vertical axis while the animal was upright (**A,D**), tilted left side down (**B,E**), or tilted left side down and then rotated 90° counterclockwise in yaw to bring the right anterior-left posterior canals to the plane of rotation (**C,F**).

the decaying time constant of the changes in the neuronal firing rate and the slow phases of yaw nystagmus for 11 VO (Figure 8B, black lines) and the two VPS neurons (Figure 8B, red lines). This was similar to the previously described relationship to rotatory nystagmus, some neurons that had a clear correlation of their neuronal firing rate to the yaw component of OKAN did not receive convergent inputs from the lateral but only from the vertical canals.

The neurons whose firing rates were related to the yaw component of OKAN were also tested by sinusoidal oscillation of the visual surround at low frequencies. All of the tested neurons were

modulated by visual surround oscillation at 0.02 Hz (Figure 3C), and about half of them were also modulated at 0.05 Hz oscillation. This was an additional confirmation that the firing rate of these neurons was related to velocity storage.

Relation of the Neuronal Discharge to the Orientation Properties of Velocity Storage

Thirteen neurons were tested by inducing yaw OKN/OKAN when animals were upright or tilted sideways up to 90° (Figure 8B). Ten neurons were classified as VO neurons and three were classified

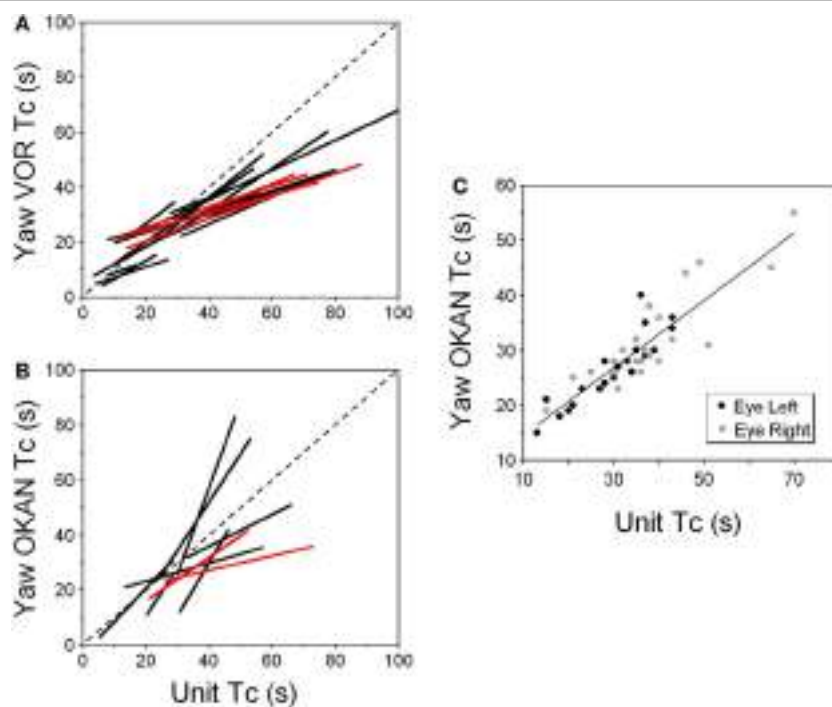


FIGURE 8 | (A,B) Relationship of the time constant of velocity storage measured from the yaw slow phase eye velocity (abscissa) during vestibular nystagmus (A) and optokinetic after-nystagmus (OKAN) (B) and measured from the changes in the neuronal firing rate (ordinate). The individual lines are regression lines for the vestibular-only (black) and VPS (red) neurons. **(C)** Relationship between the time constant of the yaw component of velocity storage tested with 60°/s optokinetic nystagmus/OKAN while the head was tilted side down at various degrees up to 90°. The time constant of the decline in neuronal firing is shown in **Figure 9**.

as VPS neurons. Twelve of the 13 (12/13) neurons had their firing rate related to the horizontal component of the OKN/OKAN. Three neurons received convergent inputs only from the lateral canal on the ipsi- (1, Type I) or contralateral (2, Type II) side. Three neurons received convergent inputs from lateral (2 ipsi-, 1 contralateral) and anterior (2 ipsi-, 1 contralateral) canals. Six neurons did not receive any convergent inputs from the lateral canals, only from vertical canals (2 ipsi- anterior, 1 ipsi- posterior and 3 contralateral posterior canals), and yet they firing rates were related to yaw rather than pitch OKN/OKAN.

According to the model, there should be no cross-coupling in the upright position, but cross-coupling to vertical would increase with the side-down tilt. Several typical examples of coding the spatial orientation of OKAN are shown in **Figures 9–11**. The VO neuron shown in **Figure 9** received convergent inputs from the contralateral lateral and anterior canals as well as static otolith input (32). When the animal was tested in the upright position, firing rate of the unit decreased with optokinetic stimulation that induced OKN/OKAN to the left (**Figure 9E**). Firing rate increased for optokinetic stimulation that induced OKN/OKAN to the right (**Figure 9A**). When the OKN/OKAN to the left was induced with the animal tilted left side down (**Figures 9B–D**, V yaw), the yaw component of the OKAN became shorter with the tilt angle, while the cross-coupled downward vertical component of OKAN (V pitch) progressively increased with the tilt angle (**Figures 9B–D**). Similar changes were observed during OKN/OKAN to the right as the animal was tilted right side down

(not shown). The same was true for OKAN to the right as the animal was tilted left side down (not shown) or right side down (**Figures 9B–D**, right side). In all cases, the changes in the neuronal firing rates were correlated only with changes of the yaw component of OKAN for both directions of rotation but not with the cross-coupled vertical component.

This unit was repeatedly tested in upright and side down tilts to obtain the relationship of neuronal firing rates to yaw and pitch OKN/OKAN (**Figure 8C**). The time constant of the yaw component of velocity storage, T_c , was largest when tested upright (two black and two gray symbols on the right in **Figure 8C**) and it progressively decreased with the tilt angle. The T_c of the decay in neuronal firing behaved similarly, and there was a tight linear relationship between the decrease in the T_c of the neuronal firing rate and the yaw component of OKAN. There was no difference for the data obtained for the slow phase eye velocities to the left or to the right (**Figure 8C**, black and gray symbols), which were associated with an increase and decrease in neuronal firing rate, except that the time constant of yaw OKAN to the right was slightly larger.

The linear regression coefficient remained approximately the same for left and right OKAN (1.27 ± 0.19) (**Figure 8C**). Similar responses were present for two other VO and three VPS neurons that received canal-related input only from the lateral canal or lateral and vertical canals (not shown). Thus, this type of neuron coded the horizontal component of velocity storage when there was cross-coupling to the pitch axis during OKN/OKAN. This

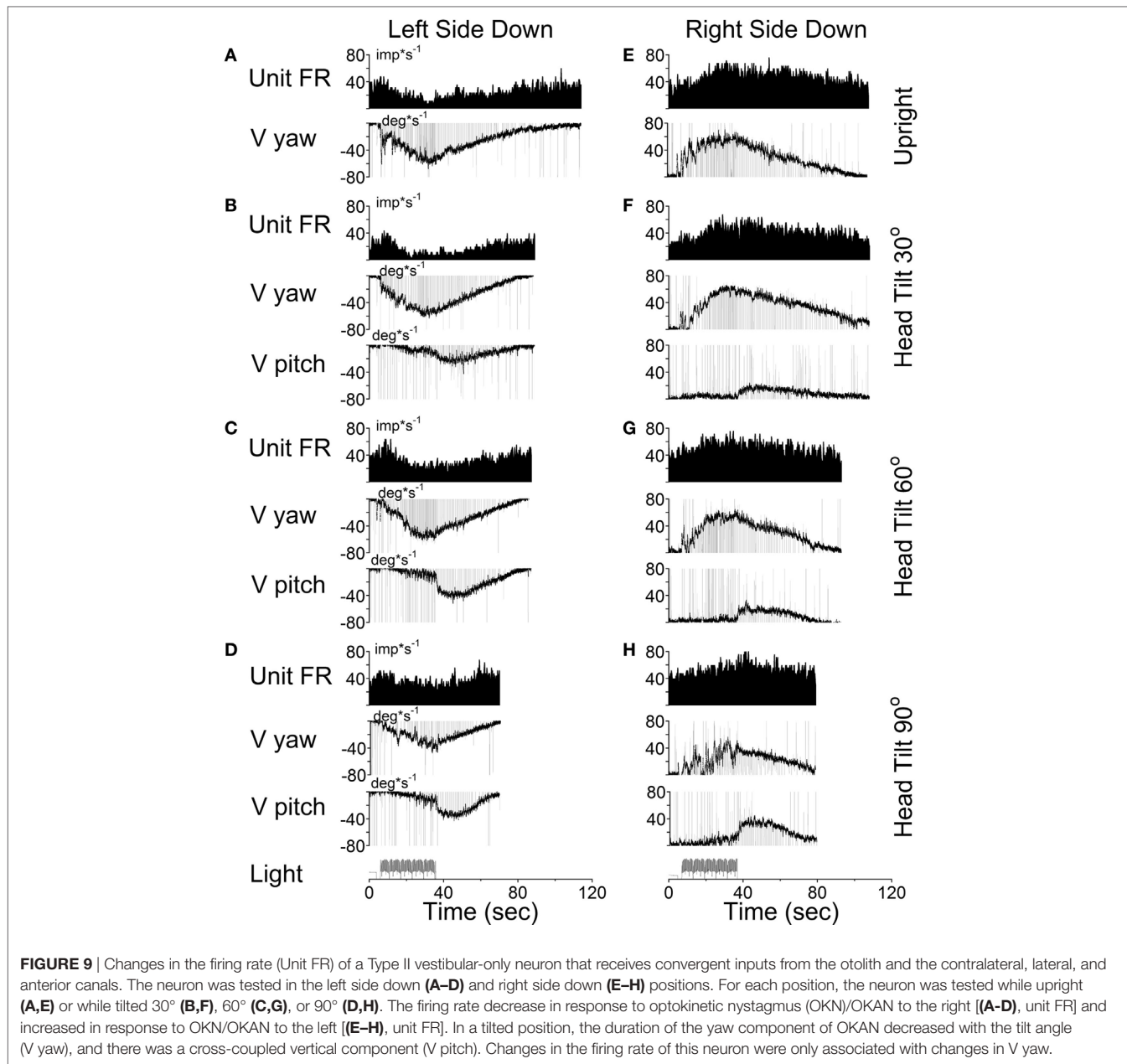


FIGURE 9 | Changes in the firing rate (Unit FR) of a Type II vestibular-only neuron that receives convergent inputs from the otolith and the contralateral, lateral, and anterior canals. The neuron was tested in the left side down (**A–D**) and right side down (**E–H**) positions. For each position, the neuron was tested while upright (**A,E**) or while tilted 30° (**B,F**), 60° (**C,G**), or 90° (**D,H**). The firing rate decrease in response to optokinetic nystagmus (OKN)/OKAN to the right [**(A–D)**, unit FR] and increased in response to OKN/OKAN to the left [**(E–H)**, unit FR]. In a tilted position, the duration of the yaw component of OKN decreased with the tilt angle (V yaw), and there was a cross-coupled vertical component (V pitch). Changes in the firing rate of this neuron were only associated with changes in V yaw.

relationship of firing rate to only yaw and not pitch OKN/OKAN indicates that the convergent input of contralateral anterior canal and otolith activity may have induced roll cross-coupling (see below), which was not tested for these units.

Thus, six (6/13) neurons including the neuron shown in **Figure 9** coded the horizontal (yaw) component of OKN/OKAN in head coordinates.

One VPS neuron received convergent input from the contralateral posterior canal (**Figure 10**). With the animal upright, this unit decreased its firing rate during OKN/OKAN to the left (**Figures 10A,D**) and increased it with OKN/OKAN to the right (not shown), regardless of the lack of the lateral canal input. When OKN/OKAN to the left was tested with the animal tilted left side down (**Figures 10B,C**), the firing rate of this neuron was

clearly modulated in relationship to the cross-coupled upward pitch component of OKAN. There was no effect of head tilt to the right (**Figures 10E,F**) or tilt in either direction during OKN/OKAN to the right (not shown). This indicates that this neuron specifically coded the cross-coupled vertical component in a specific direction. Thus, neuronal changes in this experiment reflected activation of velocity storage. Six (6/13) neurons, including the neuron shown in **Figure 10**, coded the cross-coupled (pitch) component of OKAN. Furthermore, changes observed due to the induced cross-coupled component of OKAN in tilted position reflect spatial orientation of OKAN to gravity.

This indicates that VO and VPS neurons do not form a uniform category but form a distributed class of neurons that generate the velocity storage integrator and its output (**Figure 1**).

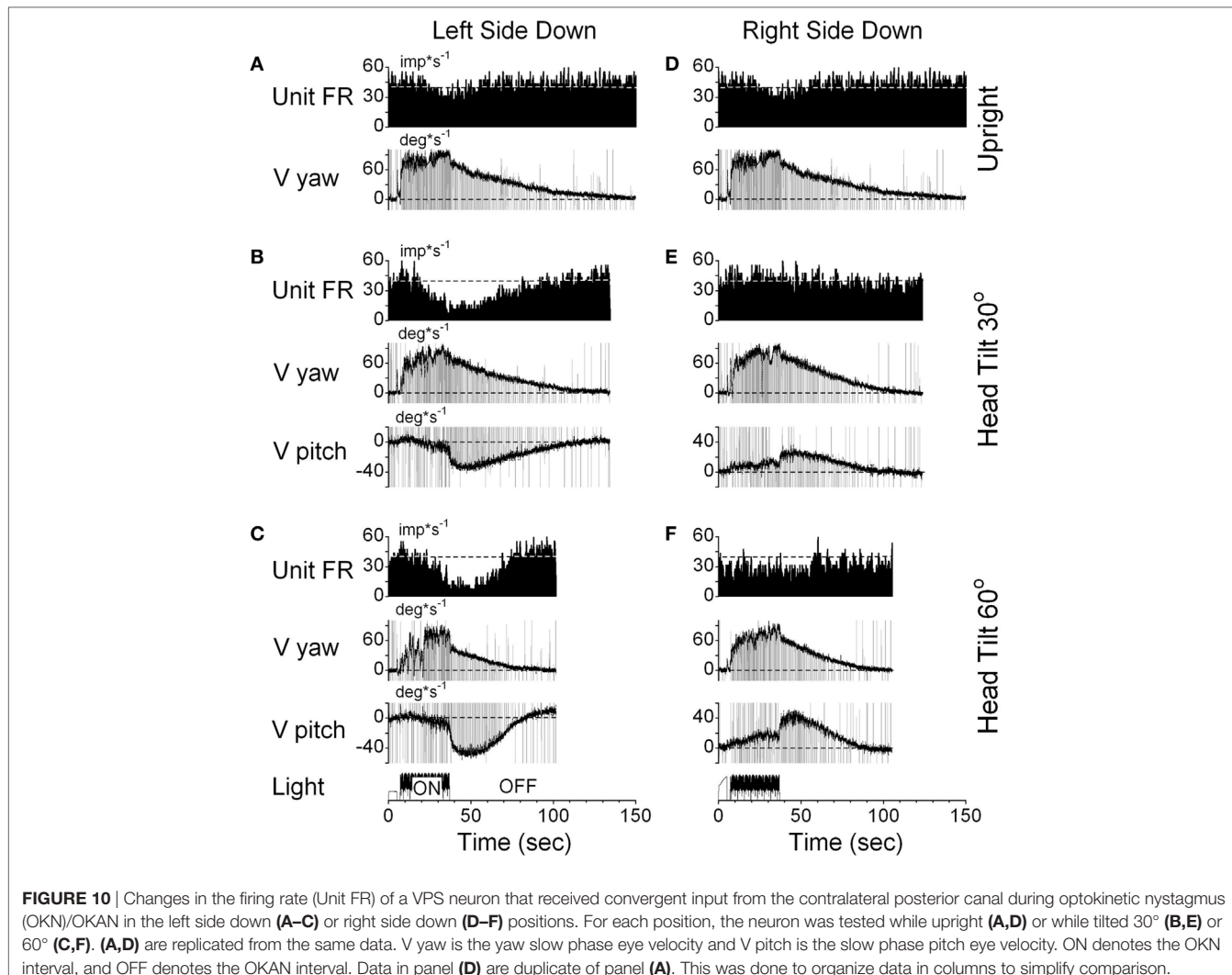


FIGURE 10 | Changes in the firing rate (Unit FR) of a VPS neuron that received convergent input from the contralateral posterior canal during optokinetic nystagmus (OKN)/OKAN in the left side down (**A–C**) or right side down (**D–F**) positions. For each position, the neuron was tested while upright (**A,D**) or while tilted 30° (**B,E**) or 60° (**C,F**). (**A,D**) are replicated from the same data. V yaw is the yaw slow phase eye velocity and V pitch is the slow phase pitch eye velocity. ON denotes the OKN interval, and OFF denotes the OKAN interval. Data in panel (**D**) are duplicate of panel (**A**). This was done to organize data in columns to simplify comparison.

This is consistent with previous findings for the one-dimensional analysis of neurons related to velocity storage (3).

It should be noted that six neurons as shown in **Figure 9**, had vertical canal-related inputs and yet changed their firing rate in relation to yaw, but not pitch OKAN. One of these neurons that received input from the ipsilateral anterior canal (32) was additionally tested during tilts forward and backward. Yaw OKN induced in these positions had only a yaw component, while OKAN cross-coupled to roll (**Figure 11**). When tested in the upright, activity of this unit slightly increased during OKN/OKAN to the left and decreased during OKN/OKAN to the right (**Figures 11A,E,I,M**). The relationship to the yaw component of OKN/OKAN remained the same when the animal was tilted up to 90° prone or right side down (not shown). When the animal was tilted left side down or supine, however, the changes in the firing rate became more evident and was associated with increased pitch and roll components (*y*), indicating a cross-coupled component from yaw (*z*). Thus, this neuron coded both of the cross-coupled components of velocity storage to roll and pitch. Specifically, cross-coupled upward pitch (**Figures 11A–D**) and CW from the

animal's point of view roll (**Figures 11E–H**) were associated with increases in the neuronal firing rate during OKN/OKAN to the left, while the cross-coupled downward pitch (**Figures 11I–L**) and CCW roll (**Figures 11M–P**) were associated with a decrease in the neuronal firing rate during OKN/OKAN to the right.

Racemic baclofen 6 mg (1.7 mg/kg) was injected IM and OKN/OKAN testing was repeated 30 min after injection. The slow phases of OKAN and changes in neuronal firing rate were completely eliminated, indicating that the velocity storage mechanism had been inactivated by the baclofen, and the firing rate of the neuron no longer had activity related to either the yaw or pitch components of the VOR (25). We did not have an opportunity to test the other five neurons for relations of their activity to cross-coupled roll OKAN. But, it is likely that at least some of them would have shown that relationship.

In summary, **Figures 9–11** demonstrate that VO and VPS neurons code various aspects of the cross-coupled components of velocity storage. Six neurons (6/13, 46%) code only the horizontal component of velocity storage while cross-coupling occurs to the vertical plane. Six neurons code cross-coupled pitch and

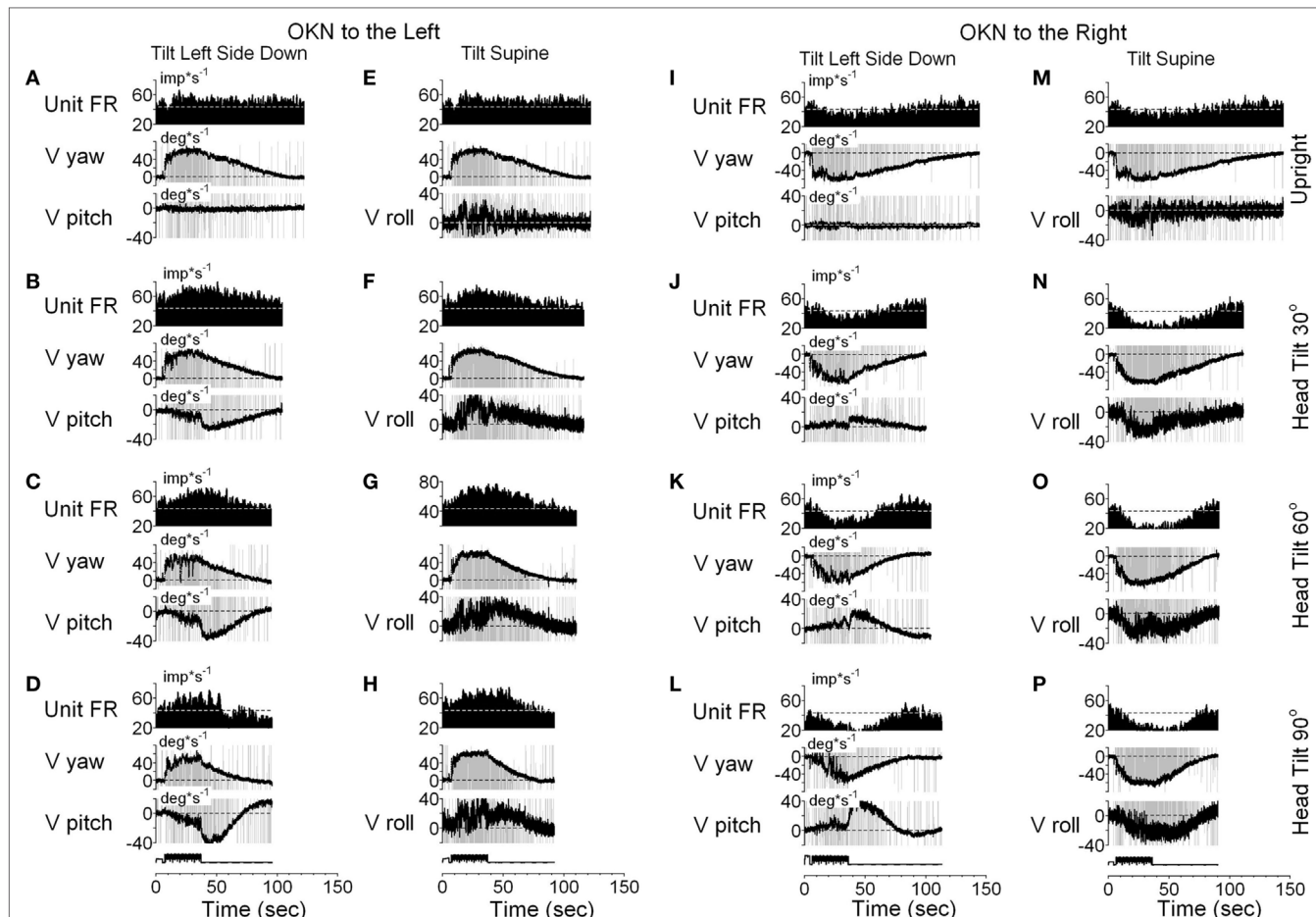


FIGURE 11 | Unit firing rates and yaw (V yaw), pitch (V pitch), and roll (V pitch) slow phase eye velocities for a VPS neuron that received input from the ipsilateral anterior canal during optokinetic nystagmus (OKN)/optokinetic after-nystagmus to the left (**A–H**) and to the right (**I–P**). This neuron was tested in the left side down (**A–D,I–L**) and supine (**E–H,M–P**) positions. In each position, the neuron was tested while upright (**A,E,I,M**) or while tilted 30° (**B,F,J,N**), 60° (**C,G,K,O**), or 90° (**D,H,L,P**). Data in panel (**E**) are duplicate of panel (**A**), and data in panel (**M**) are duplicate of panel (**I**). This was done to organize data in columns to simplify comparison.

one coded the cross-coupled roll component of OKAN (7/13, 54%). Neurons shown in **Figures 10** and **11** coded the cross-coupled vertical component of velocity storage in one (**Figure 10**, downward) or in both directions (**Figure 11**). Only one neuron, however, was tested for its relationship to the cross-coupled roll component of OKAN (**Figure 11**). Thus, the actual number of neurons that coded spatial orientation properties of velocity storage could be greater than 54%.

DISCUSSION

We characterized 33 VO and 11 vestibular-pause-saccade (VPS) neurons, recorded in the medial and SVN of alert cynomolgus monkeys. Using a newly developed technique, cells were studied for long periods during yaw rotation of the animals and visual surround while the monkeys were upright, prone and supine, and on-side.

Previous studies have shown the relationship of VO and VPS neurons to the time constant of velocity storage induced

by angular rotation and OKN (4, 17). It was further demonstrated that velocity storage is implemented by cross connections between the rostral and MVN on the left and right sides (20, 21). The cross connections are GABA_A-ergic (22–24) and are under control of the cerebellar nodulus, which is critical for controlling spatial orientation of velocity storage as well as its temporal properties (61–64). It is likely that VO neurons generate velocity storage, while VPS neurons are located in the path from the velocity storage integrator to the oculomotor plant, since their activity ceases during periods of drowsiness (3). The previous studies of velocity storage suggested that VO and VPS neurons should code all aspect of velocity storage including spatial orientation and habituation [see Ref. (15, 16, 25) for review]. However, due to technical limitations in recording of single neurons in three dimensions, a variety of tests that explore various aspects of velocity storage could not be done, limiting the understanding of how velocity storage is realized in three dimensions. The present study provides information that helps fill this gap.

All VO and VPS neurons had firing rates related to eye velocity during per- and post-rotatory nystagmus and OKAN. However, neuronal firing rates of the majority of tested neurons were tightly correlated with the horizontal component of velocity storage (**Figure 8**). Some of them (46%), however, were closely correlated with the horizontal component of velocity storage in head coordinates, regardless of head orientation in space (**Figure 9**). Other neurons were correlated with the cross-coupled components of velocity storage from yaw-to-pitch or yaw-to-roll (54%), during OKAN about tilted axes (**Figures 10 and 11**). Neuron shown in **Figure 11** is similar to the other six neurons like the one shown in **Figure 9**. It had no relation to cross-coupled vertical component of OKAN. Firing rate of this neuron was clearly correlated to cross-coupled roll component of OKAN. Unfortunately, the other six neurons were not tested with animal in prone and supine positions. Thus, actual presence of neurons that coded velocity storage in spatial coordinates could be much higher than 54%. Together, the neurons, shown in **Figures 10 and 11**, code the horizontal component of eye velocity in spatial coordinates, as the head was reoriented from the spatial vertical. Thus, this study demonstrates that the majority of VO and VPS neurons are related to various aspects of the velocity storage mechanism. The time constants of a majority of the neurons were comparable to the time constant of velocity storage determined from ocular nystagmus (**Figure 8**).

Sixty-five percent of VO and VPS neurons in this study had asymmetrical responses for rotation to the left and to the right. The existence of such neurons is not unexpected, since the firing rates of many primary vestibular afferents increase to high levels during ipsilateral rotation but decrease to 0 during contralateral rotation, i.e., these primary afferents that, presumably, provide input to VO and VPS neurons have asymmetric responses (1).

The existence of central vestibular neurons sensitive to rotation in only one direction indicates that the velocity storage signals for rotation to the left and to the right are coded by different neurons. Further, these asymmetric neurons are clustered on opposite sides of the brainstem in the medial and SVN. These data indicate that the three-dimensional velocity storage integrator is composed of directional subsets of neurons that are likely the bases for the spatial characteristics of velocity storage. The majority of them receive input from the contralateral side. Thus, the interconnections between the neural subsets on either side are critical for the maintenance of this function, since velocity storage is completely lost when the axonal projections between the left and right medial and SVN are sectioned (20, 21).

Sinusoidal oscillations have typically been used to characterize the sensitivities of central vestibular neurons (65, 66). Our study indicates that sinusoidal rotation may not provide an accurate estimate of the characteristics of those neurons with asymmetric responses, especially those related to velocity storage. It has previously been shown that the sensitivity of VO and VPS neurons to head free gaze shifts cannot be predicted based on sinusoidal head-fixed oscillations (67, 68). Our study suggests that the reason may be due to the asymmetry of many VO and VPS neurons for rotations in alternate directions.

How Neurons in This Study Fit to the Model of the Velocity Storage

This study demonstrates that VO and VPS neurons are not a uniform group of Type I and Type II neurons, consistent with earlier findings (3). Rather, the neurons recorded in this study consist of a variety of neural subgroups that implement the long time constant as well as the neurons that likely to implement the direct vestibular pathway that goes around velocity storage (**Figure 1**). The neurons that are involved in the realization of velocity storage probably project across the midline implementing a bilateral integrator, similar to that proposed for the velocity-position integrator (69, 70). Neurons that respond to rotation only in one direction also code velocity storage only for that direction. The bilateral model of velocity storage could be formed as two unilateral integrators connected to each other with cross-projections. The implementation of the velocity storage integrator in this fashion would be consistent with the abolition of velocity storage when the midline is cut (20, 21). This would also explain why the time constants of rotations in opposite directions are almost never identical (**Figures 5A–C**). It is also probable that the nodulus projects to these neurons (33), carrying otolith-related information (71) to implement the orientation properties of these velocity storage-related neurons (61, 63, 64).

We also demonstrated that some neurons coded velocity storage in head or canal coordinates. The firing rates of such neurons correlated with the horizontal (**Figure 8**) or the vertical (**Figure 7**) components of the VOR in one or both directions, but they were not related to the cross-coupled components of velocity storage. Such neurons could be involved in implementing the long time constant of the aVOR, but probably would not receive otolith information from the nodulus to be involved in spatial orientation of velocity storage. Moreover, it indicates that velocity storage may be implemented in canal coordinates and transformed to head coordinates within the vestibular nuclei. Thus, this study has demonstrated that the neural components in the vestibular nuclei have capability to not only implement the three-dimensional properties of velocity but also are part of the direct pathway around it as predicted by the model (**Figure 1**).

Summary of Our Modeling Approach as Compared to Those of Others

There have been various models put forward that attempt to give different interpretations of velocity storage and the role it plays in vestibular processing (72–74) in opposition to the 3-D mechanistic velocity storage model presented by Raphan and Cohen (15, 16). One recent model seeks to put velocity storage in context of a Bayesian model of vestibular processing (74). In this framework, semicircular canal output drives an inverse model of semicircular canal dynamics, which attempts to reconstruct rotational velocity by integrating canal signals over time, but has a low-frequency cutoff to avoid accumulation of noise in the integrator. This is followed by a second internal model, which utilizes this reconstructed rotation velocity to compute an internal estimate of tilt and inertial acceleration. This internal model too is band-limited so as to limit the accumulation of drift in the estimate of tilt/translation

over time. It is assumed that as a result of these two low-pass filters, low-frequency translation can be misinterpreted as tilt. These filters are conceptualized as two Bayesian priors of zero rotation velocity and zero linear acceleration, respectively (74) and velocity storage arises due to noise distribution of these Bayesian filters. However, regardless of how these filters are conceptualized (Bayesian or otherwise), these are global behavioral and perceptual models (75). Basing these filters on some obscure notion that they are there to separate tilt from translation (76–79) has not been related to neural activity and is not a credible approach to modeling the neural activity presented in this study. Moreover, it is beyond the scope of this study to examine and compare all models of velocity storage and how they are related to the data presented.

There are other more fundamental objections to the Bayesian tilt-translation-based model. An implication of the hypothesis that there is continual updating of the estimate of gravity in the Bayesian based model is not consistent with results obtained from centrifugation in the absence of gravity (80, 81). While in orbital space flight, gravity is imperceptible to the otoliths, and tilts of the linear acceleration vector only appear during centrifugation. Models, which depend on the continuous computation of gravity, and extracting tilt from translation based on Bayesian priors, would predict that during space flight there would be no perception of tilt or OCR during centrifugation, only perception of translation and compensatory eye movements in response to this translation. This idea had been formalized as the otolith tilt-translation reinterpretation hypothesis (82, 83). Results from flight experiments are contrary to these predictions. Centrifugation during space flight induced a clear perception of tilt (80). It also produced OCR, which was the same as that induced by similar linear acceleration on earth during static tilt (81).

A simpler explanation for the maintenance of perception and ocular tilt in the absence of gravity is that instantaneous tilt of the head is determined by a computation of head orientation relative to the net GIA, which is used as the spatial vertical reference (80, 81). Thus, there may be no need for continuous updating of the acceleration of gravity relative to the head on earth, as implied by the Observer or Bayesian based models (72, 74, 78). Orientation could simply be determined mechanistically by a three-dimensional filtering mechanism, which automatically determines the “head vertical re GIA estimate” through the eigenvectors of the system matrix, possibly controlled by the cerebellum (84–86). The neural recordings in this study and its direct relationship to the model support this hypothesis.

In contrast to the Bayesian and internal models that have shown no direct link to central vestibular neural activity, we have previously demonstrated a direct link of our model to neural activity in the central vestibular system in a number of studies. We have demonstrated that otolith polarization vectors of VO neurons can be adapted and that the polarization vector of VO neurons adapt toward the axis of gravity if animals are positioned away from spatial vertical (29, 49). Interestingly, EHV and PVP neurons (87) as well as central otolith neurons (45) have a very limited adaptive capability of their polarization vectors. The present study for the first time has related unit activity recorded

in the central vestibular system to the mechanistic three-dimensional model of velocity storage presented by Raphan and Cohen (12, 14, 16). We, therefore, reject the notion that velocity storage is an outcome of noise in differentiating tilt from translation computations (74). Moreover, we do not see how such a notion can be reflected in the central VO neurons presented in this paper. In contrast, the head vertical and its relationship to the spatial vertical are features of the Raphan–Cohen model and is reflected in the eigenvalues and eigenvectors of the system matrix, H (**Figure 1**), and is a function of differential otolith activation (12, 14).

Some Clinical Implications of Velocity Storage

The time constant of vestibular nystagmus is an important measure when evaluating vestibular abnormalities (88, 89). Typically, the time constant of velocity storage is reduced with unilateral and bilateral vestibular lesions. It can also be habituated by repeated rotations (90, 91). Such reduction reduces the susceptibility to motion sickness (25, 92, 93). This shows that velocity storage is not only critical for spatial orientation with regard to gravity, but it also serves as an input to the sympathetic system, and motion sickness susceptibility can be reduced by shortening the VOR (velocity storage) time constant (94). Studies in monkeys also demonstrate that prolonged oscillation in roll while rotating about a spatial vertical axis induces oscillatory modulations of nystagmus (95) similar to those in patients with the Mal de Debarquement Syndrome (MdDS) (94, 96, 97). Thus, changes in velocity storage are postulated to be responsible for the postural instability induced by prolong travel on water (96). Of particular significance is the fact that the MdDS impacts the body postural system, resulting in rocking, or swaying at 0.2 Hz, showing that the velocity storage integrator not only is associated with spatial orientation, eye movements and activation of the sympathetic system, but also with descending vestibulo-spinal projections that are associated with strong postural instability during the MdDS. While data in this study were obtained from monkeys they are still directly applicable to humans. The works of Jell and colleagues (98, 99) and from our laboratory (100) have shown that the observed time constant is dependent on the size and quality of the stimulus. Moreover, even when the stimulus is such that the time constants are small, the cross-coupling, which depends on the relationship of the roll, pitch, and yaw time constants, is still maintained (101). Thus, further shortening of the yaw time constant or adapting its orientation clearly reduces susceptibility to motion sickness in that rolling the head at the frequency of rocking/swaying in MdDS while velocity storage is activated by OKN significantly reduce MdDS symptoms.

CONCLUSION

This study identifies a mechanism that is widely distributed among vertebrate species that converts the activity in semicircular canal and otolith organ afferents to code angular velocity of the head in three dimensions. Located in the medial and SVN,

it has an additional component, particularly evident in primates and some mammals, namely a mechanism that orients the axis of eye rotation and probably balance to the spatial vertical. The data in this report provide the first three-dimensional study of the neurons that underlie this function. There is no reason to hypothesize that the velocity storage mechanism is involved in separating tilt from translation. There are no specific neural recordings to date that have related neural mechanisms to velocity storage and the relation of velocity storage to the tilt-translation hypothesis is unsubstantiated speculation (74, 102, 103). The data presented here is the first of its kind to clearly show neural recordings that are related to a mechanistic three-dimensional model of velocity storage [(12, 14); see Ref. (16) for review]. It is critical now to determine how orientation is controlled by the vestibulocerebellum to determine the fundamental aspect of balance, which is simply at best, is body orientation to the spatial vertical. In support of this idea, our previous findings indicate that orientation of otolith convergent input to VO and vestibular-pause-saccade (VPS) neurons could be adapted by prolong head side-down orientation (29, 87). Such plasticity suggests the possibility of development of new techniques to enhance movement and orientation in three-dimensional space.

REFERENCES

1. Goldberg JM, Fernandez C. Physiology of peripheral neurons innervating semicircular canals of the squirrel monkey. I. Resting discharge and response to constant angular accelerations. *J Neurophysiol* (1971) 34:635–60.
2. Mach E. *Grundlinien der Lehre von den Bewegungsempfindungen*. Leipzig: Engelmann (1875).
3. Reisine H, Raphan T. Neural basis for eye velocity generation in the vestibular nuclei of alert monkeys during off-vertical axis rotation. *Exp Brain Res* (1992) 92:209–26. doi:10.1007/BF00227966
4. Waespe W, Henn V. Vestibular nucleus activity during optokinetic after-nystagmus (OKAN) in the alert monkey. *Exp Brain Res* (1977) 30:323–30.
5. Raphan T, Matsuo V, Cohen B. A velocity storage mechanism responsible for optokinetic nystagmus (OKN), optokinetic after-nystagmus (OKAN), and vestibular nystagmus. In: Baker R, Berthoz A, editors. *Control of Gaze by Brain Stem Neurons*. North Holland, Amsterdam: Elsevier (1977). p. 37–47.
6. Raphan T, Matsuo V, Cohen B. Velocity storage in the vestibulo-ocular reflex arc (VOR). *Exp Brain Res* (1979) 35:229–48. doi:10.1007/BF00236613
7. Robinson DA. Linear addition of optokinetic and vestibular signals in the vestibular nucleus. *Exp Brain Res* (1977) 30:447–50.
8. Cohen B, Matsuo V, Raphan T. Quantitative analysis of the velocity characteristics of optokinetic nystagmus and optokinetic after-nystagmus. *J Physiol* (1977) 270:321–44. doi:10.1113/jphysiol.1977.sp011955
9. Mowrer OH. The influence of vision during bodily rotation upon the duration of post-rotational vestibular nystagmus. *Acta Otolaryngol* (1937) 25:351–64. doi:10.3109/00016483709127972
10. Ter Braak JWG. Untersuchungen ueber optokinetischen Nystagmus. *Arch Neerl Physiol* (1936) 21:309–76.
11. Dai MG, Raphan T, Cohen B. Characterization of yaw to roll cross-coupling in the three-dimensional structure of the velocity storage integrator. *Ann N Y Acad Sci* (1992) 656:829–31. doi:10.1111/j.1749-6632.1992.tb25266.x
12. Dai MJ, Raphan T, Cohen B. Spatial orientation of the vestibular system: dependence of optokinetic after-nystagmus on gravity. *J Neurophysiol* (1991) 66:1422–39.
13. Raphan T, Dai M, Cohen B. Spatial orientation of the vestibular system. *Ann N Y Acad Sci* (1992) 656:140–57. doi:10.1111/j.1749-6632.1992.tb25205.x
14. Raphan T, Sturm D. Modeling the spatio-temporal organization of velocity storage in the vestibulo-ocular reflex (VOR) by optokinetic studies. *J Neurophysiol* (1991) 66:1410–21.
15. Cohen B, Raphan T. The physiology of the vestibuloocular reflex (VOR). In: Highstein SM, Fay RR, Popper AM, editors. *Springer Handbook of Auditory Research. The Vestibular System*. New York: Springer (2004). p. 235–85.
16. Raphan T, Cohen B. The vestibulo-ocular reflex in three dimensions. *Exp Brain Res* (2002) 145:1–27. doi:10.1007/s00221-002-1067-z
17. Waespe W, Henn V. Neuronal activity in the vestibular nuclei of the alert monkey during vestibular and optokinetic stimulation. *Exp Brain Res* (1977) 27:523–38. doi:10.1007/BF00239041
18. Waespe W, Henn V. Conflicting visual vestibular stimulation and vestibular nucleus activity in alert monkeys. *Exp Brain Res* (1978) 33:203–11. doi:10.1007/BF00238060
19. Yokota J, Reisine H, Cohen B. Nystagmus induced by electrical stimulation of the vestibular and prepositus hypoglossi nuclei in the monkey: evidence for site of induction of velocity storage. *Exp Brain Res* (1992) 92:123–38. doi:10.1016/0006-8993(92)91436-I
20. Katz E, Vianney de Jong JM, Büttner-Ennever JA, Cohen B. Effects of midline medullary lesions on velocity storage and the vestibulo-ocular reflex. *Exp Brain Res* (1991) 87:505–20. doi:10.1007/BF00227076
21. Wearne S, Raphan T, Cohen B. Contribution of vestibular commissural pathways to spatial orientation of the angular vestibuloocular reflex. *J Neurophysiol* (1997) 78:1193–7.
22. Holstein GR, Martinelli GP, Cohen B. Immunocytochemical visualization of L-baclofen-sensitive GABA_A binding sites in the medial vestibular nucleus (MVN). *Ann N Y Acad Sci* (1992) 656:933–6. doi:10.1111/j.1749-6632.1992.tb25299.x
23. Holstein GR, Martinelli GP, Cohen B. L-baclofen-sensitive GABA_A binding sites in the medial vestibular nucleus localized by immunocytochemistry. *Brain Res* (1992) 581:175–80. doi:10.1016/0006-8993(92)90361-C
24. Holstein GR, Martinelli GP, Cohen B. The ultrastructure of GABA-immunoreactive vestibular commissural neurons related to velocity storage in the monkey. *Neuroscience* (1999) 93:171–81. doi:10.1016/S0306-4522(99)00142-6
25. Cohen B, Dai M, Yakushin SB, Raphan T. Baclofen, motion sickness susceptibility and the neural basis for velocity storage. *Prog Brain Res* (2008) 171:543–53. doi:10.1016/S0079-6123(08)00677-8
26. Cohen B, Helwig D, Raphan T. Baclofen and velocity storage: a model of the effects of the drug on the vestibulo-ocular reflex in the rhesus monkey. *J Physiol* (1987) 393:703–25. doi:10.1113/jphysiol.1987.sp016849

ETHICS STATEMENT

The surgical procedures and experimental protocol conformed to the Guide for the Care and Use of Laboratory Animals and were approved by the Institutional Animal Care and Use Committee of Icahn School of Medicine at Mount Sinai.

AUTHOR CONTRIBUTIONS

SY: planning experiments, collection of all data, data processing, data analyses, figure making, and writing of this manuscript. TR: planning experiments, data analyses, figure making, and writing of this manuscript. BC: planning experiments, figure making, and writing of this manuscript.

ACKNOWLEDGMENTS

The authors thank Evgeny Bucharin for technical support that made this project feasible. The authors also thank Rupa Mirmira for editorial support. This study was supported by NIDCD grant DC037087 to SY, by NEI grant EY04148 to TR, and by Core NIDCD Center Grant DC05204 to BC.

27. Blazquez PM, Davis-Lopez de Carrizosa MA, Heiney SA, Highstein SM. Neuronal substrates of motor learning in the velocity storage generated during optokinetic stimulation in the squirrel monkey. *J Neurophysiol* (2007) 97:1114–26. doi:10.1152/jn.00983.2006
28. Eron JN, Cohen B, Raphan T, Yakushin SB. Recording from the same cell in the vestibular nuclei over prolonged periods. *J Gravit Physiol* (2007) 14:69–70.
29. Eron JN, Cohen B, Raphan T, Yakushin SB. Adaptation of orientation vectors of otolith-related central vestibular neurons to gravity. *J Neurophysiol* (2008) 100:1686–90. doi:10.1152/jn.90289.2008
30. Sirota MG, Babaev BM, Belozerova IN, Nyrova AN, Yakushin SB, Kozlovskaya IB. Neuronal activity of nucleus vestibularis during coordinated movement of eyes and head in microgravitation. *Physiologist* (1988) 31:8–9.
31. Yakushin SB, Raphan T, Cohen B. Spatial properties of otolith units recorded in the vestibular nuclei. *Ann N Y Acad Sci* (1999) 871:458–62. doi:10.1111/j.1749-6632.1999.tb09217.x
32. Yakushin SB, Raphan T, Cohen B. Spatial properties of central vestibular neurons. *J Neurophysiol* (2006) 95:464–78. doi:10.1152/jn.00459.2005
33. Meng H, Blázquez PM, Dickman JD, Angelaki DE. Diversity of vestibular nuclei neurons targeted by cerebellar nodulus inhibition. *J Physiol* (2014) 592:171–88. doi:10.1113/jphysiol.2013.259614
34. Yakushin SB, Sheliga B, Raphan T, Cohen B. Vestibular-only (VO) neurons and the spatial orientation of velocity storage. *Soc Neurosci* (1996) 22:661.
35. Raphan T. Modeling control of eye orientation in three dimensions. I. Role of muscle pulleys in determining saccadic trajectory. *J Neurophysiol* (1998) 79:2653–67.
36. Newlands SD, Wei M. Tests of linearity in the responses of eye-movement-sensitive vestibular neurons to sinusoidal yaw rotation. *J Neurophysiol* (2013) 109:2571–84. doi:10.1152/jn.00930.2012
37. Scudder CA, Fuchs AF. Physiological and behavioral identification of vestibular nucleus neurons mediating the horizontal vestibuloocular reflex in trained rhesus monkeys. *J Neurophysiol* (1992) 68:244–64.
38. Yakushin SB, Reisine H, Büttner-Ennever J, Raphan T, Cohen B. Functions of the nucleus of the optic tract (NOT). I. Adaptation of the gain of the horizontal vestibulo-ocular reflex. *Exp Brain Res* (2000) 131:416–32. doi:10.1007/s002219900302
39. Judge SJ, Richmond BJ, Chu FC. Implantation of magnetic search coils for measurement of eye position: an improved method. *Vision Res* (1980) 20:535–8. doi:10.1016/0042-6989(80)90128-5
40. Robinson DA. A method of measuring eye movement using a scleral search coil in a magnetic field. *IEEE Trans Biomed Eng* (1963) 10:137–45. doi:10.1109/TBMEEL.1963.4322822
41. Cohen B, Kozlovskaya IB, Raphan T, Solomon D, Helwig D, Cohen N, et al. Vestibuloocular reflex of rhesus monkeys after spaceflight. *J Appl Physiol* (1992) 73:121S–31S.
42. Yakushin SB, Dai M, Suzuki J-I, Raphan T, Cohen B. Semicircular canal contributions to the three-dimensional vestibuloocular reflex: a model-based approach. *J Neurophysiol* (1995) 74:2722–38.
43. Yakushin SB, Raphan T, Buttner-Ennever JA, Suzuki J, Cohen B. Spatial properties of central vestibular neurons of monkeys after bilateral lateral canal nerve section. *J Neurophysiol* (2005) 94:3860–71. doi:10.1152/jn.01102.2004
44. Smith GA, Kastella KG, Randal DC. A stereotaxic atlas of the brainstem for *Macaca mulatta* in the sitting position. *J Comp Neurol* (1972) 145:1–24. doi:10.1002/cne.901450102
45. Eron JN, Cohen B, Raphan T, Yakushin SB. Adaptation of orientation of central otolith-only neurons. *Ann N Y Acad Sci* (2009) 1164:367–71. doi:10.1111/j.1749-6632.2009.03848.x
46. Fuchs AF, Kimm J. Unit activity in vestibular nucleus of the alert monkey during horizontal angular acceleration and eye movement. *J Neurophysiol* (1975) 38:1140–61.
47. Keller EL, Kamath BY. Characteristics of head rotation and eye movement related neurons in alert monkey vestibular nucleus. *Brain Res* (1975) 100:182–7. doi:10.1016/0006-8993(75)90257-7
48. Roy JE, Cullen KE. Selective processing of vestibular reafference during self-generated head motion. *J Neurosci* (2001) 21:2131–42.
49. Eron JN, Cohen B, Raphan T, Yakushin SB. Differential coding of head rotation by lateral-vertical canal convergent central vestibular neurons. *Prog Brain Res* (2008) 171:313–8. doi:10.1016/S0079-6123(08)00645-6
50. Dickman JD, Angelaki DE. Vestibular convergence patterns in vestibular nuclei neurons of alert primates. *J Neurophysiol* (2002) 88:3518–33. doi:10.1152/jn.00518.2002
51. Gdowski GT, McCrea RA. Neck proprioceptive inputs to primate vestibular nucleus neurons. *Exp Brain Res* (2000) 135:511–26. doi:10.1007/s00210000542
52. Sadeghi SG, Mitchell DE, Cullen KE. Different neural strategies for multimodal integration: comparison of two macaque monkey species. *Exp Brain Res* (2009) 195:45–57. doi:10.1007/s00221-009-1751-3
53. Keller EL, Daniels PD. Oculomotor related interaction of vestibular and visual stimulation in vestibular nucleus cells in alert monkey. *Exp Neurol* (1975) 46:187–98. doi:10.1016/0014-4886(75)90041-2
54. Boyle R, Büttner U, Markert G. Vestibular nuclei activity and eye movements in the alert monkey during sinusoidal optokinetic stimulation. *Exp Brain Res* (1985) 57:362–9. doi:10.1007/BF00236542
55. Singh A, Thau GE, Raphan T, Cohen B. Detection of saccades by a maximum likelihood ratio criterion. *Proc. 34th Ann. Conf. Eng. Biol.* Houston, TX (1981). 136 p.
56. Yakushin SB, Raphan T, Suzuki J-I, Arai Y, Cohen B. Dynamics and kinematics of the angular vestibulo-ocular reflex in monkey: effects of canal plugging. *J Neurophysiol* (1998) 80:3077–99.
57. Keppel G. *Design and Analysis: A Researcher's Handbook*. Englewood Cliffs, NJ: Prentice Hall (1991).
58. Schiff D, Cohen B, Raphan T. Nystagmus induced by stimulation of the nucleus of the optic tract (NOT) in the monkey. *Exp Brain Res* (1988) 70:1–14.
59. Yakushin SB, Gizzii M, Reisine H, Raphan T, Büttner-Ennever J, Cohen B. Functions of the nucleus of the optic tract (NOT). II. Control of ocular pursuit. *Exp Brain Res* (2000) 131:433–47. doi:10.1007/s002219900302
60. Reisine H, Cohen B. Stimulation and single-unit studies of velocity storage in the vestibular and prepositus hypoglossi nuclei of the monkey. *Ann N Y Acad Sci* (1992) 656:966–8. doi:10.1111/j.1749-6632.1992.tb25309.x
61. Sheliga BM, Yakushin SB, Silvers A, Raphan T, Cohen B. Control of spatial orientation of the angular vestibulo-ocular reflex by the nodulus and uvula of the vestibulocerebellum. *Ann N Y Acad Sci* (1999) 871:94–122. doi:10.1111/j.1749-6632.1999.tb09178.x
62. Solomon D, Cohen B. Stimulation of the nodulus and uvula discharges velocity storage in the vestibulo-ocular reflex. *Exp Brain Res* (1994) 102:57–68. doi:10.1007/BF00232438
63. Waespe W, Cohen B, Raphan T. Dynamic modification of the vestibulo-ocular reflex by the nodulus and uvula. *Science* (1985) 228:199–202. doi:10.1126/science.3871968
64. Wearne S, Raphan T, Cohen B. Nodulo-uvular control of the central vestibular dynamics determines spatial orientation of the angular vestibulo-ocular reflex. *Ann N Y Acad Sci* (1996) 781:364–84. doi:10.1111/j.1749-6632.1996.tb15713.x
65. Dickman JD, Angelaki DE. Dynamics of vestibular neurons during rotational motion in alert rhesus monkeys. *Exp Brain Res* (2004) 155:91–101. doi:10.1007/s00221-003-1692-1
66. Newlands SD, Lin N, Wei M. Response linearity of alert monkey non-eye movement vestibular nucleus neurons during sinusoidal yaw rotation. *J Neurophysiol* (2009) 102:1388–97. doi:10.1152/jn.090914.2008
67. Cullen KE, Roy JE, Sylvestre PA. Signal processing by vestibular nuclei neurons is dependent on the current behavioral goal. *Ann N Y Acad Sci* (2001) 942:345–63. doi:10.1111/j.1749-6632.2001.tb03759.x
68. McCrea RA, Gdowski GT, Boyle R, Belton T. Firing behavior of vestibular neurons during active and passive head movements: vestibulo-spinal and other non-eye-movement related neurons. *J Neurophysiol* (1999) 82:416–28.
69. Anastasio TJ, Robinson DA. The distributed representation of vestibulo-oculomotor signals by brain-stem neurons. *Biol Cybern* (1989) 61:79–88. doi:10.1007/BF00204592
70. Galiana HL, Outerbridge JS. A bilateral model for central neural pathways in vestibuloocular reflex. *J Neurophysiol* (1984) 51:210–41.
71. Meng H, Laurens J, Blázquez PM, Angelaki DE. In vivo properties of cerebellar interneurons in the macaque caudal vestibular vermis. *J Physiol* (2015) 593:321–30. doi:10.1113/jphysiol.2014.278523
72. Merfeld DM. Modeling the vestibulo-ocular reflex of the squirrel monkey during eccentric rotation and roll tilt. *Exp Brain Res* (1995) 106:123–34. doi:10.1007/BF00241361

73. Karmali F, Merfeld DM. A distributed, dynamic, parallel computational model: the role of noise in velocity storage. *J Neurophysiol* (2012) 108:390–405. doi:10.1152/jn.00883.2011
74. Laurens J, Angelaki DE. The functional significance of velocity storage and its dependence on gravity. *Exp Brain Res* (2011) 210:407–22. doi:10.1007/s00221-011-2568-4
75. MacNeilage PR, Ganesan N, Angelaki DE. Computational approaches to spatial orientation: from transfer functions to dynamic Bayesian inference. *J Neurophysiol* (2008) 100:2981–96. doi:10.1152/jn.90677.2008
76. Mayne R. A systems concept of the vestibular organ. In: Kornhuber HH, editor. *Handbook of Sensory Physiology, Vol VI. Vestibular System Part 2: Psychophysics < Applied Aspects and General Interpretations*. Berlin, Heidelberg, New York: Springer (1974). p. 493–580.
77. Angelaki DE, McHenry MQ, Dickman JD, Newlands SD, Hess BJ. Computation of inertial motion: neural strategies to resolve ambiguous otolith information. *J Neurosci* (1999) 19:316–27.
78. Angelaki DE, Merfeld DM, Hess BJ. Low-frequency otolith and semicircular canal interactions after canal inactivation. *Exp Brain Res* (2000) 132:539–49. doi:10.1007/s002210000364
79. Hess BJ, Angelaki DE. Internal processing of vestibulo-ocular signals. *Ann N Y Acad Sci* (1999) 871:148–61. doi:10.1111/j.1749-6632.1999.tb09181.x
80. Clément G, Moore ST, Raphan T, Cohen B. Perception of tilt (somatogravic illusion) in response to sustained linear acceleration during space flight. *Exp Brain Res* (2001) 138:410–8. doi:10.1007/s002210100706
81. Moore ST, Clément G, Raphan T, Cohen B. Ocular counterrolling induced by centrifugation during orbital space flight. *Exp Brain Res* (2001) 137:323–35. doi:10.1007/s002210000669
82. Parker DE, Reschke MF, Arrott AP, Homick JL, Lichtenberg BK. Otolith tilt-translation reinterpretation following prolonged weightlessness: implications for preflight training. *Aviat Space Environ Med* (1985) 56: 601–6.
83. Young LR. *Perception of the Body in Space: Mechanisms, Handbook of Physiology. The Nervous System Sensory Processes*. Bethesda, MD: Lippincott Williams and Wilkins (1984). p. 1023–66.
84. Paige GD, Seidman SH. Characteristics of the VOR in response to linear acceleration. *Ann N Y Acad Sci* (1999) 871:123–35. doi:10.1111/j.1749-6632.1999.tb09179.x
85. Raphan T, Wearne S, Cohen B. Modeling the organization of the linear and angular vestibulo-ocular reflexes. *Ann N Y Acad Sci* (1996) 781:348–63. doi:10.1111/j.1749-6632.1996.tb15712.x
86. Wearne S, Raphan T, Cohen B. Effects of tilt of the gravito-inertial acceleration vector on the angular vestibuloocular reflex during centrifugation. *J Neurophysiol* (1999) 81:2175–90.
87. Kolesnikova OV, Raphan T, Cohen B, Yakushin SB. Orientation adaptation of eye movement-related vestibular neurons due to prolonged head tilt. *Ann N Y Acad Sci* (2011) 1233:214–8. doi:10.1111/j.1749-6632.2011.06176.x
88. Bárány R. Untersuchungen ueber den vom Vestibularapparat des Ohres reflektorisch ausgelösten Nystagmus und seine Begleiterscheinungen. *Monatsschrift Ohrenheilkunde* (1906) 4:193–297.
89. Brandt T. *Vertigo: Its Multisensory Syndromes*. London, Berlin, New York: Springer (1998).
90. Baloh RW, Henn V, Jäger J. Habituation of the human vestibulo-ocular reflex with low-frequency harmonic acceleration. *Am J Otolaryngol* (1982) 3:235–41. doi:10.1016/S0196-0709(82)80061-6
91. Cohen H, Cohen B, Raphan T, Waespe W. Habituation and adaptation of the vestibuloocular reflex: a model of differential control by the vestibulocerebellum. *Exp Brain Res* (1992) 90:526–38. doi:10.1007/BF00230935
92. Dai M, Raphan T, Cohen B. Prolonged reduction of motion sickness sensitivity by visual-vestibular interaction. *Exp Brain Res* (2011) 210:503–13. doi:10.1007/s00221-011-2548-8
93. Bos JE, Bles W, de Graaf B. Eye movements to yaw, pitch, and roll about vertical and horizontal axes: adaptation and motion sickness. *Aviat Space Environ Med* (2002) 73:436–44.
94. Dai M, Sofroniou S, Kunin M, Raphan T, Cohen B. Motion sickness induced by off-vertical axis rotation (OVAR). *Exp Brain Res* (2010) 204(2):207–22. doi:10.1007/s00221-010-2305-4
95. Dai M, Raphan T, Cohen B. Adaptation of the angular vestibulo-ocular reflex to head movements in rotating frames of reference. *Exp Brain Res* (2009) 195:553–67. doi:10.1007/s00221-009-1825-2
96. Dai M, Cohen B, Smouha E, Cho C. Readaptation of the vestibulo-ocular reflex relieves the mal de débarquement syndrome. *Front Neurol* (2014) 5:124. doi:10.3389/fneur.2014.00124
97. Dai M, Cohen B, Cho C, Shin S, Yakushin SB. Treatment of the Mal de Débarquement syndrome, a one year follow up. *Front Neurol* (2017) 8:175. doi:10.3389/fneur.2017.00175
98. Jell RM, Ireland DJ, LaFortune S. Human optokinetic afternystagmus: slow-phase characteristics and analysis of the decay of slow-phase velocity. *Acta Otolaryngol* (1984) 98:462–71. doi:10.3109/00016488409107587
99. Jell RM, Ireland DJ, LaFortune S. Human optokinetic afternystagmus. Effects of repeated stimulation. *Acta Otolaryngol* (1985) 99:95–101. doi:10.3109/00016488509119150
100. Cohen B, Henn V, Raphan T, Dennett D. Velocity storage, nystagmus, and visual-vestibular interaction in humans. *Ann NY Acad Sci* (1981) 374:421–33. doi:10.1111/j.1749-6632.1981.tb30888.x
101. Gizzi M, Raphan T, Rudolph S, Cohen B. Orientation of human optokinetic nystagmus to gravity: a model-based approach. *Exp Brain Res* (1994) 99:347–60. doi:10.1007/BF00239601
102. Green AM, Angelaki DE. Internal models and neural computation in the vestibular system. *Exp Brain Res* (2010) 200:197–222. doi:10.1007/s00221-009-2054-4
103. Green AM, Angelaki DE. Multisensory integration: resolving sensory ambiguities to build novel representations. *Curr Opin Neurobiol* (2010) 20:353–60. doi:10.1016/j.conb.2010.04.009

Conflict of Interest Statement: The authors declare that the research was conducted in the absence of any commercial or financial relationships that could be construed as a potential conflict of interest.

Copyright © 2017 Yakushin, Raphan and Cohen. This is an open-access article distributed under the terms of the Creative Commons Attribution License (CC BY). The use, distribution or reproduction in other forums is permitted, provided the original author(s) or licensor are credited and that the original publication in this journal is cited, in accordance with accepted academic practice. No use, distribution or reproduction is permitted which does not comply with these terms.



Vestibulo-Ocular Reflex Stabilization after Vestibular Schwannoma Surgery: A Story Told by Saccades

Angel Batuecas-Caletrio^{1,2*}, Jorge Rey-Martinez³, Gabriel Trinidad-Ruiz⁴, Eusebi Matiño-Soler⁵, Santiago Santa Cruz-Ruiz^{1,2}, Angel Muñoz-Herrera^{1,2} and Nicolas Perez-Fernandez⁶

¹ Otoneurology Unit, Department of Otorhinolaryngology, University Hospital of Salamanca, IBSAL, Salamanca, Spain, ² Skull Base Unit, Department of Otorhinolaryngology, University Hospital of Salamanca, IBSAL, Salamanca, Spain, ³ Otolaryngology Unit ORL Gipuzkoa, Clinica Quiron, San Sebastian, Spain, ⁴ Otoneurology Unit, Department of Otorhinolaryngology, University Hospital of Badajoz, Badajoz, Spain, ⁵ Department of Otorhinolaryngology, Hospital General de Catalunya, Barcelona, Spain, ⁶ Otoneurology Unit, Department of Otorhinolaryngology, Clínica Universidad de Navarra, University Hospital and Medical School, University of Navarra, Pamplona, Spain

OPEN ACCESS

Edited by:

Sergio Carmona,
Instituto de Neurociencias
de Buenos Aires, Argentina

Reviewed by:

Aaron Camp,
University of Sydney, Australia

Eduardo Martín-Sanz,
Hospital de Getafe, Spain

*Correspondence:

Angel Batuecas-Caletrio
abatuc@yahoo.es

Specialty section:

This article was submitted to
Neuro-otology,
a section of the journal
Frontiers in Neurology

Received: 02 November 2016

Accepted: 11 January 2017

Published: 25 January 2017

Citation:

Batuecas-Caletrio A, Rey-Martinez J, Trinidad-Ruiz G, Matiño-Soler E, Cruz-Ruiz SS, Muñoz-Herrera A and Perez-Fernandez N (2017) Vestibulo-Ocular Reflex Stabilization after Vestibular Schwannoma Surgery: A Story Told by Saccades. *Front. Neurol.* 8:15. doi: 10.3389/fneur.2017.00015

Objective: To evaluate vestibular compensation *via* measurement of the vestibulo-ocular reflex (VOR) following vestibular schwannoma surgery and its relationship with changes in saccades strategy after surgery.

Patients: Thirty-six consecutive patients with vestibular schwannomas, without brain-stem compression, underwent surgical resection. Patients were recruited from University Hospital of Salamanca, Spain.

Methods: We assessed the age, sex, tumor size, degree of canalicular weakness, and preoperative video head impulse test (gain and saccade organization measured with PR score). Gain and saccade organization were compared with postoperative values at discharge and also at 1, 3, and 6 months. PR scores are a measure of the scatter of refixation saccades.

Results: Patients with normal preoperative caloric function had higher PR scores (saccades were scattered) following surgery compared to patients with significant pre-operative canal paresis ($p < 0.05$). VOR gain and the presence of covert/overt saccades preoperatively did not influence the PR score ($p > 0.05$), but a group of patients with very low VOR gain (<0.45) and covert/overt saccades before surgery had lower PR scores after surgery. The differences after 6 months were not significant.

Conclusion: Patients with more severe vestibular dysfunction before vestibular schwannoma surgery show significantly faster vestibular compensation following surgery, manifested by changes in VOR gain and PR score. The scatter of compensatory saccades (as measured by the PR score) may be a surrogate early marker of clinical recovery, given its relationship to the Dizziness Handicap Inventory.

Keywords: vestibular compensation, covert saccade, overt saccade, video head impulse test, PR score, vestibular schwannoma, caloric

INTRODUCTION

The head impulse test (HIT) was first described by Halmagyi and Curthoys in 1988 as a test of the vestibulo-ocular reflex (VOR) (1) and has become an established bedside assessment in the evaluation of the dizzy patient. It consists of providing a fast horizontal head thrusts while asking the subject to maintain gaze on a central target. Horizontal canal receptors ipsilateral to the direction of head movement are preferentially stimulated resulting in a reflexive eye movement with a low latency, similar velocity, and contrary direction to the head movement. In the presence of a peripheral vestibular deficit, the eyes move with the head and a “catch-up” saccade is required to bring gaze back toward the fixation target (2). The HIT is based on the detection of these “catch up” or refixation saccades.

The advent of the video HIT allowed online simultaneous recording of eye and head movements, facilitating measurement of the VOR gain (eye:head velocity) and identification of overt (occurring once the head movement is finished) (3) and covert (occurring while the head is still moving) (4, 5). In addition, the video HIT had allowed better qualitative and quantitative characterization of refixation saccades. The video HIT has a greater sensitivity and larger positive predictive value for vestibular dysfunction than the clinical HIT (6).

The taxonomy of refixation saccades captured during the video HIT is based on their latency relative to the onset of the head movement; each saccade can be analyzed individually and classified as either “overt” or “covert.” Another way to classify refixation saccades is based on the degree of synchrony of sequential refixation saccades. Using this method, saccades can be divided into two groups yielding either isochronic impulses (final look of the response is gathered) or asynchronous impulses (final look is scattered) (7). Interestingly, when the organization patterns of refixation saccades are considered, the scattered response correlates well with an uncompensated vestibular deficit in patients after surgery for a vestibular schwannoma and the gathered with a better clinical compensation (8).

Vestibular schwannoma is a slowly and irregularly growing benign tumor that induces a progressive vestibular function reduction. The main symptoms at diagnosis are hearing loss, imbalance, and tinnitus (9). The slow progressive reduction of vestibular function allows the gradual implementation of central adaptive mechanisms (vestibular compensation), which minimize vestibular schwannoma-related symptoms and influence vestibular examination (5, 10, 11–13).

After surgery for the definite and complete exeresis of the tumor, compensation has to proceed again and different mechanisms are involved, although the commissural network is one of the preferential sites to occur between the normal and damaged sides (14) and visual compensation will also contribute to vestibular compensation. In the initial postoperative phase, an intense vertigo as a manifestation of the acute modification in vestibular function is experienced in 23–49 to 66–78% of patients, leading to disequilibrium while central compensation begins to take place (15). This is paralleled by the reduction of spontaneous nystagmus intensity. Refixation saccades in the vHIT also cause temporal modifications and result in a shift from a combination

of covert and overt saccades to mainly covert ones (16); this is mirrored in the observed change from scattered to gathered saccades.

Previous studies have shown the influence of vestibular damage before vestibular schwannoma surgery in vestibular compensation, showing that a severe vestibular deficit before surgery achieves a faster recovery of patients (17). This faster compensation has been measured with different objective tests such as subjective visual vertical or computerized dynamic posturography and semiquantitative measures such as the Dizziness Handicap Inventory (18).

We have previously studied long-term (>1 year) video HIT outcomes in a group of patients who underwent vestibular schwannoma surgery (8); the majority of patients had a “stabilized” video HIT morphology, with a gathered pattern of refixation saccades. A small group of patients had a scattered pattern in the refixation saccades. With the term “stabilization,” we mean the way (in the first and medium terms) to get the definite saccadic strategy to replace the absent VOR. A greater degree of scatter correlated with worse clinical outcomes (as measured with Dizziness Handicap Inventory).

The aim of the present study was to evaluate the short- and medium-term VOR characteristics and refixation saccade changes in patients undergoing vestibular schwannoma surgery.

PATIENTS AND METHODS

Subjects

Thirty-six patients were diagnosed with a unilateral vestibular schwannoma who were prospectively scheduled for surgery between November 2011 and December 2015. All patients were subjected to retrolabyrinthine or translabyrinthine vestibular schwannoma surgery and were reviewed at 1, 3, and 6 months postoperatively.

Age, sex, tumor side, tumor size according to Koos's classification (19), canal paresis, and video HIT findings were recorded. None of the patients underwent vestibular rehabilitation after surgery during the follow-up period. Written informed consent was obtained for all patients. Because of no new or exceptional interventions, local ethical committee approval was not needed.

The study was performed in accordance with the ethical guidelines of the 1975 Declaration of Helsinki. Patients with brainstem compression or other conditions that could affect postural control were excluded.

Methods

VOR Assessment

The VOR was evaluated with the HIT. The physician stands behind the patient and grasps his or her head firmly with both hands. The patient is asked to keep looking at a stationary object on the wall that is at a distance of 90–100 cm. The head is quickly and unpredictably turned through 10–20° in the horizontal plane either to the left or the right, which permits testing of the corresponding horizontal semicircular canal. In order to register and measure head and eye velocity

during the head impulse, we have used a video HIT system (vHIT, GN Otometrics, Denmark). The patient wears a pair of lightweight, tight-fitting goggles on which is mounted a small video camera and a half-silvered mirror that reflects the image of the patient's right eye into the camera. The eye is illuminated by a low-level infrared light-emitting diode. A small sensor on the goggles measures the head movement. The whole goggle system weighs about 60 g and is secured tightly to the head to minimize goggle slippage. Calibration is performed and the procedure of vestibulo-ocular testing is initiated. The speed of head movement is measured by the sensor in the goggles, and the image of the eye is captured by the high-speed camera (250 Hz) and processed to yield eye velocity. At the end of each head turn, the head velocity stimulus and eye velocity response are displayed simultaneously on the screen so that the clinician can see how good the stimulus and response were, thereby providing a quick way to maximize the quality of the head impulse. Twenty impulses were delivered randomly in each direction. We evaluated the VOR mean gain (ratio of eye velocity to head velocity for every head rotation) and the appearance of saccades after head impulses to the right and left sides. The amplitude of the head rotation was 18–20°, and the peak head velocity of the impulse varied between 150 and 240°/s with a resultant acceleration of between 4500 and 7500°/s².

HITCal and PR Score

Vestibulo-ocular reflex data were post processed using HITCal, a software tool designed to explore and analyze vHIT default output. Original results were exported from vHIT's manufacturer software in eXtensible Markup Language format. We used HITCal to explore and obtain main variables from the records of each patient's test: mean gain, mean head amplitude, mean peak of head velocity, and mean peak of head acceleration. We also used HITCal to obtain a PR score for each test—a parameter developed to measure the aggrupation of the saccadic responses appearance in the time domain. To obtain the PR score, HITCal uses a proprietary algorithm that is summarized in **Table 1**; first step in this algorithm is to detect the saccadic responses for each eye response; in the first step, the detected saccades are not classified using the covert/overt paradigm. In the PR score algorithm, saccadic eye responses are classified attending to the order of appearance after the positive peak of velocity in head impulse. With the detected saccadic responses, the algorithm computes the PR score for each group of appearance. The PR score is based on the coefficient of variation of the (time) moment of appearance of the peak eye velocity in the saccadic response computing all the eye responses present in all the impulses recorded in the same test. In the second step, the PR scores obtained for the first and second appearance groups are computed as main parameters of an arithmetic average. Finally, to get the global PR score, this value is multiplied by a scale factor to fit it in the numeric interval of 0–100. For each vHIT test, a low PR score result (near 0) means maximum gathered, high-grouped responses. A high PR score result (near 100) means maximum scattered, poor grouped responses. HITCal software development process and source code, and PR score algorithm and methodology have been previously published by our research group (7) (**Figure 1; Table 1**).

TABLE 1 | Automated saccade analysis and PR score algorithm.

	Saccade recognition sequence	PR score algorithm
Step 1	Low pass filter of the head and eye graphs	<i>Pattern classification logic condition</i> If coefficient of variation of eye peak >12 for first saccades group or coefficient of variation >35 for second saccades group, result is scattered
Step 2	Relative max values recognition, using conditions Minimum velocity: 65°/s Minimum distance between peaks in eye graph: 15 samples Minimum distance with head velocity peak: 10 samples	Group PR score Coefficient of variation of peaks in each group The group is determined by the order of appearance of saccades
Step 3	Outlier detection, only the two first peak values with +20 or -15 difference from mean of peaks was unmarked as saccades	<i>Global PR score calculation</i> $2.5 \times (0.8 \times CV1 + 0.2 \times CV2)$, where CV1 is coefficient of variation of first registered saccades and CV2 is coefficient of variation of second registered saccades Global PR score corrections If score is >100, the value is reset to 100 If score is >35, the value is adjusted with the number of peaks detected: if only a few impulses have peaks over 35, these impulses have a low impact on the PR SCORE

Main steps in saccade recognition sequence and the PR score algorithm. For time samples, a frame rate of 250 frames per second is assumed.

Groups

Patients were classified into three groups according to the preoperative degree of canal paresis: Group A are patients with a normal caloric test, Group B are patients with a partial canal paresis from 26 to 70%, and Group C are patients with severe canal paresis (more than 71%).

Patients were also classified according to video HIT gain parameters: Group A with normal gain (≥ 0.80) and Group B with abnormal gain (≤ 0.80). In order to distinguish between patients with a mild grade of vestibular damage and patients with a severe vestibular deficit, a secondary arbitrary division was performed among Group B patients, according to whether the gain was between 0.46 and 0.79 ("low gain") or below 0.46 ("very low gain").

Finally, patients were divided in terms of the preoperative presence of overt or covert saccades: "no saccades," "only overt saccades," "only covert saccades," and "covert and overt saccades."

Statistical Analysis

All data were stored in an Excel file and analyzed using SPSS 21.0. Non-parametric tests were preferred to assess statistic significance of the differences found between quantitative variables due to sample size and Kolmogorov-Smirnov test's results. Quantitative PR score values were compared before and after the operative procedures (Wilcoxon test) to assess correlation (ρ Spearman).

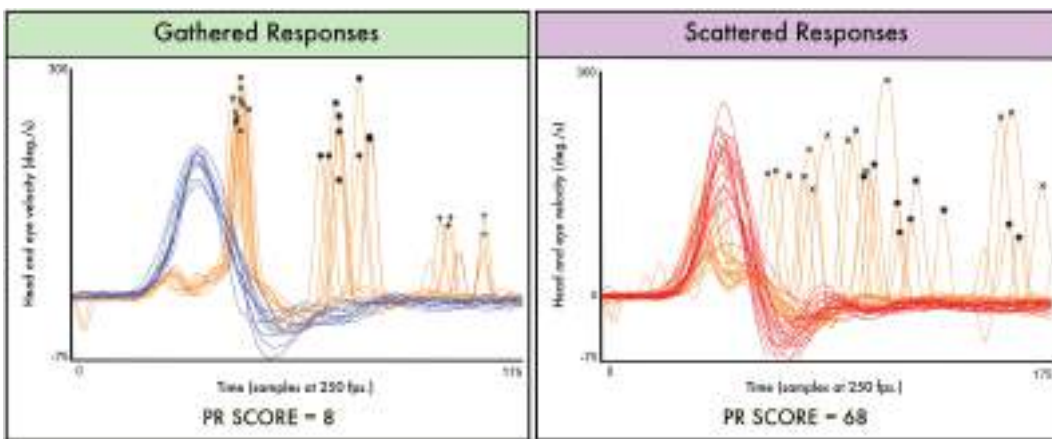


FIGURE 1 | Two real data cases are plotted to illustrate the PR score significance. In the first (left) plot, the saccadic eye responses appear mainly on a narrow interval of time; in this gathered plot, the computed PR score has a low value (PR score = 8). In the second (right) plot, the saccadic eye responses appear on a wide interval of time; even in some cases, the first responses appear after the second responses registered on other impulses; in this scattered plot, the computed PR score is much higher (PR score = 68). “X” mark is for the first group of detected saccades, “*” mark is for the second detected group, and “+” mark is for the third detected group. Y axis is head and eye velocity in degree per second, and X axis is the time domain measured in samples (at an approximated sampling frequency of 250 frames per second). Both plots and PR score measurements were obtained using the open source software HITCal 4.0 (www.mlibra.com).

RESULTS

Patients

From November 2011 to December 2015, 36 patients (21 females) were included in the study. Mean age for the total population was 52 ± 14 years. The affected side was the right in 20 patients and the left in 16 patients. There were no group differences for age, gender, or the affected side.

According to the tumor size, there were 4 grade I patients, 11 grade II patients, 17 grade III patients, and 4 grade IV patients. Surgical approaches were retrosigmoidal and translabyrinthine in 27 and 8 patients, respectively. Mean values of PR are shown in Table 2.

Caloric Test and PR Score

We studied the influence of the preoperative caloric test function upon postoperative video HIT results (Figure 2A). Mean canal paresis for all patients involved in the study was $46 \pm 42\%$ (in the lesion side in all the patients). According to the criteria elicited in the material and methods section, 9 patients were included in Group A (0–20% canal paresis), 18 patients were included in Group B (21–70% canal paresis), and 9 patients were included in Group C (71–100% canal paresis).

Mean PR score for the population before surgery was 6.8. We found that greater preoperative canal paresis was associated with higher PR scores. Thus, the group with a normal caloric test before surgery (Group A) showed a PR score of 1.2. The group with a mild vestibular deficit (Group B) presented a mean PR score of 5.6, and the PR score before surgery in the group with a severe canal paresis was 13.2; differences between groups were statistically significant ($p = 0.002$).

The inverse relationship was observed postoperatively. Thus, immediately post-surgery, PR values were higher in the group

with a normal caloric test before surgery (30.5; Group A) and compared to a PR value of 35.4 for the group with a mild canal paresis before surgery (Group B). Equally, PR score immediately after surgery in the group with a severe canal paresis before surgery (Group C) was 20.5, lower than Group B and Group A. Differences were significant between three groups in the first postoperative assessment ($p = 0.005$). In the follow-up (1 month after surgery, 3 months after surgery, and 6 months after surgery), PR values were reduced in the three groups but retained their group relationship such that they were always higher in Group A than Group B and Group C. However, differences were significant only at Post 1 ($p = 0.005$), Post 2 ($p = 0.017$), and Post 3 ($p = 0.038$) follow-up but not after Post 4, that is, 6 months after surgery, in which PR values were similar for the three groups.

VOR Gain and PR Score

Mean VOR gain before surgery was 0.71 ± 0.26 for all patients in the affected side and $0.90 (0.90 \pm 0.12)$ in the non-affected side.

Gain before surgery was considered normal (≥ 0.80) in 22 patients (Group normal) and abnormal (< 0.80) in 14 patients (Group abnormal). Mean PR score in the group with normal gain before surgery was 0.6 (± 0.3), and mean PR score in the group with abnormal gain before surgery was 8.2 (± 1.4).

After surgery, mean gain for all patients was $0.31 (\pm 0.08)$ in the operated side and $0.73 (\pm 0.06)$ in the normal side.

No significant differences were observed in the PR score before and after surgery (at discharge, 1, 3, and 6 months) for either group (normal and abnormal gain before surgery) ($p > 0.05$) (Figure 2B).

Given such a large range of “abnormal VOR gain” (0.79–0.21), we created an arbitrary threshold (0.46) to separate patients with abnormal gain and a severe deficit (very low gain) from those with a mild deficit (low gain) (Figure 2C). Thus, PR score

TABLE 2 | Mean PR values and SDs in the patient's follow-up according to the different variables.

Mean PR values			
Caloric test	Normal	Moderate canal paresis	Severe canal paresis
Pre	1.2 ± 0.6	5.6 ± 2.3	13.2 ± 4.5
Post 1	35.4 ± 7.2	30.5 ± 6.7	20.5 ± 5.6
Post 2	29.6 ± 6.1	22.9 ± 5.7	16.7 ± 5.1
Post 3	25.3 ± 4.9	18.4 ± 4.2	14.6 ± 4.3
Post 4	17.1 ± 4.1	15.6 ± 3.8	13.3 ± 3.6
Gain	Normal	Low gain	
Pre	0.6 ± 0.4	8.2 ± 3.4	
Post 1	36.6 ± 7.7	32.9 ± 8.7	
Post 2	28.7 ± 6.2	25.4 ± 7.0	
Post 3	24.2 ± 4.8	19.4 ± 6.1	
Post 4	18.3 ± 3.9	17.6 ± 5.6	
Gain	Normal	Low gain	Very low gain
Pre	0.6 ± 0.4	6.2 ± 2.8	16.4 ± 4.1
Post 1	36.6 ± 7.7	34.1 ± 9.1	25.3 ± 5.4
Post 2	28.7 ± 6.2	27.2 ± 7.8	20.1 ± 4.2
Post 3	24.2 ± 4.8	21.5 ± 5.6	18.4 ± 4.0
Post 4	18.3 ± 3.9	17.6 ± 5.1	14.3 ± 4.1
Covert saccades	Yes	No	
Pre	5.4 ± 2.3	0	
Post 1	36.2 ± 9.1	37.5 ± 8.3	
Post 2	26.6 ± 7.6	27.6 ± 7.3	
Post 3	21.8 ± 5.8	22.7 ± 5.1	
Post 4	15.7 ± 4.1	16.5 ± 4.2	
Overt saccades	Yes	No	
Pre	7.8 ± 3.4	0	
Post 1	32.6 ± 8.1	37.5 ± 8.3	
Post 2	24.5 ± 6.9	27.6 ± 7.3	
Post 3	19.7 ± 5.3	22.7 ± 5.1	
Post 4	15.3 ± 3.7	16.5 ± 4.2	
Covert and overt saccades	Yes	No	
Pre	16.8 ± 5.2	0	
Post 1	27.1 ± 7.7	37.5 ± 8.3	
Post 2	20.9 ± 5.5	27.6 ± 7.3	
Post 3	18.3 ± 3.8	22.7 ± 5.1	
Post 4	14.3 ± 3.2	16.5 ± 4.2	

was higher before surgery in the group with “very low gain” ($p = 0.009$) and lower after surgery ($p = 0.002$ in Post 1, $p = 0.017$ in Post 2, and $p = 0.035$ in Post 3) than the groups with low gain or normal gain.

Saccades and PR Score

The PR score was compared between patients with “no saccades” before surgery and those with “covert and overt” saccades before surgery (Figure 2D). Significant differences were observed in the pre-surgical evaluation ($p = 0.012$); these results were expected as from the definition of PR calculation. During follow-up, patients with refixation saccades before surgery had a significantly lower PR score at 1 week ($p = 0.001$), 1 month ($p = 0.012$), and 3 months ($p = 0.02$).

However, if the PR score is compared between patients showing isolated covert saccades before surgery (11 patients) with patients showing any saccade before surgery, no differences were obtained. The same situation was observed for patients showing isolated overt saccades (eight patients) (in both cases $p > 0.05$).

DISCUSSION

In our work, we were interested in the modification of the PR score after a definite vestibular loss in which a restoration of the VOR gain was not expected. This PR score reflects the amount of organization of refixation saccades across sequential head impulses and, indirectly, the level of vestibular disability of the patients as measured by the Dizziness Handicap Inventory (8). Saccadic reorganization is thus a useful marker of vestibular compensation following a complete unilateral vestibular ablation (18, 20). Although all patients suffer from dizziness after a vestibular schwannoma surgery, the manifestation of individual symptoms and therefore compensatory mechanisms is variable, despite a homogenous clinical syndrome (vestibular nerve transection). Our aim was to better understand these individual differences.

Our key finding is that patients with more severe vestibular dysfunction before schwannoma surgery show significantly faster vestibular compensation following surgery, manifested by changes in VOR gain and PR score. From a clinical perspective, a lower VOR gain and low PR score are more likely to cause oscillopsia during head movements, impacting negatively on the ability to carry out daily activities (21). One hypothesis is that patients with more severe preoperative canal paresis are more likely to induce central compensation (22) and thus recover more quickly post operatively (higher PR score). Second, we found a floor effect for PR scores over time; thus, regardless of preoperative canal dysfunction, there was a minimum PR score with associated refixation saccades that did not fully normalize. From a clinical perspective, such a PR score could be regarded as a target “recovery” value; it will be interesting to know in future works if this is the baseline for these patients, which represents eventually a good clinically compensated status. An elevated PR score (meaning heterochrony in refixation saccades between impulses) in the late postoperative phase would be an indicative of impaired vestibular adaptation, which is the necessary first step to compensation.

Vestibular compensation is an active process that in part impacts functionally upon the effectiveness of the VOR to stabilize gaze. When there is a chance of vestibular restoration after an acute vestibular failure (vestibular neuritis), both gain changes and saccade changes could influence the VOR contribution to vestibular compensation. But when vestibular failure is complete, this contribution can only be held by the changes in the saccades’ ability to compensate for the deficit of the VOR. The recovery of balance after vestibular schwannoma surgery is a slow process that begins early in the immediate postoperative phase and continues progressively but appears to be maximal during the first 3 months (23, 24).

When a vestibular loss is complete, visual cues both from peripheral and central vision are critical to improve the VOR (25). Indeed, in order to improve visual stabilization in relation to head

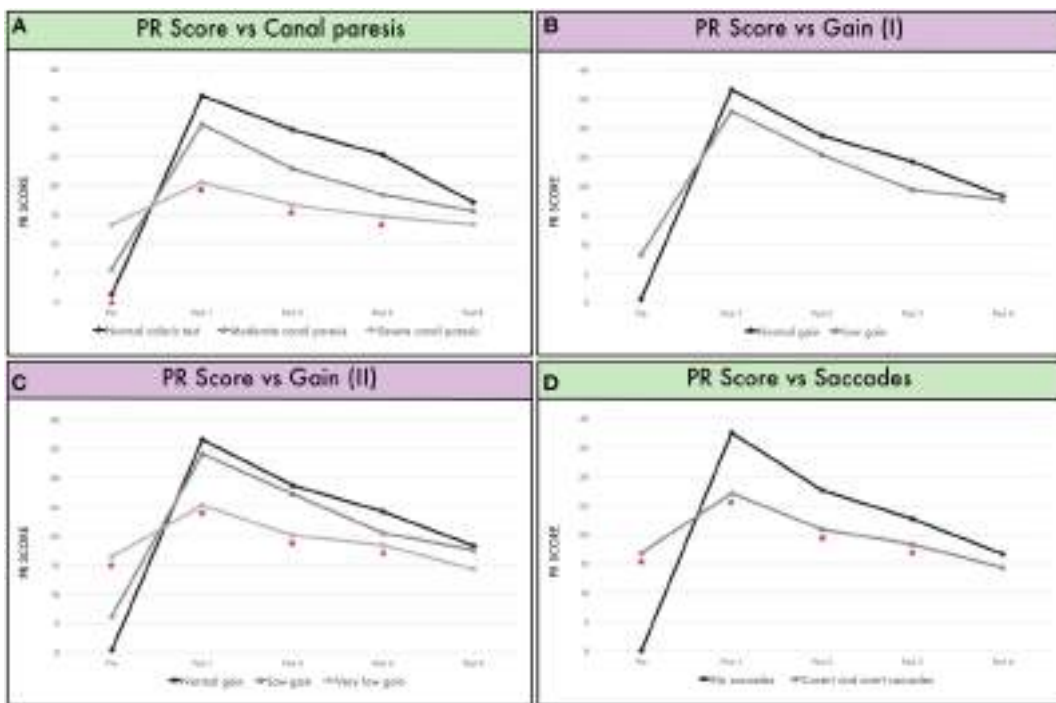


FIGURE 2 | (A) Mean PR score according to canal paresis before surgery and during follow-up. Group A are patients with a normal caloric test, Group B are patients with a partial canal paresis from 26 to 70%, and Group C are patients with a severe canal paresis (more than 71%). **(B)** Mean PR score according to gain in the vHIT before surgery. Group A showing patients with normal gain (≥ 0.80) and Group B for low gain (< 0.80). **(C)** Mean PR score according to gain in the vHIT before surgery. Group A showing patients with normal gain (≥ 0.80), Group B for low gain (< 0.80 and > 0.46), and Group C when gain < 0.46 ("very low gain"). **(D)** Mean PR score in patients without saccades (Group "no saccades") and patients with both covert and overt saccades (Group "covert and overt saccades") before surgery.

movement, the combination of modifications in the amplitude and direction of compensatory saccades and their central pre-programming are fundamental components of vestibular compensation (26, 27). Therefore, the gain of the VOR reflects the raw vestibular signal, but refixation saccades represent the resource used to solve the problem when the gain is low. The origin of such saccades has not been fully elucidated, but it is believed that quick compensatory saccades are related to pontine reticular formation and controlled by the cerebellum, with involvement of the interpositus nucleus and the nodulus (28), although also presumably under higher order cortical influence.

Previous studies showed a strong correlation between pre-operative caloric weakness and both Subjective Visual Vertical and Dizziness Handicap Inventory outcomes after surgery (18). Our finding further suggests that vestibular compensation occurs faster in patients with greater vestibular deficit before surgery (29).

The occurrence of the covert saccades was related to severity of vestibular hypofunction (25), and they are present during both predictable and unpredictable head rotations (30). Although their latency suggests that they are triggered by non-visual afferences and/or central pre-programming, they can reduce gaze error sizably for ipsilesional head rotations (25, 31) and definitely have a symbiotic relationship with the VOR, there being even an inverse

relationship between their recruitment and amplitude and the VOR gain for passive head rotations (32).

Thus, the presence of covert saccades suggests that the vestibular dysfunction has been compensated and eye-head coordination anticipates movements in the real-life situation (16).

As expected, patients with both covert and overt saccades before surgery manifest low or very low VOR gain. Given that VOR adaptation in patients with low VOR gain and saccades before surgery is a slow process, this could explain the minimal changes observed in VOR and PR scores after surgery.

In our opinion, it is very important to understand how the patient compensates for the loss of the VOR, given its implications for vestibular rehabilitation and prevention of long-term disability. In light of our findings, one can predict that patients who compensate with a "gathered pattern" saccadic strategy, with covert saccades always with the same latency, will have lower levels of disability (8) and postural instability, compared to those with a "scattered" saccadic strategy.

This is a very important consideration because VOR adaptation and the organization of the refixation saccades into a gathered pattern could be artificially induced in patients who have not developed it naturally, and improves imbalance symptoms in patients with unilateral vestibular loss and vestibular disability. Indeed, it has been demonstrated that the close relationship

between a lower value of PR and a better score in DHI is an indicative of better clinical outcomes (27).

In summary, we have shown that patients with more severe vestibular dysfunction before vestibular schwannoma surgery show significantly faster vestibular compensation following surgery, manifested by changes in VOR gain and PR score. Second, a thorough preoperative vestibular assessment in patients undergoing vestibular schwannoma surgery may identify early poor prognostic factors that could be addressed in the early postoperative stages to minimize clinical disability through promoting vestibular compensation.

REFERENCES

- Halmagyi GM, Curthoys IS. A clinical sign of canal paresis. *Arch Neurol* (1988) 45:37–9. doi:10.1001/archneur.1988.00520310043015
- Blödow A, Pannasch S, Walther LE. Detection of isolated covert saccades with the video head impulse test in peripheral vestibular disorders. *Auris Nasus Larynx* (2013) 40:348–51. doi:10.1016/j.anl.2012.11.002
- Weber KP, Aw ST, Todd MJ, McGarvie LA, Curthoys IS, Halmagyi GM. Head impulse test in unilateral vestibular loss: vestibulo-ocular reflex and catch-up saccades. *Neurology* (2008) 70:454–63. doi:10.1212/01.wnl.0000299117.48935.2e
- Tjernström F, Nyström A, Magnusson M. How to uncover the covert saccade during the head impulse test. *Otol Neurotol* (2012) 33:1583–5. doi:10.1097/MAO.0b013e318268d32f
- Batuecas-Caletrio A, Santa Cruz Ruiz S, Muñoz-Herrera A, Perez-Fernandez N. The map of dizziness in vestibular schwannoma. *Laryngoscope* (2015) 125:2784–9. doi:10.1002/lary.25402
- Yip CW, Glaser M, Frenzel C, Bayer O, Strupp M. Comparison of the bedside head-impulse test with the video head-impulse test in a clinical practice setting: a prospective study of 500 outpatients. *Front Neurol* (2016) 7:58. doi:10.3389/fneur.2016.00058
- Rey-Martinez J, Batuecas-Caletrio A, Matiño E, Perez Fernandez N. HITCal: a software tool for analysis of video head impulse test responses. *Acta Otolaryngol* (2015) 135:886–94. doi:10.3109/00016489.2015.1035401
- Batuecas-Caletrio A, Santacruz-Ruiz S, Muñoz-Herrera A, Perez-Fernandez N. The vestibulo-ocular reflex and subjective balance after vestibular schwannoma surgery. *Laryngoscope* (2014) 124:1431–5. doi:10.1002/lary.24447
- Broomfield SJ, O'Donoghue GM. Self-reported symptoms and patient experience: a British Acoustic Neuroma Association survey. *Br J Neurosurg* (2016) 30:294–301. doi:10.3109/02688697.2015.1071323
- Curthoys IS. Vestibular compensation and substitution. *Curr Opin Neurol* (2000) 13:27–30. doi:10.1097/00019052-200002000-00006
- Parietti-Winkler C, Gauchard GC, Simon C, Perrin PP. Visual sensorial preference delays balance control compensation after vestibular schwannoma surgery. *Neuroscience* (2011) 172:285–92. doi:10.1016/j.neuroscience.2010.10.059
- Nikolopoulos TP, Fortnum H, O'Donoghue G, Baguley D. Acoustic neuroma growth: a systematic review of the evidence. *Otol Neurotol* (2010) 31:478–85. doi:10.1097/MAO.0b013e3181d279a3
- Andersen JF, Nilsen KS, Vassbotn FS, Møller P, Myrseth E, Lund-Johansen M, et al. Predictors of vertigo in patients with untreated vestibular schwannoma. *Otol Neurotol* (2015) 36:647–52. doi:10.1097/MAO.0000000000000668
- Ranjbaran M, Katsarkas A, Galiana HL. Vestibular compensation in unilateral patients often causes both gain and time constant asymmetries in the VOR. *Front Comput Neurosci* (2016) 10:26. doi:10.3389/fncom.2016.00026
- Tufarelli D, Meli A, Labini FS, Badaracco C, De Angelis E, Alesii A, et al. Balance impairment after acoustic neuroma surgery. *Otol Neurotol* (2007) 28:814–21. doi:10.1097/MAO.0b013e31811f40ad
- Tjernström F, Zur O, Jahn K. Current concepts and future approaches to vestibular rehabilitation. *J Neurol* (2016) 263(Suppl 1):S65–70. doi:10.1007/s00415-015-7914-1
- Tjernström F, Fransson PA, Kahlon B, Karlberg M, Lindberg S, Siesjö P, et al. Vestibular PREHAB and gentamicin before schwannoma surgery may improve long-term postural function. *J Neurol Neurosurg Psychiatry* (2009) 11:1254–60. doi:10.1136/jnnp.2008.170878
- Batuecas-Caletrio A, Santacruz-Ruiz S, Muñoz-Herrera A, Sousa P, Otero A, Perez-Fernandez N. Vestibular compensation after vestibular schwannoma surgery: normalization of the subjective visual vertical and disability. *Acta Otolaryngol* (2013) 133:475–80. doi:10.3109/00016489.2012.757798
- Koos WT, Spetzler RF, Böck FW. Microsurgery of cerebellopontine angle tumors. In: Koos WT, Böck FW, Spetzler RF, et al., editors. *Clinical Microneurosurgery*. Stuttgart; Acton, MA: Georg Thieme (1976). p. 91–112.
- Wagner JN, Glaser M, Wowra B, Muacevic A, Goldbrunner R, Cnyrim C, et al. Vestibular function and quality of life in vestibular schwannoma: does size matter? *Front Neurol* (2011) 2:55. doi:10.3389/fneur.2011.00055
- Mohammad MT, Whitney SL, Marchetti GF, Sparito PJ, Ward BK, Furman JM. The reliability and response stability of dynamic testing of the vestibulo-ocular reflex in patients with vestibular disease. *J Vestib Res* (2011) 21:277–88. doi:10.3233/VES-2011-0430
- Scherer M, Schubert MC. High-velocity angular vestibulo-ocular reflex adaptation to position error signals. *J Neurol Phys Ther* (2010) 34:82–6. doi:10.1097/NPT.0b013e3181dde7bc
- Cohen HS, Kimball KT, Jenkins HA. Factors affecting recovery after acoustic neuroma resection. *Acta Otolaryngol* (2002) 122:841–50. doi:10.1080/00365402/000028039
- Lynn SG, Driscoll CL, Harner SG, Beatty CW, Atkinson EJ. Assessment of dysequilibrium after acoustic neuroma removal. *Am J Otol* (1999) 20:484–94.
- Schubert MC, Zee DS. Saccade and vestibular ocular motor adaptation. *Restor Neurol Neurosci* (2010) 28:9–18. doi:10.3233/RNN-2010-0523
- Sadeghi SG, Minor LB, Cullen KE. Neural correlates of sensory substitution in vestibular pathways following complete vestibular loss. *J Neurosci* (2012) 32:14685–95. doi:10.1523/JNEUROSCI.2493-12.2012
- Matíñó-Soler E, Rey-Martinez J, Trinidad-Ruiz G, Batuecas-Caletrio A, Pérez Fernández N. A new method to improve the imbalance in chronic unilateral vestibular loss: the organization of refixation saccades. *Acta Otolaryngol* (2016) 136:894–900. doi:10.3109/00016489.2016.1172730
- De Zeeuw CI, Ten Brinke MM. Motor learning and the cerebellum. *Cold Spring Harb Perspect Biol* (2015) 9:a021683. doi:10.1101/cshperspect.a021683
- Magnusson M, Kahlon B, Karlberg M, Lindberg S, Siesjö P. Preoperative vestibular ablation with gentamicin and vestibular 'prehab' enhance postoperative recovery after surgery for pontine angle tumours—first report. *Acta Otolaryngol* (2007) 127:1236–40. doi:10.1080/00016480701663433
- Della Santina CC, Cremer PD, Carey JP, Minor LB. Comparison of head thrust test with head autorotation test reveals that the vestibulo-ocular reflex is enhanced during voluntary head movements. *Arch Otolaryngol Head Neck Surg* (2002) 128:1044–54. doi:10.1001/archtol.128.9.1044
- Segal BN, Katsarkas A. Long-term deficits of goal directed vestibulo-ocular function following total unilateral loss of peripheral vestibular function. *Acta Otolaryngol* (1998) 106:102–10. doi:10.3109/00016488809107376
- Schubert MC, Migliaccio AA, Della Santina CC. Modification of compensatory saccades after a VOR gain recovery. *J Vestib Res* (2006) 16:1–7.

AUTHOR CONTRIBUTIONS

AB-C, AM-H, and SR performed surgery and visited patients after surgery. AB-C tested all the patients with vHIT. AB-C, JR-M, NP-F, and GR designed the study, wrote much of the paper, and conducted the analysis. JR-M, NP-F, ES, and AB-C have developed HitCal and PR score.

FUNDING

This study was not funded.

Conflict of Interest Statement: The authors declare that the research was conducted in the absence of any commercial or financial relationships that could be construed as a potential conflict of interest.

Copyright © 2017 Batuecas-Caletrio, Rey-Martinez, Trinidad-Ruiz, Matiño-Soler, Cruz-Ruiz, Muñoz-Herrera and Perez-Fernandez. This is an open-access article

distributed under the terms of the Creative Commons Attribution License (CC BY). The use, distribution or reproduction in other forums is permitted, provided the original author(s) or licensor are credited and that the original publication in this journal is cited, in accordance with accepted academic practice. No use, distribution or reproduction is permitted which does not comply with these terms.



Clinical Subgroups in Bilateral Meniere Disease

Lidia Frejo¹, Andres Soto-Varela², Sofía Santos-Perez², Ismael Aran³, Angel Batuecas-Caletrio⁴, Vanesa Perez-Guillen⁵, Herminio Perez-Garrigues⁵, Jesus Fraile⁶, Eduardo Martin-Sanz⁷, Maria C. Tapia⁸, Gabriel Trinidad⁹, Ana María García-Arumi¹⁰, Rocío González-Aguado¹¹, Juan M. Espinosa-Sánchez^{1,12}, Pedro Marques¹³, Paz Perez¹⁴, Jesus Benitez¹⁵ and Jose A. Lopez-Escamez^{1,16*} On Behalf of the Meniere's Disease Consortium (MeDiC)

OPEN ACCESS

Edited by:

Herman Kingma,
Maastricht University Medical Center,
Netherlands

Reviewed by:

Maurizio Barbara,
Sapienza University, Italy
Hong Ju Park,
Asan Medical Center, University of
Ulsan, South Korea

*Correspondence:

Jose A. Lopez-Escamez
antonio.lopezescamez@genyo.es

Specialty section:

This article was submitted to
Neuro-otology,
a section of the journal
Frontiers in Neurology

Received: 09 May 2016

Accepted: 07 October 2016

Published: 24 October 2016

Citation:

Frejo L, Soto-Varela A, Santos-Perez S, Aran I, Batuecas-Caletrio A, Perez-Guillen V, Perez-Garrigues H, Fraile J, Martin-Sanz E, Tapia MC, Trinidad G, García-Arumi AM, González-Aguado R, Espinosa-Sánchez JM, Marques P, Perez P, Benitez J and Lopez-Escamez JA On Behalf of the Meniere's Disease Consortium (MeDiC) (2016) Clinical Subgroups in Bilateral Meniere Disease. *Front. Neurol.* 7:182. doi: 10.3389/fneur.2016.00182

¹Otology and Neurotology Group CTS495, Department of Genomic Medicine – Centro de Genómica e Investigación Oncológica – Pfizer/Universidad de Granada/Junta de Andalucía (GENYO), Granada, Spain, ²Department of Otorhinolaryngology, Division of Otoneurology, Complejo Hospitalario Universitario, Santiago de Compostela, Spain,

³Department of Otolaryngology, Complejo Hospitalario de Pontevedra, Pontevedra, Spain, ⁴Department of Otolaryngology, Hospital Universitario Salamanca, Salamanca, Spain, ⁵Department of Otorhinolaryngology, Hospital Universitario La Fe, Valencia, Spain, ⁶Department of Otolaryngology, Hospital Miguel Servet, Zaragoza, Spain, ⁷Department of Otolaryngology, Hospital Universitario de Getafe, Getafe, Spain, ⁸Department of Otorhinolaryngology, Instituto Antóni Candela, Madrid, Spain, ⁹Department of Otorhinolaryngology, Division of Otoneurology, Complejo Hospitalario Badajoz, Badajoz, Spain,

¹⁰Department of Otorhinolaryngology, Hospital Universitario Vall d'Hebron, Barcelona, Spain, ¹¹Department of Otorhinolaryngology, Hospital Universitario Marqués de Valdecilla, Santander, Cantabria, Spain, ¹²Department of Otorhinolaryngology, Hospital San Agustín, Linares, Jaén, Spain, ¹³Department of Otorhinolaryngology, Centro Hospitalar de São João, EPE, University of Porto Medical School, Porto, Portugal, ¹⁴Department of Otorhinolaryngology, Hospital Cabueñas, Gijón, Spain, ¹⁵Department of Otolaryngology, Hospital Universitario de Gran Canaria Dr. Negrín, Las Palmas, Spain, ¹⁶Department of Otolaryngology, Instituto de Investigación Biosanitaria ibs.GRANADA, Complejo Hospitalario Universidad de Granada (CHUGRA), Granada, Spain

Meniere disease (MD) is a heterogeneous clinical condition characterized by sensorineural hearing loss, episodic vestibular symptoms, and tinnitus associated with several comorbidities, such as migraine or autoimmune disorders (AD). The frequency of bilateral involvement may range from 5 to 50%, and it depends on the duration of the disease. We have performed a two-step cluster analysis in 398 patients with bilateral MD (BMD) to identify the best predictors to define clinical subgroups with a potential different etiology to improve the phenotyping of BMD and to develop new treatments. We have defined five clinical variants in BMD. Group 1 is the most frequently found, includes 46% of patients, and is defined by metachronic hearing loss without migraine and without AD. Group 2 is found in 17% of patients, and it is defined by synchronic hearing loss without migraine or AD. Group 3, with 13% of patients, is characterized by familial MD, while group 4, that includes 12% of patients, is associated by the presence of migraine in all cases. Group 5 is found in 11% of patients and is defined by AD. This approach can be helpful in selecting patients for genetic and clinical research. However, further studies will be required to improve the phenotyping in these clinical variants for a better understanding of the diverse etiological factors contributing to BMD.

Keywords: cluster analysis, vestibular disorders, hearing loss, tinnitus, Meniere's disease, migraine, autoimmune disorders, inner ear

INTRODUCTION

Meniere's disease (MD) is a long-lasting disorder of the inner ear characterized by episodes of vertigo lasting from 20 min to hours, low-to-middle frequencies sensorineural hearing loss (SNHL, Table 1), tinnitus, and aural fullness (1). MD patients have phenotypic heterogeneity (2), and it is difficult to define the outcome of the disease in its early stages. Although the frequency of the spells of vertigo is typically greater during the earlier years (3–5), balance problems are observed during the course of the disease and might become severe if patients progress to a bilateral vestibular hypofunction (6, 7). Most of the patients start with SNHL in one ear, and it can appear in the other after several years (metachronic SNHL) (8), but a significant number of individuals show simultaneous SNHL (synchronous SNHL). Bilateral involvement is a major concern for patients because of the loss of vestibular function, and bilateral SNHL has a significant influence in the health-related quality of life in MD patients (9).

Several studies have reported contralateral ear involvement between 2 and 73% of cases, depending on the interval of follow-up and the diagnostic criteria used. However, if bilateral MD (BMD) was defined as the combination of clinical symptoms and audiometric tests, the frequency would be 2–47% (7). Some studies describe an interval of 5 years where the incidence was 10–35% (8, 10–13), while in other studies, with a follow-up of 10 years or more, the frequency of BMD ranges from 20 (14–16) to 46% (17). However, more than 20 years of follow-up have also been described, and the incidence rate of bilaterality rises up to 47% (18–22). Although there is a great disparity in the percentage of individuals with bilateral involvement, most of the studies highlighted that the number of patients with contralateral ear involvement increased with the duration of the disease (18, 21, 22).

Several comorbidities have been associated with MD, including autoimmune disorders and migraine. So, MD has been previously associated with several autoimmune diseases, such as systemic lupus erythematosus, psoriasis, or rheumatoid arthritis (6, 23), and autoimmunity has been suggested as a potential cause in MD (24) relying on the results of proteomic studies achieved in small series of patients (24–26). However, high levels of circulating immune complexes were not found in most of the patients with MD (27).

TABLE 1 | List of abbreviations.

AAO-HNS	American Academy Otolaryngology – Head Neck Surgery
AD	Autoimmune disorders/disease
AIED	Autoimmune inner ear disorder
BMD	Bilateral Meniere disease
BMD type 1	Metachronic hearing loss
BMD type 2	Synchronous hearing loss
BMD type 3	Familial Meniere disease
BMD type 4	Meniere disease + migraine
BMD type 5	Meniere disease + autoimmune disease
FMD	Familial Meniere disease
MD	Meniere disease
MRI	Magnetic resonance imaging
RCT	Randomized clinical trials
SNHL	Sensorineural hearing loss
SMD	Sporadic Meniere disease

Furthermore, autoimmune mechanisms seem to be associated with the pathogenesis of some types of SNHL (28, 29), such as sudden SNHL (30), promptly progressive bilateral SNHL (31), and MD (32–34). Additionally, several genes of the immune system have been studied in case-control studies (35–38), but they have not been replicated. Moreover, some data suggest that allelic variants of *MICA* and *TLR10* genes, involved in the innate immune response, may influence the susceptibility and time course of hearing loss of MD in European population (39, 40).

Migraine has been consistently found to be more common in MD than in the general population in case-control studies (41), but it is not clear if this association has any role in the pathophysiology of MD. Vestibular migraine (VM), the condition of episodic vestibular symptoms linked to migraine spectrum (42), may occur in some patients concomitantly with MD (43).

Genetic factors are probably relevant in a subset of patients with MD. So, familial MD was first described in 1949 by Brown (44), and many studies have described familial cases of MD (45). The genetic contribution to MD has been recently reviewed (46, 47), and there are several evidences to support a genetic origin in MD. These evidences include (a) the prevalence is higher in European descent population than in Asian (48) or African populations (49) and (b) familiar aggregation has been observed in 6% in South Korea and 8–9% in Spain (2), being

TABLE 2 | Clinical phenotype in sporadic and familial Meniere disease with at least 5 years since the onset of the disease.

Variables	FMD (n = 52)	SMD (n = 258)	p-value
Age, mean (SD)	55.5 (12.7)	61.5 (11.1)	0.001
Gender (% women)	34 (65.4)	147 (57.0)	0.28
Age of onset (SD)	39 (12.9)	44.8 (13.1)	0.003
Age of onset ≤40, n (%)	28 (53.8)	96 (37.2)	0.03
Time course (years), mean (SD)	16.3 (8.7)	16.3 (9.4)	0.96
Synchronous, n (%)	11 (21.6)	72 (27.9)	0.39
Metachronic, n (%)	40 (78.4)	186 (72.1)	
Hearing loss at diagnosis, mean (SD)	51.9 (15.5)	56.6 (17.8)	0.092
Headache, n (%)	23 (44.2)	92 (36.1)	0.27
Migraine, n (%)	13 (25.0)	44 (17.3)	0.24
Rheumatoid history, n (%)	10 (20.4)	25 (9.8)	0.048
Hearing stage, n (%)			
1	0 (0.0)	4 (1.6)	0.58
2	9 (17.6)	35 (13.6)	
3	28 (54.9)	131 (51.0)	
4	14 (27.5)	87 (33.9)	
Cardiovascular risk			
High blood pressure, n (%)	13 (26.5)	93 (39.7)	0.1
Dyslipidemia, n (%)	21 (42.0)	111 (47.6)	0.53
Type 2 diabetes, n (%)	12 (24.0)	41 (17.4)	0.32
Smoking, n (%)	15 (30)	53 (21.5)	0.2
Tumarkin crisis, n (%)	17 (35.4)	63 (25.5)	0.16
Functional Scale, n (%)			
1	9 (17.6)	53 (21.3)	0.81
2	15 (29.4)	71 (28.5)	
3	10 (19.6)	58 (23.3)	
4	7 (13.7)	35 (14.1)	
5	7 (13.7)	25 (10.0)	
6	3 (5.9)	7 (2.8)	

SMD, sporadic Meniere disease; FMD, familial Meniere disease.
Significant p values in bold.

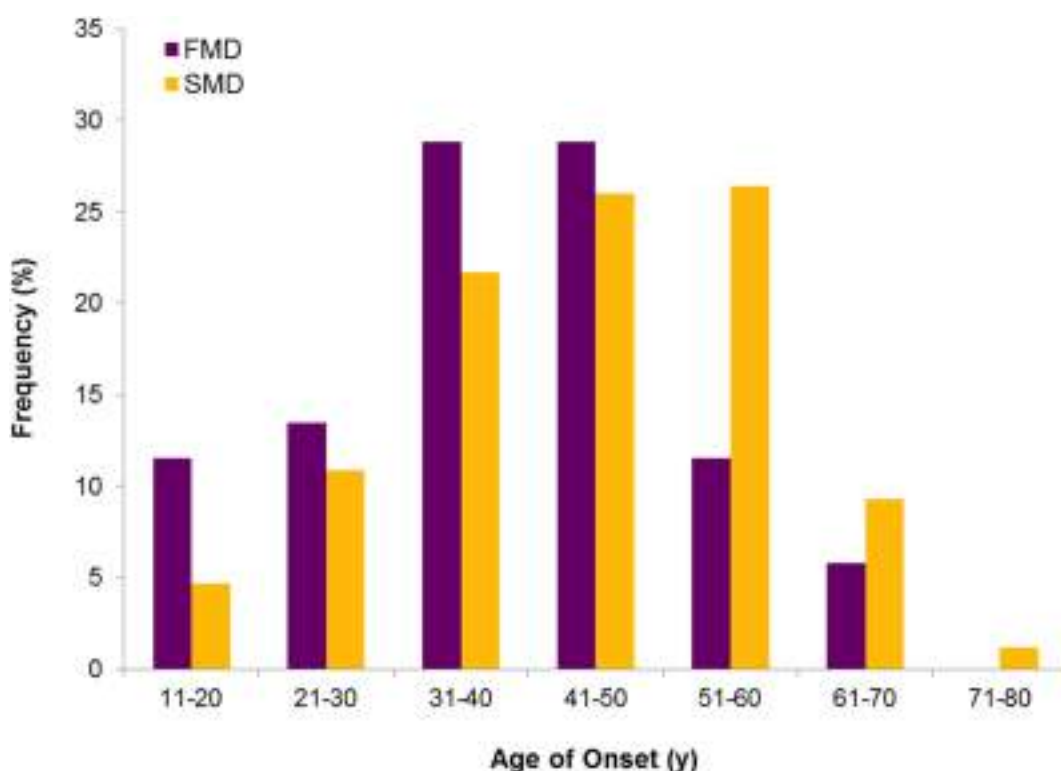


FIGURE 1 | Age of onset in bilateral Meniere disease. Distribution of frequencies in familial and sporadic cases shows an earlier onset in FMD.

TABLE 3 | Autoimmune diseases and other rheumatoid conditions observed in patients with bilateral Meniere disease.

Autoimmune diseases	N
Rheumatoid arthritis	10
Fibromyalgia	6
Arthrosis	5
Ankylosing spondylitis	5
Psoriasis	4
Hypothyroidism	3
Sjogren syndrome	3
Type 1 diabetes	2
Rosacea	2
Graves-Basedow disease	2
Systemic lupus erythematosus	2
Psoriatic arthritis	1
Autoimmune inner ear disease	1
Polymyalgia rheumatica	1
Inflammatory bowel disease	1
Cogan syndrome	1
Hip synovitis	1
Carpal tunnel syndrome	1
Undetermined	10

DTNA and *FAM136A* genes involved in autosomal dominant familial MD (50).

The aim of this study is to describe the phenotype of patients with BMD, including comorbidities such as autoimmune diseases or familial aggregation, and to perform a cluster analysis to identify clinical variants in BMD.

MATERIALS AND METHODS

Subjects

A multicenter, cross-sectional retrospective study was designed, including patients with BMD diagnosed and tracked by the Meniere's Disease Consortium. For this, the clinical records of a total of 405 patients diagnosed with definite BMD from 16 clinical centers in Spain and Portugal were reviewed in March 2016. MD diagnosis was established according to the diagnostic scale of the American Academy of Otolaryngology Head and Neck Surgery (AAO-HNS) (51). Familial MD (FMD) was defined if at least another relative (first or second degree) fulfilled all the criteria of definite or probable MD, according to the criteria established by the Barany Society International Classification for Vestibular Disorders (1). Patients with unilateral MD or bilateral BMD with less than 5 years of evolution were excluded of the study. Seven patients were excluded because of inconsistent data. This study was approved by the Institutional Review Board for Clinical Research (PI-13-1242).

Every patient underwent a complete neuro-otological evaluation, including a pure-tone audiometry, an otoscopy, nystagmus examination, and a caloric testing. A brain MRI was performed to exclude any other possible cause of neurological symptoms. Patients with simultaneous SNHL in both ears were considered to have synchronic SNHL, while metachronic SNHL was considered if an interval longer than 1 month between the first and the second ear was observed.

TABLE 4 | Clinical features of sporadic and familial bilateral Meniere disease stratified by the presence of autoimmune disease (AD).

Variables	Sporadic MD			Familial MD		
	AD+ (n = 25)	AD- (n = 230)	p-value	AD+ (n = 10)	AD- (n = 39)	p-value
Age, mean (SD)	61.7 (9.1)	61.6 (11.2)	0.94	56.5 (13.8)	55 (12.4)	0.74
Gender (% women)	18 (72.0)	128 (55.7)	0.14	6 (60.0)	26 (66.7)	0.72
Age of onset (SD)	43.4 (11.0)	45.2 (13.2)	0.5	35.9 (12.3)	40.5 (13.0)	0.31
Age of onset ≤40, n (%)	11 (44.0)	82 (35.7)	0.51	6 (60.0)	19 (48.7)	0.73
Time course (years), mean (SD)	17.4 (8.7)	16.1 (9.6)	0.52	20.7 (8.9)	14 (7.0)	0.01
Hearing loss at diagnosis, mean (SD)	57.5 (18.3)	56.7 (17.8)	0.83	52.3 (15.2)	52 (15.9)	0.96
Headache, n (%)	15 (62.5)	77 (33.5)	0.007	8 (80.0)	14 (35.9)	0.03
Migraine, n (%)	8 (33.3)	36 (15.7)	0.044	5 (50.0)	7 (17.9)	0.05
Hearing stage, n (%)						
1	0 (0.0)	4 (1.7)	0.37	0 (0.0)	0 (0.0)	0.32
2	5 (20.0)	30 (13.1)		1 (11.1)	8 (20.5)	
3	9 (36.0)	119 (52.0)		4 (44.4)	23 (59.0)	
4	11 (44.0)	76 (33.2)		4 (44.4)	8 (20.5)	
Cardiovascular risk factors						
High blood pressure, n (%)	13 (59.1)	80 (37.7)	0.07	2 (20.0)	10 (27.0)	1
Dyslipidemia, n (%)	12 (50.0)	97 (46.9)	0.83	4 (40.0)	16 (42.1)	1
Type 2 diabetes, n (%)	8 (33.3)	33 (15.8)	0.046	5 (50.0)	7 (18.4)	0.09
Smoking, n (%)	6 (28.6)	47 (21.0)	0.41	3 (30.0)	12 (30.8)	1
Tumarkin crisis, n (%)	6 (27.3)	57 (25.3)	0.8	5 (50.0)	12 (32.4)	0.46
Functional Scale, n (%)						
1	4 (17.4)	48 (21.3)	0.94	2 (20.0)	7 (17.9)	0.007
2	7 (30.4)	64 (28.4)		4 (40.0)	11 (28.2)	
3	6 (26.1)	52 (23.1)		1 (10.0)	8 (20.5)	
4	2 (8.7)	33 (14.7)		0 (0.0)	6 (15.4)	
5	3 (13.0)	22 (9.8)		0 (0.0)	7 (17.9)	
6	1 (4.3)	6 (2.7)		3 (30.0)	0 (0.0)	

Significant p values in bold.

Clinical variables studied were as follows: gender, duration of disease, age of onset, family history of MD, hearing loss at diagnosis, hearing stage defined as four-tone average of 0.5, 1, 2, and 3 kHz according to the AAO-HNS criteria (stage 1, ≤ 25 dB; stage 2, 26–40 dB; stage 3, 41–70 dB, and stage 4, > 70 dB), type of headache (migraine, tension-type headache), history of autoimmune disease (AD), cardiovascular risk factors (high blood pressure, type 2 diabetes, dyslipidemia, and smoking), Tumarkin crisis, and the Functional Scale of the AAO-HNS.

Statistical Analysis

A descriptive statistical analysis was carried out using SPSS software v.22 (SPSS Inc., Chicago, IL, USA). Data are shown as means with their SDs. Quantitative variables were compared using Student's unpaired *T*-test. Qualitative variables were compared using crosstabs and Fisher's exact test. Nominal *p*-values < 0.05 were considered statistically significant.

We carried out a two-step cluster analysis using log-likelihood distance measures, which can detect relationships within a complex dataset between patients with multiple distinct characteristics. It tries to identify homogenous groups of cases based on the distribution of some variables (input variables). The method identifies the groups by running pre-clustering first and then by using hierarchical methods to classify and to find the optimal number of clusters.

Initially, we selected variables showing differences between the clinical groups during the descriptive analysis to test its relevance as predictors of clusters. The procedure was iterated several times

until we found the minimum number of homogenous clusters. The final cluster analysis was applied using the four following categorical variables: history of autoimmune disease, onset of hearing loss (synchronous/metachronic), FMD or sporadic cases, and migraine. The four variables included produced a silhouette of cohesion and division of 0.8, indicative of good data partitioning. Two additional variables were added to the model: age of onset < 40 years old and gender, although their contribution to refine the clustering was limited.

RESULTS

Three hundred ninety-eight patients with BMD were included in the study. There were 258 sporadic cases and 52 individuals with FMD (20%). Although apparently there were no clinical differences in the phenotype between sporadic and familial cases, FMD had an earlier age of onset ($p = 0.003$) and a higher prevalence of autoimmune comorbidities (Table 2). So, the distribution of frequencies for the age of onset showed that the number of patients starting before 40 years old was significantly higher in the FMD (Figure 1). Table 3 lists the autoimmune comorbid conditions found, being rheumatoid arthritis the most common in our cohort.

The clinical features in patients with sporadic and FMD were stratified according to the presence or absence of autoimmune comorbidities. In the sporadic cases, headache and migraine were most commonly observed in patients with autoimmune background (62.5 and 33%, respectively) compared with patients without autoimmune comorbidities (33 and 16%), suggesting

a potential association between migraine and autoimmunity in patients with sporadic BMD (**Table 4**).

We also compared patients according to the onset of hearing loss (**Table 5**). One hundred three (26%) individuals developed simultaneous hearing loss in both ears (synchronous hearing loss, either symmetric or asymmetric), while 291 (73%) patients started with hearing loss in one ear and developed

TABLE 5 | Clinical features in bilateral Meniere disease according to the onset of hearing loss.

Variables	Synchronous (n = 103)	Metachronic (n = 291)	p-value
Age, mean (SD)	61 (11.0)	60.1 (11.9)	0.49
Gender (% women)	63 (61.2)	161 (55.3)	0.36
Age of onset (SD)	46.1 (12.8)	43.5 (13.2)	0.07
Age of onset ≤40, n (%)	39 (37.9)	118 (40.5)	0.73
Time course (years), mean (SD)	14.4 (8.9)	16.2 (8.9)	0.08
Family history, n (%)	39 (39.8)	119 (43.0)	0.64
FMD, n (%)	11 (13.3)	40 (17.7)	0.39
Hearing loss at diagnosis, mean (SD)	55.1 (17.0)	55.9 (17.0)	0.71
Headache, n (%)	55 (53.4)	96 (33.3)	0.0004
Migraine, n (%)	25 (24.3)	49 (17.0)	0.11
Rheumatoid history, n (%)	15 (15.0)	35 (12.2)	0.49
Hearing stage, n (%)			
1	1 (1.0)	6 (2.1)	0.004
2	27 (26.5)	34 (11.7)	
3	42 (41.2)	152 (52.4)	
4	32 (31.4)	98 (33.8)	
Cardiovascular risk			
High blood pressure, n (%)	47 (51.1)	109 (39.9)	0.068
Dyslipidemia, n (%)	53 (55.2)	121 (45.1)	0.097
Type 2 diabetes, n (%)	13 (13.5)	50 (18.5)	0.35
Smoking, n (%)	22 (21.8)	68 (24.5)	0.68
Tumarkin crisis, n (%)	24 (25.8)	69 (24.9)	0.89
Functional Scale, n (%)			
1	14 (14.0)	73 (26.0)	0.11
2	29 (29.0)	77 (27.4)	
3	26 (26.0)	55 (19.6)	
4	12 (12.0)	40 (14.2)	
5	16 (16.0)	27 (9.6)	
6	3 (3.0)	9 (3.2)	

Significant p values in bold.

the hearing loss in the contralateral ear (metachronic hearing loss). **Figure 2** compares the distribution of frequencies for the age of onset in patients with synchronous or metachronic hearing loss. There were no clinical differences between them, but the occurrence of headache was most commonly observed in synchronous hearing loss ($p = 0.0004$), and the worst hearing stage was observed in patients with metachronic hearing loss ($p = 0.004$).

We performed cluster analysis to identify groups of patients with common clinical features in BMD. **Figure 3** shows the size of the clusters, the relevance of predictors, and the contribution of each predictor to define the cluster. The best predictors for clustering were autoimmune history, FMD, migraine, and the onset of hearing loss (synchronous/metachronic). Ninety-five patients remained unclassified because of incomplete clinical data.

We have defined five clusters for BMD and ranked them according to its relative frequency (**Figure 4**). Cluster 1 is the most common, including 46.5% of patients, and it is defined by metachronic hearing loss without migraine, sporadic BMD, and no autoimmune history. Cluster 2 (17.5%) includes patients with synchronous hearing loss, sporadic BMD, no migraine, and no autoimmune history. Cluster 3 (12.9%) includes patients with FMD without migraine in 82% of patients. Cluster 4 (11.9%) consists of patients with migraine and sporadic BMD. Cluster 5 (11.2%) groups all patients with autoimmune comorbidities, being 71% sporadic and 29% FMD.

Table 6 shows the five groups found and the major clinical differences among the groups. Comparing the age of onset by groups, we observe that groups 3–5 have earlier onsets than groups 1 and 2 ($p = 0.0003$). The type of hearing loss, FMD, migraine, and autoimmune comorbidities strongly differ among groups, and these variables are the basis to assign a given patient to each cluster.

DISCUSSION

The diagnostic criteria for MD formulated by the Classification Committee of the Bárany Society state that bilateral involvement is determined by hearing loss defined in the audiogram

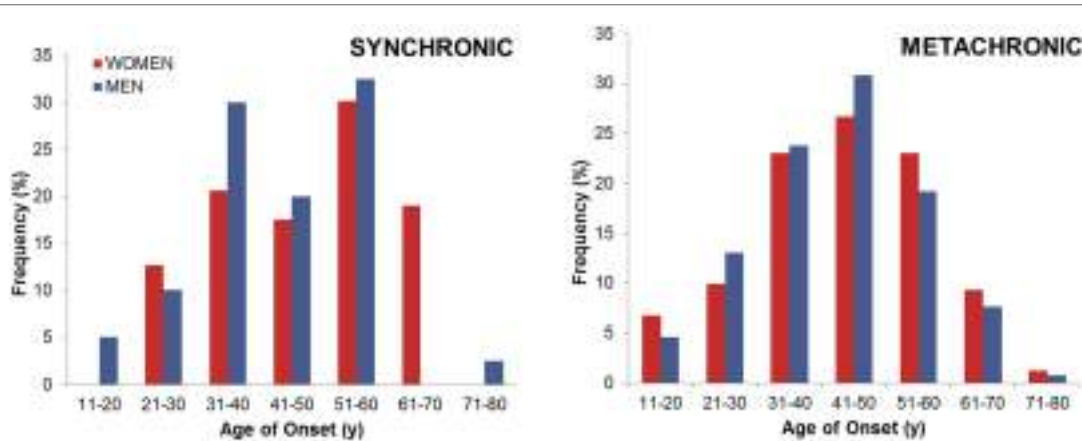


FIGURE 2 | Age of onset in bilateral Meniere disease according to the type of hearing loss observed.

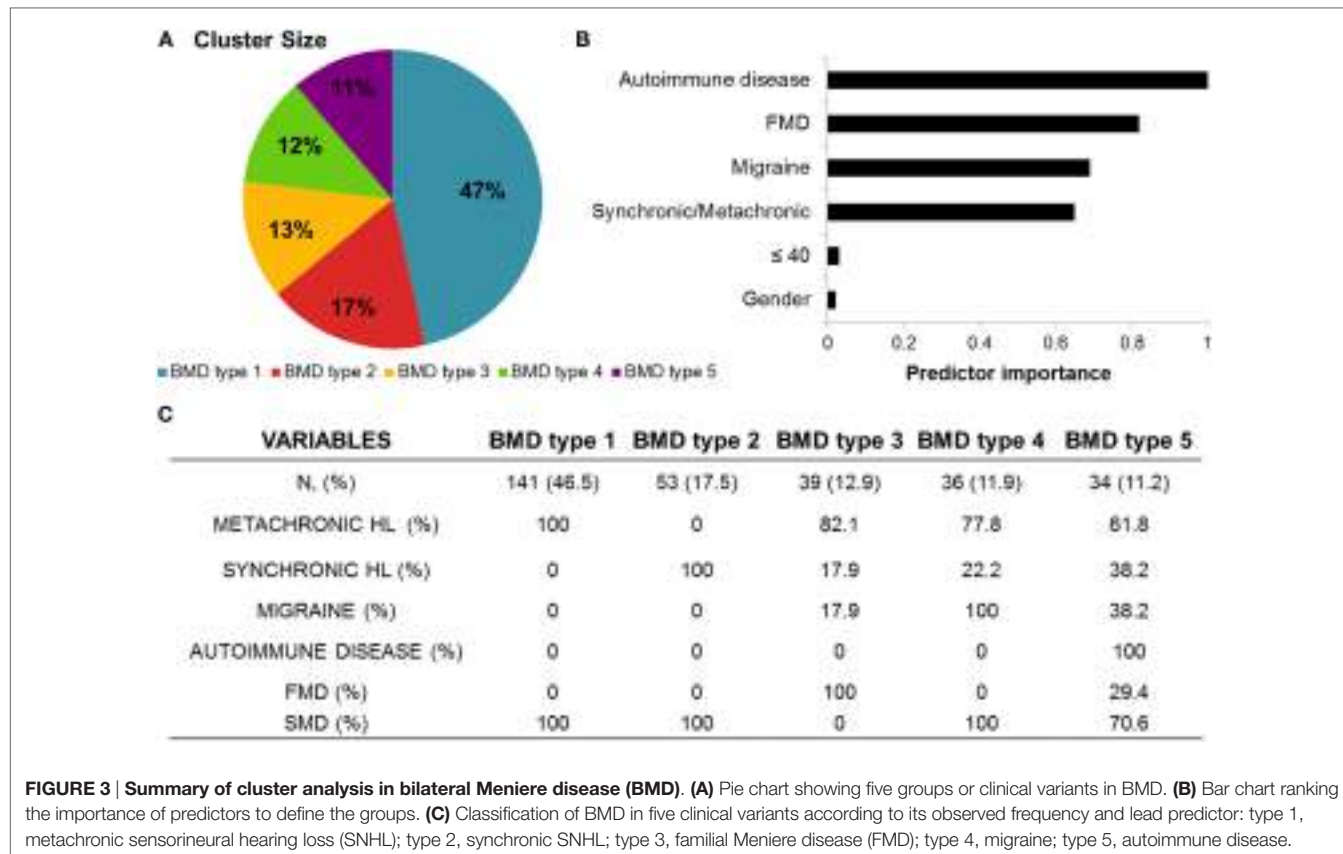


FIGURE 3 | Summary of cluster analysis in bilateral Meniere disease (BMD). (A) Pie chart showing five groups or clinical variants in BMD. (B) Bar chart ranking the importance of predictors to define the groups. (C) Classification of BMD in five clinical variants according to its observed frequency and lead predictor: type 1, metachronic sensorineural hearing loss (SNHL); type 2, synchronic SNHL; type 3, familial Meniere disease (FMD); type 4, migraine; type 5, autoimmune disease.

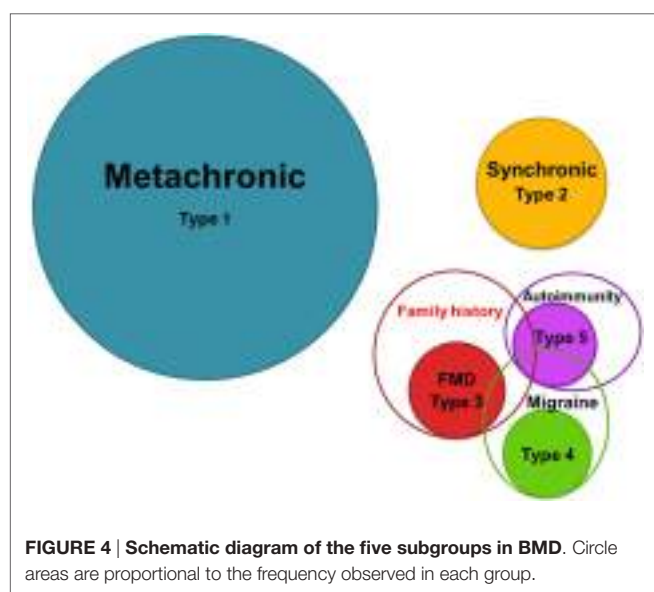


FIGURE 4 | Schematic diagram of the five subgroups in BMD. Circle areas are proportional to the frequency observed in each group.

(1). So, if the absolute thresholds for bone-conducted sound are ≥ 35 dB HL at each of two contiguous frequencies below 2000 Hz in both ears, and the patient has experienced ≥ 2 episodes of spontaneous vertigo each lasting 20 min to 12 h associated with fluctuating aural symptoms, the diagnosis of definite BMD is established. The notes added to the definition also describe a

second clinical variant when the patient develops simultaneous bilateral SNHL (symmetric or asymmetric) (1, 52), but no further clinical information was included in the definition.

Our study demonstrates that BMD is a heterogeneous disorder, and two-step cluster analysis is a very useful tool to define groups of patients with BMD according to four clinical predictors: FMD, autoimmune history, migraine, and the type of onset for hearing loss. We selected this method since it allows the inclusion of quantitative and categorical variables to define clusters (53).

We present a new classification for BMD in five groups of patients with potential etiological implications, which probably will improve the diagnostic workflow and the management of patients with BMD. Previous studies in patients with BMD were focused in the diagnosis by electrocochleography or MRI (54–56), but they did not consider the comorbidities commonly observed, such as migraine or AD in some cases. The phenotype of a patient with an episodic vestibular syndrome should not be limited to the description of the inner ear symptoms, skipping crucial information such as the familiar history of MD or migraine. Furthermore, the comorbidities of migraine or AD may explain the perception of MD as a continuum, which overlaps with migraine (57) or autoimmune inner ear disease (1, 58, 59).

The most remarkable finding in our study is that the five groups of patients identified do not overlap themselves, and each of them has a set of features able to define the group.

Bilateral MD type 1 is the most common clinical variant, and it includes patients with MD in one ear (unilateral MD), and

TABLE 6 | Clinical variants in bilateral Meniere disease (BMD) defined by two-step cluster analysis.

Variables	BMD type 1 (n = 141)	BMD type 2 (n = 53)	BMD type 3 (n = 39)	BMD type 4 (n = 36)	BMD type 5 (n = 34)	p-value
Group predictor	Metachronic SNHL	Synchronous SNHL	FMD	Migraine	AD	
Age, mean (SD)	63.3 (11.0)	62.4 (9.5)	54.7 (13.2)	54.1 (11.5)	59.7 (11.1)	0.00001
Gender (% women)	73 (51.8)	30 (56.6)	26 (66.7)	25 (69.4)	24 (70.6)	0.11
Age of onset (SD)	46.4 (13.1)	47.9 (12.0)	40 (14.5)	37 (12.5)	39.8 (11.3)	0.0003
Age of onset ≤40, n (%)	46 (32.6)	15 (28.3)	19 (48.7)	21 (58.3)	16 (47.1)	0.011
Synchronous, n (%)	0 (0.0)	53 (100.0)	7 (17.9)	8 (22.2)	13 (38.2)	3.39 × 10⁻⁴²
Metachronic, n (%)	141 (100.0)	0 (0.0)	32 (82.1)	28 (77.8)	21 (61.8)	
Family history, n (%)	18 (12.8)	7 (13.2)	39 (100.0)	7 (19.4)	19 (55.9)	1.81 × 10⁻²⁷
FMD, n (%)	0 (0.0)	0 (0.0)	39 (100.0)	0 (0.0)	10 (29.4)	4.10 × 10⁻⁵³
Headache, n (%)	22 (15.6)	20 (37.7)	14 (35.9)	36 (100.0)	23 (67.6)	4.88 × 10⁻²⁰
Migraine, n (%)	0 (0.0)	0 (0.0)	7 (17.9)	36 (100.0)	13 (38.2)	1.21 × 10⁻⁴⁴
Rheumatoid history, n (%)	0 (0.0)	0 (0.0)	0 (0.0)	0 (0.0)	34 (100.0)	2.44 × 10⁻⁶⁴
Cardiovascular risk factors						
High blood pressure, n (%)	46 (34.3)	23 (50.0)	10 (27.0)	11 (34.4)	15 (46.9)	0.15
Dyslipidemia, n (%)	58 (45.3)	26 (53.1)	16 (42.1)	13 (43.3)	15 (45.5)	0.86
Type 2 diabetes, n (%)	23 (17.8)	9 (18.4)	7 (18.4)	1 (3.2)	12 (36.4)	0.019
Smoking, n (%)	31 (22.6)	10 (18.9)	12 (30.8)	6 (17.1)	9 (29.0)	0.53

Significant p values in bold.

they develop the hearing loss in the contralateral ear (conversion from unilateral to BMD). The mean age of onset was 46 years old, comparable to BMD type 2, but it is significantly higher than it was observed in the rest of the groups (types 3, 4, or 5). BMD type 1 has no familial or autoimmune history, and patients do not have migraine, so further studies are required to investigate other concurrent comorbidities to determine contributing factors.

Bilateral MD type 2 is the second most frequently observed clinical variant, and fluctuating bilateral SNHL loss may resemble AIED, since simultaneous SNHL with vestibular symptoms can occur in 50% patients with AIED (58). However, these patients do not have any autoimmune comorbid conditions, migraine, or familial history of MD. Interestingly, BMD type 2 patients show a vascular risk profile, since 50% of them show high blood pressure, and 53% have dyslipidemia. When we compared these frequencies with BMD type 1, which do not differ in age or sex profile to BMD type 2, they were not significantly different ($p = 0.078$), but further studies should assess the role of vascular risk factors in labyrinthine microcirculation in MD.

Comparing the hearing stage for the worst ear, it seems to be worse in BMD type 1 (metachronic SNHL) than in type 2 (synchronous SNHL). Since both groups do not differ for the age of onset, duration of disease, or gender distribution, we cannot determine the reason for the severe SNHL in the first ear in BMD type 1.

Bilateral MD type 3 includes all patients with familiar history of MD, and we could subtype them in two subgroups (3a with migraine, 82%, and 3b BMD without migraine 18%). These findings confirm the early description of families with MD co-segregating migraine and MD (60) and the more recent description of FMD without migraine (2, 61, 62). According to this subtyping for FMD, there will be two types of families with MD, with and without migraine, and they reflect the genetic heterogeneity in FMD. The families include patients with uni and BMD, so epigenetic factors may influence uni or bilateral

involvement. Most of the described families have an autosomal dominant pattern of inheritance, and the participation of several genes indicate a genetic heterogeneity in FMD (2, 50). Although variable expressivity and incomplete penetrance was observed, we did not find cases with episodic ataxia in the families.

Bilateral MD type 4 is associated with migraine in all cases, but they do not have familial history of MD. This group may overlap with VM, and it may share common pathophysiological mechanisms (63). Patients with MD may show migraine symptoms even during the attacks of vertigo (57), and this finding could make difficult the differential diagnosis of VM and MD. Magnetic resonance imaging may be useful in the diagnostic evaluation of patients with the spectrum of VM/MD (MD with concurrent migraine or in cases VM and auditory symptoms) (64).

Bilateral MD type 5 could be considered as autoimmune MD, since all patients have another concurrent AD. However, this group is heterogeneous and includes patients with sporadic (71%), FMD (29%), migraine (38%), and both synchronous (38%) and metachronic SNHL (62%). Patients with BMD type 5 and migraine may have either synchronous or metachronic SNHL.

Our study has several limitations. Despite our efforts to improve phenotyping in patients with BMD, we could not classify 95 patients with BMD in any cluster, and they were excluded of the model. In fact, the largest group (BMD type 1) remains poorly characterized, since it is not associated with any particular clinical feature or etiological factor. The role of allergy in MD deserves more research efforts, since a high prevalence of sensitization to inhalant or food allergies have been reported in MD (65–67).

However, the recognizing of different subgroups of patients and the definition of clinical variants in BMD is not only the first step to improve the selection of patients for genetic and immunological studies but also for randomized clinical trials (RCT). Most of the RCT performed in MD, were not able to demonstrate any effects of diuretics (68) or betahistine (69) and had limited

effectiveness for intratympanic gentamicin (70) or steroids (71), and these results could be explained by a biased selection of patients with different etiologies. Further phenotyping of these clinical variants are needed for a better understanding of the clinical heterogeneity observed in BMD.

AUTHOR CONTRIBUTIONS

LF and JL-E conceived and designed the study. AS-V, SS-P, AB-C, VP-G, HP-G, JF, EM-S, MT, GT, AG-A, RG-A, JE-S, PM, PP, JB, and JL-E collected clinical information. LF and JL-E analyzed the data and drafted the manuscript. LF, AS-V, SS-P, AB-C, VP-G, HP-G, JF, EM-S, MT, GT, AG-A, RG-A, JE-S, PM, PP, JB, and JL-E revised and approved the final version of the manuscript.

ACKNOWLEDGMENTS

We acknowledge to all members of the *Meniere disease's Consortium (MeDiC)*, a network of clinical and research centers contributing to the study of Meniere's disease. List of participants in MeDiC: Juan Carlos Amor-Dorado (Hospital Can Misses Ibiza, Spain), IA (Complejo Hospitalario de Pontevedra, Spain),

AB-C (Hospital Universitario Salamanca, Spain), JB (Hospital Universitario de Gran Canaria Dr. Negrín, Las Palmas de Gran Canaria, Spain), JE-S (Hospital San Agustín Linares, Spain), JF (Hospital Miguel Servet, Zaragoza, Spain), AG-A (Hospital Universitario Vall d'Hebron, Barcelona, Spain), RG-A (Hospital Universitario Marqués de Valdecilla, Santander), JL-E (Complejo Hospitalario Universidad de Granada, Spain), Raquel Manrique Huarte, Nicolas Pérez-Fernandez (Clínica Universidad de Navarra, Spain), PM (Centro Hospitalar de São João, Porto, Portugal), EM-S, Ricardo Sanz (Hospital Universitario de Getafe, Madrid, Spain), Manuel Oliva Domínguez (Hospital Costa del Sol Marbella, Spain), PP (Hospital Cabueñas, Asturias, Spain), HP-G, VP-G (Hospital La Fe, Valencia, Spain), SS-P, AS-V (Complejo Hospitalario Universitario, Santiago de Compostela, Spain), MT (Instituto Antolí Candela, Madrid, Spain), Roberto Teggi (San Raffaele Scientific Institute, Milan, Italy), and GT (Complejo Hospitalario Badajoz, Spain).

FUNDING

This study was funded by a PI13/1242 Grant from ISCIII by FEDER funds from the EU.

REFERENCES

- Lopez-Escamez JA, Carey J, Chung WH, Goebel JA, Magnusson M, Mandala M, et al. Diagnostic criteria for Meniere's disease. *J Vestib Res* (2015) 25(1):1–7. doi:10.3233/VES-150549
- Requena T, Espinosa-Sánchez JM, Cabrera S, Trinidad G, Soto-Varela A, Santos-Perez S, et al. Familial clustering and genetic heterogeneity in Meniere's disease. *Clin Genet* (2014) 85(3):245–52. doi:10.1111/cge.12150
- Stahle J, Friberg U, Svedberg A. Long-term progression of Meniere's disease. *Am J Otol* (1989) 10(3):170–3.
- Belinchon A, Perez-Garrigues H, Tenias JM. Evolution of symptoms in Meniere's disease. *Audiol Neurotol* (2012) 17(2):126–32. doi:10.1159/000331945
- Perez-Garrigues H, Lopez-Escamez JA, Perez P, Sanz R, Orts M, Marco J, et al. Time course of episodes of definitive vertigo in Meniere's disease. *Arch Otolaryngol Head Neck Surg* (2008) 134(11):1149–54. doi:10.1001/archotol.134.11.1149
- Gazquez I, Soto-Varela A, Aran I, Santos S, Batuecas A, Trinidad G, et al. High prevalence of systemic autoimmune diseases in patients with Meniere's disease. *PLoS One* (2011) 6(10):e26759. doi:10.1371/journal.pone.0026759
- Huppert D, Strupp M, Brandt T. Long-term course of Meniere's disease revisited. *Acta Otolaryngol* (2010) 130(6):644–51. doi:10.3109/00016480903382808
- House JW, Doherty JK, Fisher LM, Derebery MJ, Berliner KI. Meniere's disease: prevalence of contralateral ear involvement. *Otol Neurotol* (2006) 27(3):355–61. doi:10.1097/00129492-200604000-00011
- Lopez-Escamez JA, Viciana D, Garrido-Fernandez P. Impact of bilaterality and headache on health-related quality of life in Meniere's disease. *Ann Otol Rhinol Laryngol* (2009) 118(6):409–16.
- Kitahara M, Matsubara H, Takeda T, Yazawa Y. Bilateral Meniere's disease. *Adv Otorhinolaryngol* (1979) 25:117–21. doi:10.1159/000402927
- Paparella MM, Griebel MS. Bilaterality of Meniere's disease. *Acta Otolaryngol* (1984) 97(3–4):233–7. doi:10.3109/00016488409130984
- Rosenberg S, Silverstein H, Flanzer J, Wanamaker H. Bilateral Meniere's disease in surgical versus nonsurgical patients. *Am J Otol* (1991) 12(5):336–40.
- Palaskas CW, Dobie RA, Snyder JM. Progression of hearing loss in bilateral Meniere's disease. *Laryngoscope* (1988) 98(3):287–90. doi:10.1288/00005537-198803000-00009
- Tokumasu K, Fujino A, Yoshio S, Hoshino I. Prognosis of Meniere's disease by conservative treatment: retrospective study on the time course of the disease. *Acta Otolaryngol Suppl* (1995) 519:216–8. doi:10.3109/00016489509121908
- Tokumasu K, Fujino A, Naganuma H, Hoshino I, Arai M. Initial symptoms and retrospective evaluation of prognosis in Meniere's disease. *Acta Otolaryngol Suppl* (1996) 524:43–9. doi:10.3109/00016489609124348
- Chaves AG, Boari L, Lei Munhoz MS. The outcome of patients with Meniere's disease. *Braz J Otorhinolaryngol* (2007) 73(3):346–50. doi:10.1016/S1808-8694(15)30078-1
- Balkany TJ, Sires B, Arenberg IK. Bilateral aspects of Meniere's disease: an underestimated clinical entity. *Otolaryngol Clin North Am* (1980) 13(4):603–9.
- Green JD Jr, Blum DJ, Harner SG. Longitudinal followup of patients with Meniere's disease. *Otolaryngol Head Neck Surg* (1991) 104(6):783–8. doi:10.1177/019459989110400603
- Stahle J, Friberg U, Svedberg A. Long-term progression of Meniere's disease. *Acta Otolaryngol Suppl* (1991) 485:78–83. doi:10.3109/00016489109128047
- Havia M, Kentala E. Progression of symptoms of dizziness in Meniere's disease. *Arch Otolaryngol Head Neck Surg* (2004) 130(4):431–5. doi:10.1001/archotol.130.4.431
- Friberg U, Stahle J, Svedberg A. The natural course of Meniere's disease. *Acta Otolaryngol Suppl* (1984) 406:72–7.
- Morrison AW. Predictive tests for Meniere's disease. *Am J Otol* (1986) 7(1):5–10.
- Tyrrell JS, Whinney DJ, Ukoumunne OC, Fleming LE, Osborne NJ. Prevalence, associated factors, and comorbid conditions for Meniere's disease. *Ear Hear* (2014) 35(4):e162–9. doi:10.1097/AUD.0000000000000041
- Kim SH, Kim JY, Lee HJ, Gi M, Kim BG, Choi JY. Autoimmunity as a candidate for the etiopathogenesis of Meniere's disease: detection of autoimmune reactions and diagnostic biomarker candidate. *PLoS One* (2014) 9(10):e111039. doi:10.1371/journal.pone.0111039
- Chiarella G, Saccomanno M, Scumaci D, Gaspari M, Faniello MC, Quaresima B, et al. Proteomics in Meniere disease. *J Cell Physiol* (2012) 227(1):308–12. doi:10.1002/jcp.22737
- Chiarella G, Di Domenico M, Petrolo C, Saccomanno M, Rothenberger R, Giordano A, et al. A proteomics-driven assay defines specific plasma protein signatures in different stages of Meniere's disease. *J Cell Biochem* (2014) 115(6):1097–100. doi:10.1002/jcb.24747

27. Lopez-Escamez JA, Saenz-Lopez P, Gazquez I, Moreno A, Gonzalez-Oller C, Soto-Varela A, et al. Polymorphisms of CD16A and CD32 Fcgamma receptors and circulating immune complexes in Meniere's disease: a case-control study. *BMC Med Genet* (2011) 12:2. doi:10.1186/1471-2350-12-2
28. Brand O, Gough S, Heward J. HLA, CTLA-4 and PTPN22: the shared genetic master-key to autoimmunity? *Expert Rev Mol Med* (2005) 7(23):1–15. doi:10.1017/S1462399405009981
29. McCabe BF. Autoimmune sensorineural hearing loss. *Ann Otol Rhinol Laryngol* (1979) 88(5 Pt 1):585–9. doi:10.1177/000348947908800501
30. Amor-Dorado JC, Paco L, Martin J, Lopez-Nevot MA, Gonzalez-Gay MA. Human leukocyte antigen-DQB1 and -DRB1 associations in patients with idiopathic sudden sensorineural hearing loss from a defined population of Northwest Spain. *Acta Otolaryngol* (2005) 125(12):1277–82. doi:10.1080/00016480510012228
31. Harris JP, Weisman MH, Derebery JM, Espeland MA, Gantz BJ, Gulya AJ, et al. Treatment of corticosteroid-responsive autoimmune inner ear disease with methotrexate: a randomized controlled trial. *JAMA* (2003) 290(14):1875–83. doi:10.1001/jama.290.14.1875
32. Hughes GB, Kinney SE, Barna BP, Calabrese LH. Autoimmune reactivity in Meniere's disease: a preliminary report. *Laryngoscope* (1983) 93(4):410–7.
33. Yoo TJ, Shea J Jr, Ge X, Kwon SS, Yazawa Y, Sener O, et al. Presence of auto-antibodies in the sera of Meniere's disease. *Ann Otol Rhinol Laryngol* (2001) 110(5 Pt 1):425–9. doi:10.1177/000348940111000506
34. Fattori B, Nacci A, Dardano A, Dallan I, Grossi M, Traino C, et al. Possible association between thyroid autoimmunity and Meniere's disease. *Clin Exp Immunol* (2008) 152(1):28–32. doi:10.1111/j.1365-2249.2008.03595.x
35. Furuta T, Teranishi M, Uchida Y, Nishio N, Kato K, Otake H, et al. Association of interleukin-1 gene polymorphisms with sudden sensorineural hearing loss and Meniere's disease. *Int J Immunogenet* (2011) 38(3):249–54. doi:10.1111/j.1744-313X.2011.01004.x
36. Gazquez I, Moreno A, Requena T, Ohmen J, Santos-Perez S, Aran I, et al. Functional variants of MIF, INF γ and TNF α genes are not associated with disease susceptibility or hearing loss progression in patients with Meniere's disease. *Eur Arch Otorhinolaryngol* (2013) 270(4):1521–9. doi:10.1007/s00405-012-2268-0
37. Lopez-Escamez JA, Saenz-Lopez P, Acosta L, Moreno A, Gazquez I, Perez-Garrigues H, et al. Association of a functional polymorphism of PTPN22 encoding a lymphoid protein phosphatase in bilateral Meniere's disease. *Laryngoscope* (2010) 120(1):103–7. doi:10.1002/lary.20650
38. Cabrera S, Sanchez E, Requena T, Martinez-Bueno M, Benitez J, Perez N, et al. Intronic variants in the NFKB1 gene may influence hearing forecast in patients with unilateral sensorineural hearing loss in Meniere's disease. *PLoS One* (2014) 9(11):e112171. doi:10.1371/journal.pone.0112171
39. Gazquez I, Moreno A, Aran I, Soto-Varela A, Santos S, Perez-Garrigues H, et al. MICA-STR A.4 is associated with slower hearing loss progression in patients with Meniere's disease. *Otol Neurotol* (2012) 33(2):223–9. doi:10.1097/MAO.0b013e31824296c8
40. Requena T, Gazquez I, Moreno A, Batuecas A, Aran I, Soto-Varela A, et al. Allelic variants in TLR10 gene may influence bilateral affection and clinical course of Meniere's disease. *Immunogenetics* (2013) 65(5):345–55. doi:10.1007/s00251-013-0683-z
41. Radtke A, Lempert T, Gresty MA, Brookes GB, Bronstein AM, Neuhauser H. Migraine and Meniere's disease: is there a link? *Neurology* (2002) 59(11):1700–4. doi:10.1212/01.WNL.0000036903.22461.39
42. Lempert T, Olesen J, Furman J, Waterston J, Seemungal B, Carey J, et al. Vestibular migraine: diagnostic criteria. *J Vestib Res* (2012) 22(4):167–72. doi:10.3233/VES-2012-0453
43. Neff BA, Staab JP, Eggers SD, Carlson ML, Schmitt WR, Van Abel KM, et al. Auditory and vestibular symptoms and chronic subjective dizziness in patients with Meniere's disease, vestibular migraine, and Meniere's disease with concomitant vestibular migraine. *Otol Neurotol* (2012) 33(7):1235–44. doi:10.1097/MAO.0b013e31825d644a
44. Brown MR. The factor of heredity in labyrinthine deafness and paroxysmal vertigo; Meniere's syndrome. *Ann Otol Rhinol Laryngol* (1949) 58(3):665–70.
45. Morrison AW, Bailey ME, Morrison GA. Familial Meniere's disease: clinical and genetic aspects. *J Laryngol Otol* (2009) 123(1):29–37. doi:10.1017/S0022215108002788
46. Requena T, Espinosa-Sanchez JM, Lopez-Escamez JA. Genetics of dizziness: cerebellar and vestibular disorders. *Curr Opin Neurol* (2014) 27(1):98–104. doi:10.1097/WCO.0000000000000053
47. Frejo L, Giegling I, Teggi R, Lopez-Escamez JA, Rujescu D. Genetics of vestibular disorders: pathophysiological insights. *J Neurol* (2016) 263(Suppl 1):45–53. doi:10.1007/s00415-015-7988-9
48. Lee JM, Kim MJ, Jung J, Kim HJ, Seo YJ, Kim SH. Genetic aspects and clinical characteristics of familial Meniere's disease in a South Korean population. *Laryngoscope* (2015) 125(9):2175–80. doi:10.1002/lary.25207
49. Ohmen JD, White CH, Li X, Wang J, Fisher LM, Zhang H, et al. Genetic evidence for an ethnic diversity in the susceptibility to Meniere's disease. *Otol Neurotol* (2013) 34(7):1336–41. doi:10.1097/MAO.0b013e3182868818
50. Requena T, Cabrera S, Martin-Sierra C, Price SD, Lysakowski A, Lopez-Escamez JA. Identification of two novel mutations in FAM136A and DTNA genes in autosomal-dominant familial Meniere's disease. *Hum Mol Genet* (2015) 24(4):1119–26. doi:10.1093/hmg/ddu524
51. Committee on Hearing and Equilibrium guidelines for the diagnosis and evaluation of therapy in Meniere's disease. American Academy of Otolaryngology-Head and Neck Foundation, Inc. *Otolaryngol Head Neck Surg* (1995) 113(3):181–5. doi:10.1016/S0194-5998(95)70102-8
52. Belinchon A, Perez-Garrigues H, Tenias JM, Lopez A. Hearing assessment in Meniere's disease. *Laryngoscope* (2011) 121(3):622–6. doi:10.1002/lary.21335
53. Tyler R, Coelho C, Tao P, Ji H, Noble W, Gehring A, et al. Identifying tinnitus subgroups with cluster analysis. *Am J Audiol* (2008) 17(2):S176–84. doi:10.1044/1059-0889/2008/07-0044
54. Nabi S, Parnes LS. Bilateral Meniere's disease. *Curr Opin Otolaryngol Head Neck Surg* (2009) 17(5):356–62. doi:10.1097/MOO.0b013e3283304cb3
55. Morita N, Kariya S, Farajzadeh Deroee A, Cureoglu S, Nomiya S, Nomiya R, et al. Membranous labyrinth volumes in normal ears and Meniere disease: a three-dimensional reconstruction study. *Laryngoscope* (2009) 119(11):2216–20. doi:10.1002/lary.20723
56. Nonoyama H, Tanigawa T, Tamaki T, Tanaka H, Yamamoto O, Ueda H. Evidence for bilateral endolymphatic hydrops in ipsilateral delayed endolymphatic hydrops: preliminary results from examination of five cases. *Acta Otolaryngol* (2014) 134(3):221–6. doi:10.3109/00016489.2013.850741
57. Lopez-Escamez JA, Dlugaczyk J, Jacobs J, Lempert T, Teggi R, von Brevern M, et al. Accompanying symptoms overlap during attacks in Meniere's disease and vestibular migraine. *Front Neurol* (2014) 5:265. doi:10.3389/fneur.2014.00265
58. Pathak S, Hatam LJ, Bonagura V, Vambutas A. Innate immune recognition of molds and homology to the inner ear protein, cochlin, in patients with autoimmune inner ear disease. *J Clin Immunol* (2013) 33(7):1204–15. doi:10.1007/s10875-013-9926-x
59. Eisen MD, Niparko JK. Chapter 31 – autoimmune inner ear disease. In: Eggers SDZ, Zee DS, editors. *Handbook of Clinical Neurophysiology* (Vol. 9), Elsevier (2010). p. 428–32.
60. Oliveira CA, Ferrari I, Messias CI. Occurrence of familial Meniere's syndrome and migraine in Brasilia. *Ann Otol Rhinol Laryngol* (2002) 111(3 Pt 1):229–36. doi:10.1177/00034894021100307
61. Arweiler-Harbeck D, Horsthemke B, Jahnke K, Hennies HC. Genetic aspects of familial Meniere's disease. *Otol Neurotol* (2011) 32(4):695–700. doi:10.1097/MAO.0b013e318216074a
62. Hietikko E, Kotimaki J, Kentala E, Klockars T, Sorri M, Mannikko M. Finnish familial Meniere disease is not linked to chromosome 12p12.3, and anticipation and cosegregation with migraine are not common findings. *Genet Med* (2011) 13(5):415–20. doi:10.1097/GIM.0b013e3182091a41
63. Espinosa-Sanchez JM, Lopez-Escamez JA. New Insights into pathophysiology of vestibular migraine. *Front Neurol* (2015) 6:12. doi:10.3389/fneur.2015.00012
64. Gurkov R, Kantner C, Strupp M, Flatz W, Krause E, Ertl-Wagner B. Endolymphatic hydrops in patients with vestibular migraine and auditory symptoms. *Eur Arch Otorhinolaryngol* (2014) 271(10):2661–7. doi:10.1007/s00405-013-2751-2
65. Di Berardino F, Cesari A. Gluten sensitivity in Meniere's disease. *Laryngoscope* (2012) 122(3):700–2. doi:10.1002/lary.22492
66. Derebery MJ. Allergic and immunologic features of Meniere's disease. *Otolaryngol Clin North Am* (2011) 44(3):655–66, ix. doi:10.1016/j.otc.2011.03.004
67. Powers WH. Allergic factors in Meniere's disease. *Trans Am Acad Ophthalmol Otolaryngol* (1973) 77(1):ORL22–9.

68. Thirlwall AS, Kundu S. Diuretics for Meniere's disease or syndrome. *Cochrane Database Syst Rev* (2006) (3):CD003599. doi:10.1002/14651858.CD003599.pub2
69. Adrion C, Fischer CS, Wagner J, Gurkov R, Mansmann U, Strupp M, et al. Efficacy and safety of betahistine treatment in patients with Meniere's disease: primary results of a long term, multicentre, double blind, randomised, placebo controlled, dose defining trial (BEMED trial). *BMJ* (2016) 352:h6816. doi:10.1136/bmj.h6816
70. Pullens B, van Benthem PP. Intratympanic gentamicin for Meniere's disease or syndrome. *Cochrane Database Syst Rev* (2011) (3):CD008234. doi:10.1002/14651858.CD008234.pub2
71. Phillips JS, Westerberg B. Intratympanic steroids for Meniere's disease or syndrome. *Cochrane Database Syst Rev* (2011) (7):CD008514. doi:10.1002/14651858.CD008514.pub2

Conflict of Interest Statement: The authors declare that the research was conducted in the absence of any commercial or financial relationships that could be construed as a potential conflict of interest.

Copyright © 2016 Frejo, Soto-Varela, Santos-Perez, Aran, Batuecas-Caletrio, Perez-Guillen, Perez-Garrigues, Fraile, Martin-Sanz, Tapia, Trinidad, García-Arumí, González-Aguado, Espinosa-Sánchez, Marques, Perez, Benítez and López-Escamez On Behalf of the Meniere's Disease Consortium (MeDiC). This is an open-access article distributed under the terms of the Creative Commons Attribution License (CC BY). The use, distribution or reproduction in other forums is permitted, provided the original author(s) or licensor are credited and that the original publication in this journal is cited, in accordance with accepted academic practice. No use, distribution or reproduction is permitted which does not comply with these terms.



An Exploratory Study to Detect Ménière's Disease in Conventional MRI Scans Using Radiomics

E. L. van den Burg¹, M. van Hoof¹, A. A. Postma², A. M. L. Janssen³, R. J. Stokroos¹, H. Kingma^{1,4} and R. van de Berg^{1,4*}

¹ Department of Otorhinolaryngology and Head and Neck Surgery, Maastricht University Medical Center, Maastricht, Netherlands, ² Department of Radiology, Maastricht University Medical Center, Maastricht, Netherlands, ³ Department of Methodology and Statistics, School for Public Health and Primary Care (CAPHRI), Maastricht University, Maastricht, Netherlands, ⁴ Faculty of Physics, Tomsk State University, Tomsk, Russian Federation

Objective: The purpose of this exploratory study was to investigate whether a quantitative image analysis of the labyrinth in conventional magnetic resonance imaging (MRI) scans using a radiomics approach showed differences between patients with Ménière's disease (MD) and the control group.

Materials and methods: In this retrospective study, MRI scans of the affected labyrinths of 24 patients with MD were compared to the MRI scans of labyrinths of 29 patients with an idiopathic asymmetrical sensorineural hearing loss. The 1.5- and 3-T MRI scans had been previously made in a clinical setting between 2008 and 2015. 3D Slicer 4.4 was used to extract several substructures of the labyrinth. A quantitative analysis of the normalized radiomic image features was performed in Mathematica 10. The image features of the two groups were statistically compared.

Results: For numerous image features, there was a statistically significant difference (*p*-value <0.05) between the MD group and the control group. The statistically significant differences in image features were localized in all the substructures of the labyrinth: 43 in the anterior semicircular canal, 10 in the vestibule, 22 in the cochlea, 12 in the posterior semicircular canal, 24 in the horizontal semicircular canal, 11 in the common crus, and 44 in the volume containing the reuniting duct. Furthermore, some figures contain vertical or horizontal bands (three or more statistically significant image features in the same image feature). Several bands were seen: 9 bands in the anterior semicircular canal, 1 band in the vestibule, 3 bands in the cochlea, 0 bands in the posterior semicircular canal, 5 bands in the horizontal semicircular canal, 3 bands in the common crus, and 10 bands in the volume containing the reuniting duct.

Conclusion: In this exploratory study, several differences were found in image features between the MD group and the control group by using a quantitative radiomics approach on high resolution T2-weighted MRI scans of the labyrinth. Further research should be aimed at validating these results and translating them in a potential clinical diagnostic method to detect MD in MRI scans.

Keywords: Ménière's disease, MRI, imaging, radiomics, quantitative image analysis, labyrinth, 3D models, vertigo

OPEN ACCESS

Edited by:

Jose Antonio Lopez-Escamez,
Granada University Hospital, Spain

Reviewed by:

Eduardo Martin-Sanz,
Hospital de Getafe, Spain
Raquel Manrique-Huarte,
University of Navarra Clinic, Spain

*Correspondence:

R. van de Berg
raymond.vande.berg@mumc.nl

Specialty section:

This article was submitted
to Neuro-otology,
a section of the journal
Frontiers in Neurology

Received: 24 August 2016

Accepted: 18 October 2016

Published: 07 November 2016

Citation:

van den Burg EL, van Hoof M,
Postma AA, Janssen AML,
Stokroos RJ, Kingma H and
van de Berg R (2016) An Exploratory
Study to Detect Ménière's Disease in
Conventional MRI Scans Using
Radiomics.
Front. Neurol. 7:190.
doi: 10.3389/fneur.2016.00190

INTRODUCTION

Ménière's disease (MD) is a disorder of the inner ear, which is characterized by recurrent attacks of vertigo. These attacks are accompanied by a fluctuating sensorineural hearing loss and tinnitus or a sense of fullness in the affected ear (1). The exact cause and pathophysiology of MD is unclear and includes genetic, anatomic, metabolic, endocrine, autoimmune, vascular, allergic, viral, and traumatic factors (2). Histopathologic examination in patients with MD shows a distention of Reissner's membrane (endolymphatic hydrops) in the cochlea or endolymphatic compartment of the labyrinth (3, 4). Since histopathologic examination (the gold standard) is not possible in a clinical setting, the diagnosis depends on the symptoms of MD (1, 5). For the diagnosis of definite MD, one of the criteria is that other causes of the symptoms have been excluded. Magnetic resonance imaging (MRI) is often indicated because of asymmetrical sensorineural hearing loss and to exclude other possible causes (6). However, it remains difficult to differentiate between MD and other causes of vertigo. Therefore, new imaging techniques are under investigation as a MD diagnostic, which include cone beam computed tomography (7) and MRI enhanced by invasive contrast agents such as gadolinium (8, 9). The administration of an intratympanic gadolinium injection is an invasive procedure and although adverse events are rare after intravenous contrast media, they are known to occur (10). A non-invasive imaging technique would be preferable as it could be argued that the invasiveness of this procedure does not justify the (potential) gain in diagnostic information it provides.

Here, an alternative approach is taken by analyzing quantitative data in conventional MRI scans. The evidence is increasing that with new imaging processing and analysis techniques, the evidence is increasing that with new imaging processing and analysis techniques, more information can be gathered from standard imaging modalities (11, 12). Texture analysis uses features such as the distribution of gray levels in an area or volume in an MRI scan (13). Radiomics refers to the extraction and analysis of such quantitative image features from medical images obtained with computed tomography (CT), positron emission tomography (PET), or MRI (14). These quantitative image features provide additional information about the analyzed structures that are not necessarily perceptually visible by the (neuro)radiologist. Another advantage is that standard-of-care images from the clinic can be used (14). In the process of radiomics, there are several steps to be followed (15). The first step is the acquisition of imaging (preferably standard-of-care). Second, an anatomical region has to be segmented to define the region of interest on the acquired image volume. In the study, here, this is the labyrinth. Third, quantitative image features have to be calculated from this segmentation (such as the mean of the intensities in the segmentation). Finally, these quantitative image features can be used for statistical analysis. Several recent studies have shown that radiomics can be used to obtain information about, for example, tumor phenotypes and prognosis (11, 12), tumor biomarkers (16), and distant metastasis (17). Studies have also shown structural differences in patients with amyotrophic lateral sclerosis (13) and Alzheimer's disease (18) when compared to healthy subjects.

The purpose of this exploratory study was to investigate whether a quantitative image analysis of the labyrinth in conventional MRI scans using a radiomics approach showed differences between patients with MD and the control group.

MATERIALS AND METHODS

Ethical Considerations

This study was performed in accordance with the guidelines outlined by Dutch legislation. According to the Medical Research Involving Human Subjects Act (WMO), ethical approval was not required due to the retrospective nature and anonymization of the data.

Study Population

A retrospective study was performed. Patients with MD were identified from the patient registration system from a tertiary center. Patients with definite MD according to the criteria as accepted by the American Academy of Otolaryngology-Head and Neck Surgery (AAO-HNS) (1) were included, since these were the most recent criteria for MD during the inclusion period. In retrospect, the diagnostic criteria for definite MD as formulated in 2015 by the Bárány Society (5) also apply to all the patients with MD included in this study. Furthermore, an MRI scan of the cerebellopontine angle made in two preselected MRI scanners was required for inclusion. Since this retrospective study was performed in a tertiary center, many patients with MD had an MRI scan made in another center and could therefore not be included in this study. The labyrinth affected by MD was used in the study. In case of bilateral MD, one of the labyrinths was chosen. The exclusion criterion was motion artifacts on the MRI scan (the criterion was that the inner ear should be sharply delineated). The control group consisted of patients with idiopathic asymmetrical sensorineural hearing loss. These patients were chosen as controls, since this was a retrospective study and no MRI scans from people without hearing loss were available. The labyrinth least affected by hearing loss was included in the study, because this labyrinth was considered to be most representative for a healthy person. In the clinical setting, conventional clinical tests at the discretion of the ENT specialists were performed to diagnose the patients with an idiopathic asymmetrical sensorineural hearing loss. The exclusion criteria were composed of a documented history of vertigo or balance disorders and having motion artifacts on the MRI scan. The control group was matched to the MD group by scanning date to minimize biases which might arise from differences in scanning protocols over the years.

MR Imaging

A Philips Intera MRI scanner (1.5 T) and a Philips Achieva MRI scanner (3 T) had been used to obtain the 3D High resolution T2-weighted images (Philips Nederland B.V., Eindhoven, The Netherlands). The scans had been previously made in a clinical setting between 2008 and 2015. The scan parameters were not constant, as can be seen in **Table 1**. All the scans had been previously evaluated by a radiologist.

TABLE 1 | Scan parameters.

	1.5-T MRI scanner	3-T MRI scanner
Scanning date	01-08-2012 until 17-05-2015	28-05-2008 until 31-05-2011
Repetition time (ms)	1500	2000
Echo time (ms)	Between 169 and 182	200
Slice thickness (mm)	0.6	1.0
Spacing between the slices (mm)	0.3	0.5
Echo train length	40	59
Magnetic field strength (T)	1.5	3

Scan parameters and scanning data of the included MRI scans.

Image Extraction of the Labyrinth

3D Slicer 4.4, an open source software package for visualization and image analysis (19, 20) was used to extract the (sub)volumes from the MRI scans. First, a label was created in the shape of the labyrinth for the segmentation. The labyrinth was segmented into several substructures: the cochlea, the volume containing the reuniting duct, the vestibule, the semicircular canals, and the common crus (Figure 1). The labels were used as masks for intensity data extraction and to generate 3D models to measure the surface area and the volume of the different substructures and the labyrinth.

Radiomic Feature Extraction and Statistical Analysis

Mathematica 10 (Wolfram Research, Champaign, IL, USA) was used for the radiomic feature extraction and statistical analysis. 3D models from the separate substructures were created with the edited MRI scans. These 3D models were modified by using 25 different image processing filters, resulting in a total of 26 primary radiomic features. A few examples are the entropy filter, the Laplacian filter, and the Fourier DCT filter. Every model was used to calculate 23 secondary radiomic features, which were statistical values such as the minimal intensity, the maximal intensity, and the mean intensity. The radiomic features were based on standard functions available in Mathematica 10. A list of different functions used can be found in Tables 2 and 3. In total, 598 image features were extracted. Because of differences between MRI scanners and scanning protocols, the image features were normalized. This was done by dividing the features from the different substructures of one patient by the features of the entire labyrinth of the same patient, thereby diminishing potential systematic differences introduced by different scanner's and scanner protocols (Table 1). For the statistical analysis of the radiomic image features, a permutation test was used. A two-sided *p*-value of <0.05 was considered significant.

RESULTS

Ménière's Disease Group and Control Group

In total, 24 patients who met the inclusion criteria for MD were included in this study. The control group consisted of 29 patients.

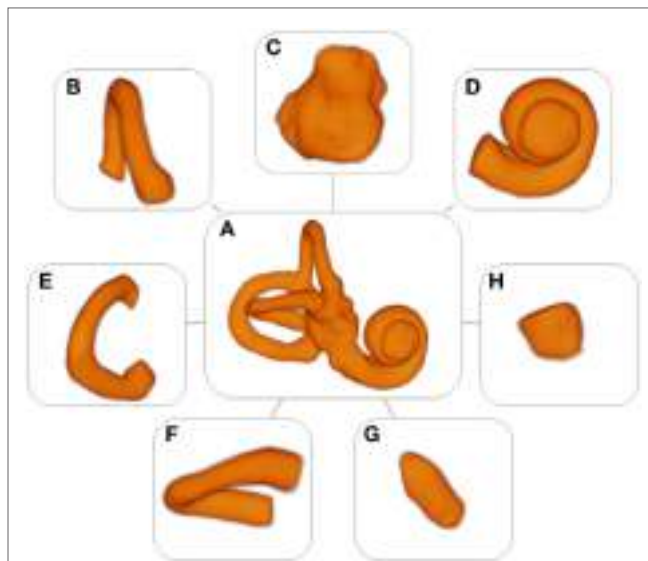


FIGURE 1 | Models of the labyrinth and its substructures. (A) Labyrinth, (B) anterior semicircular canal, (C) vestibule, (D) cochlea, (E) posterior semicircular canal, (F) horizontal semicircular canal, (G) common crus, and (H) volume containing the reuniting duct.

TABLE 2 | Primary radiomic features.

- 1 No filter
- 2 FourierDCTFilter
- 3 EdgeDetect
- 4 GradientOrientationFilter
- 5 EntropyFilter (range 1)
- 6 EntropyFilter (range 2)
- 7 EntropyFilter (range 3)
- 8 EntropyFilter (range 4)
- 9 EntropyFilter (range 5)
- 10 EntropyFilter (range 6)
- 11 LaplacianFilter
- 12 RidgeFilter
- 13 LaplacianGaussianFilter
- 14 ClusteringComponents
- 15 MorphologicalComponents
- 16 MorphologicalBinarize
- 17 DiscreteWaveletTransform (1)
- 18 DiscreteWaveletTransform (2)
- 19 DiscreteWaveletTransform (3)
- 20 DiscreteWaveletTransform (4)
- 21 DiscreteWaveletTransform (5)
- 22 DiscreteWaveletTransform (6)
- 23 DiscreteWaveletTransform (7)
- 24 DiscreteWaveletTransform (8)
- 25 ImageSaliencyFilter
- 26 ColorToneMapping

Functions used in Mathematica 10 (Wolfram Research, Champaign, IL, USA) to create the primary radiomic features.

The two groups were similar with regard to age, the labyrinth analyzed, and distribution between MRI scanners and scanning dates (Table 4). More men than women were included in both groups. The median hearing loss in the analyzed ear was higher in the MD group than in the control group.

Surface Area and Volume

The surface area and volume of the labyrinth and its separate substructures were not significantly different between the two groups (**Table 5**).

Models

A set of 53 detailed models of the labyrinth and its separate substructures were formed (**Figure 1**). These models were used to extract the radiomic image features. In addition, they provided an accurate three-dimensional image of the labyrinth and its substructures.

Radiomic Image Features

A total of 598 radiomic image features were analyzed in every substructure of the labyrinth. In all the separate substructures,

statistically significant differences between the MD group and the control group were seen in several image features (**Figures 2A–G**). **Figure 2H** shows the p-value legend. In the figures, differences are seen between the amount of statistically significant image features in the different substructures: 43 in the anterior semicircular canal, 10 in the vestibule, 22 in the cochlea, 12 in the posterior semicircular canal, 24 in the horizontal semicircular canal, 11 in the common crus, and 44 in the volume containing the reuniting duct. For example, there are more imaging features that resulted in statistical significance in the volume containing the reuniting duct and in the anterior semicircular canal than in the other substructures. Furthermore, some figures contain

TABLE 3 | Secondary radiomic features.

1	ImageMeasurements, MinIntensity
2	ImageMeasurements, MaxIntensity
3	ImageMeasurements, MeanIntensity
4	ImageMeasurements, MedianIntensity
5	ImageMeasurements, StandardDeviationIntensity
6	ImageMeasurements, TotalIntensity
7	ImageMeasurements, Skew
8	ImageMeasurements, IntensityCentroid (x-coordinate)
9	ImageMeasurements, IntensityCentroid (y-coordinate)
10	ImageMeasurements, IntensityCentroid (z-coordinate)
11	ImageMeasurements, Entropy
12	ImageMeasurements, Energy
13	DominantColors (amount)
14	DominantColors (primary)
15	VarianceCI (low)
16	VarianceCI (high)
17	Kurtosis
18	TrimmedMean
19	MeanDeviation
20	RootMeanSquare
21	Variance
22	Commonest (mean)
23	AutocorrelationTest

Functions used in Mathematica 10 (Wolfram Research, Champaign, IL, USA) to create the secondary radiomic features.

TABLE 4 | Patient demographics.

	Ménière's disease group (n = 24)	Control group (n = 29)
Age at the moment of scanning in years [median (interquartile range)]	61 (51–71)	56 (48.8–64.3)
Gender (F/M)	37.5/62.5%	13.8/86.2%
Analyzed labyrinth (left/right)	50.0/50.0%	37.9/62.1%
MRI-scanner (1.5/3 T)	41.7/58.3%	34.5/65.5%
Scanning date (range)	29-10-2008 until 17-05-2015	28-05-2008 until 26-04-2015
Distribution of scanning dates	2008 2009 2010 2011 2012 2013 2014 2015	4.2% 4.2% 4.2% 4.2% 12.5% 25.0% 33.3% 12.5%
Average hearing loss ^a in analyzed ear in dB [median (interquartile range)]	61 (42–75)	13 (8–25.5)
Bilateral MD (yes/no)	20.8/79.2%	–

Information about the Ménière's disease group and the control group.

^aThe audiogram closest to the date of scanning was used.

TABLE 5 | Surface area and volume of the labyrinth and its separate substructures.

	Ménière's disease (n = 24)	Control group (n = 29)	p-Value	
Surface area in mm ² [median (interquartile range)]	Cochlea Volume containing the reuniting duct Vestibule Anterior semicircular canal Posterior semicircular canal Horizontal semicircular canal Common crus Labyrinth	135.29 (129.08–146.86) 31.06 (25.64–35.14) 95.39 (91.97–104.12) 70.03 (63.34–74.12) 79.48 (70.77–86.47) 61.23 (50.92–68.34) 21.38 (18.86–23.78) 435.63 (412.51–478.74)	144.31 (135.91–150.45) 27.72 (25.19–31.78) 95.43 (89.78–107.69) 68.82 (61.25–77.39) 82.74 (71.33–90.04) 58.89 (50.48–65.90) 23.44 (19.85–25.82) 442.97 (413.05–473.11)	0.122 0.195 0.721 0.514 0.574 0.688 0.284 0.649
Volume in mm ³ [median (interquartile range)]	Cochlea Volume containing the reuniting duct Vestibule Anterior semicircular canal Posterior semicircular canal Horizontal semicircular canal Common crus Labyrinth	80.22 (74.96–90.51) 12.82 (9.47–14.86) 65.27 (60.04–72.31) 22.73 (17.65–26.32) 26.49 (21.43–29.49) 20.42 (14.03–23.78) 7.01 (5.61–8.21) 236.26 (202.02–272.98)	86.80 (76.04–97.29) 10.53 (9.16–12.86) 65.21 (58.07–76.90) 20.71 (17.00–25.10) 27.63 (20.16–31.04) 18.19 (13.38–21.66) 8.14 (5.84–9.15) 239.68 (207.96–267.81)	0.335 0.172 0.957 0.437 0.979 0.469 0.348 0.936

The surface area and volume of the labyrinth and its separate substructures.

vertical or horizontal bands, which show that there are several image features statistically significant in the same primary or secondary image feature. We have defined a band as three or more statistically significant image features in the same row or column. For example, **Figure 2C** shows a vertical band in the twelfth primary radiomic feature, and **Figure 2A** shows a horizontal band in the ninth secondary radiomic feature. In **Figures 2A–G**, several bands are seen: 9 bands in the anterior semicircular canal, 1 band in the vestibule, 3 bands in the cochlea, 0 bands in the posterior semicircular canal, 5 bands in the horizontal semicircular canal, 3 bands in the common crus, and 10 bands in the volume containing the reuniting duct.

DISCUSSION

Significant differences in radiomics image features between the MD group and the control group were found in all the substructures of the labyrinth. The band-like patterns shown in **Figures 2A–G** are more important than just the significant *p*-values as its interpretation is less at risk for chance findings because no corrections for multiple testing were performed. These bands indicate that primary or secondary radiomic modifications amplify features with a certain consistency. The differences found in the substructures do not necessarily reflect visually perceptible differences. Research has been performed into the histopathology

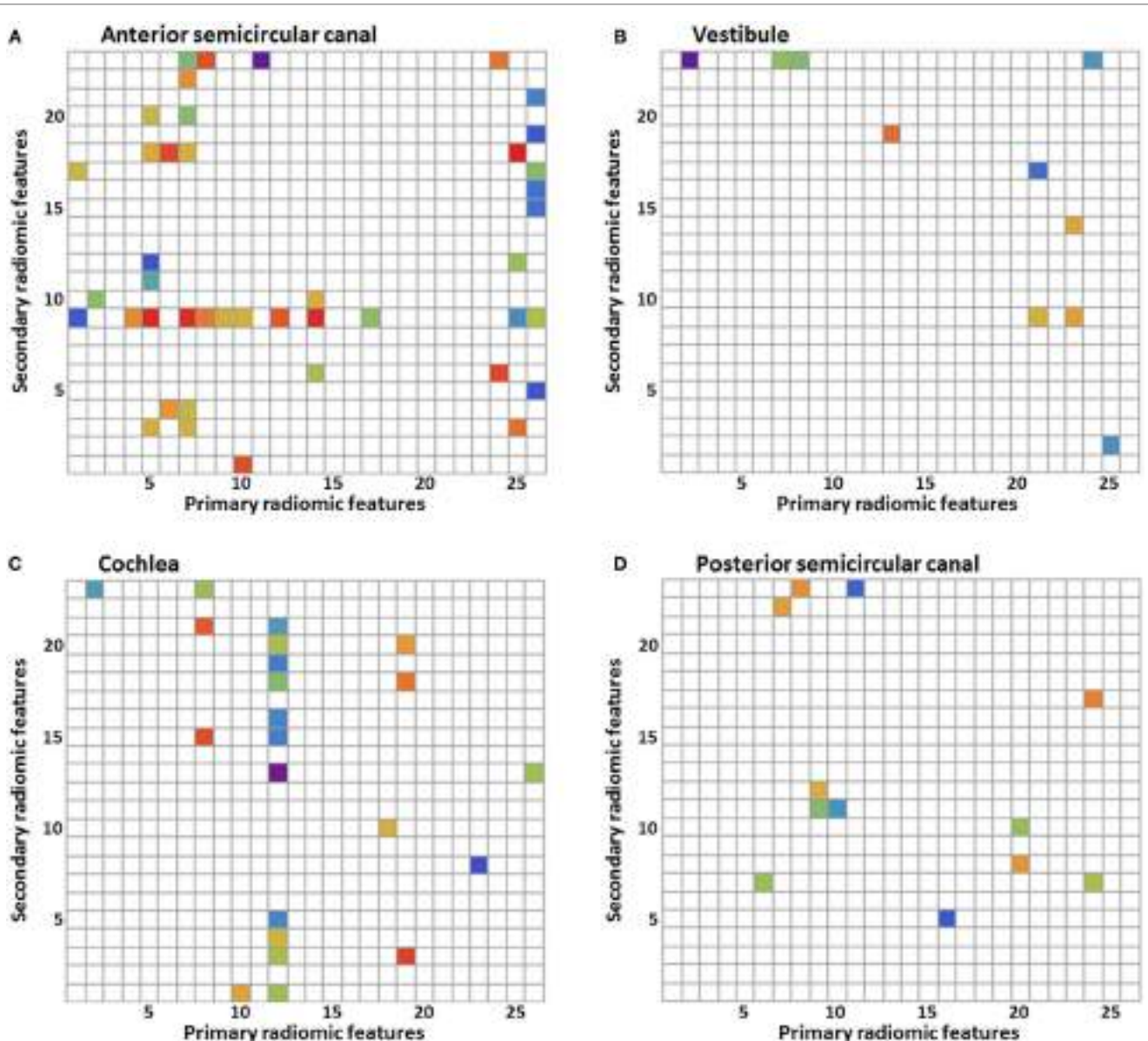
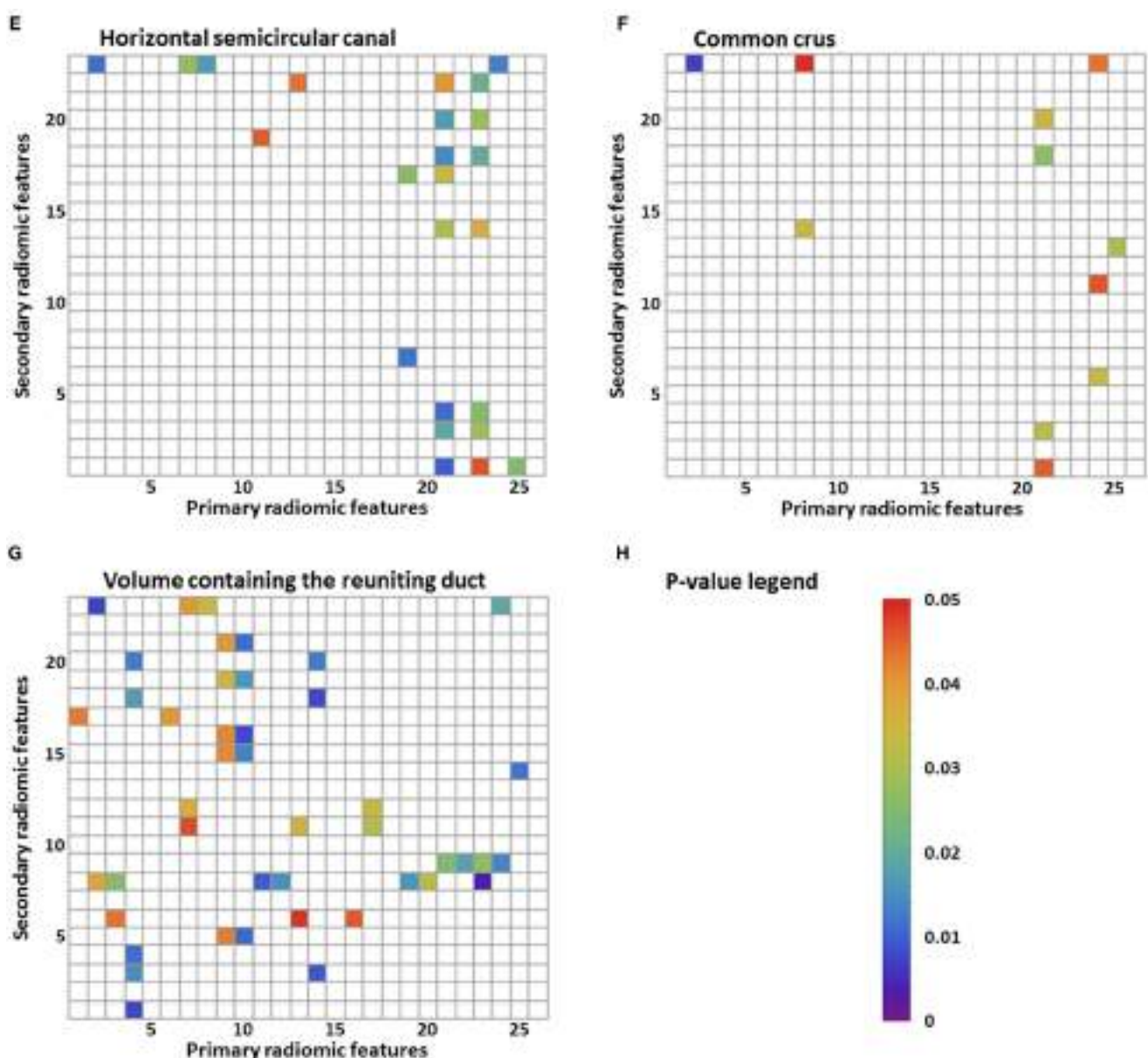


FIGURE 2 | Results of the statistical analysis of the radiomic image features.

(Continued)

**FIGURE 2 | Continued**

Every p -value <0.05 is shown in color. Primary radiomic features are shown on the x-axis; these represent the different image processing filters. The secondary radiomic features are shown on the y-axis; these are the statistical values calculated from the primary radiomic features. A list of the primary radiomic features can be found in **Table 2** and a list of the secondary radiomic features can be found in **Table 3**. A vertical band means that there are several significant image features in one primary radiomic feature, and a horizontal band means that there are several significant image features in one secondary radiomic feature. The figures represent one of the substructures of the labyrinth: (A) anterior semicircular canal, (B) vestibule, (C) cochlea, (D) posterior semicircular canal, (E) horizontal semicircular canal, (F) common crus, (G) volume containing the reuniting duct, and (H) p -value legend.

of MD (4, 21) also using proteomic techniques (22) and qualitative imaging techniques (7). This might provide an explanation for the observed differences in image features. The histopathology observed in a study of the temporal bones of patients with MD is endolymphatic hydrops (4). A distension, herniation, and rupture of the endolymph compartment were not necessarily confined to the cochlea. Pathologic changes were found to be present in the whole labyrinth, though the canals and common crus were

affected the least (21). In another study, it was suggested that an inflammatory or autoimmune reaction in the inner ear may cause damage to the epithelial layers surrounding the endolymphatic space (22). Results found in this study correspond with these findings, since a significant difference was found in all the substructures of the labyrinth. However, a meta-analysis of temporal bone reports showed that the lesion distribution was orderly from the cochlea to the saccule, utricle, ampullae, and then the canal

system (21). In our study, we did not find this order, since there were more statistically significant image features in, for example, the anterior semicircular canal than in the cochlea. The difference in image features could hypothetically be explained by the damage to or different distribution of differently charged fluids in several parts of the labyrinth, causing a different distribution of the intensities. A recent study using a proteomic approach found differences in protein composition of the inner ear fluid in MD patients in comparison to controls. The inner ear fluid of MD patients contained other immunoglobulins and its variants (22). Since γ -globulin has a higher relaxivity in serum (23), it could be a possible explanation for the differences in image features found in this study. Another study found a significant difference in the shape of the reuniting duct using cone beam CT (7). In this study, more imaging features that resulted in statistically significance were found in the volume containing the reuniting duct than in the other substructures, but this volume was also considerably smaller increasing the risk on a chance finding.

Future Clinical Implementation

The next step in exploring the application of radiomics for diagnosing patients with MD is to determine the accuracy as a diagnostic tool. For this purpose, an extensive internal and external validation is necessary. Recent research demonstrated that machine learning and radiomics can be used to predict overall survival in lung cancer patients (24). To investigate whether machine learning could be used for diagnosing MD patients, it should be trained and validated on two separate sets of data. The use of an independent test set would provide information on the diagnostic accuracy of this method. The advantage of using machine learning in combination with radiomics is that the analysis of the labyrinth could possibly be done autonomously as automatic image segmentation and registration are already feasible (25). The scalability that results from such a setup could possibly reshape diagnostics of the inner ear in the field of (neuro) radiology. In addition, it might be possible to identify patients who for some reason are difficult to diagnose by using the criteria for definite MD, for example, because of fluctuating hearing loss.

These results are promising, but radiomics cannot be used in the diagnosis of patients with MD yet. MD shows several gradations that are not yet distinguished objectively but possibly could be in the future by performing a cluster analysis on image features. Also in clinical practice, it is necessary to differentiate between three populations: patients with MD, patients with other balance disorders, and patients with complaints of dizziness which cannot be objectified (yet) (Figure 3). To enhance the differentiation between these groups, it could be helpful to cluster the relevant features to form a more robust model. Furthermore, during the last several years, several studies have been performed into the visualization of endolymphatic hydrops by using intravenous or intratympanic contrast agents such as gadolinium (8, 9, 26). Studies have been performed that have proposed a grading system for endolymphatic hydrops on MRI (27, 28) or that found a correlation between the progression of disease and endolymphatic hydrops on MRI (29). Further research is necessary to compare the radiomics method to the

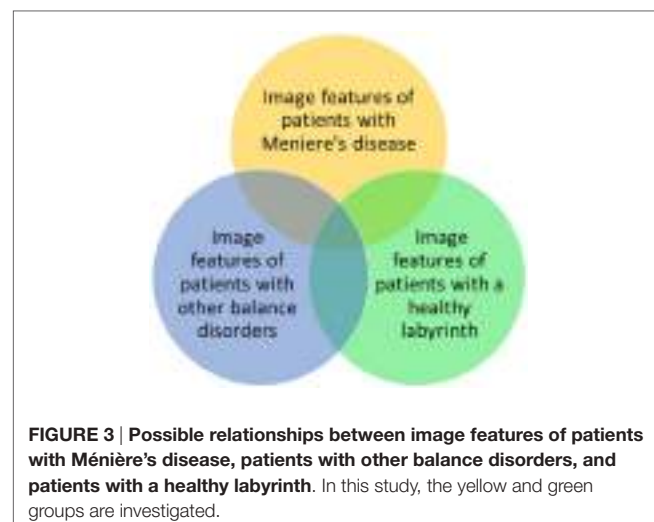


FIGURE 3 | Possible relationships between image features of patients with Ménière's disease, patients with other balance disorders, and patients with a healthy labyrinth. In this study, the yellow and green groups are investigated.

use of MRI enhanced by contrast agents, to see if similar results are found. By clustering several image features, the feasibility of a grading system in the radiomics method or a correlation between the progression of disease or progression of hearing loss can also be explored. The clustering of features can possibly also be used to separate hitherto unidentified subtypes of MD. Another advantage of the radiomics method is that no invasive contrast agents are necessary.

Limitations

A limitation in this study is that it did not include other balance disorders or other otologic conditions that could alter the composition of the labyrinth. The aim of this exploratory study instead was to investigate whether radiomic image features allow for differences to be detected between patients with MD and controls on conventional MRI scans and to provide a proof of concept for this method. Furthermore, since the aim was not to identify a single feature that could be used to diagnose a patient with MD but to identify features that could in the future be combined and used for subsequent machine learning, no correction for multiple testing was performed. Doing so would minimize false positives but could also obscure potentially important features. The statistical significant results could therefore include false positives.

Despite having two similar groups in terms of demographics (Table 4) and surface area and volume of the substructures (Table 5), confounding differences concerning the MRI scanner setup cannot be completely ruled out in this relatively small sample size (Table 1). To minimize the effect of different scan parameters, the control group was matched to the MD group by scanning date. Furthermore, by normalizing the values, it was deemed possible to compare the data, because relative differences could be analyzed. On the other hand, the variability in MRI scanners in this study might also be an advantage. If radiomics could be used clinically for the diagnosis of MD in the future, it could be more widely implemented if the method is robust and independent of the type of MRI scanner or scanning

parameters. Furthermore, we have included both unilateral and bilateral MD patients in this study, seeing that in the future the model would be more robust if both types of MD were included. Even though the etiopathogenesis might not be the same, the structural differences in the labyrinth are thought to be similar (21) and both show endolymphatic hydrops on MRI enhanced by contrast agents (30).

CONCLUSION

In this exploratory study, several differences were found in image features between the MD group and the control group by using a quantitative radiomics approach on high resolution T2-weighted MRI scans of the labyrinth. Further research should be aimed at

validating these results and translating them in a potential clinical diagnostic method to detect MD in MRI scans.

AUTHOR CONTRIBUTIONS

All the authors contributed to the design of the work presented in this paper. EB and MH designed the experiment, gathered the data, performed the analysis, and wrote the manuscript. RB designed the experiment, performed the analysis, supervised the writing, reviewed the manuscript, and edited the manuscript. AP and AJ performed the analysis, reviewed the manuscript, and edited the manuscript. RS and HK reviewed the manuscript and edited the manuscript. All the authors take full responsibility for the correctness of this paper and approved the final version.

REFERENCES

- Committee on Hearing and Equilibrium guidelines for the diagnosis and evaluation of therapy in Meniere's disease. *Otolaryngol Head Neck Surg* (1995) 113:181–5. doi:10.1016/S0194-5998(95)70102-8
- Chiarella G, Petrolo C, Cassandro E. The genetics of Meniere's disease. *Appl Clin Genet* (2015) 8:9–17. doi:10.2147/tacg.s59024
- Hallpike CS, Cairns H. Observations on the pathology of Meniere's syndrome. *J Laryngol Otol* (1938) 53:625–55. doi:10.1017/S0022215100003947
- Foster CA, Breeze RE. Endolymphatic hydrops in Meniere's disease: cause, consequence, or epiphénoménon? *Otol Neurotol* (2013) 34:1210–4. doi:10.1097/MAO.0b013e31829e83df
- Lopez-Escamez JA, Carey J, Chung W-H, Goebel JA, Magnusson M, Mandalà M, et al. Diagnostic criteria for Meniere's disease. *J Vestib Res* (2015) 25:1–7. doi:10.3233/VES-150549
- Harcourt J, Barraclough K, Bronstein AM. Meniere's disease. *BMJ* (2014) 349:g6544. doi:10.1136/bmj.g6544
- Yamane H, Iguchi H, Konishi K, Sakamaoto H, Wada T, Fujioka T, et al. Three-dimensional cone beam computed tomography imaging of the membranous labyrinth in patients with Meniere's disease. *Acta Otolaryngol* (2014) 134:1016–21. doi:10.3109/00016489.2014.913315
- Nakashima T, Naganawa S, Suguri M, Teranishi M, Sone M, Hayashi H, et al. Visualization of endolymphatic hydrops in patients with Meniere's disease. *Laryngoscope* (2007) 117:415–20. doi:10.1097/MLG.0b013e31802c300c
- Nakashima T, Naganawa S, Teranishi M, Tagaya M, Nakata S, Sone M, et al. Endolymphatic hydrops revealed by intravenous gadolinium injection in patients with Meniere's disease. *Acta Otolaryngol* (2010) 130:338–43. doi:10.1080/00016480903143986
- Rose TA, Choi JW. Intravenous imaging contrast media complications: the basics that every clinician needs to know. *Am J Med* (2015) 128:943–9. doi:10.1016/j.amjmed.2015.02.018
- Parmar C, Leijenaar RTH, Grossmann P, Rios Velazquez E, Bussink J, Rietveld D, et al. Radiomic feature clusters and prognostic signatures specific for lung and head & neck cancer. *Sci Rep* (2015) 5:11044. doi:10.1038/srep11044
- Aerts HJ, Velazquez ER, Leijenaar RT, Parmar C, Grossmann P, Carvalho S, et al. Decoding tumour phenotype by noninvasive imaging using a quantitative radiomics approach. *Nat Commun* (2014) 5:4006. doi:10.1038/ncomms5006
- de Albuquerque M, Anjos LGV, Maia Tavares de Andrade H, de Oliveira MS, Castellano G, Junqueira Ribeiro de Rezende T, et al. MRI texture analysis reveals deep gray nuclei damage in amyotrophic lateral sclerosis. *J Neuroimaging* (2016) 26:201–6. doi:10.1111/jon.12262
- Kumar V, Gu Y, Basu S, Berglund A, Eschrich SA, Schabath MB, et al. Radiomics: the process and the challenges. *Magn Reson Imaging* (2012) 30:1234–48. doi:10.1016/j.mri.2012.06.010
- Lambin P, Rios-Velazquez E, Leijenaar R, Carvalho S, van Stiphout RG, Granton P, et al. Radiomics: extracting more information from medical images using advanced feature analysis. *Eur J Cancer* (2012) 48:441–6. doi:10.1016/j.ejca.2011.11.036
- Dang M, Lysack JT, Wu T, Matthews TW, Chandarana SP, Brockton NT, et al. MRI texture analysis predicts p53 status in head and neck squamous cell carcinoma. *AJNR Am J Neuroradiol* (2015) 36:166–70. doi:10.3174/ajnr.A4110
- Coroller TP, Grossmann P, Hou Y, Rios Velazquez E, Leijenaar RT, Hermann G, et al. CT-based radiomic signature predicts distant metastasis in lung adenocarcinoma. *Radiother Oncol* (2015) 114:345–50. doi:10.1016/j.radonc.2015.02.015
- De Oliveira MS, Balthazar MLF, D'Abreu A, Yasuda CL, Damasceno BP, Cendes F, et al. MR imaging texture analysis of the corpus callosum and thalamus in amnestic mild cognitive impairment and mild Alzheimer disease. *AJNR Am J Neuroradiol* (2011) 32:60–6. doi:10.3174/ajnr.A2232
- Slicer. *BWH and 3D Slicer Contributors*. (2015). Available from: <http://www.slicer.org>
- Fedorov A, Beichel R, Kalpathy-Cramer J, Finet J, Fillion-Robin JC, Pujol S, et al. 3D Slicer as an image computing platform for the Quantitative Imaging Network. *Magn Reson Imaging* (2012) 30:1323–41. doi:10.1016/j.mri.2012.05.001
- Pender DJ. Endolymphatic hydrops and Meniere's disease: a lesion meta-analysis. *J Laryngol Otol* (2014) 128:859–65. doi:10.1017/s0022215114001972
- Kim SH, Kim JY, Lee HJ, Gi M, Kim BG, Choi JY. Autoimmunity as a candidate for the etiopathogenesis of Meniere's disease: detection of autoimmune reactions and diagnostic biomarker candidate. *PLoS One* (2014) 9:e111039. doi:10.1371/journal.pone.0111039
- Yilmaz A, Ulak FS, Batun MS. Proton T1 and T2 relaxivities of serum proteins. *Magn Reson Imaging* (2004) 22:683–8. doi:10.1016/j.mri.2004.02.001
- Parmar C, Grossmann P, Bussink J, Lambin P, Aerts HJ. Machine learning methods for Quantitative Radiomic Biomarkers. *Sci Rep* (2015) 5:13087. doi:10.1038/srep13087
- Gurkov R, Berman A, Dietrich O, Flatz W, Jerin C, Krause E, et al. MR volumetric assessment of endolymphatic hydrops. *Eur Radiol* (2015) 25:585–95. doi:10.1007/s00330-014-3414-4
- Pykkö I, Nakashima T, Yoshida T, Zou J, Naganawa S. Ménière's disease: a reappraisal supported by a variable latency of symptoms and the MRI visualisation of endolymphatic hydrops. *BMJ Open* (2013) 3:e001555. doi:10.1136/bmjjopen-2012-001555
- Barath K, Schuknecht B, Naldi AM, Schrepfer T, Bockisch CJ, Hegemann SC. Detection and grading of endolymphatic hydrops in Meniere disease using MR imaging. *AJNR Am J Neuroradiol* (2014) 35:1387–92. doi:10.3174/ajnr.A3856
- Gurkov R, Flatz W, Louza J, Strupp M, Ertl-Wagner B, Krause E. In vivo visualized endolymphatic hydrops and inner ear functions in patients with electrocochleographically confirmed Meniere's disease. *Otol Neurotol* (2012) 33:1040–5. doi:10.1097/MAO.0b013e31825d9a95
- Fiorino F, Pizzini FB, Beltramello A, Barbieri F. Progression of endolymphatic hydrops in Meniere's disease as evaluated by magnetic resonance imaging. *Otol Neurotol* (2011) 32:1152–7. doi:10.1097/MAO.0b013e31822a1ce2
- Gu X, Fang ZM, Liu Y, Huang ZW, Zhang R, Chen X. Diagnostic advantages of intratympanically gadolinium contrast-enhanced magnetic resonance

imaging in patients with bilateral Meniere's disease. *Am J Otolaryngol* (2015) 36:67–73. doi:10.1016/j.amjoto.2014.10.003

Conflict of Interest Statement: The authors declare that the research was conducted in the absence of any commercial or financial relationships that could be construed as a potential conflict of interest.

Copyright © 2016 van den Burg, van Hoof, Postma, Janssen, Stokroos, Kingma and van de Berg. This is an open-access article distributed under the terms of the Creative Commons Attribution License (CC BY). The use, distribution or reproduction in other forums is permitted, provided the original author(s) or licensor are credited and that the original publication in this journal is cited, in accordance with accepted academic practice. No use, distribution or reproduction is permitted which does not comply with these terms.



The Skull Vibration-Induced Nystagmus Test of Vestibular Function—A Review

Georges Dumas^{1,2*}, Ian S. Curthoys³, Alexis Lion^{2,4}, Philippe Perrin^{2,5} and Sébastien Schmerber^{1,6}

¹Department of Oto-Rhino-Laryngology, Head and Neck Surgery, University Hospital, Grenoble, France, ²EA 3450 DevAH, Development, Adaptation and Disadvantage, Faculty of Medicine and UFR STAPS, University of Lorraine, Villers-lès-Nancy, France, ³Vestibular Research Laboratory, School of Psychology, the University of Sydney, Sydney, NSW, Australia, ⁴Sports Medicine Research Laboratory, Luxembourg Institute of Health, Strassen, Luxembourg, ⁵Department of Paediatric Oto-Rhino-Laryngology, University Hospital of Nancy, Vandoeuvre-lès-Nancy, France, ⁶INSERM UMR 2015, Grenoble, France

OPEN ACCESS

Edited by:

Richard Lewis,
Harvard University, USA

Reviewed by:

Bernard Cohen,
Icahn School of Medicine at Mount
Sinai, USA
Shinichi Iwasaki,
University of Tokyo, Japan

*Correspondence:

Georges Dumas
GDumas@chu-grenoble.fr

Specialty section:

This article was submitted to
Neuro-otology,
a section of the journal
Frontiers in Neurology

Received: 18 August 2016

Accepted: 30 January 2017

Published: 09 March 2017

Citation:

Dumas G, Curthoys IS, Lion A, Perrin P and Schmerber S (2017)
The Skull Vibration-Induced Nystagmus Test of Vestibular Function—A Review.
Front. Neurol. 8:41.
doi: 10.3389/fneur.2017.00041

A 100-Hz bone-conducted vibration applied to either mastoid induces instantaneously a predominantly horizontal nystagmus, with quick phases beating away from the affected side in patients with a unilateral vestibular loss (UVL). The same stimulus in healthy asymptomatic subjects has little or no effect. This is skull vibration-induced nystagmus (SVIN), and it is a useful, simple, non-invasive, robust indicator of asymmetry of vestibular function and the side of the vestibular loss. The nystagmus is precisely stimulus-locked: it starts with stimulation onset and stops at stimulation offset, with no post-stimulation reversal. It is sustained during long stimulus durations; it is reproducible; it beats in the same direction irrespective of which mastoid is stimulated; it shows little or no habituation; and it is permanent—even well-compensated UVL patients show SVIN. A SVIN is observed under Frenzel goggles or videonystagmoscopy and recorded under videonystagmography in absence of visual-fixation and strong sedative drugs. Stimulus frequency, location, and intensity modify the results, and a large variability in skull morphology between people can modify the stimulus. SVIN to 100 Hz mastoid stimulation is a robust response. We describe the optimum method of stimulation on the basis of the literature data and testing more than 18,500 patients. Recent neural evidence clarifies which vestibular receptors are stimulated, how they cause the nystagmus, and why the same vibration in patients with semicircular canal dehiscence (SCD) causes a nystagmus beating toward the affected ear. This review focuses not only on the optimal parameters of the stimulus and response of UVL and SCD patients but also shows how other vestibular dysfunctions affect SVIN. We conclude that the presence of SVIN is a useful indicator of the asymmetry of vestibular function between the two ears, but in order to identify which is the affected ear, other information and careful clinical judgment are needed.

Keywords: skull vibration, nystagmus, vertigo, high frequencies, vestibular disease

Abbreviations: BCV, bone-conducted vibration; SCC, semicircular canal; SPV, slow-phase eye velocity; SVIN, skull vibration-induced nystagmus; SVINT, skull vibration-induced nystagmus test; UVL, unilateral vestibular loss; pUVL, partial unilateral vestibular loss; tUVL, total unilateral vestibular loss; VOR, vestibulo-ocular reflex.

INTRODUCTION—HISTORICAL BACKGROUND

Von-Bekesy in 1935 (1) reported that vibration applied to the skull induced reflexes and motion illusions which he attributed to stimulation of vestibular receptors. Lucke in 1973 (2) first described how 100 Hz mastoid vibration-induced nystagmus (VIN) in a patient with a unilateral vestibular loss (UVL), and in 1999 that result was confirmed and extended by Hamann and Schuster (3) and Dumas et al. (4, 5). Dumas et al. described a systematic clinical analysis of the skull vibration-induced nystagmus (SVIN) in patients after total (tUVL) [after surgery for vestibular schwannoma (VS)] or partial (pUVL) UVL and reported more recently SVIN in superior semicircular canal dehiscence (SCD) patients (6, 7).

Shortly after Lucke's observation, Young et al. (8) reported that squirrel monkey primary afferents from semicircular canals (SCC) and otoliths were activated by bone-conducted vibration (BCV). That report presaged the likely explanation of SVIN and the neural basis of SVIN is considered below.

Vibration-induced nystagmus has been described in various inner ear diseases (**Table 1**); most publications address cranial BCV stimulations (2–7, 9–25, 27–29, 41–43, 45) but others deal with cervical and cranial vibrations (26, 30, 31) and a few with cervical stimulations only (32–34, 40, 44). This review is only mainly restricted to BCV with cranium stimulations which are now more clearly documented by physiology (35–39). We propose for clarity to term it the skull vibration-induced nystagmus test (SVINT).

METHODS—PRACTICAL CONDITIONS

Test Procedure

The examiner performs stimulation either by standing in front of (or behind) the patient to use his dominant hand for more reproducibility (46, 47). The vibrator must be firmly held and applied perpendicularly to the skin over the mastoid process, posteriorly to the auricle, at the level of the external acoustic meatus (**Figure 1**). Stimulation applied on the tip of the mastoid process must be avoided, as it can induce activation of proprioceptive afferents from the trapezius and sternocleidomastoid muscles (47). A pressure of about 10 N is applied. It is recommended that three stimulation trials of each mastoid be given using 100 Hz with each stimulus lasting about 5–10 s. Eye movements can be visualized either under Frenzel goggles or, preferably, observed using video procedures such as videonystagmoscopy or recorded under videonystagmography 2D or 3D. Testing must be done in complete absence of any visual fixation of either eye (47). The average slow-phase velocity (SPV) of SVIN after tUVL is 10.83°/s (SD = 6.82; n = 45) (10, 26). The simplest procedure is to use only mastoid stimulation as described above (3, 12, 23, 24); one may use also vertex stimulation (4, 26, 29). The technical and practical conditions of the test are presented in **Figure 1**.

Stimulation

Different vibrators are available [VVIB 3F or VVIB 100 Hz (Synapsys, France) or ISV 1 or IP 500 (Amplifon, France) or

VVSED 500 (Euro Clinic, Italy) or NC 70209 (North Coast Medical, USA)] (**Figure 1**). The vibrator should preferably have a circular contact surface 20 mm in diameter covered with a thin felt or thin rubber.

Pressure and acceleration measures have shown that for optimum mastoid stimulation the force should be around 10 N or 1 kg (46). For such mastoid stimulation the spread or radiation of vibration to neck muscles is small (46). **Figure 2** shows the SVINT topographic optimization using piezoelectric sensors. Vibration applied to one mastoid is very efficiently transmitted to the opposite mastoid for frequencies under 0.25 kHz (48–54); conversely vertex and cervical stimulations are less efficient for vibrations energy transfer to mastoid (close to the vestibule end organ). A small part of vibrations radiates to cervical region and *vice versa*.

Stimulus Location

For most vestibular pathologies, mastoid stimulation elicits higher SVIN SPV than vertex or cervical stimulation (4, 5, 9, 10, 19–24, 26). Mastoid stimulation will predominantly stimulate labyrinthine receptors in both labyrinths, with only small stimulation of cervical muscle proprioceptors (46). For the cranial midline location, the comparison of the SVIN SPV measured at the frontal location (Fz), vertex (Vx), bregma, occipital, and sub-occipital locations at 100 and 60 Hz in 15 UVL patients did not show significant differences (46). BCV applied to the frontal location is considerably less efficient than mastoid vibration in eliciting SVIN (26) and for vibration transfer to the promontory (54–56).

However, in cases of SCD or other pathologies associated with a third window, vertex stimulation is more efficient than mastoid stimulation (7). This may occur because the pressure transmission from cerebrospinal fluid (*via* middle temporal fossa fistula) is enhanced in this condition (50, 57, 58).

Stimulus Frequency

In measures on patients with tUVL, a large range of frequencies (40–150 Hz) have been shown to induce SVIN. Stimulation at 20 Hz is not effective, and progressively stronger responses are obtained for stimuli between 60 to 120 Hz (28), with around 100 Hz being optimal. In clinical practice, the frequency of stimulation used by Karlberg et al. (13) was 92 Hz, Lackner and Graybiel (11) was 120 Hz, and Magnusson et al. (31) was 85 Hz, and it was 100 Hz for the following: Manzari et al. (42), Ohki et al. (12), Park et al. (24), Koo et al. (19), Xie et al (20), and Dumas et al. (27).

In patients with pUVL, similar results are observed but with significant smaller slow-phase eye velocities (SPV) of SVIN. SVIN SPV were significantly higher at 100 Hz and 60 Hz than at 30 Hz (27). Recently our group has shown SPV was optimal at 100 Hz by testing SVIN frequencies from 10 to 700 Hz delivered by a Brüel & Kjaer Minishaker 4810 (Naerum, Denmark) in 15 common and severe UVL patients. No responses were observed at 10 or 500 Hz.

TABLE 1 | Synoptic table of results in literature.

Reference	Level of evidence	Study design	Sample size (n)	Pathology	Record	Stimulus location	Stimulus frequency Hz (amplitude mm)	Main contribution, comments
Lücke 1973 (2)	3	RCS	65	Unilateral vestibular loss (UVL) patients, central patients	Frenzel	Face cranium vertex necknape	100	First incidental observation of a vibration-induced nystagmus (VIN) in a UVL patient
Lackner and Graybiel 1974 (11)	2	PCS	6	Normal subjects	Frenzel	Face, mastoids, cervical	40–280 optimal 120–180	Vibrations induce postural, visual illusions, rare VIN in normal subjects
Yagi and Ohyama 1996 (32)	3	PCS	11	UVL	VNG3D	Dorsal neck muscles	115 (1 mm)	Vibrations induce in UVL compensated patients a VIN (Hor and Vert components) related to vestibular decompensation
Strupp et al. 1998 (33)	2	PCS	25	VN	VNG, SVSA	Neck muscles	100	Somatosensory substitution of vestibular function in UVL patients
Popov et al. 1999 (40)	2	PCS	4	UVL	Scleral, coils, visual illusions	Neck vibration	90 (0.5 mm)	Propriogryal illusion secondary to vibration-induced eye movement (COR)
Hamann and Schuster 1999 (3)	3	RCS	60	Peripheral UVL benign positional paroxysmic vertigo	VNS VNG2D	Mastoid	60, 100	In UVL, a lesionnal VIN is observed in peripheral diseases and seldom in BPPV and in central patients. Optimal stim 60 Hz
Dumas et al. 1999 (4)	3	RCS	80	UVL: TUVL (TA, VNT) PUVL (MD, VN, VS)	VNS, VNG3D	Mastoid, vertex	100 (0.2 mm)	VIN: 3 components in TUVL. VIN characteristics, technical conditions, sensitivity, specificity
Dumas et al. 2000 (5)	3	RCS	46	UVL	VNS, VNG3D	Mastoid, vertex	20–150 (0.2 mm)	VIN SPV amplitude; location and frequency stimulus optimization. A vestibular Weber test
Karlberg et al. 2003 (13)	3	PCS	18	UVL (VN, VNT)	Scleral Coils, SVH	Mastoid, posterior neck	92 (0.6 mm)	SVH shift is explained by vibration-induced ocular torsion whose magnitude is related to the extent of UVL deficit
Ohki et al. 2003 (12)	3	RCS	100	UVL (VN, MD, VS)	VNG	Mastoid, forehead	100	In UVL patients VIN is correlated with CaT hypofunction
Nuti and Mandala 2005 (21)	3	RCS	28	VN	VNG	Mastoid	60–120	Sensitivity 75%, specificity 100% VIN beats usually toward the intact side
Magnusson et al. 2006 (31)	2	PCS	10	Normal subjects	Posture	Mastoid, neck	85 (1 mm) 55 (0.4 mm)	Cervical muscle afferents play a dominant role over vestibular afferents during bilateral vibration of the neck
Dumas et al. 2007 (10)	3	RCS	4,800	TUVL, PUVL, brainstem lesion	VNS, VNG	Mastoid, vertex	100 (1 mm)	VIN is observed in 98% TUVL, 75% PUVL, 34% BSL

(Continued)

TABLE 1 | Continued

Reference	Level of evidence	Study design	Sample size (n)	Pathology	Record	Stimulus location	Stimulus frequency Hz (amplitude mm)	Main contribution, comments
Hong et al. 2007 (22)	3	RCS	52	MD Unilat	VNS, VNG, head-shaking-nystagmus (HSN), CaT	Mastoid	100	VIN is usually correlated with CaT hypofunction. VIN beats frequently ipsilaterally toward MD side
White et al. 2007 (41)	3	RCS	8	SCD	VNS, VNG 2D	Mastoid, vertex, suboccip.	100	Vibrations induce a torsional VIN beating toward the SCD and down beating suggesting the stimulation of the dehiscent SSCC
Dumas et al. 2008 (26)	3	RCS	131	TUVL (TA, VNT)	VNS, VNG 2D 3D	Mastoid, vertex (cervical)	100 (1 mm)	VIN: 3 components (H,V,T), SVINT: a bilateral stimulation, sensitivity 98%, specificity 94%, SPV:10.7%/s; SD = 7.5, VIN is always beating toward the intact side
Manzari et al. 2008 (42)	3	RCS	16	SCD	VNG3D	Mastoid	100	Vibrations induce a VIN with a torsional component beating toward the lesion side
Park et al. 2008 (23)	3	RCS	19	VN	VNG	Mastoid	100	Clinical significance of VIN
			22	Controls				
Park et al. 2010 (24)	2	PCS	26	VN	VNG	Mastoid	100	VIN clinical significance, reliability
Aw et al. 2011 (43)	3	RCS	17	SCD	Scleral coils	Mastoid	500	Eye slow torsional component ViVOR is directed toward the intact side: vibrations stimulate the anterior dehiscent canal
Dumas et al. 2011 (27)	3	RCS	99	PUVL (VN, VS, MD, CL)	VNG 2D	Mastoid, vertex	30, 60, 100 (1 mm)	Sensitivity 75%. VIN beats toward safe side in 91%. skull vibration-induced nystagmus test complements CaT, HST in vestibular multifrequential analysis
Kawase 2011 (44)	3	RCS	14	7 pre-surgical VS, 7 post-surgical VS	VNG, SVV	Neck muscles	110	Ipsilat. vibrations increase SVV deviation, VIN is correlated to SVV alteration, VIN is not modified by the side of the stimulation
Koo et al. 2011 (19)	3	RCS	74	VS	VNG	Mastoid	100	Comparison of sensitivity of VIN and other vestibular tests in the YAW axis in VN. VIN is observed in 86% of cases in correlation with CaT Hypofunction. VIN beats toward the intact side in 98%
			24	Controls	HST CaT			VIN is observed in 86% of cases in correlation with CaT Hypofunction. VIN beats toward the intact side in 98%
Dumas et al. 2013 (30)	2	RCS	9	Profound compensated long-standing UVL	VNG 2D, posturog	Mastoid, vertex (cervical)	100	VIN beats toward the intact side in 100% of cases, No measurable postural changes in EC condition in long standing compensated severe UVL patients
			12	Control				
Xie et al. 2013 (20)	3	RCS	112	UVL	VNG, HST CaT	Mastoids	100	VIN is observed in 91% of peripheral UVL. It is more frequent and important when CaT canal paresis augments. VIN usually beats toward the healthy side except in MD
			30	Controls				VIN specificity is 100%

(Continued)

TABLE 1 | Continued

Reference	Level of evidence	Study design	Sample size (n)	Pathology	Record	Stimulus location	Stimulus frequency Hz (amplitude mm)	Main contribution, comments
Dumas et al. 2014 (7)	RCS	17	SCD (unilateral)	VNG 3D, cVEMP, Cat, VHT	Mastoid, vertex	60,100 (1 mm)	In Unilat SCD, a VIN is observed in 86% cases. Horizontal and Torsional components beat toward lesion side. The VIN vert. component is most often up beating. Higher responses are obtained on vertex location	
Park et al. 2014 (25)	RCS	11	SCD		Mastoid	100	VIN horizontal component beats toward the lesion side	
Lee et al. 2015 (45)	RCS	87	MD	VNG	Mastoid	100	In MD, VIN and HSN are not always in the same direction	
Dumas et al. 2016 (46)	PCS	11	Normal subjects	Piezoelectric sensor	Mastoid; vertex; neck	100	Vibration transfer is more efficient from one mastoid to the other one	

RCS, Retrospective Clinical Study; PCS, Prospective Clinical Study; tUVL, total unilateral vestibular lesion; pUVL, partial unilateral vestibular lesion; VNL, vestibular neuritis; MD, Meniere's disease; VS, vestibular Schwannoma; CL, chemical labyrinthectomy (Gentamicin); SCD, superior semicircular canal dehiscence; TA, translabryrinthine approach (for VS surgery); VNT, vestibular neurotomy; BS1, brainstem lesion; VNG, videonystagmography; VNS, videonystagmometry; 3D, 3-dimensional study of the nystagmus; 2D, 2-dimensional study; SSC, scleral searching coils; SVH, subjective visual vertical; SVR, subjective visual horizontal; SVSA, subjective visual straight ahead; Cat, caloric test; cVEMP, cervical evoked myogenic potentials; VIN, vibration induced nystagmus; HSN, head shaking nystagmus; COR, cervico-ocular reflex; EC, eye closed

RESULTS – MAIN LEADS FOR INTERPRETATION (Box 1)

In tUVL patients, 100 Hz BCV applied to either mastoid induces a low velocity (~10°/s) predominantly horizontal nystagmus beating away from the affected side, irrespective of which mastoid is stimulated (3–5, 9, 10, 13, 26) (Figure 3). The nystagmus is precisely stimulus-locked: it starts with stimulation onset and stops at stimulation offset, with no post-stimulation reversal and is reproducible.

SVIN Habituation or Fatigue after Long Period of Stimulation in tUVL

Three-dimensional recordings of 100-Hz long duration SVIN in tUVL patients during stimulation lasting 3 min demonstrated that the SVIN horizontal component persisted during stimulation with little SPV decrease, whereas first the vertical and then torsional components disappeared. These results suggest a moderate per-stimulatory adaptation (28). The brief repeated stimulation in the usual test does not show signs of habituation.

SVIN Acts as a Vestibular Weber Test

In tUVL, for 100 Hz BCV mastoid stimulation, SVIN is observed in 98% of patients and beats toward the healthy side in 100% of cases (26). In addition, there was no correlation between the SVIN SPV value and which side was stimulated—either mastoid was equally effective in generating the SVIN ($P = 0.17$; $n = 20$). These results indicate that SVIN is due to stimulation of vestibular receptors on the intact side (26), and in this way, SVIN is a “vestibular Weber test” (5, 10, 27) (Figure 3). In accord with that description: in total bilateral vestibular lesions (26) and in symmetrical partial bilateral vestibular lesions, no SVIN was observed (27). Similar results are observed in severe pUVL as showed in Figure 4.

Arguments for SVIN Being a Global Vestibular Stimulus

Three-dimensional eye movement recordings show that the response to SVIN is not purely horizontal (Figure 3). In 43 tUVL patients (10, 26) 100 Hz mastoid stimulation, the 3D recordings revealed a SVIN with horizontal, torsional, and vertical component in 98, 75, and 47% of cases, respectively. These observations suggest a primary participation of the horizontal SCC and/or utricle (for generating the horizontal component), of the posterior or superior SCC and/or sacculus (for the vertical component) and superior and posterior SCC and/or otolithic structures (for the torsional component). In SCD (7), the SVIN revealed a primarily torsional, a primarily horizontal, and a primarily vertical (up-beating in 80% of cases) component in 40, 30, and 30% of cases, respectively. These results suggest that the superior dehiscent SCC is not the only stimulated structure (the up-beating vertical component suggests the possible stimulation of the posterior SCC or sacculus) (7).

SVIN Is Not Influenced by Vestibular Compensation Mechanisms

Dumas et al. observed in 98% of 131 surgical tUVL patients that 100 Hz mastoid vibration induced a SVIN. In well-compensated

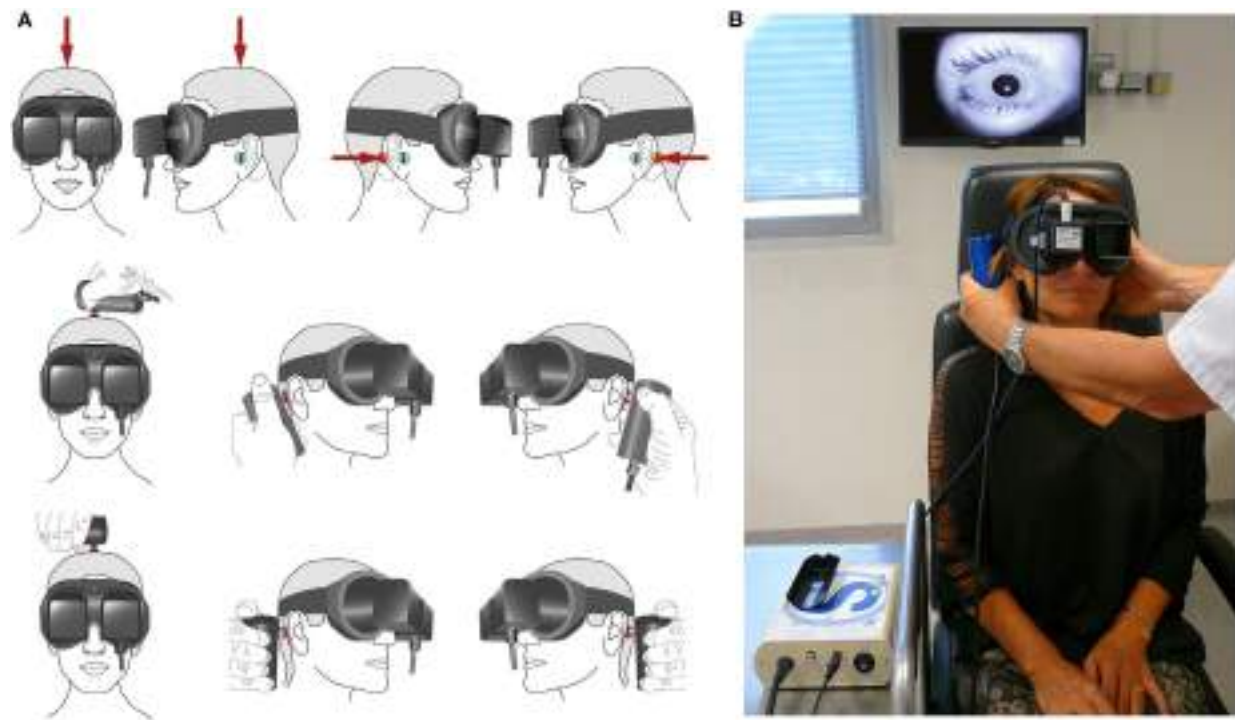


FIGURE 1 | **Skull vibration-induced nystagmus test technique in clinical practice.** **(A)** Principle of stimulation: the examiner can face the subject, as in the first example. The vibrator cylindrical contact is applied perpendicularly to the designated surface (red spot) with a pressure of about 10 N or 1 kg on the vertex or each mastoid process [level to the external acoustic meatus (Green spot)]. The examiner uses the other hand to maintain and immobilize the subject's head. The same type of stimulation can be performed with the examiner behind the subject (second example situation). Stimulation must avoid the mastoid tip to prevent from muscular vibration radiation and proprioceptive involvement. **(B)** Mastoid stimulation; examiner in front of the subject; the other hand immobilizes the head. 3F Synapsys stimulator (France). Videonystagmographic recording (Collin ORL, France).

patients SVIN was not modified at 6 months, or 2 years, or 10 years (**Figure 3**) or up to 23 years post surgery (26). In another study measuring SVIN, the subjective visual vertical (SVV) and postural changes in a population of severe chronic compensated UVL patients (median: 32 ± 25 months) revealed a normalization of the SVV and of postural results but persistence in all patients of SVIN (30). Similarly, Hamann and Schuster (3, 59) observed that in a series of 14 unilateral unoperated VS, patients had a SVIN in 80% of cases (most of them had a chronic evolution and complained of no vestibular imbalance and had a compensated vestibular dysfunction). Ohki et al. (12) demonstrated that in 19, unoperated, long lasting VS and 15 long standing VN, a SVIN beating toward the intact side was observed in 60 and 70% of cases, respectively.

SVINT Sensitivity and Specificity

The sensitivity of SVIN in tUVL ($n = 131$), pUVL ($n = 78$), and brainstem lesion ($n = 36$) was 98, 75, and 30%, respectively. Specificity was 94% ($n = 95$ controls) (10, 26, 27). SVINT is significantly more sensitive for detecting peripheral disease than central brainstem lesions (BSLs) ($P = 0.04$) (10, 27) (**Figure 5**). The presence and direction of SVIN is strongly correlated with caloric hypofunction (26), and a SVIN is observed in 90% of UVL patients when caloric test hypofunction is higher than 50% (12).

SVINT Is More Sensitive for Identifying Peripheral Than Central Diseases

In central or BSLs, Kheradmand and Zee (60) reported a more frequent down-beating SVIN. In BSLs, a SVIN with horizontal components beating toward the healthy side may also be observed (27) as reported by Dumas and Schmerber in cavernous hemangiomas (61). Hamann and Schuster described a SVIN in 10% of central diseases (3).

SVIN IN VARIOUS PATIENT CONDITIONS

Table 1 summarizes the clinical evidence of cervical and BCVs on nystagmus. The selection criteria of publications in this comprehensive table are based on the following process.

Data sources: the following search criteria were used from inception through June 2016 in PubMed, Embase, Cochrane Library for key words: Skull/Head Vibrations, Vibration-Induced Nystagmus, Bone conducted vibrations, cranial vibrations, cervical vibrations, consequences on posture, vestibulo-ocular-reflex (VOR) and subjective visual vertical (SVV), high frequencies, low frequencies, and nystagmus.

Data selection: in total, 1,723 articles were retrieved among which 1,222 satisfied to eligible criteria: vestibular structures

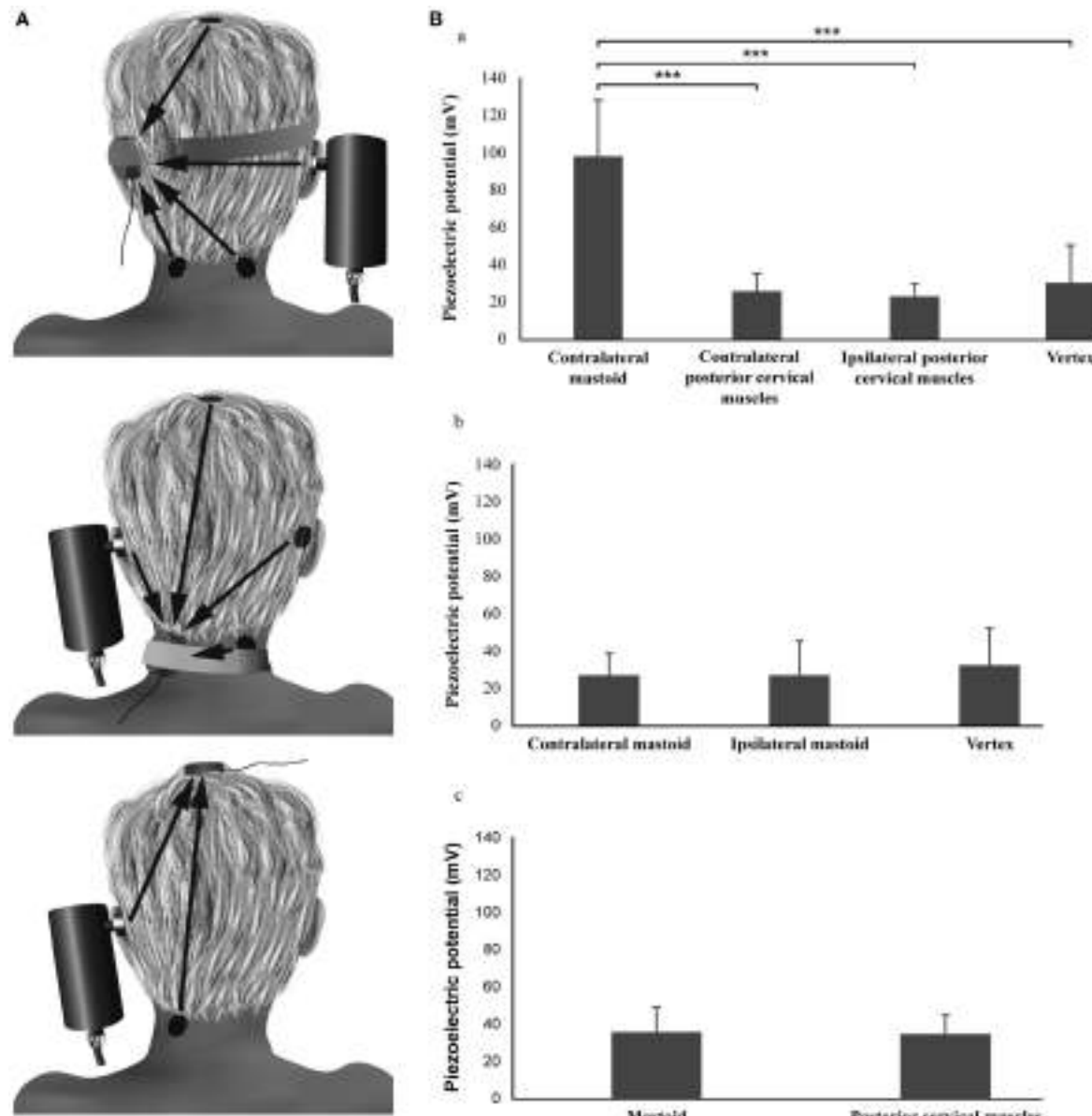


FIGURE 2 | Topographic optimization analysis of the skull vibration-induced nystagmus test. **(A)** Procedure. **(B)** Results: the piezoelectric potentials (millivolts) recorded on the mastoid are significantly different according to the location of the stimulation (Friedman test, $P < 0.001$): the values obtained during the vibratory stimulation of the contralateral mastoid are higher than those obtained after vertex or ipsilateral and contralateral posterior cervical muscle vibrations (Wilcoxon tests, $P < 0.001$). No difference is observed between vertex and posterior cervical muscle stimulation locations (Wilcoxon tests, $P > 0.05$). The piezoelectric potentials recorded on the vertex or the posterior cervical muscles are not different according to the location of the stimulation (Friedman test and Wilcoxon test, $P > 0.05$).

involved, reproducibility, stimulus frequencies and location optimization, VIN characteristics, comparison with results in caloric test (CaT), ocular vestibular evoked myogenic potential (oVEMP), cervical evoked myogenic potentials (cVEMP), and first level examination tests.

Data extraction: critical appraisal and direct interest retained 29 clinical studies. Were retained series with sufficient number of participants, satisfactory directness of evidence (level 2 or 3), and low risk of bias.

The SVINT reveals instantaneously in UVL patients a vibration-induced nystagmus (SVIN) and so meets the need in clinical practice for a rapid, easy to perform, first-line examination test, completing the battery of common clinical tests exploring low or middle range vestibular frequencies by using higher frequency stimulations at 100 Hz. This test provides clinical guidance for further explorations or imaging as a mild, non-invasive bedside examination test with a valuable cost/efficiency rate (47, 60, 62, 63).

BOX 1 | Main clinical outcomes.

Skull vibration-induced nystagmus (SVIN) optimal frequency stimulation is 100 Hz and shows a primarily horizontal component; the best location is the mastoid process in most peripheral diseases except in SCD and other labyrinthine pathologies associated with a third window (higher responses are obtained on vertex). Both labyrinths are concomitantly stimulated, and a SVIN beating away from the lesion side is the result of the stimulation of the intact side in tUVL. In partial unilateral vestibular lesions (pUVL), a SVIN beating toward the intact side is usually obtained on mastoid process stimulation. But in SCD, SVIN beats toward the lesion side. The SVIN SPV is correlated in tUVL with the total caloric efficiency on the healthy ear. No responses are observed in bilateral areflexia or symmetrical hypofunctions. The SVIN is definitive and not modified at repetitive controls and long lasting re-tests. The sensitivity is 98% in tUVL and the specificity 94% in normal subjects. In pUVL, sensitivity is 75% and SVIN beats toward the intact side in 91% of cases. No significant alteration of the vestibulo-spinal reflex analyzed with posturography is observed in chronic compensated unilateral vestibular lesion (UVL) in eye-closed condition. SVIN Test is more sensitive to reveal peripheral than central neurological diseases. A 100 Hz BCV stimulates both canal and otolith structures in animals but SVIN in clinic is more relevant and is a good marker for canal lesions which it is well correlated to.

In summary, in unilateral peripheral vestibular lesions, SVIN is of the lesional type and beats usually toward the intact side. However, there are exceptions of this rule in partial vestibular lesions related to a combination of responses of the intact side and the residual responses of the lesion side. We report below various clinical situations highlighting these exceptions.

Unilateral Vestibular Loss (UVL)

Two main goals of SVIN are to indicate the symmetry of the two labyrinths and lesion lateralization. Whereas the evidence is clear that SVIN indicates asymmetry, care must be taken in inferring lateralization of which side is the affected labyrinth.

In tUVL, results are simple, permanent, and consistent: whatever the stimulus frequency (40–150 Hz) and location on the skull (mastoid or vertex) the quick phase of the resulting SVIN (horizontal and torsional components) beats away from the affected ear and toward the intact side in 98% of cases (26). Karlberg et al. independently reported similar results after vestibular neurectomy (13). Results are less clear-cut in pUVL.

Total Unilateral Vestibular Loss (tUVL)

This condition is observed after surgical cases (translabyrinthine approaches, vestibular neurectomy) (Figure 3) or temporal bone fractures.

In tUVL, a SVIN observed in 98% of patients was always beating toward the intact side (100% of cases), and the SVIN SPV horizontal component was correlated with the total caloric efficiency on the intact side ($P = 0.03$; $n = 20$) (26). These results suggest a predominantly horizontal SCC contribution to SVIN (26) since the caloric test stimulates primarily the horizontal SCC.

In cases of tUVL, the axis of eye rotation (i.e., the relative magnitudes of horizontal, torsional, vertical eye velocity) may change with the stimulus location (mastoid or vertex) but the quick phase direction (right or left) remains unchanged with different locations (26). These results correlate closely with

those obtained by concomitant caloric and head-shaking test results (10, 26).

With less complete unilateral vestibular loss (pUVL), the results are not as clear cut.

Partial Unilateral Vestibular Loss (pUVL)

A SVIN is observed in 75% of cases. This condition is observed in vestibular neuritis (VN), Menière's disease, preoperative VSs, and intratympanic gentamicin (ITG). The nystagmus direction beats toward the healthy side in 91% of those cases (27). In pUVL, SVIN was significantly more frequently observed (90% of cases) when caloric testing revealed a hypofunction higher than 50% (10, 12, 27). Hamann and Schuster suggested that SVIN stimulated the horizontal SCC since they observed a SVIN correlated with the caloric hypofunction but not with cVEMP or SVV results (3, 10).

In pUVL explored with caloric (low frequency test at 0.003 Hz), HST (midrange frequency at 2 Hz), and SVINT (high frequency), it was demonstrated that the three tests were not always positive at the same time. A SVIN was observed in 20% of patients with normal calorics. Conversely caloric was positive in 22% of patients with normal SVINT. This was noteworthy in Meniere's Disease (MD) and VS (27). In MD, nystagmus direction observed at 100 Hz with SVINT may be different from head-shaking-nystagmus (HSN) direction and be associated with a normal caloric test performed on the same day (10, 27, 60, 64). Responses may be different dependent on stimulus frequency (SVIN direction at 30 Hz is different at 100 Hz in 10% of pUVL), and discordant results between caloric test, HST, SVINT are observed in 30% of pUVL patients (27).

There are other exceptions: reports of 100 Hz SVIN causing nystagmus beating toward, rather than away from, the affected ear; in 15.5% Meniere's Disease patients tested, 10% of VN, and 8% of pre-surgery VS cases (27). Similar exceptions have been described by Modugno et al. (15), Karkas et al. (16), Hamann and Schuster (3), Freyss et al. (17), and Negrevergne et al. (18).

Superior Semicircular Canal Dehiscence (SCD)

In contrast to the result in UVL is the result in SCD where the nystagmus beats toward the affected ear, suggesting that the vibration activates the canal with the SCD. In unilateral SCD Dumas et al. (7) reported that the torsional and horizontal quick phases of SVIN beat usually toward the lesion side (Figure 6). In SCD, SVINT is positive in 82% of cases while caloric and HST are usually negative (7). Other authors (41–43) have also reported in SCD a prevalent stimulation of the superior SCC on the lesion side and observed a torsional SVIN beating toward the lesion side. This result is consistent with the BC facilitation inherent in this third window pathology (65–69). These results correspond to the acoumetry (Weber test) and the side of the conductive hearing loss as described by our group (7) and confirmed by Park et al. (25).

A SVIN is observed in between 82 and 100% of SCD patients (7, 41). Many authors agree that the stimulation of patients with a dehiscent anterior canal provokes a SVIN

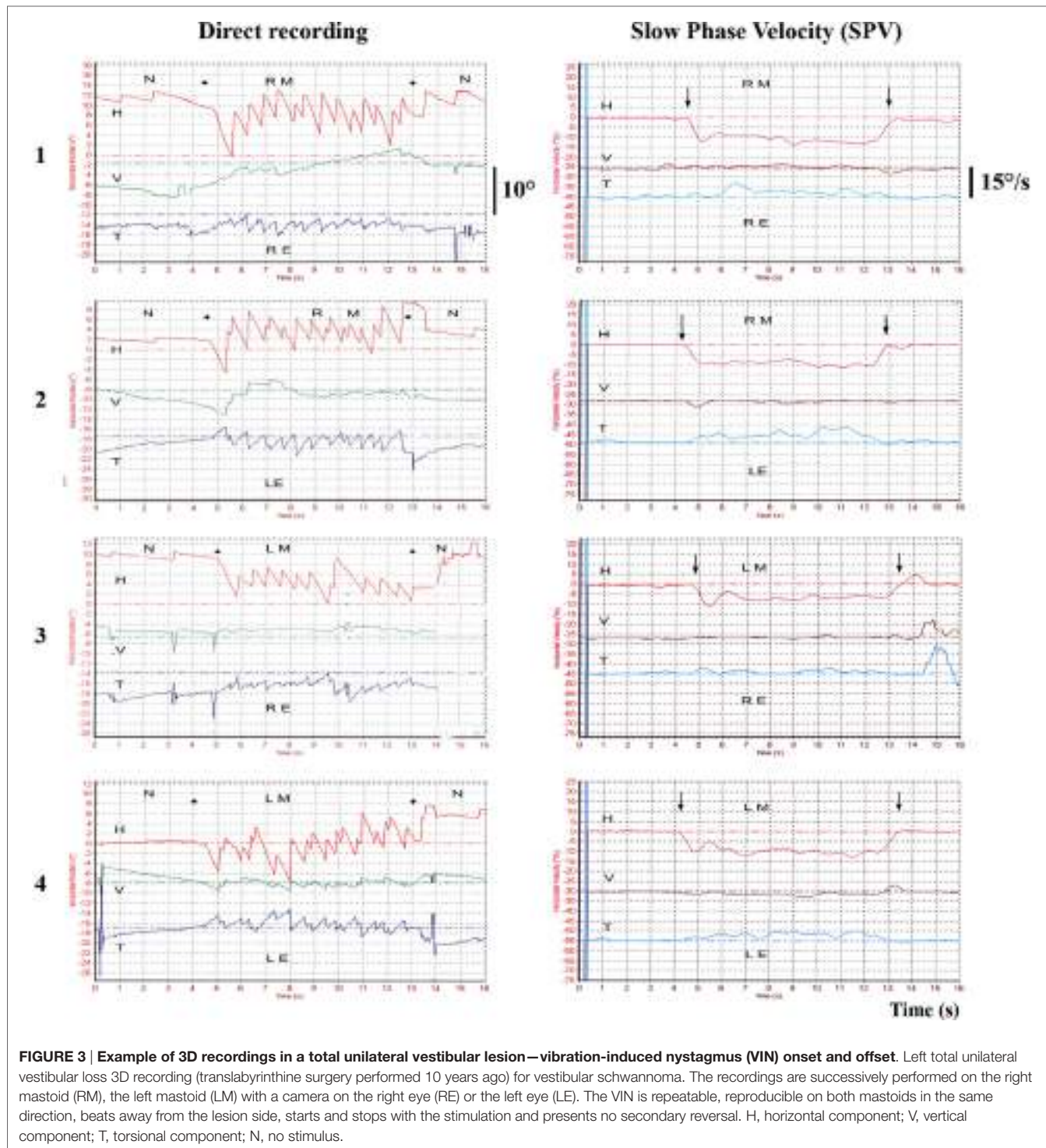


FIGURE 3 | Example of 3D recordings in a total unilateral vestibular lesion—vibration-induced nystagmus (VIN) onset and offset. Left total unilateral vestibular loss 3D recording (translabyrinthine surgery performed 10 years ago) for vestibular schwannoma. The recordings are successively performed on the right mastoid (RM), the left mastoid (LM) with a camera on the right eye (RE) or the left eye (LE). The VIN is repeatable, reproducible on both mastoids in the same direction, beats away from the lesion side, starts and stops with the stimulation and presents no secondary reversal. H, horizontal component; V, vertical component; T, torsional component; N, no stimulus.

with torsional component beating toward the lesion side (6, 7, 41–43). This is opposite to the usual direction after UVL in which the unaffected ear shows the greater response. The observation of a SVIN horizontal component beating toward the lesion side is probably correlated with the concomitant stimulation of the ipsilateral horizontal SCC and/or utricle

(25, 35) (Figure 6). The vertical most often up-beating SVIN suggests a more global stimulation than the sole anterior SCC (7). This pathology is associated with an increase sensitivity of inner ear structures to high frequencies. Our group described in SCD patients a SVIN observed up to 500 or 700 Hz stimulation.

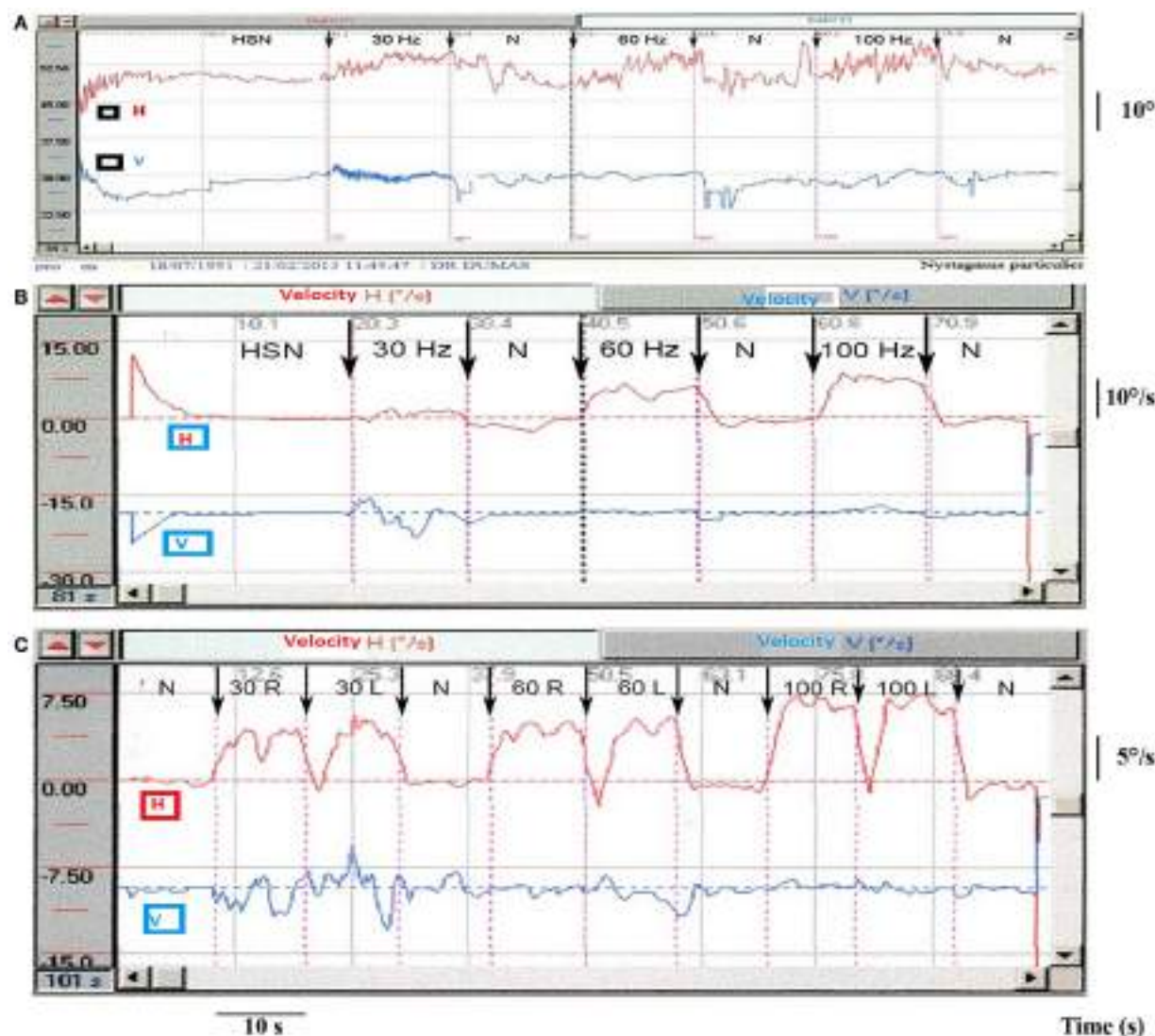


FIGURE 4 | Partial unilateral vestibular lesions [vibration-induced nystagmus (VIN) 2D recording]. (A) Example of right vestibular neuritis or acute peripheral vestibular disorder (APVD). Direct recording of head-shaking-nystagmus (HSN) and VIN at 30, 60, and 100 Hz. When skull vibration-induced nystagmus test (SVINT) is performed after the HST, it is recommended to observe an interval between the two tests (about 2 min) to avoid interference of HSN on VIN due to a possible second HSN reversal phase. (B) Same patient, right APVD: recording of the eye slow-phase velocity (SPV). (C) Right chemical labyrinthectomy (intratympanic gentamicin): 2D recording of the VIN SPV; SVINT 30 Hz [right mastoid (RM)-left mastoid (LM)]; 60 Hz (RM-LM); 100 Hz (RM-LM) protocol.

Vestibular Neuritis (VN)

Park et al. described SVIN in 63% of cases ($n = 38$) (23); Nuti and Mandala observed a SVIN in 75% ($n = 28$), a caloric hypofunction in 93%, and positive HIT in 64% of cases (21). Dumas et al. observed SVIN in 90% and a caloric hypofunction in 100% ($n = 18$) (29); Karlberg et al. described in 100% of VN an ipsilesional tonic shift of torsional eye position (13). SVIN is most often beating toward the intact side (Figures 4A,B) but a SVIN beating toward the lesion side has been described in 10% of cases (6, 27). To summarize, a SVIN is observed in 63–100% of cases in VN usually beating toward the intact side (13, 21, 23, 27, 29) (Figure 4).

Vestibular Schwannoma (VS)

In unoperated VS, SVIN has been described in 44–78% of cases (15, 16).

Modugno et al. (15) observed a SVIN in 44% of his 86 cases of VS beating toward the lesion side in 26% of cases; Freyss et al. (17) observed SVIN in 65% of 51 preoperative patients while the caloric (unilateral separate ear infusion) demonstrated an hypofunction in 72% of cases and a significant vestibular asymmetry after simultaneous bilateral irrigation in 95% of cases. The SVIN beats toward the lesion side in 6% of cases. Dumas et al. reports a SVIN in 64%, a positive HST in 40%, and caloric hypofunction in 75% of 25 VS (29). In that series,

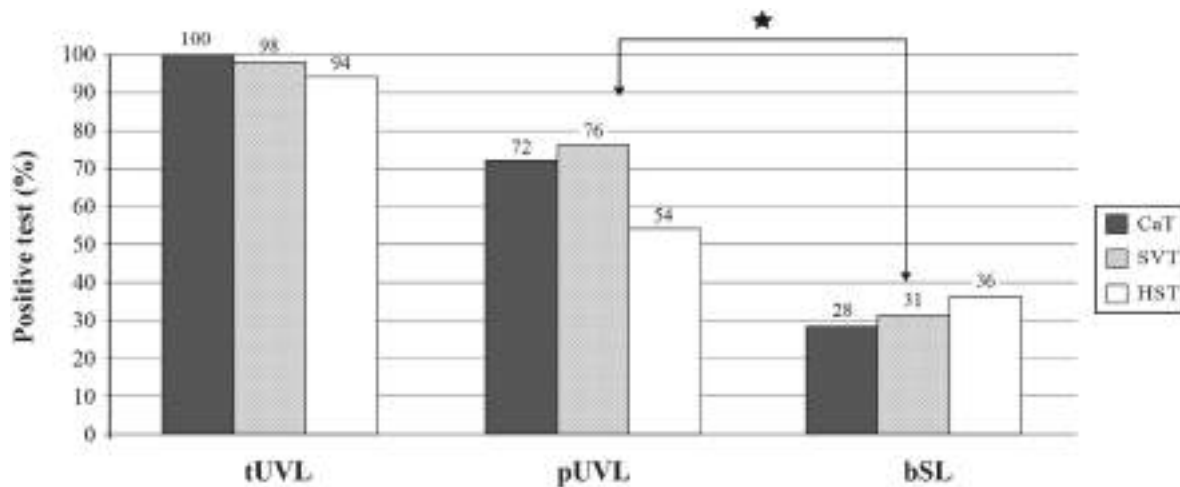


FIGURE 5 | Skull vibration-induced nystagmus test (SVINT) is more sensitive to identify peripheral than central diseases. Comparative sensitivity of caloric test (CaT), SVINT, and head-shaking test (HST) in populations of total unilateral vestibular lesions (tUVL) ($n = 131$), of partial unilateral vestibular lesions (pUVL) ($n = 78$), and brainstem lesions (BSL) ($n = 36$). SVINT is more sensitive to reveal peripheral than central lesions ($P = 0.04$).

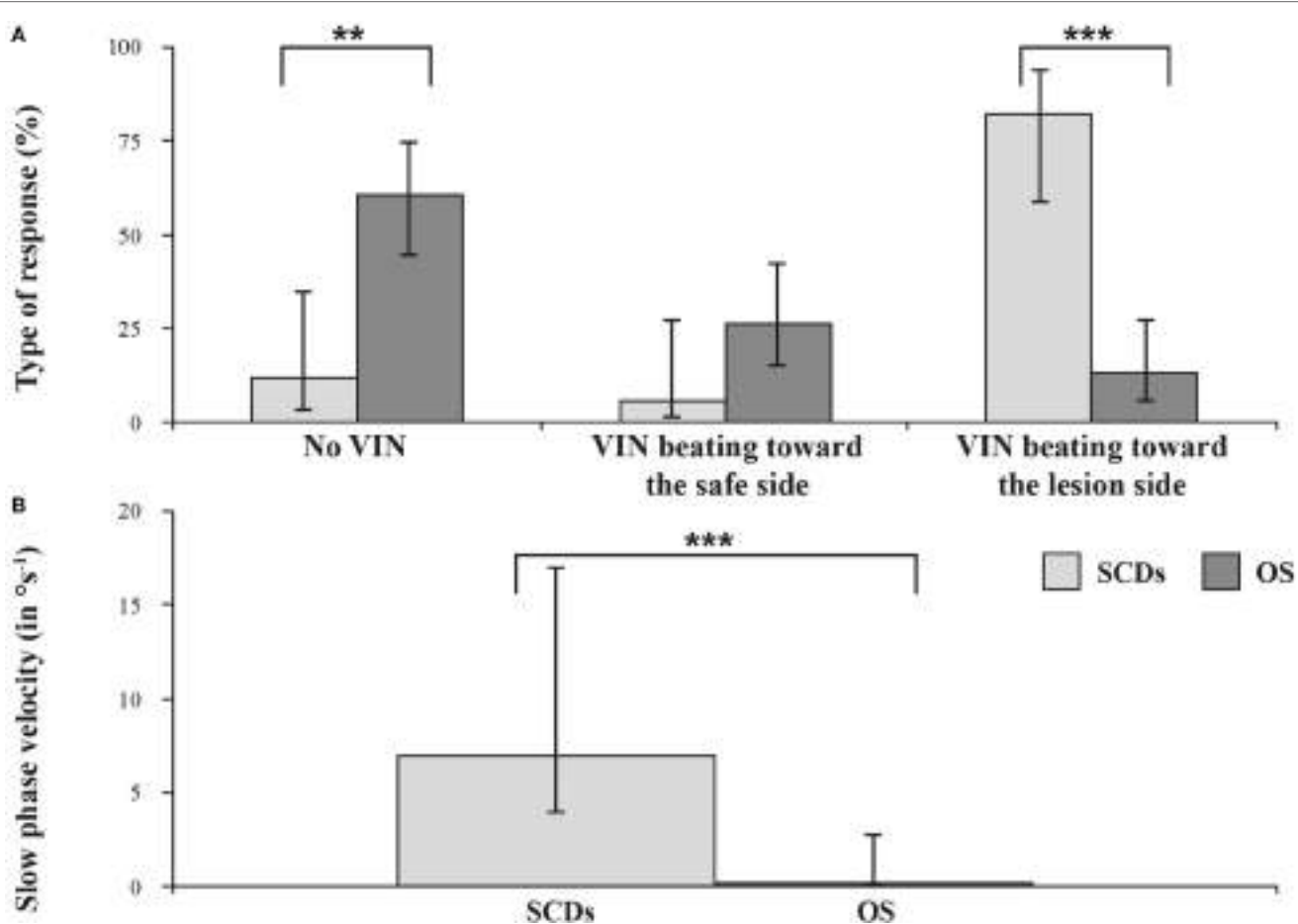


FIGURE 6 | Results in conductive hearing loss observed in unilateral SCD and otosclerosis (OS). Vibration-induced nystagmus (VIN) acts as a vestibular Weber Test. Skull vibration-induced nystagmus test (SVINT)—percentages (with 95% confidence interval) of no VIN, VIN beating toward the healthy side, and VIN beating toward the lesion side (**A**) and median (with interquartile range) of the slow-phase velocity of the VIN (**B**) observed in superior canal dehiscence (SCD) and otosclerosis (OS) patients (** $P < 0.001$, *** $P < 0.0001$).

the test positivity depends on the VS size (SVIN is observed in only 45% of stages 1 and 2). In another study of 70 patients, a SVIN was reported in 78% while HST was positive in 51% and caloric in 83% of cases (16). A SVIN beating toward the lesion side is observed in 10% of cases (16). Hamann identifies in 15 unoperated VS (59) a SVIN in 80% of patients with unilateral lesion and notes its absence in the only case with bilateral VS. This author does not describe precisely the nystagmus direction but suggests in most cases a nystagmus beating away from the affected ear (59).

Negrevergne et al. (18) reported in 100 unoperated VS that the results of SVIN and caloric were not always positive at the same time. SVINT was positive in 72% of cases, but a SVIN beating toward the intact side or toward the lesion side was observed in 49% and in 23% of cases, respectively.

Meniere's Disease (MD)

Hong et al. (22) analyzed 52 MD (between attacks) and observed a SVIN in 71% of cases beating toward the lesion side in 27% of cases. The SVIN observation was correlated with the severity of caloric hypofunction. Dumas et al. reported a SVIN in 71% of MD (most of them observed in a pre-attack or a period close to a recent attack) with caloric test results modified in 64% (29). This same author described an "irritative" SVIN beating toward the lesion side in 15.5% of cases and a frequent discordance with other tests such as caloric test or HST in 30% of cases (27). Lee (45) observed a SVIN more often in the irritative phase (63% of cases) and more rarely in quiescent periods (28% of cases). SVIN and HSN directions are discordant in 38% of MD during the irritative phase. To summarize, SVIN is observed in 28–71% of MD patients cases (usually related to the proximity of an acute period) and is often of the irritative type (22, 29).

SVIN after Intratympanic Gentamicin (ITG)

Junet et al. (70) observed an SVIN to 100 Hz BCV in 100% of patients treated for disabling MD by ITG after seven injections with the nystagmus beating toward the intact side. After one injection, 75% showed such an SVIN. Accordingly the strength of SVIN is a guide to the severity of the deafferentation (**Figure 4C**). After efficient ITG in responding patients SVIN direction is correlated and concordant with the lesion nystagmus obtained in other vestibular tests and the caloric test hypofunction.

Otosclerosis (OS)

A SVIN of low intensity is seldom observed in otosclerosis and is as often directed toward the intact as toward the lesioned side (7) (**Figure 6**).

Benign Positional Paroxysmic Vertigo (BPPV)

In BPPV, SVINT is seldom observed (3) and is positive only in Lindsay–Hemenway syndrome (BPPV associated with a strong ipsilateral caloric hypofunction) (10).

SVIN CLINICAL VALUE

A Complement to Other Vestibular Tests

Skull vibration-induced nystagmus can be conducted where caloric tests cannot, for example, where there are middle ear malformations or tympanic membrane perforations or external acoustic meatus atresia. It is useful when caloric test results are modified after middle ear surgery (radical mastoidectomy or tympanoplasty) and show a false vestibular hyperexcitability (due to thermic conduction modifications). In such cases, it can substitute for the water caloric test and give informative data. This test is less invasive and challenging for elderly, arthritic, and vascular patients than HST or HIT. In conductive hearing loss with normal tympanic membrane, it can suggest an SCD if it induces a characteristic SVIN beating toward the lesion side and still observable at high frequency stimulations. This diagnosis can be confirmed by audiometric low frequency air-bone gap (bone-conducted facilitation) for the affected side related to the existence of a third window in this pathology, the stapedial reflex preservation, and further by a dedicated (targeted) imaging. In all other peripheral pathologies associated with a vestibular hypofunction, the SVIN usually beats toward the intact side. Thus, SVIN test (SVINT) provides useful information and suggests a possible hypofunctioning side (10, 27, 29).

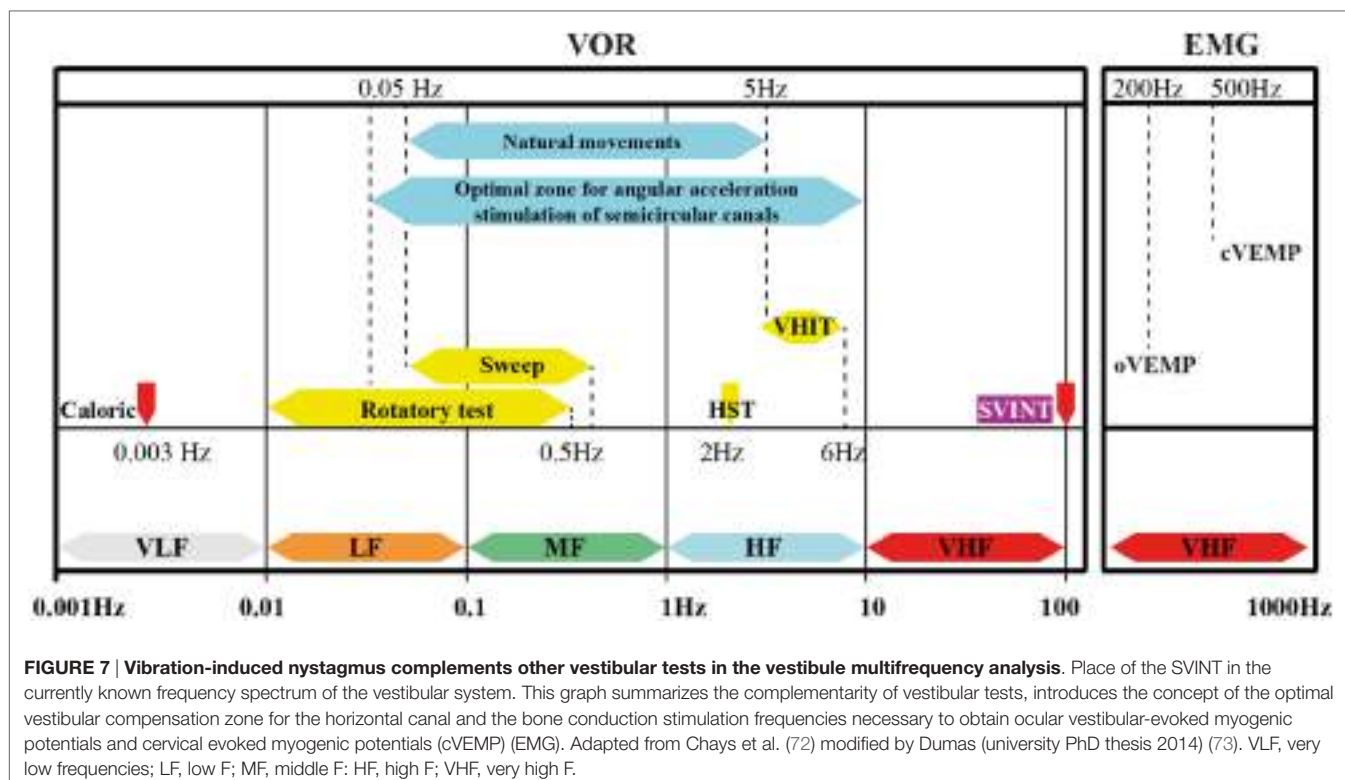
Skull vibration-induced nystagmus test is useful for revealing false bilateral areflexia: such patients have no responses for caloric test and rotatory test (for low frequencies), no HSN, and no responses to vHIT for the six SCC (middle range frequencies) but show a SVIN proving that residual sensory hair cells at least on one side are still present and responding at high frequencies. Hence, a patient with a so-called bilateral vestibular areflexia should be documented not only with the caloric test, vHIT, and otolithic tests but also with SVIN (27).

Kheradmand and Zee (60) and Huh and Kim (62) mentioned SVIN as a part of other first-line examination tests in clinical practice and describe a nystagmus in UVL with the quick phase usually beating away from the paretic ear. Dumas et al. proposed SVIN since 1997 and 2000 (4, 5, 9), insisted on SVINT benefit as a simple test to reveal vestibular asymmetry and described the characteristics of the SVIN which was later designed as a suitable bedside clinical test and an adjunct to the caloric test (4, 5, 10, 12, 14, 24, 26–30, 47). This test has been proposed in occupational medicine (71). In clinical practice, SVINT may be part of a first-line bedside examination screening when combined with the HST, HIT (or VHIT), and possibly caloric test (or Barany test) (47, 72).

Skull vibration-induced nystagmus is a recent complementary test which allows the study of vestibular frequency spectrum at higher frequencies (10, 28, 47, 72) (**Figure 7**) and has extended the field of vestibular exploration which has been restricted to the low frequencies of the caloric test and rotatory test. SVINT does not replace but complements the caloric test.

Inconvenience

In case of bilateral total or symmetrical partial lesion, SVINT is negative since it does not analyze separately each side as the



caloric test (47). This test uses extraphysiological stimulations since in daily life usual stimulations are between 0.5 and 5 Hz (Figure 7) (72).

Tolerance and Adverse Effects

The test acceptability has been validated in more than 18,500 subjects (73). Some patients with recent acute peripheral vestibular disorder described lateropulsion sensations (usually toward the intact side), while other subjects with SCD may report nausea when the test is repeated. These mild manifestations usually do not prevent continuation of the examination. One subject reported transient tinnitus.

The series of 18,500 patients reported in Dumas PhD thesis (73) noted the absence of significant side effect and signaled the advantage of this test upon HST and HIT in elderly patients with vascular problems or cervical arthritis. It is recommended to perform this test cautiously in certain situations (recently operated otosclerosis, retinal detachment, history of recent cerebral hematoma, poorly controlled anticoagulant therapy) (47).

Numerous authors using BCV do not mention any noxious effect in more restraint series (3, 11–13, 23, 24, 64).

CERVICAL VIBRATIONS

Yagi and Ohyama (32) suggested in UVL patients stimulated on posterior cervical muscles that the VIN observed is the consequence of vestibular decompensation provoked by the massive proprioceptive inputs in brain stem vestibular nuclei where cervical afferents are well represented. Vibrations at 100 Hz have been

described to correspond to optimal frequencies to stimulate muscle spindles (74). This conclusion may be moderated considering the possible concomitant stimulation of labyrinthine receptors because of vibrations diffusion (46) and since one knows that in UVL patients VIN SPV measured on Mastoid is more efficient than cervical posterior vibrations (10, 26).

Strupp et al. (33) explained perceptual and oculomotor effects of neck muscle vibration in VN as ipsilateral somatosensory substitution of vestibular function.

Iwasa et al.'s (34) proposal to use vibration to determine a cervical origin in vertigo was not further confirmed. They described, in vertigo with possible cervical origin, a postural sway toward the side contralateral to the vibratory nystagmus obtained in the absence of caloric test modification. These results are difficult to interpret and not totally convincing in the perspective of the VIN after cervical stimulations as an indicator of cervical proprioceptive pathology. Popov et al. (40) demonstrated in bilateral areflexive patients that neck vibrations induce a vertical upward slow eye movement and a fast phase downward and that the propriocegry illusion is secondary to vibration-induced eye movement mediated by the cervico-ocular reflex. Kawase et al. (44) demonstrated in UVL patients (VS) that neck vibrations increase significantly SVV shift and that the presence of VIN and magnitude of SVV are correlated.

Other muscular stimulations in normal subjects either cervical or to inferior limbs have been proposed: they modify posture and head position but usually induce no nystagmus (75, 76). In UVL patients, cervical stimulations induce a VIN but not inferior limb stimulations (30).

THE NEURAL BASIS—EVIDENCE FROM ANIMAL EXPERIMENTS

The evidence for establishing the basis of SVIN comes from recordings from single primary SCC and otolithic afferents in anesthetized guinea pigs in response to BCV using frequencies and intensities comparable to those used in the clinical testing of SVIN in human (subjects and patients)—100 Hz BCV of the skull (36–38). The predominantly horizontal component of SVIN leads to the hypothesis that it is the horizontal SCC which is activated by this stimulus.

Primary vestibular afferents with irregular resting discharge were activated during low-frequency vibration of the stereotaxic frame by a hand-held Brüel and Kjaer minishaker 4810. They were identified as canal neurons by their response to angular acceleration in canal planes or as otolith neurons by their response to static pitch stimulation, and/or by neurobiotin staining. A triaxial linear accelerometer on the skull showed that the strength of the BCV stimulation in these studies was similar to that used to generate SVIN in human patients when BCV is delivered to the mastoid by a hand-held massager or dedicated device (3–5, 26, 27).

Many primary otolithic afferent neurons from the utricular or saccular macule with irregular resting discharge can be activated at low intensity by a full range of BCV frequencies from less than 100 Hz up to 2,000 Hz, with a very low threshold of about 0.02 g peak-to-peak at 500 Hz (38). When activated, the cells show phase-locking of the action potential to individual cycles of the stimulus waveform, similar to that found in auditory afferents (77). At high frequencies, the neurons do not fire on every cycle but each action potential is phase-locked to approximately the same phase angle of the vibration stimulus, so every single cycle of the waveform is the effective stimulus for the vestibular receptor/afferent.

In contrast irregular horizontal SCC neurons are not activated even by high intensity (>2 g p-p) 500 Hz BCV (78). However, as the frequency is decreased to around 100 Hz, these irregular semicircular canal neurons from both the horizontal and anterior canals show activation with phase-locked firing to 100 Hz vibration and up to about 200–300 Hz (Figure 8), but no activation at higher frequencies.

This activation of SCC neurons at 100 Hz occurs even though the stimulus is a linear not an angular acceleration, and the frequency is above the highest reported upper frequency response of canal-cupula mechanical models of the horizontal canal (79). With phase locking, the 100 Hz stimulus frequency puts a limit of 100 spikes/s on the firing rate. This is above the average neural resting discharge rate of irregular semicircular canal afferents in primates (80), and such an increase in firing would also be produced by a real maintained small angular acceleration and so one would expect a horizontal eye movement response (horizontal nystagmus) to such an increased firing rate in alert animals (81).

At 500 Hz, BCV otolith neurons are clearly activated at low threshold and high sensitivity whereas semicircular canal neurons show no change in firing rate to intense 500 Hz stimuli (37, 38). This dissociation is the reason that 500 Hz BCV is used in specific

clinical tests of otolith function in human patients (63, 82). However, at low frequencies around 100–200 Hz, and at stimulus levels used clinically, both otolith and semicircular canal neurons are activated. If we could have delivered even higher amplitude linear accelerations at 500 Hz, we may well have activated canal neurons but such very large linear accelerations are above the values used clinically and are impractical and painful for human subjects and patients and recording neurons would be beyond challenging.

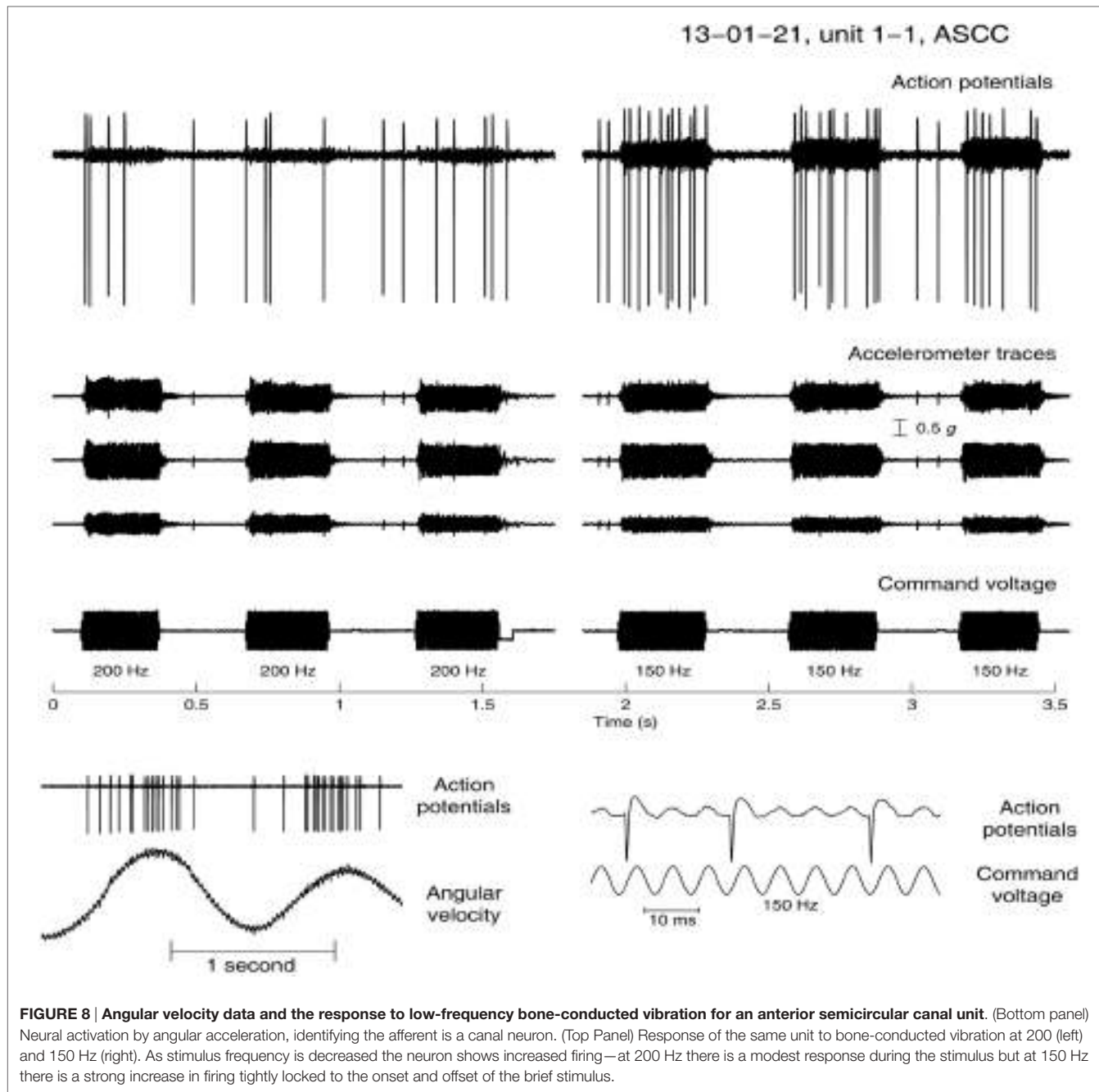
How Could These Results Explain the SVIN Results?

Vibration is very efficiently transmitted through the head of both guinea pigs and humans (78). As a result, the 100 Hz vibration stimulus applied to one mastoid is an effective stimulus for vestibular receptors in both labyrinths and so would be expected to cause phase-locked activation in irregular afferents from both labyrinths. Presumably healthy subjects with both labyrinths intact do not show SVIN since both labyrinths will be activated and an enhanced firing rate, phase-locked to the 100 Hz stimulus, will occur in both vestibular nerves simultaneously and so their effects on generating horizontal eye movements presumably cancel at the level of the vestibular nuclei. In patients with UVL, the irregular horizontal canal neurons on the remaining healthy side will be activated by vibration of either mastoid, and so the increased neural firing in afferents from that healthy labyrinth will not be canceled and will result in a drive to generate a predominantly horizontal nystagmus, with quick phases directed away from the affected side. Simultaneous activation of nerves from both lateral canals in cats results in cancellation of canal-induced eye movements (83).

Anterior canal neurons are also activated by the same 100 Hz (and probably posterior canals also). In other words, it is likely that all canals in a labyrinth are activated by the imposed 100 Hz mastoid BCV. So why is the nystagmus direction horizontal? The cancellation principle implies that the eye movements induced by simultaneous anterior and posterior canal activation in the one labyrinth are opposite, and so cancel, leaving just the horizontal component driving the eye movement response.

The neural results predict the following

- (1) in patients with a left UVL, the 100 Hz BCV stimulation will activate irregular neurons in the healthy right labyrinth, which will not be canceled by input from the affected left labyrinth. The result will be a slow-phase eye movement to the patient's left and quick phases to the patient's right, i.e., a horizontal nystagmus beating away from the affected (left) side.
- (2) in patients with a dehiscence of the anterior semicircular canal in the left labyrinth—the BCV stimulation will strongly activate the irregular canal afferents from the left side and not be canceled at the vestibular nuclei by the input from the right side. This will cause a horizontal nystagmus with slow phases to the patient's right and quick phases to the patient's left [i.e., a horizontal nystagmus beating toward the affected (left) side]. Moreover, in artificially created SCD, the



labyrinth becomes more sensitive to high frequency stimulations for both otolith and semicircular canal receptors (84).

Onset and Offset

In human patients, the nystagmus starts abruptly at the onset of the stimulus and finishes abruptly at the termination of the stimulus—there is no after nystagmus (4, 5, 26, 29) (Figure 3). The recordings of phase-locked activation in irregular canal and otolith neurons shows precisely the same abrupt onset and termination of phase-locked neural activation, since the mechanism of this vibration-induced activation does not involve canal-cupula mechanics (35).

The absence of any evidence of velocity storage may be due to the simultaneous otolithic activation “dumping” any canal-induced nystagmus (“tilt dumping”).

The response of single semicircular canal neurons to low-frequency BCV stimulation appears to explain the major phenomena of SVIN (Box 2). Curthoys et al. (78) demonstrated in guinea pigs that at 75 dB and 500 Hz (delivered by bone-anchored vibrators) only irregular afferent fibers issuing from otolithic vestibular structures responded; there were no responses at these frequencies issuing from SCC afferents.

In a more recent work (36), the authors studied in guinea pigs responses to a wider range of frequencies and demonstrated that

BOX 2 | Summary.

- Why SVIN occurs in patients with asymmetric vestibular function but not in healthy subjects:* 100 Hz BCV activates semicircular canal neurons in intact (normally encased) labyrinths, and in healthy subjects the simultaneous neural input from both labyrinths would be expected to cancel, whereas in unilateral patients the input from the healthy side is unopposed so cancellation does not occur.
- Why the nystagmus direction is horizontal in UVL patients:* the vibration probably activates sensitive canal neurons in all canals, in both labyrinths, but the anterior and posterior canal inputs in each labyrinth will cancel, leaving just the horizontal canal activation driving the eye movement.
- Why 100 Hz BCV mastoid stimulation of patients with UVL causes nystagmus with quick phases beating away from the affected side:* the unopposed neural drive from the intact labyrinth will cause slow phases away from the healthy side and quick phases toward the healthy side (i.e., away from the affected side).
- Why 100 Hz BCV mastoid stimulation of patients with SCD causes nystagmus with quick phases beating toward the affected side:* the neural drive from the side with the SCD will have lower threshold and higher firing rate and so will not be fully canceled by the activation from the healthy ear resulting in slow phases away from the affected side and quick phases toward the affected side.
- Why these respective responses in patients are independent of which mastoid is stimulated:* the vibration stimulation is conducted so effectively to both labyrinths, independently of which side is stimulated.
- Why the onset and offset of the nystagmus is so abrupt, unlike other nystagmus attributed to horizontal canal activation by angular acceleration:* the vibration stimulus causes immediate phase-locked activation of canal neurons which ceases at stimulus offset.
- Why high frequency vibrations at 100 Hz which are beyond the mechanical cut off frequencies of canal mechanism:* BCV induces inner ear fluid displacements which deflect type I receptors and so activates irregular afferent neurons.

at 100 Hz in normally encased labyrinths both canal and otolithic irregular fibers were activated. Lower stimulus intensity (in g) is, however, required to elicit responses from otolithic structures than from canals. For frequencies at 500 Hz or higher, only otolithic afferents from the striola region of utricular or saccular macula were activated (36, 78).

Vibration-induced nystagmus requires not only integrity of the peripheral end organ (type 1 inner ear hair cells), afferent neurons with irregular discharges, and integration in the vestibular nucleus for production of the slow phase but also structures of the brain stem to restore the eye position by quick phases (pontine reticula formation). Clinical interpretation of VIN in term of topography and side of a lesion needs a careful analysis and we emphasize that although SVIN is robust and the 100-Hz mastoid vibration stimulus is superficially simple, care must be taken with patient testing, stimulus presentation, response measurement, and the interpretation of the results (Box 3).

CONCLUSION

Skull vibration-induced nystagmus test, a recent, robust, non-invasive examination test, has opened a new area of vestibular exploration as it allows without side effects a simple non-invasive, rapid clinical test to vestibular high frequencies. SVINT is a useful tool to indicate a lesion side and reveals instantaneously, even in chronic or compensated patients, a SVIN in case of

BOX 3 | SVIN validity criteria.

The induced nystagmus starts with stimulation, stops with its withdrawal, and does not present any secondary reversal. It is sustained, reproducible, and beats in the same direction either after left and/or right mastoid (RM) process stimulation, is often less intense or absent after vertex stimulation (except in case of superior SCD). Nystagmus is usually absent or discordant in subjects with no vestibular disorders: in 10% of cases, false-positive nystagmus is observed at 60 Hz with right-beating nystagmus on the RM and left-beating nystagmus on the left mastoid (inconsistent directions). A SVIN slow-phase velocity SPV greater than 2°/s is also required to validate the test.

vestibular asymmetry as a vestibular Weber test. SVINT is a reliable, fast, first-line test. The optimal frequency to induce a SVIN is 100 Hz.

Skull vibration-induced nystagmus test is useful to complement information of other common vestibular tests in the multifrequency analysis of vestibular function. Yet, it gives no specific information on vestibular pathways exact topographic alteration and reveals modifications related with a lesion located in any point of the vestibulo-ocular reflex pathway. Noteworthy, it is significantly more sensitive to reveal peripheral than central lesions.

Skull vibration-induced nystagmus test is not influenced by vestibular compensation and could be advisable as an additional data and an adjunct in forensic or occupational medicine. It brings complementary information to classical SCC test explorations, cVEMP, and oVEMP. Its use in clinical practice seems to predict a wider development as a future promising first-line test.

AUTHOR NOTES

The skull vibration-induced nystagmus test was the subject of the PhD thesis entitled “Influence of vibratory stimulation applied to the skull and neck muscles on equilibrium function. Physiological interpretations and applications to pathology. Development and validation of a new vestibular investigation test: the skull vibration-induced nystagmus test or Dumas test” presented at the University of Lorraine (Nancy), September 18, 2014. Thesis Jury Members: S. Caudron, France; A. Charpiot, France; N. Deggouj, Belgium; P. Denise, France; H. Kingma, The Netherlands; M. Magnusson, Sweden; P. Perrin, France; S. Schmerber, France; D. Vibert, Switzerland.

AUTHOR CONTRIBUTIONS

All authors listed, have made substantial, direct and intellectual contribution to the work, and approved it for publication.

ACKNOWLEDGMENTS

The authors thank the UEM CHU Grenoble, the institute of health Luxembourg, and the DRCI Grenoble for their scientific support; Mrs. Hernandez of the Biomedical Department Grenoble for the material supply; P. Jousse from the Neuroradiology Department for drawings and figures.

REFERENCES

- Von-Békésy G. Über akustische Reizung des Vestibularapparates. *Arch Ges Physiol* (1935) 236:59–72. doi:10.1007/BF01752324
- Lucke K. [A vibratory stimulus of 100 Hz for provoking pathological nystagmus (author's transl)]. *Z Laryngol Rhinol Otol* (1973) 52(10):716–20.
- Hamann KF, Schuster EM. Vibration-induced nystagmus – a sign of unilateral vestibular deficit. *ORL J Otorhinolaryngol Relat Spec* (1999) 61(2):74–9. doi:10.1159/000027645
- Dumas G, Michel J, Lavieille JP, Charachon R, Ouedraogo E. [Clinical value of the cranial vibratory test. A 3D analysis of the nystagmus]. *J Fr ORL* (1999) 48:13–21.
- Dumas G, Michel J, Lavieille JP, Ouedraogo E. [Semiologic value and optimum stimuli trial during the vibratory test: results of a 3D analysis of nystagmus]. *Ann Otolaryngol Chir Cervicofac* (2000) 117(5):299–312.
- Dumas G, Perrin P, Morel N, N'Guyen DQ, Schmerber S. [Skull vibratory test in partial vestibular lesions – influence of the stimulus frequency on the nystagmus direction]. *Rev Laryngol Otol Rhinol (Bord)* (2005) 126(4):235–42.
- Dumas G, Lion A, Karkas A, Perrin P, Perrottino F, Schmerber S. Skull vibration-induced nystagmus test in unilateral superior canal dehiscence and otosclerosis: a vestibular Weber test. *Acta Otolaryngol* (2014) 134(6):588–600. doi:10.3109/00016489.2014.888591
- Young ED, Fernandez C, Goldberg JM. Responses of squirrel monkey vestibular neurons to audio-frequency sound and head vibration. *Acta Otolaryngol* (1977) 84(5–6):352–60. doi:10.3109/00016487709123977
- Dumas G, Michel J. Valeur sémiologique du test de vibration osseux crânien. In: IPSEN, editor. *XXXI ème Symposium International d'Otoneurologie*. Liège (1997).
- Dumas G, De Waele C, Hamann KF, Cohen B, Negrevergne M, Ulmer E, et al. [Skull vibration induced nystagmus test]. *Ann Otolaryngol Chir Cervicofac* (2007) 124(4):173–83. doi:10.1016/j.aorl.2007.05.001
- Lackner JR, Graybiel A. Elicitation of vestibular side effects by regional vibration of the head. *Aerospace Med* (1974) 45(11):1267–72.
- Ohki M, Murofushi T, Nakahara H, Sugasawa K. Vibration-induced nystagmus in patients with vestibular disorders. *Otolaryngol Head Neck Surg* (2003) 129(3):255–8. doi:10.1016/S0194-5998(03)00529-1
- Karlberg M, Aw ST, Black RA, Todd MJ, MacDougall HG, Halmagyi GM. Vibration-induced ocular torsion and nystagmus after unilateral vestibular deafferentation. *Brain* (2003) 126(Pt 4):956–64. doi:10.1093/brain/awg091
- Dumas G, Lavieille J, Schmerber S, Sauvage J. Le test vibratoire osseux crânien. *Rev SFORL* (2004) 82:8–14.
- Modugno G, Brandolini C, Piras G, Raimondi M, Ferri G. *Bone Vibration-Induced Nystagmus (VIN) Is Useful in Diagnosing Vestibular Schwannoma (VS)*. Sixth International Conference on Acoustic Neuroma; 2011. Los Angeles: International Conference on Acoustic Neuroma (2011).
- Dumas G, Karkas A, Schmerber S. Skull high-frequency vibration-induced nystagmus test for vestibular function assessment in vestibular schwannoma. In: Neurooma I, editor. *Sixth International Conference on Acoustic Neuroma*; 2011. Los Angeles (2011).
- Freyss G, De-Waele C, Ledjedel S. Efficacité comparative des explorations vestibulaires caloriques (épreuves unilatérales et bilatérales simultanées) et vibratoires dans la détection des neurinomes de l'acoustique. In: IPSEN, editor. *XXXVI ème Symposium de la Société Internationale d'Otoneurologie*; 2006. Paris (2006).
- Negrevergne M, Ribeiro S, Moraes CL, Maunsell R, Morata GC, Darrouzet V. [Video-nystagmography and vibration test in the diagnosis of vestibular schwannoma. Review of 100 cases]. *Rev Laryngol Otol Rhinol (Bord)* (2003) 124(2):91–7.
- Koo JW, Kim JS, Hong SK. Vibration-induced nystagmus after acute peripheral vestibular loss: comparative study with other vestibulo-ocular reflex tests in the yaw plane. *Otol Neurotol* (2011) 32:466–71. doi:10.1097/MAO.0b013e31820d9685
- Xie S, Guo J, Wu Z, Qiang D, Huang J, Zheng Y, et al. Vibration-induced nystagmus in patients with unilateral peripheral vestibular disorders. *Indian J Otolaryngol Head Neck Surg* (2013) 65(4):333–8. doi:10.1007/s10270-013-0638-6
- Nuti D, Mandala M. Sensitivity and specificity of mastoid vibration test in detection of effects in vestibular neuritis. *Acta Otorhinolaryngol Ital* (2005) 25:271–6.
- Hong SK, Koo JW, Kim JS, Park MH. Implication of vibration induced nystagmus in Menière's disease. *Acta Otolaryngol Suppl* (2007) 127(558):128–31. doi:10.1080/03655230701625019
- Park H, Hong SC, Shin J. Clinical significance of vibration-induced nystagmus and head-shaking nystagmus through follow-up examinations in patients with vestibular neuritis. *Otol Neurotol* (2008) 29(3):375–9. doi:10.1097/MAO.0b013e318169281f
- Park H, Lee Y, Park M, Kim J, Shin J. Test-retest reliability of vibration-induced nystagmus in peripheral dizzy patients. *J Vestib Res* (2010) 20(6):427–31. doi:10.3233/VES-2010-0389
- Park JH, Kim HJ, Kim JS, Koo J. Costimulation of the horizontal semicircular canal during skull vibrations in superior canal dehiscence syndrome. *Audiol Neurotol* (2014) 19:175–83. doi:10.1159/000358002
- Dumas G, Perrin P, Schmerber S. Nystagmus induced by high frequency vibrations of the skull in total unilateral peripheral vestibular lesions. *Acta Otolaryngol* (2008) 128:255–62. doi:10.1080/00016480701477677
- Dumas G, Karkas A, Perrin P, Chahine K, Schmerber S. High-frequency skull vibration-induced nystagmus test in partial vestibular lesions. *Otol Neurotol* (2011) 32:1291–301. doi:10.1097/MAO.0b013e31822f0b6b
- Dumas G, Schmerber S, Lavieille JP. [Nystagmus and vibratory test: evidence for mechanism. Material conditions and methods in the fast detection of unilateral vestibular lesions]. *Ann Otolaryngol Chir Cervicofac* (2003) 120(5):286–95.
- Dumas G, De-Waele C, Tran-Ba-Huy P, Chays A. *Test vibratoire osseux crânien*. In: *Electrophysiologie en ORL*. Paris: Société Française d'Oto-rhino-laryngologie et de Chirurgie de la Face et du Cou (2008). p. 154–9.
- Dumas G, Lion A, Gauchard G, Herpin G, Magnusson M, Perrin P. Clinical interest of postural and vestibulo-ocular reflex changes induced by cervical muscles and skull vibration in compensated unilateral vestibular lesion patients. *J Vestib Res* (2013) 23:41–9. doi:10.3233/VES-130468
- Magnusson M, Andersson G, Gomez S, Johansson R, Martensson A, Karlberg M, et al. Cervical muscle afferents play a dominant role over vestibular afferents during bilateral vibration of neck muscles. *J Vestib Res* (2006) 16(3):127–36.
- Yagi T, Ohya Y. Three-dimensional analysis of nystagmus induced by neck vibration. *Acta Otolaryngol* (1996) 116(2):167–9. doi:10.3109/00016489609137815
- Strupp M, Arbusow V, Dieterich M, Sautier W, Brandt T. Perceptual and oculomotor effects of neck muscle vibration in vestibular neuritis. Ipsilateral somatosensory substitution of vestibular function. *Brain* (1998) 121(Pt 4):677–85. doi:10.1093/brain/121.4.677
- Iwasa H, Yagi T, Kamio T. Diagnostic significance of neck vibration for the cervical vertigo. *Adv Otorhinolaryngol* (1983) 30:268–70.
- Curthoys IS, Grant JW. How does high frequency sound or vibration activate vestibular receptors? *Exp Brain Res* (2015) 233(3):691–9. doi:10.1007/s00221-014-4192-6
- Curthoys IS, Vulovic V, Pogson J, Sokolic L. *Responses of Guinea Pig Primary Vestibular Afferents to Low Frequency (50–100Hz) Bone Conducted Vibration (BCV) – The Neural Basis of Vibration Induced Nystagmus*. Program No. 574.06 2012 Neuroscience Meeting Planner. New Orleans, LA: Society for Neuroscience (2013).
- Curthoys IS, Vulovic V, Burgess AM, Manzari L, Sokolic L, Pogson J, et al. Neural basis of new clinical vestibular tests: otolithic neural responses to sound and vibration. *Clin Exp Pharmacol Physiol* (2014) 41:371–80. doi:10.1111/1440-1681.12222
- Curthoys IS, Vulovic V, Burgess AM, Sokolic L, Goonetilleke SC. The response of guinea pig primary utricular and saccular irregular neurons to bone-conducted vibration (BCV) and air-conducted sound (ACS). *Hear Res* (2016) 331:131–43. doi:10.1016/j.heares.2015.10.019
- Bozovic D, Hudspeth AJ. Hair-bundle movements elicited by transepithelial electrical stimulation of hair cells in the sacculus of the bullfrog. *Proc Natl Acad Sci U S A* (2003) 100(3):958–63. doi:10.1073/pnas.0337433100
- Popov KE, Lekhel H, Faldon M, Bronstein AM, Gresty MA. Visual and oculomotor responses induced by neck vibration in normal subjects and labyrinthine defective patients. *Exp Brain Res* (1999) 128(3):343–52. doi:10.1007/s002210050854
- White JA, Hughes GB, Ruggieri PN. Vibration-induced nystagmus as an office procedure for the diagnosis of superior semicircular canal dehiscence. *Otol Neurotol* (2007) 28(7):911–6. doi:10.1097/MAO.0b013e31812f7222

42. Manzari L, Modugno GC, Brandolini C, Pirodda A. Bone vibration-induced nystagmus is useful in diagnosing superior semicircular canal dehiscence. *Audiol Neurotol* (2008) 13(6):379–87. doi:10.1159/000148201
43. Aw ST, Aw GE, Todd MJ, Bradshaw AP, Halmagyi GM. Three-dimensional vibration-induced vestibulo-ocular reflex identifies vertical semicircular canal dehiscence. *J Assoc Res Otolaryngol* (2011) 12(5):549–58. doi:10.1007/s10162-011-0274-3
44. Kawase T, Maki A, Takata Y, Miyazaki H, Kobayashi T. Effects of neck muscle vibrations on subjective visual vertical comparative effects on nystagmus. *Eur Arch Otorhinolaryngol* (2011) 268(6):823–7. doi:10.1007/s00405-010-1467-9
45. Lee S-U, Kee HJ, Sheen SS, Choi BY, Koo JW, Kim J-S. Head-shaking and vibration-induced nystagmus duringan between the attacks of unilateral Menière's disease. *Otol Neurotol* (2015) 36(5):865–72. doi:10.1097/MAO.0000000000000743
46. Dumas G, Lion A, Perrin P, Ouedraogo E, Schmerber S. Topographic analysis of the skull vibration-induced nystagmus test with piezoelectric accelerometers and force sensors. *Neuroreport* (2016) 27(5):318–22. doi:10.1097/WNR.0000000000000539
47. Dumas G, Perrin P, Ouedraogo E, Schmerber S. How to perform the skull vibration induced nystagmus test (SVNT). *Eur Ann Otorhinolaryngol Head Neck Dis* (2016) 133(5):343–8. doi:10.1016/j.anorl.2016.04.002
48. Franke E. Response of the human skull to mechanical vibrations. *J Acoust Soc Am* (1956) 28:1277–84. doi:10.1121/1.1908622
49. Jahn AF, Tonndorf J. Lateralization of bone-conducted sounds. *Am J Otolaryngol* (1982) 3(2):133–40. doi:10.1016/S0196-0709(82)80044-6
50. Stenfelt S, Goode RL. Bone-conducted sound: physiological and clinical aspects. *Otol Neurotol* (2005) 26(6):1245–61. doi:10.1097/01.mao.0000187236.10842.d5
51. Wever E, Bray C. The nature of bone conduction as shown in the electrical response of the cochlea. *Ann Otol Rhinol Laryngol* (1936) 45:822–30. doi:10.1177/000348943604500323
52. Stenfelt S, Puria S, Hato N, Goode RL. Basilar membrane and osseous spiral lamina motion in human cadavers with air and bone conduction stimuli. *Hear Res* (2003) 181(1–2):131–43. doi:10.1016/S0378-5955(03)00183-7
53. Nolan M, Lyon DJ. Transcranial attenuation in bone conduction audiometry. *J Laryngol Otol* (1981) 95(6):597–608. doi:10.1017/S0022215100091155
54. Kirikai I. An experimental study on the fundamental mechanism of bone conduction. *Acta Otolaryngol Suppl* (1959) 145:1–111.
55. Von-Bekesy G. Zur Theorie des Hörens bei der Schallaufnahme durch Knöchenleitung. *Ann Physik* (1932) 132(13):111–36. doi:10.1002/andp.1932405109
56. Richter U, Brinkmann K. Threshold of hearing by bone conduction. A contribution to international standardization. *Scand Audiol* (1981) 10(4):235–7. doi:10.3109/01050398109076186
57. Tonndorf J. Compressional bone conduction in cochlear models. *J Acoust Soc Am* (1962) 34:1127–31. doi:10.1121/1.1918259
58. Sohmer H, Freeman S, Geal-Dor M, Adelman C, Savion I. Bone conduction experiments in humans, a fluid pathway from bone to ear. *Hear Res* (2000) 146:81–8. doi:10.1016/S0378-5955(00)00099-X
59. Hamann KF. Le Nystagmus de Vibration vis à vis du Neurinome de l'acoustique. In: IPSEN, editor. *XXXVI^e Symposium de la Société Internationale d'Otoneurologie de langue Française 2002. 24-25 Mai. Marrakech* (2002). p. 47.
60. Kheradmand A, Zee D. The bedside examination of the vestibulo-ocular reflex (VOR): an update. *Rev Neurol* (2012) 168:710–9. doi:10.1016/j.neuro.2012.07.011
61. Dumas G, Schmerber S. Cavernous haemangiomas: hearing and vestibular inaugural symptoms. *Ann Otolaryngol Chir Cervicofac* (2004) 121(5):272–81. doi:10.1016/S0003-438X(04)95520-X
62. Huh YE, Kim JS. Bedside evaluation of dizzy patients. *J Clin Neurol* (2013) 9:203–13. doi:10.3988/jcn.2013.9.4.203
63. Curthoys IS. The interpretation of clinical tests of peripheral vestibular function. *Laryngoscope* (2012) 122:1342–52. doi:10.1002/lary.23258
64. Ulmer E, Chays A, Bremond G. [Vibration-induced nystagmus: mechanism and clinical interest]. *Ann Otolaryngol Chir Cervicofac* (2004) 121(2):95–103. doi:10.1016/S0003-438X(04)95495-3
65. Minor LB, Solomon D, Zinreich JS, Zee DS. Sound- and/or pressure-induced vertigo due to bone dehiscence of the superior semicircular canal. *Arch Otolaryngol Head Neck Surg* (1998) 124(3):249–58.
66. Minor LB. Superior canal dehiscence syndrome. *Am J Otol* (2000) 21(1):9–19. doi:10.1016/S0196-0709(00)80105-2
67. Rosowski JJ, Songer JE, Nakajima HH, Brinsko KM, Merchant SN. Clinical, experimental, and theoretical investigations of the effect of superior semicircular canal dehiscence on hearing mechanisms. *Otol Neurotol* (2004) 25(3):323–32. doi:10.1097/00129492-200405000-00021
68. Songer JE, Rosowski JJ. The effect of superior canal dehiscence on cochlear potential in response to air-conducted stimuli in chinchilla. *Hear Res* (2005) 210(1–2):53–62. doi:10.1016/j.heares.2005.07.003
69. Songer JE, Rosowski JJ. A mechano-acoustic model of the effect of superior canal dehiscence on hearing in chinchilla. *J Acoust Soc Am* (2007) 122(2):943–51. doi:10.1121/1.2747158
70. Junet P, Karkas A, Dumas G, Quesada JL, Schmerber S. Vestibular results after intratympanic gentamicin therapy in disabling Menière's disease. *Eur Arch Otorhinolaryngol* (2016) 273(10):3011–8. doi:10.1007/s00405-015-3889-x
71. Beatrice F, Karkas A, Bucolo S, Palermo A, Perrottino F, Lion A, et al. Benefit of skull vibration-induced nystagmus test in occupational medicine. *Rev Laryngol Otol Rhinol* (2014) 135(1):1–6.
72. Chays A, Florent A, Ulmer E. *Les Vertiges*. Paris: Masson (2004). 213 p.
73. Dumas G. *Influence of Vibratory Stimulations Applied to Skull and Cervical Muscles on Equilibrium Function. Physiological Interpretation and Applications in Pathology. Development and Validation of a New Vestibular Test: The Skull Vibration Induced Nystagmus Test or Dumas Test*. Ph.D. thesis, University of Lorraine, Perrin P, Schmerber S Thesis directors (2014).
74. Perrin P, Lestienne F. In: Masson, editor. *Mécanismes de l'équilibration humaine. Exploration fonctionnelle, application au sport et à la rééducation*. Paris, Milan, Barcelona (1994). 168 p.
75. Roll JP, Vedel JP, Bibot E. Eye, head and skeletal muscle spindle feedback in the elaboration of body references. *Prog Brain Res* (1989) 80:113–23. doi:10.1016/S0079-6123(08)62204-9
76. Dumas G. *Validation d'un test de l'équilibration chez des sportifs de haut niveau*. Master's thesis, Nancy, UFR en Sciences et Techniques des Activités Physiques et Sportives, Nancy I (2001).
77. Rose JE, Brugge JF, Anderson DJ, Hind JE. Phase-locked response to low-frequency tones in single auditory nerve fibers of the squirrel monkey. *J Neurophysiol* (1967) 30(4):769–93.
78. Curthoys IS, Kim J, McPhedran SK, Camp AJ. Bone conducted vibration selectively activates irregular primary otolithic vestibular neurons in the guinea pig. *Exp Brain Res* (2006) 175:256–67. doi:10.1007/s00221-006-0544-1
79. Hartmann R, Klinke R. Discharge properties of afferent-fibers of the goldfish semicircular canal with high-frequency stimulation. *Pflügers Arch* (1980) 388:111–21. doi:10.1007/bf00584116
80. Haque A, Angelaki DE, Dickman JD. Spatial tuning and dynamics of vestibular semicircular canal afferents in rhesus monkeys. *Exp Brain Res* (2004) 155:81–90. doi:10.1007/s00221-003-1693-0
81. Waespe W, Henn V. Velocity response of vestibular nucleus neurons during vestibular, visual, and combined angular-acceleration. *Exp Brain Res* (1979) 37:337–47. doi:10.1007/BF00237718
82. Iwasaki S, Smulders YE, Burgess AM, McGarvie LA, Macdougall HG, Halmagyi GM, et al. Ocular vestibular evoked myogenic potentials to bone conducted vibration of the midline forehead at Fz in healthy subjects. *Clin Neurophysiol* (2008) 119:2135–47. doi:10.1016/j.clinph.2008.05.028
83. Cohen B, Suzuki J-I, Bender MB. Eye movements from semicircular canal nerve stimulation in the cat. *Ann Otol Rhinol Laryngol* (1964) 73:153–69. doi:10.1177/000348946407300116
84. Curthoys IS. The new vestibular stimuli: sound and vibration—anatomical, physiological and clinical evidence. *Exp Brain Res* (2017). doi:10.1007/s00221-017-4874-y

Conflict of Interest Statement: IC is an unpaid consultant to GN Otometrics. The other authors declare no conflict of interest.

Copyright © 2017 Dumas, Curthoys, Lion, Perrin and Schmerber. This is an open-access article distributed under the terms of the Creative Commons Attribution License (CC BY). The use, distribution or reproduction in other forums is permitted, provided the original author(s) or licensor are credited and that the original publication in this journal is cited, in accordance with accepted academic practice. No use, distribution or reproduction is permitted which does not comply with these terms.



The Video Head Impulse Test

G. M. Halmagyi^{1*}, Luke Chen¹, Hamish G. MacDougall², Konrad P. Weber^{3,4}, Leigh A. McGarvie¹ and Ian S. Curthoys²

¹Neurology Department, Institute of Clinical Neurosciences, Royal Prince Alfred Hospital, Camperdown, NSW, Australia,

²Vestibular Research Laboratory, School of Psychology, The University of Sydney, Sydney, NSW, Australia, ³Department of Ophthalmology, University Hospital Zurich, University of Zurich, Zurich, Switzerland, ⁴Department of Neurology, University Hospital Zurich, University of Zurich, Zurich, Switzerland

In 1988, we introduced impulsive testing of semicircular canal (SCC) function measured with scleral search coils and showed that it could accurately and reliably detect impaired function even of a single lateral canal. Later we showed that it was also possible to test individual vertical canal function in peripheral and also in central vestibular disorders and proposed a physiological mechanism for why this might be so. For the next 20 years, between 1988 and 2008, impulsive testing of individual SCC function could only be accurately done by a few aficionados with the time and money to support scleral search-coil systems—an expensive, complicated and cumbersome, semi-invasive technique that never made the transition from the research lab to the dizzy clinic. Then, in 2009 and 2013, we introduced a video method of testing function of each of the six canals individually. Since 2009, the method has been taken up by most dizzy clinics around the world, with now close to 100 refereed articles in PubMed. In many dizzy clinics around the world, video Head Impulse Testing has supplanted caloric testing as the initial and in some cases the final test of choice in patients with suspected vestibular disorders. Here, we consider seven current, interesting, and controversial aspects of video Head Impulse Testing: (1) introduction to the test; (2) the progress from the head impulse protocol (HIMPs) to the new variant—suppression head impulse protocol (SHIMPs); (3) the physiological basis for head impulse testing; (4) practical aspects and potential pitfalls of video head impulse testing; (5) problems of vestibulo-ocular reflex gain calculations; (6) head impulse testing in central vestibular disorders; and (7) to stay right up-to-date—new clinical disease patterns emerging from video head impulse testing. With thanks and appreciation we dedicate this article to our friend, colleague, and mentor, Dr Bernard Cohen of Mount Sinai Medical School, New York, who since his first article 55 years ago on compensatory eye movements induced by vertical SCC stimulation has become one of the giants of the vestibular world.

OPEN ACCESS

Edited by:

Bernard Cohen,
Icahn School of Medicine at Mount
Sinai, United States

Reviewed by:

David Samuel Zee,
Johns Hopkins University,
United States
Jorge Kattah,
University of Illinois College
of Medicine Peoria, United States

*Correspondence:

G. M. Halmagyi
gmh@icn.usyd.edu.au

Specialty section:

This article was submitted
to Neuro-otology,
a section of the journal
Frontiers in Neurology

Received: 21 April 2017

Accepted: 22 May 2017

Published: 09 June 2017

Citation:

Halmagyi GM, Chen L,
MacDougall HG, Weber KP,
McGarvie LA and Curthoys IS (2017)
The Video Head Impulse Test.
Front. Neurol. 8:258.
doi: 10.3389/fneur.2017.00258

Abbreviations: AC, anterior canal; AICA, anterior inferior cerebellar artery; AT, ataxia telangiectasia; ATD, ascending tract of Deiter's; AVS, acute vestibular syndrome; aWE, acute Wernicke's encephalopathy; BVL, bilateral vestibular loss; CS-DI, compensatory saccade dysconjugacy index; GD, Gaucher's disease; HC, horizontal canal; HIMP, the generic name for the head impulse test protocol; HIT, head impulse test; INO, internuclear ophthalmoplegia; ION, inferior olivary nucleus; LARP, the plane of the left anterior-right posterior canals; MLE, medial longitudinal fasciculus; NPH, nucleus prepositus hypoglossi; PC, posterior canal; PCS, posterior circulation stroke; PICA, posterior inferior cerebellar artery; RALP, the plane of the right anterior-left posterior canals; SCA 6, spinocerebellar atrophy type 6; SCC, semicircular canal; SHIMP, the generic name for the suppression head impulse test protocol; vHIT, video head impulse test; VN, vestibular neuritis; VOG, video-oculography; VOR, vestibulo-ocular reflex; VOR-DI, VOR dysconjugacy index.

INTRODUCTION

In 1984, we tested a patient with bilateral vestibular schwannomas who had had both vestibular nerves surgically sectioned (1). We measured the horizontal smooth compensatory eye movements in response to passive, low-frequency (0.2 Hz), low-acceleration, sinusoidal horizontal rotations, first while the patient stared at an earth-fixed LED target in an otherwise totally dark room, and then, while he imagined the target after it had been switched off. Even without any vestibular sensory input, this patient could nonetheless generate reasonably smooth compensatory eye movement responses to that stimulus, which shows that low-frequency, low-acceleration head rotation is not a valid indicator of semicircular canal (SCC) function. In response to this stimulus, other oculomotor control mechanisms can generate the compensatory eye movements.

However, when staring at the earth-fixed target during small, fast, passive unpredictable horizontal head turns ($\sim 15^\circ$, $100^\circ/\text{s}$, $1,000^\circ/\text{s}^2$), for the first 100 ms or so, he could not generate any eye movement response to keep his gaze on target so that his gaze went with his head. Eye movement responses to small, brief, fast, unpredictable horizontal head turns (head impulses) are, in contrast to passive, slow, predictable head turns, a valid indicator of SCC function. The angular acceleration of a head impulse—up to $4,000^\circ/\text{s}^2$ —is what occurs during normal head movements. A head impulse is a purely vestibular test because it is too fast for other oculomotor control systems (such as smooth pursuit, optokinetic, cervico-ocular reflex). The head impulse test (HIT) can be done in a normally lit room—visual stimuli do not play a role in generating the response, which means this purely vestibular test can be done anywhere—a dark room is not

necessary so long as the head turn is fast—above $150^\circ/\text{s}$, passive and unpredictable.

FROM HEAD IMPULSES TO SHIMPs

The Standard HIT

In the HIT, the clinician turns the patient's head abruptly and unpredictably in the plane of a SCC pair, about 15° in about 100 ms, and observes the instantaneous compensatory eye movement response (Figure 1A). During each head impulse, the eye movement response of a healthy subject will compensate for head turn and gaze will stay fixed on the earth-fixed fixation target (Figure 2A); however, the eyes of a patient without vestibular function (an “avestibular” patient) will move with the head so that the patient has to make a corrective saccade at the end of each head impulse in order to return his gaze to the earth-fixed target (Figure 3A). This “overt” corrective or catch-up saccade observed by the clinician is the clinical sign of canal paresis (2). The contrast is that during the head turn subjects with normal SCC function make smooth compensatory eye movements, which keep gaze on the earth-fixed target, and do not need to make catch-up saccades. The overt catch-up saccades are useful because clinicians can observe them even in bedridden patients. But of course the major drawback of any clinical sign of canal paresis is that it is subjective—there is no objective verifiable record of exactly what the patient did.

The usual measure of the adequacy of the vestibulo-ocular response (VOR) is gain. Gain is a general term to cover the ratio of output to input in any dynamic system. To measure the VOR gain, we calculate the ratio of the area under the eye velocity curve, to the area under the head velocity curve, during the head impulse

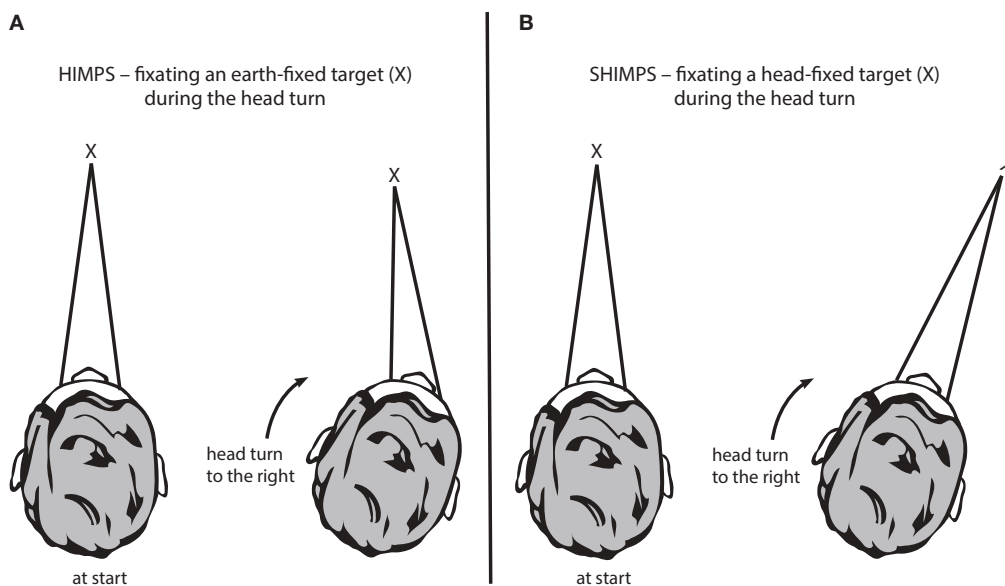


FIGURE 1 | The two test protocols for testing semicircular canal function. **(A)** In the HIMPs protocol (the classical test protocol), the person is required to maintain fixation on an earth-fixed target during a small, unpredictable, passive, head turn. Healthy subjects will not make any saccades at all or only small saccades. **(B)** In the SHIMPs protocol, the head turn is identical but the instructions are different—the person must maintain fixation on a head-fixed target (a spot from a head-mounted laser projected onto the wall in front of the subject). Healthy subjects make large saccades (see text for explanation).

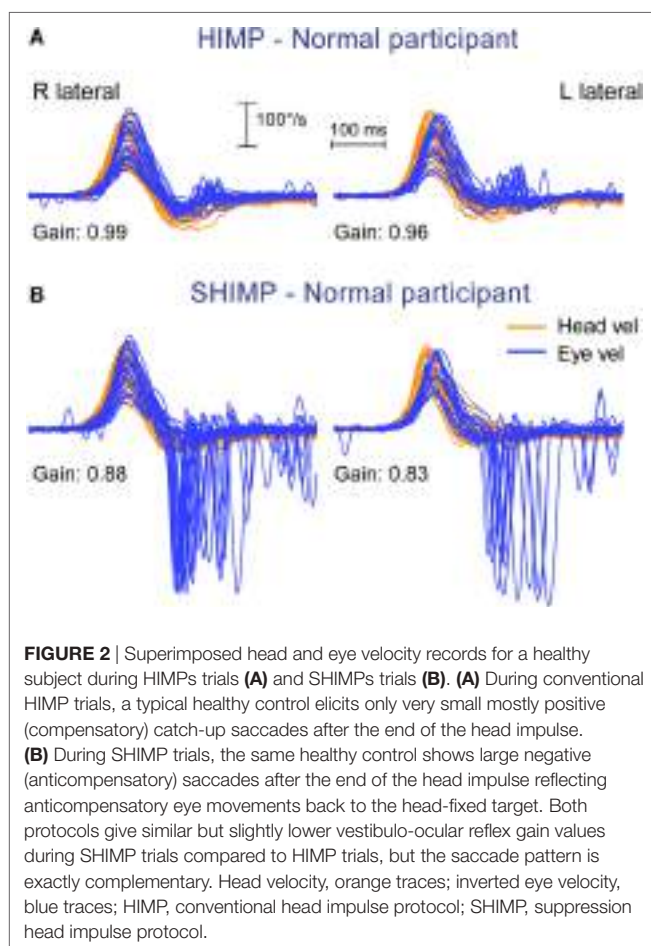


FIGURE 2 | Superimposed head and eye velocity records for a healthy subject during HIMP trials (**A**) and SHIMP trials (**B**). (**A**) During conventional HIMP trials, a typical healthy control elicits only very small mostly positive (compensatory) catch-up saccades after the end of the head impulse. (**B**) During SHIMP trials, the same healthy control shows large negative (anticompensatory) saccades after the end of the head impulse reflecting anticompen-satory eye movements back to the head-fixed target. Both protocols give similar but slightly lower vestibulo-ocular reflex gain values during SHIMP trials compared to HIMP trials, but the saccade pattern is exactly complementary. Head velocity, orange traces; inverted eye velocity, blue traces; HIMP, conventional head impulse protocol; SHIMP, suppression head impulse protocol.

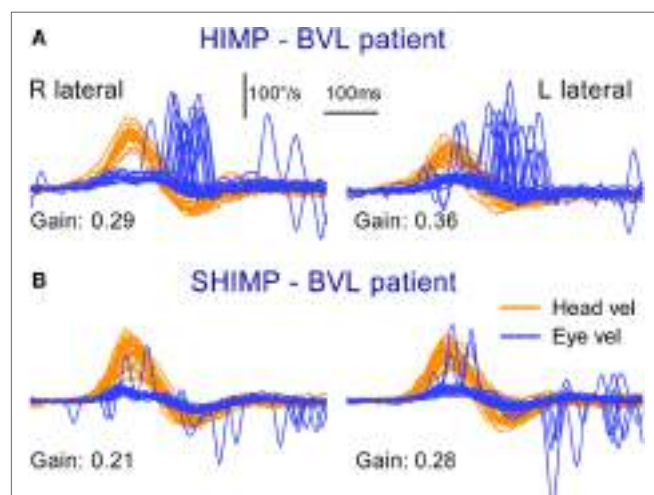


FIGURE 3 | Superimposed head and eye velocity records for a patient with BVL during HIMP trials (**A**) and SHIMP trials (**B**). The results for a typical patient with complete BVL showing a reversed saccadic pattern during HIMP and SHIMP compared to a healthy control (**Figure 2**). (**A**) During standard HIMP trials, the patient with BVL elicits mostly overt positive (compensatory) catch-up saccades after the head impulse. (**B**) During SHIMP, the same patient with BVL shows only very few downward (anticompen-satory) saccades after the end of the head impulse back to the head-fixed target. Both protocols give similar but slightly lower vestibulo-ocular reflex gain values during SHIMP compared to HIMP, but there is a complementary saccade pattern, which is reversed compared to healthy controls. Head velocity, orange traces; inverted eye velocity, blue traces. BVL, bilateral vestibular loss; HIMP, conventional head impulse protocol; SHIMP, suppression head impulse protocol. Reproduced with permission of Wolters Kluwer from the study by MacDougall et al. (3); <http://www.neurology.org>.

(4–7) (see Calculating VOR Gain). Normal VOR gain is close to 1.0. Patients with unilateral vestibular loss (UVL) have a reduced VOR gain during the head turn to their affected ear (usually less than 0.7) and so their slow phases do not compensate for head turn, with the result that their eyes move with the head, and they need to make corrective saccades for head impulses toward their affected ear (**Figure 4A**), thus identifying the side of loss.

Some patients make catch-up saccades during the head impulse, and these are not detectable by the clinician: they are “covert” catch-up saccades (8). They showed the need for an objective record of eye movement and head movement during head impulses. After about 10 years of development, MacDougall et al. came up with a high-speed head-mounted camera on tight-fitting goggles with head velocity sensors, and software for accurate objective measures of the head and eye velocity. The camera measures the center of the pupil, and valid measures require an excellent image of the eye, uncontaminated by the eye lid (see below). This is what has become the widely used video head impulse test (vHIT) (5).

The function of each and every canal can be measured individually with vHIT (4, 9, 10), and there is not much decrement of the VOR with age (11, 12). vHIT can quantify the absolute level of canal function after treatment with systemic (13) or intratympanic gentamicin (14) and measure bilateral loss of

vestibular function (15–17) (see Quantitative Head Impulse Test in Central Vestibular Disorders and New Clinical Disease Patterns Emerging from 3D Video Head Impulse Testing). Tracking the pattern of covert saccades after UVL shows that there are changes in the timing and pattern of the saccades which may be related to the adequacy of vestibular compensation. Some patients may use covert saccades to obscure the retinal slip that must occur because of their inadequate VOR (18). vHIT allows for the measurement of the pattern of these covert saccades for addressing the important question of the role of covert saccades in recovery after vestibular loss (19–23).

The vHIT rather than caloric test is becoming the first test for patients with suspected vestibular disorders (24, 25). It is fast, innocuous, repeatable and provides objective quantitative data about each of the SCCs.

Must the loss of SCC function be profound for head impulse testing to detect it? No. The published evidence shows that vHIT may detect mild impairment of canal function. Weber et al. (13) showed that different patients had different levels of bilaterally impaired SCC function on head impulse testing after systemic gentamicin—they did not all show “profound” loss of SCC function, and indeed some patients had small losses in function. The results showed a continuous spectrum of VOR gains on head impulse testing in different patients from almost normal to complete bilateral vestibular loss (BVL). More recently, vHIT has been

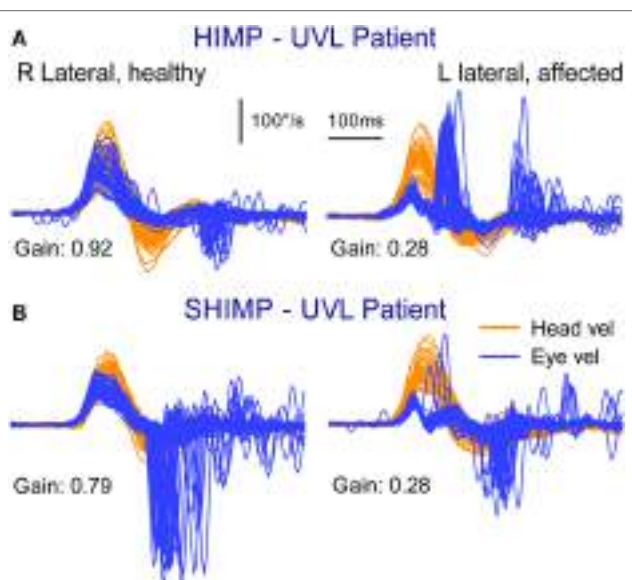


FIGURE 4 | Superimposed head and eye velocity records for a patient with unilateral vestibular loss (UVL) during HIMP trials (A) and SHIMP trials (B). (A) For rotations to their healthy (right) side, the patient shows the usual HIMP pattern of slow compensatory eye movement with few saccades. During rotations to the affected (left) side, there is a reduced slow-phase eye velocity and covert and overt saccades. (B) For rotations to their affected side, there are few SHIMP saccades, whereas for rotations to their healthy left side, there are many large SHIMP saccades. Reproduced with permission of Wolters Kluwer from the study by MacDougall et al. (3); <http://www.neurology.org>.

shown to detect mild loss of function: Marques et al. (14) found a single ITG dose only reduced VOR function using vHIT by an average of 26%—again modestly impaired SCC function rather than being a “profound” loss. Finally, the tight bands of vHIT gain for healthy subjects, which we have published (12), show that even small losses of canal function are detectable. So, just as an audiogram detects a mild impairment of auditory function, so the HIT detects mild impairment of vestibular function.

The SHIMP Variant

In the standard vHIT, the patient is required to stare at an earth-fixed target during the head impulse. If their VOR is not adequate, the patient must make a corrective saccade to return fixation to the target. vHIT is the measurement system, and we now call the whole protocol HIMP (as abbreviation for Head IMPulse testing). (Since HIMP is a recently introduced term, we will use the terms vHIT and HIMP interchangeably in this review.) In the SHIMP (“Suppression Head IMPulses”) variant, the patient stares at a *head-fixed* target during the head turn (Figure 1B). The head turn stimulus is exactly the same in HIMPs and SHIMPs—brief, passive, unpredictable, high-acceleration head turns—but in the SHIMPs protocol, the subject is required to fixate a target *which moves with the head*—a spot from a head-mounted laser projected on the wall in front of the subject (3). We call this new variant protocol SHIMP because we expected suppression of the VOR to dominate. Healthy subjects suppress their VOR frequently in

daily life (reading a book on a bus) but VOR suppression in this passive, high-acceleration vHIT protocol takes around 80 ms from the onset of the head turn (26), so VOR suppression is just starting around the end of the head impulse stimulus. (Note that we have used these new terms since the HIMP and SHIMP protocols can be used with or without the vHIT goggles. SHIMP is even easier to carry out at the bedside than HIMPs, and the corrective saccade is much easier for the clinician to see.)

The results from the SHIMP testing protocol complement the original HIMP protocol: in the SHIMPs protocol it is healthy individuals who make a large corrective saccade (Figure 2B), and the patients without vestibular function who do not make a saccade (Figure 3B). Why do healthy subjects need to make a corrective saccade? Because during the head impulse the VOR drives their eyes opposite to head, and healthy subjects do not suppress their VOR during the early stage (first ~80 ms) of the head turn. Consequently, their gaze is driven by their VOR off the head-fixed target. For example, as the head is turned to the left, the VOR keeps the gaze fixed in space by rotating the eyes in the head to the right, and so at the end of the impulse the target is to the left of the subject’s gaze so the healthy subject has to make a large leftward saccade to regain the target. This is an anticomplementary saccade, since it is in the same direction as head rotation (left). At the other extreme, for a patient with complete vestibular loss (Figure 3B), their absent VOR does not drive their eyes off the head-fixed target at all during the head impulse, so at the end of the impulse the avestibular patient’s eyes are still on target so they do not make any corrective saccade. In SHIMPs, it is the patients without vestibular function who do not make corrective saccades—exactly the converse of HIMPs. Patients with UVL show large SHIMP saccades for head turns to their healthy side and small or absent SHIMP saccades for head turns to their affected side (Figure 4B). In the SHIMPs protocol, the size of the corrective saccade is an indicator of VOR gain—healthy subjects make large saccades, whereas patients with vestibular loss make small saccades or no saccades at all, and a recent study used saccade size as an extra indicator of canal function (27). However, care is needed in interpreting the size of the saccades since there are many factors that affect the peak saccadic eye velocity—for example, the extent of overshoot of head turn, the peak head velocity of the impulse, and even the duration of the head impulse. It is important to avoid any predictive clues about the direction of head turn to avoid an early anticipatory saccade in the direction of head movement. Nevertheless, the results show that saccadic velocity can be used to index SCC function (27). So the SHIMPs protocol provides two measures of SCC function—VOR gain and the size (velocity) of the corrective saccade. VOR gain, measured from the slow-phase eye velocity, is similar for both HIMPs and SHIMPs (3), and SHIMPs has the advantage of effectively removing the covert saccades, which cause problems in gain measurement in the standard HIMPs protocol (see Figure 4).

THE PHYSIOLOGICAL BASIS OF THE HIT

The basic physiology underlying both HIMPs and SHIMPs is the same. A head turn causes fluid displacement in the SCCs, which deflects the cupula, deflects hair bundles of receptor hair cells,

triggers action potentials in primary SCC afferents which project to vestibular nuclei, thence to eye muscle motoneurons of both eyes, and so the resulting conjugate eye movement corrects for the head turn and gaze remains stable even during an unpredictable head turn (28). It is important to understand how the eye movement response is driven and there are some special features:

- The onset of eye movement response is fast—its latency is about 8 ms from onset of the head turn stimulus to the onset of the eye movement response (29).
- The stimulus causes compensatory movement of both eyes, although detailed measures show the two eyes are not exactly conjugate (30).
- The major direct neural pathways governing this response are known.
- Cerebellar input governs transmission through these pathways, and it is that cerebellar input which is responsible for VOR suppression (see also Cerebellum below).

The vHIT provides time series records of the eye movement response to head impulses and of the corrective saccades which occur in patients with UVL. In some patients, there are aspects of the response which initially appear puzzling: for example, why are there compensatory saccades to head impulses to the healthy side in UVL patients (8, 19). This section shows how the established neural connections explain the VOR response in healthy subjects and in patients with UVL. These are not some computer generated fantasies, they are evidence based—built on the hard-won neural evidence.

Rotational testing of SCC function has a major drawback. The one head movement causes complementary stimulation of canals on both sides of the head. The physiology of the canal-ocular pathways shows that for testing patients with low peak head velocities the input from the healthy ear can determine the results for both directions of horizontal rotation. The contribution from the healthy ear can be ruled out by using high-acceleration head impulses, which silence the input from the opposite side. If low velocity (low acceleration) head impulses are used, the remaining healthy ear can drive the eye movement response. That is why high velocity stimuli are mandatory. The essential reason is that for most head impulses the response is made up of two components—a dominant excitatory drive from the side to which the head is turned—and a smaller, indirect, functionally excitatory, drive from the opposite ear.

Normal head movements have very high accelerations—4,000°/s² and above (31, 32), and so the eye movement response must have a very short latency and be accurate. The response is very fast: about 8 ms from the onset of the head movement stimulus to the onset of the eye movement response (29). It is likely that the onset response is due to the action of the very fast type I receptors and irregular afferents from the central region at the crest of the crista. Receptors of the horizontal canal (HC) are not all uniform—there are two types; type I, amphora shaped receptors with short stiff hair bundles, enveloped by a calyx afferent ending [see Ref. (33, 34) for reviews]. These type I receptors predominate at the crest of the crista and intracellular recordings have shown the very fast dynamic responses of these receptors (35, 36).

The neural pathway for these fast direct projections is shown in **Figure 5A**. The schema is similar for the following figures that show the consequences of canal activation.

The point of view for these schematic figures is a view looking down on the brainstem and the two eyes. The neural structures involved in the responses are labeled, as are the synapses with each synapse in this direct circuit numbered. The papers providing the evidence about each projection and the synapse are given in the accompanying **Table 1**. The literature on the anatomy and physiology of the vestibulo-ocular projections is immense, but rather than pointing the reader to a book or a huge review we have listed in **Table 1** the selected references for each projection and each synapse.

Primary afferents from each labyrinth are excitatory and project to the vestibular nuclei; some neurons project from the vestibular nuclei to the contralateral abducens nuclei. One set of axons from abducens project directly to the lateral rectus, another group of abducens neurons (the internuclear neurons) project to the medial rectus of the contralateral eye via the medial longitudinal fasciculus (MLF) and the oculomotor nucleus (III). The connections of particular importance for understanding the eye movement to vestibular stimulation are the fibers between the two vestibular nuclei. These are the commissural fibers and they are functionally inhibitory, so each vestibular nucleus acts to inhibit some neurons in the contralateral vestibular nucleus. With head stationary, the activity of the two vestibular nuclei are presumed to be in equilibrium.

There are two other projections of importance which, for simplicity, are not shown here, because their action complements the action of other projections.

- (1) Some excitatory type I neurons in the vestibular nucleus project in the ascending tract of Deiter's (ATD) directly to the ipsilateral III nucleus (63) and so activate the ipsilateral medial rectus (complementing the excitatory input to III from the contralateral abducens internuclear neurons).
- (2) Some type I neurons in the vestibular nucleus are inhibitory and project to the ipsilateral abducens nucleus (48) and so complement the decreased input from the contralateral type I vestibular nucleus neurons during head turns.

The aim of the series of images (**Figures 5B,C** and **6A,B**) is to show how the documented anatomical structure and evidence from physiology and neural projection (**Figure 5A**) proceeds from labyrinth stimulation to eye movement response, how unilateral loss affects the system, and how, after a UVL, the system responds to head turns to the healthy and affected ear. In these figures, the two blue ellipses represent the vestibular nuclei with the darker blue representing increased activation. The orange arrows represent the functionally inhibitory fibers between the two vestibular nuclei and the width of the arrows indicates the strength of the projection.

In a healthy subject during an abrupt head turn to the left, receptor and afferents in the left HC are activated and *simultaneously* receptors and afferents from the right HC are silenced. The excitation of the left labyrinth afferents projects to, and activates, neurons in the left vestibular nucleus, and neurons in that nucleus project activation (blue lines) to the contralateral abducens

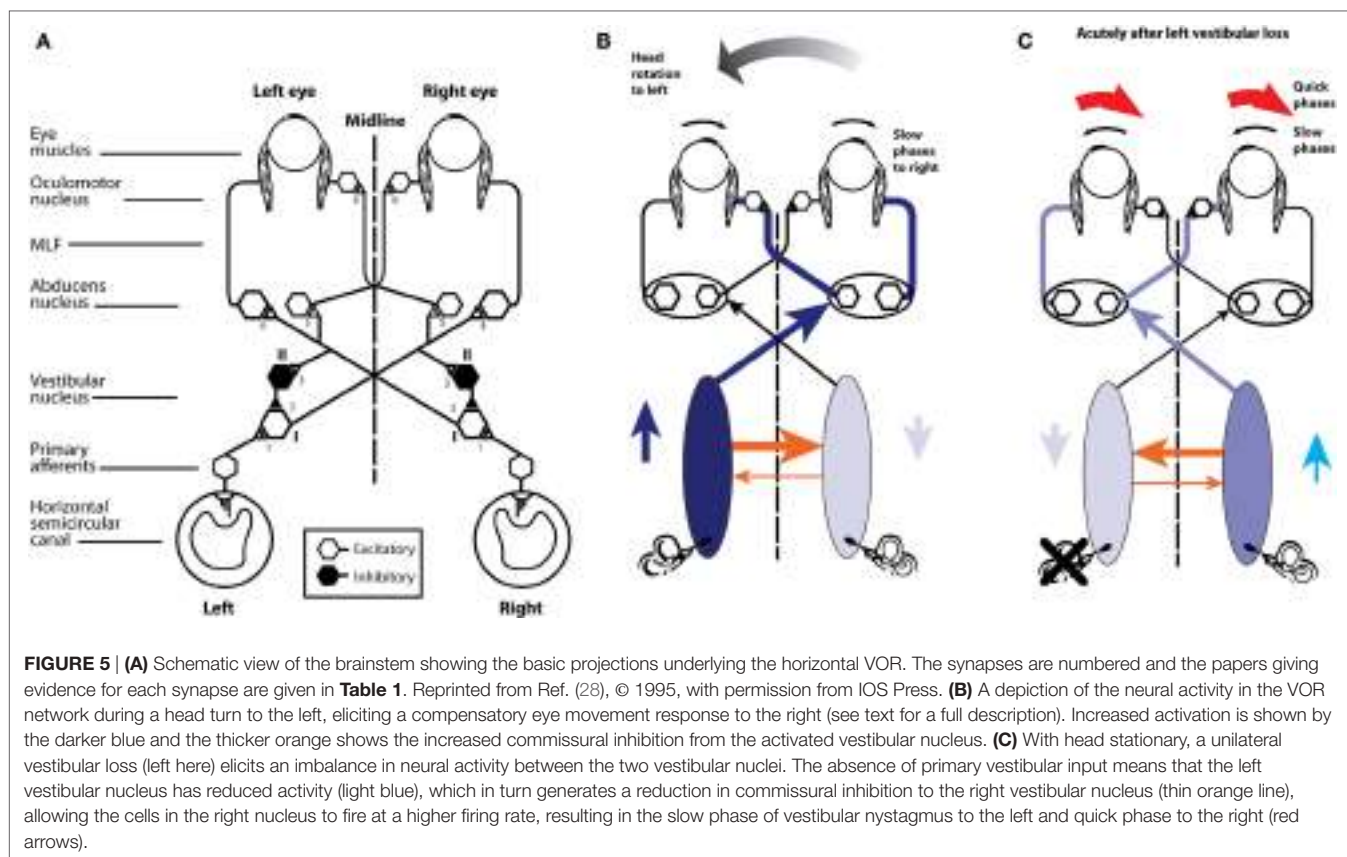


TABLE 1 | Selected references providing the anatomical and physiological evidence for the projections depicted in **Figure 5A**.

1. Excitatory projections from HC receptors to type I vestibular nucleus neurons (37–43) (type I neurons increase their firing during ipsilateral horizontal rotations)
2. Inhibitory projections from type II vestibular nucleus neurons to type I excitatory neurons (44–47) (type II neurons are inhibitory and decrease their firing during ipsilateral horizontal rotations)
3. Excitatory projections from type I vestibular nucleus neurons to the contralateral vestibular nucleus to inhibitory type II neurons (47–49)
4. Excitatory projections from type I vestibular nucleus neurons to contralateral abducens motoneurons and internuclear neurons (50–58)
5. Excitatory projections from type I vestibular neurons to contralateral internuclear neurons (48, 55, 57)
6. Excitatory projections from abducens internuclear neurons to the contralateral III nucleus (59–62)

nucleus, generating the slow-phase eye movement to the right, compensating for head turn. Some neurons in abducens nucleus (so-called internuclear neurons) project via the MLF to the contralateral oculomotor nucleus and thus activate the medial rectus muscle of the left eye. In this way, there are synergistic movements of both eyes—both eyes rotate to compensate for head turn and so both eyes remain on the fixation target during the head turn. While these excitatory processes are in action, there are exactly complementary effects exerted by projections from the right labyrinth; the head turn acts to silence the primary afferents from

the right SCC, so they project less excitation to the right vestibular nucleus, resulting in reduced excitation of the left abducens and reduced activation of the right medial rectus. So for both eyes, there is simultaneous excitation of one set of eye muscles and simultaneously reduced excitation of the opposing muscles, allowing for a smooth eye movement response of both eyes.

Importantly, however, these direct effects are complemented by the functionally inhibitory connections between the two vestibular nuclei. During the leftward head turn, the excitation of neurons in the left vestibular nucleus acts to further reduce the resting activity of the neurons in the right vestibular nucleus, *via* the functionally inhibitory commissural fibers. But the neurons in the right vestibular nucleus are already firing at a low firing rate because of reduced input from the right SCC. As a result of the reduced activity in the right vestibular nucleus, the neurons in the left vestibular nuclei receive less inhibition from the right vestibular nucleus. In this way, the functionally inhibitory commissural connections act to enhance the difference in neural activity between the two vestibular nuclei.

So the simple excitation from the left labyrinth is complemented by another source of activation—the reduction in inhibition (called disinhibition). As the right horizontal canal decreases activity, cells in the right vestibular nuclei also decrease activity. Thus they exert less inhibition (i.e., they disinhibit) the neurons in the activated left nucleus, allowing these left vestibular nucleus neurons to fire at a higher rate. This is the key—the normal compensatory eye movement response is due to the combined effect

of two functional excitatory components—excitation and disinhibition. Note that the reduced activity in the right vestibular nucleus is enhanced by the increased firing (and thus increased functional inhibition) from the left vestibular nucleus neurons.

If the left labyrinth is damaged (Figure 5C), the afferent neurons from the left labyrinth cease firing and so neurons in the left (ipsilesional) vestibular nucleus have a low firing rate. Thus, these silenced neurons exert less inhibition on cells in the right vestibular nuclei which project to and activate abducens neurons. This reduced inhibition from the left vestibular nucleus allows cells in the right vestibular nucleus to fire at a higher firing rate than their usual resting rate. This imbalance in firing rate between the two vestibular nuclei is equivalent to the imbalance caused by a real head rotation to the right, and the consequence is slow-phase eye movements away from the healthy right side and quick phases away from the affected left side. This is spontaneous vestibular nystagmus with slow phases to the left and quick phases to the

right. [The cause of the quick phase is due to a separate group of burst neurons—see Ref. (64).] The higher firing rate of cells in the right vestibular nucleus acts to further inhibit the vestibular nucleus neurons on the left side, which already had their activity decreased by the absence of afferent input from the left labyrinth. Once again the functionally inhibitory commissural neurons act to enhance the imbalance in neural activity between the two vestibular nuclei. Over time the imbalance in neural activity between the two vestibular nuclei reduces and as it does so the spontaneous nystagmus declines as vestibular compensation takes place and equilibrium returns (28).

Now consider testing the horizontal VOR of a patient with a left vestibular loss (Figure 6). First giving them a head turn to their healthy (right) side (6 A). This is also called a contralateral head turn. The stimulus will result in the usual increase in firing of afferents from the remaining right labyrinth projecting to the right vestibular nucleus and thence to the left abducens, to

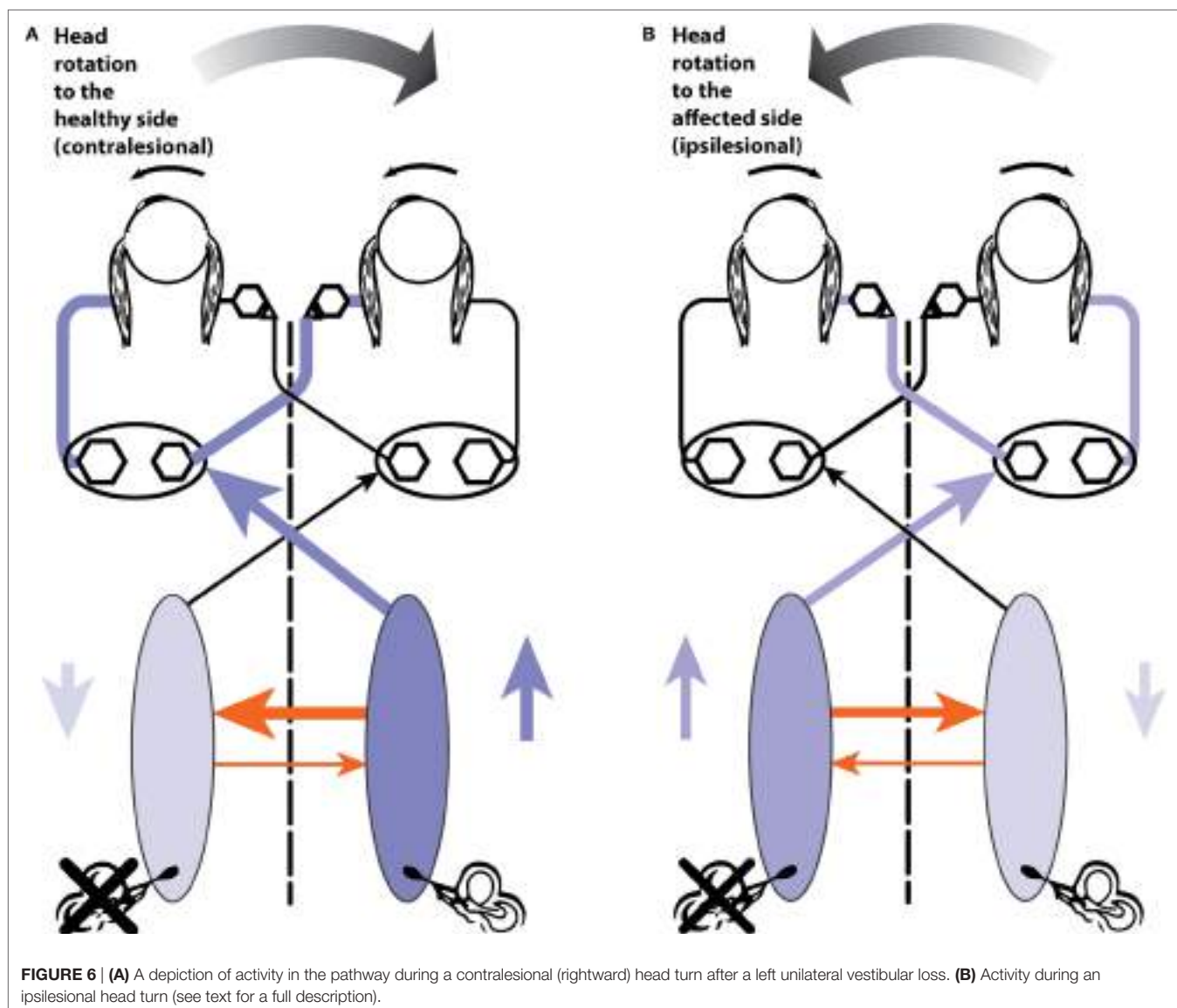


FIGURE 6 | (A) A depiction of activity in the pathway during a contralateral (rightward) head turn after a left unilateral vestibular loss. **(B)** Activity during an ipsilesional head turn (see text for a full description).

generate a compensatory slow-phase eye movement to the left, just as occurs in response to a rightward head turn in a healthy person, but with one important difference. Now the increase in neural activity in the right vestibular nucleus on the healthy side is not complemented by reduction in inhibition from the lesioned side. The disinhibition is missing. The overall result will be a compensatory eye movement whose eye velocity does not quite match (and so does not exactly compensate for) head velocity, because although it has the excitatory component it is missing the disinhibitory component which healthy subjects have. Because of that absent disinhibitory component the eye position at the end of the head turn to the healthy side will be a little short of the target, so the patient probably will, at the end of this head impulse to the intact side, need to make a (small) compensatory saccade to get their fixation back to target. In other words, there may be a small saccade in UVL patients, even for head turns to their healthy side. This is not a deficiency in the explanation—quite the contrary—it is exactly in line with what is expected by the neural connections that physiological experiments so painstakingly demonstrated. [It is worth noting that this small compensatory saccade will not happen in all patients—it depends on many things—how large is the vestibular loss, how large is the overshoot in the head turn, how big the fixation target is, how well the patient can see the target, and how far off target their final fixation is, and their criterion for deciding if they need to make a saccade at all (is “near enough good enough”)].

The evidence supporting this interpretation based on disinhibition is that for rotations to the healthy side in patients with surgically verified unilateral loss, there is not only a reduction in VOR gain for rotations to the affected side but also a significant reduction in VOR gain for rotations to the healthy side—see Figure 7 of Ref. (65)—often resulting in small overt saccades in UVL patients for rotations to the healthy side (8). The gain reduction is not large but the use of vHIT shows it, because even very small saccades have high velocity and so are easy to detect from the eye velocity records.

Head turns to the lesioned side in a UVL patient will cause an initial compensatory eye movement. Why? When there are no remaining receptors on the left side to be activated. What can cause any compensatory eye movement? The head turn will cause a decrease in activity of receptors in the healthy labyrinth, leading to decreased neural input to the right vestibular nucleus. In turn, this reduction will act to reduce inhibition on cells in the left vestibular nucleus. A reduction in inhibition is an excitatory drive, so the neurons in the left vestibular nuclei will fire at a higher rate and project to abducens neurons and so drive the eye to compensate for the head turn, at least initially. At high head accelerations, this disinhibitory drive will be short lasting—as soon as the neurons in the right vestibular labyrinth and nucleus are driven to silence there can be no further reduction in commissural inhibition, and so the effective excitation will cease. In patients with bilateral loss, there will not be any disinhibition and so there will be no early eye velocity response and the eye velocity records should be flat for both directions of head turn.

It should be noted that there are descending projections from the cerebellum, which can modulate the transmission through the vestibular nucleus and are responsible for the voluntary

suppression of the VOR in many situations. However, evidence is that in human subjects in response to abrupt, passive, high-acceleration head impulses, VOR suppression only starts to operate after a delay of around 80 ms (26).

PRACTICAL ASPECTS AND POTENTIAL PITFALLS OF VIDEO HEAD IMPULSE TESTING

Video head impulse test allows dynamic testing of vestibular function even in bed-bound patients, without the necessity of a specialized equipment, such as a motorized rotating chair, or the need for special testing conditions—such as total darkness. It is a quick, objective test that can be used to test the dynamic function of all six SCCs (9). It is of special value in testing vestibular function in young children (67–70). The effectiveness of intratympanic injection of gentamicin for treatment of Menière’s disease is now being monitored by vHIT measures of canal function after injection (14). vHIT is now being used to screen potential stroke patients in the emergency room. The vertigo which incoming patients report may be of peripheral origin from VN or central origin from a brainstem or cerebellar stroke. vHIT testing helps resolve this major question: patients with normal VOR on vHIT are more likely to have had a stroke (71).

Many studies have reported the sensitivity and specificity of vHIT with respect to the caloric test. The clear conclusion from such studies is that, not surprisingly, these two different tests give different results. One mistake has been to assume that the caloric is the “gold standard” of horizontal canal function. That is not correct—the caloric is just one test of canal function, just as vHIT is. vHIT uses the natural physiological stimulus of head rotation. The caloric relies on thermal conduction and probably buoyancy to generate a cupula displacement in an artificial, non-physiological manner (because heat is not the natural stimulus for SCC stimulation). The important question is the sensitivity and specificity of vHIT, not against the caloric test, but for detecting surgically verified absent horizontal canal function, and with our colleagues de Waele and Chiaravano, we have shown that the sensitivity and specificity of vHIT for detecting surgically verified absent HC function are both 1.0 (Curthoys, deWaele, and Chiaravano, unpublished data).

It is now clear that many patients (especially those with Menière’s disease) do have normal horizontal canal function—as shown by vHIT, responses to high-acceleration horizontal head rotation, but have reduced or absent caloric responses (72–76). It has been suggested that this dissociation between vHIT and caloric results may be an indicator of Menière’s disease (77, 78). McGarvie et al. (74, 75) have suggested that this dissociation between vHIT and caloric results may occur because hydrops of Menière’s disease dilates the labyrinth and so affects the mechanism by which caloric stimulation activates canal receptors, but that hydrops has little effect on canal-cupula responses to rotation.

In summary, the two testing protocols, HIMPs and SHIMPs, are complementary ways of testing SCC function, and the vHIT system provides the objective records of head velocity and eye velocity for determining the level of semicircular canal function.

Pitfalls in Video Head Impulse Testing

Since its introduction (4, 5), head impulse testing has become one of the primary frontline vestibular tests in many institutions around the world. The ability to quickly measure the VOR response of all six SCCs in the standard clinical setting has greatly improved our diagnostic accuracy.

However, as with any new test, there are pitfalls for the operators who are not personally experienced with the practical aspects of the test. To minimize these pitfalls, it is important to be aware of what vHIT is measuring since it reduces a complex three-dimensional biological response to one that can be measured with a simpler two-dimensional system. Furthermore, the measurement sensors themselves are mounted in a set of goggles, which are connected to the head in such a way that the measurements truly reflect the head motion in space and the pupil motion within the head. The following outlines some of the potential sources of artifacts and describes techniques to minimize them.

Head Motion Measurement

A three-dimensional inertial sensor (IMU) is mounted in the goggles, with the primary sensor stimulus planes notionally set along the head stimulus axes [horizontal, left anterior-right posterior (LARP), and right anterior-left posterior (RALP)]. The output of the various systems is the head velocity in a given plane. In order to accurately transduce the head stimulus, two basic requirements need to be met. The first is obviously that the goggles are tightly linked to the skull, as the stimulus is actually applied to the head but is transduced at the goggles level. The second is that the plane of the stimulus matches the appropriate sensing plane of the goggles. For example, if the goggles are mounted on the face such that the horizontal head velocity sensor axis does not match the axis of the applied “horizontal” head impulse, then the measured head stimulus will be lower than the actual head velocity by a factor of the cosine of the angle between the axes. Within a range of $\pm 10^\circ$ between the axes, this effect is negligible, with the effect being less than 1.5%. However, as the angle increases, the effect becomes more pronounced, reaching 10% at just over 25° . This will artificially increase the gain, calculated as eye velocity divided by head velocity (either instantaneous or over the period of the impulse). Therefore, the stimulus axis and the appropriate sensor axis should be aligned as closely as possible for the most accurate measurement of head motion. It should also be noted that an additional source of variation is the range of orientations of the horizontal canal planes in the skull between individuals—mean and standard deviation of the plane of the horizontal canal with respect to Reid’s baseline is $25.12 \pm 5.62^\circ$ ($n = 20$). So 2SDs give a range of around 11° —ranging from 36 to 14° (79, 80). These sources of variation (81) may contribute to the variation of VOR gain values between individuals.

Eye Movement Measurement

While actual eye movements are complex three-dimensional rotations with horizontal, vertical, and torsional components, vHIT currently only tracks horizontal and vertical movements of the center of the image of the pupil as captured by the high-speed video cameras. The output of the measurement is eye velocity (horizontally and vertically), as calculated from the motion of

the “center of mass” of the pupil image in pixels across the image sensor, combined with the geometrical compensation required when a captured, flat video image represents a three-dimensional eyeball rotation (82). This has various consequences when we are trying to minimize artifacts. The first and most obvious is that the camera and the head motion sensor are both mounted in the goggles. If there is no real movement of head in space or eye in head, but there is a movement of the goggles with respect to the face, it will be measured as both an eye velocity and a head velocity. An example of this is a movement of the goggles pulled by the operator moving the skin on the head during the start of the impulse. During a normal horizontal impulse, this type of effect will produce an artifactual “biphasic” eye velocity superimposed on the actual eye velocity as the goggles “lead,” and then “lag,” the head. The converse may occur if the goggles are way too loose and initially “lag” the skull. It is usually only obvious when there is no or minimal true VOR response (83). Once again, to minimize this, the goggles need to be tightened on the subject’s head as tightly as feasible and the operator should hold the head so that skin movement does not move the goggles on the skull.

For horizontal impulses, the two-dimensional eye velocity measurement does not of itself introduce any significant artifacts. A horizontal head stimulus will elicit a horizontal eye velocity, and gaze elevations or depressions within $\pm 15^\circ$ will only have a minimal effect on the measured eye velocity (84). However, for the vertical impulses, the situation is more complex, and gaze direction has a major effect on the measured VOR (Figure 7) (10).

For example, a head stimulus in only the LARP plane will produce a vertical response if gaze is also in the LARP plane (66), a roll response if gaze is in the RALP plane and a combined roll and vertical response if gaze is directed straight ahead. Consequently, as the gaze moves away from the plane of stimulation, the measured vertical component of the eye velocity reduces as the roll component increases. There is also a further level of complexity to the vertical impulse response and gaze combination, in that it is physically very difficult to produce a pure LARP stimulus without in any way stimulating the canals of the RALP plane. While the gaze is maintained in the LARP plane, this is not important, as stimulus to the RALP plane will only induce a roll response, which is not measurable. However, as gaze moves out of the LARP plane toward the RALP plane, then a head stimulus that also contains a (small) RALP component will begin to also elicit a vertical eye response, further confounding the measured response. Therefore, it is of major importance to maintain gaze as close to the stimulated head plane as is possible (Figure 7). If gaze does drift out of the plane of stimulus, the results will start to show an apparent “reduced gain” combined with an apparent “delay” of the eye signal, and an absence of corrective vertical saccades.

The other major source of artifact, particularly for the vertical tests, is that of eyelid interference with the pupil image. Once again, if we consider the actual output of the test, we can see how the effects occur. With an average impulse at $200^\circ/\text{s}$, the head motion from takeoff to the zero velocity crossing takes about 150 ms. With camera frame rates of 250–220 frames per second, depending on the system used, about 40 images of the pupil will be collected during the impulse. As eye velocity is calculated from the geometrically compensated change in the position of the

"center of mass" of the pupil between successive images, then a small apparent change in this position can lead to a large recorded velocity. The eyelid briefly touching the pupil image can produce a range of artifacts, depending on the stimulus direction and the way in which it interferes with the image (**Figure 8**).

In our experience, the usual transient eyelid "flick" is the upper eyelid briefly covering the top of the pupil image and then uncovering it, all during the impulse. If an anterior canal (AC) is being stimulated as this occurs, the head is being rotated downward and the eye is rotating upward. As the eyelid touches the top of the pupil, the pupil image will reduce in height and "center of mass" of the pupil image will appear to slow down its upward

trajectory. This will reverse as the eyelid uncovers the top of the image, producing an apparent increase in upward velocity. So, an eyelid "flick" during an anterior impulse will produce an apparent, biphasic velocity slow down followed by an apparent speeding up, both superimposed on the actual upward eye velocity. If this eyelid "flick" happens during a posterior impulse (which is a rarer situation), then the eye is moving downward during the impulse. As the upper eyelid touches the top of the pupil image, the "center of mass" will appear to move even further downward, with an apparent rapid increase in velocity, returning to the true eye velocity as the pupil is uncovered. This can have the appearance of a covert saccade superimposed on the true vertical eye

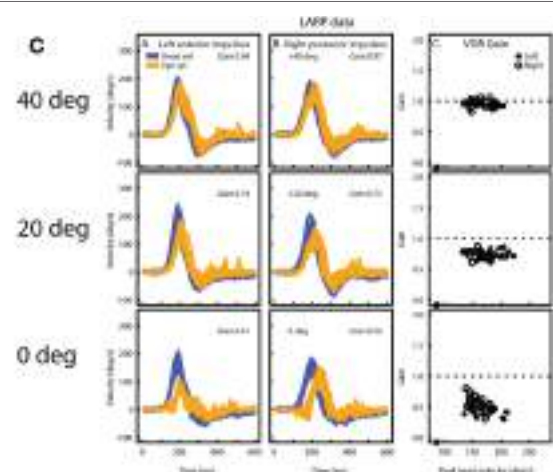
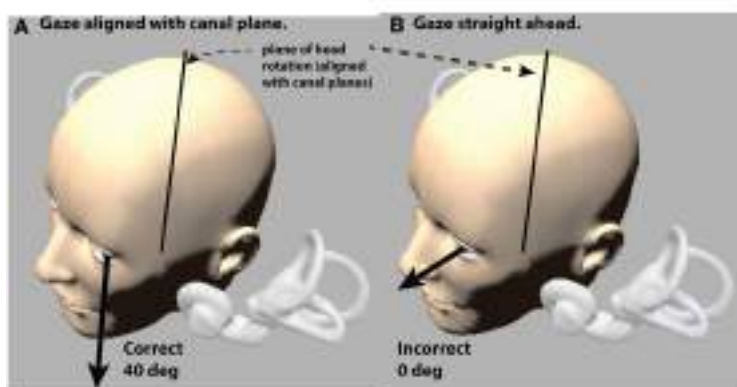


FIGURE 7 | The effect of gaze angle on measurements of the eye movement during vertical head impulses. Because the video camera only measures horizontal and vertical components (not torsional components as yet), it is necessary to arrange the test situation so that there is minimal contribution of torsion to the eye movement response to vertical canal stimulation (66). This is achieved by gaze being directed along the plane of the canals under test (**A**). If gaze is straight ahead (**B**), there is a substantial reduction in vertical eye velocity (and VOR gain) and the reduction is shown in (**C**)—eye velocity from the same subject with only gaze direction changing. Reproduced with permission from the study by McGarvie et al. (10).

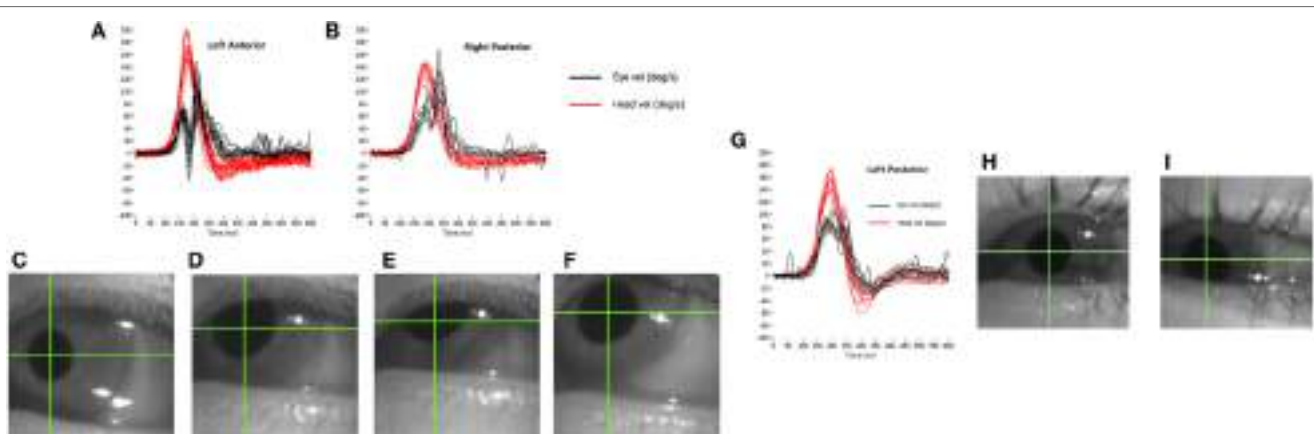


FIGURE 8 | How eyelid obstruction of the pupil during the head impulse generates artifactual eye movement records. (**A,B**) show the results of an eyelid flick touching the top of the pupil: biphasic for the anterior response (**A**) and uniphasic for the posterior response (**B**). The lower panels show stills from a grossly exaggerated version of how this occurs during the anterior impulse: the pupil starts in the centre of the vertical range (**C**), then is moving upwards as the eyelid "flicks" down to touch the top of the pupil (**D,E**), producing an apparent deceleration of the motion. As the eyelid then moves back up (**F**), the center of mass appears to accelerate upward. (**G–I**) A set of posterior canal impulses (**G**) in the situation where the pupil slides behind a stationary lower eyelid as it moves downward during the stimulus (**H,I**).

velocity, as in this case the effect is uniphasic as pupil and upper eyelid are initially moving in the same direction. Both of these situations can be seen in **Figure 8**, an extreme case of a subject with a normal VOR and a reflexive large, quick “flick down” of the upper eyelid in response to each impulse.

Although these artifacts appear obvious on the velocity traces, they are almost impossible to see by eye on the video image as they happen so quickly. More recent systems allow recording and replay of the video image, which should be used if these artifacts are suspected.

A variation of these effects occurs when the eyelid does not “flick,” but the pupil slides under it as the eye moves upward during an anterior stimulus. In this case, the eye velocity curve can look like a “table-top,” with a velocity plateau during the impulse. This is due to the “center of mass” still appearing to move upward as the pupil image reduces in height until the head velocity drops to a point at which the two signals rematch. A clue to the artifactual nature of this type of eyelid effect is a “table-top” like eye velocity profile, with no catch-up saccades after the impulse. The same situation can occur with the pupil running behind the lower eyelid as the eye moves downward during a posterior head impulse, as shown in **Figure 8**. Once again, use the playback of the video recording to confirm these artifacts, and aggressively tuck the eyelids out of the way to avoid such situations.

Basic Geometrical Considerations

The final factors to consider when optimizing the vHIT are the basic geometrical considerations of the test. Even though head rotation is the primary stimulus, the head rotation axis rarely occurs around the eye actually being measured. As such, in addition to the rotation response, there is a variable, within-space translation of the eye combined with the gain-changing effect of target distance. In comparison between subjects, these effects can be noticeable. The geometrical difference in the stimulus between a subject with an upright flexible neck and a subject with a head carried forward and a stiff neck can be appreciable, particularly when we consider that the eye being measured is always to one side of the center line to the target. While these effects are usually small, an operator wishing to optimize the test output should bear them in mind and adjust the test environment accordingly.

Taking note of the basics of how the test works and the factors that are actually measured will hopefully improve the diagnostic accuracy and ease of the video head impulse in the years ahead. The ability to measure the VOR response of all six SCCs is a dramatic step forward in enabling us to help our dizzy patients.

CALCULATING VOR GAIN

While the vHIT has become a valuable addition to vestibular testing—one issue remains controversial: the method for calculating VOR gain (7). For vHIT, we calculate the gain of the slow-phase VOR response by comparing head and eye velocity using a “wide window” from the beginning of the impulse until the head velocity returns to (or crosses) 0°/s (4). Instantaneous or “narrow-window” gain calculations that were traditionally used for search-coil recordings are not reliable for vHIT because some goggle movement is practically unavoidable when manually

delivering passive head impulses using force applied *via* the flexible skin and flesh. The “wide window” method is less sensitive to movement of the goggles with respect to the skull (and eyes) because these movements are biphasic, with an acceleration and deceleration component that tend to cancel out.

Figure 9 shows an exaggerated model of the “Bump Artifact” (gray), which affects any video goggle system. In this example, a calculation of gain using the traditional search-coil method (with a narrow window at peak head acceleration—vertical green line) produces large errors (nominal values shown in red). Similarly, an instantaneous or narrow-window gain calculation around any other point (e.g. peak head velocity) will also produce errors. The exception to this would be the point at ~75 ms where, in this example, the coil eye velocity (blue) and video eye velocity (cyan) cross over (have the same value). Unfortunately, it is not possible to know the latency of this point (which varies between trials, subjects, and operators) without simultaneous search-coil recordings, which are impractical for routine clinical applications.

Simultaneous search-coil and video recordings (on the same eye) are feasible in the laboratory and provide: a powerful tool for validating vHIT systems; an objective measure of the “Bump Artifact”; and a method to compare the performance of various gain calculation methods (5). Without simultaneous search-coil recordings, a vHIT system developer or user might easily remain ignorant to the existence of the problem and effectiveness of the proposed solution. In 2014, Agrawal et al. (85) attempted to validate an instantaneous gain calculation using simultaneous search-coil measures. Unfortunately, they measured the right eye with a search coil and the left eye with video rather than doing simultaneous recordings of the same eye. Since we know that the eye-movement responses during head impulses are not completely conjugate (30), this instantaneous gain validation was rather less compelling.

A simple position gain is calculated from the ratio of the areas under the desaccaded eye velocity and head velocity traces after “covert” saccades are removed. This simplified rotational position gain is a convenient and sufficiently accurate approximation of the actual eye rotation required to maintain fixation on a target at least 1 m in front of the subject for horizontal and vertical head impulses (9). In other situations, for example with a close fixation point, this simplification can be less than adequate. A more sophisticated conception of gain that can be used with many different head movements and target positions would be one that compares measured eye movement responses and the ideal eye movement response that would be required to maintain fixation.

An “ideal” gain calculation factors in the geometric consequences of fixation distance but also of eye translation, which is part of any head rotation around an axis that is usually offset from one or both eyes. With the single exception of head pitch around an axis that passes through the center of both eyes, all head rotations produce some translation of the eyes. **Figure 10A** shows a very simple example of horizontal head rotation (around the Z axis). With a fixation point closer than 1 m (the minimum suggested distance), a 20° rotation of the head (around its center) would require an ideal eye movement rotation response of ~22° in the left eye and ~21° in the right eye. The difference between the head and eye rotations is caused by the translation of the eyes

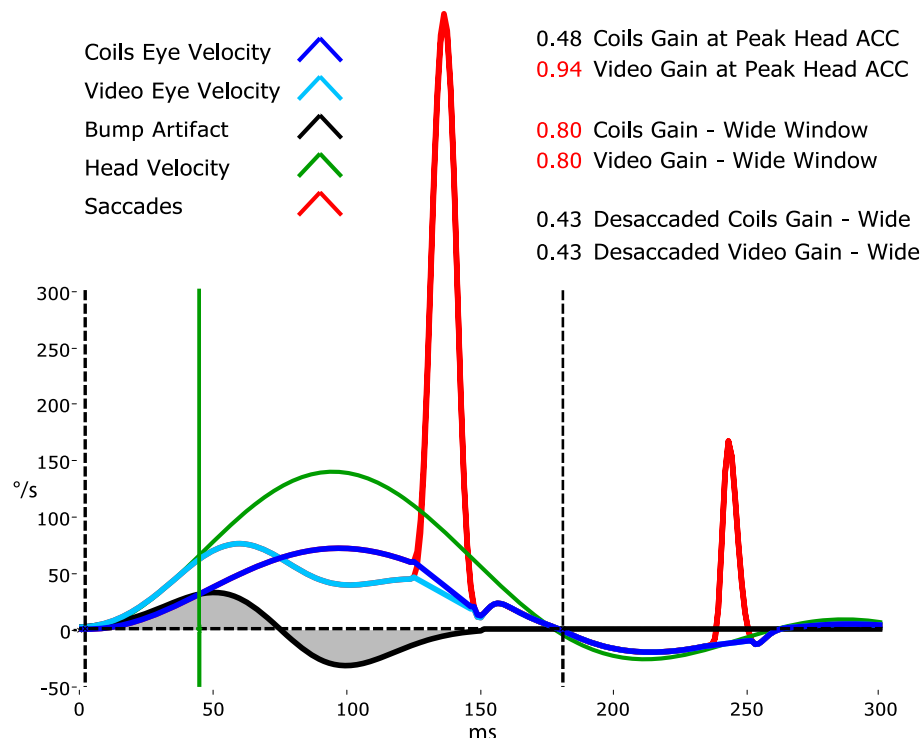


FIGURE 9 | A model of head impulse gain calculation. The figure shows a slow-phase eye velocity response recorded by search coils (blue trace) and by video—video head impulse test (vHIT) (cyan trace) with compensatory “catch-up” saccades (red). The difference between these two traces is the goggle movement “bump artifact” (black trace) that is practically unavoidable for any video goggle system. Traditional VOR gain measurements over a narrow window that is usually centered on peak head acceleration (vertical green line) are very sensitive to contamination by this artifact (red gain values). For vHIT, we measure gain over a “wide window” from the beginning of the head impulse until the head velocity returns to 0°/s (vertical black dashed lines). This gain calculation method is relatively unaffected by the biphasic “bump artifact” (gray shaded areas) because the positive component (caused by manual acceleration of the head) and the negative component (deceleration) tend to cancel out during the impulse. Gains calculated using this wide window method are very similar for video and coils and quite comparable to the traditional narrow window gain measurement method for search coils.

during the head rotation. With a fixation point further than a meter, these differences become less significant and the simplified calculation of gain using eye rotation vs head rotation is acceptable. In other situations such as the very close fixation point shown in **Figure 10B**, a simple gain calculation would not be sufficient and gain would best be calculated as ratio of measured slow-phase eye response to the ideal eye responses of ~27° and ~30° in the left and right eyes, respectively.

The issues concerning the calculation of gain vs the ideal eye movement response is particularly clear when considering head “heaves” or linear head movements (86), where a comparison between eye rotation and head rotation would obviously be meaningless. **Figures 10C,D** show linear head movements with far and close fixation points and very different “ideal” eye movement rotation responses required to maintain fixation. With these linear head movements, it only really makes sense to calculate gain as a ratio of measured eye movement response to the ideal eye movement response, and since almost every head movement (including “pure” rotations) involves some translation of the eyes it would be beneficial to consider these geometric consequences in various situations. Considering the geometry and ideal gain would help in the interpretation of small differences in simple gain between the two eyes, between different head

turn directions, for different head turn axes (LARP, RALP), with unusual fixation distances and eccentricities, and where gain and catch-up saccade patterns do not match perfectly. Ideal gain calculations require accurate measurement of (or valid assumptions about) the geometry of head movements and target locations in six degrees-of-freedom, so in practice it is often better to keep simple gain calculations valid by understanding the limitations of the idealizations on which they are based, and not to interpret departures from these assumptions as indicators of vestibular dysfunction.

QUANTITATIVE HIT IN CENTRAL VESTIBULAR DISORDERS

Central vestibular disorders are caused by lesions in the vestibular pathways, which include vestibular nuclei in the brainstem, ascending projections in the MLF, vestibulocerebellum, thalamus, and parieto-insular vestibular cortex (87). Clinical manifestations include vertigo, imbalance, and localizing neurological deficits. Lesions vary in nature but may be due to acute ischemia, demyelination, and metabolic disorders.

Clinical HIT can be performed quickly for individual SCCs to qualitatively assess the vestibulo-ocular reflex (2). It is the

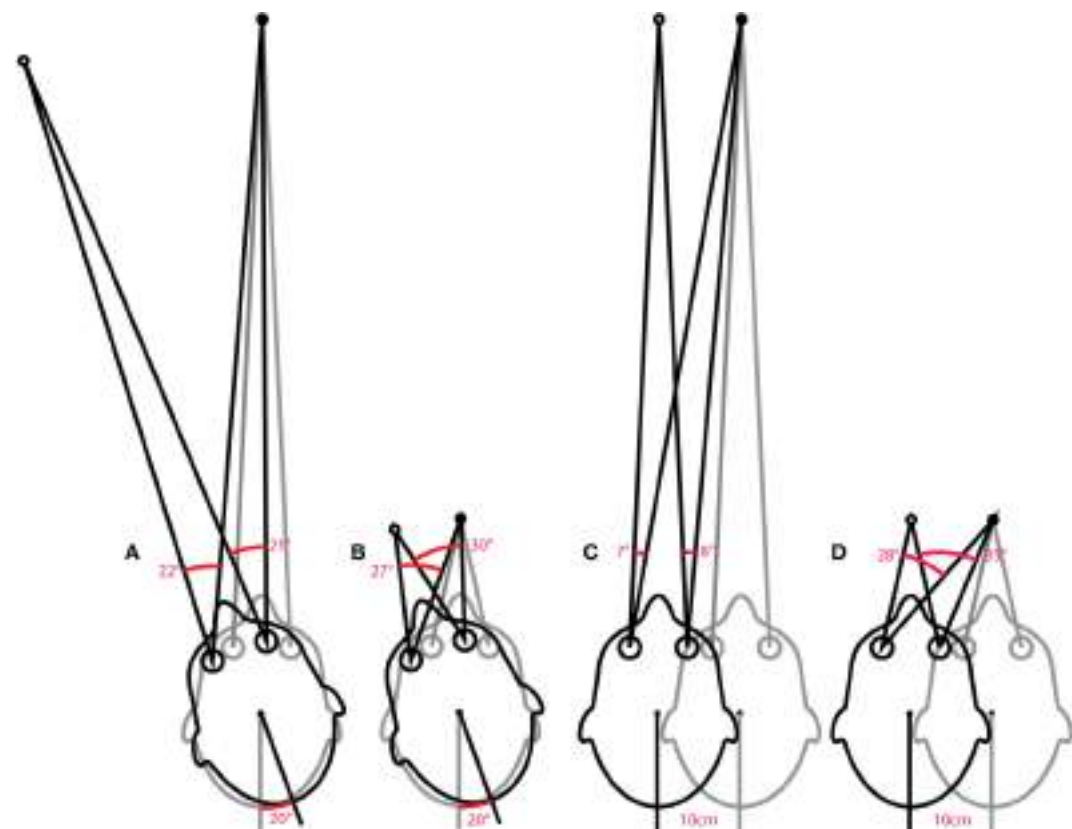


FIGURE 10 | Issues in how VOR performance should be calculated. The ideal eye movement response is one that is compensatory (i.e., maintains fixation) during head impulses with a fixation point: far (**A**) and close (**B**), and for linear “head heaves”: far (**C**) and close (**D**). Even in this simple example in one (horizontal) plane, with head rotation around a single point (or for purely linear translations), the calculation of an ideal eye movement response must factor in the geometric consequences of fixation distance, gaze eccentricity, interocular distance, head size (rotation radius), etc. The ideal eye movement rotation responses for a 20° head rotation and a 10 cm head translation are different: for the head rotation for the two eyes, and for the two fixation distances. With more natural head movements, in six degrees-of-freedom, these calculations are more complicated. Although technologies to track head movements and target positions in six degrees-of-freedom are improving rapidly, it is still convenient for video head impulse test to approximate gain calculations with simplified head rotation vs eye-rotation calculations. Such a convenient simplification does however require an understanding of the limitations and some diligence in minimizing departures from the assumptions such as a distant fixation point.

most important test in differentiating central from peripheral vestibular disorders, especially when traditional neurological deficits may be subtle or absent, such as in acute vestibular syndrome (AVS) (88, 89), subclinical internuclear ophthalmoplegia (90, 91), and early Wernicke’s encephalopathy (92, 93). HIT gain and compensatory saccades can be quantified using search coils (8, 94), or high-speed video-oculography (VOG) (4, 5). In this review, we discuss some advances in quantitative HIT in central vestibular disorders.

Published research articles employ either search coil and/or VOG to record HIT in central vestibular disorders. For search-coil studies, there are binocular or monocular (left eye) recordings, and horizontal-only or individual SCC plane HIT (95). For VOG studies, there are monocular (right eye) recording and horizontal-only or modified-individual SCC plane HIT (66). Search coil is the gold standard in eye movement recording, but is semi-invasive and non-portable. VOG has inferior spatiotemporal resolution but is non-invasive and portable.

Acute Vestibular Syndrome

Acute vestibular syndrome is commonly due to VN (96, 97) but is closely mimicked by posterior circulation stroke (PCS) (98, 99). A negative clinical horizontal HIT, or the absence of compensatory saccade, is a strong predictor of PCS (88, 89) but its interpretation is dependent on examiner experience (100). vHIT gain can differentiate VN from PCS with sensitivity of 88% and specificity of 92% (101), which is comparable to clinical HIT (102, 103). Search-coil measurement yields better sensitivity of 94–97% and specificity of 90–100% for detecting PCS (104). It demonstrates a spectrum of horizontal VOR gain and compensatory saccade abnormalities in different subgroups of PCS compared to VN. In contrast to unilateral gain deficit and corresponding large compensatory saccade amplitude, PCS involving the anterior inferior cerebellar artery (AICA) territory (AICA stroke) leads to more symmetric bilateral VOR gain reduction and smaller saccades, while posterior inferior cerebellar artery (PICA) territory PCS (PICA stroke) typically leads to symmetrical mild reduction in VOR gain with smallest saccades (**Figure 11**).

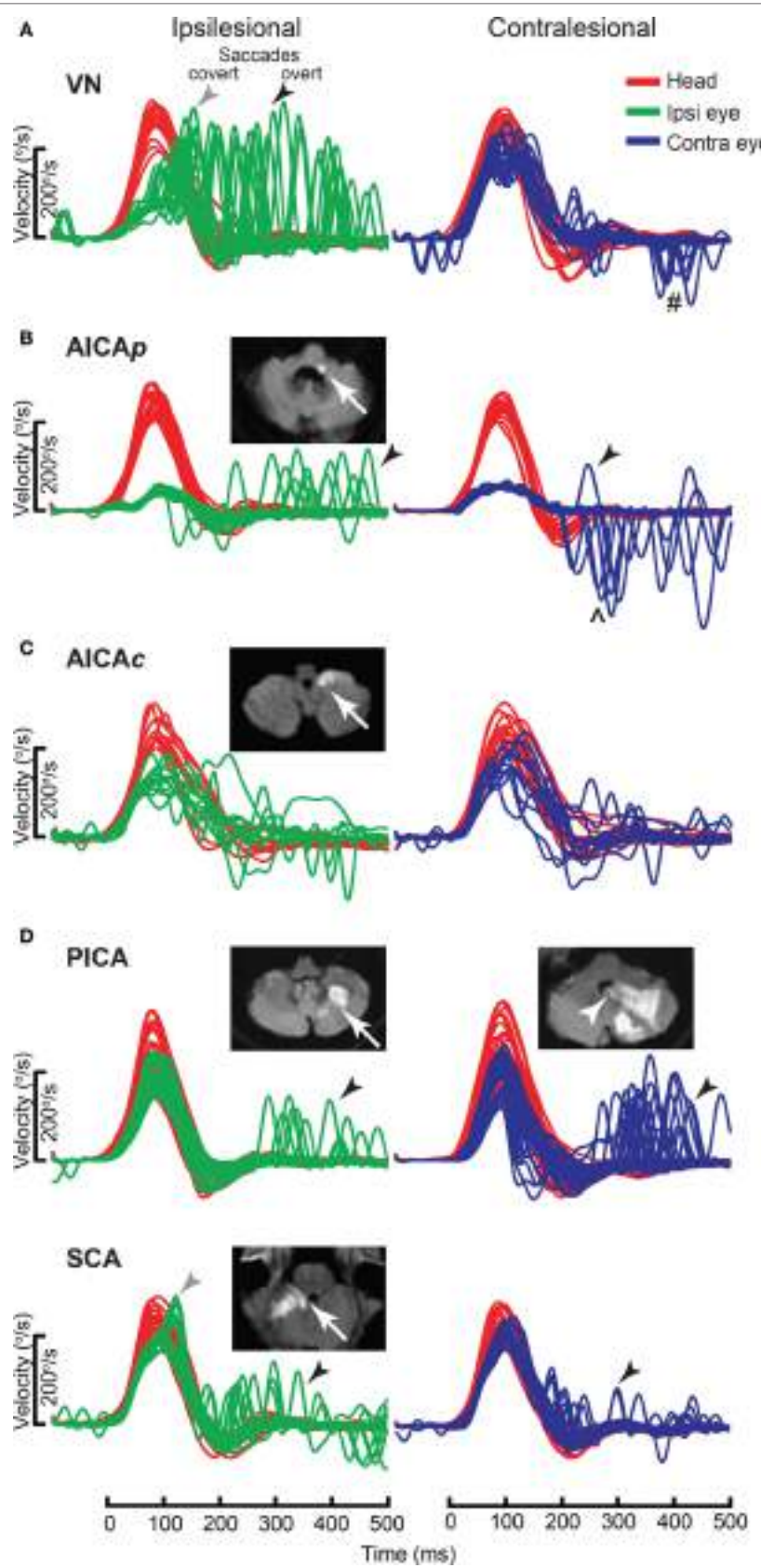
**FIGURE 11 |** Continued

FIGURE 11 | Continued

Examples of head impulse test (HIT) results. (1) Posterior circulation stroke (PCS) and vestibular neuritis (VN). Examples of HIT in PCS and VN, displayed as time series of inverted eye (ipsilesional: green, contralateral: blue) to head (red) impulse velocities. **(A)** In VN, ipsilateral gain deficit (mean 0.16) led to large overt (black arrows) saccades (cumulative amplitude: 9.1°, mean) and frequent covert saccades (73% of trials). Contralateral gain was mildly reduced (0.72), matched by small overt saccades (1.2°). Saccades occurring in the direction of contralateral impulses (#) were quick phases of spontaneous nystagmus. **(B)** In anterior inferior cerebellar artery-peripheral (AICA_p) stroke due to left vestibular nuclear infarction (white arrow), gains were bilaterally deficient (ipsilesional: 0.11, contralateral: 0.21) and overt saccades were present bilaterally, larger after ipsilesional (5.7°) than contralateral (3.3°) trials. Compared to VN, overt saccades were 63% smaller after ipsilesional trials but 2.8 times larger after contralateral trials. Anticompenatory saccades (*) were dominant after contralateral trials. **(C)** In anterior inferior cerebellar artery-central (AICAc) stroke due to isolated right floccular infarction, gains were asymmetrically reduced (ipsilesional: 0.55, contralateral: 0.75) with few small overt saccades (ipsilesional trials: 2.7°, contralateral trials: 2.1°). **(D)** Upper: in posterior inferior cerebellar artery (PICA) stroke involving the left cerebellar hemisphere and nodulus (white arrowhead), gains were symmetrical (ipsilesional: 0.85, contralateral: 0.82) with frequent overt saccades, larger after contralateral (4.3°) than ipsilesional (2.8°) trials. Lower: in superior cerebellar artery (SCA) stroke involving the superior vermis, gains were mildly reduced bilaterally (ipsilesional: 0.66, contralateral: 0.71) with small overt saccades (ipsilesional trials: 2.2°, contralateral trials: 1.2°). Reproduced from the study by Chen et al. (104), used with permission from Wolters Kluwer Health, Inc.

Anterior inferior cerebellar artery stroke causes ipsilateral vestibular loss, conceivably due to labyrinth and lateral pontine involvement (105, 106); the unexpected contralateral gain reduction is speculated to involve the inhibitory and excitatory projections of the floccular target neurons in the ipsilateral vestibular nuclei, reciprocal commissural inhibitory inter-vestibular nuclei connections, and possibly adaptive changes in the flocculus (107). PICA stroke, which sometimes affects nodulus/uvula, causes on average 20% reduction in gain, a finding that has been demonstrated with search coil (104) but not VOG (108). Such reduction is only modest, perhaps because only 20% of nodulus targeting neurons, including position-velocity-pause neurons, in the vestibular nuclei, are sensitive to eye movement (109).

In VN, saccade amplitude (mean: ipsilateral 8.5°, contralateral 1.3°) and asymmetry are expected to mirror gain reduction (mean: ipsilateral 0.22, contralateral 0.76) and asymmetry. In AICA stroke, although ipsilesional gain reduction is similar to VN, saccade amplitude is smaller, perhaps invoking the flocculus that can influence saccades (110, 111). Experimental lesion of the flocculus causes postsaccadic drift, which can be backward (112). As contralateral gain is reduced more than occurs in VN, saccade amplitude is correspondingly larger. Thus, AICA stroke could produce bilaterally positive clinical HIT (mean: ipsilateral 4.7°, contralateral 3.3°), since clinical detection threshold varies from 1–2° (113) to 3–4° (104). The practical implication is that bilateral positive clinical HIT does not localize to only the peripheral vestibular system (108), and AICA stroke should be considered in the differential diagnosis. Finally in PICA stroke, saccades occur more frequently and/or are collectively larger during contralateral HIT, potentially representing refixating eye movements as a result of dorsal vermal lesion causing ipsilesional saccadic hypometria (114, 115).

Specific Central Vestibular Lesions

Cerebellum

Cerebellar lesions have variable effect on VOR. Diffuse or degenerative processes can cause asymmetric VOR gain, higher for anterior SCC (AC), and can alter the axis of eye rotation (116). Whereas horizontal VOR evoked by rotation is increased in both ataxia telangiectasia (117) and spinocerebellar atrophy type 6 (SCA 6), it is decreased in response to horizontal (118) and individual SCC HIT in SCA 6 (119). Such selectivity for stimulus frequency is perhaps related to degeneration of flocculus (107), and vestibular nucleus, where processing of linear and non-linear pathway inputs

(120, 121) might take place. Finally, acute unilateral tonsillar lesion does not affect VOR gain (122). Anatomical-physiological correlation in focal cerebellar lesions may not be exact, since non-lesioned parts of cerebellum may participate in learning and adaptation.

Nucleus Prepositus Hypoglossi (NPH)

Acute lesion of NPH produces a distinctive pattern of abnormal SCC function, resulting in contralateral horizontal SCC (HC) hypofunction but bilateral AC hyperfunction (123). Contralateral HC impairment may be explained by a loop of stronger crossed inhibitory projections from NPH to inferior olive nucleus (ION), inter-NPH inhibitory connections and inhibitory climbing fibers from ION reaching contralateral flocculus. Based on these known connections, ipsilateral NPH lesion could result in increased inhibition of ipsilesional ION, disinhibition of contralateral flocculus, and increased inhibition of contralateral vestibular nucleus. The bilateral AC hyperfunction can also be explained by the same loop, since ipsilateral AC pathway is preferentially inhibited by flocculus (124).

Vestibular Nucleus

Acute vestibular nucleus lesion leads to UVL, selective for HC and posterior canal (PC) while sparing the AC (125). Since the anterior SCC afferents project to both superior as well as medial vestibular nuclei (126, 127), lesion of medial vestibular nuclei could possibly only affect HC and PC function. Contralateral HC and PC function is also reduced, possibly due to adaptive change mediated by inhibitory interneurons.

Medial Longitudinal Fasciculus

Disruption of the MLF produces internuclear ophthalmoplegia (INO), a dysconjugate horizontal eye movement disorder classically characterized by abducting eye nystagmus and adducting eye slowing during horizontal saccades (128–130). Such dysconjugacy can be clinically subtle or silent, but can be quantified by a versional dysconjugacy index (91, 131). The horizontal SCC afferents enter the medial vestibular nuclei, which send projections to the contralateral abducens nucleus, from which two projections arise: directly to the contralateral lateral rectus, responsible for abduction, and via crossed abducens interneurons ascending in ipsilateral MLF, responsible for adduction (**Figure 5A**). There is an extra-MLF pathway for horizontal VOR that arises from the lateral vestibular nucleus and projects to the ipsilateral oculomotor

nucleus *via* ATD (63, 132, 133). The MLF also carries projections from anterior and posterior SCCs, but some secondary neurons in superior vestibular nucleus that received projection from anterior SCC travel outside the MLF in the crossed central tegmental tract or brachium conjunctivum (134). The functional consequence is that contralateral posterior SCC function is selectively impaired relative to anterior SCC function, as demonstrated in a case of acute unilateral INO (135).

In both unilateral and bilateral INOs (Figure 12), horizontal VOR dysconjugacy is less severe than compensatory saccade dysconjugacy. This discrepancy might be because of some contribution of ATD in driving adduction during VOR, relative to no contribution from the damaged MLF in driving adduction during

saccade. Vertical-torsional VOR is impaired, both for anterior and posterior SCC, but is relatively more severe for posterior SCC. This dissociation between anterior and posterior SCC function is less obvious in bilateral INO, potentially related to relative strength of extra-MLF pathways for anterior SCC signals (136), on-off direction asymmetry of the paired vertical SCC (137) and higher sensitivity of secondary neurons to angular acceleration (138).

Metabolic Disorders

Acute Wernicke's Encephalopathy (aWE)

Acute Wernicke's encephalopathy, a medical emergency, is due to thiamine deficiency, and if untreated leads to permanent

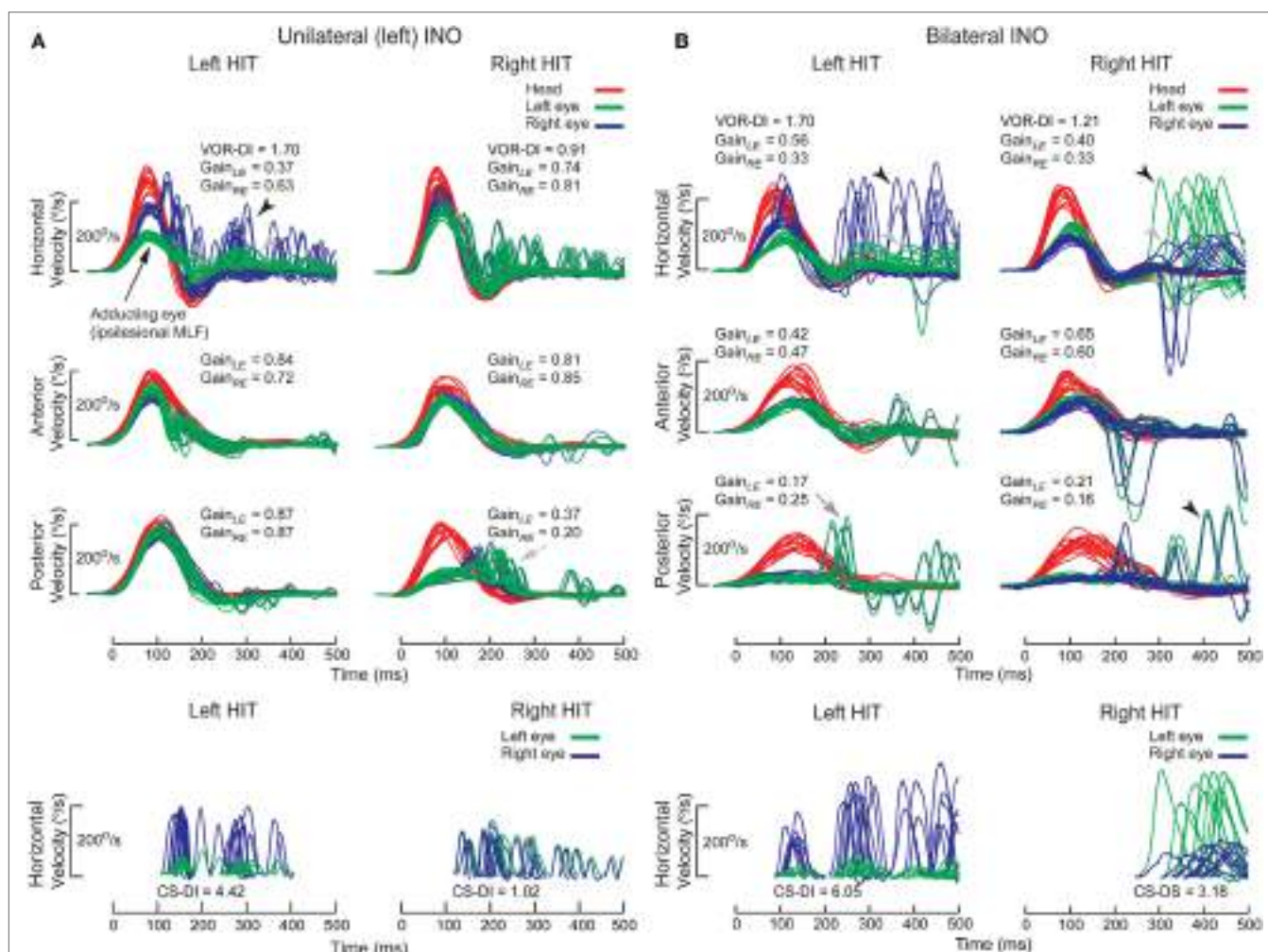


FIGURE 12 | Examples of head impulse test (HIT) results. (2) Internuclear ophthalmoplegia. Binocular search-coil recording of head (red) and eye (left: green, right: blue) in internuclear ophthalmoplegia. **(A)** Top: in left internuclear ophthalmoplegia (INO) during ipsilesional horizontal canal (HC) (i.e., leftward) plane (HC) impulses, vestibulo-ocular reflex (VOR) was dysconjugate: gains were lower for the abducting than adducting eye, as measured by the VOR dysconjugacy index (VOR-DI), the ratio of abducting to adducting eye gain. During contralateral HC impulses, conjugacy was maintained. Abducting eye gains during either HC impulses were mildly reduced, possibly due to additional partial abducens nerve or supranuclear gaze involvement. All vertical canal function was preserved except for contralateral posterior canal (PC). Bottom: saccades elicited during ipsilesional HC impulses were also dysconjugate, as measured by the compensatory saccade dysconjugacy index (CS-DI), but more severely affected than VOR-DI. **(B)** Top: in bilateral INO during HC impulses to either side, dysconjugacy was present, albeit asymmetrically in this case. Abducting eye gains were lower compared to unilateral INO, possibly due to defective disinhibition of the medial rectus motoneurons by the excitatory abducens interneurons, which are normally inhibited by type 1 vestibular neurons. All vertical canal function was impaired, but anterior canal was relatively less affected than PC. Bottom: like in unilateral INO, CS-DI was more severely affected than VOR-DI.

neurological deficits (139). The classic triad of altered mental status, ocular motor abnormality, and ataxia may not be present, and form fruste cases without overt encephalopathy present with acute bilateral vestibular loss (BVL) selectively affecting horizontal but not vertical VOR (92). Such dissociation might be characteristic of aWE, as has been demonstrated by search-coil and VOG recordings of individual SCC plane HIT (93, 140) (**Figure 13**). Presumably, thiamine deficiency has selective and profound detrimental effect on the medial vestibular nucleus. Rapid recognition and prompt treatment with thiamine replacement can improve neurological function.

Gaucher's Disease (GD)

Gaucher's disease is a hereditary metabolic disorder due to glucocerebrosidase deficiency leading to multi-organ deposition of glucocerebroside (141). Its hallmark eye movement abnormality is saccade slowing, more selectively for horizontal than vertical saccades (142, 143). HIT demonstrates both horizontal and vertical VOR loss and prolonged VOR onset latency, with very small compensatory saccades during horizontal HIT and relatively more frequent saccades during vertical HIT (**Figure 14**). The BVL is likely due to neuronal loss in the vestibular nuclei (141), while preferential involvement of horizontal over vertical saccades could be ascribed to relatively more severe involvement of pontine paramedian reticular formation (horizontal saccade generator) over rostral interstitial of the MLF (vertical saccade generator). However, this is not the case in postmortem examination, presumably because of the advanced disease stage (144).

NEW CLINICAL DISEASE PATTERNS EMERGING FROM 3D VIDEO HEAD IMPULSE TESTING

With the widespread use of vHIT for all six SCCs in daily clinical practice, not only are classic vestibular disease patterns, such as superior vestibular neuritis (VN) confirmed, but also new and exciting disease patterns are emerging. Together with cervical vestibular-evoked myogenic potentials (cVEMPs) for measuring saccular function, ocular vestibular evoked myogenic potentials (oVEMPs) for measuring utricular function and audiometry for testing cochlear input, it is now possible to assess the function of all six suborgans of each labyrinth completely (145).

Superior Vestibular Neuritis

The classic and most frequently encountered clinical pattern of UVL is that of superior VN (146, 147). These patients often present with an AVS and spontaneous horizontal-torsional nystagmus beating toward the healthy side. The vHIT—applicable directly in the emergency room—reveals loss of lateral and AC function with sparing of the PC, making the diagnosis of superior VN. In addition to the classic horizontal catch-up saccade upon rotation of the head toward the affected side, D'Onofrio (148) also described an oblique upward catch-up saccade after head rotation toward the healthy side. This catch-up saccade is thought to be caused by an isolated activation of the remaining inferior SCC contralateral to the head rotation, which drives the eyes downward, resulting in an oblique upward catch-up saccade (148). This results from the obligatory shift in VOR axis that occurs with UVL (29). Loss of utricular function—as confirmed by oVEMP

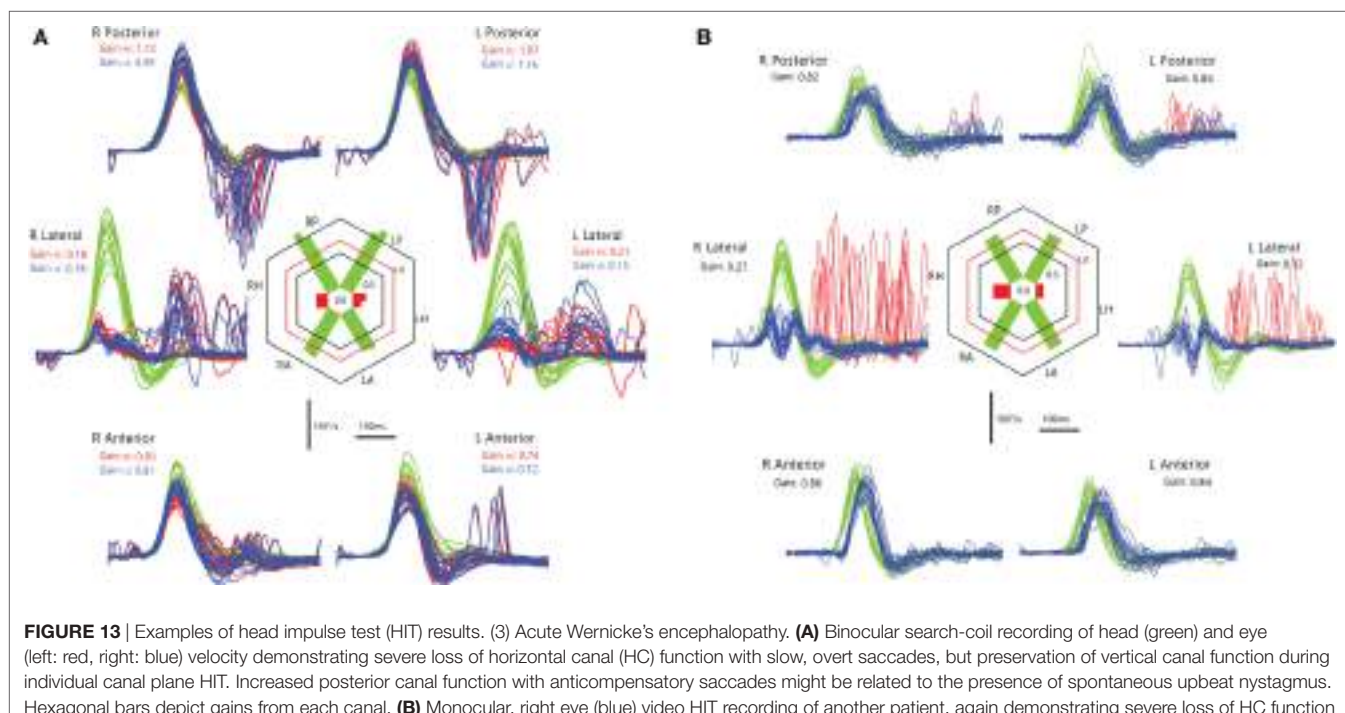


FIGURE 13 | Examples of head impulse test (HIT) results. (3) Acute Wernicke's encephalopathy. **(A)** Binocular search-coil recording of head (green) and eye (left: red, right: blue) velocity demonstrating severe loss of horizontal canal (HC) function with slow, overt saccades, but preservation of vertical canal function during individual canal plane HIT. Increased posterior canal function with anticomplementary saccades might be related to the presence of spontaneous upbeat nystagmus. Hexagonal bars depict gains from each canal. **(B)** Monocular, right eye (blue) video HIT recording of another patient, again demonstrating severe loss of HC function with preservation of vertical canal function. Reproduced from the study by Akdal et al. (93), used with permission from Elsevier.

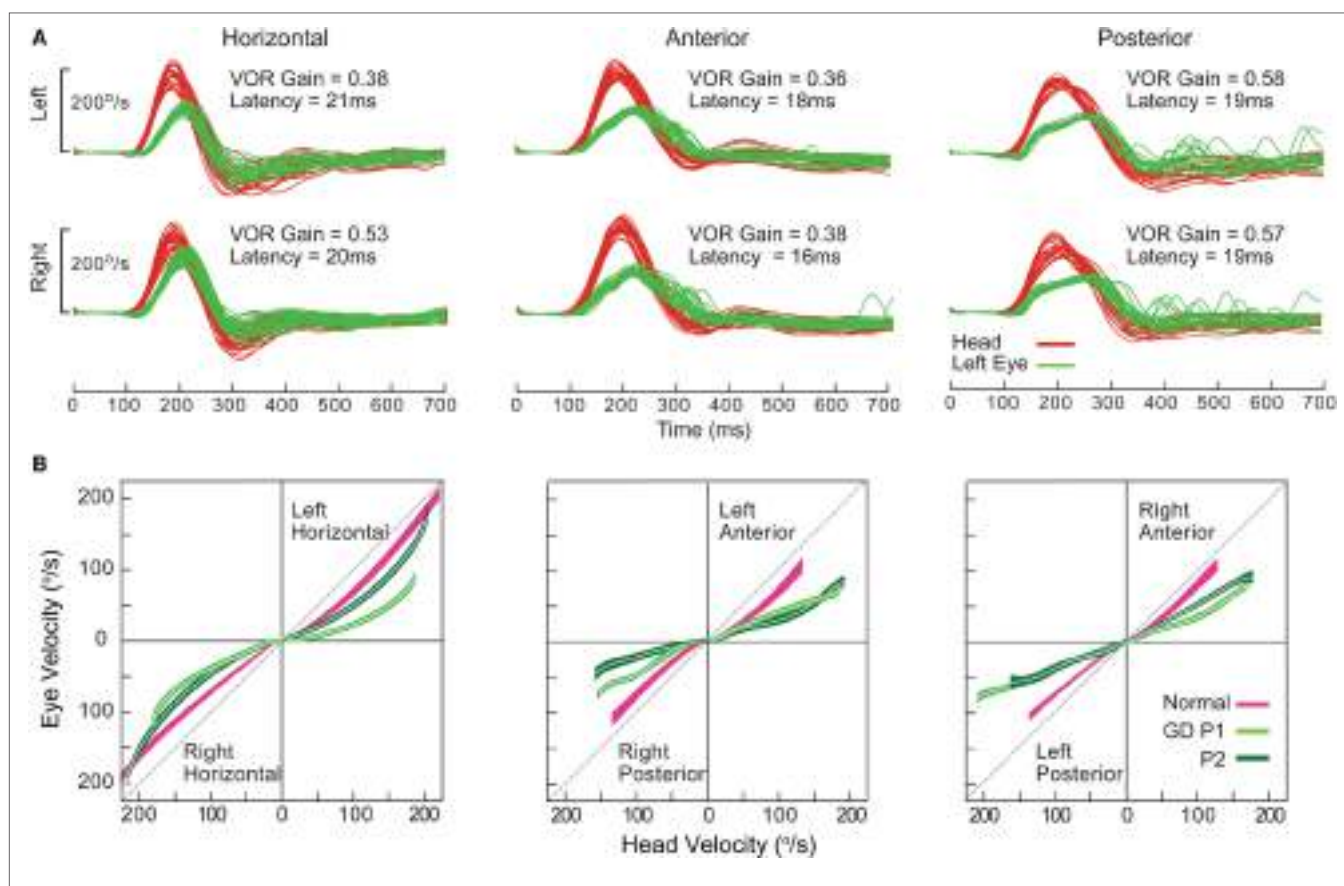


FIGURE 14 | Examples of head impulse test results. (4) Gaucher's disease (GD). **(A)** Monocular search-coil recording of head (red) and left eye in patient 1 (P1) with GD. Gains for each canal were substantially reduced, but there was a paucity of compensatory saccades especially during horizontal canal impulses. Vestibulo-ocular reflex (VOR) onset latency was prolonged. **(B)** Phase-plane plots of eye versus head velocity for normal (pink), patient 1 (P1, light green), and patient 2 (P2, dark green). Normal phase-plane plot is slightly curved but approximates the diagonal (dotted gray line), indicating near matching of eye to head velocity. In both P1 and P2, due to gain deficit and latency delay, the curve is markedly deviated from the diagonal. Reproduced from the study by Chen et al. (143), used with permission from Springer.

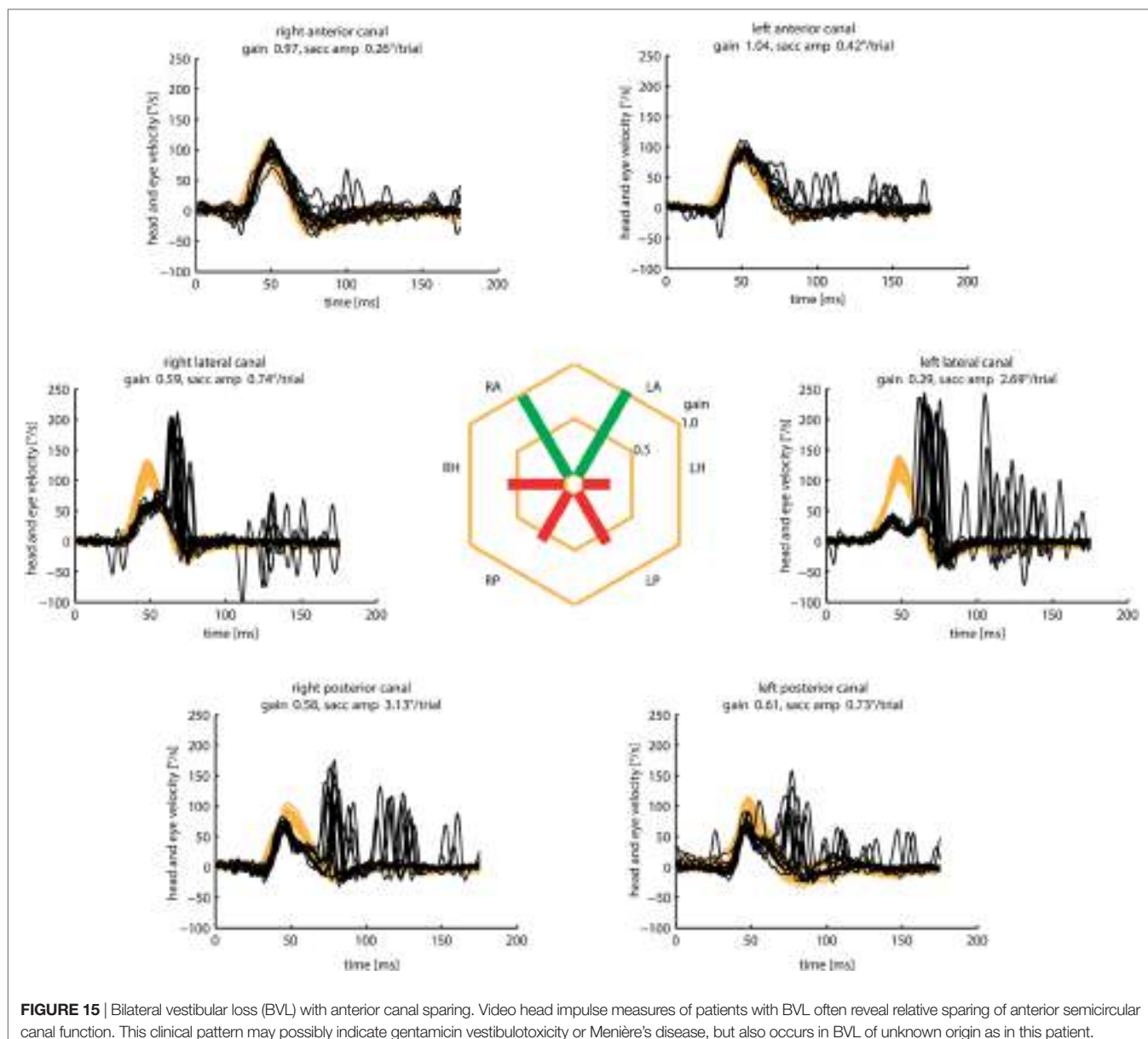
testing—may complete the clinical pattern. The constellation can be explained by the anatomy of the superior branch of the vestibular nerve, which innervates the lateral and superior canal, as well as the utricle. The susceptibility of the superior branch for VN may be explained by the tight bony canal surrounding the vestibular nerve (149). The pattern of damage with sparing of the PC may also explain the propensity of these patients to benign paroxysmal positional vertigo. Weeks or months after the attack, debris from the affected canals may fall into the PC, which is still fully functional, and may cause recurrent attacks of positional vertigo.

Inferior Vestibular Neuritis

The clinical counterpart of superior VN is inferior VN (146, 150). Here, only the PC is affected, often associated with tinnitus and hearing loss and saccular deficits measured with cVEMPs (146, 150–152). As there is little spontaneous nystagmus and normal caloric response, these do not fulfill the criteria of classic VN and may be mistaken as a central vestibular disorder. In these cases, detection of PC loss in vHIT may help differentiating between a peripheral and central vestibular disease.

Bilateral Vestibular Loss with Anterior SCC Sparing

Outside specialized balance centers, the diagnosis of BVL is often delayed or missed (153), because the characteristic symptoms of postural imbalance and oscillopsia (154–156)—often without vertigo—are not recognized. Once the suspicion has been raised, the clinical diagnosis is often straightforward based on three simple clinical bedside tests: the HIT, dynamic visual acuity, and the Romberg test on rubber foam (157). The etiology of BVL, however, still remains undetermined in about 50% of the cases despite intensive investigations (158). With the advent of vHIT, it is now possible to routinely assess the function of all six SCCs independently (4, 5, 9). Based on these investigations, characteristic patterns of SCC hypofunction started to emerge in patients with BVL: anterior SCC function was selectively spared in about 60% of these patients (Figure 15). As it turned out, AC sparing, determined by gain values (>0.7) and cumulative catch-up saccade amplitudes ($<0.73^\circ/\text{trial}$), were associated with aminoglycoside vestibulotoxicity and Menière's disease (17). Therefore, routine vHIT measures of all six SCCs may help to identify the underlying cause in patients with BVL.



Unilateral and Bilateral Loss of PC Function

Isolated loss of posterior SCC function was found in about 2% of patients with vHIT assessment of all six SCCs (159). Thorough vestibular work-up of these patients, including oVEMP and cVEMP for testing otolith function, as well as audiograms to assess cochlear function, revealed associated vestibular deficits in more than 80% of these patients. These associated deficits were most frequent in patients with vestibular Schwannoma or a history of VN and often the patients were at risk for concomitant BPPV.

AUTHOR CONTRIBUTIONS

IC wrote Sections "Introduction," "From Head Impulses to SHIMPs," and "The Physiological Basis of the Head Impulse

Test," LM wrote Section "Practical Aspects and Potential Pitfalls of Video Head Impulse Testing," HM wrote Section "Calculating VOR Gain," LC and GH wrote Section "Quantitative Head Impulse Test in Central Vestibular Disorders," and KW wrote Section "New Clinical Disease Patterns Emerging from 3D Video Head Impulse Testing." GH and IC assembled the paper, and all authors revised it.

ACKNOWLEDGMENTS

We are very grateful for the help of many colleagues in the work reported here, extending back some 33 years! There are too many people to acknowledge individually with one exception: we are very grateful to Ann Burgess who has done such valuable work in preparing this paper and has given such excellent help over so many years in the research reported here.

FUNDING

HM is supported by a Senior/Principal Research Fellowship from the Garnett Passe and Rodney Williams Memorial Foundation. Much of the work reported here has been supported by this

foundation: we are very grateful for their continued support, and for that of the National Health and Medical Research Foundation of Australia. The Trustees of the Royal Prince Alfred Hospital Neurology Department have continuously supported our vestibular research since 1979.

REFERENCES

- Halmagyi GM, Curthoys IS. Human compensatory slow eye movements in the absence of vestibular function. In: Graham MD, Kemink JL, editors. *The Vestibular System: Neurophysiologic and Clinical Research*. New York: Raven Press (1987). p. 471–9.
- Halmagyi GM, Curthoys IS. A clinical sign of canal paresis. *Arch Neurol* (1988) 45:737–9. doi:10.1001/archneur.1988.00520310043015
- MacDougall HG, McGarvie LA, Halmagyi GM, Rogers SJ, Manzari L, Burgess AM, et al. A new saccadic indicator of peripheral vestibular function based on the video head impulse test. *Neurology* (2016) 87:410–8. doi:10.1212/wnl.0000000000002827
- MacDougall HG, McGarvie LA, Halmagyi GM, Curthoys IS, Weber KP. The video Head Impulse Test (vHIT) detects vertical semicircular canal dysfunction. *PLoS One* (2013) 8:e61488. doi:10.1371/journal.pone.0061488
- MacDougall HG, McGarvie LA, Halmagyi GM, Curthoys IS. The video head impulse test: diagnostic accuracy in peripheral vestibulopathy. *Neurology* (2009) 73:1134–41. doi:10.1212/WNL.0b013e3181bacf85
- Mantokoudis G, Saber Tehrani AS, Wozniak A, Eibenberger K, Kattah JC, Gude CI, et al. Impact of artifacts on VOR gain measures by video-oculography in the acute vestibular syndrome. *J Vestib Res* (2016) 26:375–85. doi:10.3233/ves-160587
- Cleworth TW, Carpenter MG, Honegger F, Allum JHJ. Differences in head impulse test results due to analysis techniques. *J Vestib Res* (2017) (in press).
- Weber KP, Aw ST, Todd MJ, McGarvie LA, Curthoys IS, Halmagyi GM. Head impulse test in unilateral vestibular loss – vestibulo-ocular reflex and catch-up saccades. *Neurology* (2008) 70:454–63. doi:10.1212/01.wnl.0000299117.48935.2e
- MacDougall HG, McGarvie LA, Halmagyi GM, Curthoys IS, Weber KP. Application of the video head impulse test to detect vertical semicircular canal dysfunction. *Otol Neurotol* (2013) 34:974–9. doi:10.1097/MAO.0b013e3182d676d
- McGarvie LA, Martinez-Lopez M, Burgess AM, MacDougall HG, Curthoys IS. Horizontal eye position affects measured vertical VOR gain on the video head impulse test. *Front Neurol* (2015) 6:58. doi:10.3389/fneur.2015.00058
- Yang CJ, Lee JY, Kang BC, Lee HS, Yoo MH, Park HJ. Quantitative analysis of gains and catch-up saccades of video-head-impulse testing by age in normal subjects. *Clin Otolaryngol* (2016) 41:532–8. doi:10.1111/coa.12558
- McGarvie LA, MacDougall HG, Halmagyi GM, Burgess AM, Weber KP, Curthoys IS. The video head impulse test (vHIT) of semicircular canal function – age-dependent normative values of VOR gain in healthy subjects. *Front Neurol* (2015) 6:154. doi:10.3389/fneur.2015.00154
- Weber KP, Aw ST, Todd MJ, McGarvie LA, Curthoys IS, Halmagyi GM. Horizontal head impulse test detects gentamicin vestibulotoxicity. *Neurology* (2009) 72:1417–24. doi:10.1212/WNL.0b013e3181a18652
- Marques P, Manrique-Huarte R, Perez-Fernandez N. Single intratympanic gentamicin injection in Meniere's disease: VOR change and prognostic usefulness. *Laryngoscope* (2015) 125:1915–20. doi:10.1002/lary.25156
- Judge PD, Janky KL, Barin K. Can the video head impulse test define severity of bilateral vestibular hypofunction? *Otol Neurotol* (2017) 38:730–6. doi:10.1097/mao.0000000000001351
- Kang KW, Lee C, Kim SH, Cho HH, Lee SH. Bilateral vestibulopathy documented by video head impulse tests in superficial siderosis. *Otol Neurotol* (2015) 36:1683–6. doi:10.1097/mao.0000000000000865
- Tarnutzer AA, Bockisch CJ, Buffone E, Weiler S, Bachmann LM, Weber KP. Disease-specific sparing of the anterior semicircular canals in bilateral vestibulopathy. *Clin Neurophysiol* (2016) 127:2791–801. doi:10.1016/j.clinph.2016.05.005
- MacDougall HG, Curthoys IS. Plasticity during vestibular compensation: the role of saccades. *Front Neurol* (2012) 3:21. doi:10.3389/fneur.2012.00021
- Batuecas-Caletro A, Santacruz-Ruiz S, Munoz-Herrera A, Perez-Fernandez N. The vestibulo-ocular reflex and subjective balance after vestibular schwannoma surgery. *Laryngoscope* (2014) 124:1431–5. doi:10.1002/lary.24447
- Mantokoudis G, Saber Tehrani AS, Wong AL, Agrawal Y, Wenzel A, Carey JP. Adaptation and compensation of vestibular responses following superior canal dehiscence surgery. *Otol Neurotol* (2016) 37:1399–405. doi:10.1097/mao.00000000000001196
- Matino-Soler E, Rey-Martinez J, Trinidad-Ruiz G, Batuecas-Caletro A, Perez Fernandez N. A new method to improve the imbalance in chronic unilateral vestibular loss: the organization of refixation saccades. *Acta Otolaryngol* (2016) 136:894–900. doi:10.3109/00016489.2016.1172730
- Rey-Martinez J, Batuecas-Caletro A, Matino E, Perez Fernandez N. HITCal: a software tool for analysis of video head impulse test responses. *Acta Otolaryngol* (2015) 135:886–94. doi:10.3109/00016489.2015.1035401
- Wettstein VG, Weber KP, Bockisch CJ, Hegemann SC. Compensatory saccades in head impulse testing influence the dynamic visual acuity of patients with unilateral peripheral vestibulopathy. *J Vestib Res* (2016) 26:395–402. doi:10.3233/ves-160591
- Rambold HA. Economic management of vertigo/dizziness disease in a county hospital: video-head-impulse test vs. caloric irrigation. *Eur Arch Otorhinolaryngol* (2015) 272:2621–8. doi:10.1007/s00405-014-3205-1
- van Esch BF, Nobel-Hoff GE, van Benthem PP, van der Zaag-Loonen HJ, Bruintjes TD. Determining vestibular hypofunction: start with the video-head impulse test. *Eur Arch Otorhinolaryngol* (2016) 273:3733–9. doi:10.1007/s00405-016-4055-9
- Crane BT, Demer JL. Latency of voluntary cancellation of the human vestibulo-ocular reflex during transient yaw rotation. *Exp Brain Res* (1999) 127:67–74. doi:10.1007/s002210050774
- Shen Q, Magnani C, Sterkers O, Lamas G, Vidal PP, Sadoun J, et al. Saccadic velocity in the new suppression head impulse test: a new indicator of horizontal vestibular canal paresis and of vestibular compensation. *Front Neurol* (2016) 7:160. doi:10.3389/fneur.2016.00160
- Curthoys IS, Halmagyi GM. Vestibular compensation: a review of the oculomotor, neural, and clinical consequences of unilateral vestibular loss. *J Vestib Res* (1995) 5:67–107. doi:10.1016/0957-4271(94)00026-X
- Aw ST, Halmagyi GM, Haslwanter T, Curthoys IS, Yavor RA, Todd MJ. Three-dimensional vector analysis of the human vestibuloocular reflex in response to high-acceleration head rotations. II. responses in subjects with unilateral vestibular loss and selective semicircular canal occlusion. *J Neurophysiol* (1996) 76:4021–30.
- Weber KP, Aw ST, Todd MJ, McGarvie LA, Pratap S, Curthoys IS, et al. Inter-ocular differences of the horizontal vestibulo-ocular reflex during impulsive testing. *Prog Brain Res* (2008) 171:195–8. doi:10.1016/s0079-6123(08)00626-2
- Grossman GE, Leigh RJ, Abel LA, Lanska DJ, Thurston SE. Frequency and velocity of rotational head perturbations during locomotion. *Exp Brain Res* (1988) 70:470–6. doi:10.1007/BF00247595
- Grossman GE, Leigh RJ, Bruce EN, Huebner WP, Lanska DJ. Performance of the human vestibuloocular reflex during locomotion. *J Neurophysiol* (1989) 62:264–72.
- Curthoys IS. The new vestibular stimuli: sound and vibration -anatomical, physiological and clinical evidence. *Exp Brain Res* (2017) 235:957–72. doi:10.1007/s00221-017-4874-y
- Curthoys IS, Vulovic V, Burgess AM, Sokolic L, Goonetilleke SC. The response of guinea pig primary utricular and saccular irregular neurons to bone-conducted vibration (BCV) and air-conducted sound (ACS). *Hear Res* (2016) 331:131–43. doi:10.1016/j.heares.2015.10.019

35. Eatock RA, Songer JE. Vestibular hair cells and afferents: two channels for head motion signals. *Annu Rev Neurosci* (2011) 34:501–34. doi:10.1146/annrev-neuro-061010-113710
36. Songer JE, Eatock RA. Tuning and timing in mammalian type I hair cells and calyceal synapses. *J Neurosci* (2013) 33:3706–24. doi:10.1523/jneurosci.4067-12.2013
37. Carpenter MB. Vestibular nuclei – afferent and efferent projections. *Prog Brain Res* (1988) 76:5–15. doi:10.1016/S0079-6123(08)64487-8
38. Gacek RR. Afferent and efferent innervation of the labyrinth. *Adv Otorhinolaryngol* (1982) 28:1–13. doi:10.1159/000406732
39. Goldberg JM. Afferent diversity and the organization of central vestibular pathways. *Exp Brain Res* (2000) 130:277–97. doi:10.1007/s002210050033
40. Ishizuka N, Sasaki S, Mannen H. Central course and terminal arborizations of single primary vestibular afferent-fibers from the horizontal canal in the cat. *Neurosci Lett* (1982) 33:135–9. doi:10.1016/0304-3940(82)90240-3
41. Precht W, Shimazu H. Functional connections of tonic and kinetic vestibular neurons with primary vestibular afferents. *J Neurophysiol* (1965) 28:1014–28.
42. Sato F, Sasaki H. Morphological correlations between spontaneously discharging primary vestibular afferents and vestibular nucleus neurons in the cat. *J Comp Neurol* (1993) 333:554–66. doi:10.1002/cne.90330408
43. Sato F, Sasaki H, Ishizuka N, Sasaki SI, Mannen H. Morphology of single primary vestibular afferents originating from the horizontal semicircular canal in the cat. *J Comp Neurol* (1989) 290:423–39. doi:10.1002/cne.902900310
44. Markham CH, Yagi T, Curthoys IS. Contribution of contralateral labyrinth to 2nd order vestibular neuronal-activity in cat. *Brain Res* (1977) 138:99–109. doi:10.1016/0006-8993(77)90786-7
45. Shimazu H. Excitatory and inhibitory premotor neurons related to horizontal vestibular nystagmus. In: Asanuma H, Wilson VJ, editors. *Integration in the Nervous System*. Tokyo: Igaku-shoin (1979). p. 123–43.
46. Shimazu H. Neuronal organization of the premotor system controlling horizontal conjugate eye movements and vestibular nystagmus. In: Desmedt JE, editor. *Motor Control Mechanisms in Health and Disease*. New York: Raven Press (1983). p. 565–88.
47. Shimazu H, Precht W. Inhibition of central vestibular neurons from contralateral labyrinth and its mediating pathway. *J Neurophysiol* (1966) 29:467–92.
48. Nakao S, Sasaki S, Schor RH, Shimazu H. Functional organization of premotor neurons in the cat medial vestibular nucleus related to slow and fast phases of nystagmus. *Exp Brain Res* (1982) 45:371–85. doi:10.1007/bf01208597
49. Kasahara M, Uchino Y. Selective mode of commissural inhibition induced by semicircular canal afferents on secondary vestibular neurones in cat. *Brain Res* (1971) 34:366–9. doi:10.1016/0006-8993(71)90288-5
50. Ishizuka N, Mannen H, Sasaki S, Shimazu H. Axonal branches and terminations in the cat abducens nucleus of secondary vestibular neurons in the horizontal canalsystem. *Neurosci Lett* (1980) 16:143–8. doi:10.1016/0304-3940(80)90334-1
51. Maciewicz RJ, Eagen K, Kaneko CRS, Highstein SM. Vestibular and medullary brain-stem afferents to abducens nucleus in cat. *Brain Res* (1977) 123:229–40. doi:10.1016/0006-8993(77)90476-0
52. Maeda M, Shimazu H, Shinoda Y. Rhythmic activities of secondary vestibular efferent fibers recorded within abducens nucleus during vestibular nystagmus. *Brain Res* (1971) 34:361–5. doi:10.1016/0006-8993(71)90287-3
53. Maeda M, Shimazu H, Shinoda Y. Nature of synaptic events in cat abducens motoneurons at slow and quick phase of vestibular nystagmus. *J Neurophysiol* (1972) 35:279–96.
54. McCrea RA, Strassman A, Highstein SM. Morphology and physiology of abducens motoneurons and internuclear neurons intracellularly injected with horseradish-peroxidase in alert squirrel-monkeys. *J Comp Neurol* (1986) 243:291–308. doi:10.1002/cne.902430302
55. McCrea RA, Strassman A, May E, Highstein SM. Anatomical and physiological characteristics of vestibular neurons mediating the horizontal vestibulo-ocular reflex of the squirrel monkey. *J Comp Neurol* (1987) 264:547–70. doi:10.1002/cne.902640408
56. McCrea RA, Yoshida K, Berthoz A, Baker R. Eye-movement related activity and morphology of 2nd order vestibular neurons terminating in the cat abducens nucleus. *Exp Brain Res* (1980) 40:468–73. doi:10.1007/BF00236156
57. Nakao S, Sasaki S. Firing pattern of interneurons in abducens nucleus related to vestibular nystagmus in cat. *Brain Res* (1978) 144:389–94. doi:10.1016/0006-8993(78)90166-x
58. Shinoda Y, Yoshida K. Dynamic characteristics of responses to horizontal head angular acceleration in vestibuloocular pathway in cat. *J Neurophysiol* (1974) 37:653–73.
59. Baker R, Highstein SM. Physiological identification of interneurons and motoneurons in abducens nucleus. *Brain Res* (1975) 91:292–8. doi:10.1016/0006-8993(75)90551-x
60. Buttner-Ennever JA, Akert K. Medial rectus subgroups of the oculomotor nucleus and their abducens inter-nuclear input in the monkey. *J Comp Neurol* (1981) 197:17–27. doi:10.1002/cne.901970103
61. Highstein SM, Baker R. Excitatory termination of abducens inter-nuclear neurons on medial rectus motoneurons – relationship to syndrome of inter-nuclear ophthalmoplegia. *J Neurophysiol* (1978) 41:1647–61.
62. Nakao S, Sasaki S. Excitatory input from interneurons in the abducens nucleus to medial rectus moto-neurons mediating conjugate horizontal nystagmus in the cat. *Exp Brain Res* (1980) 39:23–32. doi:10.1007/BF00237066
63. Reisine H, Highstein SM. The ascending tract of Deiters' conveys a head velocity signal to medial rectus motoneurons. *Brain Res* (1979) 170:172–6. doi:10.1016/0006-8993(79)90949-1
64. Curthoys IS. Generation of the quick phase of horizontal vestibular nystagmus. *Exp Brain Res* (2002) 143:397–405. doi:10.1007/s00221-002-1022-z
65. Halmagyi GM, Curthoys IS, Cremer PD, Henderson CJ, Todd MJ, Staples MJ, et al. The human horizontal vestibulo-ocular reflex in response to high-acceleration stimulation before and after unilateral vestibular neurectomy. *Exp Brain Res* (1990) 81:479–90. doi:10.1007/BF02423496
66. Migliaccio AA, Cremer PD. The 2D modified head impulse test: a 2D technique for measuring function in all six semi-circular canals. *J Vestib Res* (2011) 21:227–34. doi:10.3233/ves-2011-0421
67. Hamilton SS, Zhou G, Brodsky JR. Video head impulse testing (vHIT) in the pediatric population. *Int J Pediatr Otorhinolaryngol* (2015) 79:1283–7. doi:10.1016/j.ijporl.2015.05.033
68. Khater AM, Afifi PO. Video head-impulse test (vHIT) in dizzy children with normal caloric responses. *Int J Pediatr Otorhinolaryngol* (2016) 87:172–7. doi:10.1016/j.ijporl.2016.06.030
69. Nassif N, Balzanelli C, Redaelli de Zinis LO. Preliminary results of video Head Impulse Testing (vHIT) in children with cochlear implants. *Int J Pediatr Otorhinolaryngol* (2016) 88:30–3. doi:10.1016/j.ijporl.2016.06.034
70. Ross LM, Helminski JO. Test-retest and interrater reliability of the video head impulse test in the pediatric population. *Otol Neurotol* (2016) 37:558–63. doi:10.1097/mao.0000000000001040
71. Newman-Toker DE, Curthoys IS, Halmagyi GM. Diagnosing stroke in acute vertigo: The HINTS Family of Eye Movement Tests and the future of the "Eye ECG". *Semin Neurol* (2015) 35:506–21. doi:10.1055/s-0035-1564298
72. Blodow A, Helbig R, Wichmann N, Wenzel A, Walther LE, Bloching MB. [Video head impulse test or caloric irrigation? Contemporary diagnostic tests for vestibular schwannoma]. *HNO* (2013) 61:781–5. doi:10.1007/s00106-013-2752-x
73. Mahringer A, Rambold HA. Caloric test and video-head-impulse: a study of vertigo/dizziness patients in a community hospital. *Eur Arch Otorhinolaryngol* (2014) 271:463–72. doi:10.1007/s00405-013-2376-5
74. McGarvie LA, Curthoys IS, MacDougall HG, Halmagyi GM. What does the dissociation between the results of video head impulse versus caloric testing reveal about the vestibular dysfunction in Meniere's disease? *Acta Otolaryngol* (2015) 135:859–65. doi:10.3109/00016489.2015.1015606
75. McGarvie LA, Curthoys IS, MacDougall HG, Halmagyi GM. What does the head impulse test versus caloric dissociation reveal about vestibular dysfunction in Meniere's disease? *Ann N Y Acad Sci* (2015) 1343:58–62. doi:10.1111/nyas.12687
76. Zellhuber S, Mahringer A, Rambold HA. Relation of video-head-impulse test and caloric irrigation: a study on the recovery in unilateral vestibular neuritis. *Eur Arch Otorhinolaryngol* (2014) 271:2375–83. doi:10.1007/s00405-013-2723-6
77. McCaslin DL, Jacobson GP, Bennett ML, Gruenwald JM, Green AP. Predictive properties of the video head impulse test: measures of caloric symmetry and self-report dizziness handicap. *Ear Hear* (2014) 35:e185–91. doi:10.1097/aud.0000000000000047
78. McCaslin DL, Rivas A, Jacobson GP, Bennett ML. The dissociation of video head impulse test (vHIT) and bithermal caloric test results provide topographical localization of vestibular system impairment in patients with "definite" Meniere's disease. *Am J Audiol* (2015) 24:1–10. doi:10.1044/2014_aaja-14-0040

79. Blanks RH, Curthoys IS, Markham CH. Planar relationships of the semicircular canals in man. *Acta Otolaryngol* (1975) 80:185–96. doi:10.3109/00016487509121318
80. Curthoys IS, Blanks RH, Markham CH. Semicircular canal functional anatomy in cat, guinea pig and man. *Acta Otolaryngol* (1977) 83:258–65. doi:10.3109/00016487709128843
81. Bradshaw AP, Curthoys IS, Todd MJ, Magnussen JS, Taubman DS, Aw ST, et al. A mathematical model of human semicircular canal geometry: a new basis for interpreting vestibular physiology. *J Assoc Res Otolaryngol* (2010) 11:145–59. doi:10.1007/s10162-009-0195-6
82. Moore ST, Haslwanter T, Curthoys IS, Smith ST. A geometric basis for measurement of three-dimensional eye position using image processing. *Vision Res* (1996) 36:445–59. doi:10.1016/0042-6989(95)00130-1
83. Suh MW, Park JH, Kang SI, Lim JH, Park MK, Kwon SK. Effect ofoggle slippage on the Video Head Impulse Test outcome and its mechanisms. *Otol Neurotol* (2017) 38:102–9. doi:10.1097/mao.0000000000001233
84. Fetter M, Hain TC, Zee DS. Influence of eye and head position on the vestibuloocular reflex. *Exp Brain Res* (1986) 64:208–16. doi:10.1007/BF00238215
85. Agrawal Y, Schubert MC, Migliaccio AA, Zee DS, Schneider E, Lehnen N, et al. Evaluation of quantitative head impulse testing using search coils versus video-oculography in older individuals. *Otol Neurotol* (2014) 35:283–8. doi:10.1097/MAO.0b013e3182995227
86. Kessler P, Tomlinson D, Blakeman A, Rutka J, Ranalli P, Wong A. The high-frequency/acceleration head heave test in detecting otolith diseases. *Otol Neurotol* (2007) 28:896–904. doi:10.1097/MAO.0b013e3181256543
87. Dieterich M. Central vestibular disorders. *J Neurol* (2007) 254:559–68. doi:10.1007/s00415-006-0340-7
88. Newman-Toker DE, Kattah JC, Alvernia JE, Wang DZ. Normal head impulse test differentiates acute cerebellar strokes from vestibular neuritis. *Neurology* (2008) 70:2378–85. doi:10.1212/01.wnl.0000314685.01433.0d
89. Kattah JC, Talkad AV, Wang DZ, Hsieh YH, Newman-Toker DE. HINTS to diagnose stroke in the acute vestibular syndrome: three-step bedside oculomotor examination more sensitive than early MRI diffusion-weighted imaging. *Stroke* (2009) 40:3504–10. doi:10.1161/STROKEAHA.109.551234
90. Flipse JP, Straathof CS, Van der Steen J, Van Leeuwen AF, Van Doorn PA, Van der Meche FG, et al. Binocular saccadic eye movements in multiple sclerosis. *J Neurol Sci* (1997) 148:53–65. doi:10.1016/S0022-510X(96)05330-0
91. Frohman EM, Frohman TC, O'Suilleabhain P, Zhang H, Hawker K, Racke MK, et al. Quantitative oculographic characterisation of internuclear ophthalmoparesis in multiple sclerosis: the versional dysconjugacy index Z score. *J Neurol Neurosurg Psychiatry* (2002) 73:51–5. doi:10.1136/jnnp.73.1.51
92. Kattah JC, Dhanani SS, Pula JH, Mantokoudis G, Tehrani ASS, Toker DEN. Vestibular signs of thiamine deficiency during the early phase of suspected Wernicke encephalopathy. *Neurology* (2013) 80:3460–8. doi:10.1212/01.cpn.0000435749.32868.91
93. Akdal G, MacDougall HG, Chen L, Tanriverdizade T, Yigitaslan O, Halmagyi GM. Selective impairment of horizontal vestibulo-ocular reflexes in acute Wernicke's encephalopathy. *J Neurol Sci* (2016) 365:167–8. doi:10.1016/j.jns.2016.04.013
94. Aw ST, Todd MJ, Aw GE, Weber KP, Halmagyi GM. Gentamicin vestibulotoxicity impairs human electrically evoked vestibulo-ocular reflex. *Neurology* (2008) 71:1776–82. doi:10.1212/01.wnl.0000335971.43443.d9
95. Cremer PD, Halmagyi GM, Aw ST, Curthoys IS, McGarvie LA, Todd MJ, et al. Semicircular canal plane head impulses detect absent function of individual semicircular canals. *Brain* (1998) 121(Pt 4):699–716. doi:10.1093/brain/121.4.699
96. Baloh RW. Clinical practice. Vestibular neuritis. *N Engl J Med* (2003) 348:1027–32. doi:10.1056/NEJMcp021154
97. Strupp M, Brandt T. Chapter 25 – vestibular neuritis. In: Scott DZE, David SZ, editors. *Handbook of Clinical Neurophysiology* (Vol. 9). Amsterdam: Elsevier (2010). p. 315–32. doi:10.1016/S1567-4231(10)09025-8
98. Choi KD, Lee H, Kim JS. Vertigo in brainstem and cerebellar strokes. *Curr Opin Neurol* (2013) 26:90–5. doi:10.1097/WCO.0b013e32835c5edd
99. Kim HA, Yi HA, Lee H. Recent advances in cerebellar ischemic stroke syndromes causing vertigo and hearing loss. *Cerebellum* (2016) 15:781–8. doi:10.1007/s12311-015-0745-x
100. Jorns-Haderli M, Straumann D, Palla A. Accuracy of the bedside head impulse test in detecting vestibular hypofunction. *J Neurol Neurosurg Psychiatry* (2007) 78:1113–8. doi:10.1136/jnnp.2006.109512
101. Mantokoudis G, Saber Tehrani A, Wozniak A, Eibenberger K, Kattah JC, Gude CI, et al. VOR gain by head impulse video-oculography differentiates acute vestibular neuritis from stroke. *Otol Neurotol* (2015) 36:457–65. doi:10.1097/MAO.0000000000000638
102. Tarnutzer AA, Berkowitz AL, Robinson KA, Hsieh YH, Newman-Toker DE. Does my dizzy patient have a stroke? A systematic review of bedside diagnosis in acute vestibular syndrome. *CMAJ* (2011) 183:E571–92. doi:10.1503/cmaj.100174
103. Newman-Toker DE, Kerber KA, Hsieh YH, Pula JH, Omron R, Saber Tehrani AS, et al. HINTS outperforms ABCD2 to screen for stroke in acute continuous vertigo and dizziness. *Acad Emerg Med* (2013) 20:986–96. doi:10.1111/acebm.12223
104. Chen L, Todd M, Halmagyi GM, Aw S. Head impulse gain and saccade analysis in pontine-cerebellar stroke and vestibular neuritis. *Neurology* (2014) 83:1513–22. doi:10.1212/WNL.0000000000000906
105. Lee H, Kim JS, Chung EJ, Yi HA, Chung IS, Lee SR, et al. Infarction in the territory of anterior inferior cerebellar artery: spectrum of audiovestibular loss. *Stroke* (2009) 40:3745–51. doi:10.1161/STROKEAHA.109.564682
106. Lee H. Audiovestibular loss in anterior inferior cerebellar artery territory infarction: a window to early detection? *J Neurol Sci* (2012) 313:153–9. doi:10.1016/j.jns.2011.08.039
107. Park HK, Kim JS, Strupp M, Zee DS. Isolated floccular infarction: impaired vestibular responses to horizontal head impulse. *J Neurol* (2013) 260:1576–82. doi:10.1007/s00415-013-6837-y
108. Newman-Toker DE, Saber Tehrani AS, Mantokoudis G, Pula JH, Gude CI, Kerber KA, et al. Quantitative video-oculography to help diagnose stroke in acute vertigo and dizziness: toward an ECG for the eyes. *Stroke* (2013) 44:1158–61. doi:10.1161/STROKEAHA.111.000033
109. Meng H, Blazquez PM, Dickman JD, Angelaki DE. Diversity of vestibular nuclei neurons targeted by cerebellar nodulus inhibition. *J Physiol* (2014) 592:171–88. doi:10.1113/jphysiol.2013.259614
110. Miles FA, Fuller JH, Braitman DJ, Dow BM. Long-term adaptive changes in primate vestibuloocular reflex III. Electrophysiological observations in flocculus of normal monkeys. *J Neurophysiol* (1980) 43:1437–76.
111. Noda H, Suzuki DA. The role of the flocculus of the monkey in saccadic eye movements. *J Physiol* (1979) 294:317–34. doi:10.1113/jphysiol.1979.sp012932
112. Zee DS, Yamazaki A, Butler PH, Guer G. Effects of ablation of flocculus and paraflocculus of eye movements in primate. *J Neurophysiol* (1981) 46:878–99.
113. Ludvigh E. Amount of eye movement objectively perceptible to the unaided eye. *Am J Ophthalmol* (1949) 32:649–50. doi:10.1016/0002-9394(49)91415-4
114. Sato H, Noda H. Saccadic dysmetria induced by transient functional decortication of the cerebellar vermis [corrected]. *Exp Brain Res* (1992) 88:455–8. doi:10.1007/BF02259122
115. Takagi M, Zee DS, Tamargo RJ. Effects of lesions of the oculomotor vermis on eye movements in primate: saccades. *J Neurophysiol* (1998) 80:1911–31.
116. Walker MF, Zee DS. Cerebellar disease alters the axis of the high-acceleration vestibuloocular reflex. *J Neurophysiol* (2005) 94:3417–29. doi:10.1152/jn.00375.2005
117. Shaikh AG, Marti S, Tarnutzer AA, Palla A, Crawford TO, Straumann D, et al. Ataxia telangiectasia: a “disease model” to understand the cerebellar control of vestibular reflexes. *J Neurophysiol* (2011) 105:3034–41. doi:10.1152/jn.00721.2010
118. Kremmyda O, Kirchner H, Glasauer S, Brandt T, Jahn K, Strupp M. False-positive head-impulse test in cerebellar ataxia. *Front Neurol* (2012) 3:162. doi:10.3389/fneur.2012.00162
119. Huh YE, Kim JS, Kim HJ, Park SH, Jeon BS, Kim JM, et al. Vestibular performance during high-acceleration stimuli correlates with clinical decline in SCA6. *Cerebellum* (2015) 14:284–91. doi:10.1007/s12311-015-0650-3
120. Lasker DM, Hullar TE, Minor LB. Horizontal vestibuloocular reflex evoked by high-acceleration rotations in the squirrel monkey. III. Responses after labyrinthectomy. *J Neurophysiol* (2000) 83:2482–96.
121. Palla A, Straumann D. Recovery of the high-acceleration vestibulo-ocular reflex after vestibular neuritis. *J Assoc Res Otolaryngol* (2004) 5:427–35. doi:10.1007/s10162-004-4035-4
122. Lee SH, Park SH, Kim JS, Kim HJ, Yunusov F, Zee DS. Isolated unilateral infarction of the cerebellar tonsil: ocular motor findings. *Ann Neurol* (2014) 75:429–34. doi:10.1002/ana.24094

123. Kim SH, Zee DS, du Lac S, Kim HJ, Kim JS. Nucleus prepositus hypoglossi lesions produce a unique ocular motor syndrome. *Neurology* (2016) 87:2026–33. doi:10.1212/WNL.0000000000003316
124. Zhang Y, Partsalis AM, Highstein SM. Properties of superior vestibular nucleus flocculus target neurons in the squirrel monkey. I. General properties in comparison with flocculus projecting neurons. *J Neurophysiol* (1995) 73:2261–78.
125. Kim HJ, Lee SH, Park JH, Choi JY, Kim JS. Isolated vestibular nuclear infarction: report of two cases and review of the literature. *J Neurol* (2014) 261:121–9. doi:10.1007/s00415-013-7139-0
126. Hirai N, Uchino Y. Superior vestibular nucleus neurones related to the excitatory vestibulo-ocular reflex of anterior canal origin and their ascending course in the cat. *Neurosci Res* (1984) 1:73–9. doi:10.1016/0168-0102(84)90032-4
127. Carpenter MB, Cowie RJ. Connections and oculomotor projections of the superior vestibular nucleus and cell group 'y'. *Brain Res* (1985) 336:265–87. doi:10.1016/0006-8993(85)90653-5
128. Zee DS. Internuclear ophthalmoplegia: pathophysiology and diagnosis. *Baillieres Clin Neurol* (1992) 1:455–70.
129. Frohman EM, Frohman TC, Zee DS, McColl R, Galetta S. The neuro-ophthalmology of multiple sclerosis. *Lancet Neurol* (2005) 4:111–21. doi:10.1016/S1474-4422(05)00992-0
130. Frohman TC, Galetta S, Fox R, Solomon D, Straumann D, Filippi M, et al. Pearls & Oy-sters: the medial longitudinal fasciculus in ocular motor physiology. *Neurology* (2008) 70:e57–67. doi:10.1212/01.wnl.0000310640.37810.b3
131. Frohman TC, Frohman EM, O'Suilleabhain P, Salter A, Dewey RB Jr, Hogan N, et al. Accuracy of clinical detection of INO in MS: corroboration with quantitative infrared oculography. *Neurology* (2003) 61:848–50. doi:10.1212/01.WNL.0000085863.54218.72
132. Highstein SM, Reisine H. The ascending tract of Deiters' and horizontal gaze. *Ann N Y Acad Sci* (1981) 374:102–11. doi:10.1111/j.1749-6632.1981.tb30864.x
133. Nguyen LT, Baker R, Spencer RF. Abducens internuclear and ascending tract of deiters inputs to medial rectus motoneurons in the cat oculomotor nucleus: synaptic organization. *J Comp Neurol* (1999) 405:141–59. doi:10.1002/(SICI)1096-9861(19990308)405:2<141::AID-CNE1>3.0.CO;2-R
134. Zwergal A, Strupp M, Brandt T, Buttner-Ennever JA. Parallel ascending vestibular pathways: anatomical localization and functional specialization. *Ann N Y Acad Sci* (2009) 1164:51–9. doi:10.1111/j.1749-6632.2009.04461.x
135. Cremer PD, Migliaccio AA, Halmagyi GM, Curthoys IS. Vestibulo-ocular reflex pathways in internuclear ophthalmoplegia. *Ann Neurol* (1999) 45:529–33. doi:10.1002/1531-8249(199904)45:4<529::AID-ANA18>3.0.CO;2-H
136. Mitsacos A, Reisine H, Highstein SM. The superior vestibular nucleus: an intracellular HRP study in the cat. I. Vestibulo-ocular neurons. *J Comp Neurol* (1983) 215:78–91. doi:10.1002/cne.902150107
137. Reisine H, Raphan T. Neural basis for eye velocity generation in the vestibular nuclei of alert monkeys during off-vertical axis rotation. *Exp Brain Res* (1992) 92:209–26. doi:10.1007/BF00227966
138. Shimazu H, Precht W. Tonic and kinetic responses of cat's vestibular neurons to horizontal angular acceleration. *J Neurophysiol* (1965) 28:991–1013.
139. Sechi G, Serra A. Wernicke's encephalopathy: new clinical settings and recent advances in diagnosis and management. *Lancet Neurol* (2007) 6:442–55. doi:10.1016/S1474-4422(07)70104-7
140. Choi KD, Oh SY, Kim HJ, Kim JS. The vestibulo-ocular reflexes during head impulse in Wernicke's encephalopathy. *J Neurol Neurosurg Psychiatry* (2007) 78:1161–2. doi:10.1136/jnnp.2007.121061
141. Winkelmann MD, Banker BQ, Victor M, Moser HW. Non-infantile neuronopathic Gaucher's disease: a clinicopathologic study. *Neurology* (1983) 33:994–1008. doi:10.1212/WNL.33.8.994
142. Benko W, Ries M, Wiggs EA, Brady RO, Schiffmann R, Fitzgibbon EJ. The saccadic and neurological deficits in type 3 Gaucher disease. *PLoS One* (2011) 6:e22410. doi:10.1371/journal.pone.0022410
143. Chen L, Halmagyi GM, Todd MJ, Aw ST. Vestibular and saccadic abnormalities in Gaucher's Disease. *JIMD Rep* (2014) 13:111–8. doi:10.1007/8904_2013_264
144. Wong K, Sidransky E, Verma A, Mixon T, Sandberg GD, Wakefield LK, et al. Neuropathology provides clues to the pathophysiology of Gaucher disease. *Mol Genet Metab* (2004) 82:192–207. doi:10.1016/j.mgme.2004.04.011
145. Curthoys IS. The interpretation of clinical tests of peripheral vestibular function. *Laryngoscope* (2012) 122:1342–52. doi:10.1002/lary.23258
146. Aw ST, Fetter M, Cremer PD, Karlberg M, Halmagyi GM. Individual semi-circular canal function in superior and inferior vestibular neuritis. *Neurology* (2001) 57:768–74. doi:10.1212/WNL.57.5.768
147. Halmagyi GM, Weber KP, Curthoys IS. Vestibular function after acute vestibular neuritis. *Restor Neurol Neurosci* (2010) 28:37–46. doi:10.3233/RNN-2010-0533
148. D'Onofrio F. Vertical eye movements during horizontal head impulse test: a new clinical sign of superior vestibular neuritis. *Acta Otorhinolaryngol Ital* (2013) 33:418–24.
149. Gianoli G, Goebel J, Mowry S, Poomipannit T. Anatomic differences in the lateral vestibular nerve channels and their implications in vestibular neuritis. *Otol Neurotol* (2005) 26:489–94. doi:10.1097/01.mao.0000169787.99835.9f
150. Halmagyi GM, Aw ST, Karlberg M, Curthoys IS, Todd MJ. Inferior vestibular neuritis. *Ann N Y Acad Sci* (2002) 956:306–13. doi:10.1111/j.1749-6632.2002.tb02829.x
151. Chihara Y, Iwasaki S, Murofushi T, Yagi M, Inoue A, Fujimoto C, et al. Clinical characteristics of inferior vestibular neuritis. *Acta Otolaryngol (Stockh)* (2012) 132:1288–94. doi:10.3109/00016489.2012.701326
152. Kim JS, Kim HJ. Inferior vestibular neuritis. *J Neurol* (2012) 259:1553–60. doi:10.1007/s00415-011-6375-4
153. van de Berg R, van Tilburg M, Kingma H. Bilateral vestibular hypofunction: challenges in establishing the diagnosis in adults. *ORL J Otorhinolaryngol Relat Spec* (2015) 77:197–218. doi:10.1159/000433549
154. Dandy WE. Results of removal of acoustic tumors by the unilateral approach. *Arch Surg* (1941) 42:1026–33. doi:10.1001/archsurg.1941.01210120061006
155. Atkin A, Bender MB. Ocular stabilization during oscillatory head movements – vestibular system dysfunction and relation between head and eye velocities. *Arch Neurol* (1968) 19:559–66. doi:10.1001/archneur.1968.00480060029003
156. Crawford J. Living without a balancing mechanism. *N Engl J Med* (1952) 246:458–60. doi:10.1056/NEJM195203202461207
157. Petersen JA, Straumann D, Weber KP. Clinical diagnosis of bilateral vestibular loss: three simple bedside tests. *Ther Adv Neurol Disord* (2013) 6:41–5. doi:10.1177/1756285612465920
158. Zingler VC, Cnyrim C, Jahn K, Weintz E, Fernbacher J, Frenzel C, et al. Causative factors and epidemiology of bilateral vestibulopathy in 255 patients. *Ann Neurol* (2007) 61:524–32. doi:10.1002/ana.21102
159. Tarnutzer AA, Bokisch CJ, Buffone E, Weber KP. Association of posterior semicircular canal hypofunction on video-head-impulse testing with other vestibulo-cochlear deficits. *Clin Neurophysiol* (2017). doi:10.1016/j.clinph.2017.04.029

Conflict of Interest Statement: IC, GH, HM, and LM are unpaid consultants to GN Otometrics, Taastrup, Denmark, but have received support from GN Otometrics for travel and attendance at conferences and workshops. For all other authors, the research was conducted in the absence of any commercial or financial relationships that could be construed as a potential conflict of interest.

Copyright © 2017 Halmagyi, Chen, MacDougall, Weber, McGarvie and Curthoys. This is an open-access article distributed under the terms of the Creative Commons Attribution License (CC BY). The use, distribution or reproduction in other forums is permitted, provided the original author(s) or licensor are credited and that the original publication in this journal is cited, in accordance with accepted academic practice. No use, distribution or reproduction is permitted which does not comply with these terms.



Superior Canal Dehiscence Syndrome: Lessons from the First 20 Years

Bryan K. Ward^{1*}, John P. Carey¹ and Lloyd B. Minor²

¹ Department of Otolaryngology-Head and Neck Surgery, Johns Hopkins University School of Medicine, Baltimore, MD, USA

² Department of Otolaryngology-Head and Neck Surgery, Stanford University School of Medicine, Stanford, CA, USA

OPEN ACCESS

Edited by:

Bernard Cohen,
Icahn School of Medicine
at Mount Sinai, USA

Reviewed by:

Eric Smouha,
Icahn School of Medicine
at Mount Sinai, USA
Gregory T. Whitman,
Massachusetts Eye and
Ear Infirmary, USA

*Correspondence:

Bryan K. Ward
bward15@jhmi.edu

Specialty section:

This article was submitted
to Neuro-otology,
a section of the journal
Frontiers in Neurology

Received: 25 January 2017

Accepted: 13 April 2017

Published: 28 April 2017

Citation:

Ward BK, Carey JP and Minor LB (2017) Superior Canal Dehiscence Syndrome: Lessons from the First 20 Years. *Front. Neurol.* 8:177.
doi: 10.3389/fneur.2017.00177

Superior semicircular canal dehiscence syndrome was first reported by Lloyd Minor and colleagues in 1998. Patients with a dehiscence in the bone overlying the superior semicircular canal experience symptoms of pressure or sound-induced vertigo, bone conduction hyperacusis, and pulsatile tinnitus. The initial series of patients were diagnosed based on common symptoms, a physical examination finding of eye movements in the plane of the superior semicircular canal when ear canal pressure or loud tones were applied to the ear, and high-resolution computed tomography imaging demonstrating a dehiscence in the bone over the superior semicircular canal. Research productivity directed at understanding better methods for diagnosing and treating this condition has substantially increased over the last two decades. We now have a sound understanding of the pathophysiology of third mobile window syndromes, higher resolution imaging protocols, and several sensitive and specific diagnostic tests. Furthermore, we have a treatment (surgical occlusion of the superior semicircular canal) that has demonstrated efficacy. This review will highlight some of the fundamental insights gained in SCDS, propose diagnostic criteria, and discuss future research directions.

Keywords: superior semicircular canal dehiscence syndrome, vestibular diseases, autophony, vertigo, labyrinth diseases

INTRODUCTION

In 1998, Minor et al. described a series of patients with symptoms of chronic disequilibrium and sound- or pressure-induced vertigo and nystagmus in the plane of the superior semicircular canal (1). Computed tomography (CT) imaging revealed a bony dehiscence over the superior semicircular canal in these patients, and a few underwent surgery to plug and resurface the superior semicircular canal, after which the primary symptoms improved. As additional patients were recognized, symptoms of bone conduction hyperacusis (i.e., hearing internal noises transmitted loudly to the affected ear) and pulsatile tinnitus became prominent features (2). The name superior canal dehiscence syndrome (SCDS) was used to describe patients with these unique symptoms associated with the presence of a bony dehiscence over the superior semicircular canal.

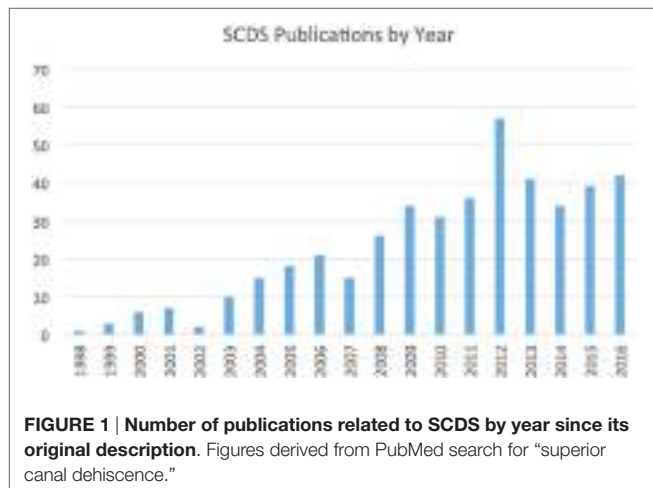
The syndrome has subsequently been modeled as a third mobile window in the labyrinth (3). Sound pressure entering the oval window via the stapes normally exits at the elastic round window. Superior canal dehiscence presents a novel low-impedance pathway for pressure entering at the oval window to dissipate through the labyrinth instead of the cochlea. For air-conducted sound, the result is a loss of energy and corresponding increase in thresholds for hearing. However, for bone-conducted sound, the opposite is true: the low impedance of the dehiscence permits bone-conducted

sound to access the perilymph of the inner ear *via* the labyrinth, and the free communication of the perilymph with the cochlea results in hearing bone-conducted sounds better than normal. This “bony hyperacusis” manifests as symptoms of autophony (hearing one’s own voice as loud or distorted); pulsatile tinnitus; and audible eye movements, footsteps, chewing, bowel movements, etc. The laboratory correlates are not only audiometric air-bone gaps, but characteristic negative bone conduction thresholds; yet, stapedial reflexes remain intact, a contradistinction from the characteristics of conductive hearing loss due to fixation of the stapes or other ossicles (4, 5). In addition, pressure gradients between the oval window and dehiscence cause flow of endolymph in the superior canal ampulla, causing vertigo and nystagmus corresponding to either excitation or inhibition of the superior canal. These pressure gradients can be generated in the ampullofugal (excitatory) direction by loud sound, positive pressure applied to the external auditory canal, or Valsalva against pinched nostrils. Conversely, ampullopetal (inhibitory) flow results from increases in intracranial pressure (e.g., Valsalva against closed glottis) or negative pressure applied to the external auditory canal (6). The third mobile window model has support not only from considerable clinical experience (7–9), including improvement or resolution of symptoms and signs with surgery that occludes and seals the bony defect, but also a growing experimental evidence as well (10–12).

Since the first publication, over 600 cases of SCDS have been reported, and research productivity directed at understanding better methods for diagnosing and treating this condition has substantially increased (Figure 1). This review will highlight some of the fundamental insights gained in SCDS, propose diagnostic criteria, and discuss future research directions.

HISTORICAL CONTEXT

Symptoms of sound-induced vertigo or dizziness have been recognized as a clinical complaint of patients related to the labyrinth for at least 70 years (13). In the early twentieth century Pietro Tullio observed in pigeons that when a hole was made in a semicircular canal, the labyrinth became responsive to externally applied sound stimuli, inducing eye and head movements in the plane



of the fenestrated canal (14, 15). Subsequent work by Huizinga attributed this observation to creating a new low-resistance pathway through the inner ear (16). Cawthorne described Tullio’s phenomenon in patients who had undergone fenestration procedures for otosclerosis in which the stapes was not fixed, creating a “third window” in the inner ear (17), Figure 2. Hennebert also identified patients with congenital syphilis in whom pressure applied to the ear canal produced vestibular symptoms and signs (18). We now commonly apply the term Tullio phenomenon to the symptom of vertigo in response to loud sound and Hennebert sign to the same symptoms and eye movements in response to an externally applied pressure at the ear canal.

David Robinson’s development of the magnetic scleral search coil allowed both improved accuracy of eye movement measurements and the recording of three-dimensional eye movements (19). With increased attention directed to observing eye movements in patients with Tullio phenomenon, several groups identified patients with vertical and torsional eye movements in response to loud sounds or pressure (20–22). A key insight that led to the discovery of SCDS was observing that when patients were exposed to pressure changes or loud sounds they had eye movements in the plane of the ipsilateral superior semicircular canal, linking their symptoms to anatomy. High-resolution CT imaging revealed a dehiscence in the bone over the superior semicircular canal in these patients, creating a “third window” as described by Cawthorne (1).

ETIOLOGY

Evolutionary adaptations have allowed the auditory and vestibular organs to maintain close proximity yet functional independence (23). The presence of a dehiscence can disturb this independence, leading both to alterations in the way sounds are transmitted to the ear and to vertigo in response to sound. The underlying pathophysiology of SCDS is the presence of a third mobile window in the inner ear, in addition to the oval and round windows (1). As a result of a dehiscence in the otic capsule, inner ear biomechanics are altered, such that low-frequency acoustic stimuli of high intensities may create a traveling wave toward the dehiscence, stimulating the vestibular end organs (3, 24). This shunting of acoustic energy creates both a distortion to sound perception, causing hyperacusis and reverberation, and sound-and pressure-evoked vertigo and dizziness (10, 25).

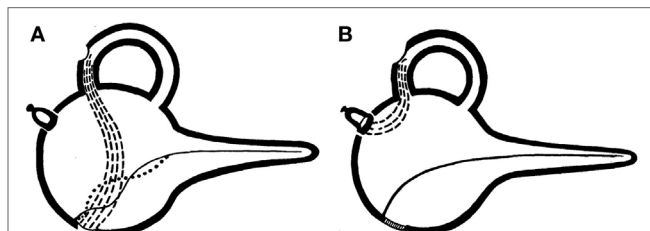


FIGURE 2 | Original graphical demonstrations by Cawthorne of the third mobile window effect. (A) Demonstrates the effect of semicircular canal fenestration in otosclerosis with a fixed stapes footplate and two mobile windows and (B) third mobile window established via semicircular canal fenestration in a patient with a mobile stapes footplate.

The etiology of SCDS is unknown, but it appears not to be cephalic displacement of the labyrinth during development (26). Currently, there are two primary theories: congenital and acquired. Based on the results of a large temporal bone study at Johns Hopkins (27), we believe SCDS is primarily a congenital phenomenon. From that study, temporal bones that showed thinning or dehiscence over the superior semicircular canal did not have evidence of bony remodeling except in rare cases (i.e., one patient with a meningioma). Others have found similar results in a patient who had confirmed SCDS during life (28). While otic capsule bone differs from the rest of the skeleton in having low bone turnover, the otic capsule is thought to develop for several years after birth. Many groups have observed that the prevalence of a dehiscence on CT is high in infants but decreases during the first decade of life (29–32), providing some support for the congenital theory. SCDS affects both ears in about 25% of patients, also consistent with congenital predisposition (33). Although there are a few cases of familial SCDS (34, 35) and a new report that indicates a high prevalence of canal dehiscence in patients with CDH23 variants (Usher syndrome type 1D) (36), strong genetic correlates have not been identified.

In as many as one quarter of cases, however, another inciting injury such as a traumatic head injury or Valsalva initiates symptoms (37). Many surgeons have noticed that patients with SCDS often have numerous tegmen defects (2, 38–40) as well as a dehiscent geniculate ganglion (41, 42), with some groups arguing that this supports a congenital etiology, and a few to speculate that over many years the slow pulsations of the brain and cerebrospinal fluid that surrounds it may lead to the development of both SCDS and tegmen defects (43). Intracranial hypertension has been hypothesized as contributing to SCDS; however, patients with SCDS tend not to be obese (44), suggesting obesity is not a mediator in the development of SCDS. Supporting the acquired theory is the observation on CT imaging of increasing thinning of the bone over the superior semicircular canal with advanced age (45, 46) and a few cases in which radiographic progression has been observed (47). Unusual cases of abnormalities of the middle and posterior cranial fossae have been identified as causing cases of SCDS (48–51), but these are exceptional.

Aside from dehiscence of the superior semicircular canal, several other sources of labyrinthine dehiscence can lead to symptoms similar to those in SCDS, including that of the posterior semicircular canal (52, 53), lateral semicircular canal (17, 54), vestibular aqueduct (55), facial nerve (56), internal auditory canal (57), and the carotid canal (58, 59). Merchant and Rosowski synthesized many of these reports and broadly proposed that any dehiscence of the inner ear can lead to an inner ear conductive hearing loss from a third mobile window (60). Beyond frank dehiscence, however, we have suggested that focal thinning—perhaps accompanied by pinpoint dehiscences—of otic capsule bone can in some cases transmit pressure and cause symptoms of SCDS (61), and others have suggested that a more global thinning in some conditions such as Paget's disease (60, 62) can lead to similar phenomena. Nakajima and colleagues have emphasized that any opening, even pinpoint ones, can sufficiently alter the impedance of the otic capsule to cause a functional third mobile window (12, 63).

SYMPTOMS

The most common symptoms of SCDS include bone conduction hyperacusis, autophony, pulsatile tinnitus, and sound- or pressure-induced vertigo (2, 37). Some of the internal noises that patients report as being particularly disturbing include hearing their eyeballs move, hearing their footfalls loudly, chewing, belching, or borborygmi. Patients also experience aural fullness. Chronic disequilibrium is common, and many patients with SCDS often report a sensation of "brain fog" that may be related to vestibular contributions to attention and other aspects of cognition (64). Patulous Eustachian tube dysfunction can also present with autophony, voice distortion, and pulsatile tinnitus (65). In patulous Eustachian tube dysfunction, hearing one's nasal breathing and symptom relief when in supine position are commonly thought to be distinguishing features; however, although breath autophony is uncommon in SCDS, half of patients with SCDS may experience symptom relief when supine (66).

Many patients with SCDS also have migraine, but this may represent the high prevalence of migraine in the general population and that SCDS is an effective migraine trigger. Some unusual symptoms have included a patient with tinnitus with head movements in the plane of the affected semicircular canal (67), as well as vertical head movements when hearing a loud sound. The vestibular system influences reflexes that control the neck musculature, as evidenced by the early vestibular physiology studies performed in pigeons and referenced above. It is therefore particularly interesting that a few patients can develop involuntary head movements in response to loud sounds, and that these movements occur in the plane of the superior semicircular canal (6). Vestibular contributions to the muscles controlling head movements may explain the neck muscular strain reported by some patients with SCDS.

Whether SCDS is progressive is unclear. It appears that the hearing loss does not significantly change over time (68). There have been reported cases of worsening conductive hearing loss over time and cases have been reported in which symptoms progressed over many years (35, 47, 69), while at least one case developed rapid mixed hearing loss (70). If SCDS is related to a congenital predisposition, patients may develop worsening symptoms as the dehiscence becomes larger with increasing age. As a result, pediatric patients may present differently than adults (69). Despite the high prevalence of an anatomic dehiscence noted on CT in young children (described above), only a few cases of pediatric SCDS has been reported (71), even fewer of whom underwent surgical repair (72).

DIAGNOSIS

Imaging

Computed tomography imaging demonstrating a dehiscence is an important diagnostic feature of SCDS, but it is not sufficient for diagnosis and may mislead the ordering physician. On review of 1,000 temporal bones, the prevalence of a dehiscent superior semicircular canal is 0.5% (27), yet as many as 9% of patients may have a dehiscence on a coronal temporal bone CT with 1-mm slice thickness (73). Higher resolution studies can improve diagnostic

accuracy. For the diagnosis of SCDS, temporal bone CT images should be obtained with slice thickness less than 1 mm (ideally 0.625 mm or less) and reformatted in the planes of the superior semicircular canal (Pöschl view) and orthogonal to it (Stenvers view). Due to volume averaging and other factors, however, CT imaging can still overcall a dehiscence (74). Furthermore, many patients with CT evidence of a dehiscence are asymptomatic, perhaps reflecting the protective role of inelastic dura in preventing pressure transmission through some bony dehiscences. In addition to a dehiscence of CT imaging, therefore, patients must also have both symptoms consistent with the syndrome and physiological evidence of a third mobile window.

Magnetic resonance imaging (MRI) has been explored as a possible alternative to CT for diagnosis (75, 76); and some centers routinely perform MRI (in addition to CT) to better evaluate the skull base for vascular malformations, masses, or encephaloceles prior to surgery. It has been our preference to reserve MRI only for cases of persistent symptoms after an initial attempt at surgery. If an MRI is performed, the best sequences for viewing the semicircular canals are heavily T2 weighted and have a variety of names depending on the MRI manufacturer (e.g., FIESTA, CISS). In these sequences, semicircular canal fluid signal is bright; loss of this signal can be useful for assessing adequacy of prior surgical plugging (77).

Clinical Exam

Fortunately, for diagnostic purposes a variety of abnormal physiologic findings have been observed in SCDS that can provide evidence of a third mobile window. In many of the first patients described by Minor et al., eye movements or nystagmus in the plane of the superior semicircular canal were observed, a critical finding that led to localizing the source of symptoms to the superior semicircular canal (6). In our practice, this test is performed during the clinic visit using an audiometer during which a range of different frequency tones are played to the ear at varying intensity while monitoring the patient's eye movements with video-oculography or Frenzel lenses. This finding is not observed in all patients (2), and when observed is not always in the plane of the superior semicircular canal. When the Tullio phenomenon elicits eye movements not in the plane of the superior semicircular canal, however, clinicians should consider alternative diagnoses due to the rarity of this finding. As mentioned above, approximately 20% of patients have head movements in the plane of the superior semicircular canal during this evaluation. Paradoxically, patients with larger dehiscence length (typically >5 mm) also can have impaired function of the affected superior semicircular canal due to "autoplugging" in which temporal dura herniates through the dehiscence and compresses the membranous duct (6).

Pure Tone Audiometry

On pure tone audiometry, one of the more common findings is a large air-bone gap at the lower frequencies (250, 500, and 1,000 Hz). As a result, many early cases were suspected of having otosclerosis; it is important to perform acoustic reflexes, as these are commonly normal in SCDS. There have been a few cases reported in which patients have both otosclerosis and SCDS, but these cases are atypical (78–80). Increased dehiscence length has

been shown to correlate with larger air-bone gaps (63, 81), and this is predicted on modeling of a dehiscence as well (63). In many patients, the bone conduction threshold at these frequencies is negative or better than normal. In order to capture this, however, audiometers must be calibrated appropriately, and audiologists need to be aware of the need to test bone conduction thresholds below 0 dB hearing level. A clinical assessment that is oftentimes confirmatory of negative bone conduction thresholds is Weber tuning fork testing, in which a struck 512 Hz tuning fork will be heard more loudly in the ear with greater bone conduction hyperacusis (i.e., negative thresholds). Sometimes, the tuning fork can be heard in the affected ear when placed on the medial malleolus or other distant bony prominences (82).

Vestibular-Evoked Myogenic Potentials (VEMPs)

Vestibular-evoked myogenic potentials are electromyographic potential reflex tests that in the non-dehiscent ear are thought to reflect function of the saccule (cervical VEMP) or utricle (ocular VEMP) (83). The cervical VEMP involves an inhibitory neural reflex pathway from the saccule to the ipsilateral sternocleidomastoid muscle. The ocular VEMP involves an excitatory pathway from the utricle to the contralateral inferior oblique muscle. In SCDS, these tests are frequently abnormal, as the affected ear is especially sensitive to the auditory or vibratory stimuli used to evoke these myogenic potentials. Patients with SCDS frequently have lower than normal thresholds for cervical VEMP responses to an audible click or tone burst and elevations in the ocular VEMP amplitude responses. Ocular VEMP amplitudes in particular have been found to be highly sensitive and specific for the diagnosis of an intraoperative confirmed dehiscence (84, 85). We therefore believe VEMPs to be an essential component to the diagnostics of SCDS.

Electrocochleography (ECoG)

Electrocochleography was formerly a popular test for endolymphatic hydrops associated with Meniere's disease. Arts et al. identified that patients with SCDS consistently have elevations in the summing potential (SP) to action potential (AP) ratio, and that this abnormality corrects after surgical plugging of the affected canal (86, 87). These findings have subsequently been observed by us and others (88, 89). While the results have not yet correlated with postoperative hearing outcomes, changes such as rapid rises in the SP are often observed during surgery and likely reflect changes in inner ear biomechanics during vestibular surgery. The clinical utility of this test for diagnosis and intraoperative use is still under investigation; nevertheless, ECoG appears to reflect the presence of a third mobile window, similar to the other diagnostic testing described above.

Diagnostic Criteria

The diagnosis of SCDS is based on the combination of CT evidence of a dehiscence, patient symptoms, and evidence of abnormal pressure transmission via a third mobile window (see **Figure 3**, for an example case). We synthesized the following diagnostic criteria for superior semicircular canal dehiscence syndrome

based on patients from our institution who had SCDS, underwent surgery, and reported improvement in symptoms (**Table 1**).

TREATMENT

Canal Plugging and Resurfacing

There are no known effective medical treatments for SCDS. While some patients with SCDS are content to have an explanation for their symptoms, some (about half in our experience) pursue surgery. We offer surgery to patients when we can relate their

symptoms to SCDS and when the patient can tell themselves that their symptoms are debilitating. As part of the original series on SCDS reported by Minor et al., a few patients underwent surgical resurfacing and/or plugging of the superior semicircular canal by middle cranial fossa approach and experienced resolution of symptoms (1). The goal of surgery is elimination of the third mobile window pathophysiology. A few of the original patients that underwent resurfacing alone without plugging experienced recurrence of symptoms after surgery (37). Since this report, it has been our practice to plug the affected canal in order to

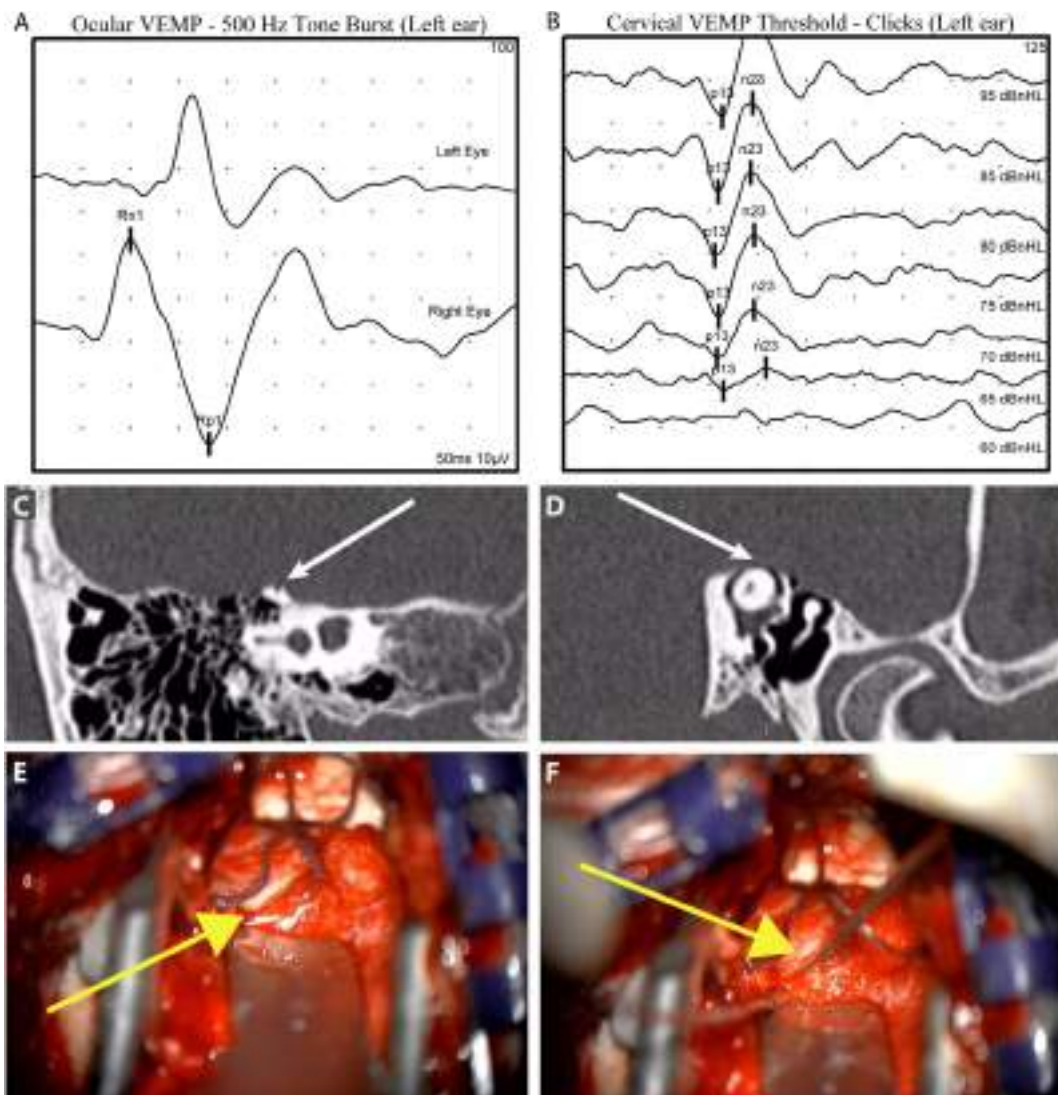


FIGURE 3 | Illustrative case to demonstrate diagnostic and intraoperative findings: a 40-year-old man presented with 6 years of left aural fullness, pulsatile tinnitus, vocal distortion, and hearing his eyeballs move in his left ear. Ocular vestibular-evoked myogenic potentials (VEMPs) indicated elevated amplitude responses to 500 Hz tone bursts [(A), 47.3 μ V, normal range 0–17 μ V] and cervical VEMPs with low thresholds in response to clicks [(B), 65 dB nHL, normal range \geq 80 dB nHL], both suggestive of a third mobile window syndrome involving the left ear. High-resolution computed tomography imaging with 0.6-mm slice thickness demonstrated a dehiscence of the left superior semicircular canal when image reconstructions were made orthogonal to the plane of the superior canal [(C), Stenvers view] and in the plane of the superior canal [(D), Pöschl view]. He elected to proceed with surgery via middle cranial fossa approach. The dehiscence measured 5 mm \times 1 mm [(E), yellow arrow] and was plugged with a combination of autologous materials including fascia, bone dust, and bone chips [(F)]. The middle cranial fossa was resurfaced with hydroxyapatite cement. Autophony improved after surgery, hearing was preserved, and vestibular dysfunction was limited to the superior semicircular canal as determined by clinical head impulse testing in all semicircular canal planes.

TABLE 1 | Proposed diagnostic criteria for superior canal dehiscence syndrome (SCDS).

Patients should meet the following conditions:

1. High-resolution computed tomography images (≤ 0.625 -mm slice thickness) reformatted in the plane of the superior SCC demonstrating a dehiscence
2. At least one of the following symptoms consistent with SCDS
 - A. Bone conduction hyperacusis (in the form of autophony, audible eye movements, audible footsteps, etc.)
 - B. Sound-induced vertigo
 - C. Pressure-induced vertigo (*via* nasal or glottic Valsalva or pressure applied to the external auditory canal)
 - D. Pulsatile tinnitus
3. At least one of the following diagnostic tests indicating a third mobile window
 - A. Negative bone conduction thresholds on pure tone audiometry
 - B. Enhanced VEMP responses (low cervical VEMP thresholds or high ocular VEMP amplitudes)
 - C. Elevated summating potential to action potential ratio on electrocochleography in the absence of a sensorineural hearing loss

SCC, semicircular canal; VEMP, vestibular-evoked myogenic potential.

VEMP thresholds should be compared to laboratory norms.

obtain a watertight seal with a combination of fascia, bone dust, and bone chips. The middle cranial fossa is then resurfaced with fascia and hydroxyapatite cement. At this time, numerous other groups have reported their series' with other plugging materials used such as bone wax (11) or bone dust and fibrin glue (90), and with reductions in patient symptoms reported regardless of plugging materials used. Resurfacing material also varies and can include cartilage, fascia, bone dust, fibrin glue, and hydroxyapatite cement. The transmastoid approach to plugging the canal has also been used in many cases with excellent results (38, 90–92). Prior to pursuing surgery, however, control of migraine is critical to avoid exacerbation of migraine after surgery and to distinguish treatable symptoms that are unlikely to be helped by repairing a dehiscence. Jung et al. recently showed patients with migraine have worse dizziness handicap than those without migraine, including after surgery (93).

The selection of surgical approach to repair the dehiscent canal should be based on the patient's anatomy (42) and on the experience of the treating surgeon. The middle cranial fossa approach is familiar to neurotologists and allows the advantages of directly observing the dehiscent canal and providing assurance that the canal is adequately plugged on either side of the dehiscence. In some cases in which the dehiscence is located adjacent to the superior petrosal sinus or the more posterior aspect of the canal near the common crus, the transmastoid approach is preferred. Alternatively, an angled endoscope may extend visualization for plugging *via* middle cranial fossa approach (94). Furthermore, in some cases the transmastoid approach is not feasible due to a contracted mastoid with a low-hanging tegmen. We feel a significant disadvantage of the transmastoid approach is the lack of directly seeing the dehiscence, thereby risking inadequate plugging on either side of the dehiscence. Some have suggested this can be circumvented by elevating dura over the dehiscence *via* the mastoid and using a mirror to ensure the canal is adequately plugged (92).

Patients generally do well after surgery to plug the affected semicircular canal, with improvements in autophony (9), dizziness

handicap (8), and overall health-related quality of life (95). This corresponds with elimination of the third mobile window, as has been demonstrated by the normalization of cervical VEMP thresholds (96), the ocular VEMP amplitudes (96), the elevated SP to AP ratio (86, 89), and the low-frequency air-bone gap (97). After surgical plugging, patients have expected reduction in the function of the superior semicircular canal (7, 98). About one-third of patients have a temporary pan-labyrinthine hypofunction (99), and approximately 15% have plugging material that also impacts function of the posterior semicircular canal (7). Benign paroxysmal positional vertigo has been reported in up to 25% of patients (100). Perhaps surprisingly in the history of otology, exposing and manipulating the membranous labyrinth at surgery only rarely results in a significant loss of hearing, even in patients undergoing revision surgery (97, 101–103). Approximately 25% of patients, however, develop a high-frequency sensorineural hearing loss (97, 104). In our experience, the recurrence rate from plugging and resurfacing of the canal is quite low (77). Furthermore, patients who undergo revision surgery for SCDS tend to do well, but the success rates are lower than in primary surgery.

Round Window Procedures

Some otologic surgeons have recently begun offering a procedure to reinforce the round window by a variety of methods as an attempt to dampen SCDS symptoms (105, 106). This procedure is proposed as a minimally invasive approach that might provide relief from SCDS symptoms. The proponents argue that stiffening the round window partially dampens one of the three inner ear windows, leaving the oval window and the dehiscence as the primary remaining inner ear windows. Lempert and other proponents of horizontal semicircular canal fenestration invoked a similar philosophy in the early treatment of otosclerosis (107), bypassing the fixed oval window and using instead the round window and a new semicircular canal fenestration to restore compression and rarefaction of inner ear fluids. There have been significant advancements in the understanding of inner ear biomechanics that would suggest that these approaches should induce vertigo, by shunting acoustic energy preferentially across vestibular sensory epithelia. This in fact appears to be the case with complete round window occlusion in two patients with SCDS who subsequently had the process reversed (106).

Furthermore, occlusion of the round window is thought to induce a hearing loss (108, 109). In the series by Silverstein et al., hearing loss was the only subjective survey measure that did not improve after round window reinforcement (106), others have reported a conductive hearing loss (105), and additional series of patients undergoing round window reinforcement by some of the authors have shown a mild hearing loss with this surgery in the non-dehiscent ear (110, 111). Among patients who have had this procedure performed elsewhere, we have observed that if successful, round window reinforcement has provided only temporary relief for SCDS and that some have reported hearing loss and new tinnitus. Whether this transient relief is caused by a reduction in hearing or some other mechanism remains to be determined, and thus far there has not been a proposed model to explain how this alteration in physiology can improve symptoms. We believe

this surgery requires additional study before it is recommended to patients.

FUTURE DIRECTIONS

There are many interesting remaining questions in SCDS. As described above, the etiology of SCDS remains unknown, in particular an explanation is needed for why patients tend to present later in life if this is primarily a congenital phenomenon. In some cases, symptoms occur after a traumatic incident or sudden increase in intracranial pressure leading to symptom onset. However, many patients do not report an inciting event. It may therefore be some combination of congenital and acquired pathology (112). Identifying the etiology is important for purposes of treatment, for if the etiology can be identified, research toward medical management may become feasible.

Comparative outcomes among surgical approaches are lacking, in part due to a lack of a well-designed disease-specific outcome measure in SCDS to assess for symptom improvement. A validated outcome measure would be a significant step forward in assessing post-intervention outcomes. We believe plugging the canal by middle cranial fossa approach currently is the gold standard for treatment based on the available data. This procedure reduces function of the superior semicircular canal and poses additional risk to the inner ear. While the outcome from canal plugging is supported by reductions in symptoms, improvements in quality of life, and a low risk of recurrence, methods of effectively addressing the pathology without producing impaired inner ear function would be desirable. Perhaps, individually fabricated 3D-printed reconstructions could prevent the third mobile window phenomena without risks of disease recurrence or persistence that have been observed with resurfacing alone (113).

While we know from temporal bone studies and surveys of CT imaging the approximate prevalence of an anatomic dehiscence, we still do not know the prevalence or incidence of SCDS or whether there are modifiable risk factors. For diagnosis, there are many available tests that appear to represent the abnormal pressure transmission associated with a third mobile window

(ocular and cervical VEMPs, pure tone audiometry, and ECoG), nevertheless, improved CT imaging techniques such as cone beam or flat panel CT may improve diagnostic accuracy. A recent study observed that some patients with SCDS may also have endolymphatic hydrops as determined by MRI with intratympanic gadolinium (114). This observation needs to be confirmed in a larger, well-defined population, for if confirmed, it may have implications for etiology.

Finally, we have identified some patients with thin, but not frankly dehiscent bone over the superior semicircular canal (i.e., near dehiscence) at the time of surgery (61). These patients often have symptoms of SCDS, physiologic evidence of a third mobile window, and in some cases are noted to have compliance of the thin bone at the time of surgery. On the other hand, these patients tended not to fair as well after surgical repair. It remains to be determined whether patients with thin bone over the superior semicircular canal have poorer outcomes, and additional data are needed.

CONCLUSION

Although there are still unanswered questions, superior semicircular canal dehiscence syndrome has become one of the most well-described vestibular disorders. Its physiologic basis is well established through tremendous progress over the last 20 years. This has been the result of a combination of several developments including our collective understanding of novel methods of vestibular testing, development of high-resolution imaging, and pioneering surgeries demonstrating the safety and efficacy of semicircular canal plugging. Consistent diagnostic criteria and a disease-specific outcome measure would allow improved ability to compare treatment outcomes in developing even safer and more enduring therapies.

AUTHOR CONTRIBUTIONS

BW reviewed literature and wrote the initial draft. JC and LM performed critical analysis of the initial draft and revisions.

REFERENCES

- Minor LB, Solomon D, Zinreich JS, Zee DS. Sound- and/or pressure-induced vertigo due to bone dehiscence of the superior semicircular canal. *Arch Otolaryngol Head Neck Surg* (1998) 124:249–58. doi:10.1001/archotol.124.3.249
- Minor LB. Superior canal dehiscence syndrome. *Am J Otol* (2000) 21:9–19. doi:10.1016/S0196-0709(00)80105-2
- Rosowski JJ, Songer JE, Nakajima HH, Brinsko KM, Merchant SN. Clinical, experimental, and theoretical investigations of the effect of superior semicircular canal dehiscence on hearing mechanisms. *Otol Neurotol* (2004) 25: 323–32. doi:10.1097/00129492-200405000-00021
- Mikulec AA, McKenna MJ, Ramsey MJ, Rosowski JJ, Herrmann BS, Rauch SD, et al. Superior semicircular canal dehiscence presenting as conductive hearing loss without vertigo. *Otol Neurotol* (2004) 25:121–9. doi:10.1097/00129492-200403000-00007
- Minor LB, Carey JP, Cremer PD, Lustig LR, Streubel S-O, Ruckenstein MJ. Dehiscence of bone overlying the superior canal as a cause of apparent conductive hearing loss. *Otol Neurotol* (2003) 24:270–8. doi:10.1097/00129492-200303000-00023
- Cremer PD, Minor LB, Carey JP, Della Santina CC. Eye movements in patients with superior canal dehiscence syndrome align with the abnormal canal. *Neurology* (2000) 55:1833–41. doi:10.1212/WNL.55.12.1833
- Carey JP, Migliaccio AA, Minor LB. Semicircular canal function before and after surgery for superior canal dehiscence. *Otol Neurotol* (2007) 28:356–64. doi:10.1097/01.mao.0000253284.40995.d8
- Crane BT, Minor LB, Carey JP. Superior canal dehiscence plugging reduces dizziness handicap. *Laryngoscope* (2008) 118:1809–13. doi:10.1097/MLG.0b013e31817f18fa
- Crane BT, Lin FR, Minor LB, Carey JP. Improvement in autophony symptoms after superior canal dehiscence repair. *Otol Neurotol* (2010) 31:140–6. doi:10.1097/MAO.0b013e3181bc39ab
- Carey JP, Hirvonen TP, Hullar TE, Minor LB. Acoustic responses of vestibular afferents in a model of superior canal dehiscence. *Otol Neurotol* (2004) 25:345–52. doi:10.1097/00129492-200405000-00024
- Cheng YS, Kozin ED, Remenschneider AK, Nakajima HH, Lee DJ. Characteristics of wax occlusion in the surgical repair of superior canal dehiscence in human temporal bone specimens. *Otol Neurotol* (2016) 37:83–8. doi:10.1097/MAO.0000000000000916
- Pisano DV, Niesten MEF, Merchant SN, Nakajima HH. The effect of superior semicircular canal dehiscence on intracochlear sound pressures. *Audiol Neurotol* (2012) 17:338–48. doi:10.1159/000339653
- Cawthorne T. The effect on hearing in man of removal of the membranous lateral semicircular canal. *Acta Otolaryngol* (1948) 36:145–9. doi:10.3109/00016484809122648

14. Addams-Williams J, Wu K, Ray J. The experiments behind the Tullio phenomenon. *J Laryngol Otol* (2014) 128:223–7. doi:10.1017/S0022215114000280
15. Tullio P. *The Ear and the Genesis of Language and Writing*. Berlin, Wien: Urban & Schwarzenberg (1929).
16. Huizinga E. The physiological and clinical importance of experimental work on the pigeon's labyrinth. *J Laryngol Otol* (1955) 69:260–8. doi:10.1017/S0022215100050635
17. Cawthorne T. Otosclerosis. *J Laryngol Otol* (1955) 69:437–56. doi:10.1017/S0022215100050933
18. Hennebert C. A new syndrome in hereditary syphilis of the labyrinth. *Press Med Belg Brux* (1911) 63:467.
19. Robinson D. A method of measuring eye movement using a scleral search coil in a magnetic field. *IEEE Trans Biomed Eng* (1963) 10:137–45.
20. Colebatch JG, Rothwell JC, Bronstein A, Ludman H. Click-evoked vestibular activation in the Tullio phenomenon. *J Neurol Neurosurg Psychiatry* (1994) 57:1538–40. doi:10.1136/jnnp.57.12.1538
21. Deecke L, Mergner T, Plester D. Tullio phenomenon with torsion of the eyes and subjective tilt of the visual surround. *Ann N Y Acad Sci* (1981) 374:650–5. doi:10.1111/j.1749-6632.1981.tb30908.x
22. Dieterich M, Brandt T, Fries W. Otolith function in man. Results from a case of otolith Tullio phenomenon. *Brain* (1989) 112(Pt 5):1377–92. doi:10.1093/brain/112.5.1377
23. Carey J, Amin N. Evolutionary changes in the cochlea and labyrinth: solving the problem of sound transmission to the balance organs of the inner ear. *Anat Rec A Discov Mol Cell Evol Biol* (2006) 288A:482–90. doi:10.1002/ar.a.20306
24. Grieser BJ, Kleiser L, Obrist D. Identifying mechanisms behind the Tullio phenomenon: a computational study based on first principles. *J Assoc Res Otolaryngol* (2016) 17:103–18. doi:10.1007/s10162-016-0553-0
25. Hirvonen TP, Carey JP, Liang CJ, Minor LB. Superior canal dehiscence: mechanisms of pressure sensitivity in a chinchilla model. *Arch Otolaryngol Head Neck Surg* (2001) 127:1331–6. doi:10.1001/archotol.127.11.1331
26. Potyagaylo VL, Delta Santina CC, Minor LB, Carey JP. Superior canal dehiscence is not due to cephalic displacement of the labyrinth. *Ann N Y Acad Sci* (2005) 1039:498–502. doi:10.1196/annals.1325.053
27. Carey JP, Minor LB, Nager GT. Dehiscence or thinning of bone overlying the superior semicircular canal in a temporal bone survey. *Arch Otolaryngol Head Neck Surg* (2000) 126:137–47. doi:10.1001/archotol.126.2.137
28. Teixido M, Kung B, Rosowski JJ, Merchant SN. Histopathology of the temporal bone in a case of superior canal dehiscence syndrome. *Ann Otol Rhinol Laryngol* (2012) 121:7–12. doi:10.1177/000348941212100102
29. Chen EY, Paladin A, Phillips G, Raske M, Vega L, Peterson D, et al. Semicircular canal dehiscence in the pediatric population. *Int J Pediatr Otorhinolaryngol* (2009) 73:321–7. doi:10.1016/j.ijporl.2008.10.027
30. Meiklejohn DA, Corrales CE, Boldt BM, Sharon JD, Yeom KW, Carey JP, et al. Pediatric semicircular canal dehiscence. *Otol Neurotol* (2015) 36:1383–9. doi:10.1097/MAO.0000000000000811
31. Saxby AJ, Gowdy C, Fandiño M, Chadha NK, Kozak FK, Sargent MA, et al. Radiological prevalence of superior and posterior semicircular canal dehiscence in children. *Int J Pediatr Otorhinolaryngol* (2015) 79:411–8. doi:10.1016/j.ijporl.2015.01.001
32. Sugihara EM, Babu SC, Kitsko DJ, Haupert MS, Thottam PJ. Incidence of pediatric superior semicircular canal dehiscence and inner ear anomalies. *Otol Neurotol* (2016) 37:1370–5. doi:10.1097/MAO.0000000000001194
33. Watters KF, Rosowski JJ, Sauter T, Lee DJ. Superior semicircular canal dehiscence presenting as postpartum vertigo. *Otol Neurotol* (2006) 27:756–68. doi:10.1097/01.mao.0000227894.27291.9f
34. El Hadi T, Sorrentino T, Calmels M-N, Fraysse B, Deguine O, Marx M. Spontaneous tegmen defect and semicircular canal dehiscence. *Otol Neurotol* (2012) 33:591–5. doi:10.1097/MAO.0b013e31824bae10
35. Niesten MEF, Lookabaugh S, Curtin H, Merchant SN, McKenna MJ, Grolman W, et al. Familial superior canal dehiscence syndrome. *JAMA Otolaryngol Head Neck Surg* (2014) 140:363. doi:10.1001/jamaoto.2013.6718
36. Noonan KY, Russo J, Shen J, Rehm H, Halbach S, Hopp E, et al. CDH23 related hearing loss. *Otol Neurotol* (2016) 37:1583–8. doi:10.1097/MAO.0000000000001210
37. Minor LB. Clinical manifestations of superior semicircular canal dehiscence. *Laryngoscope* (2005) 115:1717–27. doi:10.1097/01.mlg.0000178324.55729.b7
38. Brantberg K, Bergenius J, Mendel L, Witt H, Tribukait A, Ygge J. Symptoms, findings and treatment in patients with dehiscence of the superior semicircular canal. *Acta Otolaryngol* (2001) 121:68–75. doi:10.1080/000164801300006308
39. Nadaraja GS, Gurgel RK, Fischbein NJ, Anglemeyer A, Monfared A, Jackler RK, et al. Radiographic evaluation of the tegmen in patients with superior semicircular canal dehiscence. *Otol Neurotol* (2012) 33:1245–50. doi:10.1097/MAO.0b013e3182634e27
40. Suryanarayanan R, Lesser TH. “Honeycomb” tegmen: multiple tegmen defects associated with superior semicircular canal dehiscence. *J Laryngol Otol* (2010) 124:560. doi:10.1017/S0022215109991411
41. Isaacson B, Vrabec JT. The radiographic prevalence of geniculate ganglion dehiscence in normal and congenitally thin temporal bones. *Otol Neurotol* (2007) 28:107–10. doi:10.1097/01.mao.0000235968.53474.77
42. Lookabaugh S, Kelly HR, Carter MS, Niesten MEF, McKenna MJ, Curtin H, et al. Radiologic classification of superior canal dehiscence. *Otol Neurotol* (2014) 36:118–25. doi:10.1097/MAO.0000000000000523
43. Schutt CA, Neubauer P, Samy RN, Pensak ML, Kuhn JJ, Herschovitch M, et al. The correlation between obesity, obstructive sleep apnea, and superior semicircular canal dehiscence. *Otol Neurotol* (2015) 36:551–4. doi:10.1097/MAO.0000000000000555
44. Jan TA, Cheng YS, Landegger LD, Lin BM, Srikanth P, Niesten MEF, et al. Relationship between surgically treated superior canal dehiscence syndrome and body mass index. *Otolaryngol Head Neck Surg* (2017) 156:722–7. doi:10.1177/0194599816686563
45. Davey S, Kelly-Morland C, Phillips JS, Nunney I, Pawaroo D. Assessment of superior semicircular canal thickness with advancing age. *Laryngoscope* (2015) 125:1940–5. doi:10.1002/lary.25243
46. Jackson NM, Allen LM, Morell B, Carpenter CC, Givens VB, Kakade A, et al. The relationship of age and radiographic incidence of superior semicircular canal dehiscence in pediatric patients. *Otol Neurotol* (2014) 36:99–105. doi:10.1097/MAO.0000000000000660
47. Lookabaugh S, Niesten MEF, Owoc M, Kozin ED, Grolman W, Lee DJ. Audiologic, cVEMP, and radiologic progression in superior canal dehiscence syndrome. *Otol Neurotol* (2016) 37:1393–8. doi:10.1097/MAO.0000000000001182
48. Bae JS, Lim HW, An YS, Park HJ. Acquired superior semicircular canal dehiscence confirmed by sequential CT scans. *Otol Neurotol* (2013) 34:e45–6. doi:10.1097/MAO.0b013e31828d6753
49. Crane BT, Carey JP, McMenomey S, Minor LB. Meningioma causing superior canal dehiscence syndrome. *Otol Neurotol* (2010) 31:1009–10. doi:10.1097/MAO.0b013e3181a32d85
50. Goddard JC, Go JL, Friedman RA. Fibrous dysplasia causing superior canal dehiscence. *Otol Neurotol* (2013) 34:e1–2. doi:10.1097/MAO.0b013e3182355642
51. Koo J-W, Hong SK, Kim D-K, Kim JS. Superior semicircular canal dehiscence syndrome by the superior petrosal sinus. *J Neurol Neurosurg Psychiatry* (2010) 81:465–7. doi:10.1136/jnnp.2008.155564
52. Cremer PD, Migliaccio AA, Pohl DV, Curthoys IS, Davies L, Yavor RA, et al. Posterior semicircular canal nystagmus is conjugate and its axis is parallel to that of the canal. *Neurology* (2000) 54:2016–20. doi:10.1212/WNL.54.10.2016
53. Krombach GA, DiMartino E, Schmitz-Rode T, Prescher A, Haage P, Kinzel S, et al. Posterior semicircular canal dehiscence: a morphologic cause of vertigo similar to superior semicircular canal dehiscence. *Eur Radiol* (2003) 13:1444–50. doi:10.1007/s00330-003-1828-5
54. Zhang L-C, Sha Y, Dai C-F. Another etiology for vertigo due to idiopathic lateral semicircular canal bony defect. *Auris Nasus Larynx* (2011) 38:402–5. doi:10.1016/j.anl.2010.11.003
55. Merchant SN, Nakajima HH, Halpin C, Nadol JB, Lee DJ, Innis WP, et al. Clinical investigation and mechanism of air-bone gaps in large vestibular aqueduct syndrome. *Ann Otol Rhinol Laryngol* (2007) 116:532–41. doi:10.1177/000348940711600709
56. Blake DM, Tomovic S, Vazquez A, Lee HJ, Jyung RW. Cochlear-facial dehiscence – a newly described entity. *Laryngoscope* (2014) 124:283–9. doi:10.1002/lary.24223

57. Karlberg M, Annertz M, Magnusson M. Mondini-like malformation mimicking otosclerosis and superior semicircular canal dehiscence. *J Laryngol Otol* (2006) 120:419–22. doi:10.1017/S0022215106000934
58. Kim HHS, Wilson DF. A third mobile window at the cochlear apex. *Otolaryngol Head Neck Surg* (2006) 135:965–6. doi:10.1016/j.otohns.2005.04.006
59. Lund AD, Palacios SD. Carotid artery-cochlear dehiscence: a review. *Laryngoscope* (2011) 121:2658–60. doi:10.1002/lary.22391
60. Merchant SN, Rosowski JJ. Conductive hearing loss caused by third-window lesions of the inner ear. *Otol Neurotol* (2008) 29:282–9. doi:10.1097/mao.0b013e318161ab24
61. Ward BK, Wenzel A, Ritzl EK, Gutierrez-Hernandez S, Della Santina CC, Minor LB, et al. Near-dehiscence: clinical findings in patients with thin bone over the superior semicircular canal. *Otol Neurotol* (2013) 34:1421–8. doi:10.1097/MAO.0b013e318287ef6
62. Wackym PA, Wood SJ, Siker DA, Carter DM. Otic capsule dehiscence syndrome: superior semicircular canal dehiscence syndrome with no radiographically visible dehiscence. *Ear Nose Throat J* (2015) 94:E8–24.
63. Niesten MEF, Stieger C, Lee DJ, Merchant JP, Grolman W, Rosowski JJ, et al. Assessment of the effects of superior canal dehiscence location and size on intracochlear sound pressures. *Audiol Neurotol* (2015) 20:62–71. doi:10.1159/000366512
64. Bigelow RT, Agrawal Y. Vestibular involvement in cognition: visuospatial ability, attention, executive function, and memory. *J Vestib Res* (2015) 25:73–89. doi:10.3233/VES-150544
65. Poe DS. Diagnosis and management of the patulous eustachian tube. *Otol Neurotol* (2007) 28:668–77. doi:10.1097/mao.0b013e31804d4998
66. Zhou G, Gopen Q, Poe DS. Clinical and diagnostic characterization of canal dehiscence syndrome: a great otologic mimicker. *Otol Neurotol* (2007) 28:920–6. doi:10.1097/MAO.0b013e31814b25f2
67. Nam E-C, Lewis R, Nakajima HH, Merchant SN, Levine RA. Head rotation evoked tinnitus due to superior semicircular canal dehiscence. *J Laryngol Otol* (2010) 124:333–5. doi:10.1017/S0022215109991241
68. Patel NS, Hunter JB, O'Connell BP, Bertrand NM, Wanna GB, Carlson ML. Risk of progressive hearing loss in untreated superior semicircular canal dehiscence. *Laryngoscope* (2016) 127:1181–6. doi:10.1002/lary.26322
69. Hegemann SCA, Carey JP. Is superior canal dehiscence congenital or acquired? A case report and review of the literature. *Otolaryngol Clin North Am* (2011) 44:377–82. doi:10.1016/j.otc.2011.01.009
70. Wilkinson EP, Liu GC, Friedman RA. Correction of progressive hearing loss in superior canal dehiscence syndrome. *Laryngoscope* (2008) 118:10–3. doi:10.1097/MLG.0b013e31814b8d67
71. Lee GS, Zhou G, Poe D, Kenna M, Amin M, Ohlms L, et al. Clinical experience in diagnosis and management of superior semicircular canal dehiscence in children. *Laryngoscope* (2011) 121:2256–61. doi:10.1002/lary.22134
72. McCall AA, McKenna MJ, Merchant SN, Curtin HD, Lee DJ. Superior canal dehiscence syndrome associated with the superior petrosal sinus in pediatric and adult patients. *Otol Neurotol* (2011) 32:1312–9. doi:10.1097/MAO.0b013e31822e5b0a
73. Williamson RA, Vrabec JT, Coker NJ, Sandlin M. Coronal computed tomography prevalence of superior semicircular canal dehiscence. *Otolaryngol Head Neck Surg* (2003) 129:481–9. doi:10.1016/S0194-5998(03)01391-3
74. Curtin HD. Superior semicircular canal dehiscence syndrome and multi-detector row CT. *Radiology* (2003) 226:312–4. doi:10.1148/radiol.2262021327
75. Browaeys P, Larson TL, Wong ML, Patel U. Can MRI replace CT in evaluating semicircular canal dehiscence? *AJNR Am J Neuroradiol* (2013) 34:1421–7. doi:10.3174/ajnr.A3459
76. Krombach GA, Martino E, Martiny S, Prescher A, Haage P, Buecker A, et al. Dehiscence of the superior and/or posterior semicircular canal: delineation on T2-weighted axial three-dimensional turbo spin-echo images, maximum intensity projections and volume-rendered images. *Eur Arch Otorhinolaryngol* (2006) 263:111–7. doi:10.1007/s00405-005-0970-x
77. Sharon JD, Pross SE, Ward BK, Carey JP. Revision surgery for superior canal dehiscence syndrome. *Otol Neurotol* (2016) 37:1096–103. doi:10.1097/MAO.0000000000001113
78. Hope A, Fagan P. Latent superior canal dehiscence syndrome unmasked by stapedotomy for otosclerosis. *J Laryngol Otol* (2010) 124:428–30. doi:10.1017/S0022215109991654
79. Pritchett CV, Spector ME, Kileny PR, Heidenreich KD, El-Kashlan HK. Surgical treatment of hearing loss when otosclerosis coexists with superior semicircular canal dehiscence syndrome. *Otol Neurotol* (2014) 35:1163–7. doi:10.1097/MAO.0000000000000047
80. Yang CJ, Kim SA, Lee HS, Park HJ. A case of superior semicircular canal dehiscence syndrome with coexisting otosclerosis. *Korean J Otorhinolaryngol Head Neck Surg* (2016) 59:68. doi:10.3342/kjorhns.2016.59.1.68
81. Chien WW, Janky K, Minor LB, Carey JP. Superior canal dehiscence size: multivariate assessment of clinical impact. *Otol Neurotol* (2012) 33:810–5. doi:10.1097/MAO.0b013e318248eac4
82. Watson SR, Halmagyi GM, Colebatch JG. Vestibular hypersensitivity to sound (Tullio phenomenon): structural and functional assessment. *Neurology* (2000) 54:722–8. doi:10.1212/WNL.54.3.722
83. Curthoys IS. The interpretation of clinical tests of peripheral vestibular function. *Laryngoscope* (2012) 122:1342–52. doi:10.1002/lary.23258
84. Janky KL, Nguyen KD, Welgampola M, Zuniga MG, Carey JP. Air-conducted oVEMPs provide the best separation between intact and superior canal dehiscent labyrinths. *Otol Neurotol* (2013) 34:127–34. doi:10.1097/MAO.0b013e318271c32a
85. Zuniga MG, Janky KL, Nguyen KD, Welgampola MS, Carey JP. Ocular versus cervical VEMPs in the diagnosis of superior semicircular canal dehiscence syndrome. *Otol Neurotol* (2013) 34:121–6. doi:10.1097/MAO.0b013e31827136b0
86. Adams ME, Kileny PR, Telian SA, El-Kashlan HK, Heidenreich KD, Mannarelli GR, et al. Electrocochleography as a diagnostic and intraoperative adjunct in superior semicircular canal dehiscence syndrome. *Otol Neurotol* (2011) 32:1506–12. doi:10.1097/MAO.0b013e3182382a7c
87. Arts HA, Adams ME, Telian SA, El-Kashlan H, Kileny PR. Reversible Electrococleographic abnormalities in superior canal dehiscence. *Otol Neurotol* (2009) 30:79–86. doi:10.1097/MAO.0b013e31818d1b51
88. Park JH, Lee SY, Song J-J, Choi BY, Koo J-W. Electrococleographic findings in superior canal dehiscence syndrome. *Hear Res* (2015) 323:61–7. doi:10.1016/j.heares.2015.02.001
89. Wenzel A, Ward BK, Ritzl EK, Gutierrez-Hernandez S, Della Santina CC, Minor LB, et al. Intraoperative neuromonitoring for superior semicircular canal dehiscence and hearing outcomes. *Otol Neurotol* (2015) 36:139–45. doi:10.1097/MAO.0000000000000642
90. Agrawal SK, Parnes LS. Transmastoid superior semicircular canal occlusion. *Otol Neurotol* (2008) 29:363–7. doi:10.1097/MAO.0b013e3181616c9d
91. Crovetto M, Areitio E, Elexpuru J, Aguayo F. Transmastoid approach for resurfacing of superior semicircular canal dehiscence. *Auris Nasus Larynx* (2008) 35:247–9. doi:10.1016/j.anl.2007.06.010
92. Powell HRF, Khalil SS, Saeed SR. Outcomes of transmastoid surgery for superior semicircular canal dehiscence syndrome. *Otol Neurotol* (2016) 37:e228–33. doi:10.1097/MAO.0000000000001103
93. Jung DH, Lookabaugh SA, Owoc MS, McKenna MJ, Lee DJ. Dizziness is more prevalent than autophony among patients who have undergone repair of superior canal dehiscence. *Otol Neurotol* (2014) 36:126–32. doi:10.1097/MAO.0000000000000531
94. Carter MS, Lookabaugh S, Lee DJ. Endoscopic-assisted repair of superior canal dehiscence syndrome. *Laryngoscope* (2014) 124:1464–8. doi:10.1002/lary.24523
95. Remenschneider AK, Owoc M, Kozin ED, McKenna MJ, Lee DJ, Jung DH. Health utility improves after surgery for superior canal dehiscence syndrome. *Otol Neurotol* (2015) 36:1695–701. doi:10.1097/MAO.0000000000000886
96. Welgampola MS, Myrie OA, Minor LB, Carey JP. Vestibular-evoked myogenic potential thresholds normalize on plugging superior canal dehiscence. *Neurology* (2008) 70:464–72. doi:10.1212/01.wnl.0000299084.76250.4a
97. Ward BK, Agrawal Y, Nguyen E, Della Santina CC, Limb CJ, Francis HW, et al. Hearing outcomes after surgical plugging of the superior semicircular canal by a middle cranial fossa approach. *Otol Neurotol* (2012) 33:1386–91. doi:10.1097/MAO.0b013e318268d20d
98. Janky KL, Zuniga MG, Ward B, Carey JP, Schubert MC. Canal plane dynamic visual acuity in superior canal dehiscence. *Otol Neurotol* (2014) 35:844–9. doi:10.1097/MAO.0000000000000336
99. Agrawal Y, Migliaccio AA, Minor LB, Carey JP. Vestibular hypofunction in the initial postoperative period after surgical treatment of superior semicircular canal dehiscence. *Otol Neurotol* (2009) 30:502–6. doi:10.1097/MAO.0b013e3181a32d69

100. Barber SR, Cheng YS, Owoc M, Lin BM, Remenschneider AK, Kozin ED, et al. Benign paroxysmal positional vertigo commonly occurs following repair of superior canal dehiscence. *Laryngoscope* (2016) 126:2092–7. doi:10.1002/lary.25797
101. Beyea JA, Agrawal SK, Parnes LS. Transmastoid semicircular canal occlusion: a safe and highly effective treatment for benign paroxysmal positional vertigo and superior canal dehiscence. *Laryngoscope* (2012) 122:1862–6. doi:10.1002/lary.23390
102. Goddard JC, Wilkinson EP. Outcomes following semicircular canal plugging. *Otolaryngol Head Neck Surg* (2014) 151:478–83. doi:10.1177/0194599814538233
103. Van Haesendonck G, Van de Heyning P, Van Rompaey V. Retrospective cohort study on hearing outcome after transmastoid plugging in superior semicircular canal dehiscence syndrome: our experience. *Clin Otolaryngol* (2016) 41:601–6. doi:10.1111/coa.12539
104. Niesten MEF, McKenna MJ, Herrmann BS, Golman W, Lee DJ. Utility of cVEMPs in bilateral superior canal dehiscence syndrome. *Laryngoscope* (2013) 123:226–32. doi:10.1002/lary.23550
105. Nikkar-Esfahani A, Whelan D, Banerjee A. Occlusion of the round window: a novel way to treat hyperacusis symptoms in superior semicircular canal dehiscence syndrome. *J Laryngol Otol* (2013) 127:705–7. doi:10.1017/S0022215113001096
106. Silverstein H, Kartush JM, Parnes LS, Poe DS, Babu SC, Levenson MJ, et al. Round window reinforcement for superior semicircular canal dehiscence: a retrospective multi-center case series. *Am J Otolaryngol* (2014) 35:286–93. doi:10.1016/j.amjoto.2014.02.016
107. Lempert J. Physiology of hearing; what have we learned about it following fenestration surgery? *AMA Arch Otolaryngol* (1952) 56:101–13. doi:10.1001/archotol.1952.00710020120001
108. Borrman A, Arnold W. Non-syndromal round window atresia: an autosomal dominant genetic disorder with variable penetrance? *Eur Arch Otorhinolaryngol* (2007) 264:1103–8. doi:10.1007/s00405-007-0305-1
109. Elliott SJ, Ni G, Verschuur CA. Modelling the effect of round window stiffness on residual hearing after cochlear implantation. *Hear Res* (2016) 341:155–67. doi:10.1016/j.heares.2016.08.006
110. Silverstein H, Wu Y-HE, Hagan S. Round and oval window reinforcement for the treatment of hyperacusis. *Am J Otolaryngol* (2015) 36:158–62. doi:10.1016/j.amjoto.2014.10.014
111. Silverstein H, Ojo R, Daugherty J, Nazarian R, Wazen J. Minimally invasive surgery for the treatment of hyperacusis. *Otol Neurotol* (2016) 37:1482–8. doi:10.1097/MAO.0000000000001214
112. Park JH, I S, Choi HS, Lee SY, Kim J-S, Koo J-W. Thickness of the bony otic capsule: etiopathogenetic perspectives on superior canal dehiscence syndrome. *Audiol Neurotol* (2015) 20:243–50. doi:10.1159/000371810
113. Kozin ED, Remenschneider AK, Cheng S, Nakajima HH, Lee DJ. Three-dimensional printed prosthesis for repair of superior canal dehiscence. *Otolaryngol Head Neck Surg* (2015) 153:616–9. doi:10.1177/0194599815592602
114. Sone M, Yoshida T, Morimoto K, Teranishi M, Nakashima T, Naganawa S. Endolymphatic hydrops in superior canal dehiscence and large vestibular aqueduct syndromes. *Laryngoscope* (2016) 126:1446–50. doi:10.1002/lary.25747

Conflict of Interest Statement: The authors declare that the research was conducted in the absence of any commercial or financial relationships that could be construed as a potential conflict of interest.

The reviewer, ES, and handling Editor declared their shared affiliation, and the handling Editor states that the process nevertheless met the standards of a fair and objective review.

Copyright © 2017 Ward, Carey and Minor. This is an open-access article distributed under the terms of the Creative Commons Attribution License (CC BY). The use, distribution or reproduction in other forums is permitted, provided the original author(s) or licensor are credited and that the original publication in this journal is cited, in accordance with accepted academic practice. No use, distribution or reproduction is permitted which does not comply with these terms.



Balance Screening of Vestibular Function in Subjects Aged 4 Years and Older: A Living Laboratory Experience

Maria Carolina Bermúdez Rey^{1,2}, **Torin K. Clark**^{1,2,3} and **Daniel M. Merfeld**^{1,2,4*}

¹Jenks Vestibular Physiology Laboratory, Massachusetts Eye and Ear Infirmary, Boston, MA, United States, ²Otolaryngology, Harvard Medical School, Harvard University, Boston, MA, United States, ³Smead Aerospace Engineering Sciences, University of Colorado, Boulder, CO, United States, ⁴Otolaryngology, The Ohio State University, Columbus, OH, United States

OPEN ACCESS

Edited by:

Bernard Cohen,
Icahn School of Medicine at
Mount Sinai, United States

Reviewed by:

Aaron Camp,
University of Sydney, Australia
Bryan Kevin Ward,
Johns Hopkins University,
United States

*Correspondence:

Daniel M. Merfeld
merfeld.6@osu.edu

Specialty section:

This article was submitted
to Neuro-Otology,
a section of the journal
Frontiers in Neurology

Received: 21 July 2017

Accepted: 13 November 2017

Published: 28 November 2017

Citation:

Bermúdez Rey MC, Clark TK and
Merfeld DM (2017) Balance
Screening of Vestibular Function
in Subjects Aged 4 Years and Older:
A Living Laboratory Experience.
Front. Neurol. 8:631.
doi: 10.3389/fneur.2017.00631

To better understand the various individual factors that contribute to balance and the relation to fall risk, we performed the modified Romberg Test of Standing Balance on Firm and Compliant Support, with 1,174 participants between 4 and 83 years of age. This research was conducted in the Living Laboratory® at the Museum of Science, Boston. We specifically focus on balance test condition 4, in which individuals stand on memory foam with eyes closed, and must rely on their vestibular system; therefore, performance in this balance test condition provides a proxy for vestibular function. We looked for balance variations associated with sex, race/ethnicity, health factors, and age. We found that balance test performance was stable between 10 and 39 years of age, with a slight increase in the failure rate for participants 4–9 years of age, suggesting a period of balance development in younger children. For participants 40 years and older, the balance test failure rate increased progressively with age. Diabetes and obesity are the two main health factors we found associated with poor balance, with test condition 4 failure rates of 57 and 19%, respectively. An increase in the odds of having fallen in the last year was associated with a decrease in the time to failure; once individuals dropped below a time to failure of 10 s, there was a significant 5.5-fold increase in the odds of having fallen in the last 12 months. These data alert us to screen for poor vestibular function in individuals 40 years and older or suffering from diabetes, in order to undertake the necessary diagnostic and rehabilitation measures, with a focus on reducing the morbidity and mortality of falls.

Keywords: balance, aging, vestibular, screening, falls

INTRODUCTION

Falls are a leading cause of injury and death throughout the world. In 2003 in the US, fatal falls or hospitalizations for hip fractures occurred at a rate of approximately 36.8 per 100,000 people aged 65 and older (1). According to the World Health Organization (WHO) (2), “falls and consequent injuries are major public health problems. ... Falls lead to 20–30% of mild to severe injuries, and are the underlying cause of 10–15% of all emergency department visits. ... Falls [also] account for 40% of all injury deaths.”

Mobility changes with age are complex [e.g., (3)]. The WHO notes that biological factors, including age, interact with behavioral, environmental, and socioeconomic risks to yield fall risk (2). As a pertinent example for the data reported herein, postural control (i.e., “balance”) results from a combination of various subcomponents, such as biomechanics, movement strategies, sensory function, sensory integration, cognitive processing, etc. (4)—each of which can individually (or in combination) be impacted by dysfunction. Therefore, interventions ideally will vary by the individual case. For example, fall prevention for someone who suffers from poor vestibular function (e.g., vestibular hypofunction) will likely differ—at least in part—from fall prevention for someone with poor proprioception.

We focus herein on vestibular contributions to balance and falls because, as noted earlier: (a) the vestibular system is fundamental for balance (5–11) and (b) recent data show large increases in vestibular perceptual thresholds begin after age 40 (12). Data from patients with vestibular disorders demonstrate the crucial role that the vestibular system plays for balance control (5–11) as do some studies that combine vestibular modeling with empirical balance data (8, 13, 14).

Because balance testing provides a screening test for all vestibular organs (e.g., semicircular canals and otoliths) as well as central sensory integration, one standard screening used to approximate the prevalence of vestibular dysfunction is the fourth condition of a modified Romberg Test of Standing Balance on Firm and Compliant Support Surfaces (modified Romberg Test) (15, 16). Subjects must rely on their vestibular system for test condition 4 (C4), because the contribution of visual and kinesthetic cues are eliminated/reduced by closing the eyes and standing on thick memory foam, respectively. Therefore, failure to complete C4 of this modified Romberg test provides a proxy for vestibular dysfunction.

This modified Romberg test was performed during the National Health and Nutrition Examination Survey (NHANES) between 2001 and 2004, on US adults aged 40 years and older. Data show a C4 failure rate of 35.4% (15). In contrast, in a similar population study of 3,267 Korean adults aged 40 or older, data show a C4 failure rate of just 1.84% (16). The main methodological difference between these two balance studies was that for the American study, balance testing was performed with feet together (15), while for the Korean study, participants were asked to stand with their feet 10 cm apart (16), which provided a broader base of stability.

The US study reported that subjects who failed the same C4 test condition were 6.3 times more likely to have fallen in the past year (15). While speculative, our recent article showed calculations that combined the findings of these (and other) studies to suggest that 48,000 to 152,000 accidental deaths in the US each year might correlate with vestibular dysfunction (12). Even the lowest estimate, which would place this as the 10th leading cause of death, conveys the importance of understanding vestibular contributions to falls in otherwise healthy, but aging humans.

We are aware of only one earlier population study that performed balance testing focused on vestibular contributions for subjects younger than 20 years (17). This study included subjects between the age of 7 and 81. For sensory organization test number

6 (SOT6), which is considered a vestibular test condition, data showed a broad balance performance plateau between the ages of about 20 and 50 with performance degrading below the age of 20 and above the age of 50. However, this study did not correlate balance and fall history.

Given that there are no recent studies analyzing the vestibular contributions to balance in both children and adults, we intend to build upon the Agrawal study by testing a broader age group (participants 4 years of age and older) using the same modified Romberg test (15). We decided to use the version of the modified Romberg Test in which testing was performed with feet together because this is the one that has been used more extensively in the US population (15, 18, 19), it is more challenging than when performed using a wider stance (16), and it is the one that our group previously used to correlate with vestibular perceptual threshold data (12).

MATERIALS AND METHODS

This research was conducted in the Living Laboratory® at the Museum of Science, Boston, where all participants were museum visitors. Living Laboratory® is an innovative model for educating the public about human health and behavior. Museum visitors have the chance to engage in one-on-one conversations with scientists from their own community and participate in active research studies (20). During our time at the museum, one of the goals was to increase awareness of balance, including the importance of a normal and functional vestibular system for daily living (e.g., for balance).

All interested museum visitors aged 4 years or older were eligible to participate. For minors, the presence of a legal guardian was required. Subjects were excluded from balance testing if they were unable to stand unassisted, weighed more than 275 pounds, had a foot or leg amputation, were dizzy or lightheaded at the time of the test, or had a waist circumference that could not accommodate our largest standard safety gait belt (approximately 150 cm). Details on the number of subjects excluded are provided in the Section “Results.”

Informed consent was obtained from all subjects or their guardians as dictated by the Declaration of Helsinki. A waiver of documentation of consent was approved by the institutional ethical committee at the Massachusetts Eye and Ear Infirmary and the Museum of Science, since providing name and signature on the informed consent form would have provided the only Personally Identifiable Information collected for this study.

If eligible, participants filled out a questionnaire collecting demographic information (age, race, ethnicity, education), two questions regarding history of falls and dizziness in the last year, and cardiovascular risks. Subsequently subjects performed the modified Romberg test (details below). All study data were collected and managed using REDCap™ (Research Electronic Data Capture) electronic data capture tools hosted at the Massachusetts Eye and Ear Infirmary. REDCap™ is a secure, web-based application designed to support data capture for research studies (21). The Supplementary Material includes the exact text that the subjects responded to via a REDCap™ link. To avoid any impact of balance testing on subjective reports, the questionnaire was

always completed prior to the balance test. Details of each of these aspects are provided below.

Questionnaire

Exact wording of the questionnaire is provided in the Supplementary Material; here we provide a summary of the questions/items. Sex was grouped as male or female. Age at interview was collected in years. Height was recorded in feet and inches and weight in pounds. Ethnicity was grouped as American Indian/Alaska Native, Asian, White, Native Hawaiian or other Pacific Islander, Black or African American, and more than one race, following the NIH suggestion. In addition, participants were asked if they identified themselves as Hispanic/Latino or not. To estimate the presence of hypertension and diabetes, the following questions were used (each with yes/no answers): Do you have hypertension/high blood pressure? Do you take any blood pressure medication? Do you have diabetes/high blood sugar? Do you take any medication to lower blood sugar?

For subjects aged 18 or older, educational information, current smoking, pregnancy, and history of dizziness or balance impairment were also collected. Education was grouped as some high school, high school graduate including General Equivalency Diploma, some college, college graduate, and advanced degree. Current smoking included the number of years smoked and the current number of cigarettes smoked per day. In case a woman indicated she was pregnant, weeks of pregnancy were registered. Balance and dizziness was assessed *via* two questions: “during the past 12 months, have you had dizziness or difficulty with balance?” and “during the past 12 months, have you had difficulty with falling?”

Balance Testing

The modified Romberg test we used had four conditions. Each condition must be passed in order to move to the next condition. All conditions were performed standing with feet together and arms crossed. To pass the first condition (C1), each participant had to stand on the floor (firm surface) for 15 s with eyes open. To pass the second condition (C2), they had to stand on the floor for 15 s with eyes closed. To pass the third condition (C3), they had to stand on memory foam with eyes open for 30 s. To pass the final condition (C4), they had to stand on the foam with eyes closed for 30 s. This C4 test condition primarily assesses vestibular function, since visual contributions are eliminated and the foam makes kinesthetic cues unreliable (15, 22). The balance test was scored on a pass/fail basis. Failure was defined as participants needing to open their eyes, move their feet or arms to maintain stability, or be supported by the experimenter to prevent a fall before the timed trial duration. All subjects were allowed up to two attempts to complete each condition. For the two conditions (C3 and C4) requiring a foam pad, a Sunmate medium density foam pad (16 in × 18 in × 3 in") was used. Testing was performed by one of the authors (María Carolina Bermúdez Rey or Torin K. Clark).

Statistical Analysis

We calculated the prevalence of failing the C4 balance test condition, which serves as a proxy for vestibular dysfunction. Therefore, we will sometimes refer to the C4 balance test condition as the

“vestibular test condition.” A Fisher’s exact test was used to test for prevalence differences. Multiple logistic regression was used to estimate the odds of failing the vestibular condition in association with various sociodemographic and cardiovascular risk factors and to estimate the odds of reporting a fall associated with failing the vestibular condition. We fit our multiple logistic regression model mimicking the approach of Agrawal et al. (15), except where inappropriate (e.g., educational level was not included in the model fits with child and adolescent subjects). Collinearity between predictor variables was assessed with Chi-squared tests of association. Adjusting for multiple comparisons, significant associations were not found for most predictor variables; exceptions are noted in the Discussion. Five percent ($p < 0.05$) was the statistical criteria applied throughout. Analyses were performed using SAS statistical software (SAS Institute Inc., Cary, NC, USA).

RESULTS

A total of 1,227 museum goers filled out the initial questionnaire. Of these, 27 were excluded and 26 withdrew before completing the study, leaving a sample of 1,174 participants. Of these 1,174, none failed to complete conditions C1, C2, or C3. The overall prevalence of failure to complete C4 in this Living Laboratory experience was 11.24% (Table 1). The C4 failure rate was stable between 10 and 39 years of age, with a slight increase in the failure rate for participants 4–9 years of age. Above 40 years of age, the C4 failure rate increased significantly with age (Figure 1A). Among all adults (aged 18 years and older), the C4 failure rate was 12.65% [95% confidence interval (CI): 10.36–15.24%], while it was 21.70% (95% CI: 17.58–26.30%) for participants aged 40 years and older.

When looking at the influence of demographic characteristics, C4 failure rates did not differ by sex, race, or ethnicity (Table 1), nor did they differ by education level for adults aged 40 years and older (Table 2). Regarding cardiovascular risk factors in adults, C4 failure rate was significantly increased in individuals with a history of hypertension or a history of diabetes for the overall population, and a significant difference by body mass index (Table 3). There was no difference between smokers and non-smokers. Adults who reported a history of dizziness were more likely to fail C4, as were adults who reported falling in the past year (Table 3).

To take into account the potential effect of demographic characteristics and cardiovascular risk factors on the association between age and C4 failure, multivariate analyses were performed, noting a persistent influence of age on the odds of not completing C4 (“Adjusted OR” in Table 1 and Figure 1B). Analyses were performed in the overall population as well as in two subsamples: participants aged 18 years and older and those 40 years and older. For all three groups, increasing age was associated with increased odds of not completing C4; due to the similarity of the results, we only show data for the overall population (Table 1).

A self-reported history of diabetes was associated with a significant increase in the odds of not completing C4 in adjusted analyses (Figure 2), both for the overall population and the two subsamples (Table 3 shows the subsample of adults). The C4 failure rate among adults with diabetes was 57% (95% CI: 29–82%).

TABLE 1 | C4 failure rate by demographic factors and unadjusted and adjusted odds of failing C4 for participants 4 and older.

Characteristic	No. (%) of participants	Prevalence of C4 failure (95% CI) (%)	p-Value	C4 failure	
				Unadjusted OR (95% CI)	Adjusted OR (95% CI) ^a
All participants	1,174	11.24 (9.49–13.19)	–		
Sex					
Male	465 (39.61)	13.33 (10.38–16.76)	0.0728	1 (reference)	1 (reference)
Female	709 (60.39)	9.87 (7.78–12.31)		0.71 (0.49–1.04)	0.59 (0.39–0.89)
Age (years)					
4–9	201 (17.12)	10.45 (6.58–15.53)	<0.0001	3.20 (1.18–8.69)	3.04 (1.09–8.44)
10–19	283 (24.11)	6.01 (3.54–9.44)		1.75 (0.63–4.84)	1.73 (0.61–4.90)
20–29	184 (15.67)	5.43 (2.64–9.77)		1.57 (0.53–4.71)	1.65 (0.54–4.98)
30–39	142 (12.10)	3.52 (1.15–8.03)		1 (reference)	1 (reference)
40–49	165 (14.05)	9.70 (5.64–15.27)		2.94 (1.05–8.24)	3.04 (1.05–8.74)
50–59	84 (7.16)	15.48 (8.51–25.01)		5.01 (1.72–14.62)	4.37 (1.43–13.40)
60–69	75 (6.39)	34.67 (24.04–46.54)		14.53 (5.29–39.99)	15.35 (5.32–44.33)
≥70	40 (3.41)	60.00 (43.33–75.14)		41.01 (13.76–122.62)	44.60 (14.09–141.17)
Race^b					
White	987 (85.01)	11.35 (9.44–13.49)	0.5795	1 (reference)	1 (reference)
Black or African American	25 (2.15)	8.00 (0.98–26.03)		0.68 (0.16–2.92)	0.51 (0.10–2.76)
Asian	80 (6.89)	7.50 (2.80–15.61)		0.63 (0.27–1.49)	0.75 (0.28–2.00)
Other (American Indian, Hawaiian, and more than one race)	69 (5.94)	14.49 (7.17–25.04)		1.32 (0.66–2.66)	1.33 (0.60–2.94)
Ethnicity^c					
Non-Hispanic	1,097 (94.24)	10.94 (9.15–12.94)	0.1651	1 (reference)	1 (reference)
Hispanic	67 (5.76)	16.42 (8.49–27.48)		1.61 (0.74–3.22)	2.18 (0.99–4.90)

^aAdjusted for sex, age, race, ethnicity, and history of diabetes, and hypertension.

^bData were missing for 13 participants.

^cData were missing for 10 participants.

Bold text identifies a statistically significant finding. The p value shown for age ($p < 0.0001$) is the result of a statistical test comparing all age groups in the same test. When analyzed separately (as pairs), there was no significant difference in the prevalence of C4 failure for the following pairs: 4–9 vs. 10–19, 4–9 vs. 20–29, 4–9 vs. 40–49, 4–9 vs. 50–59, 10–19 vs. 20–29, 10–19 vs. 30–39, 10–19 vs. 40–49, 20–29 vs. 30–39, 20–29 vs. 40–49, and 40–49 vs. 50–59 years (p values between 0.09 and –0.84). The other 16 pairs show a significant difference in the prevalence of C4 failure, with p values ranging from 0.04 to 0.00000001. OR, odds ratio.

Surprisingly, females had significantly lower odds of not completing C4 (i.e., increased odds of completing C4) in the multivariate analyses adjusting for age, race ethnicity and cardiovascular risk factors (Table 1). In our sample, adult females were significantly associated with having lower body mass index, which we further consider in the section “Discussion.”

History of hypertension, smoking, self-reported dizziness and history of falls did not increase the odds of not completing C4 following adjusted analyses, both for the overall population and the two subsamples (Table 3 shows the subsample of adults). Having a history of hypertension was significantly associated with age, self-reported dizziness, and body mass index. When we refit the model without a history of hypertension as a predictor, it did not impact the significance of the other variables (not shown). For adults, failure to complete C4 was similarly not associated with an increase in the odds of self-reported dizziness or history of falls, even after adjusted analyses (Table 4).

When looking at time to failure in the last test condition (where 30 s corresponds to passing C4), there was no statistically significant difference between age groups ($p = 0.9121$, data not shown). However, for adults, as the time to failure shortened, there was a significant increase in both the prevalence and the odds of falling (defined as self-reported history of falling in the last year) (Figure 3). Only 1.7% of adults who passed C4 by maintaining balance for 30 s reported falls in the previous year, whereas for those

who were only able to maintain balance for less than 10 s, fall prevalence was 8.5%—five times higher than for participants who passed C4 (Table 5). Consistent with this prevalence finding, the odds of falling increased as the time to failure shortened, reaching statistical significance only for participants who failed in less than 10 s, having a 5.6-fold increase in the odds of falling (Table 5).

DISCUSSION

These findings suggest that vestibular contributions to balance are relatively stable between the ages of 10–39, with the lowest C4 failure rate for participants 30–39 years of age (3.52%). As a novel finding, there was a slightly higher C4 failure rate (10.45%) for participants 4–9 years of age, presumably representing the development of balance in younger individuals. Above age 40, as previous studies have shown (15, 16, 19), the C4 failure rate increased markedly and progressively, reaching a rate of 60% above age 70, making balance deficits due to poor vestibular function fairly common. This general pattern also occurred in an earlier study of balance using the computerized posturography SOT6 as the “vestibular condition” (17). Furthermore, our rate of C4 failure for adults aged 40 years and older (21.70%) is comparable with the 35% rate reported from the NHANES study (15), as is the pattern of increase seen as participants become

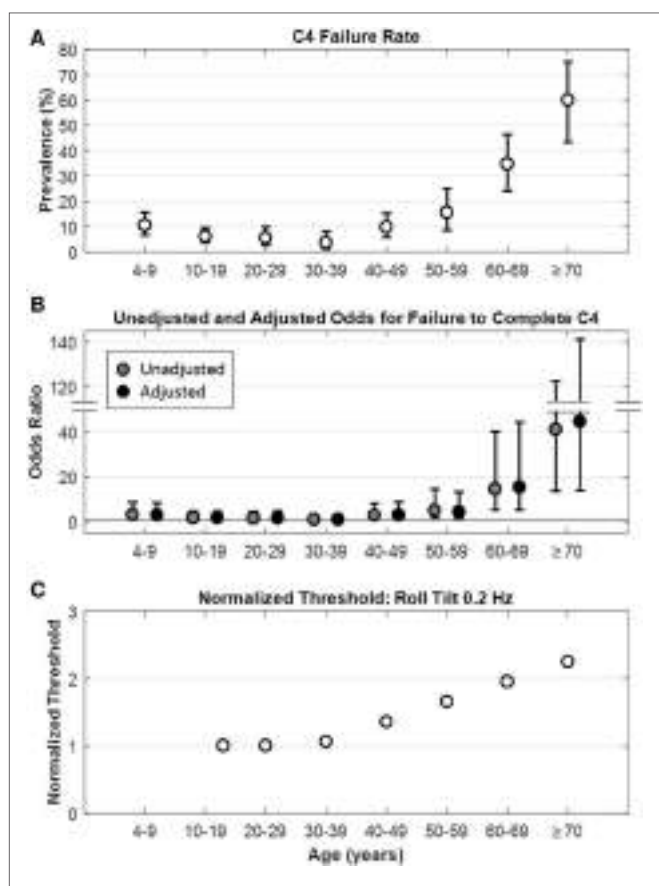


FIGURE 1 | Relationship between age and C4 failure. **(A)** Rate of C4 failure as a function of age ($p < 0.0001$), whiskers show $\pm 95\%$ confidence intervals. **(B)** Unadjusted (●) and adjusted (●) odds ratios for failure to complete C4 by age. Whiskers show $\pm 95\%$ confidence intervals. Gray horizontal line is the line of null effect. Odds ratios were adjusted for sex, age, race, ethnicity, and history of diabetes and hypertension. **(C)** Model fit for roll tilt 0.2 Hz thresholds as a function of age in healthy participants, from Bermúdez Rey et al. (12).

TABLE 2 | C4 balance test failure rate by educational level in adults 40 and older.

Characteristic	Number of participants	C4 balance test, % failure (95% CI)	p-Value
All participants	364	21.70 (17.58–26.30)	—
Educational level			
Some high school	6 (1.65)	33.33 (4.33–77.72)	0.547
High school graduate including GED	15 (4.13)	33.33 (11.82–61.62)	
Some college	78 (21.49)	24.36 (15.35–35.40)	
College graduate	116 (31.96)	18.97 (12.28–27.29)	
Advanced degree	148 (40.77)	20.95 (14.70–28.39)	

older. Our lower C4 failure rate may have resulted from selection bias, owing to the general degree of health required for someone to be able to visit a museum in comparison to the health of the general population.

Here, we find the vestibular contributions to balance degrade with age above 40. We have previously shown that vestibular

perceptual thresholds increase with age above the age of about 40 (Figure 1C) (12). These two data sets support the idea that only after age 40 do age effects on the vestibular system become substantial enough to alter balance function or vestibular perception thresholds in the general adult population.

Our recent study also showed that variations in vestibular function measured directly in healthy “normals”—specifically, variations in vestibular perceptual roll tilt thresholds—were highly correlated with balance function. Specifically, we reported strong correlations between healthy subjects’ inability to complete C4 with increasing yaw rotation (1.04 vs. 1.43°/s), y-translation (0.69 vs. 1.05 cm/s), z-translation (1.62 vs. 3.67 cm/s), and roll tilt (0.40s vs. 0.76°/s at 0.2 Hz) thresholds (12). These self-motion perceptual thresholds have previously been shown to be 2–50× higher in fully compensated patients suffering total vestibular loss (23), suggesting a dominant role of the vestibular system. Consistent with earlier findings linking age and balance deficits [e.g., (17, 24–26)], we too reported that increasing age was linked to these balance test failures. But even when age was considered as an independent factor, balance test failures were still correlated with higher roll tilt thresholds at both 0.2 and 1 Hz. The fact that only roll tilt thresholds (and not the other thresholds measured) correlated with balance test failures after adjusting for age shows that this is not due to a general vestibular degradation. Rather, the fact that only roll tilt thresholds correlated with C4 failure suggests (but does not prove) a causal contribution since roll tilt vestibular cues are directly relevant to postural control in the roll plane. Furthermore, that the effect was particularly prominent at 0.2 Hz suggests the importance of both the semicircular canals and otoliths, since roll tilt thresholds near this frequency have been shown to require the integration of sensory cues from the canals and otoliths (27).

As we mentioned, females had significantly higher odds of completing C4 in the multivariate analyses adjusting for age, race ethnicity and cardiovascular risk factors. We do not know how to interpret that sex showed a significant effect on the odds of failing C4. Since we chose to use the standard statistical criterion ($p = 0.05$), it is certainly possible that this could be one of the 1 in 20 random effects that happen to appear significant when tested. Alternatively, the museum population could have led to some sort of selection bias—either in who attended the museum or who agreed to participate. For example, we note adult females in our population had a significantly lower body mass index. This association makes it difficult to attribute the reduced odds of failing C4 to either sex or body mass index. Of course, there could be a real effect of sex on balance. Since C4 is the vestibular condition, this would potentially suggest that age-matched women had better vestibular function, but this hypothesis is not consistent with our recent comprehensive testing of vestibular thresholds that found no significant difference in five different vestibular thresholds (12). We are not aware of any other studies establishing substantive sex differences for either balance tasks or vestibular measures.

When we look at health factors associated with a higher rate of C4 failure, self-reported history of diabetes stands out at 57% (95% CI: 29–82%)—a percentage almost as high as the one for individuals 70 years of age and above—and with a 4.3

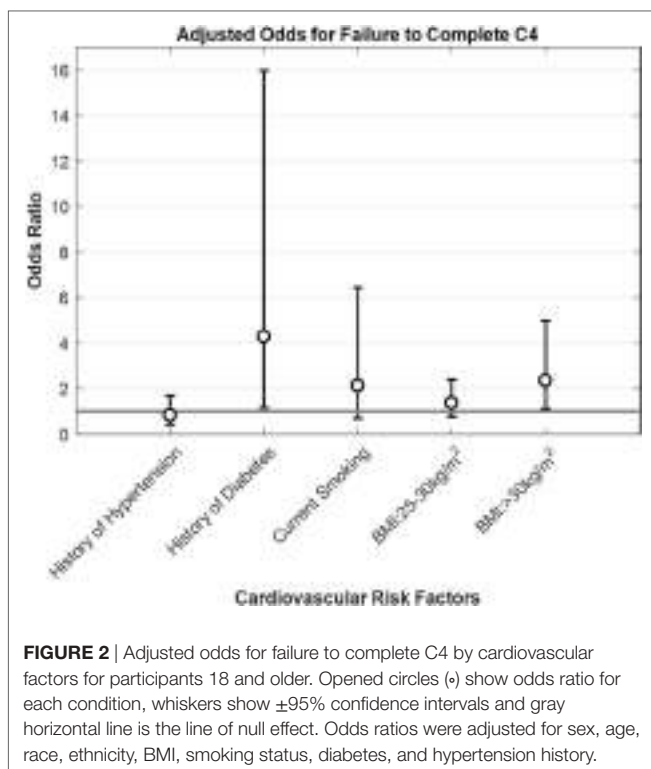
TABLE 3 | C4 failure rate and odds for cardiovascular factors for participants 18 and older.

Characteristic	No. (%) of participants	Prevalence of C4 failure (95% CI) (%)	p-Value	C4 failure	
				Unadjusted OR (95% CI)	Adjusted OR (95% CI) ^a
All participants	751	12.65 (10.36–15.24)	–		
History of hypertension^b					
No	667 (88.93)	10.49 (8.27–13.07)	< 0.0001	1 (reference)	1 (reference)
Yes	83 (11.07)	30.12 (20.53–41.18)		3.68 (2.06–6.40)	0.83 (0.41–1.69)
History of diabetes mellitus^b					
No	736 (98.13)	11.82 (9.58–14.38)	< 0.0001	1 (reference)	1 (reference)
Yes	14 (1.87)	57.14 (28.86–82.34)		9.95 (2.93–35.46)	4.29 (1.15–15.99)
Smokers^c					
No	713 (95.19)	12.62 (10.27–15.29)	0.7973	1 (reference)	1 (reference)
Yes	36 (4.81)	13.89 (4.67–29.50)		1.12 (0.33–3.00)	2.13 (0.70–6.44)
BMI (kg/m²)					
<25	402 (53.53)	9.45 (6.78–12.74)	0.0116	1 (reference)	1 (reference)
25–30	253 (33.69)	15.42 (11.20–20.46)		1.75 (1.08–2.81)	1.36 (0.78–2.39)
30≤	96 (12.78)	18.75 (11.51–28.00)		2.21 (1.20–4.08)	2.35 (1.11–4.98)
Self-reported dizziness^b					
No	666 (88.80)	11.56 (9.23–14.24)	0.0146	1 (reference)	1 (reference)
Yes	84 (11.20)	21.43 (13.22–31.74)		2.09 (1.10–3.78)	1.36 (0.66–2.77)
History of falls					
No	734 (97.87)	12.26 (9.98–14.86)	0.041	1 (reference)	1 (reference)
Yes	16 (2.13)	31.25 (11.02–58.66)		3.25 (0.86–10.42)	2.21 (0.53–9.17)

^aAdjusted for sex, age, race, ethnicity, BMI, smoking status, as well as diabetes and hypertension history.^bData were missing for one participant.^cData were missing for two participants.

Bold text identifies a statistically significant finding.

OR, odds ratio.

**FIGURE 2** | Adjusted odds for failure to complete C4 by cardiovascular factors for participants 18 and older. Opened circles (•) show odds ratio for each condition, whiskers show $\pm 95\%$ confidence intervals and gray horizontal line is the line of null effect. Odds ratios were adjusted for sex, age, race, ethnicity, BMI, smoking status, diabetes, and hypertension history.

(95% CI: 1.15–15.99) increase in the odds of failing the C4 test condition, which supports the suggestion that diabetes mellitus is a risk factor for vestibular dysfunction (18, 28, 29). It is well

known that diabetics have an increased risk of falling (18, 30), which has been attributed primarily to peripheral neuropathy (31–34). Studies have shown the association between diabetes and altered vestibular tests, like cervical vestibular-evoked myogenic potentials and ocular VEMP (35, 36), head thrust dynamic visual acuity testing (36), vestibulo-ocular reflex, and optokinetic reflex (37).

Furthermore, studies have demonstrated the role of vestibular function in the risk of falling for people suffering diabetes (18, 38). Having determined that diabetes increases the risk of falls, it is even more important to develop a screening tool that allows us to establish if the risk is higher due to poor vestibular function. In the case that this is proven to be true, potentially helpful therapies focused on vestibular rehabilitation (39) could be initiated in a prompt manner, when pertinent. The urgency of this matter is highlighted because of the increased risk of hip, foot, and spine fractures in adults suffering diabetes, that is not attenuated after adjustment for diabetes-related complications (40), thus increasing morbidity and mortality of a potential fall.

A second health factor that deserves a special mention is BMI. In this study, as BMI increases, the rate of failure of C4 increases too (Table 3), going from 9.45% (95% CI: 6.78–12.74%) for people with $BMI < 25 \text{ kg/m}^2$ (normal range) to 18.75% (95% CI: 11.51–28.00%) for individuals with $BMI \geq 30 \text{ kg/m}^2$ (obese). More importantly, there was a significant 2.4-fold increase in the odds of failing C4 for $BMI \geq 30 \text{ kg/m}^2$, after adjusting for sex, age, race, ethnicity, smoking status, as well as diabetes and hypertension history. This suggests an association between obesity and poor vestibular function. A large national German study

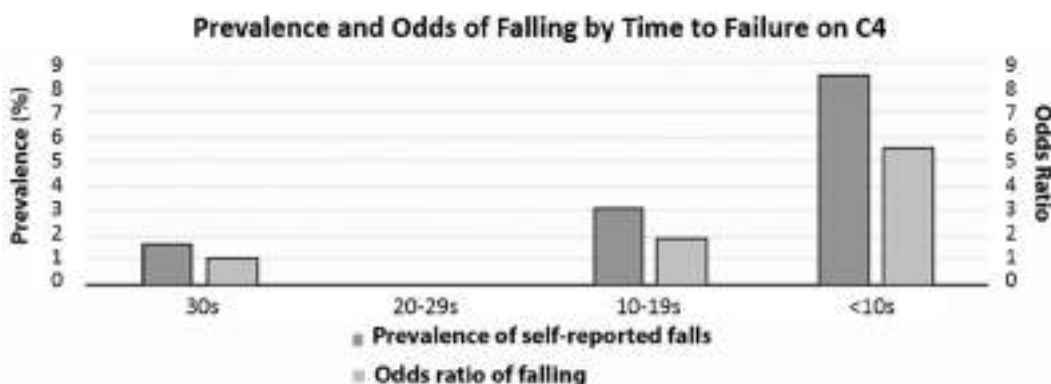
TABLE 4 | Prevalence and odds of self-reported dizziness and history of falls for participants who passed and failed the vestibular balance test condition (C4).

C4 balance test failure	Self-reported dizziness			History of falls		
	Prevalence	Unadjusted OR	Adjusted OR ^a	Prevalence	Unadjusted OR	Adjusted OR ^a
No	10.08 (7.88–12.64)	1 (reference)	1 (reference)	1.68 (0.84–2.98)	1 (reference)	1 (reference)
Yes	18.95 (11.63–28.28)	2.09 (1.10–3.78)	1.39 (0.69–2.80)	5.26 (1.73–11.86)	3.25 (0.86–10.42)	2.0 (0.47–8.50)

^aAdjusted for sex, age, race, ethnicity, BMI, smoking status, and history of diabetes and hypertension.

Bold text identifies a statistically significant finding.

OR, odds ratio.

**FIGURE 3** | Prevalence and odds of falling by time to failure of C4. Dark gray bars show % of C4 failure and light gray bars show odds ratio of falling. None of the 16 participants who failed C4 between 20 and 29 s self-reported falls in the last 12 months.**TABLE 5** | Prevalence and odds of falling with time to failure on C4.

Time to failure (s)	N	Prevalence (95% CI)	OR (95% CI)
30	656	1.7 (0.8–3.0)	1 (reference)
20–29	16	0	ND
10–19	32	3.1 (0.1–16.2)	1.9 (0.2–15.1)
<10	47	8.5 (2.4–20.4)	5.5 (1.7–17.9)

Bold text identifies a group that is statistically significantly different from the reference group.

OR, odds ratio; ND, no data.

(41), found a significant 1.8-fold increase in the odds of having vestibular vertigo both for individuals categorized as overweight (BMI 25–30 kg/m²) or obese (BMI ≥ 30 kg/m²). Furthermore, posturography differences between obese subjects and their lean counterparts have been reported by multiple studies, both in children (42, 43) and adults (42, 44–46). Given that more than one-third (36.5%) of US adults and about 17% of US children and adolescents meet obesity criteria (47), an effort to elucidate if obesity might contribute to vestibular dysfunction (e.g., via glycation or another mechanism) and to establish if treating obesity improves either vestibular function or balance performance might impact public health.

As in the Agrawal study (15), these data show that individuals who fail C4 were more likely to report having dizziness and a history of falls. In both studies, when performing unadjusted analyses, those who reported a history of falling were significantly more likely to fail C4. Unexpectedly, for our data when we performed

the adjusted analysis accounting for other factors, there was no significant increase in the odds of falling for people who fail C4 (Table 3). This differs from the findings reported earlier (15) but may be due to the small number of individuals who reported falls in our study (16 of 751 of participants 18 and older) and/or may be related to a possible sampling bias described earlier whereby individuals who go to the museum may be healthier than a random population sampling. Specifically, while speculative, individuals who have recently (e.g., in the past year) fallen may decide to go to the Museum less frequently than individuals who have not recently fallen. We note that while not significant, the estimated odds for failing C4 was 2.2 for individuals who reported falling in the last year.

We did notice an increase in the odds of having fallen in the last year as performance times on C4 decrease. Specifically, once individuals dropped below a time failure of 10 s, there was a significant 5.5-fold increase in the odds of having fallen (Table 5). This failure time of 10 s is lower than the trial duration identified by a previous study (20 s) as the threshold at which the risk of falling rises (19). Of all people who fail C4, individuals who fall before 10 s might be the ones who benefit the most from therapies that focus on balance enhancement and fall risk reduction, especially if they have diabetes, osteoporosis or other factors that predispose individuals to fractures.

We note that failing C4 of our modified Romberg test only suggests poor vestibular function, but is not able to confirm the presence of vestibular dysfunction or to diagnose the exact vestibular modality (modalities) affected (i.e., rotational transduced

via semicircular canals, translational transduced *via* saccule or utricle, or tilt *via* central integration of canal and otolith cues). Thus further correlations between balance abnormalities and objective measures of each vestibular modality, as in our earlier study (12), are imperative. This knowledge can be used for the purpose of better understanding the role of vestibular function for balance and how poor vestibular function contributes to the risk of falls, and to design and test vestibular rehabilitation techniques. Since such clinical vestibular tests take time and require health care resources, which are limited, it is not difficult to envision using a simple balance test as a screen to determine who needs full vestibular function tests (e.g., a comprehensive set of perceptual threshold assays).

ETHICS STATEMENT

This study was carried out in accordance with the recommendations of Massachusetts Eye and Ear Infirmary institutional review board, with informed consent from all subjects. Informed consent was obtained from all subjects or their guardians in accordance with the Declaration of Helsinki; due to the minimal risk characteristics of this study, a waiver of documentation of consent was granted. The protocol was approved by the institutional ethical committee.

REFERENCES

1. Centers for Disease Control and Prevention (CDC). Fatalities and injuries from falls among older adults—United States, 1993–2003 and 2001–2005. *MMWR Morb Mortal Wkly Rep* (2006) 55(45):1221–4.
2. WHO. *WHO Global Report on Falls Prevention in Older Age*. Geneva: World Health Organization (2008).
3. Varma VR, Hausdorff JM, Studenski SA, Rosano C, Camicioli R, Alexander NB, et al. Aging, the central nervous system, and mobility in older adults: interventions. *J Gerontol A Biol Sci Med Sci* (2016) 71(11):1451–8. doi:10.1093/gerona/glw080
4. Horak FB. Postural orientation and equilibrium: what do we need to know about neural control of balance to prevent falls? *Age Ageing* (2006) 35 (Suppl 2):ii7–11. doi:10.1093/ageing/afl077
5. Nashner LM, Black FO, Wall C III. Adaptation to altered support and visual conditions during stance: patients with vestibular deficits. *J Neurosci* (1982) 2(5):536–44.
6. Horak F, Nashner L, Diener H. Postural strategies associated with somatosensory and vestibular loss. *Exp Brain Res* (1990) 82(1):167–77. doi:10.1007/BF00230848
7. Allum J, Adkin A, Carpenter M, Held-Ziolkowska M, Honegger F, Pierchala K. Trunk sway measures of postural stability during clinical balance tests: effects of a unilateral vestibular deficit. *Gait Posture* (2001) 14(3):227–37. doi:10.1016/S0966-6362(01)00132-1
8. Peterka RJ. Sensorimotor integration in human postural control. *J Neurophysiol* (2002) 88(3):1097–118.
9. Mergner T, Schweigart G, Maurer C, Blumle A. Human postural responses to motion of real and virtual visual environments under different support base conditions. *Exp Brain Res* (2005) 167(4):535–56. doi:10.1007/s00221-005-0065-3
10. Stapley PJ, Ting LH, Kuifu C, Everaert DG, Macpherson JM. Bilateral vestibular loss leads to active destabilization of balance during voluntary head turns in the standing cat. *J Neurophysiol* (2006) 95(6):3783–97. doi:10.1152/jn.00034.2006
11. Macpherson JM, Everaert DG, Stapley PJ, Ting LH. Bilateral vestibular loss in cats leads to active destabilization of balance during pitch and roll rotations of the support surface. *J Neurophysiol* (2007) 97(6):4357–67. doi:10.1152/jn.01338.2006
12. Bermúdez Rey MC, Clark TK, Wang W, Leeder T, Bian Y, Merfeld DM. Vestibular perceptual thresholds increase above the age of 40. *Front Neurol* (2016) 7:162. doi:10.3389/fneur.2016.00162
13. Cenciarini M, Peterka RJ. Stimulus-dependent changes in the vestibular contribution to human postural control. *J Neurophysiol* (2006) 95(5):2733–50. doi:10.1152/jn.00856.2004
14. van der Kooij H, Peterka RJ. Non-linear stimulus-response behavior of the human stance control system is predicted by optimization of a system with sensory and motor noise. *J Comput Neurosci* (2011) 30(3):759–78. doi:10.1007/s10827-010-0291-y
15. Agrawal Y, Carey JP, Della Santina CC, Schubert MC, Minor LB. Disorders of balance and vestibular function in US adults. Data from the National Health and Nutrition Examination Survey, 2001–2004. *Arch Intern Med* (2009) 169(10):938–44. doi:10.1001/archinternmed.2009.66
16. Koo JW, Chang MY, Woo SY, Kim S, Cho YS. Prevalence of vestibular dysfunction and associated factors in South Korea. *BMJ Open* (2015) 5(10):e008224. doi:10.1136/bmjjopen-2015-008224
17. Peterka R, Black FO, Schoenhoff M. Age-related changes in human postural control: motor coordination tests. *J Vestibular Res* (1990) 1:87–96.
18. Agrawal Y, Carey JP, Della Santina CC, Schubert MC, Minor LB. Diabetes, vestibular dysfunction, and falls: analyses from the National Health and Nutrition Examination Survey. *Otol Neurotol* (2010) 31(9):1445–50. doi:10.1097/MAO.0b013e3181f2f035
19. Agrawal Y, Carey JP, Hoffman HJ, Sklare DA, Schubert MC. The modified Romberg Balance Test: normative data in U.S. adults. *Otol Neurotol* (2011) 32(8):1309–11. doi:10.1097/MAO.0b013e31822e5bee
20. Museum of Science. *Living Lab and National Living Lab*. Boston: Museum of Science (2017). Available from: <https://www.mos.org/collaborations/living-lab-and-national-living-lab>
21. Harris PA, Taylor R, Thielke R, Payne J, Gonzalez N, Conde JG. Research electronic data capture (REDCap) – a metadata-driven methodology and workflow process for providing translational research informatics support. *J Biomed Inform* (2009) 42(2):377–81. doi:10.1016/j.jbi.2008.08.010

AUTHOR CONTRIBUTIONS

MB and DM designed the study and assisted in acquisition of data, statistical analyses and interpretation, and manuscript preparation. TC also assisted in acquisition and interpretation of data and manuscript preparation. All authors approved the final version of this article.

ACKNOWLEDGMENTS

This research was supported by NIH/NIDCD R01-DC01458 and R01-DC014924. The authors thank Living Laboratory personnel at the Museum of Science, Boston, especially, Justin Harris, for opening the doors for us. We also thank Adrian Priesol, Csilla Haburcakova, Faisal Karmali, Gregory Whitman, Koeun Lim, Niek Beckers, Raquel Galvan-Garza, Richard Lewis, Ryan Anderson, Susan King, and Yasha Iravantchi, for their help collecting data, and Carol Brennan, Jillian Howard, Garyfallia Pagonis, and Suzanne Day, for their support throughout the project.

SUPPLEMENTARY MATERIAL

The Supplementary Material for this article can be found online at <http://www.frontiersin.org/article/10.3389/fneur.2017.00631/full#supplementary-material>.

22. Shumway-Cook A, Horak FB. Assessing the influence of sensory interaction of balance. Suggestion from the field. *Phys Ther* (1986) 66(10):1548–50. doi:10.1093/ptj/66.10.1548
23. Valko Y, Lewis RF, Priesol AJ, Merfeld DM. Vestibular labyrinth contributions to human whole-body motion discrimination. *J Neurosci* (2012) 32(39):13537–42. doi:10.1523/JNEUROSCI.2157-12.2012
24. Peterka RJ, Black FO. Age-related changes in human posture control: sensory organization tests. *J Vestib Res* (1990) 1(1):73–85.
25. Cohen H, Heaton LG, Congdon SL, Jenkins HA. Changes in sensory organization test scores with age. *Age Ageing* (1996) 25(1):39–44. doi:10.1093/ageing/25.1.39
26. Cenciarini M, Loughlin PJ, Sparto PJ, Redfern MS. Stiffness and damping in postural control increase with age. *IEEE Trans Biomed Eng* (2010) 57(2):267–75. doi:10.1109/TBME.2009.2031874
27. Lim K, Karmali F, Nicoucar K, Merfeld DM. Perceptual precision of passive body tilt is consistent with statistically optimal cue integration. *J Neurophysiol* (2017) 117(5):2037–52. doi:10.1152/jn.00073.2016
28. D'Silva LJ, Lin J, Staeker H, Whitney SL, Kluding PM. Impact of diabetic complications on balance and falls: contribution of the vestibular system. *Phys Ther* (2016) 96(3):400. doi:10.2522/ptj.20140604
29. Hewston P, Deshpande N. Falls and balance impairments in older adults with type 2 diabetes: thinking beyond diabetic peripheral neuropathy. *Can J Diabetes* (2016) 40(1):6–9. doi:10.1016/j.jcjd.2015.08.005
30. Crews RT, Yalla SV, Fleischer AE, Wu SC. A growing troubling triad: diabetes, aging, and falls. *J Aging Res* (2013) 2013:342650. doi:10.1155/2013/342650
31. Richardson JK, Ching C, Hurvitz EA. The relationship between electromyographically documented peripheral neuropathy and falls. *J Am Geriatr Soc* (1992) 40(10):1008–12. doi:10.1111/j.1532-5415.1992.tb04477.x
32. Brown SJ, Handsaker JC, Bowling FL, Boulton AJ, Reeves ND. Diabetic peripheral neuropathy compromises balance during daily activities. *Diabetes Care* (2015) 38(6):1116–22. doi:10.2337/dc14-1982
33. Vinik AI, Vinik EJ, Colberg SR, Morrison S. Falls risk in older adults with type 2 diabetes. *Clin Geriatr Med* (2015) 31(1):89–99.viii. doi:10.1016/j.cger.2014.09.002
34. Timar B, Timar R, Gaiță L, Oancea C, Levai C, Lungeanu D. The impact of diabetic neuropathy on balance and on the risk of falls in patients with type 2 diabetes mellitus: a cross-sectional study. *PLoS One* (2016) 11(4):e0154654. doi:10.1371/journal.pone.0154654
35. Konukseven O, Polat SB, Karahan S, Konukseven E, Ersoy R, Cakir B, et al. Electrophysiologic vestibular evaluation in type 2 diabetic and prediabetic patients: air conduction ocular and cervical vestibular evoked myogenic potentials. *Int J Audiol* (2015) 54(8):536–43. doi:10.3109/14992027.2014.971887
36. Ward BK, Wenzel A, Kalyani RR, Agrawal Y, Feng AL, Polydefkis M, et al. Characterization of vestibulopathy in individuals with type 2 diabetes mellitus. *Otolaryngol Head Neck Surg* (2015) 153(1):112–8. doi:10.1177/0194599815576717
37. Nicholson M, King J, Smith PF, Darlington CL. Vestibulo-ocular, optokinetic and postural function in diabetes mellitus. *Neuroreport* (2002) 13(1):153–7. doi:10.1097/00001756-200201210-00035
38. Walley M, Anderson E, Pippen MW, Maitland G. Dizziness and loss of balance in individuals with diabetes: relative contribution of vestibular versus somatosensory dysfunction. *Clin Diabetes* (2014) 32(2):76–7. doi:10.2337/diaclin.32.2.76
39. Han BI, Song HS, Kim JS. Vestibular rehabilitation therapy: review of indications, mechanisms, and key exercises. *J Clin Neurol* (2011) 7(4):184–96. doi:10.3988/jcn.2011.7.4.184
40. Gilbert MP, Pratley RE. The impact of diabetes and diabetes medications on bone health. *Endocr Rev* (2015) 36(2):194–213. doi:10.1210/er.2012-1042
41. Neuhauser HK, von Brevern M, Radtke A, Lezius F, Feldmann M, Ziese T, et al. Epidemiology of vestibular vertigo: a neurotologic survey of the general population. *Neurology* (2005) 65(6):898–904. doi:10.1212/01.wnl.0000175987.59991.3d
42. Menegoni F, Tacchini E, Bigoni M, Vismara L, Priano L, Galli M, et al. Mechanisms underlying center of pressure displacements in obese subjects during quiet stance. *J Neuroeng Rehabil* (2011) 8:20. doi:10.1186/1743-0003-8-20
43. Steinberg N, Nemet D, Kohen-Raz R, Zeev A, Pantanowitz M, Eliakim A. Posturography characteristics of obese children with and without associated disorders. *Percept Mot Skills* (2013) 116(2):564–80. doi:10.2466/25.10.26.PMS.116.2.564-580
44. Teasdale N, Hue O, Marcotte J, Berrigan F, Simoneau M, Doré J, et al. Reducing weight increases postural stability in obese and morbid obese men. *Int J Obes (Lond)* (2007) 31(1):153–60. doi:10.1038/sj.ijo.0803360
45. Menegoni F, Galli M, Tacchini E, Vismara L, Cavigoli M, Capodaglio P. Gender-specific effect of obesity on balance. *Obesity (Silver Spring)* (2009) 17(10):1951–6. doi:10.1038/oby.2009.82
46. Cruz-Gómez NS, Plascencia G, Villanueva-Padrón LA, áuregui-Renaud KJ. Influence of obesity and gender on the postural stability during upright stance. *Obes Facts* (2011) 4(3):212–7. doi:10.1159/000329408
47. Ogden CL, Carroll MD, Fryar CD, Flegal KM. *Prevalence of Obesity among Adults and Youth: United States, 2011–2014*. Hyattsville, MD: NCHS Data Brief, U.S. Department of Health and Human Services, Centers for Disease Control and Prevention, National Center for Health Statistics (2015).

Conflict of Interest Statement: The authors declare that the research was conducted in the absence of any commercial or financial relationships that could be construed as a potential conflict of interest.

Copyright © 2017 Bermúdez Rey, Clark and Merfeld. This is an open-access article distributed under the terms of the Creative Commons Attribution License (CC BY). The use, distribution or reproduction in other forums is permitted, provided the original author(s) or licensor are credited and that the original publication in this journal is cited, in accordance with accepted academic practice. No use, distribution or reproduction is permitted which does not comply with these terms.



Multivariate Analyses of Balance Test Performance, Vestibular Thresholds, and Age

Faisal Karmali^{1,2*}, María Carolina Bermúdez Rey^{1,2}, Torin K. Clark^{1,2,3}, Wei Wang^{2,4} and Daniel M. Merfeld^{1,2}

¹Jenks Vestibular Physiology Laboratory, Mass Eye and Ear Infirmary, Boston, MA, United States, ²Otolaryngology, Harvard Medical School, Harvard University, Boston, MA, United States, ³Smead Aerospace Engineering Sciences, University of Colorado, Boulder, CO, United States, ⁴Division of Sleep Medicine, Brigham and Women's Hospital, Boston, MA, United States

OPEN ACCESS

Edited by:

Bernard Cohen,
Icahn School of Medicine at
Mount Sinai, United States

Reviewed by:

Kathleen Cullen,
McGill University, Canada
Aaron Camp,
University of Sydney,
Australia

*Correspondence:

Faisal Karmali
faisal_karmali@yahoo.com

Specialty section:

This article was submitted
to Neuro-Otology,
a section of the journal
Frontiers in Neurology

Received: 17 July 2017

Accepted: 13 October 2017

Published: 08 November 2017

Citation:

Karmali F, Bermúdez Rey MC,
Clark TK, Wang W and Merfeld DM
(2017) Multivariate Analyses of
Balance Test Performance,
Vestibular Thresholds, and Age.
Front. Neurol. 8:578.

doi: 10.3389/fneur.2017.00578

We previously published vestibular perceptual thresholds and performance in the Modified Romberg Test of Standing Balance in 105 healthy humans ranging from ages 18 to 80 (1). Self-motion thresholds in the dark included roll tilt about an earth-horizontal axis at 0.2 and 1 Hz, yaw rotation about an earth-vertical axis at 1 Hz, y-translation (interaural/lateral) at 1 Hz, and z-translation (vertical) at 1 Hz. In this study, we focus on multiple variable analyses not reported in the earlier study. Specifically, we investigate correlations (1) among the five thresholds measured and (2) between thresholds, age, and the chance of failing condition 4 of the balance test, which increases vestibular reliance by having subjects stand on foam with eyes closed. We found moderate correlations (0.30–0.51) between vestibular thresholds for different motions, both before and after using our published aging regression to remove age effects. We found that lower or higher thresholds across all threshold measures are an individual trait that account for about 60% of the variation in the population. This can be further distributed into two components with about 20% of the variation explained by aging and 40% of variation explained by a single principal component that includes similar contributions from all threshold measures. When only roll tilt 0.2 Hz thresholds and age were analyzed together, we found that the chance of failing condition 4 depends significantly on both ($p = 0.006$ and $p = 0.013$, respectively). An analysis incorporating more variables found that the chance of failing condition 4 depended significantly only on roll tilt 0.2 Hz thresholds ($p = 0.046$) and not age ($p = 0.10$), sex nor any of the other four threshold measures, suggesting that some of the age effect might be captured by the fact that vestibular thresholds increase with age. For example, at 60 years of age, the chance of failing is roughly 5% for the lowest roll tilt thresholds in our population, but this increases to 80% for the highest roll tilt thresholds. These findings demonstrate the importance of roll tilt vestibular cues for balance, even in individuals reporting no vestibular symptoms and with no evidence of vestibular dysfunction.

Keywords: vestibular, balance, perception, thresholds, aging, multivariate

INTRODUCTION

Deficits in postural control and resulting falls have profound public health implications (>31,000 deaths and >800,000 hospitalizations/year) (2). Sensory feedback plays a critical role in postural control (3–10). A number of studies have linked vestibular function and falls. One epidemiological study (11) showed that failure to complete the condition 4 of the Modified Romberg foam test (12–14), which is commonly considered a balance assay of vestibular function, was highly correlated with “difficulty with falling” in the past 12 months. Another epidemiological study reported that 80% of fallers admitted to an Emergency department in the UK had symptoms of vestibular impairment (15). Most recently, we reported significant correlations between failure to complete the Modified Romberg foam balance test and roll tilt perceptual thresholds in the dark (1). These roll tilt perceptual thresholds were previously shown to primarily be a measure of vestibular function (16). These findings complement previous studies showing that vestibular dysfunction negatively impacts clinical balance test performance (3, 4, 6, 17–20). While speculative, a previous manuscript (1) also provided statistical calculations that emphasize the significance of the problem, suggesting that falls associated with vestibular function might cause somewhere between 50,000 and 150,000 deaths in America each year. This would rank vestibular dysfunction somewhere between number 10 and number 3 on the list of leading causes of death in the United States¹ (21).

The aforementioned studies emphasize the importance of understanding the connections between vestibular function (and dysfunction), age, and falls. Therefore, we decided to perform another set of analyses on our previously published data set (1) of 105 subjects between 18 and 80 year of age who had been prescreened to be suffering no vestibular symptoms. There was no evidence for differences in the thresholds of males and females, but statistically significant threshold increases above the age of 40 were reported for all five motions investigated: roll tilt about an earth-horizontal axis at 0.2 and 1 Hz, yaw rotation about an earth-vertical axis at 1 Hz, y-translation (interaural/lateral) at 1 Hz, and z-translation (vertical) at 1 Hz. These threshold data were best modeled by a two-segment age model having a constant baseline below an age cutoff around 40 years of age with thresholds increasing above the age of 40. Building on these findings, this manuscript focuses on correlations—both correlations in the threshold measures themselves and correlations between thresholds, age, and failing the vestibular part (condition 4) of the Modified Romberg test.

Correlations between thresholds and balance are important because they might help us intervene to prevent falls *via* (a) warnings (e.g., verbal) from a clinician informing patients about

their individual fall risk, (b) rehabilitation/training (22, 23), or (c) *via* the use of prosthetics/aids like canes, balance feedback devices (24), vestibular prosthesis (25–28), vibro-tactile shoes (29), stochastic resonance of the vestibular system (30–33), and/or orthotic devices (34).

Understanding the correlations between thresholds for different types of motion (e.g., yaw rotation and interaural translation) is also important as it could provide clues regarding the mechanism that causes increased thresholds with age (1). To further explore this, we used principal component analysis (PCA) to understand the structure underlying intersubject variability in thresholds. Moreover, given the vital importance that thresholds might play in predicting fall risk, understanding correlations between thresholds may improve fall risk evaluation.

As detailed in Section “Discussion,” these multivariate analyses yield new findings that were not presented in our previous study. First, while our previous univariate analysis found that all five threshold measures were correlated with chance of failing condition 4, these new multivariate analyses show that only roll tilt 0.2 Hz has a statistically significant correlation after taking into account the relationship between the threshold measures. While the previous analyses found that thresholds are correlated with chance of failing condition 4 even after adjusting for age effects, the new analyses show how the chance of failing depends on the combination of age and roll tilt 0.2 Hz thresholds. We provide correlation coefficients between all threshold measures both before and after age adjustment. Furthermore, new analyses determine the structure of variation in thresholds, including the effects of aging and individual differences.

MATERIALS AND METHODS

Subjects

As previously described (1), 105 subjects (54 females, 51 males) participated, ranging from 18 to 80 years old. Subjects were excluded if they reported, *via* a questionnaire, any major health problems (e.g., a history of neurological, otologic, vestibular, and chronic uncontrolled diseases) or any history of vestibular symptoms. The study was approved by the MEEI Human Studies Committee, and written informed consent was obtained from all subjects as dictated by the Declaration of Helsinki.

Balance Testing

The modified Romberg test of standing balance on firm and compliant support surfaces (14) was used to assess balance function (12, 13). Subjects stand with arms crossed and feet together. The test has four conditions, each of which was scored as pass/fail. Each condition must be passed to progress to the next, with two attempts permitted for each condition, according to the following criteria. In condition 1, the subject must stand on the floor for 15 s with eyes open. In condition 2, the subject must stand on the floor for 15 s with eyes closed. In condition 3, the subject must stand on memory foam with eyes open for 30 s. In condition 4, the subject must stand on the foam with

¹According to the 2010 national vital statistics report (21), the following are the leading causes of death in United States: (1) heart disease (598,000), (2) cancer (575,000), (3) chronic respiratory diseases (138,000), (4) stroke (129,000), (5) accidents (121,000), (6) Alzheimer’s (83,000), (7) diabetes (69,000), (8) kidney diseases (50,000), (9) influenza and pneumonia (50,000), and (10) suicide (38,000). All death rates are rounded to nearest thousand.

eyes closed for 30 s. A fail occurred when subjects did any of the following before the allotted time for each trial: move their feet for stability, open their eyes, or release their arms. Condition 4 primarily assesses vestibular function (11, 14), since visual contributions are eliminated and the foam makes kinesthetic cues unreliable. Six subjects did not perform the balance test and were not included in the balance analyses in this study.

Vestibular Threshold Measurements

The detailed methods used to assay perceptual threshold have been published (1, 16, 35, 36). Upright subjects in the dark were seated in a chair with a helmet to reduce head movement and a five-point harness. The chair was mounted on a Moog 6DOF motion platform that delivered single-cycle acceleration motion stimuli. Subjects listened to white noise through noise-canceling headphones, both to indicate when motion was occurring and to mask other auditory cues. To improve efficiency (37), stimuli magnitudes were selected using an adaptive three-down, one-up staircase (37, 38), in which stimuli become smaller after three consecutive correct responses, and larger after one incorrect response. The staircase followed parameter estimation by sequential testing (PEST) rules (39). The direction (e.g., left/right) was determined randomly for each trial. Testing occurred in blocks of 100 trials, and each trial consisted of a motion stimulus followed by a response. Subjects reported their perception of motion direction using buttons in their left or right hand and were required to report a perception for every trial.

Each subject participated in five blocks of testing lasting approximately 3 h—one block for each of the five types of motion—with the following “motion type” conditions: (1) “yaw 1 Hz”—yaw rotations about an earth-vertical axis at 1 Hz (i.e., a motion duration of 1 s), with an initial stimulus of 4°/s; (2) “Y 1 Hz”—y-translations (lateral/interaural) along an earth-horizontal axis at 1 Hz, with an initial stimulus of 4 cm/s; (3) “Z 1 Hz”—z-translations (superior-inferior) along an earth-vertical axis at 1 Hz, with an initial stimulus of 16 cm/s; (4) “Roll tilt 1 Hz”—ear-down tilts about a head-centered earth-horizontal axis at 1 Hz, with an initial stimulus of 3°/s; and (5) “Roll tilt 0.2 Hz”—the same at 0.2 Hz, with an initial stimulus of 2°/s. Motions at 1 Hz were selected to focus on either the semicircular canals (SCCs) or otolith organs and because 100 trials can be completed in less than 10 min; roll tilt 0.2 Hz was used to study integration of otolith and SCC cues (40).

Threshold (σ) was determined for each block by fitting a Gaussian cumulative distribution psychometric function (41, 42) to the binary responses. The mean of the Gaussian (μ) is often called the “vestibular bias” and corresponds to the stimulus for which there is an equal likelihood of a left vs. right response (or up vs. down).

Data Analysis

All analyses were performed using Matlab R2014b (Mathworks, MA, USA). All statistical analyses were conducted using log-transformed thresholds (e.g., geometric means for across subject averages) because vestibular thresholds have been shown to demonstrate a lognormal distribution across subjects (1, 43, 44).

Correlation coefficients were calculated using Pearson’s correlation. When statistical tests were performed on correlations across the thresholds for different motion types, yielding ten statistical tests, a Bonferroni correction was used for multiple comparisons, using a critical value (p_c) of $0.05/10 = 0.005$. PCA was performed after standardizing log-transformed thresholds by subtracting the mean from all values and dividing by the SD.

Multiple variable logistic regression was used to model the relationship between the chance of failing condition 4 of the balance test and thresholds, age and sex; logistic regression was used because of the binary pass/fail nature of the dependent variable. The Matlab command fitglm with a binomial distribution was used to perform logistic regressions. Stepwise regression (45) was used for variable selection using the Matlab command stepwiseglm, which uses a forward and backward stepwise procedure and a Bayesian information criteria (BICs). All regressions included an intercept term, which was statistically significant in all analyses.

Analyses were also performed on age-adjusted thresholds. Our previous publication (1) determined that a piecewise model best described the effect of aging on vestibular thresholds, with a constant baseline below 42.5 years, followed by a linear increase above this age cutoff. Each motion type had unique baseline and slope values. For subjects younger than the age cutoff, the age-adjusted threshold was simply their threshold. For subjects older than the age cutoff, we determine each age-adjusted threshold using this equation:

$$\text{age adjusted threshold} = e^{\log(\text{threshold}) - \log(\text{slope} \cdot [\text{age} - \text{cutoff}] + \text{baseline}) + \log(\text{baseline})}$$

$$= \text{threshold} \cdot \frac{\text{baseline}}{\text{slope} \cdot [\text{age} - \text{cutoff}] + \text{baseline}}$$

Effectively, this factored out known changes with age by modifying any threshold above the age cutoff—leaving only threshold variations after removing the effect of age. Note that subtraction of the threshold from the model is done after log transformation because of the lognormal threshold distribution.

RESULTS

Threshold Correlations

Thresholds

We applied the published age fitting model (1) to compute the age-adjusted thresholds (Figure 1) which are simply the thresholds after removing the average age effect. Results are segmented by sex to illustrate that there is no effect of sex even after age adjustment, which confirms our previous report of no statistically significant differences between females and males in any threshold measure. Results are also segmented by subjects who passed (○) and failed (×) condition 4 of the balance test and show that subjects who failed condition 4 tended to have higher roll tilt thresholds. Older subjects also tended to fail condition 4 more than younger subjects (i.e., more failures on right side of plots).

To further explore the relationship between age, thresholds and balance, we determined the average thresholds for different age groups segmented by results of condition 4 of the balance

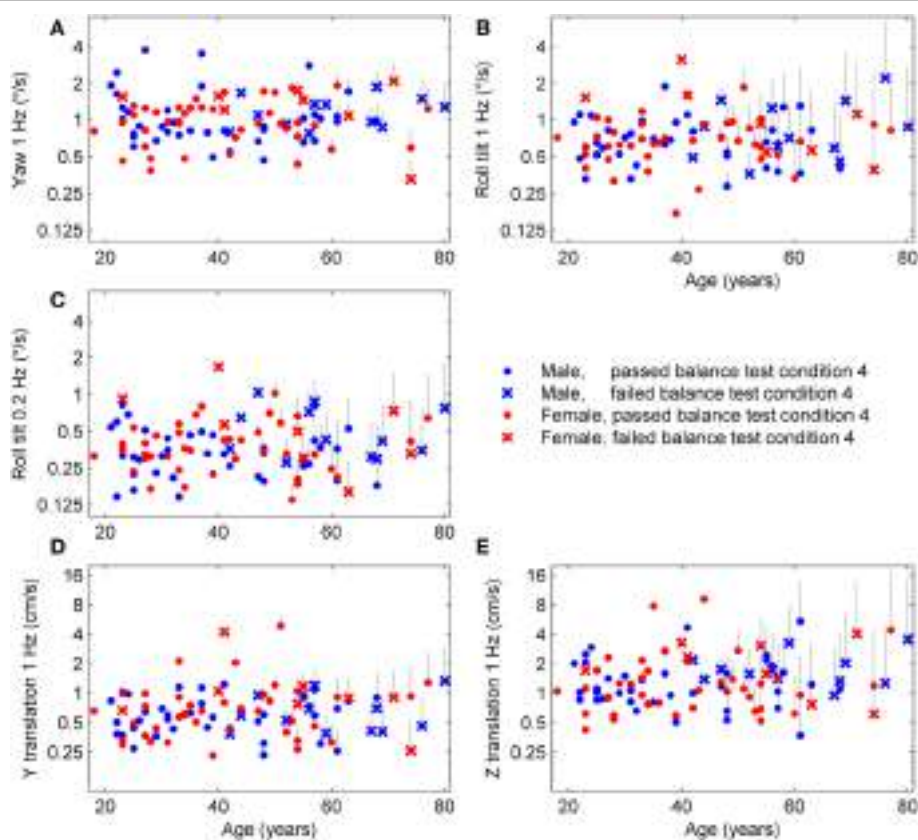


FIGURE 1 | Age-adjusted thresholds for each subject and each of the five motion types. The published aging regression (1) found that thresholds had a constant baseline until 42.5 years, then increased at different rates for each of the five threshold measures. Thresholds for each subject above 42.5 years were adjusted to leave only variations independent of age. **(A)** The gray lines show the decrease in yaw threshold applied to each subject, with the top of the line showing the uncorrected threshold and the symbol at the bottom of the line showing the age-adjusted threshold. **(B–E)** Results for the four other threshold measures.

TABLE 1 | Thresholds segmented by age group and results of condition 4 of the balance test, with 95% confidence intervals.

Age (years)	No. subjects	Yaw 1 Hz (/s)	y-translation 1 Hz (cm/s)	z-translation 1 Hz (cm/s)	Roll tilt 1 Hz (/s)	Roll tilt 0.2 Hz (/s)
All	105	1.11 (1.01–1.23)	0.78 (0.69–0.89)	1.97 (1.68–2.30)	0.93 (0.83–1.04)	0.46 (0.41–0.51)
18–29	29	1.06 (0.87–1.28)	0.61 (0.48–0.79)	1.36 (1.04–1.77)	0.70 (0.60–0.82)	0.37 (0.31–0.44)
30–39	20	1.04 (0.86–1.26)	0.64 (0.52–0.79)	1.26 (0.95–1.67)	0.65 (0.52–0.81)	0.37 (0.30–0.46)
40–49	19	0.99 (0.83–1.20)	0.79 (0.59–1.05)	1.91 (1.44–2.53)	0.92 (0.71–1.18)	0.46 (0.37–0.59)
50–59	21	1.16 (0.93–1.44)	0.99 (0.75–1.29)	2.81 (2.23–3.53)	1.19 (1.00–1.42)	0.57 (0.45–0.72)
60–80	16	1.45 (1.14–1.85)	1.15 (0.87–1.53)	4.35 (2.86–6.61)	1.74 (1.29–2.35)	0.67 (0.50–0.88)
Passed balance	79	1.04 (0.94–1.16)	0.69 (0.61–0.79)	1.62 (1.37–1.92)	0.81 (0.71–0.91)	0.40 (0.36–0.45)
18–29	24	0.98 (0.79–1.21)	0.51 (0.43–0.60)	1.14 (0.93–1.40)	0.63 (0.55–0.73)	0.34 (0.29–0.41)
30–39	20	1.04 (0.86–1.26)	0.64 (0.52–0.79)	1.26 (0.95–1.67)	0.65 (0.52–0.81)	0.37 (0.30–0.46)
40–49	13	0.87 (0.70–1.09)	0.70 (0.52–0.95)	1.75 (1.18–2.60)	0.81 (0.62–1.05)	0.39 (0.32–0.47)
50–59	14	1.16 (0.91–1.48)	0.97 (0.66–1.41)	2.43 (1.84–3.19)	1.17 (0.94–1.46)	0.52 (0.38–0.69)
60–80	8	1.37 (1.03–1.83)	1.18 (0.77–1.81)	3.80 (1.97–7.35)	1.45 (1.00–2.10)	0.58 (0.40–0.84)
Failed balance	20	1.43 (1.19–1.71)	1.05 (0.81–1.35)	3.67 (2.79–4.84)	1.55 (1.18–2.04)	0.76 (0.60–0.95)
18–29	1	1.56 (1.56–1.56)	0.67 (0.67–0.67)	1.71 (1.71–1.71)	1.53 (1.53–1.53)	0.92 (0.92–0.92)
30–39	0	–	–	–	–	–
40–49	5	1.25 (0.98–1.58)	1.03 (0.50–2.11)	2.29 (1.85–2.84)	1.34 (0.76–2.34)	0.78 (0.48–1.27)
50–59	6	1.43 (1.14–1.81)	1.03 (0.74–1.44)	4.12 (3.04–5.59)	1.18 (0.83–1.67)	0.70 (0.49–1.01)
60–80	8	1.53 (1.05–2.25)	1.13 (0.78–1.63)	4.97 (3.02–8.19)	2.10 (1.36–3.23)	0.77 (0.52–1.13)

test (Table 1; Figure 2). While detailed statistical analyses of this relationship will follow, we note a tendency toward higher thresholds for subjects who failed condition 4 in comparison to those who passed condition 4.

Correlations between Vestibular Threshold Measures
We examined correlations between threshold measures for each motion type, since these correlations have important practical implications and also provide some insight into the

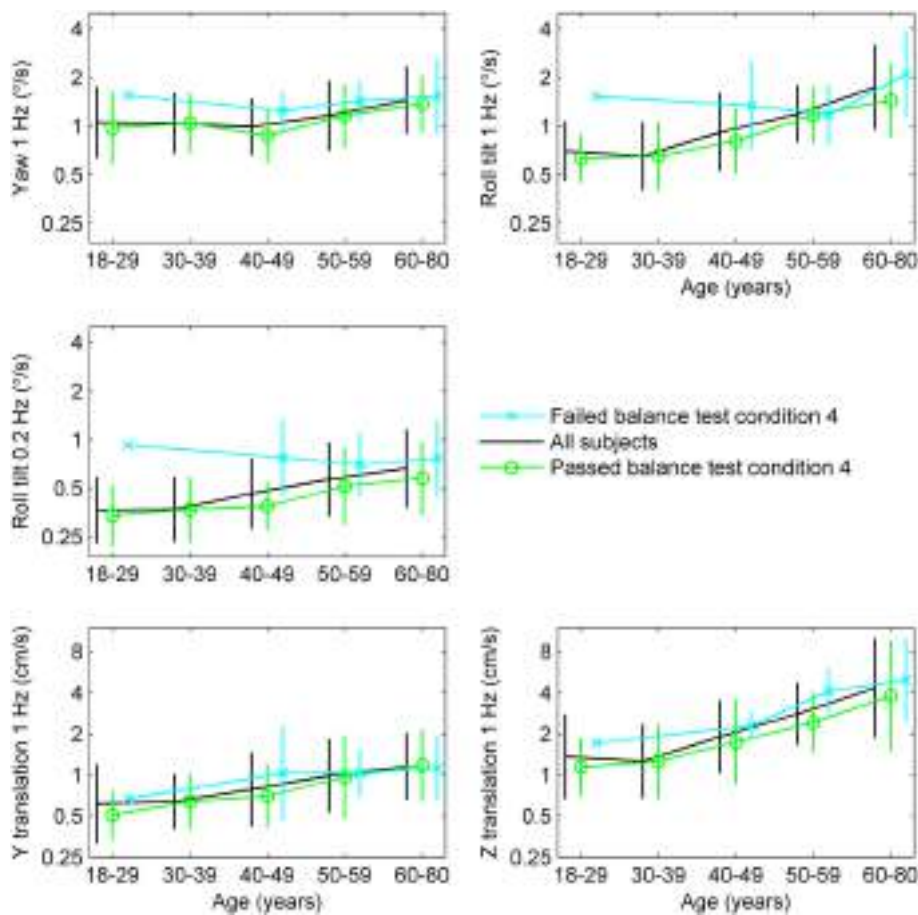


FIGURE 2 | Thresholds segmented by age group and results of condition 4 of the balance test, with error bars showing SD.

shared organs and mechanisms underlying vestibular sensation. **Figure 3** shows the relationship between thresholds across subjects. For example, **Figure 3A** shows the relationship between roll tilt 0.2 Hz thresholds and roll tilt 1 Hz thresholds. In this case, the correlation coefficient was $r_a = 0.63$ for all subjects, and $r_p = 0.50$ for only subjects who passed condition 4 of the balance test. Each threshold pair had a positive, statistically significant (multiple comparison, $p < 0.005$) correlation.

Since all thresholds increase with age, some correlations may occur because of the aging process. To focus on correlation due to factors other than aging, we performed the same analysis on age-adjusted thresholds (**Figure 1**). **Figure 4** shows the relationships between these age-adjusted thresholds. All correlation coefficients decreased somewhat (**Table 2**) compared with unadjusted thresholds, but all remained statistically significant (multiple comparison, $p < 0.005$) when calculated for all subjects. Thus, age alone does not explain these correlations. Section “Discussion” provides our interpretation of these correlation coefficients, including the observation that the lowest correlation coefficients were between yaw thresholds and the other four thresholds. When calculated for subjects who passed condition 4, most correlation coefficients were statistically significant, with

a few exceptions ($p = 0.01$, $p = 0.02$, $p = 0.02$) that did not reach statistical significance after multiple comparisons correction (p_c of $0.05/10 = 0.005$).

Structure Underlying Variation in Vestibular Thresholds

We examined the underlying structure of the relationship between thresholds. This was done using PCA, which determines principal components that are a weighted combination of each of the other measures such that they explain most of the variation within the data. The PCA analysis yielded similar results for unadjusted thresholds (**Table 3**) and age-adjusted threshold (**Table 4**). The contribution shows the variation in the data explained by each component. Since age adjustment explains 20.7% of the variation in the data (1), we also determined the variation explained by each component as a fraction of the remaining 79.3% of the variation (**Table 5**, second row). For comparison, the variation explained by each component for the unadjusted thresholds is shown (**Table 5**, first row).

More than half of intersubject variability is explained by the first component, suggesting a relatively low-dimensional structure underlying thresholds and vestibular sensory precision. Its projection remains (i.e., the weights remain) surprisingly

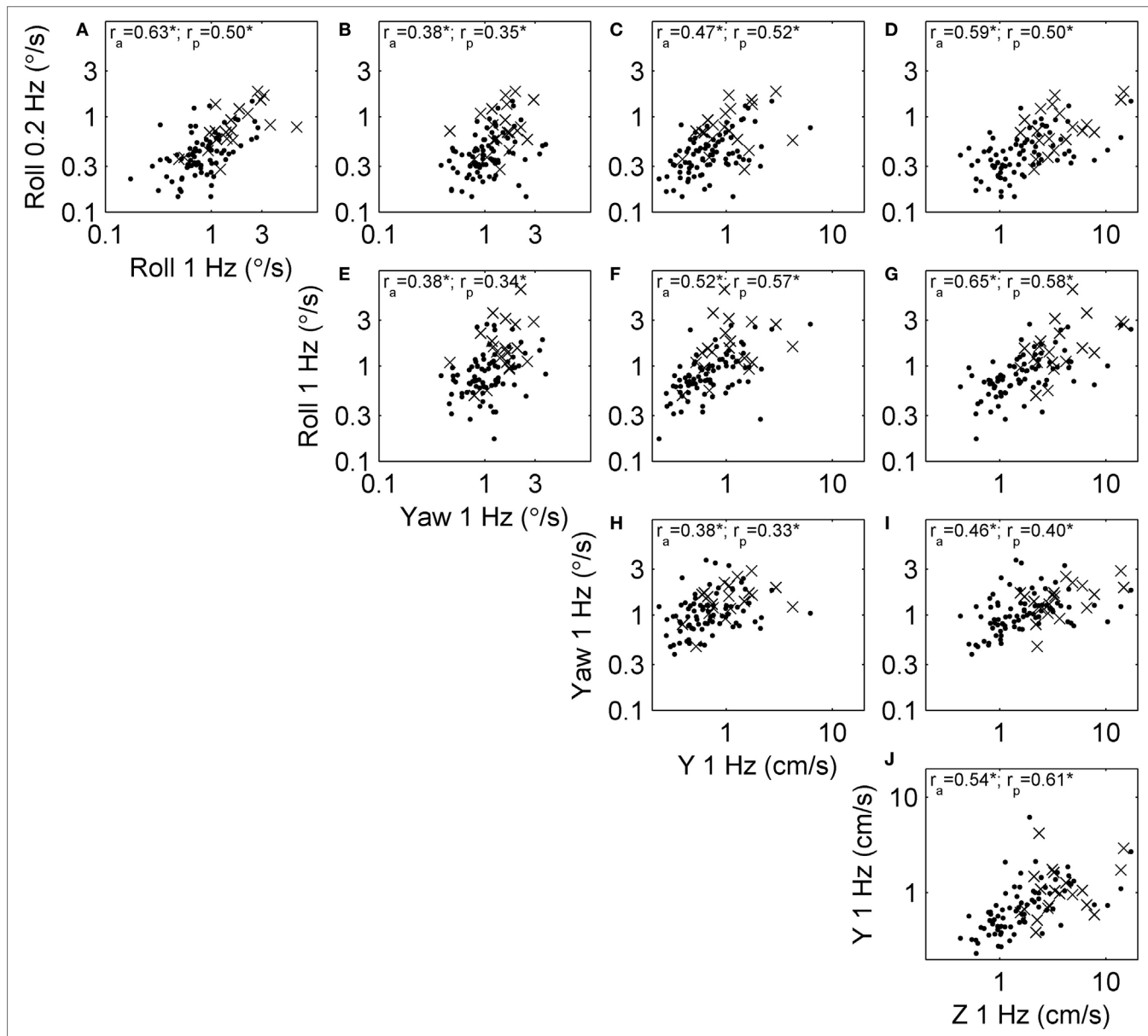


FIGURE 3 | Scatterplots showing the relationship between each of the threshold measures across subjects. Each subject is shown, and segmented into those who passed (dots) and failed (x) condition 4 of the balance test. Correlation coefficients were calculated using log-transformed thresholds, including the correlation across all subjects (r_a) and only those who passed condition 4 (r_p). All correlations were significant at the $p < 0.005$ level (indicated by *). **(A)** The relationship between roll tilt 0.2 Hz thresholds and roll tilt 1 Hz thresholds across subjects. **(B–J)** The relationships between other corresponding pairs of thresholds.

similar after age adjustment, suggesting that lower or higher thresholds across all measures are an important individual trait. For unadjusted thresholds, the first component has a contribution of 60% (Table 3). After age adjustment, the first component has a contribution of 52% (Table 4), which is 41% (Table 5) of the total variance ($52\% \cdot 79.3\% = 41\%$). This shows that much of the variation due to age was included in the first principal component. The remaining components are more difficult to interpret, but the second component may allow a decoupling of yaw and roll thresholds, concomitant with their low correlation.

Correlations with Condition 4 of the Modified Romberg Foam Test

The Relationship between Vestibular Thresholds and Condition 4 of the Modified Romberg Foam Test

Our previous study (1) examined the basic relationship between failing condition 4 of the Modified Romberg test and vestibular thresholds. However, those analyses only looked at the relationship between each individual threshold and the chance of failing the test, without performing multivariate analyses. Specifically, we performed single-variable logistic regressions between failures and each age-adjusted threshold. There were statistically

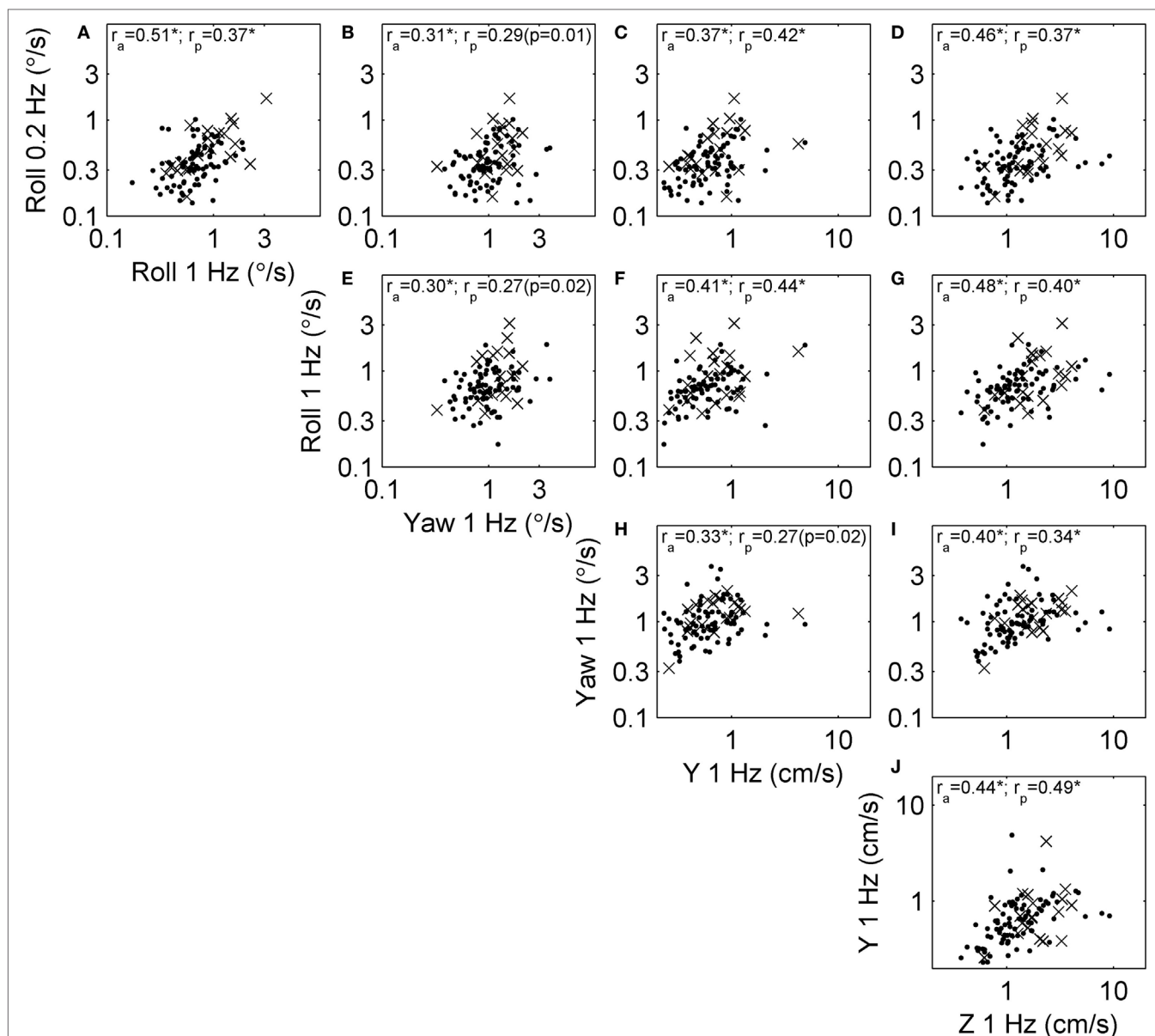


FIGURE 4 | Scatterplots showing the relationship between each of the age-adjusted threshold measures across subjects. This repeats that analysis shown in **Figure 3** in a way that focuses on correlation due to factors other than aging. Each subject is shown, and segmented into those who passed (dots) and failed (x) condition 4 of the balance test. Correlation coefficients were calculated using log-transformed, age-adjusted thresholds, including the correlation across all subjects (r_a) and only those who passed condition 4 (r_p). Most correlations were statistically significant at the $p < 0.005$ level (indicated by *), with exceptions noted by the actual p value. **(A)** The relationship between roll tilt 0.2 Hz thresholds and roll tilt 1 Hz thresholds across subjects. **(B–J)** The relationships between other corresponding pairs of thresholds.

significant correlations with roll 0.2 Hz ($p = 0.003$) and roll 1 Hz ($p = 0.02$) thresholds, a suggestion of possible correlation with yaw 1 Hz ($p = 0.09$) and y-translation 1 Hz ($p = 0.09$) thresholds, and a non-significant correlation for z-translation ($p = 0.50$) thresholds. Given that thresholds may be correlated with each other, a weakness of this analysis was that it did not determine if the covariation between thresholds described above could have resulted in an artifact of some thresholds being correlated with the chance of failing condition 4.

Here, we further explore this relationship using multivariate analyses. The 99 subjects who did balance testing all passed conditions 1, 2, and 3. 79 subjects passed condition 4, while 20 failed. **Table 6** shows the results of a multiple variable logistic regression to predict the chance of failing condition 4 based on age and vestibular thresholds. This analysis found that only roll tilt 0.2 Hz thresholds had a statistically significant ($p = 0.046$) relationship to the chance of failing condition 4. Sex and all other thresholds were not significant, with $p > 0.47$. In

TABLE 2 | The reduction in correlation coefficients due to age adjustment of thresholds.

	Roll 1 Hz	Yaw	Y	Z
Roll 0.2 Hz	–27% (0.63 to 0.51)	–17% (0.38 to 0.31)	–21% (0.47 to 0.37)	–27% (0.59 to 0.46)
Roll 1 Hz		–21% (0.38 to 0.30)	–24% (0.52 to 0.41)	–31% (0.65 to 0.48)
Yaw			–14% (0.38 to 0.33)	–12% (0.46 to 0.40)
Y				–18% (0.54 to 0.44)

Differences shown for coefficients calculated across all subjects (r_a).

TABLE 3 | Principal component analysis (PCA) of log-transformed thresholds for all subjects.

	First	Second	Third	Fourth	Fifth
Contribution (%)	60	14	11	8	7
Yaw	0.37	0.90	–0.16	0.08	0.13
Y	0.43	–0.04	0.87	0.22	0.02
Z	0.49	–0.07	–0.07	–0.62	–0.60
Roll tilt 1 Hz	0.48	–0.31	–0.19	–0.29	0.75
Roll tilt 0.2 Hz	0.46	–0.29	–0.41	0.69	–0.25

The five components are listed (first, second, etc.). The contribution shows the variation in the data explained by each component. The coefficients show the weight given to each threshold when combined to form each component. Thresholds were standardized before PCA. The component with the largest contribution is shown in bold.

TABLE 4 | Principal component analysis of age-adjusted, log-transformed thresholds for all subjects.

	First	Second	Third	Fourth	Fifth
Contribution (%)	52	15	13	10	10
Yaw	0.38	0.84	–0.29	–0.22	0.15
Y	0.43	0.03	0.85	–0.28	–0.07
Z	0.48	0.05	0.00	0.82	–0.30
Roll tilt 1 Hz	0.47	–0.40	–0.15	0.03	0.77
Roll tilt 0.2 Hz	0.46	–0.38	–0.41	–0.45	–0.53

The component with the largest contribution is shown in bold.

TABLE 5 | Variance explained by each principal component after considering the variance explained by age adjustment.

	Age	First	Second	Third	Fourth	Fifth
Thresholds (%)	–	60	14	11	8	7
Age-adjusted thresholds (%)	21	41	12	10	8	8

The first row shows the results for log-transformed thresholds without age adjustment. The second row shows the results for age-adjusted, log-transformed thresholds. The component with the largest contribution is shown in bold.

particular, roll tilt 1 Hz thresholds were not significantly associated with the chance of failing condition 4, even though our previous single-variable regression found a statistically significant relationship. This was likely due to the correlations between roll tilt 0.2 Hz and roll tilt 1 Hz thresholds described above, which demonstrates the importance of the multiple variable analysis. **Figure 5** shows logistic regression curves depicting the

TABLE 6 | Results of a multiple logistic regression to predict the chance of failing condition 4 of the balance test based on age and log-transformed vestibular thresholds.

	Estimate	SE	t-Stat	p-Value
(Intercept)	–3.24	1.39	–2.34	0.0193
Age	0.0457	0.0278	1.65	0.100
Sex	0.349	0.639	0.546	0.585
Yaw 1 Hz	0.543	0.763	0.711	0.477
Y 1 Hz	–0.484	0.700	–0.692	0.489
Z 1 Hz	0.173	0.600	0.289	0.773
Roll tilt 1 Hz	0.502	0.751	0.668	0.504
Roll tilt 0.2 Hz	1.51	0.757	2.00	0.0457*

*Signifies statistical significance ($p < 0.05$).

dependency of failing condition 4 on age and each threshold measure. **Figure 5A** shows that younger subjects tend to pass (O) the balance test while older subjects tend to fail (X), with the logistic regression curve showing that the chance of failing the balance test is 4% for an 18 years old, and increases to 45% for an 80 years old. Each curve is generated by holding the other five variables at the median value of their sample, so it does not show the combined influence of multiple variables. **Figure 5B** shows that subjects with low roll tilt 0.2 Hz thresholds tend to pass (O) the balance test while subjects with higher thresholds tend to fail (X), with the logistic regression curve showing that the chance of failing the balance test is near 0% for the lowest roll tilt 0.2 Hz thresholds in our population, and increases to 61% for the highest thresholds. **Figures 5C–F** show the results for other thresholds, confirming the weak relationship between these variables and the chance of failing condition 4.

Since the regression revealed that many variables had little or no effect on the chance of failing condition 4, we aimed to create a simplified model that included only relevant variables. We used a stepwise procedure (45) to determine which variables to include in the model. **Table 7** shows the results for the simplified model, which includes only age and roll tilt 0.2 Hz thresholds, both of which were statistically significant. This model had a lower BIC value than the complete model (85.4 vs. 106). To further confirm this model selection, we also investigated models that included: (1) each threshold without age, (2) age + each threshold, and (3) age + roll tilt 0.2 Hz thresholds + each other threshold. The selected model provided better fits than each of these, according to BIC values (these models are detailed in Section “Model Comparisons” in Appendix). We also considered a model that included age, roll tilt 0.2 Hz threshold and an interaction term between the two, but the interaction term was not significant ($p = 0.054$), and had slightly worse fit quality (BIC 85.8 vs. 85.4) so we focus on the simpler model.

Both age and roll tilt 0.2 Hz thresholds had a statistically significant contribution to the chance of failing condition 4. **Figure 6** shows the chance of failing condition 4 vs. both age and roll tilt 0.2 Hz thresholds. Generally it shows that the chance of failing condition 4 increases with both age and roll tilt 0.2 Hz thresholds. It emphasizes that for older subjects with high thresholds, the chance of failing is very high, approaching 90%. **Figure 7A** shows the dependency of failing condition 4 on age for different roll tilt thresholds. For example, for subjects whose

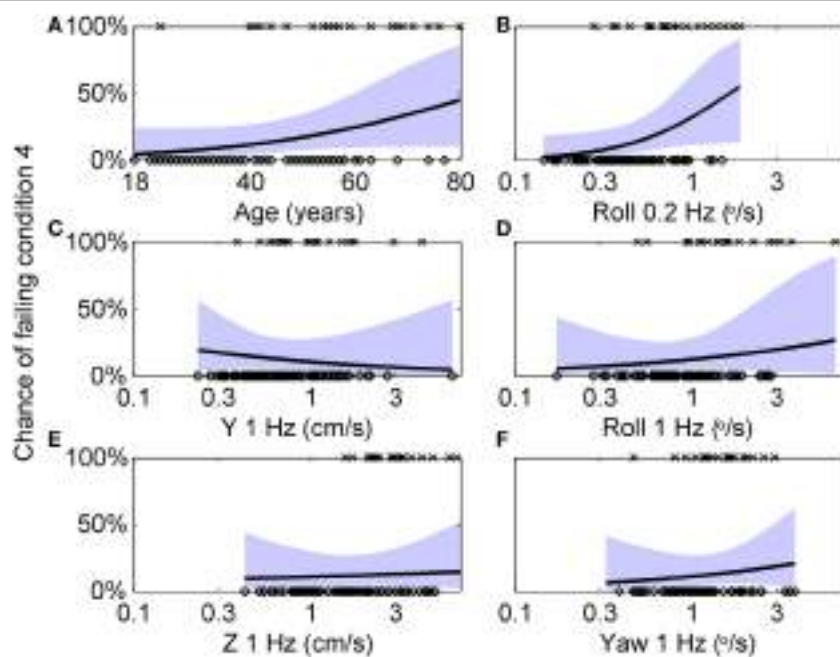


FIGURE 5 | Logistic regression curves showing the dependency of failing condition 4 on age and each threshold measure. **(A)** Circles (○) indicate individual subjects who passed condition 4, while crosses (x) indicate subjects who failed condition 4. A logistic curve showing the dependency of the chance of failing condition 4 on age, with the shaded area showing the 95% confidence intervals. Each curve is generated by holding the other five variables at the median value of their sample, so it does not show the combined influence of multiple variables. **(B–F)** Similar analyses for each of the five threshold measurements.

TABLE 7 | Results of a multiple logistic regression after application of a stepwise algorithm to provide a simplified model.

	Estimate	SE	t-Stat	p-Value
(Intercept)	-2.99	1.29	-2.32	0.0202
Age	0.0551	0.0222	2.48	0.0131*
Roll tilt 0.2 Hz	1.72	0.623	2.76	0.00584*

Regression was performed on log-transformed thresholds.

*Signifies statistical significance ($p < 0.05$).

roll tilt 0.2 Hz thresholds are in the 75th percentile, the chance of failing increases from 6% at age 18 to 68% at age 80. **Figure 7B** shows the dependency of failing condition 4 on roll tilt thresholds for subjects of different ages. For example, at 60 years old, the chance of failing is roughly 5% for the lowest roll tilt thresholds, which does not differ much from younger subjects. However, this increases to 80% for the highest roll tilt thresholds.

We also examined the relationship between the chance of failing condition 4 and age-adjusted thresholds shown in **Figure 1**. **Table 8** shows the results of stepwise logistic regression using age-adjusted, log-transformed thresholds. Roll tilt 0.2 Hz thresholds and age were the only selected contributors and both were statistically significant, as for the unadjusted thresholds. While the coefficient for roll tilt 0.2 Hz thresholds was roughly the same for the age-adjusted and unadjusted thresholds, the coefficient of age was larger when age-related changes were removed from the threshold data. As detailed in

Section “Discussion,” this is likely due to age effects, both vestibular and non-vestibular, being removed from the threshold measure, causing a stronger effect of age on the chance of failing condition 4. We compared regression models that included various combinations of age-adjusted thresholds and found that the selected model had the lowest BIC value (these models are detailed in Section “Model Comparisons” in Appendix).

We also examined whether a relationship existed between failing condition 4 and vestibular bias. Since a large bias in any direction may indicate the presence of erroneous sensory information, analyses were performed using the absolute value of bias, normalized by the subject’s threshold. No significant contribution was found from bias in any of the five motion axes ($p > 0.1$), and only age was predictive of the chance of failing ($p = 0.0006$).

The Relationship between Principal Components and Modified Romberg Foam Test Performance

Since principal components incorporate contributions from all threshold measures, there is a possibility that a latent variable created by projecting all thresholds into a principal component would be a better predictor of the chance of failing condition 4 than using only the roll 0.2 Hz threshold. To evaluate this, we performed a logistic regression using latent variables created using the first and second principal components. For unadjusted, log-transformed thresholds, we found that the first component alone had a statistically significant relationship with the chance of failing condition 4 ($p = 0.013$), while age ($p = 0.12$) and the second component ($p = 0.77$) did not. Interestingly, a model that

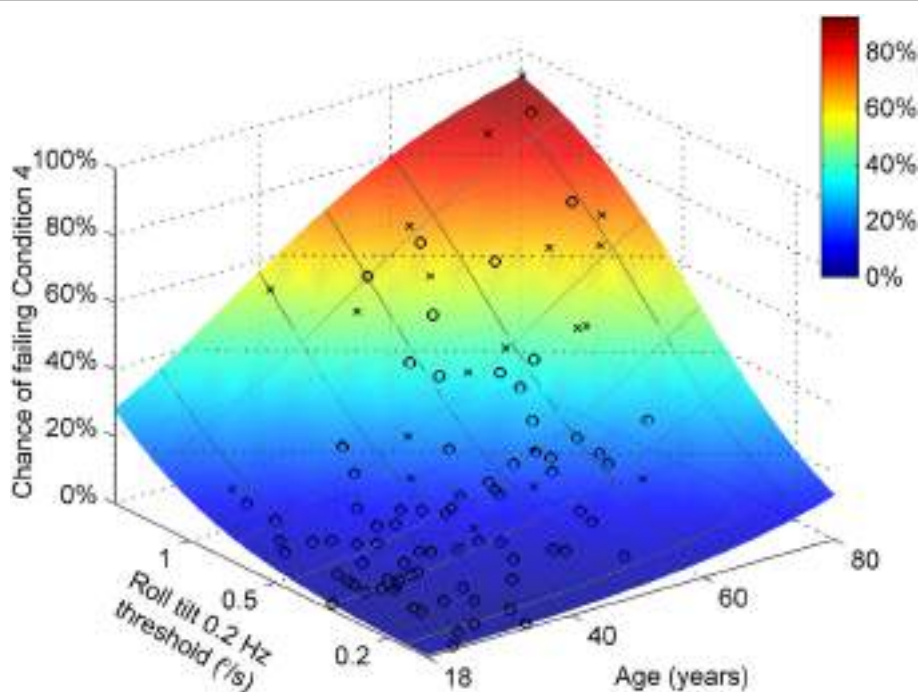


FIGURE 6 | Logistic regression results showing the chance of failing condition 4 vs. both age and roll tilt 0.2 Hz thresholds determined using the model in **Table 7**. Symbols show subjects who passed (○) and failed (×) condition 4.

included only the first principal component (BIC 85.2) provided a similar fit quality to age + roll tilt 0.2 Hz thresholds (BIC 85.4), and slightly better fit quality than roll tilt 0.2 Hz thresholds alone (BIC 88.0) or age + first component (BIC 86.9). These results suggest that the first principal component includes both vestibular and age effects. We performed a similar analysis for age-adjusted, log-transformed thresholds. We found that age ($p = 0.00033$) and the first component ($p = 0.010$) had a statistically significant relationship with the chance of failing condition 4, while the second component ($p = 0.65$) did not. In this case, a model that included age + first component (BIC 86.1) provided a similar fit quality to age + roll tilt 0.2 Hz thresholds (BIC 84.9), and a better fit quality than the first component alone (BIC 99.8).

DISCUSSION

We report correlations among the five thresholds measured, and between thresholds, age and the chance of failing condition 4 of the Modified Romberg balance test. We found moderate correlations (0.30–0.51) between vestibular thresholds, even while using age-adjusted thresholds. PCA suggest that lower or higher thresholds across all threshold measures are an individual trait which account for roughly 60% of the variation in the population; this can be further portioned into about 20% of variation being explained by aging and about 40% of the variation being explained by the first component that represents common variations across the five vestibular thresholds measured.

When only roll tilt 0.2 Hz thresholds and age were analyzed together, we found that the chance of failing condition 4 depends significantly on both ($p = 0.006$ and $p = 0.013$, respectively). An analysis incorporating more variables found that the chance of failing condition 4 depended significantly only on roll tilt 0.2 Hz thresholds ($p = 0.046$) and not age ($p = 0.10$), sex, nor any of the other four threshold measures, suggesting that some of the age effect might be captured by the fact that vestibular thresholds increase with age. This contrasts with our published univariate analyses which found a significant correlation with all five thresholds, and did not examine their combined contributions.

Illustrating the importance of considering both age and vestibular thresholds, at 60 years of age the average chance of failing condition 4 is 43%, but this ranges from roughly 5% for the lowest roll tilt thresholds in our population to 80% for the highest roll tilt thresholds. As a second illustration, at the median 0.2 Hz roll tilt threshold, the chance of failing condition 4 is 12%, but this ranges from roughly 3% at 18 years to 50% at 80 years.

We emphasize that these were subjects who qualified as healthy normals. Subjects who reported dizziness, imbalance, or other vestibular symptoms on the mandatory healthy questionnaire were excluded. Thus, we are characterizing how normal variability in human balance depends on “subclinical” intersubject differences in vestibular precision. In this way, our study complements previous work showing that vestibular dysfunction negatively impacts clinical balance test performance (3, 4, 6, 17–20).

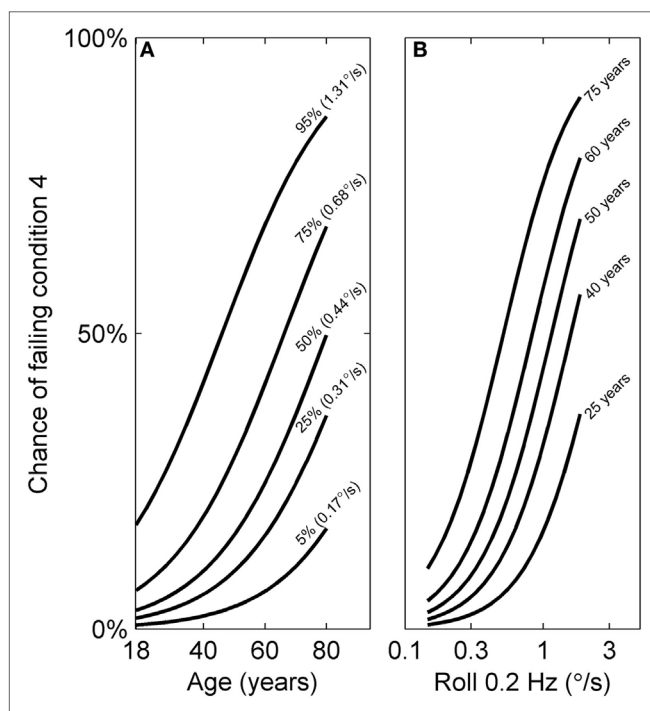


FIGURE 7 | Logistic curves showing the chance of failing condition 4 vs. both age and roll tilt 0.2 Hz thresholds determined using the model in

Table 7. **(A)** The dependency of failing condition 4 on age is shown for different roll tilt thresholds, which have been determined for the 5th, 25th, 50th, 75th, and 95th percentile within our sample. **(B)** The dependency of failing condition 4 on roll tilt 0.2 Hz thresholds for different ages (25, 40, 50, 60, and 75 years old). These curves are also shown in gray in **Figure 6**.

TABLE 8 | Results of a multiple logistic regression after application of a stepwise algorithm to provide a simplified model.

Estimate	SE	t-Stat	p-Value
(Intercept)	-4.05	1.21	0.000834
Age	0.0867	0.0231	0.000171*
Roll tilt 0.2 Hz	1.75	0.618	0.004723*

Analyses were done using age-adjusted, log-transformed thresholds.

*Signifies statistical significance ($p < 0.05$).

New Contributions of This Study Compared with Our Previous Study

While our previous study (1) investigated some of the same topics as this study, several new and significant results are described herein. The previous study briefly stated that statistically significant correlations existed between threshold measures; this study visualizes these relationships and provides correlation coefficients both for unadjusted and age-adjusted thresholds. The PCA results are new.

The previous study, using single-variable logistic regression, reported that without age adjustment, all five threshold measures had a statistically significant correlation with the chance of failing condition 4 ($p < 0.007$). Even after age adjustment, the previous study reported statistically significant correlations for roll tilt 0.2 Hz thresholds ($p = 0.003$) and roll tilt 1 Hz

thresholds ($p = 0.02$), a suggestion of possible correlation with yaw rotation thresholds ($p = 0.09$) and z-translation thresholds ($p = 0.09$), and not significant results for y-translation thresholds ($p = 0.50$). By contrast, the new multiple variable analysis found that only roll tilt 0.2 Hz thresholds and age had a statistically significant contribution to the chance of failing condition 4. The difference between the two results arises because the multiple variable analysis adjusts for the correlations between thresholds, while the single-variable regression fits do not. This study also shows the chance of failing condition 4 for different combinations of age and roll tilt 0.2 Hz thresholds, while the previous study provided an odds ratio for the chance of failing as a function of thresholds only. While the previous analyses showed that threshold was a significant contributor to chance of failing condition 4, even after age adjustment, it did not show the relative contribution of age and roll tilt 0.2 Hz thresholds (Figure 6).

Interpretation of Correlation Coefficients

Even after age adjustment, the correlation coefficients between different threshold measures ranged from 0.30 to 0.51, which are moderate correlations. We now consider three possibilities for how these correlations may arise from: (1) anatomical variations that impact all peripheral organs similarly, (2) shared peripheral organs, and/or (3) shared processing of cues.

The first principal component included relatively similar contributions from all thresholds, consistent with anatomical variation that impacts all organs or a common central cause. However, this does not explain the differences in correlation coefficients between threshold measures for different motion directions.

Correlations may arise from shared peripheral sensory organs. The largest coefficient (0.51) was between roll tilt 0.2 Hz and roll tilt 1 Hz thresholds, which may be explained by the shared superior and posterior SCC cues. Shared otolith cues may explain the next largest correlations, between roll tilt (both 0.2 and 1 Hz) and Z thresholds (0.46, 0.48), between Y and Z thresholds (0.44) and between roll tilt (both 0.2 and 1 Hz) and Y thresholds (0.41, 0.37). Finally, the lowest coefficients were between yaw thresholds and all others, which may be explained by separate yaw cues from the horizontal SCC. In particular, yaw and roll thresholds had the lowest coefficients (0.30, 0.31), which indicates that even within the SCCs, each canal plane has some unique characteristics. This supports the view that peripheral changes are either a less predominant cause of the variations or may be somewhat different for different end organs.

Correlations may arise from shared processing of vestibular cues. There is substantial evidence for spatial orientation internal models that combine otolith and SCC cues (46–53). In addition, there is evidence that there are separate streams of processing for the components of rotation that are about an earth-vertical vs. earth-horizontal axes (54–56). More specifically, yaw rotations about an earth-vertical axis only receive useful motion cues from the SCC, while tilts and translation about an earth-horizontal axis require SCC–otolith integration to disambiguate tilt and translation. This may result in our

earth-vertical yaw rotation thresholds having lower correlations with the other threshold measures, all of which required SCC-otolith integration.

We note that multiple comparisons correction strictly applies to the case of a small number of rejections of the null hypothesis among a large group in which the null hypothesis is not rejected. In our correlations between thresholds, the null hypothesis was rejected in 17 of 20 comparisons, so the remaining three may not have occurred by chance.

Structure Underlying Variation in Vestibular Thresholds

Principal component analysis found that one component accounts for roughly 60% of the variation in the population. After age adjustment, 21% of variation is explained by aging and 41% of the variation is explained by the first component. The projection of the first component hardly changes after age adjustment, suggesting that lower or higher thresholds across all measures are an important individual trait. A possible interpretation of this component is that it represents (or partially represents) physiologic/biologic age (57, 58), which account for variations not explained by chronologic age (i.e., in years). It could also arise from anatomical or physiological covariation across subjects.

The remaining components (two through five) account for 40% of variation, and are more difficult to interpret, especially since they each explain roughly 10% of the total variation. The second component may allow a decoupling of yaw and roll thresholds, consistent with their low correlation. These components also include measurement imprecision by definition. For example, we have used simulations to estimate that when thresholds are determined using 100 trials and a three-down, one-up staircase, the predicted coefficient of variation is 18% (37). This accounts for only random effects, and does not consider “real world” effects like subjects losing concentration, fatigue and other lapses.

Balance Test Results

From Correlation to Expression of Fundamental Causes

Although correlations do not prove causation, a few factors convince us that the regression results are an expression of roll tilt 0.2 Hz thresholds as a fundamental cause of changes in balance performance. We describe these in detail below, but begin with a summary: (1) the converse relationship, that changes in balance cause changes in vestibular function, seems less likely; (2) among the thresholds we measured, roll tilt 0.2 Hz thresholds assay the cues that provide the most physically relevant sensory feedback for postural control; and (3) if covariate(s) of vestibular thresholds were responsible for the correlation between thresholds and chance of failing condition 4, it is unlikely that they would only covary with roll tilt 0.2 Hz thresholds.

First, while evidence from patients with vestibular deficits shows that vestibular function plays a causal role in the control of balance (3, 4, 6, 17–20), no evidence exists (to the best of our

knowledge) that changes in balance cause changes in vestibular function. While vestibular sensory feedback has been shown to affect postural control, it is less clear how changes in balance caused by aging would affect vestibular function.

Second, the physiologic ability to remain upright depends on the sensation of gravitational direction, and thus roll tilt cues would be one of the fundamental cues required to control balance (59, 60). We have shown that roll tilt 0.2 Hz thresholds depend on both otolith cues about the direction of gravity as well as SCC cues about angular rotation (40). Thus, the regression results are consistent with this physical prediction. This argument is strengthened by the lack of statistically significant correlations between chance of failing condition 4 and vestibular cues (e.g., yaw rotation) that do not have a direct theoretical rationale for contributing to postural control.

Third, we consider the possibility that vestibular thresholds are covariates of another variable that is the true primary underlying cause of balance dysfunction, since we did not quantify all of the many contributors to balance (e.g., biomechanics, muscle strength, proprioception, and vision—when available, movement strategies, sensory integration, cognitive processing, etc.) (4). For example, both muscle strength and vestibular function decline with age, and thus are likely correlated across subjects. Since muscle strength is correlated with fall risk (61) and balance performance (62), one could imagine that a regression between vestibular function and balance performance could give a positive result that arises because of covariation between vestibular function and muscle strength. However, if this were true, it is unlikely that only a single vestibular threshold out of five would be correlated with covariates, but we find only a single vestibular threshold is correlated with the chance of failing condition 4. Furthermore, it would be an unlikely coincidence that roll tilt 0.2 Hz threshold would be correlated with the chance of failing condition 4 because of covariates, given the physical explanation described earlier.

We conducted further analyses to provide additional support that covariates are unlikely to explain our correlations. We performed a multiple variable logistic regression between age, Y, Z, yaw, and roll tilt 1 Hz thresholds (i.e. all measures except for roll tilt 0.2 Hz thresholds) and found that none of the thresholds had a statistically significant relationship with the chance of failing condition 4 ($Y\ p = 0.71$; $Z\ p = 0.46$; $yaw\ p = 0.40$; $roll\ tilt\ 1\ Hz\ p = 0.16$). We compared this to the multiple variable logistic regression that included the same variables as well as roll tilt 0.2 Hz thresholds. The difference between these fits was statistically significant (χ^2 -statistic, $p = 0.037$) showing that adding the roll tilt 0.2 Hz thresholds as a regression variable yielded significant model fit improvements even after all of the other available variables (including their various covariations) had already been included in the fit. A similar analysis in which each of the four other thresholds was dropped from the model did not yield a statistically significant difference from the model that included the five thresholds (χ^2 -statistic, $p > 0.39$).

Sagittal vs. Frontal Plane Motion

Balance requires control of orientation relative to gravity in both the sagittal (anterioposterior) and frontal (mediolateral) planes,

and roll tilt thresholds only assay the cues that provide feedback about motion in the frontal plane. Future studies could measure pitch thresholds to determine the cues relevant to sagittal control, and to estimate the relative importance of sagittal and frontal mechanisms to the chance of failing condition 4. There is some evidence that the task we used in which the feet were together primarily challenges frontal plane control, since the rates of failing condition 4 were >20 vs. 1.8% in a similar task with a wide stance (63), which provides less frontal plane challenge and presumably similar sagittal plane challenge. Therefore, we hypothesize that, for the task we used, the chance of failing condition 4 would have a stronger correlation with roll tilt thresholds than pitch thresholds.

Model Comparison

A number of models performed similarly well at predicting the chance of failing condition 4, with BIC values between 84.9 and 86.9: (i) first principal component of thresholds, (ii) age + roll tilt 0.2 Hz thresholds, (iii) age + first principal component of age-adjusted thresholds, (iv) age + roll tilt 0.2 Hz age-adjusted thresholds, and (v) age + first principal component of thresholds. Since age + roll tilt 0.2 Hz thresholds relies on less data than PCA, and since it does not require the additional step of age adjustment, the simplicity of this model may make it preferable.

We found that age had a larger coefficient when roll tilt 0.2 Hz thresholds were age-adjusted vs. when they were unadjusted. Since vestibular age effects were removed from the threshold measure, it is unsurprising that this causes age itself to have a stronger effect on the chance of failing condition 4. Furthermore, age serves as a proxy for the various contributors to balance which we did not measure (i.e., non-vestibular). Thus, we propose that the effects of age on vestibular thresholds also covaried with these non-vestibular factors, and when the covarying age effects were removed from the roll tilt 0.2 Hz thresholds, the age coefficient was adjusted to capture just the non-vestibular age effects on the chance of failing condition 4.

Related to this, we also note that while age is statistically significant in the model that includes roll tilt 0.2 Hz thresholds and age, in the models that include age, sex and all five thresholds, age is not statistically significant ($p = 0.10$). The most likely explanation for this is that since vestibular thresholds vary with age, the age effect is spread among age and the vestibular thresholds, decreasing the effect size for each variable and making it harder to reach the level of statistical significance. This explanation is supported by the fact that in the same regression using age-adjusted thresholds (Section “Model Comparisons” in Appendix), age is still statistically significant ($p = 0.00026$). An alternate explanation is that adding additional variables to the model increases variability overall and makes it less likely that each variable will reach statistical significance without a corresponding increase in the number of subjects. Another explanation that we cannot refute at this time is that vestibular thresholds might serve as a biomarker for physiologic/biologic age (57, 58).

We also performed a regression that predicted the chance of failing condition 4 based on age ($p = 0.42$), roll tilt 0.2 Hz threshold ($p = 0.017$) and an interaction term ($p = 0.054$). Since the

interaction term did not strictly reach the criteria for statistical significance, we did not present it in the Results. We note that this may have occurred because our population was not extremely large, and because there were not many subjects that were either older with low thresholds, or younger with high thresholds. We speculate that in a study with a larger population, each of these terms might be statistically significant.

We found no evidence that vestibular biases were correlated with the chance of failing condition 4. We can only speculate about the reasons. Perceptual biases may be unrelated to motor errors. The brain may be better at compensating for biases in balance vs. in perception. Alternatively, only large biases may have an effect on balance, and our subjects may not have exhibited large enough biases to demonstrate a relationship. Finally, the measured biases may reflect cognitive processes rather than having a sensory origin (64).

Unique Aspects of Yaw Rotation

We noted a few ways in which yaw rotation threshold responses differ from those of other motions, in addition to those that have been previously reported; we summarize them here. First, while our previous study presented an age regression that fit well across all five threshold measures, when fits were done to individual threshold measures, only yaw rotation did not have a statistically significant ($p = 0.087$) age effect (1); qualitatively, it also seems that the age cutoff may be higher for yaw rotation. Other studies also reported the lack of statistically significant changes in yaw thresholds with age (65–67). Second, yaw rotation thresholds have the weakest correlation with other threshold measures; specifically, the lowest correlation coefficients were between yaw thresholds and the other four thresholds. Third, velocity storage has different properties for yaw rotation vs. other motions, including less dependence on otolith cues for yaw rotation even with the subject supine (68), and a longer time constant for yaw rotations about an earth-vertical axis (69). Finally, the yaw plane plays a unique role during navigation (70). Different and/or more extensive processing for yaw rotation may result in reduced age effects.

BRIEF SUMMARY

We investigated correlations between thresholds and multiple variable correlations between thresholds and the chance of failing condition 4 of the Modified Romberg balance test, which increases vestibular reliance by having subjects stand on foam with eyes closed. We found that the chance of failing condition 4 depends significantly on both roll tilt 0.2 Hz thresholds ($p = 0.006$) and age ($p = 0.013$). We also found moderate correlations (0.30–0.51) among the five vestibular thresholds, even after using our published aging regression to remove most aging effects.

ETHICS STATEMENT

The study was approved by the MEEI Human Studies Committee and written informed consent was obtained from all subjects as dictated by the Declaration of Helsinki.

AUTHOR CONTRIBUTIONS

MB, TC, and DM designed the study and collected the data. FK, WW, DM, and TC performed statistical analyses and interpretation. FK drafted the manuscript and WW, DM, TC, and MB provided critical feedback on the manuscript.

REFERENCES

- Bermúdez Rey M, Clark T, Wang W, Leeder T, Bian Y, Merfeld D. Vestibular perceptual thresholds increase above the age of 40. *Front Neurol* (2016) 7(162):162. doi:10.3389/fneur.2016.00162
- CDC. *Web-Based Injury Statistics Query and Reporting System (WISQARS)*. Atlanta, GA: National Center for Injury Prevention and Control (2014).
- Nashner LM, Black FO, Wall C III. Adaptation to altered support and visual conditions during stance: patients with vestibular deficits. *J Neurosci* (1982) 2(5):536–44.
- Horak F, Nashner L, Diener H. Postural strategies associated with somatosensory and vestibular loss. *Exp Brain Res* (1990) 82(1):167–77. doi:10.1007/BF00230848
- Peterka RJ, Benolken MS. Role of somatosensory and vestibular cues in attenuating visually induced human postural sway. *Exp Brain Res* (1995) 105(1):101–10. doi:10.1007/BF00242186
- Peterka RJ. Sensorimotor integration in human postural control. *J Neurophysiol* (2002) 88(3):1097–118. doi:10.1152/jn.00605.2001
- Horak FB. Postural orientation and equilibrium: what do we need to know about neural control of balance to prevent falls? *Age Ageing* (2006) 35(Suppl 2):ii7–11. doi:10.1093/ageing/afl077
- Goodworth AD, Peterka RJ. Influence of bilateral vestibular loss on spinal stabilization in humans. *J Neurophysiol* (2010) 103(4):1978–87. doi:10.1152/jn.01064.2009
- van der Kooij H, Peterka RJ. Non-linear stimulus-response behavior of the human stance control system is predicted by optimization of a system with sensory and motor noise. *J Comput Neurosci* (2011) 30(3):759–78. doi:10.1007/s10827-010-0291-y
- Shumway-Cook A, Woollacott MH. *Motor Control Translating Research into Clinical Practice*. Philadelphia: Lippincott Williams & Wilkins (2012).
- Agrawal Y, Carey JP, Della Santina CC, Schubert MC, Minor LB. Disorders of balance and vestibular function in US adults: data from the National Health and Nutrition Examination Survey, 2001–2004. *Arch Intern Med* (2009) 169(10):938–44. doi:10.1001/archinternmed.2009.66
- Shumway-Cook A, Horak FB. Assessing the influence of sensory interaction on balance: suggestion from the field. *Phys Ther* (1986) 66(10):1548–50. doi:10.1093/ptj/66.10.1548
- Horak FB. Clinical measurement of postural control in adults. *Phys Ther* (1987) 67(12):1881–5. doi:10.1093/ptj/67.12.1881
- CDC. *Balance Procedures Manual*. NHANES (2003). Available from: <https://www.cdc.gov/nchs/data/nhanes/ba.pdf>
- Pothula VB, Chew F, Lesser TH, Sharma AK. Falls and vestibular impairment. *Clin Otolaryngol Allied Sci* (2004) 29(2):179–82. doi:10.1111/j.0307-7772.2004.00785.x
- Valko Y, Lewis RF, Priesol AJ, Merfeld DM. Vestibular labyrinth contributions to human whole-body motion discrimination. *J Neurosci* (2012) 32(39):13537–42. doi:10.1523/JNEUROSCI.2157-12.2012
- Allum J, Adkin A, Carpenter M, Held-Ziolkowska M, Honegger F, Pierchala K. Trunk sway measures of postural stability during clinical balance tests: effects of a unilateral vestibular deficit. *Gait Posture* (2001) 14(3):227–37. doi:10.1016/S0966-6362(01)00132-1
- Mergner T, Schweigart G, Maurer C, Blumle A. Human postural responses to motion of real and virtual visual environments under different support base conditions. *Exp Brain Res* (2005) 167(4):535–56. doi:10.1007/s00221-005-0065-3
- Stapley PJ, Ting LH, Kuifu C, Everaert DG, Macpherson JM. Bilateral vestibular loss leads to active destabilization of balance during voluntary head turns in the standing cat. *J Neurophysiol* (2006) 95(6):3783–97. doi:10.1152/jn.00034.2006
- Macpherson JM, Everaert DG, Stapley PJ, Ting LH. Bilateral vestibular loss in cats leads to active destabilization of balance during pitch and roll rotations of the support surface. *J Neurophysiol* (2007) 97(6):4357–67. doi:10.1152/jn.01338.2006
- Heron M. Deaths: leading causes for 2010. *Natl Vital Stat Rep* (2013) 62(6):1–96.
- Han BI, Song HS, Kim JS. Vestibular rehabilitation therapy: review of indications, mechanisms, and key exercises. *J Clin Neurol* (2011) 7(4):184–96. doi:10.3988/jcn.2011.7.4.184
- Hall CD, Herdman SJ, Whitney SL, Cass SP, Clendaniel RA, Fife TD, et al. Vestibular rehabilitation for peripheral vestibular hypofunction: an evidence-based clinical practice guideline: from the American physical therapy association neurology section. *J Neurol Phys Ther* (2016) 40(2):124–55. doi:10.1097/NPT.0000000000000120
- Sienko KH, Vichare VV, Balkwill MD, Wall C III. Assessment of vibrotactile feedback on postural stability during pseudorandom multidirectional platform motion. *IEEE Trans Biomed Eng* (2010) 57(4):944–52. doi:10.1109/TBME.2009.2036833
- Chiang B, Fridman GY, Dai C, Rahman MA, Della Santina CC. Design and performance of a multichannel vestibular prosthesis that restores semicircular canal sensation in rhesus monkey. *IEEE Trans Neural Syst Rehabil Eng* (2011) 19(5):588–98. doi:10.1109/TNSRE.2011.2164937
- Merfeld DM, Lewis RF. Replacing semicircular canal function with a vestibular implant. *Curr Opin Otolaryngol Head Neck Surg* (2012) 20(5):386–92. doi:10.1097/MOO.0b013e328357630f
- Van De Berg R, Guinand N, Guyot J-P, Kingma H, Stokroos RJ. The modified ampullar approach for vestibular implant surgery: feasibility and its first application in a human with a long-term vestibular loss. *Front Neurol* (2012) 3:18. doi:10.3389/fneur.2012.00018
- Golub JS, Ling L, Nie K, Nowack A, Shepherd SJ, Bierer SM, et al. Prosthetic implantation of the human vestibular system. *Otol Neurotol* (2014) 35(1):136. doi:10.1097/MAO.0000000000000003
- Priplata AA, Patritti BL, Niemi JB, Hughes R, Gravelle DC, Lipsitz LA, et al. Noise-enhanced balance control in patients with diabetes and patients with stroke. *Ann Neurol* (2006) 59(1):4–12. doi:10.1002/ana.20670
- Scinicariello AP, Inglis JT, Collins JJ. The effects of stochastic monopolar galvanic vestibular stimulation on human postural sway. *J Vestib Res* (2002) 12(2–3):77–85.
- Pal S, Rosengren SM, Colebatch JG. Stochastic galvanic vestibular stimulation produces a small reduction in sway in Parkinson's disease. *J Vestib Res* (2009) 19(3–4):137–42. doi:10.3233/VES-2009-0360
- Mulavara AP, Fiedler MJ, Kofman IS, Wood SJ, Serrador JM, Peters B, et al. Improving balance function using vestibular stochastic resonance: optimizing stimulus characteristics. *Exp Brain Res* (2011) 210(2):303–12. doi:10.1007/s00221-011-2633-z
- Goel R, Kofman I, Jeevarajan J, De Dios Y, Cohen HS, Bloomberg JJ, et al. Using low levels of stochastic vestibular stimulation to improve balance function. *PLoS One* (2015) 10(8):e0136335. doi:10.1371/journal.pone.0136335
- Goodworth AD, Kunsman M, DePietro V, LaPenta G, Miles K, Murphy J. Characterization of how a walking boot affects balance. *J Prosthet Orthot* (2014) 26(1):54–60. doi:10.1097/JPO.0000000000000014

ACKNOWLEDGMENTS

This research was supported by NIH/NIDCD R01-DC01458, R01-DC014924 and R03-DC013635. The authors also thank Raquel Galvan-Garza, Wangsong Gong, Bob Grimes, Csilla Haburcakova, Kristen Kirk, Rick Lewis, Koeun Lim, and Yongwoo Yi.

35. Grabherr L, Nicoucar K, Mast FW, Merfeld DM. Vestibular thresholds for yaw rotation about an earth-vertical axis as a function of frequency. *Exp Brain Res* (2008) 186(4):677–81. doi:10.1007/s00221-008-1350-8
36. Chaudhuri SE, Karmali F, Merfeld DM. Whole body motion-detection tasks can yield much lower thresholds than direction-recognition tasks: implications for the role of vibration. *J Neurophysiol* (2013) 110(12):2764–72. doi:10.1152/jn.00091.2013
37. Karmali F, Chaudhuri SE, Yi Y, Merfeld DM. Determining thresholds using adaptive procedures and psychometric fits: evaluating efficiency using theory, simulations, and human experiments. *Exp Brain Res* (2016) 234(3):773–89. doi:10.1007/s00221-015-4501-8
38. Leek MR. Adaptive procedures in psychophysical research. *Percept Psychophys* (2001) 63(8):1279–92. doi:10.3758/BF03194543
39. Taylor MM. PEST: efficient estimates on probability functions. *J Acoust Soc Am* (1967) 41:782–7. doi:10.1121/1.1910407
40. Lim K, Karmali F, Nicoucar K, Merfeld DM. Perceptual precision of passive body tilt is consistent with statistically optimal cue integration. *J Neurophysiol* (2017) 117(5):2037–52. doi:10.1152/jn.00073.2016
41. McCullagh PNJA. *Generalized Linear Models*. London, New York: Chapman & Hall/CRC (1989).
42. Chaudhuri SE, Merfeld DM. Signal detection theory and vestibular perception: III. Estimating unbiased fit parameters for psychometric functions. *Exp Brain Res* (2013) 225(1):133–46. doi:10.1007/s00221-012-3354-7
43. Benson AJ, Spencer MB, Stott JR. Thresholds for the detection of the direction of whole-body, linear movement in the horizontal plane. *Aviat Space Environ Med* (1986) 57(11):1088–96.
44. Benson AJ, Hutt EC, Brown SF. Thresholds for the perception of whole body angular movement about a vertical axis. *Aviat Space Environ Med* (1989) 60(3):205–13.
45. Mathworks. *Create Generalized Linear Regression Model by Stepwise Regression*. Mathworks (2017). Available from: <https://www.mathworks.com/help/stats/stepwiselm.html>
46. Merfeld DM. Modeling the vestibulo-ocular reflex of the squirrel monkey during eccentric rotation and roll tilt. *Exp Brain Res* (1995) 106(1):123–34. doi:10.1007/BF00241361
47. Glasauer S, Merfeld DM. Modeling three-dimensional responses during complex motion stimulation. In: Fetter M, Haslwanter T, Misslisch H, Tweed D, editors. *Three-Dimensional Kinematics of Eye, Head and Limb Movements*. Amsterdam: Harwood Acad (1997) p. 387–98.
48. Angelaki DE, McHenry MQ, Dickman JD, Newlands SD, Hess BJM. Computation of inertial motion: neural strategies to resolve ambiguous otolith information. *J Neurosci* (1999) 19(1):316–27.
49. Mergner T, Glasauer S. A simple model of vestibular canal-otolith signal fusion. *Ann N Y Acad Sci* (1999) 871(1):430–4. doi:10.1111/j.1749-6632.1999.tb09211.x
50. Merfeld DM, Zupan LH. Neural processing of gravitoinertial cues in humans. III. Modeling tilt and translation responses. *J Neurophysiol* (2002) 87(2):819–33. doi:10.1152/jn.00485.2001
51. Zupan LH, Merfeld DM, Darlot C. Using sensory weighting to model the influence of canal, otolith and visual cues on spatial orientation and eye movements. *Biol Cybern* (2002) 86(3):209–30. doi:10.1007/s00422-001-0290-1
52. Green AM, Angelaki DE. Resolution of sensory ambiguities for gaze stabilization requires a second neural integrator. *J Neurosci* (2003) 23(28):9265–75.
53. Green AM, Angelaki DE. An integrative neural network for detecting inertial motion and head orientation. *J Neurophysiol* (2004) 92(2):905–25. doi:10.1152/jn.01234.2003
54. Raphan T, Matsuo V, Cohen B. Velocity storage in the vestibulo-ocular reflex arc (VOR). *Exp Brain Res* (1979) 35(2):229–48. doi:10.1007/BF00236613
55. Green AM, Shaikh AG, Angelaki DE. Sensory vestibular contributions to constructing internal models of self-motion. *J Neural Eng* (2005) 2(3):S164–79. doi:10.1088/1741-2560/2/3/S02
56. Angelaki DE, Cullen KE. Vestibular system: the many facets of a multimodal sense. *Annu Rev Neurosci* (2008) 31:125–50. doi:10.1146/annurev.neuro.31.060407.125555
57. Krishnamurthy J, Torrice C, Ramsey MR, Kovalev GI, Al-Regaiey K, Su L, et al. Ink4a/Arf expression is a biomarker of aging. *J Clin Invest* (2004) 114(9):1299–307. doi:10.1172/JCI22475
58. Ressler S, Bartkova J, Niederegger H, Bartek J, Scharffetter-Kochanek K, Jansen-Dürr P, et al. p16INK4A is a robust in vivo biomarker of cellular aging in human skin. *Aging Cell* (2006) 5(5):379–89. doi:10.1111/j.1474-9726.2006.00231.x
59. Goodworth AD, Peterka RJ. Influence of stance width on frontal plane postural dynamics and coordination in human balance control. *J Neurophysiol* (2010) 104(2):1103–18. doi:10.1152/jn.00916.2009
60. Goodworth AD, Peterka RJ. Sensorimotor integration for multisegmental frontal plane balance control in humans. *J Neurophysiol* (2012) 107(1):12–28. doi:10.1152/jn.00670.2010
61. Moreland JD, Richardson JA, Goldsmith CH, Clase CM. Muscle weakness and falls in older adults: a systematic review and meta-analysis. *J Am Geriatr Soc* (2004) 52(7):1121–9. doi:10.1111/j.1532-5415.2004.52310.x
62. Fukagawa NK, Wolfson L, Judge J, Whipple R, King M. Strength is a major factor in balance, gait, and the occurrence of falls. *J Gerontol A Biol Sci Med Sci* (1995) 50(Special_Issue):64–7. doi:10.1093/gerona/50A.Special_Issue.64
63. Koo J-W, Chang MY, Woo S-Y, Kim S, Cho Y-S. Prevalence of vestibular dysfunction and associated factors in South Korea. *BMJ Open* (2015) 5(10):e008224. doi:10.1136/bmjjopen-2015-008224
64. Garcia-Perez MA, and Alcala-Quintana R. Shifts of the psychometric function: distinguishing bias from perceptual effects. *Q J Exp Psychol (Hove)*. (2013) 66: 319–37. doi:10.1080/17470218.2012.708761
65. Seemungal B, Gunaratne I, Fleming I, Gresty M, Bronstein A. Perceptual and nystagmic thresholds of vestibular function in yaw. *J Vestib Res* (2004) 14(6):461–6.
66. Roditi RE, Crane BT. Directional asymmetries and age effects in human self-motion perception. *J Assoc Res Otolaryngol* (2012) 13(3):381–401. doi:10.1007/s10162-012-0318-3
67. Chang NY, Hiss MM, Sanders MC, Olomu OU, MacNeilage PR, Uchanski RM, et al. Vestibular perception and the vestibulo-ocular reflex in young and older adults. *Ear Hear* (2014) 35(5):565–70. doi:10.1097/AUD.0000000000000052
68. Bockisch CJ, Straumann D, Haslwanter T. Human 3-D aVOR with and without otolith stimulation. *Exp Brain Res* (2005) 161(3):358–67. doi:10.1007/s00221-004-2080-1
69. Bertolini G, Ramat S. Velocity storage in the human vertical rotational vestibulo-ocular reflex. *Exp Brain Res* (2011) 209(1):51–63. doi:10.1007/s00221-010-2518-6
70. Taube JS. The head direction signal: origins and sensory-motor integration. *Annu Rev Neurosci* (2007) 30:181–207. doi:10.1146/annurev.neuro.29.051605.112854

Conflict of Interest Statement: The authors declare that the research was conducted in the absence of any commercial or financial relationships that could be construed as a potential conflict of interest.

Copyright © 2017 Karmali, Bermúdez Rey, Clark, Wang and Merfeld. This is an open-access article distributed under the terms of the Creative Commons Attribution License (CC BY). The use, distribution or reproduction in other forums is permitted, provided the original author(s) or licensor are credited and that the original publication in this journal is cited, in accordance with accepted academic practice. No use, distribution or reproduction is permitted which does not comply with these terms.

APPENDIX

A. Model Comparisons

We investigated a number of logistic regression models to find the most appropriate descriptor of our results (**Table A1**). Models are listed in ascending order of the BIC, with lower values indicating better models. This comparison shows that there are two categories of models that best describe the data, with none of the five models clearly better than the others. The first is age and roll 0.2 Hz, with or without age adjustment. The second is the first PCA component, with or without the age term included, and with or without age adjustment.

TABLE A1 | Comparison of logistic regression models.

Model	p-Values of each coefficient	BIC	AIC
1 + Age + roll 0.2 Hz (age adjusted)	0.00017 0.0047	84.9	77.1
1 + First PCA component	0.000075	85.2	80
1 + Age + roll 0.2 Hz	0.013 0.0058	85.4	77.7
1 + Age + first PCA component (age adjusted)	0.00032 0.0087	86.1	78.3
1 + Age + first PCA component	0.098 0.013	86.9	79.1
1 + Roll 0.2 Hz	0.000081	88	82.8
1 + Age + yaw + roll 0.2 Hz	0.014 0.36 0.014	89.2	78.8
1 + Age + roll 1 Hz	0.040 0.036	89.3	81.5
1 + Age + roll 1 Hz + roll 0.2 Hz	0.063 0.42 0.039	89.4	79

(Continued)

TABLE A1 | Continued

Model	p-Values of each coefficient	BIC	AIC
1 + Age + sex + roll 0.2 Hz	0.016 0.42 0.0055	89.4	79
1 + First PCA component + second PCA component	0.000087 0.54	89.4	81.6
1 + Age + Z + roll 0.2 Hz	0.063 0.52 0.018	89.6	79.3
1 + Age + Y + roll 0.2 Hz	0.012 0.63 0.0072	89.8	79.4
1 + Age + first PCA component + second PCA component (age adjusted)	0.00033 0.010 0.65	90.5	80.1
1 + Age + Z	0.026 0.090	91.1	83.3
1 + Age + first PCA component + second PCA component	0.12 0.013 0.77	91.4	81
1 + Age + yaw	0.00060 0.11	91.4	83.6
1 + Age + Y	0.0010 0.43	93.4	85.7
1 + Age + Y + roll 1 Hz + roll 0.2 Hz	0.055 0.53 0.37 0.033	93.6	80.6
1 + First PCA component (age adjusted)	0.0052	99.8	94.6
1 + Age + yaw + Y + Z + roll 1 Hz + roll 0.2 Hz	0.084 0.41 0.41 0.75	102	83.6
1 + First PCA component + second PCA component (age adjusted)	0.52 0.044	104	96.4
1 + Age + sex + yaw + Y + Z + roll 1 Hz + roll 0.2 Hz (age adjusted)	0.00026 0.54 0.45	105	84.3
1 + Age + sex + yaw + Y + Z + roll 1 Hz + roll 0.2 Hz	0.46 0.67 0.47 0.047	106	85.3

Most models included an intercept term (indicated by 1+). Most analyses used log-transformed thresholds, and some used age-adjusted, log-transformed thresholds (indicated by age adjusted). The second column shows the p values for each term, excluding the intercept term. The third and fourth terms show the Bayesian information criterion (BIC) and Akaike information criterion (AIC) for each model, with a lower value indicating a better model.

PCA, principal component analysis.



Treatment of the Mal de Debarquement Syndrome: A 1-Year Follow-up

Mingjia Dai¹, Bernard Cohen¹, Catherine Cho^{2,3}, Susan Shin¹ and Sergei B. Yakushin^{1*}

¹ Department of Neurology, Icahn School of Medicine at Mount Sinai, New York, NY, USA, ² Department of Neurology, NYU Langone Medical Center, New York, NY, USA, ³ Department of Otolaryngology, NYU Langone Medical Center, New York, NY, USA

OPEN ACCESS

Edited by:

Dominik Straumann,
University of Zurich, Switzerland

Reviewed by:

Pierre-Paul Vidal,
Université Paris Descartes, France
Fumiuki Goto,
Tokyo Medical Center (NHO), Japan

*Correspondence:

Sergei B. Yakushin
sergei.yakushin@mssm.edu

Specialty section:

This article was submitted
to Neuro-otology,
a section of the journal
Frontiers in Neurology

Received: 23 February 2017

Accepted: 13 April 2017

Published: 05 May 2017

Citation:

Dai M, Cohen B, Cho C, Shin S and
Yakushin SB (2017) Treatment of the
Mal de Debarquement Syndrome:
A 1-Year Follow-up.
Front. Neurol. 8:175.

doi: 10.3389/fneur.2017.00175

The mal de debarquement syndrome (MdDS) is a movement disorder, occurring predominantly in women, is most often induced by passive transport on water or in the air (classic MdDS), or can occur spontaneously. MdDS likely originates in the vestibular system and is unfamiliar to many physicians. The first successful treatment was devised by Dai et al. (1), and over 330 MdDS patients have now been treated. Here, we report the outcomes of 141 patients (122 females and 19 males) treated 1 year or more ago. We examine the patient's rocking frequency, body drifting, and nystagmus. The patients are then treated according to these findings for 4–5 days. During treatment, patients' heads were rolled while watching a rotating full-field visual surround (1). Their symptom severity after the initial treatment and at the follow-up was assessed using a subjective 10-point scale. Objective measures, taken before and at the end of the week of treatment, included static posturography. Significant improvement was a reduction in symptom severity by more than 50%. Objective measures were not possible during the follow-up because of the wide geographic distribution of the patients. The treatment group consisted of 120 classic and 21 spontaneous MdDS patients. The initial rate of significant improvement after a week of treatment was 78% in classic and 48% in spontaneous patients. One year later, significant improvement was maintained in 52% of classic and 48% of spontaneous subjects. There was complete remission of symptoms in 27% (32) of classic and 19% (4) of spontaneous patients. Although about half of them did not achieve a 50% improvement, most reported fewer and milder symptoms than before. The success of the treatment was generally inversely correlated with the duration of the MdDS symptoms and with the patients' ages. Prolonged travel by air or car on the way home most likely contributed to the symptomatic reversion from the initial successful treatment. Our results indicate that early diagnosis and treatment can significantly improve results, and the prevention of symptomatic reversion will increase the long-term benefit in this disabling disorder.

Keywords: vestibular, adaptation, rocking, swaying, bobbing, velocity storage, sea legs, disembarking syndrome

INTRODUCTION

The mal de débarquement syndrome (MdDS) is a maladapted vestibular movement disorder characterized by continuous rocking, swaying, or bobbing that can follow a cruise, flight, or ground transport (the classic MdDS) and can also occur spontaneously (1–7). The continuous oscillating movements are often accompanied by additional symptoms, such as bouncing while walking, intolerance to lights and noises and crowds, impaired cognition, lack of mental clarity (i.e., brain fog), blurry vision, anxiety, depression, and lethargy. These symptoms are generally relieved temporarily while riding in a car or a plane, but return promptly when the ride ends and can persist for months or years. At present, MdDS is not widely recognized by the medical community, and, until recently, there was no effective treatment. While MdDS has been classified as a rare, disabling disease, with the wide interest in cruises, there is a steady stream of patients who contract this illness.

Experimental human and animal studies have provided insight into the neural structures and mechanisms involved in producing this syndrome. MdDS likely originates from the vestibular system since people without vestibular function have the same or better postural stability after 200 miles of sea voyage (8), and the syndrome does not occur in monkeys with short-time constants of the vestibular-ocular reflex (VOR), i.e., in animals without velocity storage (9). Thus, MdDS does not occur in subjects with severe vestibular damage. VOR moves the eyes to stabilize gaze in space during rotation of the head around any axis. Head movements in yaw produce horizontal eye movements. Pitch head movements produce vertical eye movements, and roll head movements produce ocular torsion (10). Thus, simple head roll along the naso-occipital axis only produces torsional eye movements and/or nystagmus without a component in pitch (11, 12). There are situations, however, where the VOR occurs across more than one axis. For example, if the head rolls while the body is rotating in yaw, there is activation of the semicircular canals in both pitch and roll. As the head is turned, the vertical canals are brought into the plane of rotation, producing vertical nystagmus and a strong sensation of tumbling in pitch (9, 13, 14). Similar results were also produced by roll while rotating in cynomolgus monkeys (14). This is an unusual vestibular stimulus that we designate as a cross-axis-coupled stimulus (9) because the third axis of eye movement is produced by a cross-product of the other two axes (15) and has been used in training astronauts for mitigating motion sickness susceptibility (9, 16–18). A cross-axis-coupled stimulus can alter velocity storage of the VOR (19, 20) to produce persistent, abnormal eye movements (1, 14, 21).

The VOR is composed of three components: yaw, pitch, and roll. All three are the subject of adaptation (22). Adaptation of the VOR can occur in a specific context across different axes (23). Contextual adaptation is long lasting, and the changes induced by 1 h of training can last for several days (24–27). As described in the paragraph above, simultaneous rotation about yaw and oscillation in roll induces oscillation in pitch (9, 14). If a subject is adapted to that context, then, similar to cross-axis adaptation, simple oscillation in roll can induce adaptive compensatory eye oscillations in pitch. This finding became the bases for the

hypotheses of the underlying mechanism of MdDS (1). Cruise ships frequently change their course. In addition, the ships are constantly rocking side to side at ≈ 0.2 Hz (28). Most of the people become motion sick from such a complex stimulus; however, others are well adapted and feel fine while in motion. On disembarkment, however, small head motions, side to side with every step, induce a sensation of gravitational pull forward and backward. When motionless, however, the patient experiences a sensation of constant rocking at ≈ 0.2 Hz.

We reasoned that if the notion of MdDS caused by maladaptation of the VOR holds true, a reversed VOR stimulus should mitigate or even cure the MdDS symptoms. Based on these findings, a treatment for MdDS was devised that consisted of rolling the head at the frequency of body rocking, while the subjects viewed a slowly moving visual surround. This postulate was tested in 24 MdDS patients employing cross-axis visual coupling (1). The results were promising: 75% of the MdDS patients had significant improvement in a 12-month observation, which was the first successful treatment of this debilitating illness. Since then, 330 MdDS patients have been treated with a similar initial success rate. This report documents the follow-up of 141 of these treated patients who had a year observation, of whom 120 had the classic MdDS and 21 had the spontaneous MdDS.

MATERIALS AND METHODS

Patient Selection

Subjects were screened with a brief interview and an intake form. The inclusion criteria were reports of continuous rocking, swaying, and/or bobbing, which had persisted for at least 3 weeks. Their symptoms were temporarily relieved during car rides (1) and returned immediately after the rides had ended. They had no history of head or neck trauma, Lyme disease, vestibular disease, or major neurological or vascular disorders. For all patients if the oscillating sensation began less than 3 days after a passive motion event, it was designated as the classic form of MdDS. If the oscillating sensation was not preceded by a motion event or it took place more than 3 days after a motion event, it was designated as the spontaneous form of MdDS. The patients were referred by medical doctors, physiotherapists, or former patients, or were self-referred. Many had completed neurologic and otologic workups including MRIs. These studies were generally normal.

Treatment Procedure

The clinical treatment has been detailed in our previous study (1). A critical aspect was to establish the frequency of the rocking and swaying. Static posturography for stability was performed using a Wii board that measured rocking and sway (1). The dominant oscillating frequency was determined from the power spectra of the recorded center of pressure (COP) (29). If the body movements were not expressed physically, the patients were asked to move their arm attached to an acceleration sensor at the frequency of the internally sensed movement.

During the treatment, the head was rolled from side to side at the measured frequency while they watched the movement of vertical stripes projected onto the wall of an enclosure that surrounded them. The direction of the horizontal optokinetic (OKN)

stimulus was predetermined based on the Fukuda stepping test, circular body rotation, or spontaneous horizontal nystagmus that was due to the maladaptation of the VOR (14). In some cases, the direction of OKN could not be determined. If so, an arbitrary direction was tested for ≈ 30 s to see whether it was effective to improve the symptoms. If the symptoms became worse or there was no effect, the direction of drum rotation was reversed. The patients were treated 10–120 min a day for 4–5 consecutive days. On the first and last day, their balance was measured by posturography, and they were asked to rate their level of MdDS severity and to describe their symptoms.

Subjective Measures

The levels of subjective severity were reported on a simplified 10-point scale before and after treatment. A score of 10 was the most severe symptoms that they had experienced. A score of 5 was moderate, and they scored 0 if they were completely symptom free. The subjective score was based on the patient's own experiences as well as being dependent on their initial severity level before the treatment. There has been no unified self-scoring index system, and the self-ratings were used for the percentage change in subjective severity as an assessment of treatment effects.

Survey Process

The patients were asked to report the status of the MdDS severity and specific symptoms retrospectively at 2 weeks and 3, 6, and 12 months after treatment. The common symptoms reported are listed in Table 1.

Assessment of Treatment

A reduction of the symptom severity by more than 50% was deemed a clinically significant improvement or success of treatment. The treatment results of symptom severity were related to the forms of MdDS, duration, age, gender, and posturography.

The displacement of COP over a 20-s period was measured, and the root mean square (RMS) of the postural displacement was computed (30) to compare the postural stability before and

after the treatment (1). The total trajectory length (maximum excursion) of the COP deviation was computed over 20 s.

Statistics

ANOVA and Student's *t*-tests were used to establish the statistical significance of the findings.

RESULTS

Demographics and Attributions

One hundred forty-one patients of 155 who were treated a year or more ago and who responded to our follow-up formed the basis for this report. The average age of the female patients was 49 ± 13 years and for male was 38 ± 13 years. There were 120 classic cases with 100 females and 20 males, a ratio of 5:1. Thus, classic MdDS was more common in women than in men. The spontaneous group was composed of 2 males and 19 females, also a strong female predominance. Since the spontaneous group is small, the majority of the statistical analyses was performed for patients with classic MdDS. In the classic group, there were 56 individuals in whom the MdDS was triggered by a cruise (47%); 30 (25%) by boating; 23 (19%) by air flights; 7 (6%) by car, bus, or train rides; and the others by playing video games, rafting, or scuba diving.

In the spontaneous group, nine patients (43%) could not recall a particular event that preceded their MdDS. One had had classic MdDS that had remitted years ago. The MdDS in eight patients was preceded by a period of stress and anxiety from switching medication, severe headache, surgery, or heavy drinking. In the remaining three patients, one reported that his MdDS was triggered by an episode of benign paroxysmal positional vertigo. A brief motion triggered the other two patients: one due to a sudden drop of a helicopter and the other due to a 360° spin of a vehicle on ice.

Primary Symptoms

Symptoms associated with MdDS were reported widely and differently, and they are listed in Table 1. Many patients experienced more than one type of motion. The primary symptoms were related to their motion sensation, either observable physically or perceived internally. The most common sensation was rocking, i.e., an oscillation back and forth, recorded or reported in 95% of the patients. Next most common sensations were swaying, i.e., side to side, in 55% and bobbing up and down in 43% of patients. In addition, bouncing while walking, which was labeled as "trampoline walking," was often a complaint. There were variations in trampoline walking. Some patients felt that they were pushed as if they were walking on an airport moving walkway, others experienced "moon walking" up and down in a slow motion, and the others felt side-to-side bouncing for each step as if they were walking on a floating dock. These bounces could be felt only in some parts of the body, i.e., in the head, trunk, and legs or feet. Besides the motion sensations, some patients also experienced a steady pulling sensation on the body in a particular direction when standing still. This was labeled as "gravity pulling." Falling backward due to the backward pulling was most common.

TABLE 1 | Percentage of the symptom occurrence.

Symptoms	Pretreatment	A year later
Rocking	80	42
Swaying	73	44
Bobbing	46	32
Gravity pulling	54	39
Trampoline walking	29	30
Fatigue	62	54
Unstable in crowds	51	60
Brain fog	53	49
Sensitivity to fluorescent lights	51	48
Sensitivity to computer screens	54	40
Anxiety	49	41
Depression	38	23
Fullness of the ears	39	23
Tinnitus	33	27
Fussy vision	37	29
Clumsiness	37	37
Head pressure	28	32

Additional Symptoms

These were mainly secondary to the primary problem of incessant motion. They occurred immediately or days or months after the onset of the MdDS. They included light or sound sensitivity, head pressure, heaviness of the body, brain unclarity (fog), fuzzy vision, claustrophobia, agoraphobia, stress, anxiety, fatigue, insomnia, and depression, and they were not uncommon. The symptoms could be exaggerated by physical or visual motions, hormonal changes, weather changes, stress, and fatigue. The symptoms could also be aggravated by coffee (28%) and alcohol (21%). Some patients had prolonged motion after-sensations (aftereffects), i.e., those that followed a motion or movement (31). The persistent symptoms were incapacitating, and many even were unable to continue working.

About half of the patients developed heightened motion and visual sensitivity. As a result, they experienced motion sickness as well as migraine-like symptoms, such as headache, pulsating head pressure, and woozy and queasy feelings. Most of them, however, did not have a clear history of migraine or motion sickness predating their MdDS.

Initial Posttreatment Results

The average score of severity for the classic group before treatment was 6.1 ± 1.9 . Immediately after treatment, the average score was 2.4 ± 2.1 ($P < 0.0001$, $N = 120$), with a rate of success of 78%. Twenty-three became asymptomatic (19%) after the treatment. In the spontaneous group, the average score of severity before treatment was 6.6 ± 1.8 . After treatment, the average score was 2.5 ± 2.8 ($P < 0.001$, $N = 21$), with a rate of success of 48%.

Postural Instability and Subjective Improvement

Static posturography was recorded before and a week after treatment for 105 patients, and the relationship in improvement between the subjective measure and postural stability was determined for patients who reported >50% improvement. These data are shown in **Figure 1**. The median value of the self-reported improvement was 75% (**Figure 1A**), which was better than the median values of improvement in swaying (63%; **Figure 1B**), rocking (55%; **Figure 1C**), or maximum body excursion (38%; **Figure 1D**). These data indicate that postural improvement was concomitant with subjective improvement, but there was not a simple quantitative relationship between the subjective measure and the postural stability. The actual traces of postural frequency were predominantly at 0.2 Hz, which is roughly 90° phase shifted from the sway (**Figure 1E1**). After treatment, there was no predominant frequency (**Figure 1F2**). The rocking combined with swaying (**Figure 1E1** and 2) formed a circular progression of the trunk around the stationary feet. This circular progression (CW) can be best seen in the trajectory plots of the COP deviation (**Figure 1G**) recorded by a Wii board. After treatment, the circular progression disappeared together with a smaller COP trajectory (**Figure 1H**). In these examples, the RMS of sway before treatment was 11 and 5 mm after treatment. The RMS of rocking before treatment was 25 and 10 mm after treatment. The disappearance of a dominant oscillating frequency and the reduction of the

RMS of rocking and sway provided objective data supporting the efficacy of treatment. The average rocking frequency for all classic patients was 0.23 ± 0.16 Hz (ranging from 0.02 to 1.0 Hz), which was significantly lower than the sway frequency (0.29 ± 0.17 Hz, ranging from 0.06 to 0.8 Hz, $P = 0.011$). There was no difference in rocking ($P = 0.46$, ANOVA) and swaying frequencies ($P = 0.44$, ANOVA) between age groups.

One-Year Follow-up

Symptoms Reported from Follow-ups

Table 1 shows the percentage of all patients who experienced the spontaneous symptoms before the treatment and thereafter for a year. The patients did not specifically grade the severity for each of the symptoms. A year later, 38, 29, and 14% of patients who initially experienced rocking, swaying, or bobbing were free of these symptoms respectively. Meanwhile, 15% had recovered from gravity pulling. For some, although the symptoms were still lingering a year later, they were much milder and infrequent compared to the pretreatment period.

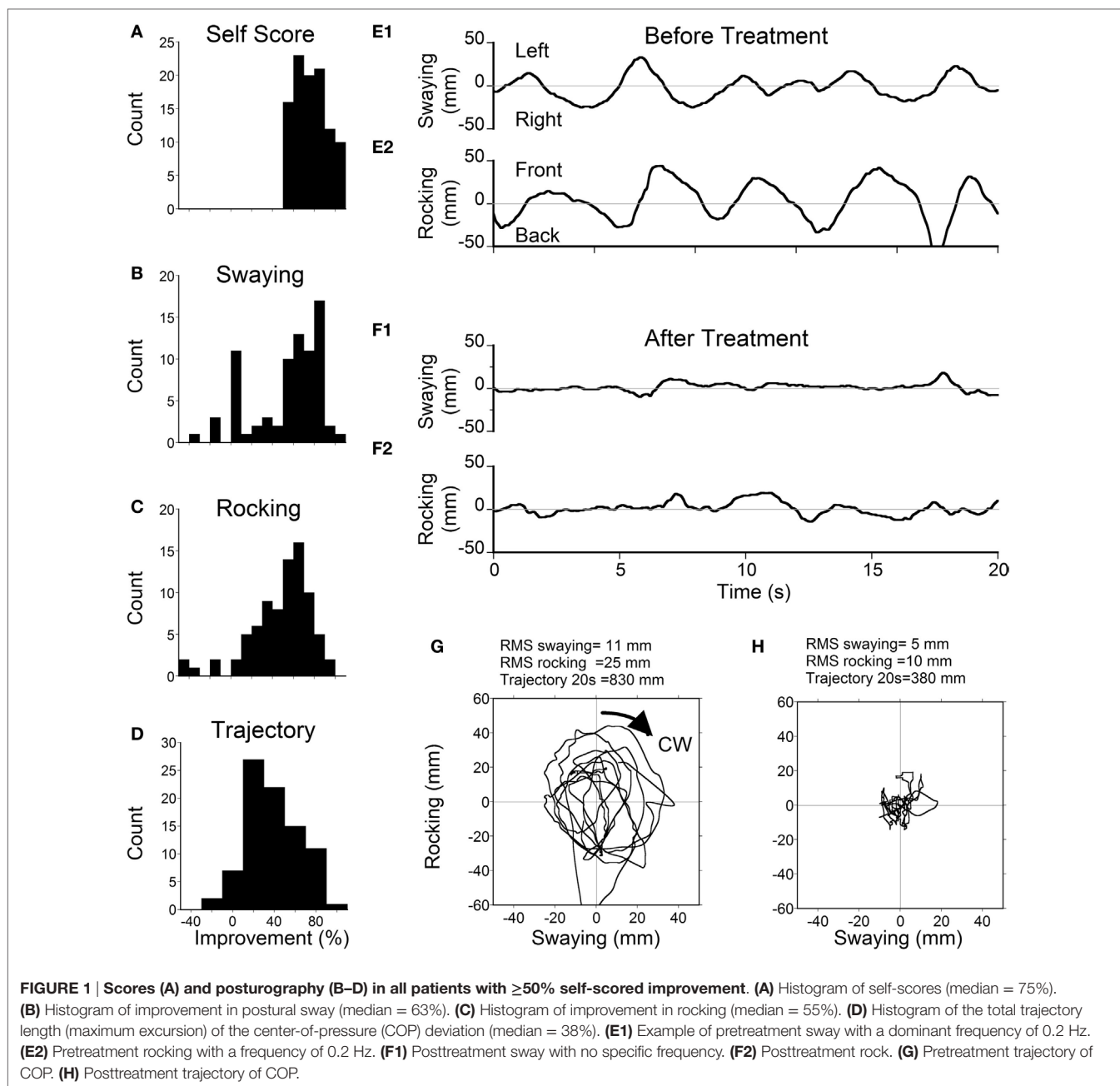
In the classic group, there was a significant setback 2 weeks after treatment. The rate of subjective improvement dropped to 42% from the initial 78%. A year later, the rate increased to 53% (**Figure 2**), and 32 patients did not experience any symptoms (27%). There was also a significant setback in the spontaneous group. The rate dropped to 14% at week 2 from the initial 48%. It climbed back to 48% a year later, however (**Figure 2**). There was no difference in the improvement rate between classic and spontaneous groups at 1 year. Interestingly, nine classic patients and three spontaneous patients, who did not improve initially, were significantly improved 1 year later.

Difference between Genders

The most striking difference was the heavy predominance of the MdDS in females, in both the classic and spontaneous groups. Effects of treatment were similar, however, in both genders (80% for male and 75% for female). The success rate dropped to 55% in male patients and 53% in female patients a year after treatment (**Figure 3**). Small gender differences were noted at week 2, and the improvement rate dropped to 39% in females but less in males (55%).

Effects of Symptom Duration on Treatment

The 120 classic patients were examined for the effects of symptom duration of MdDS on treatment (**Figure 4**). The patients were divided into three groups based on the duration of the illness; 1 year or less (Group 1, $N = 53$), more than 1 year to 3 years (Group 2, $N = 34$), and more than 3 years (Group 3, $N = 33$). The initial rate of success was higher in Group 1 (85%). This was followed by Group 2 (79%) and Group 3 (64%). The success rate decreased to 47% (Group 1), 35% (Group 2), and 39% (Group 3) at week 2 when they returned home. There was a recovery in Group 1 (62%) and Group 2 (56%) at a year but not in Group 3 (30%). There was no difference between Groups 1 and 2 over a year ($P = 0.07$, repeated measures, ANOVA), but there was a significant difference between Groups 1 and 3 ($P = 0.0003$) and Groups 2 and 3 ($P = 0.013$). Thus, in general, the treatment was less successful for those with MdDS for more than 3 years.



There were exceptions, however. Seven patients whose history was greater than 9 years (from 9 to 27 years) had a better outcome than Group 3 as a collective. The initial rate was 71% that declined to 57% after week 2 but still held at 43% after a year.

Effect of Age on Treatment

The average age for patients with classic MdDS was 48 ± 14 years (**Figure 5A**). This was similar to the mean age in our prior study (1). These patients were divided into three age groups: less than 40 years (Group 1, $N = 28$), 40–60 years (Group 2, $N = 70$), and greater than 60 years (Group 3, $N = 22$). The initial effect was better in the oldest patients (Group 3, 86% improvement). This was followed by Group 2 (79%) and then by Group 1 (66%).

The initial rate of success dropped to 42% at 2 weeks for all three groups (**Figure 5B**). There were no significant differences between Groups 1 and 2 in the success rates over a year after the initial improvement at week 1 (**Figure 5B**; $P = 0.99$, ANOVA). Despite the higher initial success rate in patients who were older than 60 years, they were not able to maintain this improvement. Their rate of improvement declined to below that in the younger groups (**Figure 5B**; $P < 0.0004$). Groups 1 and 2 recovered to 53% and Group 3 did not improve over a year (**Figure 5B**).

Recurrent MdDS

Recurrent episodes of MdDS were experienced by 23% of the classic patients (25 of 120). They experienced a relapse due to

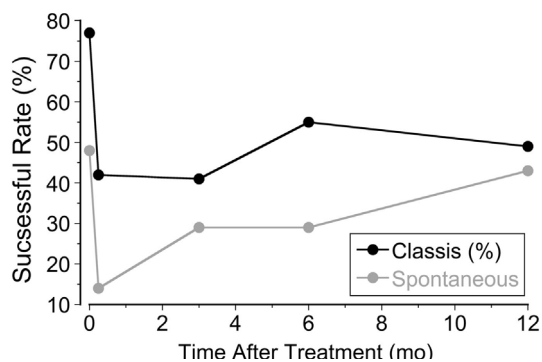


FIGURE 2 | Percentage of patients improved at week 1, week 2, month 3, month 6, and month 12 after treatment.

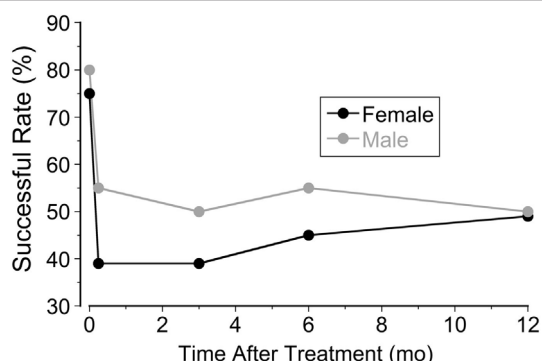


FIGURE 3 | Improvement rates in female and male patients at week 1, week 2, month 3, month 6, and month 12 after treatment.

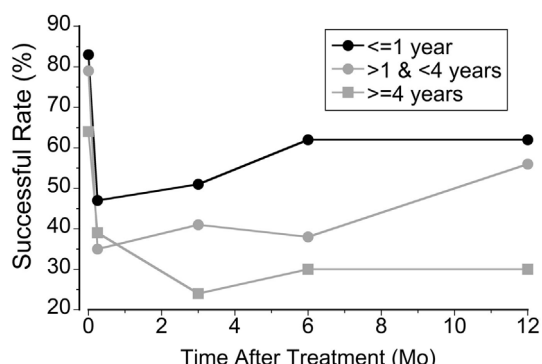


FIGURE 4 | The relationship between the rate of success and the duration of mal de debarquement syndrome at week 1, week 2, month 3, month 6, and month 12 after treatment.

another cruise, boating, a long haul flight, or an extreme stress, or they had a slow regression after a period of remission. There was no difference in age or gender between patients who had recurrent episodes or a single episode of MdDS. The initial improvement in these two groups was approximately the same

(67% in patients with recurrent episodes versus 72% in patients with a single episode). A year later, 63% of patients with recurrent episodes had improved, but only 50% of patients with a single episode were better.

Progression over a Year between Long-term Successful and Unsuccessful Groups

The classic patients were divided into two groups: those in whom 50% improvement had occurred in 12 months and those with a lesser successful rate. Sixty-two were successful, and 58 were unsuccessful. Their progression over a year is shown in **Figure 6**. The pretreatment severity score for the successful group was not different from that of the unsuccessful group (5.7 ± 1.9 versus 6.3 ± 1.8 ; $P = 0.08$). There was a smaller rebound of the average score in the successful group from 1.7 ± 1.5 at week 1 to 2.5 ± 2.1 at week 2 (47% increase). There was a larger rebound in the unsuccessful group from 2.7 ± 2.2 at week 1 to 5.3 ± 2.4 at week 2 (96% increase). Despite the small rebound at week 2 in the successful group, the improvement by more than 50% was maintained at any given time of the year. These data indicate that when the rebound at week 2 was small, the improvement would last, and *vice versa*. Of note is that some of our successful patients had an additional motion sickness treatment that desensitized their motion and visual sensitivity (32), which in turn may actually have reduced the chance of reversion. More study is needed to investigate the relationship between the visual–motion sensitivity and the reversion of MdDS.

While there was no such 50% improvement over a year in the unsuccessful group after the larger rebound at week 2, however, there was a statistically significant reduction in severity between the pretreatment and at month 12 ($P = 0.005$). These accompanied their general feelings of less and milder symptoms.

DISCUSSION

Summary of Findings

Using a full-field visual stimulus while the head was rolled the severity of MdDS symptoms was successfully improved by $\geq 50\%$ immediately after the treatment in 78% of 120 classic patients and in 48% of 21 spontaneous patients. The improvement was also shown in posturography findings (**Figure 1**). In the classic cases, the initial improvement rate of subjective findings regressed to 42% over 2 weeks upon returning home, but rose to 52%, 12 months later. The success rate of spontaneous cases fell to 14% 2 weeks after treatment, but then rose to 48%, 12 months later (**Figure 2**). For patients who did not have a 50% reduction, there was still a statistically significant reduction in subjective symptoms a year later compared to the pretreatment level ($P = 0.005$). There was a marked preponderance of females with MdDS, but there was essentially no difference in the response to treatment between genders (**Figure 3**). There was also the same tendency for a reduced rate of success in patients who had had the MdDS for long periods (**Figure 4**), or they were of an advance age (**Figure 5**). This was not universal, however. There were three patients with more than 20 years of symptom duration who were treated successfully. Thus, we were able to essentially reproduce the beneficial results of treatment for MdDS, a condition that

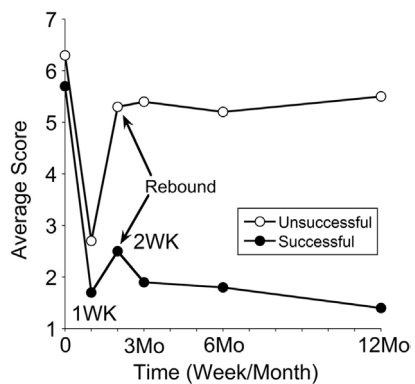
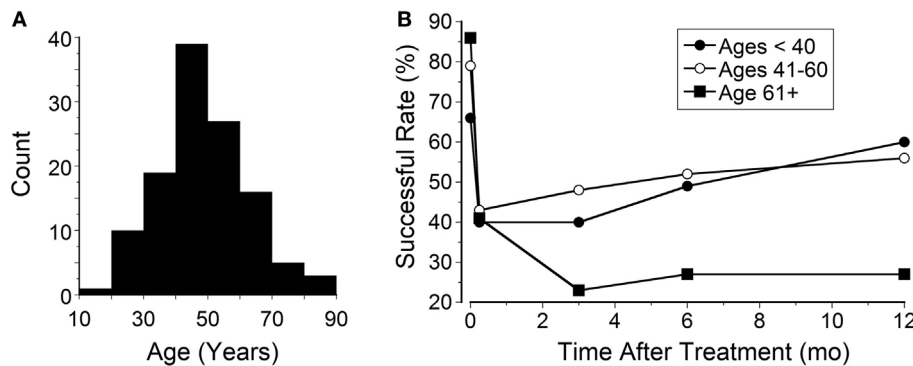


FIGURE 6 | Progression in severity scores over a year in treatment-successful and treatment-unsuccessful groups. Time 0 is pretreatment, followed by posttreatments at week 1, week 2, month 3, month 6, and month 12. The symptom rebound at week 2 is indicated by arrows. The SDs of the data set were not shown, which are from 1.0 to 2.0.

had had no successful treatment prior to our earlier study (1). The medical community is generally unaware that the MdDS is a characteristic set of signs and symptoms, and the patients who came to us most frequently had a full medical workup with many medical tests, costing thousands of dollars by the time that these patients were diagnosed and referred. The knowledge that there is such a syndrome and further that it can be successfully treated would be a benefit to both patients and the medical system.

There was a significant reversion in improvements when patients traveled back home at week 2, more in women than in men (Figure 2). There are many reasons to account for the reversion. The major factors most probably were the long duration of traveling and anxiety. The rate of reversion when traveling home was higher in this study (36%) than in the previous study, in which only about 22% of successfully treated patients had a regression of symptoms (1). The reason for this difference is not clear, but in the previous study, most patients lived nearby and did not have to travel long distances to return home. More than half of the patients also developed heightened visual and motion sensitivity following the onset of the MdDS. When their

oscillating symptoms were treated, there were still a portion of patients who were susceptible to visual and motion stimuli, such as intolerance to fluorescent lights, flickering screens, and busy patterns. Some of them reported that their symptoms had reverted when they were exposed to patterned hallway or extreme lighting conditions. The subjects were asked to take a small dose of a benzodiazepine when traveling home, but it did not always produce the desired result.

One of the interesting outcomes from this follow-up is that when there was no or less reversion, the improvement was sustainable, and *vice versa* (Figure 6). Thus, the avoidance of the reversion in the first 2 weeks could be vital to retain the treatment effects. On the other hand, if this setback in the first 2 weeks could be reverted back to the week 1 posttreatment level using an effective home-based treatment, it might help those patients with reversions.

The Neural Basis of the MdDS

Mal de débarquement, or sea legs, is a natural phenomenon after some sea voyages, ordinarily only lasting for up to 24 h, even after long voyages (33, 34). It can also occur from other transport modalities. This is different from the MdDS that can last for weeks, months, or years (1, 2, 4, 35). The neural basis for the MdDS was shown in humans and monkey experiments to be produced by a combination of roll with rotation (14, 21) that caused a deviation of the yaw axis eigenvector from gravity, i.e., the axis around which the eyes rotate in upright and tilted positions.

The neuronal activity responsible for MdDS is probably in the velocity storage integrator located in the vestibular-only (VO) neurons in the medial and superior vestibular nuclei (36). Monkeys without velocity storage and very short VOR time constants do not develop abnormal responses to roll while rotating, and the same is true for humans without velocity storage, confirming that the MdDS is a vestibular phenomenon, arising in the brainstem. The VO neurons are GABA_b-ergic, and their axons cross the brainstem (37, 38), and they send activity into the reticulospinal and vestibulospinal pathways (39). Thus, they could provide the vestibulospinal activity to produce the rocking, swaying, and bobbing to the body and limbs. VO neuron activity can also reach the oculomotor system through velocity-pause-saccade neurons, but the activity in these neurons

disappears in drowsiness, although the vestibulospinal activity and the rocking persist during drowsiness (36). The velocity storage integrator is under the control of the nodulus in lobule 10 of the vermis of the vestibulocerebellum (40–43). As far as is known, there is no structural or pathologic process that involves the brainstem of those individuals who suffer from the MdDS.

In an accompanying hypothesis (this volume), we postulate that the neurons on both sides of the brainstem oscillate with the activity flowing back and forth, at about 0.2 Hz to activate the body and legs into rocking and swaying at 0.2 Hz. The source of the 0.2 Hz drive is unknown, but it is likely to originate in the nodulus of the vestibulocerebellum, which exerts control over the velocity storage system (42–47). Such activity, which has been found in the cerebellar cortex of the nodulus in the rabbit (48), can be brief or can last for years. Why and how the activity is generated continuously is not understood, but it is clear that the MdDS is an illness without significant pathology that has been determined, at least at this time. Therefore, if appropriate maneuvers or drugs are found to stop the oscillations, subjects can be restored to normality, even after having suffered with the incessant oscillations for many years.

For these reasons, we believe that the other symptoms that accompany the MdDS, i.e., anxiety, brain fog, depression, sensitivity to sound and light, and headaches are likely to be due to the inability to turn off the incessant oscillations. Such symptoms have been widely noted and are exhaustively detailed in a recent article by Van Ombergen et al. (7). Since the process producing the MdDS most likely originates in the velocity storage mechanism in the brainstem, magnetic cortical stimulation is likely to be ineffective in producing long-term relief.

Limits of the Study

1. We investigated the relationship between self-scored severity and postural instability in patients we have treated successfully (**Figure 1**). The successful patients had improvement in sway, rocking, and the maximum excursion of the COP of the body. Moreover, the oscillations related to rocking and swaying disappeared in the successful patients. However, the degrees of the improvement in postural stability were lower than the median value of the self-scored improvement that was 78%. Thus, while the postural data are roughly correlated with the tendency of subjective improvement, the quantitative relation is not fully established at present.
2. Because of the widespread origin of the patients, it was impossible to do posturography after the patients left our treatment facility. While the posturography provided an objective measure, there was a portion of patients who did not have a physical sign of instability rather than a sensation of internal motion. Therefore, the measure of the success of treatment at present mainly depends on the patient's subjective assessment of their status.
3. We used a 10-point scale to assess the overall severity of the MdDS. Although the scale has been commonly used clinically, it has not been verified, and it is not certain how it may have varied among the many patients of different ages, genders, and

experiences. At present, there is no standard indexing system to estimate the severity of the MdDS that encompasses all physiological and emotional aspects of the MdDS symptoms. It is certain that a major component should be related to the oscillating sensations, since those are the major features of the MdDS. With a better scoring system, the interindividual difference in reporting the severity may be reduced to allow a better estimate.

4. Although we had a large sampling size, one inadequacy was our failure to have a placebo-controlled crossover design of treatment. Unfortunately, the resources were not available, and it was not possible, particularly in patients who flew to New York from the Midwest, Florida, the West Coast, Canada, Europe, or Australia and spent a week in New York to accomplish the extra study that is likely to be unsuccessful in relieving the patients' symptoms and signs.
5. Sea legs are common for short periods after many experiences on the sea, but it is not clear why the oscillation can persist for months or years in some people, and particularly in women, centered around menopausal age. There is a similar preponderance of women experiencing motion sickness, with activation of the autonomic system, but why there is this gender predominance is not clear.

CONCLUSION

Despite the setback from the initial effectiveness of the treatment, we are pleased that we still achieved a significant improvement in about 50% of classic and spontaneous MdDS patients after 1 year of observation. Thus, the treatment we developed is reproducible (1). If the reversion problem can be resolved, more than 75% of MdDS patients will benefit from this treatment.

ETHICS STATEMENT

This retrospective human study was performed in accordance with the Helsinki Declaration of 1975, as revised in 2013 (49) and was approved by the IRB of Mount Sinai School of Medicine with an exemption of informed consent.

AUTHOR CONTRIBUTIONS

MD and SY contributed to research design, data collection, data processing, making figures, and writing of this manuscript. BC and CC contributed to research design and writing of this manuscript. SS referred patients for treatment, and contributed to discussion of treatment results and writing of manuscript.

ACKNOWLEDGMENTS

We are particularly grateful to Abraham Shulman, M.D., Emeritus Professor of NeuroOtology, and the Martha Entenmann Tinnitus Research Center, Inc., at the Department of Otolaryngology, Dow State Medical Center, who donated a complete rotational and optokinetic setup. We also thank Dmitri Ogorodnikov for technical and engineering support and Rupa Mirmira for editorial assistance.

REFERENCES

- Dai M, Cohen B, Smouha E, Cho C. Readaptation of the vestibulo-ocular reflex relieves the mal de debarquement syndrome. *Front Neurol* (2014) 5:124. doi:10.3389/fneur.2014.00124
- Brown JJ, Baloh RW. Persistent mal de debarquement syndrome: a motion-induced subjective disorder of balance. *Am J Otolaryngol* (1987) 8:219–22. doi:10.1016/S0196-0709(87)80007-8
- Hain TC, Hanna PA, Rheinberger MA. Mal de debarquement. *Arch Otolaryngol Head Neck Surg* (1999) 125:615–20. doi:10.1001/archotol.125.6.615
- Cha YH, Brodsky J, Ishiyama G, Sabatti C, Baloh RW. Clinical features and associated syndromes of mal de debarquement. *J Neurol* (2008) 255:1038–44. doi:10.1007/s00415-008-0837-3
- Cha YH, Debleick C, Wu AD. Double-blind sham-controlled cross-over trial of repetitive transcranial magnetic stimulation for mal de debarquement syndrome. *Otol Neurotol* (2016) 37:805–12. doi:10.1097/MAO.0000000000001045
- Hain TC, Cherchi M. Mal de debarquement syndrome. *Handb Clin Neurol* (2016) 137:391–5. doi:10.1016/B978-0-444-63437-5.00028-5
- Van Ombergen A, Van Rompaey V, Maes LK, Van De Heyning PH, Wuyts FL. Mal de debarquement syndrome: a systematic review. *J Neurol* (2016) 263:843–54. doi:10.1007/s00415-015-7962-6
- Fregley AR, Graybiel A. *Residual Effects of Storm Conditions at Sea upon Postural Equilibrium Functioning of Vestibular Normal and Vestibular Defective Human Subjects*. NSAN-935. Pensacola, FL, USA: Naval School of Aviation Medicine (1965).
- Dai M, Kunin M, Raphan T, Cohen B. The relation of motion sickness to the spatial-temporal properties of velocity storage. *Exp Brain Res* (2003) 151:173–89. doi:10.1007/s00221-003-1479-4
- Cohen B, Raphan T. The physiology of the vestibuloocular reflex. In: Highstein SM, Fay RR, Popper AN, editors. *The Vestibular System*. New York: Springer (2004). p. 235–85.
- Cohen B, Tokumasu K, Goto K. Semicircular canal nerve eye and head movements. *Arch Ophthalmol* (1966) 76:523–31. doi:10.1001/archophth.1966.03850010525010
- Yakushin SB, Xiang Y, Cohen B, Raphan T. Dependence of the roll angular vestibuloocular reflex (aVOR) on gravity. *J Neurophysiol* (2009) 102:2616–26. doi:10.1152/jn.00245.2009
- Graybiel A, Wood CD. Rapid vestibular adaptation in a rotary environment by means of controlled head movements. *Aerospace Med* (1969) 40:638–43.
- Dai M, Raphan T, Cohen B. Adaptation of the angular vestibulo-ocular reflex to head movements in rotating frames of reference. *Exp Brain Res* (2009) 195:553–67. doi:10.1007/s00221-009-1825-2
- Dai M, Raphan T, Cohen B. Spatial orientation of the vestibular system: dependence of optokinetic after nystagmus on gravity. *J Neurophysiol* (1991) 66:1422–38.
- Guedry FE, Collins WE, Graybiel A. Vestibular habituation during repetitive complex stimulation: a study of transfer effects. *J Appl Physiol* (1964) 19:1005–15.
- Guedry FE, Benson AJ. Coriolis cross-coupling effects: disorienting and nauseogenic or not? *Aviat Space Environ Med* (1978) 49:29–35.
- Young LR, Hecht H, Lyne L, Sienko K, Cheung C, Kavelaars J. Artificial gravity: head movements during short-radius centrifugation. *Acta Astronaut* (2001) 49:215–26. doi:10.1016/S0094-5765(01)00100-X
- Raphan T, Matsuo V, Cohen B. Velocity storage in the vestibulo-ocular reflex arc (VOR). *Exp Brain Res* (1979) 35:229–48. doi:10.1007/BF00236613
- Raphan T, Cohen B. The vestibulo-ocular reflex (VOR) in three dimensions. *Exp Brain Res* (2002) 145:1–27. doi:10.1007/s00221-002-1067-z
- Guedry FE Jr, Graybiel A. Compensatory nystagmus conditioned during adaptation to living in a rotating room. *J Appl Physiol* (1962) 17: 398–404.
- Bello S, Paige GD, Highstein SM. The squirrel monkey vestibulo-ocular reflex and adaptive plasticity in yaw, pitch, and roll. *Exp Brain Res* (1991) 87:57–66. doi:10.1007/BF00228506
- Shelhamer M, Robinson DA, Tan HS. Context-specific adaptation of the gain of the vestibulo-ocular reflex in humans. *J Vestib Res* (1992) 2:89–96.
- Pettorossi VE, Panichi R, Botti FM, Kyriakareli A, Ferraresi A, Faralli M, et al. Prolonged asymmetric vestibular stimulation induces opposite, long-term effects on self-motion perception and ocular responses. *J Physiol* (2013) 591:1907–20. doi:10.1113/jphysiol.2012.241182
- Schubert MC, Migliaccio AA, Minor LB, Clendaniel RA. Retention of VOR gain following short-term VOR adaptation. *Exp Brain Res* (2008) 187:117–27. doi:10.1007/s00221-008-1289-9
- Yakushin SB, Bukharina SE, Raphan T, Buettner-Ennever J, Cohen B. Adaptive changes in the angular VOR: duration of gain changes and lack of effect of nodulo-uvulaectomy. *Ann N Y Acad Sci* (2003) 1004:78–93. doi:10.1196/annals.1303.009
- Yakushin SB, Palla A, Haslwanter T, Bockisch CJ, Straumann D. Dependence of adaptation of the human vertical angular vestibulo-ocular reflex on gravity. *Exp Brain Res* (2003) 152:137–42. doi:10.1007/s00221-003-1543-0
- Schmitke RT. Shipsway, roll, and yaw motions in oblique seas. *SNAME Trans* (1978) 86:26–46.
- Demura S, Kitabayashi T, Noda M. Power spectrum characteristics of sway position and velocity of the center of pressure during static upright posture for healthy people. *Percept Mot Skills* (2008) 106:307–16. doi:10.2466/pms.106.1.307-316
- Brandt T, Krafczyk S, Malsbenden I. Postural imbalance with head extension: improvement by training as a model for ataxia therapy. *Ann N Y Acad Sci* (1981) 374:636–49. doi:10.1111/j.1749-6632.1981.tb30907.x
- Lewis RF. Frequency-specific mal de debarquement. *Neurology* (2004) 63:1983–4. doi:10.1212/01.WNL.0000144701.94530.6A
- Dai M, Raphan T, Cohen B. Prolonged reduction of motion sickness sensitivity by visual-vestibular interaction. *Exp Brain Res* (2011) 210:503–13. doi:10.1007/s00221-011-2548-8
- Cohen H. Vertigo after sailing a nineteenth century ship. *J Vestib Res* (1996) 6:31–5. doi:10.1016/0957-4271(95)02004-7
- Gordon CR, Spitzer O, Dowec I, Melamed Y, Shupak A. Clinical features of mal de debarquement: adaptation and habituation to sea conditions. *J Vestib Res* (1995) 5:363–9. doi:10.1016/0957-4271(95)00005-Z
- Cha YH. Mal de debarquement. *Semin Neurol* (2009) 29:520–7. doi:10.105/s-0029-1241038
- Reisine H, Raphan T. Neural basis for eye velocity generation in the vestibular nuclei of alert monkeys during off-vertical axis rotation. *Exp Brain Res* (1992) 92:209–26. doi:10.1007/BF00227966
- Holstein GR, Martinelli GP, Wearne S, Cohen B. Ultrastructure of vestibular commissural neurons related to velocity storage in the monkey. *Neuroscience* (1999) 93:155–70. doi:10.1016/S0306-4522(99)00141-4
- Katz E, Vianney de Jong JM, Büttner-Ennever JA, Cohen B. Effects of midline medullary lesions on velocity storage and the vestibulo-ocular reflex. *Exp Brain Res* (1991) 87:505–20. doi:10.1007/BF00227076
- McCall AA, Miller DM, Yates BJ. Descending influences on vestibulospinal and vestibulosympathetic reflexes. *Front Neurol* (2017) 8:112. doi:10.3389/fneur.2017.00112
- Wearne S, Raphan T, Waespe W, Cohen B. Control of the three-dimensional dynamic characteristics of the angular vestibulo-ocular reflex by the nodulus and uvula. *Prog Brain Res* (1997) 114:321–34. doi:10.1016/S0079-6123(08)63372-5
- Sheliga BM, Yakushin SB, Silvers A, Raphan T, Cohen B. Control of spatial orientation of the angular vestibulo-ocular reflex by the nodulus and uvula of the vestibulocerebellum. *Ann N Y Acad Sci* (1999) 871:94–122. doi:10.1111/j.1749-6632.1999.tb09178.x
- Solomon D, Cohen B. Stimulation of the nodulus and uvula discharges velocity storage in the vestibulo-ocular reflex. *Exp Brain Res* (1994) 102:57–68. doi:10.1007/BF00232438
- Angelaki DE, Hess BJ. Lesion of the nodulus and ventral uvula abolish steady-state off-vertical axis otolith response. *J Neurophysiol* (1995) 73:1716–20.
- Angelaki DE, Hess BJ. The cerebellar nodulus and ventral uvula control the torsional vestibulo-ocular reflex. *J Neurophysiol* (1994) 72(3):1443–7.
- Cohen H, Cohen B, Raphan T, Waespe W. Habituation and adaptation of the vestibulo-ocular reflex: a model of differential control by the vestibulo-cerebellum. *Exp Brain Res* (1992) 90(3):526–38. doi:10.1007/BF00230935
- Laurens J, Angelaki DE. The functional significance of velocity storage and its dependence on gravity. *Exp Brain Res* (2011) 210(3–4):407–22. doi:10.1007/s00221-011-2568-4

47. Singleton GT. Relationships of the cerebellar nodulus to vestibular function: a study of the effects of nodulectomy on habituation. *Laryngoscope* (1967) 77(9):1579–619. doi:10.1288/00005537-196709000-00001
48. Barmack NH, Shojaku H. Vestibularly induced slow oscillations in climbing fiber responses of Purkinje cells in the cerebellar nodulus of the rabbit. *Neuroscience* (1992) 50:1–5. doi:10.1016/0306-4522(92)90376-D
49. World Medical Association. World Medical Association Declaration of Helsinki: ethical principles for medical research involving human subjects. *JAMA* (2013) 310:2191–4. doi:10.1001/jama.2013.281053

Conflict of Interest Statement: Patients payed for this treatment to the Department of Neurology Icahn School of Medicine at Mount Sinai.

Copyright © 2017 Dai, Cohen, Cho, Shin and Yakushin. This is an open-access article distributed under the terms of the Creative Commons Attribution License (CC BY). The use, distribution or reproduction in other forums is permitted, provided the original author(s) or licensor are credited and that the original publication in this journal is cited, in accordance with accepted academic practice. No use, distribution or reproduction is permitted which does not comply with these terms.



Hypothesis: The Vestibular and Cerebellar Basis of the Mal de Debarquement Syndrome

Bernard Cohen^{1*}, Sergei B. Yakushin¹ and Catherine Cho^{2,3}

¹Department of Neurology, Icahn School of Medicine at Mount Sinai, New York, NY, United States,

²Department of Neurology, NYU School of Medicine, New York, NY, United States, ³Department of Otolaryngology, NYU School of Medicine, New York, NY, United States

OPEN ACCESS

Edited by:

David Samuel Zee,
Johns Hopkins University,
United States

Reviewed by:

Dominik Straumann,
University of Zurich, Switzerland
Pierre-Paul Vidal,
Université Paris Descartes, France

*Correspondence:

Bernard Cohen
bernard.cohen@mssm.edu

Specialty section:

This article was submitted to
Neuro-Otology,
a section of the journal
Frontiers in Neurology

Received: 26 May 2017

Accepted: 12 January 2018

Published: 05 February 2018

Citation:

Cohen B, Yakushin SB and Cho C (2018) Hypothesis: The Vestibular and Cerebellar Basis of the Mal de Debarquement Syndrome. *Front. Neurol.* 9:28.
doi: 10.3389/fneur.2018.00028

The Mal de Debarquement syndrome (MdDS) generally follows sea voyages, but it can occur after turbulent flights or spontaneously. The primary features are objective or perceived continuous rocking, swaying, and/or bobbing at 0.2 Hz after sea voyages or 0.3 Hz after flights. The oscillations can continue for months or years and are immensely disturbing. Associated symptoms appear to be secondary to the incessant sensation of movement. We previously suggested that the illness can be attributed to maladaptation of the velocity storage integrator in the vestibular system, but the actual neural mechanisms driving the MdDS are unknown. Here, based on experiments in subhuman primates, we propose a series of postulates through which the MdDS is generated: (1) The MdDS is produced in the velocity storage integrator by activation of vestibular-only (VO) neurons on either side of the brainstem that are oscillating back and forth at 0.2 or 0.3 Hz. (2) The groups of VO neurons are driven by signals that originate in Purkinje cells in the cerebellar nodulus. (3) Prolonged exposure to roll, either on the sea or in the air, conditions the roll-related neurons in the nodulus. (4) The prolonged exposure causes a shift of the pitch orientation vector from its original position aligned with gravity to a position tilted in roll. (5) Successful treatment involves exposure to a full-field optokinetic stimulus rotating around the spatial vertical countering the direction of the vestibular imbalance. This is done while rolling the head at the frequency of the perceived rocking, swaying, or bobbing. We also note experiments that could be used to verify these postulates, as well as considering potential flaws in the logic. Important unanswered questions: (1) Why does the MdDS predominantly affect women? (2) What aspect of roll causes the prolongation of the tilted orientation vector, and why is it so prolonged in some individuals? (3) What produces the increase in symptoms of some patients when returning home after treatment, and how can this be avoided? We also posit that the same mechanisms underlie the less troublesome and shorter duration Mal de Debarquement.

Keywords: vestibular-only neurons, nodulus, baclofen, rocking, swaying, bobbing, gravity, orientation vector

Abbreviations: G, gravity; GIA, gravitoinertial acceleration; GABA, gamma amino butyric acid; Hz, per second; MdD, Mal de Debarquement, also sometimes known as "Land sickness"; MdDS, Mal de Debarquement syndrome; OKN, optokinetic nystagmus; PAN, periodic alternating nystagmus; VO neurons, vestibular-only neurons; VPS neurons, velocity-pause-saccade neurons; VOR, vestibulo-ocular reflex.

DEFINITIONS

Brain fog	disruption of ability to think clearly
Classic MdDS	MdDS arising from travel on the sea or in the air
Spontaneous MdDS	MdDS generally arising after exposure to motion, but without known exposure to sea or air travel
Dutch roll	flutter of wings and fuselage of aircraft when banking in turbulent weather
Gravity pulling	Sensation of being pulled in one particular direction MdDS
Pitch orientation vector	Vector generally directed toward the spatial vertical that underlies balance
Rocking	movement or sensation of movement forward and back, generally at 0.2 Hz
Swaying	movement or sensation of movement from side-to-side, frequently with a rotary component
Bobbing	sensation of vertical movement of the head and body, generally not associated with actual movement
Roll while rotating	rotation of monkeys in darkness about a vertical axis at 60°/s for several hours while oscillating ±20° at 0.1 Hz in roll
Pitch while rotating	rotation of monkeys in darkness at 60°/s for several hours around a vertical axis while oscillating at 0.1 Hz at ±20° in pitch at 0.1 Hz

INTRODUCTION

The Mal de Débarquement Syndrome (MdDS) is composed of primary and secondary symptoms. The major primary effects are the continuous rocking, swaying, bobbing, or continuous sensations of these phenomena at 0.2 Hz after being on the sea or 0.3 Hz after turbulent flight (1, 2). These symptoms cease briefly when riding in a car (1–8). The patients also frequently experience a sensation of “pulling” in specific directions (“gravity pulling”) (2). The MdDS pathology can be extended over months or years, giving a sense of continuous oscillatory motion that seriously affects the lives of the sufferers, who are predominantly middle-aged women. The incessant rocking, swaying, and/or bobbing are frequently associated with a host of symptoms such as brain fog, sensitivity to sound and fluorescent lights, headaches, inability to work, depression, and suicidal tendencies (2, 4, 6, 9, 10).

Neither the cause for nor the changes in neural activity producing the MdDS are known (4, 6, 7), but there have been many hypotheses to explain the source of the MdDS. These include “vestibular adaptation” or “defective readaptation” (3–5, 11), although the specifics of the vestibular adaptation were not detailed. The MdDS has also been attributed to various cerebral processes that involve the vestibular projections to the cerebral cortex (7), overactivity of the hippocampus and entorhinal cortex (7), interaction of cerebral processes (7, 12), increased sensitivity of the cerebrospinal pathways (13), and modulation of general activity following loss of gray matter in the prefrontal cortex, entorhinal cortex, and cerebellum (14). These studies led to the use of transcranial magnetic stimulation that produced transient relief of symptoms (7, 13) but not to prolonged disappearance of the symptoms of the MdDS. It has also been proposed that the MdDS is a vestibular analog of the Charles Bonnet syndrome,

with the recurrent oscillations reflecting a loss of vestibular input (15). However, the function of the semicircular canals is generally intact in these individuals. Thus, there is an inherent difference between the Charles Bonnet sufferers, in whom the loss of vision is the precipitating cause for the visual hallucinations (16, 17) and the MdDS where there is no loss of vestibular function.

There have also been attempts to quell the symptoms with medication. These medications include GABA_a agonists like diazepam or clonazepam, nortriptyline, verapamil, and topiramate. Generally, these produced only mild or moderate reduction of symptoms (4, 12). Vestibular rehabilitation has generally been unsuccessful in stopping the sensed or actual movements of the MdDS, and extensive medical workups that include MRI’s, tests of vestibular function with video nystagmography, and tests of auditory and otolith function have all been normal. It has been estimated that the costs of these normal tests extend into the thousands of dollars. Until recently, there has been no successful treatment of the MdDS, nor is it clear how and where the process is generated in the central nervous system.

In 2014, Dai et al. (1) introduced the first successful treatment of the MdDS, and several hundred patients have been successfully treated since that time (2). However, the succession of the neural events that produce the MdDS is still relatively obscure. In this paper, we present a hypothesis composed of a number of postulates that presumably will explain the neural basis of the internal structure responsible for this condition. Other than the proposed maladaptation of the velocity storage integrator in the vestibulo-ocular reflex (VOR) (1), there is no theory detailing the neural pathways involved in generating the incessant rocking, swaying, and/or bobbing or a sense of these oscillations that are the main features of the illness (1). Though important questions remain, it is the first such analysis of the vestibular and cerebellar components that we believe are responsible for generating the MdDS.

The vestibular basis for the treatment came from experiments on the monkey (18). The monkeys were rotated for several hours in darkness while oscillating in roll. Afterward, the animals had horizontal spontaneous nystagmus and unusual vertical positional nystagmus when their heads were rolled to either side. The quick phases of the vertical nystagmus were upward when the head was rolled to one side and downward when the head was rolled to the other side (18), similar to the vertical positional nystagmus with head roll in the MdDS patients (1). These changes persisted for about 18 h and were never induced in monkeys that had very short VOR time constants, i.e., in animals that had appropriate vestibular responses to angular acceleration but no velocity storage. This was modeled, and it was concluded that the positional nystagmus had been produced by cross-coupling of the pitch orientation eigenvector that had been shifted in roll after exposure to roll while rotating. A similar shift in the pitch orientation vector was not produced by pitch while rotating. It was presumed that the pitch while rotating only strengthened the pitch orientation vector in its alignment along the spatial vertical (see Ref. (19–22) for a more complete description of the characteristics of velocity storage). The striking similarities between the reversal of vertical positional nystagmus with head roll to either side in the monkeys and in the MdDS patients

suggested that a primate analog of the human disorder had been created in the monkey by the roll while rotating. This included vestibular imbalance, as shown by the tendency of the patients to march to one side on the Fukuda stepping test, and the occasional spontaneous nystagmus, which was observed consistently in monkeys. In these subjects, the direction of the slow phases of the nystagmus and the direction of the postural deviation in the Fukuda test in the MdDS patients were always congruent, indicating that a vestibular imbalance had been created.

Long-lasting changes were never produced in monkeys by pitch while rotating, specifically implicating the roll system in the MdDS. Similar vertical nystagmus had also been previously produced in humans by extended exposure to a slow rotating room for several days in which the subjects intermittently made roll head movements. This induced vertical positional nystagmus for several hours thereafter when they rolled their heads (23, 24). Since only roll while rotating caused the abnormal eye movements in monkeys, not pitch while rotating, and similar vertical nystagmus with head roll was produced in humans (23), we postulated that the roll encountered during voyages was responsible for the generation of the MdDS (1).

It can be questioned whether there is a significant amount of roll especially on cruise ships that are the most common source of the MdDS patients. The stability of boats depends not only on the size of the vessel but also on the extent of the wind and waves as well as the direction of the boat's progress. The sea is not always calm, and there are multiple reports of vessels being capsized in rough waters as reported by the Marine Accident Investigation Branch. A search of the literature revealed measurements of roll in the Bass Strait (between Australia and Tasmania) in a ship of 11,000 t deadweight, 603.7 ft in length and 77.6 ft in width (25). The ship had an average roll of $\pm 6.3^\circ$, an average pitch of $\pm 1.9^\circ$, and an average heave of 7.2 ft. The Bass Straight is 190 miles wide and 120 miles long. This was likely to have been very rough conditions, and the sea in cruises between Florida and the West Indies might generally be calmer. Additionally, there are roll stabilizers, i.e., planar strips of metal attached to the keel that can reduce roll. However, many although not all of the trips are in the Atlantic, and there can be strong weather that produces larger waves in any sea. Even large ships will roll if they encounter waves obliquely. Thus, there can be substantial roll, depending on the size of the waves despite the cruise ship's roll stabilizers. While it is true that people walk around the deck in cruise ships, nevertheless, they are in stable positions for 6–8 h when they sleep at night or when they are sitting down for meals or in chairs to relax. Therefore, there can be adequate exposure to roll in cruise ships on the sea, particularly in heavy weather.

There have been no recent studies specifically on roll during flight in turbulent air, to our knowledge, although Dutch roll was described in light planes when banking in rough weather (26). Flutter of the wing tips and fuselage at 3–3.5 Hz has been generated in transport aircraft in turbulent conditions. See more details in the link provided (<https://www.youtube.com/watch?v=kOBbAFzXrRg>). Similar oscillations could contribute to the 0.3 Hz body oscillations in some MdDS patients after extended flights in turbulent weather.

A striking finding was that there was a sharp peak in the average frequency of rocking and the perceived rocking in both our 2014 and 2017 papers at 0.2 Hz (Figure 1A). There was more spread in swaying (Figure 1B), probably due to the variation in determining the period of swaying, i.e., pitching was easier to observe and sense than swaying. The significance of the relatively conserved 0.2 Hz frequency (1 cycle/5 s) is that it signifies that a similar process is likely to be producing the rocking in virtually all of the MdDS patients after sea voyages. This implies that the frequency is being internally generated and is sensitive to an external stimulus of 0.2 Hz. The 0.2 Hz frequency is too slow to be produced by lesions of the inferior olive, since frequencies of such phenomena like palatal myoclonus typically have frequencies of about 1 Hz (27). Therefore, there should be another, separate source for the 0.2 and 0.3 Hz signals in the brainstem and cerebellum to account for the changes that are presumed to arise in the velocity storage integrator.

Modulation of roll depends heavily on the integrity of the cerebellar nodulus (28–31). This suggests that the nodulus may play an important part in the generation of the MdDS. In normal monkeys and humans, the orientation of the axis of eye velocity is always aligned with the spatial vertical or the gravitoinertial acceleration (GIA) during rotation, regardless of the position of the head in space (20, 21, 30–35). The underlying postulate for the generation of the MdDS was that the pitch orientation vector of the system had been transformed from its original position along gravity to a tilted position in roll (1). The purpose of the treatment was to bring the orientation vector back to the spatial vertical by activating the velocity storage integrator with an optokinetic stimulus that rotated around the spatial vertical. Thus, the proposed treatment was to roll the head of the affected subjects at the frequency of their perceived or actual rocking, swaying, or bobbing, while activating the velocity storage integrator with a low-frequency, constant velocity, full-field, optokinetic stimulus rotating around the spatial vertical against the direction of their

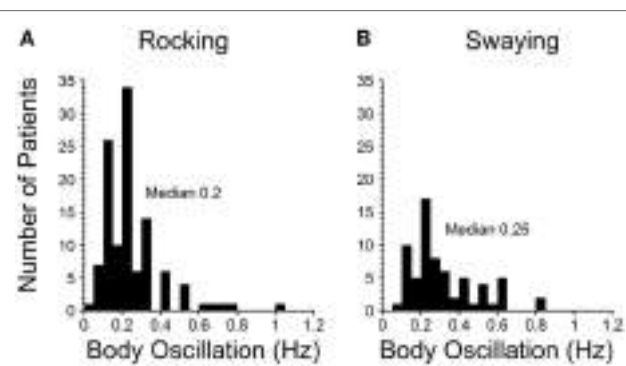


FIGURE 1 | Frequencies of rocking (A) and swaying (B) in Mal de Débarquement Syndrome patients (2). The frequencies were determined on a Nintendo Wii board. The rocking frequencies were tightly centered around a maximum at 0.2 Hz, more for the rocking than the swaying. When there was no actual rocking or swaying, the perceived frequencies were determined with the elbow stabilized on a board, and the patient moved the forearm at the frequency of the perceived movement.

vestibular imbalance. Presumably, this reoriented the integrator back to gravity or the GIA. If the correct direction of the vestibular imbalance was not chosen during the treatment, the body oscillations became worse, supporting the postulate that it was the conflict between the tilted orientation vector and the spatial vertical that had produced the MdDS.

As a result, it was possible to relieve the constant rocking, swaying, and/or bobbing in 70% of the original 24 patients after the second week of treatment, an improvement that was generally maintained in the original group when they returned home, and at follow-up after a year (1). In an additional 141 MdDS patients, the 2-week success rate was 80% (2); however, the rate of symptom reduction fell to 44% after 1 year, possibly due to stress experienced by these patients during long flights or rides home after treatment. This drop in efficacy must be addressed in future studies, but it should be emphasized that this was the first and only successful treatment for the MdDS.

The implication of these results is that the underlying cause for the MdDS is a disturbance in the control of roll at a specific direction and frequency, which is approximately 0.2 Hz after sea voyages and 0.3 Hz after turbulent flight. The fact that there was a difference in the sensed or actual oscillations implies that an external 0.2 or 0.3 Hz component of the roll on the sea or in the air was provoking the prolonged response to roll, but the highly specific oscillation frequencies across a wide range of MdDS patients strongly implies that those frequencies were recognized and perpetuated in the central nervous system. As will be shown below, we think that it is likely that the storage mechanism involves the nodulus of the vestibulocerebellum.

The treatment devised by Dai et al. (1) significantly reduced the symptoms by readapting the velocity storage mechanism to normality. This indicates that there had been no primary structural lesions in the vestibulocerebellar system that had caused the symptoms. This was essentially verified by the rapid return to normality, even after having suffered with the major symptoms for up to 20 years (2). However, the neural basis of the process that involved the velocity storage mechanism in the VOR has remained unclear. Here, a hypothesis composed of a number of postulates is proposed to explain how these findings are produced in the brainstem and cerebellum. First, however, we consider some of the requirements of such a proposal.

THEORETICAL DEMANDS OF AN MdDS GENERATION HYPOTHESIS

The recurrent direction-changing nystagmus in periodic alternating nystagmus (PAN) after cerebellar lesions offers a potential scheme to explain the continuous sensations of rocking, swaying, and bobbing of the MdDS patients. PAN occurs after cerebellar lesions and causes a reversal of the direction of the slow and quick phases of nystagmus at frequencies of about once every 2–3 min (36). This has been interpreted as recurrent activation of groups of neurons on each side of the brainstem, i.e., as an adaptive process that can continuously reverse the direction of the nystagmus (37, 38). We have also reproduced the continuous reversal of the direction of horizontal nystagmus in the monkey

by ablation of the nodulus and uvula (31, 39). In both studies, the recurrent cycle was terminated by an IM injection of the GABA_B agonist baclofen, similar to the effect of baclofen on the PAN (36). The PAN is, of course, considerably slower than the recurrent oscillations in the MdDS, but this analogy shows that there can be oscillation between neural groups on each side of the brainstem.

MdDS GENERATION HYPOTHESIS

Based on new findings from a three-dimensional study of the characteristics of vestibular-only (VO) neurons in the medial and superior vestibular nuclei (40), it is proposed that there is a similar situation that produces the MdDS, namely, oscillation between the VO neuronal groups on each side of the brainstem at frequencies of 0.2 or 0.3 Hz, controlled by output from the cerebellar nodulus that produces the MdDS.

RELEVANT QUESTIONS

Previous studies of velocity storage have primarily been done on oculomotor aspects of vestibular activation, while the current interest is in head, neck, body, and leg movements or the perception of such movements. Therefore, there should be specific activation of the neural elements that would cause excitation of the body and limbs rather than the eyes. There should also be neurons that control different neural groups on either side of the brainstem to activate different parts of the body and limbs. If such an arrangement exists, these neural groups should have substantial connections between them that could monitor and maintain the oscillations. The VO neurons characteristically have a time constant during rotation of 15–25 s (40, 41), but these neurons are capable of responding at a much faster rate, i.e., up to 450 impulses/s (42, 43). As suggested earlier, there should be adaptable elements in these structures to account for the proposed shift in the pitch orientation vector that drives them into oscillation when confronted with exposure to head roll on the sea or in the air. Finally, there should be access to a 0.2 or 0.3 Hz signal from a structure that directly connects to these neural groups and sequentially drives them.

The VO neurons in the medial and superior vestibular nuclei meet these criteria. They are the neural structures that convert the time constant of the hair cells in the cupula of 4–4.5 s (42) into the VOR time constants of 15–25 s or longer (19–22, 44). The VO neurons receive direct input from the semicircular canals and output to the neck, body, and limbs through vestibulo- and reticulocollic and vestibulo- and reticulospinal pathways (45–48). They have little direct output to the oculomotor system, and presumably contact the oculomotor system primarily through the VPS neurons (48), although there are also some direct vestibulo-oculomotor projections. As shown by Boyle and McCrea et al., the VO neurons reflect the imposed accelerations on the head and body, but do not go into action during volitional turns of the head (45–47). There are other vestibular neurons related to eye velocity that are activated during volitional head or head and body oscillations (49–51). Thus, there is a clear separation between the

vestibular neurons that respond to passive head or head and body oscillations, as against a complex set of neurons in the vestibular nuclei that respond to visual input, volitional turns of the head or efference copy (45).

The VO neurons, however, are out of volitional control, and we postulate that the rocking, swaying and bobbing during the MdDS is generated by the VO neurons that similarly are not subject to efference copy, volitional control, or response of cortical or visual input. This is consistent with the finding during the MdDS that the patients have little or no active control of imposed rocking, swaying, and/or bobbing, or of the sensations associated with these movements. Of interest, drowsiness does not affect the rocking, swaying, or bobbing of the MdDS patients, and these oscillations or the perception of these oscillations persist even when the MdDS patients are not alert (Yakushin, Cohen, persoal communication).

The mixture of neurons that respond to passive head movement, voluntary head movement, and efference copy demonstrate that activity generated in the vestibular system can be overt or silent when viewed in terms of muscular activity. Thus, we assume that perceived rocking, swaying, and bobbing that is not observable in many of the MdDS patients does not mean that vestibulospinal and reticulospinal tracts are not active, but simply that the activity is not always manifest.

The VO neurons have extensive axonal connections to VO neurons on the other side of the brainstem and use GABA_B as the primary inhibitory agonist (52–54). Injections of baclofen caused a dramatic reduction in activity of VO neurons (22, 40, 55), and when the crossing axons were severed, velocity storage permanently disappeared (54, 56). Since we propose velocity storage is intimately involved in production of the MdDS (1), the disappearance of velocity storage when the connecting VO neurons in the brainstem were inhibited or severed supports our hypothesis that the VO neurons are involved in the production of the MdDS.

When examined in three dimensions, a majority of VO neurons on each side of the brainstem are primarily activated by rotation to the contralateral side and fail to respond to ipsilateral rotation (40). They also receive vertical canal and otolith inputs. Since these neurons project to the head, neck, body, and limbs through different components of the reticulospinal and vestibulospinal pathways, they each can activate a different set of head, neck, body, and limb movements, which could result in the rocking, swaying, and bobbing as well as the “gravity pulling” of the MdDS. Exactly how this is done is still not known, however.

EVIDENCE THAT THE ORIENTATION VECTOR CAN BE MODIFIED BY EXPOSURE TO ROLL

The experiments in monkeys using roll while rotating produced modification of the pitch orientation vector for up to 18 h (18). In other experiments, Eron et al. (57, 58) also have demonstrated that it is possible to condition the polarization vector of VO neurons by putting monkeys on their sides (in

roll) for 30–60 min. This shifts the otolith polarization vector toward gravity in the side-down or rolled position. The shift in the habituated orientation of the neuron persisted for periods of several hours. Thus, the orientation of the VO neurons can be altered for substantial periods by exposure to roll. Changes in their polarization vectors, while not as profound, were also found in canal-related neurons that were located in the direct pathway of the VOR (59). Such changes could also be involved in the “gravity pulling” by altering the vertical canal and otolith inputs to the VO neurons.

A POTENTIAL CEREBELLAR SOURCE OF THE 0.2 OR 0.3 Hz BODY OSCILLATIONS

A large body of experimental data indicates that the nodulus and part of the uvula exert powerful control of the VO neurons and the velocity storage integrator. The VO neurons receive substantial input from the nodulus (31, 60–63). Pathways from the lateral portions of the nodulus cause disappearance of velocity storage and electrical stimulation of the nodulus, presumably activating these pathways, also causes a loss of velocity storage (64). This region of the nodulus is likely to discharge activity in velocity storage during visual suppression (19, 65) as well as loss of stored activity in velocity storage during “tilt-dumps” (20, 33, 39). In contrast, pathways from the central portions of the nodulus provide activity responsible for orienting the axis of eye velocity to the spatial vertical (20, 66). These functions are lost after nodulus lesions (30, 31). Habituation of the dominant time constant of the VOR is also controlled by the nodulus and is lost after nodulus lesions (67, 68). Therefore, there is extensive neural control of the VO neurons and of the velocity storage integrator through this structure (30, 31). Lesions of the nodulus also result in alternating nystagmus every 5 min (31, 39). Thus, the nodulus has a role in maintaining temporal adaptation of processes in the vestibular nuclei, that presumably can identify the source of the drive on neuronal groups in the brainstem that produce the PAN. Of note, this alternating nystagmus is eliminated by the action of baclofen, similar to the elimination of activity in VO neurons by the IM injection of baclofen (40, 55).

Nodulus lesions also cause a loss of roll eye movements and torsional nystagmus (28, 29), confirming the close association of the nodulus to roll. Thus, the tilted state of the pitch orientation vector in roll during the MdDS would be a natural function of the neural structure of the nodulus, as would the ability of the roll component of the nodulus to be modified by extensive exposure to roll on water or in the air.

Although the origin of the 0.2 and 0.3 Hz signal driving the VO neurons has yet to be discovered in monkeys or humans, this signal is present in the nodulus of the rabbit. In a comprehensive series of experiments, Barmack and Shojaku et al. (69–74) showed that there was a massive input from the vestibular nerve to the nodulus (73). A striking aspect of this is that about 70% of vestibular fibers in Scarpà's ganglion project directly to the nodulus through the inferior olives, bypassing the vestibular nuclei. This input arises predominantly in the anterior and posterior canals that sense active or passive roll movements of

the head and/or of the head and body. This activity is also transmitted through the medial and inferior vestibular nuclei to the inferior olives, where the individual planes of one anterior and the contralateral posterior semicircular canals are represented in individual neurons. The combined anterior and posterior canal activation in roll is also separately represented in another inferior olive nucleus (69). The combined activity that represents roll head and/or head and body in space is then transmitted by climbing fiber and mossy fiber inputs to the Purkinje cells in the contralateral nodulus. Thus, there is a powerful input to the nodulus continuously detailing the passive and active head and/or head and body movements in roll. Otolith neurons also sense the roll position of the head and/or the head and body relative to gravity and the GIA, and transmit this activity to the inferior olives and thence to the nodulus. The nodulus also receives a mossy fiber input from the dorsal cap of Kooy in the inferior olive that originates in the subcortical visual system in the nucleus of the optic tract that carries optokinetic-generated activity to the vestibular nuclei and the nodulus.

In their experiments, coordinated firing of the nodular and uvular Purkinje cells (**Figure 2A**) was produced by rolling the head and body statically and dynamically around the long axis at 0.2 Hz (**Figure 2B**). The 0.2 Hz oscillation in roll was chosen because it was the frequency that gave the best coordinated responses in the Purkinje cells on repeated testing at different frequencies of oscillation (Barmack, personal communication). The

coordinated firing of the Purkinje cells at 0.2 Hz ceased in most cells, when the roll stimulus ended, and the cells returned to their irregular spontaneous activity. In about 15% of the Purkinje cells, however, the 0.2 Hz firing frequency faded and then returned for 300–400 s. Thus, it was possible to induce after-activity in some neurons at the preceding 0.2 Hz frequency that considerably outlasted the exciting 0.2 Hz roll oscillation (70). If such activity were present in the human nodulus, and if it were sufficiently prolonged, presumably it could supply activation of the output pathways to the VO neurons, and initiate the sense of swaying, rocking, and/or bobbing. Moreover, in a small number of Purkinje cells, it was possible to change the frequency of the after-activity to 0.3 Hz, as experienced in the MdDS after turbulent flight. A 0.1 Hz frequency was also induced that could be related to the spread in frequencies shown in **Figure 1**. They also encountered Purkinje cells that had a continuous 0.2 Hz firing rate that could maintain the preference of the Purkinje cells to oscillate at 0.2 Hz. Thus, there was activity in the rabbit nodulus and uvula that could have potentially caused activation of VO neurons that outlasted the roll stimulus that had induced the original activity. If this activity existed in humans, it could explain the frequency of the body rocking (**Figure 1**).

This work provides a potential neural basis for the 0.2 and 0.3 Hz oscillations in Purkinje cell firing that could be responsible for the 0.2 and 0.3 Hz oscillations in rocking, swaying, and bobbing of the MdDS patients. One may question whether results in rabbit as well as in monkey can be appropriately applied to humans. The rabbit's eyes are centered $\pm 85^\circ$ from the midline of the head; whereas, the monkey and human have the fovea centered $\pm 7^\circ$ from the midline. Of course, there are many other differences between rabbits and humans. However, the vestibular system does not follow this rule. Baker and Straka and other colleagues have done extensive studies of the vestibular and oculomotor systems in fish and frogs (75–80). They note that "although the projections of the neurons vary among species, similar subgroups of major vestibular projection neurons originate from homologous segmental positions in the hindbrain of mammals, birds, and amphibians."

Thus, it is striking that the semicircular canal to vestibular nuclei and inferior olive connections are very similar across mammalian species. For example, the angles of the planes of the semicircular canals and the insertions of the eye muscles driven by the semicircular canals lie in the same planes in humans, monkeys, goldfish, and sharks (81–83). Moreover, the eye movements induced by the canals are also the same across species in rabbits, dogs, cats, and monkeys (81, 82, 84). A striking example of the similar morphology of the end organs is that the planes of the semicircular canals are the same in monkeys and humans as in a brachiosaurus dinosaur that has been extinct for 155 million years (85). Of course, the dinosaur labyrinth is magnitudes bigger than the monkey labyrinth, but the planes of the canals are the same.

Baker and Straka conclude: "these comparative attributes among vertebrates suggest that, from basic wiring through function, the vestibular blueprint was established quite early during vertebrate evolution and, from the viewpoint of structure more than function, has been largely conserved throughout ~400

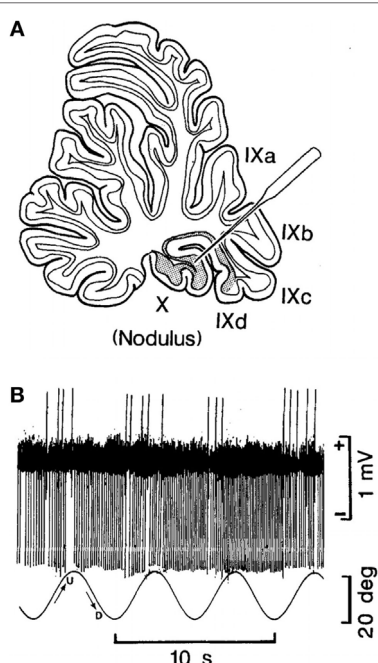


FIGURE 2 | (A) Site of recording of the neuron of the nodulus shown in **(B)**. **(B)** Climbing Fiber-driven Purkinje cell activity from the site shown in **(B)**. The Purkinje cell fired three to five times. Each time, the animal was rolled into the left side-down position. The oscillation in roll is shown by the bottom trace. The oscillation amplitude is shown by the bar on the right, and the time base by the lowest trace. This figure is reprinted with permission. For further details, see the article by Barmack and Shojaku (70).

million years of vertebrate phylogeny (75).” From this, we postulate that the findings in the rabbit can be applied to monkeys and humans and that the driving frequency established in the nodular Purkinje cells are manifest in the VO neurons to produce the rocking, swaying, and bobbing of the MdDS in humans.

DISCUSSION

In this paper, we posit that the MdDS is produced by a deviation of the pitch orientation vector from the spatial vertical to one side in roll. Further, the deviation of the pitch orientation vector occurs as a function of contextual learning after prolonged exposure to roll on the sea or in the air. If the pitch orientation vector is displaced in roll, it should cause positional nystagmus. Consistent with this, many of the MdDS patients had a unique type of vertical positional nystagmus when their heads were put in roll on either side; the quick phases were up when the head was on one side and down when the head was on the other side (1). Most patients also had a vestibular imbalance, manifested by marching to one side in the Fukuda stepping test. The unusual vertical positional nystagmus was also produced in monkeys after extensive exposure to roll while rotating. This occurred in association with a vestibular imbalance manifested by spontaneous nystagmus in darkness (18). This provided the basis for recognizing that a similar process had produced the MdDS in monkeys as in humans. Such vertical positional nystagmus was also produced in humans after long exposure to a slow rotating room when they rolled their heads to the side (23, 24). The experiments in monkeys also demonstrated that such responses to roll while rotating only occurred in monkeys with a long VOR time constant, that considerably outlasted the 4.5–5.0 s input from the hair cells in the semicircular canals to steps of rotational velocity (42). Such time constants are produced in the velocity storage integrator, providing evidence that the MdDS was generated in velocity storage.

From this, it was postulated that the pitch orientation vector had been transformed from its original position along gravity to a lateral position in roll. It was further postulated that this shift had been produced by cross-coupling that had altered the position of the pitch orientation vector. The failure of pitch while rotating to cause a shift in the pitch orientation vector was interpreted as having strengthened, not modified, the pitch orientation vector. Model predictions were consistent with this hypothesis.

The finding that modification of the pitch orientation vector, i.e., its return to the spatial vertical, was produced by viewing low velocity, full-field optokinetic stimulation oriented around the spatial vertical confirmed this hypothesis. Thus, there was internal consistency between the conditions in both the MdDS patients and the response to roll while rotating. The ability to reverse the MdDS symptoms with a low velocity, full-field, optokinetic stimulus rotating against the direction of the vestibular imbalance, further strengthened the hypothesis that the optokinetic nystagmus (OKN) stimulus had countered the lateral tilt of the pitch orientation vector in roll. This conclusion was also supported by the disappearance of the rocking, swaying, and bobbing and the subjective symptoms after such treatment (1, 2).

EVALUATION OF SPECIFIC ASPECTS OF THE HYPOTHESIS

The mechanics of the basis for oscillation were also considered: namely, it was proposed that the MdDS is produced by repetitive oscillation of groups of VO neurons on either side of the medial and superior vestibular nuclei. These neurons project excitatory activity to muscles in the head, neck, body, and limbs that could produce the repetitive rocking, swaying, and/or bobbing or the sensation that these motions have occurred (40). This could explain why spontaneous nystagmus was not prominent in the MdDS patients. Instead they generally manifested their vestibular imbalance through the body and limbs, as evidenced by the lateral movement on the Fukuda stepping test. This would be expected if the primary site of activation of the MdDS movements was in the VO neurons that primarily project to the head, neck, limbs, and body, and not to the oculomotor system. Rather, it is believed that the major projection of the VO neurons that are sensing body rotation is to the body, and not to the eyes (48). The proposed link to the oculomotor system from the VO neurons is through the VPS neurons, and these neurons become inactivated during drowsiness along with the eye movements, whereas the VO neurons continue their activity unchanged (13, 43). Similarly, in agreement with this, the perceived rocking, swaying, and bobbing continue even when the MdDS patients are drowsy. These findings are consistent with the clinical state and support the conclusion that the VO neurons are at the basis of the MdDS.

Finally, we propose that the signal driving the 0.2 and 0.3 Hz oscillations impinges on the VO neurons through projections from the nodulus. Since the nodulus has been shown to have a close association with roll (28, 29, 69–74), the exposure to repetitive roll while on the sea or in the air is presumably the trigger for the syndrome. As yet, the source of the 0.2 Hz signal, postulated to come from the nodulus, has not been found in humans or subhuman primates, but the findings by Barmack and Shojaku indicate that a preferred 0.2 Hz oscillation is present in the nodulus of the rabbit, and that the climbing fiber-driven Purkinje cells are readily excited by a 0.2 or a 0.3 Hz oscillation in roll. Such a signal may also be present in the human nodulus.

The same organization is probably also responsible for the generation of the commonly experienced Mal de Debarquement (MdD). It is likely that the less intrusive MdD is also produced by a transient shift of the orientation vector in roll, but fortunately, this is short-lived in most individuals. The underlying basis for the difference in durations of the MdD and the MdDS are not known, but presumably involve different tendencies for continued activation of nodulus Purkinje cells in the two conditions. Nor is it obvious why women are much more susceptible to development of MdDS than men. A similar propensity is also prevalent in migraine and motion sickness. If our postulate that the changes in the underlying frequency of nodular Purkinje cells is at the heart of the syndrome, then experiments in male and female monkeys and rabbits could prove interesting. It would also be important to determine if the effects of tilt of the body axis and exposure to brief flashes of light during recording of optokinetic after-nystagmus cause discharge in velocity storage (19, 65). Both of these functions have been demonstrated to originate in the nodulus (19, 30, 65).

POSSIBLE EXPERIMENTAL INVESTIGATION OF UNPROVEN ASSUMPTIONS

The postulate that the VO neurons were set into oscillation through an inhibitory link across the brainstem is presented without specific evidence that this actually occurs in the MdDS patients. For that reason, it would be important to have registration of VO neurons in monkeys with long VOR time constants after they had been exposed to several hours of roll while rotating that produced the vertical positional nystagmus when their heads were put in roll on either side of the midline. This preparation could also be useful in determining if the 0.2 Hz oscillation in the Purkinje cells in the rabbit were similar to those in primates. It is also possible to determine if the pitch orientation axis is aligned with the spatial vertical in recordings of neurons in the nodulus. If so, then it could be determined if the pitch orientation vector was tilted after generation of an MdDS analog in monkeys and whether it was possible to reorient the pitch orientation vector by exposure to a slowly moving, full-field OKN stimulus moving about the spatial vertical. It also might be possible to force a shift in the pitch orientation vector by exposure to roll while rotating, and to determine how much tilt of the OKN axis was sufficient to produce a tilt in the pitch orientation vector. Finally, it might also be possible to determine if the pitch orientation vector is actually strengthened after exposure to pitch while rotating (18).

Similarly, the hypothesis that exposure to an optokinetic stimulus oriented to gravity induces reversion of the pitch orientation vector could explain the finding that the body oscillations disappear briefly when the MdDS patients ride in cars (3–5). Presumably, some aspect of the visual streaming or the oscillations of the automobile temporarily restore the orientation vector back to the spatial vertical. This could be studied experimentally by blocking vision during the car rides, or by determining if rides on smooth, flat surfaces in well sprung cars fail to affect the sensations of the MdDS.

It would also be of interest to tilt the axis of rotation of the OKN when treating MdDS patients to determine whether tilts of the axis of the OKN stimulus failed to induce abolition of the MdDS, and if so, by how much tilt of the axis of rotation. The importance of the vestibular imbalance could also be studied by combining rotation at various velocities with the MdDS to determine whether it made the perception or actual oscillations better or worse, as does rotating the OKN stimulus during treatment against or in the direction of the vestibular imbalance. Finally, it would be of interest to reduce the time constant of the velocity storage integrator using the paradigm that was used to reduce velocity storage in motion sickness (66), and test the hypothesis that the MdDS could be improved by habituating or shortening the time constants of the VO neurons.

A critical experiment would also be to determine if the yaw axis orientation vector was tilted from the spatial vertical during off-vertical axis rotation (OVAR) in patients with the MdDS, and whether such a tilt reverted to its orientation to gravity after the patients had been successfully treated (20, 66). Such an

experiment could provide proof of the tilted orientation vector hypothesis.

The syndrome considered in this manuscript is dependent on the presence of a velocity storage integrator and does not exist in monkeys and presumably in humans with a short VOR time constant. Velocity storage, as noted above, is not a recently developed phenomenon, since it is also present in the goldfish, evolved hundreds of millions of years ago (75). Ernst and Thomas have shown that it is possible to activate cross axis firing of neurons on each side of the vestibular nuclei of the goldfish with continuous rotation, as in humans (37, 38). The goldfish also have prominent cerebella with many similar connections as in mammals (75). Consequently, it could also be of interest if it were possible to produce cross-brain stem activation of vestibular units by roll while rotating in the goldfish. The point is that this type of cerebellar-driven oscillation of neurons in the vestibular nuclei may be a very old phenomenon. If so, then it would be of interest to determine if cerebellar-driven vestibular activity is an intrinsic phenomenon crossing species from fish to man.

QUALIFICATIONS TO THE MdDS HYPOTHESIS

Two major qualifications could invalidate the hypothesis presented in this paper. First, there has been heavy emphasis on the speculation that the syndrome produced in the monkey by roll while rotating is essentially the same as that of the MdDS in humans. This was based primarily on the finding of abnormal positional nystagmus and a vestibular imbalance in both humans and monkeys. However, there were significant differences between these two that were encountered. Namely, there was more activation of spontaneous nystagmus in the monkeys than in humans in whom spontaneous nystagmus was rarely present. This suggested that the vestibulo-ocular component was larger in the monkeys than in humans. It could have been related to the differences in generation of the mdDS. The monkeys were rotated in yaw for several hours, whereas the humans presumably got their MdDS after prolonged exposure to roll, without the concomitant yaw axis rotation. More important, perhaps, was the difference in body movements. Rocking, swaying, and/or bobbing was never observed in the monkeys after roll while rotating, but such movements or the perception of such movements were a cardinal feature of the MdDS. Of course, there was no manifest movement in many of the humans, only the sensation of movement, and it could not be ascertained whether the monkeys also had a sensation of movement, not manifest by rocking, swaying, and/or bobbing. If the VO neurons were driven by the nodulus, such activity would be expected. However, the monkeys studied in the 2009 paper were always chaired when out of their cages, so that it is possible that weak oscillations of limbs were never observed (18). If monkeys were to be used in Future studies, it would be important to have implanted EMG electrodes to determine if weak oscillations were present in the muscles after exposure to roll.

Second, heavy emphasis was placed on the origin of the role of the nodulus in perpetuating the body oscillations or the

perception of the body oscillations. This postulate depended on data from the rabbit. However, there was little direct evidence that such activation of nodular Purkinje cells was also present in the individuals with the MdDS. If such activity does not exist in humans, then an important part of this hypothesis would be invalidated.

Despite these differences, the hypothesis that the pitch orientation vector had been tilted in roll that led to the treatment generated a therapy that was successful in a majority of the MdDS patients, for the first time (1, 2). If the study using OVAR can be performed, then it could potentially provide support for this portion of the hypothesis. However, these qualifications must be kept in mind in evaluating whether the hypothesis is generally valid.

OTHER TREATMENT NECESSITIES

A major criticism of the therapeutic results is that they were obtained without adequate controls. This largely accrued because there was no significant support for such a study. The patients were desperate for relief after having had the MdDS for years without relief, and some were even suicidal. Also, this was the first successful treatment for the MdDS, and the results in the initial study were statistically significant (1). Moreover, the patients were coming for treatment from all over the country and the world and were not able to return for motor studies without support. The fact that many of the patients had had their illness for many years without relief despite a wide range of investigative steps, extensive drug treatment, and prolonged physiotherapy without significant improvement rendered treatment, even without controls to be a necessity. Presumably, given the strong positive results, even though they were largely reported by telephone, provide the preliminary data to support a complete, controlled study. Such a study is now under consideration.

A significant problem remains in the treatment of the MdDS, namely, that there was a substantial reversion back to the rocking, swaying, and/or bobbing after treatment. This was generally attributed to oscillations during the ride home (2). Initial efforts to

reduce this reversion with oral baclofen have not been successful. This might be due to its limited ability to cross the blood-brain barrier (86–89).

Intramuscular injections of baclofen in monkeys caused the disappearance of any vestige of velocity storage in the VO neurons (22, 40, 55). If our hypotheses that the MdDS is produced by VO neuronal activity are correct, suppression of VO neuron activity could stop the uncontrollable oscillations of the body during the MdDS. If the 0.2 or 0.3 Hz signals are coming from the cerebellum, however, we do not have the appropriate drugs to affect cerebellar circuitry, aside from the GABA_A and GABA_B inhibitory agonists, and more research is necessary on this subject.

Since cruises on the sea continue to be an attractive vacation, it is likely that we will continue to have numerous people who are afflicted by this malady. However, while it was originally considered to be untreatable, and people have even been driven to suicide by this condition, there appears to be the possibility of finally correcting the position of the pitch orientation vector so that it stays permanently on its appropriate orientation to the spatial vertical. Of course, adequate therapy demands reduction in the host of associated symptoms such as brain fog, sensitivity to sound and fluorescent lights, headaches, inability to work, depression, and suicidal tendencies that accompany the MdDS (2, 4, 6, 7, 9, 10, 13–15), but this must be addressed in detail when the uncontrolled body movements or the sensation of these movements ceases.

AUTHOR CONTRIBUTIONS

All authors contributed to the generation of this manuscript.

ACKNOWLEDGMENTS

We thank Larry Cornman at the Aviation Applications Program of the UCAR for information on aircraft characteristics in turbulent weather. We thank Richard Lewis, MD, for helpful criticisms, and Rupa Mirmira for editorial assistance.

REFERENCES

- Dai M, Cohen B, Smouha E, Cho C. Readaptation of the vestibulo-ocular reflex relieves the Mal de Débarquement Syndrome. *Front Neurol* (2014) 5:124. doi:10.3389/fneur.2014.00124
- Dai M, Cohen B, Cho C, Shin S, Yakushin S. Treatment of the Mal de Débarquement Syndrome, a one year follow-up. *Front Neurol* (2017) 8:175. doi:10.3389/fneur.2017.00175
- Hain TC, Hanna PA, Rheinberger MA. Mal de Débarquement. *Arch Otolaryngol Head Neck Surg* (1999) 125:615–20. doi:10.1001/archotol.125.6.615
- Hain TC, Cherchi M. Mal de Débarquement Syndrome. *Handb Clin Neurol* (2016) 137:391–5. doi:10.1016/B978-0-444-63437-5.00028-5
- Lewis RF. Frequency-specific Mal de Débarquement. *Neurology* (2004) 63:1983–4. doi:10.1212/01.WNL.0000144701.94530.6A
- Cha YH. Mal de Débarquement. *Semin Neurol* (2009) 29:520–7. doi:10.1055/s-0029-1241038
- Cha YH. Mal de Débarquement Syndrome: new insights. *Ann N Y Acad Sci* (2015) 1343:63–8. doi:10.1111/nyas.12701
- Arroll MA, Attree EA, Cha YH, Dancey CP. The relationship between symptom severity, stigma, illness intrusiveness and depression in Mal de Débarquement Syndrome. *J Health Psychol* (2016) 21:1339–50. doi:10.1177/1359105314553046
- Macke A, LePorte A, Clark BC. Social, societal, and economic burden of Mal de Débarquement Syndrome. *J Neurol* (2012) 259:1326–30. doi:10.1007/s00415-011-6349-6
- Van Ombergen A, Van Rompaey V, Maes LK, Van de Heyning PH, Wuyts FL. Mal de Débarquement Syndrome: a systematic review. *J Neurol* (2016) 263:843–54. doi:10.1007/s00415-015-7962-6
- Mair IWS. The Mal de Débarquement Syndrome. *J Audiol Med* (1996) 5:21–5.
- Ghavami Y, Haider YM, Ziai KN, Moshtaghi O, Bhatt J, Lin HW, et al. Management of Mal de Débarquement Syndrome as vestibular migraines. *Laryngoscope* (2016) 127:1670–5. doi:10.1002/lary.26299
- Clark BC, LePorte A, Clark S, Hoffman RL, Quick A, Wilson TE, et al. Effects of persistent Mal de Débarquement Syndrome on balance, psychological traits, and motor cortex excitability. *J Clin Neurosci* (2013) 20:446–50. doi:10.1016/j.jocn.2012.06.004
- Cha YH, Chakrapani S. Voxel based morphometry alterations in Mal de Débarquement Syndrome. *PLoS One* (2015) 10:e0135021. doi:10.1371/journal.pone.0135021
- Moeller L, Lempert T. Mal de Débarquement: pseudo-hallucinations from vestibular memory? *J Neurol* (2007) 254:813–5. doi:10.1007/s00415-006-0440-4
- Kazui H, Ishii R, Yoshida T, Ikezawa K, Takaya M, Tokunaga H, et al. Neuroimaging studies in patients with Charles Bonnet Syndrome. *Psychogeriatrics* (2009) 9:77–84. doi:10.1111/j.1479-8301.2009.00288.x

17. Schadlu AP, Schadlu R, Shepherd JB III. Charles Bonnet Syndrome: a review. *Curr Opin Ophthalmol* (2009) 20:219–22. doi:10.1097/ICU.0b013e328329b643
18. Dai M, Raphan T, Cohen B. Adaptation of the angular vestibulo-ocular reflex to head movements in rotating frames of reference. *Exp Brain Res* (2009) 195:553–67. doi:10.1007/s00221-009-1825-2
19. Raphan T, Matsuo V, Cohen B. Velocity storage in the vestibulo-ocular reflex arc (VOR). *Exp Brain Res* (1979) 35:229–48. doi:10.1007/BF00236613
20. Raphan T, Cohen B. The vestibulo-ocular reflex in three dimensions. *Exp Brain Res* (2002) 145:1–27. doi:10.1007/s00221-002-1067-z
21. Cohen B, Raphan T. The physiology of the vestibuloocular reflex (VOR). In: Hignstein SM, Fay RR, Popper AN, editors. *The Vestibular System*. New York, NY: Springer New York (2004). p. 235–85.
22. Cohen B, Dai M, Yakushin SB, Raphan T. Baclofen, motion sickness susceptibility and the neural basis for velocity storage. *Prog Brain Res* (2008) 171:543–53. doi:10.1016/S0079-6123(08)00677-8
23. Guedry FE Jr, Graybiel A. Compensatory nystagmus conditioned during adaptation to living in a rotating room. *J Appl Physiol* (1962) 17:398–404. doi:10.1152/jappl.1962.17.3.398
24. Brown JJ, Baloh RW. Persistent Mal de Debarquement Syndrome: a motion-induced subjective disorder of balance. *Am J Otolaryngol* (1987) 8:219–22. doi:10.1016/S0196-0709(87)80007-8
25. Hibbert GK, Lesser GR. *Measuring Vessel Motions Using a Rapid-Deployment Device on Ships of Opportunity*. OMC International Pty Ltd (2015).
26. Hunsaker JC. Dynamical stability of aeroplanes. *Proc Natl Acad Sci U S A* (1916) 2:278–83. doi:10.1073/pnas.2.5.278
27. Shaikh AG, Hong S, Liao K, Tian J, Solomon D, Zee DS, et al. Oculopalatal tremor explained by a model of inferior olive hypertrophy and cerebellar plasticity. *Brain* (2010) 133:923–40. doi:10.1093/brain/awp323
28. Angelaki DE, Hess BJ. The cerebellar nodulus and ventral uvula control the torsional vestibulo-ocular reflex. *J Neurophysiol* (1994) 72:1443–7. doi:10.1152/jn.1994.72.3.1443
29. Angelaki DE, Hess BJ. Lesion of the nodulus and ventral uvula abolish steady-state off-vertical axis otolith response. *J Neurophysiol* (1995) 73: 1716–20. doi:10.1152/jn.1995.73.4.1716
30. Wearne S, Raphan T, Waespe W, Cohen B. Control of the three-dimensional dynamic characteristics of the angular vestibulo-ocular reflex by the nodulus and uvula. *Prog Brain Res* (1997) 114:321–34. doi:10.1016/S0079-6123(08)63372-5
31. Wearne S, Raphan T, Cohen B. Control of spatial orientation of the angular vestibuloocular reflex by the nodulus and uvula. *J Neurophysiol* (1998) 79:2690–715. doi:10.1152/jn.1998.79.5.2690
32. Matsuo V, Cohen B. Vertical optokinetic nystagmus and vestibular nystagmus in the monkey: up-down asymmetry and effects of gravity. *Exp Brain Res* (1984) 53:197–216. doi:10.1007/BF00238150
33. Dai MJ, Raphan T, Cohen B. Spatial orientation of the vestibular system: dependence of optokinetic after-nystagmus on gravity. *J Neurophysiol* (1991) 66:1422–39. doi:10.1152/jn.1991.66.4.1422
34. Raphan T, Sturm D. Modeling the spatiotemporal organization of velocity storage in the vestibuloocular reflex by optokinetic studies. *J Neurophysiol* (1991) 66:1410–21. doi:10.1152/jn.1991.66.4.1410
35. Schnabolk C, Raphan T. Modeling 3-D slow phase velocity estimation during off-vertical-axis rotation (OVAR). *J Vestib Res* (1992) 2:1–14.
36. Halmagyi GM, Rudge P, Gresty MA, Leigh RJ, Zee DS. Treatment of periodic alternating nystagmus. *Ann Neurol* (1980) 8:609–11. doi:10.1002/ana.410080611
37. Leigh RJ, Robinson DA, Zee DS. A hypothetical explanation for periodic alternating nystagmus: instability in the optokinetic-vestibular system. *Ann N Y Acad Sci* (1981) 374:619–35. doi:10.1111/j.1749-6632.1981.tb30906.x
38. Ernst RD, Thomas JA. *Instabilities in Eye Movement Control: A Model of Periodic Alternating Nystagmus*. (1998). p. 138–44.
39. Waespe W, Cohen B, Raphan T. Dynamic modification of the vestibulo-ocular reflex by the nodulus and uvula. *Science* (1985) 228:199–202. doi:10.1126/science.3871968
40. Yakushin SB, Raphan T, Cohen B. Coding of velocity storage in the vestibular nuclei. *Front Neurol* (2017) 8:386. doi:10.3389/fneur.2017.00386
41. Scudder CA, Fuchs AF. Physiological and behavioral identification of vestibular nucleus neurons mediating the horizontal vestibuloocular reflex in trained rhesus monkeys. *J Neurophysiol* (1992) 68:244–64. doi:10.1152/jn.1992.68.1.244
42. Goldberg JM, Fernandez C. Physiology of peripheral neurons innervating semicircular canals of the squirrel monkey. I. Resting discharge and response to constant angular accelerations. *J Neurophysiol* (1971) 34:635–60. doi:10.1152/jn.1971.34.4.635
43. Reisine H, Raphan T. Unit activity in the vestibular nuclei of monkeys during off-vertical axis rotation. *Ann N Y Acad Sci* (1992) 656:954–6. doi:10.1111/j.1749-6632.1992.tb25305.x
44. Mach E. *Grundlinean der Lehre von den Bewegungsempfindungen*. Leipzig: Endelmann (1875).
45. Boyle R, Belton T, McCrea RA. Responses of identified vestibulospinal neurons to voluntary eye and head movements in the squirrel monkey. *Ann N Y Acad Sci* (1996) 781:244–63. doi:10.1111/j.1749-6632.1996.tb15704.x
46. McCrea RA, Gdowski GT, Boyle R, Belton T. Firing behavior of vestibular neurons during active and passive head movements: vestibulo-spinal and other non-eye-movement related neurons. *J Neurophysiol* (1999) 82:416–28. doi:10.1152/jn.1999.82.1.416
47. Gdowski GT, Boyle R, McCrea RA. Sensory processing in the vestibular nuclei during active head movements. *Arch Ital Biol* (2000) 138:15–28. doi:10.4449/aib.v138i1.274
48. McCall AA, Miller DM, Yates BJ. Descending influences on vestibulospinal and vestibulosympathetic reflexes. *Front Neurol* (2017) 8:112. doi:10.3389/fneur.2017.00112
49. Cullen KE, Belton T, McCrea RA. A non-visual mechanism for voluntary cancellation of the vestibulo-ocular reflex. *Exp Brain Res* (1991) 83:237–52. doi:10.1007/BF00231150
50. McCrea RA, Cullen KE. Responses of vestibular and prepositus neurons to head movements during voluntary suppression of the vestibuloocular reflex. *Ann N Y Acad Sci* (1992) 656:379–95. doi:10.1111/j.1749-6632.1992.tb25223.x
51. Cullen KE, Chen-Huang C, McCrea RA. Firing behavior of brain stem neurons during voluntary cancellation of the horizontal vestibuloocular reflex. II. Eye movement related neurons. *J Neurophysiol* (1993) 70:844–56. doi:10.1152/jn.1993.70.2.828
52. Holstein GR, Martinelli GP, Cohen B. L-Baclofen-sensitive GABA_A binding sites in the medial vestibular nucleus localized by immunocytochemistry. *Brain Res* (1992) 581:175–80. doi:10.1016/0006-8993(92)90361-C
53. Holstein GR, Martinelli GP, Degen JW, Cohen B. GABAergic neurons in the primate vestibular nuclei. *Ann N Y Acad Sci* (1996) 781:443–57. doi:10.1111/j.1749-6632.1996.tb15719.x
54. Holstein GR, Martinelli GP, Wearne S, Cohen B. Ultrastructure of vestibular commissural neurons related to velocity storage in the monkey. *Neuroscience* (1999) 93:155–70. doi:10.1016/S0306-4522(99)00140-2
55. Cohen B, Helwig D, Raphan T. Baclofen and velocity storage: a model of the effects of the drug on the vestibulo-ocular reflex in the rhesus monkey. *J Physiol* (1987) 393:703–25. doi:10.1113/jphysiol.1987.sp016849
56. Katz E, Vianney de Jong JM, Buettner-Ennever J, Cohen B. Effects of midline medullary lesions on velocity storage and the vestibulo-ocular reflex. *Exp Brain Res* (1991) 87:505–20. doi:10.1007/BF00227076
57. Eron JN, Cohen B, Raphan T, Yakushin SB. Adaptation of orientation vectors of otolith-related central vestibular neurons to gravity. *J Neurophysiol* (2008) 100:1686–90. doi:10.1152/jn.90289.2008
58. Eron JN, Cohen B, Raphan T, Yakushin SB. Adaptation of orientation of central otolith-only neurons. *Ann N Y Acad Sci* (2009) 1164:367–71. doi:10.1111/j.1749-6632.2009.03848.x
59. Kolesnikova OV, Raphan T, Cohen B, Yakushin SB. Orientation adaptation of eye movement-related vestibular neurons due to prolonged head tilt. *Ann N Y Acad Sci* (2011) 1233:214–8. doi:10.1111/j.1749-6632.2011.06176.x
60. Meng H, Blazquez PM, Dickman JD, Angelaki DE. Diversity of vestibular nuclei neurons targeted by cerebellar nodulus inhibition. *J Physiol* (2014) 592:171–88. doi:10.1113/jphysiol.2013.259614
61. Voogd J, Bigar F. Topographical distribution of olivary and corticonuclear fibers in the cerebellum: a review. *The Inferior Olivary Nucleus: Anatomy and Physiology*. New York: Raven Press (1980):207–34.
62. Voogd J. The importance of fiber connections in the comparative anatomy of the mammalian cerebellum. In: Llinás R, editor. *Neurology of Cerebellar Evolution and Development*. (1969). p. 493–514.
63. Voogd J, Gerrits NM, Ruigrok TJ. Organization of the vestibulocerebellum. *Ann N Y Acad Sci* (1996) 781:553–79. doi:10.1111/j.1749-6632.1996.tb15728.x

64. Solomon D, Cohen B. Stimulation of the nodulus and uvula discharges velocity storage in the vestibulo-ocular reflex. *Exp Brain Res* (1994) 102:57–68. doi:10.1007/BF00232438
65. Cohen B, Matsuo V, Raphan T. Quantitative analysis of the velocity characteristics of optokinetic nystagmus and optokinetic after-nystagmus. *J Physiol* (1977) 270:321–44. doi:10.1113/jphysiol.1977.sp011955
66. Dai M, Kunin M, Raphan T, Cohen B. The relation of motion sickness to the spatial-temporal properties of velocity storage. *Exp Brain Res* (2003) 151:173–89. doi:10.1007/s00221-003-1479-4
67. Singleton GT. Relationships of the cerebellar nodulus to vestibular function: a study of the effects of nodulectomy on habituation. *Laryngoscope* (1967) 77:1579–619. doi:10.1288/00005537-196709000-00001
68. Cohen H, Cohen B, Raphan T, Waespe W. Habituation and adaptation of the vestibuloocular reflex: a model of differential control by the vestibulocerebellum. *Exp Brain Res* (1992) 90:526–38. doi:10.1007/BF00230935
69. Barmack NH, Fagerson M, Fredette BJ, Mugnaini E, Shojaku H. Activity of neurons in the beta nucleus of the inferior olive of the rabbit evoked by natural vestibular stimulation. *Exp Brain Res* (1993) 94:203–15. doi:10.1007/BF00230288
70. Barmack NH, Shojaku H. Vestibularly induced slow oscillations in climbing fiber responses of Purkinje cells in the cerebellar nodulus of the rabbit. *Neuroscience* (1992) 50:1–5. doi:10.1016/0306-4522(92)90376-D
71. Shojaku H, Barmack NH, Mizukoshi K. Influence of vestibular and visual climbing fiber signals on Purkinje cell discharge in the cerebellar nodulus of the rabbit. *Acta Otolaryngol Suppl* (1991) 481:242–6. doi:10.3109/00016489109131391
72. Barmack NH, Baughman RW, Eckenstein FP, Shojaku H. Secondary vestibular cholinergic projection to the cerebellum of rabbit and rat as revealed by choline acetyltransferase immunohistochemistry, retrograde and orthograde tracers. *J Comp Neurol* (1992) 317:250–70. doi:10.1002/cne.903170303
73. Barmack NH, Baughman RW, Errico P, Shojaku H. Vestibular primary afferent projection to the cerebellum of the rabbit. *J Comp Neurol* (1993) 327:521–34. doi:10.1002/cne.903270405
74. Barmack NH, Shojaku H. Vestibular and visual climbing fiber signals evoked in the uvula-nodulus of the rabbit cerebellum by natural stimulation. *J Neurophysiol* (1995) 74:2573–89. doi:10.1152/jn.1995.74.6.2573
75. Straka H, Baker R. Vestibular blueprint in early vertebrates. *Front Neural Circuits* (2013) 7:182. doi:10.3389/fncir.2013.00182
76. Glover JC. The organization of vestibulo-ocular and vestibulospinal projections in the chicken embryo. *Eur J Morphol* (1994) 32:193–200.
77. Glover JC. Neuroepithelial ‘compartments’ and the specification of vestibular projections. *Prog Brain Res* (2000) 124:3–21. doi:10.1016/S0079-6123(00)24004-1
78. Diaz C, Glover JC. Comparative aspects of the hodological organization of the vestibular nuclear complex and related neuron populations. *Brain Res Bull* (2002) 57:307–12. doi:10.1016/S0361-9230(01)00673-6
79. Straka H, Baker R, Gilland E. Rhombomeric organization of vestibular pathways in larval frogs. *J Comp Neurol* (2001) 437:42–55. doi:10.1002/cne.1268
80. Straka H, Baker R, Gilland E. The frog as a unique vertebrate model for studying the rhombomeric organization of functionally identified hindbrain neurons. *Brain Res Bull* (2002) 57:301–5. doi:10.1016/S0361-9230(01)00670-0
81. Cohen B, Suzuki JI, Bender MB. Eye movements from semicircular canal nerve stimulation in the cat. *Ann Otol Rhinol Laryngol* (1964) 73:153–69. doi:10.1177/000348946407300116
82. Suzuki JI, Cohen B, Bender MB. Compensatory eye movements induced by vertical semicircular canal stimulation. *Exp Neurol* (1964) 9:137–60. doi:10.1016/0014-4886(64)90013-5
83. Ezure K, Graf W. A quantitative analysis of the spatial organization of the vestibulo-ocular reflexes in lateral- and frontal-eyed animals – I. Orientation of semicircular canals and extraocular muscles. *Neuroscience* (1984) 12:85–93. doi:10.1016/0306-4522(84)90140-4
84. Suzuki JI, Cohen B. Head, eye, body and limb movements from semicircular canal nerves. *Exp Neurol* (1964) 10:393–405. doi:10.1016/0014-4886(64)90031-7
85. Clarke AH. On the vestibular labyrinth of *Brachiosaurus brancai*. *J Vestib Res* (2005) 15:65–71.
86. van Bree JB, Heijligers-Feijen CD, de Boer AG, Danhof M, Breimer DD. Stereoselective transport of baclofen across the blood-brain barrier in rats as determined by the unit impulse response methodology. *Pharm Res* (1991) 8:259–62. doi:10.1023/A:1015812725011
87. Deguchi Y, Inabe K, Tomiyasu K, Nozawa K, Yamada S, Kimura R. Study on brain interstitial fluid distribution and blood-brain barrier transport of baclofen in rats by microdialysis. *Pharm Res* (1995) 12:1838–44. doi:10.1023/A:1016263032765
88. Abbott NJ, Romero IA. Transporting therapeutics across the blood-brain barrier. *Mol Med Today* (1996) 2:106–13. doi:10.1016/1357-4310(96)88720-X
89. Drugbank, Baclofen, Canadian Institute of Health Research. Alberta Innovates –Health Solutions. The Metalomics Innovation Center (2005).

Conflict of Interest Statement: The authors declare that the research was conducted in the absence of any commercial or financial relationships that could be construed as a potential conflict of interest.

Copyright © 2018 Cohen, Yakushin and Cho. This is an open-access article distributed under the terms of the Creative Commons Attribution License (CC BY). The use, distribution or reproduction in other forums is permitted, provided the original author(s) and the copyright owner are credited and that the original publication in this journal is cited, in accordance with accepted academic practice. No use, distribution or reproduction is permitted which does not comply with these terms.



Vestibular Modulation of Sympathetic Nerve Activity to Muscle and Skin in Humans

Elie Hammam¹ and Vaughan G. Macefield^{1,2,*†}

¹ School of Medicine, Western Sydney University, Sydney, NSW, Australia, ² Neuroscience Research Australia, Sydney, NSW, Australia

OPEN ACCESS

Edited by:

Bernard Cohen,
Icahn School of Medicine
at Mount Sinai, United States

Reviewed by:

André Diedrich,
Vanderbilt University,
United States
Pierre-Paul Vidal,
Université Paris Descartes,
France

*Correspondence:

Vaughan G. Macefield
v.macefield@westernsydney.edu.au

†Present address:

Vaughan G. Macefield,
Mohammed Bin Rashid University
of Medicine and Health Sciences,
Dubai, United Arab Emirates

Specialty section:

This article was submitted
to Neuro-otology,
a section of the journal
Frontiers in Neurology

Received: 29 January 2017

Accepted: 26 June 2017

Published: 26 July 2017

Citation:

Hammam E and Macefield VG (2017)
Vestibular Modulation of
Sympathetic Nerve Activity to
Muscle and Skin in Humans.
Front. Neurol. 8:334.
doi: 10.3389/fneur.2017.00334

We review the existence of vestibulosympathetic reflexes in humans. While several methods to activate the human vestibular apparatus have been used, galvanic vestibular stimulation (GVS) is a means of selectively modulating vestibular afferent activity *via* electrodes over the mastoid processes, causing robust vestibular illusions of side-to-side movement. Sinusoidal GVS (sGVS) causes partial entrainment of sympathetic outflow to muscle and skin. Modulation of muscle sympathetic nerve activity (MSNA) from vestibular inputs competes with baroreceptor inputs, with stronger temporal coupling to the vestibular stimulus being observed at frequencies remote from the cardiac frequency; “super entrainment” was observed in some individuals. Low-frequency (<0.2 Hz) sGVS revealed two peaks of modulation per cycle, with bilateral recordings of MSNA or skin sympathetic nerve activity, providing evidence of lateralization of sympathetic outflow during vestibular stimulation. However, it should be noted that GVS influences the firing of afferents from the entire vestibular apparatus, including the semicircular canals. To identify the specific source of vestibular input responsible for the generation of vestibulosympathetic reflexes, we used low-frequency (<0.2 Hz) sinusoidal linear acceleration of seated or supine subjects to, respectively, target the utricular or saccular components of the otoliths. While others had discounted the semicircular canals, we showed that the contributions of the utricle and saccule to the vestibular modulation of MSNA are very similar. Moreover, that modulation of MSNA occurs at accelerations well below levels at which subjects are able to perceive any motion indicates that, like vestibulospinal control of posture, the vestibular system contributes to the control of blood pressure through potent reflexes in humans.

Keywords: galvanic vestibular stimulation, linear acceleration, muscle sympathetic nerve activity, skin sympathetic nerve activity, vestibular system, vestibulosympathetic reflexes

OVERVIEW OF BLOOD PRESSURE AND THE NERVOUS SYSTEM

The autonomic nervous system controls most visceral functions of the body automatically, without the requirement for conscious control. The efferent outflow comprises three subdivisions: the enteric nervous system, which deals exclusively with gastrointestinal function, and the sympathetic (thoracolumbar) and parasympathetic (craniosacral) nervous systems. The latter two subdivisions are regularly thought of as operating in parallel and antagonistic (1). While this is true in many organs that receive dual innervation, such as the pupil of the eye and the heart, control of blood flow

in the systemic circulation is governed exclusively by the sympathetic nervous system (2). Similarly, vestibular-mediated changes in peripheral blood flow are brought about *via* the sympathetic nervous system, giving rise to the term “vestibulosympathetic reflex” (3). Accordingly, this review is focused on the relationship of the vestibular input and its effect on the sympathetic output to muscle and skin. Microelectrode recordings from postganglionic sympathetic axons in motor fascicles of human peripheral nerves have revealed that muscle sympathetic nerve activity (MSNA), which occurs as bursts of activity coupled to the cardiac cycle *via* the arterial baroreflex, consists only of vasoconstrictor impulses (4). Given that the skeletal muscle vascular beds make up a significant proportion of cardiac output, muscle vasoconstrictor drive contributes importantly to the control of blood pressure (5). Conversely, skin sympathetic nerve activity (SSNA) is primarily involved in thermoregulation and emotional expression, supplying cutaneous blood vessels, sweat glands, and hairs (4).

VESTIBULOSYMPATHETIC REFLEXES IN HUMANS

In this review, we explore the role of the vestibular system in cardiovascular control in humans, with particular reference to interactions between the vestibular system and sympathetic outflow to muscle and skin. We shall assume that the reader has a good knowledge of the anatomy and physiology of the vestibular apparatus, and refer the reader to a recent comprehensive review of the anatomical and physiological substrates supporting the existence of vestibulosympathetic reflexes (3). While studies in animals clearly provided overwhelming evidence for the anatomical and physiological pathways describing the influence of the vestibular apparatus on the cardiovascular system, its role in humans has been more difficult to explore and establish. Much like the animal work using different methodologies, research conducted on human participants has employed both physiological and electrical stimulation, with the inherent strengths and weaknesses associated with these approaches. Throughout this review, emphasis will be placed on studies that have directly recorded MSNA and SSNA in awake human subjects *via* intraneuronal microelectrodes (microneurography). Moreover, we shall aim to highlight evidence in which differences in vestibular modulation of MSNA and SSNA exist.

CALORIC STIMULATION

Caloric stimulation is a technique that delivers cold or warm water to the tympanic membrane *via* the ear canal, producing nystagmus (involuntary eye movements) and, hence, indicating that vestibulo-ocular reflexes have been activated. In short, this method produces a thermal gradient within the semicircular canals (the horizontal canals in particular) that leads to increased endolymphatic flow and stimulation of vestibular hair cells. Employing this natural stimulation, Costa et al. (6) recorded MSNA to unilateral caloric stimulation using warm water irrigation but found no evidence of increased sympathetic outflow to the leg (6). On the other hand, Cui and colleagues

employed bilateral caloric stimulation, using both hot- and cold-water irrigation, and concluded that caloric stimulation decreases SSNA (7) and transiently increases MSNA and that these responses are proportional to the degree of nystagmus (8). It is not clear why there is a discrepancy in the findings of these two groups, but it is possible that the differences are due to the different means by which caloric stimuli were delivered (9). It is also worth pointing out that Ray and colleagues (10, 11) found no modulation of sympathetic nerve activity to either muscle or skin during active horizontal rotations of the head, another method that stimulates the horizontal semicircular canals. Finally, it is important to note that the aforementioned studies limited the stimulations to the horizontal canals, as the vertical canals cannot be selectively stimulated in human subjects. Of course, while this means that there is a possibility that the vertical canals play a role in cardiovascular control, studies in animals strongly argue against this (12).

HEAD-DOWN NECK FLEXION (HDNF)

Another means of stimulating the vestibular apparatus physiologically in humans is HDNF. The method entails laying the subject prone with the head and body aligned and by tilting the head downward the maneuver creates an altered gravitational input to the otolith organs. As a response to this stimulus, Essandoh, Normand, and their colleagues demonstrated decreases in arterial pressure and blood flow to the limbs (13, 14). However, it was Shortt and Ray (15) who recorded MSNA and demonstrated that the method leads to an increase in burst frequency and heart rate—increases that were sustained throughout the 10 min of HDNF (15). The same response was not evident during recording of SSNA (16), emphasizing the independence of sympathetic outflow to muscle and skin. Furthermore, studies outlined that the MSNA response is dependent on the magnitude of the stimulus (17) and is the same to the upper limbs as it is to the lower limbs (18, 19), contrary to what is reported in animal studies (20–22). However, in addition to stimulating both the utricle and saccule, HDNF activates several non-vestibular inputs capable of increasing sympathetic outflow—in particular, afferents from muscle (and other) receptors in the neck (23).

OFF-VERTICAL AXIS ROTATION (OVAR)

Another approach to investigate the roles of the otolith organs is OVAR—a method well-known to produce motion sickness (24) and widely used to study vestibular-ocular reflexes (25–27). The technique involves continuous horizontal rotation of the seated body at a constant velocity, with—as its name suggests—the axis of rotation being tilted (15°) from vertical. Initially, the semicircular canals are activated by the angular acceleration, but as the fluid in the semicircular canals starts to move at the same velocity as the head, the semicircular canals no longer provide a signal of rotational motion after ~ 12 s (28). This rotational steady state provides linear acceleration allowing the otolith organs to be activated; by keeping the neck aligned with the body axis, this eliminates neck movement and, in turn, sustaining constant afferent input. Indeed, Yates and Bronstein (29) showed that

individual vestibular afferents start to fire as soon as the nose-up position is passed during OVAR (29). In humans, Kaufmann and colleagues applied OVAR while recording MSNA to study the vestibulosympathetic reflex across a wide range of rotational velocities and found that in the nose-up position there was an increase in MSNA to the lower limbs. The reflexive increase in neural traffic occurred within a short latency (0.4 s)—too quick to be attributed to the baroreflex that has a minimal latency of 1.22 s to the lower limbs (30). These data provided evidence of a vestibulosympathetic reflex, originating from the otolith, contributing to peripheral blood pressure control. Indeed, a recent study that applied centrifugal forces to astronauts pre and post spaceflight demonstrated that depression of otolithic function following space travel leads to a temporary depression of blood pressure control on Earth—a transient dysfunction that reverses with the “re-conditioning” of the gravitational accelerometers, i.e., the otolithic organs (31). By contrast, OVAR applied in the nose-down position caused a decrease in MSNA (32)—results conflicting those seen in HDNF (15). The discrepancies shown in these studies may be due to the different means of stimulating the vestibular apparatus, such as changes in posture and, hence, changes in vestibular input with respect to gravity, and the use of dynamic stimuli and neck displacements in one study but not in the other study. Accordingly, this leads to a need for an experimental design to selectively activate vestibular inputs without acting on other non-vestibular inputs.

GALVANIC VESTIBULAR STIMULATION (GVS)

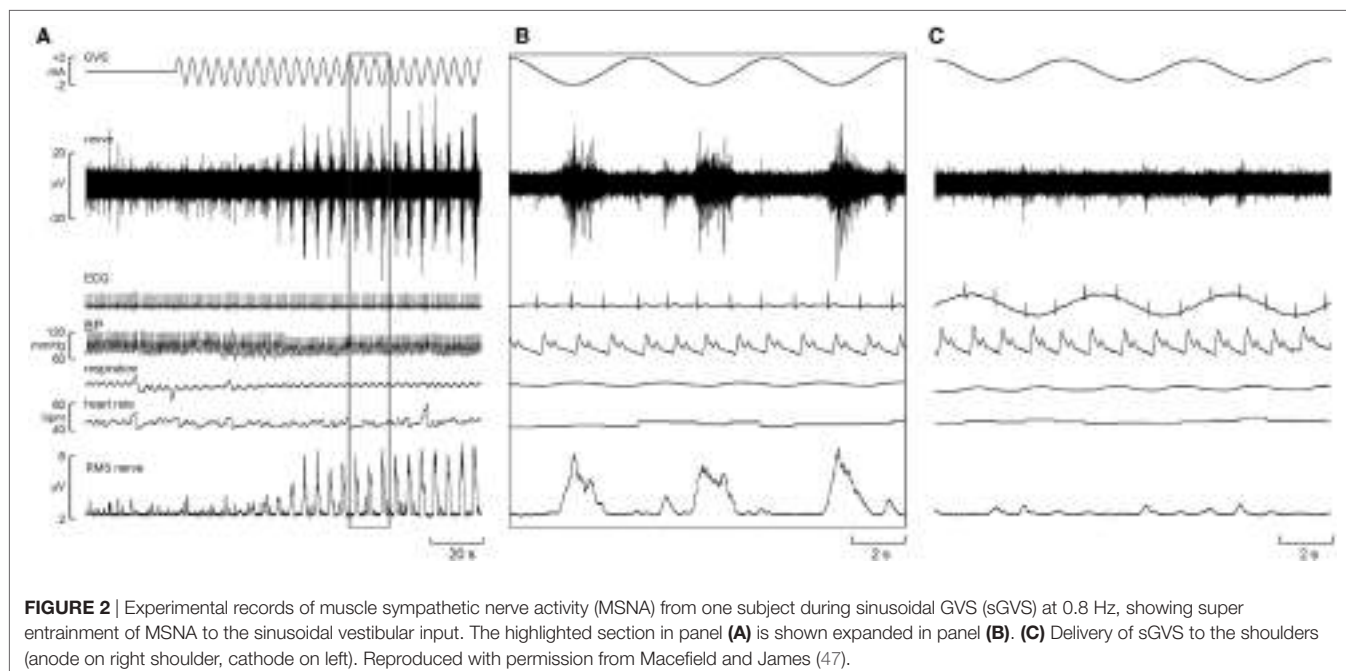
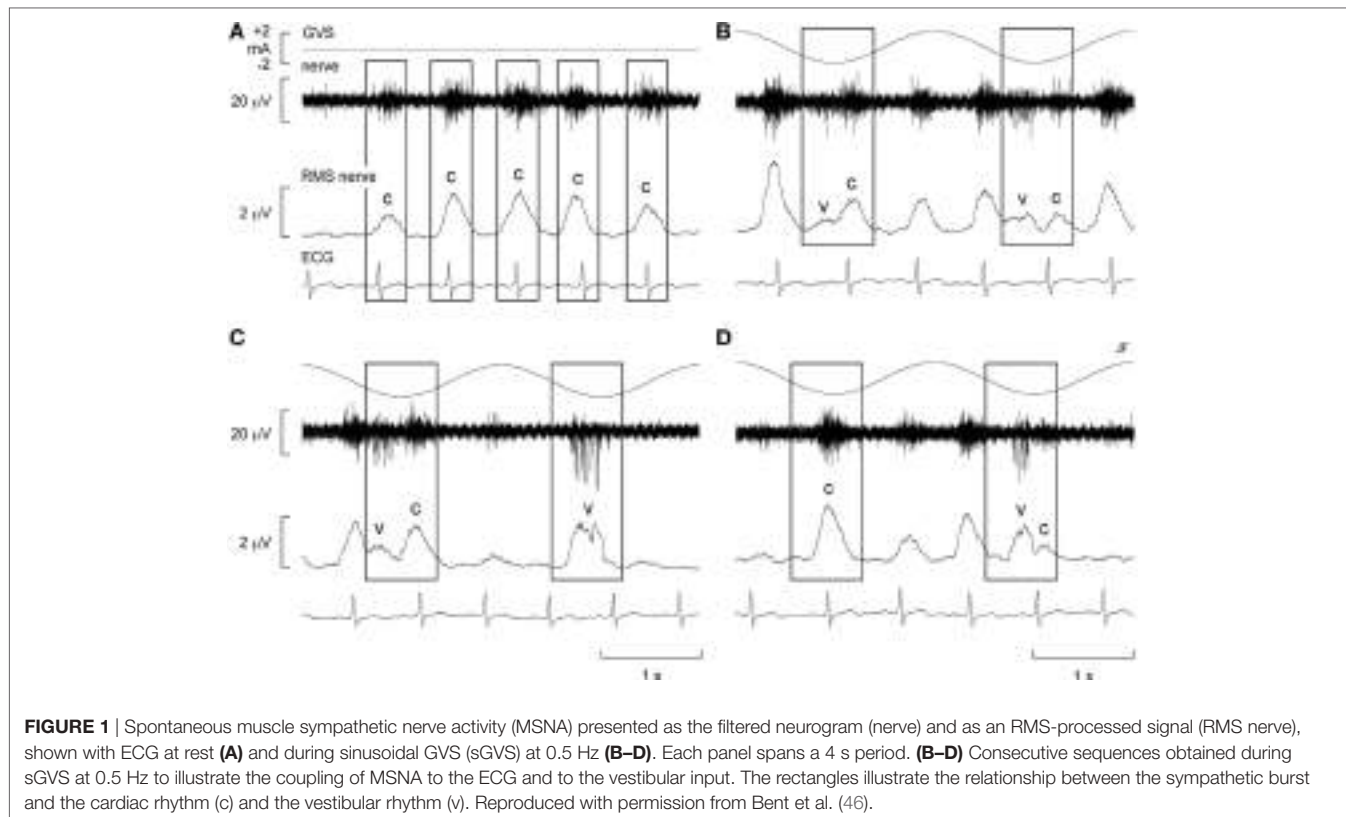
Galvanic vestibular stimulation is a means of stimulating afferents in the vestibular nerves through weak electrical stimuli applied to the mastoid processes, and was initially used to study the contributions of the vestibular system to control of eye movements, locomotion, and posture (33, 34) and has since been used by our group to study vestibulosympathetic reflexes in humans. It provides a selective form of stimulation to the vestibular apparatus (35–37), though it has been pointed out that GVS is less selective than other methods, resulting in an overall stimulation of vestibular nerves rather than specific components (9). Goldberg et al. (35) made direct recordings from vestibular afferents in primates during application of GVS. They showed in the squirrel monkey that when cathodal GVS was applied in the perilymphatic space, or anodal GVS applied at a more proximal point, both caused excitatory responses in vestibular afferents (35). GVS stimulates the hair cell axon terminals of the vestibular afferents and alter their firing (35). Cathodal currents depolarize and, thus, increase the firing rate of vestibular afferents, whereas anodal currents hyperpolarize and thereby decrease their firing rate. As noted above, a limitation of GVS is that it cannot discriminate between the vestibular end organs (semicircular canals or otolith organs). However, animal research has shown that the response to GVS is predominantly otolithic (38–40), and other evidence strongly argues against a contribution from the semicircular canals in the vestibular control of sympathetic nerve activity (6, 10, 11). Thus, one can assume that any changes in sympathetic outflow

in humans during GVS can be attributed to activation of the otolith organs (9, 38–40). A particular advantage offered by GVS is that it is selective to the vestibular system: it does not modulate neck afferents (as in HDNF), cause fluid shifts in the body (as in OVAR), or influence any other physiological parameter that may affect sympathetic outflow—such as heart rate, blood pressure, or respiration (9, 33).

Bolton et al. (41) first applied GVS in the form of a 1 s step to examine the vestibular contributions to cardiovascular control, in particular its effect on sympathetic outflow to muscle vascular beds in the lower limbs. The investigators found that the application of a 2 mA current across the mastoid processes in a binaural, bipolar fashion adequately modified the firing of vestibular afferents because subjects reported strong perceptual illusions of sway toward the anode. However, despite being delivered at different times following the heart beat, with a delay of 0, 200, 400, or 600 ms following the R-wave of the ECG, GVS failed to cause a net change in MSNA but did cause short-latency bursts of SSNA. Therefore, it was concluded that the short duration of electrical vestibular stimuli did not interact with the baroreceptors, nor did they cause modulation of MSNA, but did excite cutaneous vasoconstrictor and sudomotor neurones (41).

Alternatively, Voustianiouk et al. (42) employed dynamic stimuli in the form of brief trains (30 ms) of 10 pulses of GVS and found a clear modulation of MSNA. While many animal studies demonstrated cardiovascular responses to trains of electrical stimuli delivered to the vestibular system (43–45), Voustianiouk and colleagues clearly showed that short-latency vestibulosympathetic reflexes do exist in humans. The authors concluded that these reflexes might contribute to the control of arterial blood pressure, especially during rapid postural changes (42). To further investigate, our laboratory used continuous (as opposed to intermittent) dynamic GVS to study vestibular modulation of muscle sympathetic outflow (46). Vestibular afferents were stimulated using continuous sinusoidal (0.5–0.8 Hz) stimulation (2 mA) to the mastoid processes (46). Participants experienced strong perceptual illusions of “rocking in a boat” or “swinging from side to side in a hammock,” at a frequency matching that of the stimulation. Interestingly, this study showed that overall MSNA increased by 156% and that sinusoidal GVS (sGVS) was able to cyclically modulate MSNA (**Figure 1**). For this and subsequent studies using sGVS, we used cross-correlation analyses to identify temporal coupling between the occurrence of sympathetic nerve activity and the peak of the sinusoidal vestibular stimulus (i.e., the peak of the sinusoid) or the peak of the ECG (i.e., the R-wave). This approach allows one to quantify vestibular or cardiac modulation in terms of the modulation index—the magnitude of the temporal coupling of sympathetic outflow to a reference event, be it the vestibular stimulus or the heart beat.

Furthermore, there was evidence of generation of *de novo* sympathetic bursts to the dynamic GVS: two bursts of MSNA could be generated per cardiac interval (46), with one burst being temporally coupled to the sinusoidal vestibular input and the other to the baroreceptor (cardiac) input (**Figure 1**). This observation showed that the vestibular system exerts a significant influence on sympathetic outflow to muscle, and that



this may operate independently of the arterial baroreceptors in the control blood pressure (46). Recently, we provided evidence of “super entrainment” of MSNA, in which a burst of MSNA is very strongly coupled to a phase of sGVS (47). As shown in **Figure 2**, this strong temporal coupling was clearly generated by

stimulation of the vestibular nerves, as applying the same current to the shoulders failed to induce any modulation.

To further explore the effect of sGVS on sympathetic outflow, in separate studies, our laboratories exposed participants to a wider range of frequencies (0.2–2.0 Hz, 200 cycles, ± 2 mA)

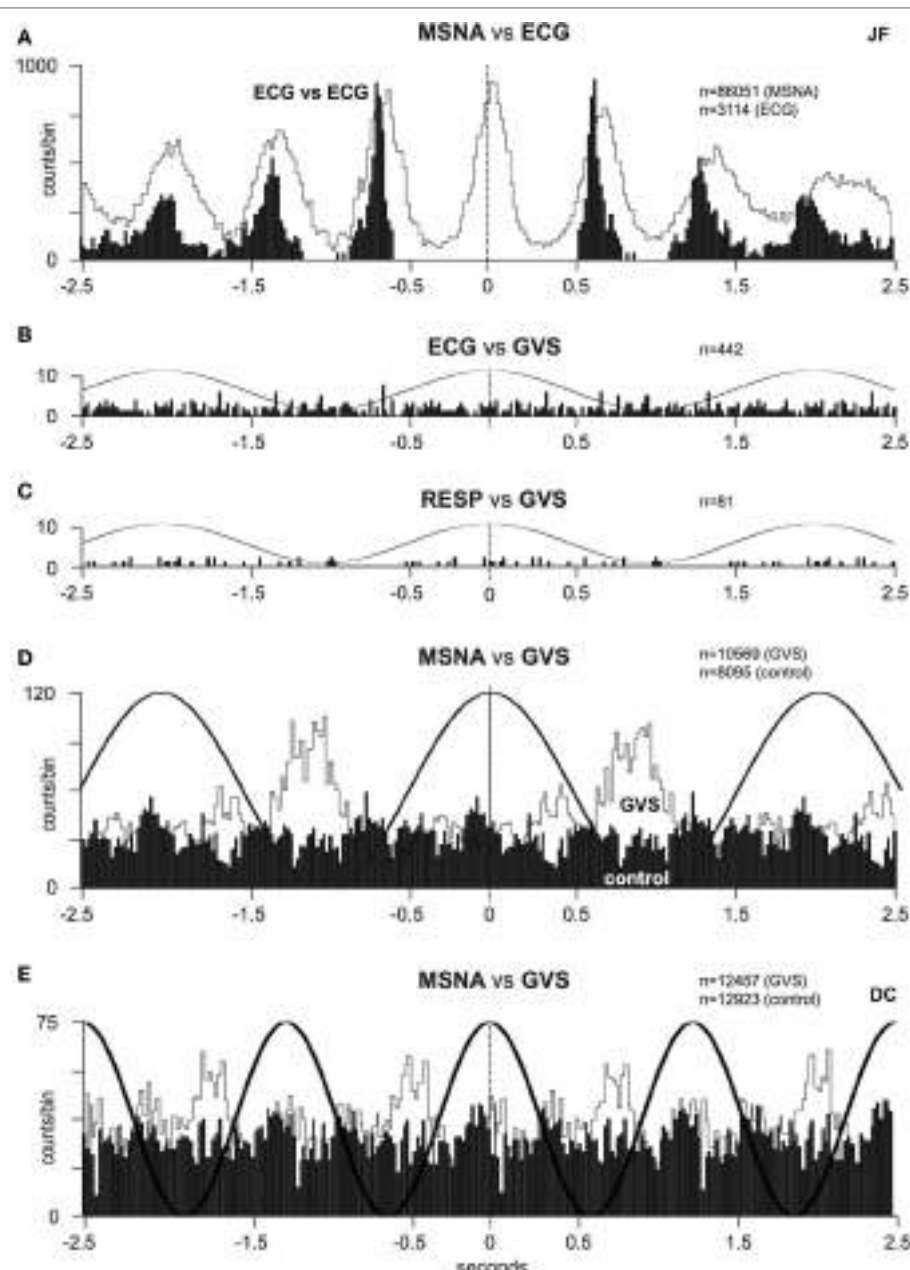


FIGURE 3 | (A) Cross-correlation histograms of the relationship between muscle sympathetic nerve activity (MSNA) and R-waves of the ECG (white histogram) and autocorrelogram of the ECG (black histogram). **(B,C)** Cross-correlation histograms between ECG and sinusoidal GVS (sGVS) and respiration (inspiratory peaks) and sGVS. A 0.5 Hz sine wave has been superimposed on the histogram to illustrate the timing of the galvanic vestibular stimulation; it has been inverted for clarity. **(D,E)** Cross-correlation histograms of MSNA with respect to the vestibular input (GVS), in white, or to a control sine wave (control), in black. Data in panels **(A–D)** are from the same subject represented in **Figure 1**; data in panel **(E)** were obtained from another subject. 20 ms bins in all panels. n = the numbers of counts comprising the histograms. Reproduced with permission from Bent et al. (46).

during recordings of both muscle and SSNA (48, 49). Similarly, in both of these studies, all of the subjects reported robust vestibular illusions, though these were reduced at the higher frequencies. Cross-correlation analysis revealed partial phase locking of both muscle and skin to the cyclic vestibular input, with the vestibular modulation of MSNA found to be greatest at 0.2 Hz and lowest at 0.8 Hz—the latter being the frequency closest to

the cardiac rhythm. **Figure 3** shows cross-correlation histograms between MSNA and ECG (**Figure 3A**) and 0.5 Hz sinusoidal GVS (**Figure 3D**). It can be seen that the cardiac modulation of MSNA is higher than the vestibular modulation, and that GVS has no direct effect on ECG (**Figure 3B**) or respiration (**Figure 3C**). The cross-correlation histogram between MSNA and GVS, delivered at 0.8 Hz, is shown for another subject in **Figure 3E**. Unlike the

vestibular modulation of MSNA, the vestibular modulation of SSNA was high at all frequencies of stimulation. This prompted further investigation to better understand the modulation of MSNA. In an extension of the latter study, sGVS was delivered at the resting heart rate of a given subject and at frequencies (0.1, 0.2, 0.3, and 0.6 Hz) above and below the central cardiac frequency. Results confirmed that vestibular modulation of MSNA was significantly reduced when it coincides with the cardiac rhythm, confirming the competitive nature of vestibular and baroreceptor inputs. This further highlights the dominance of the arterial baroreceptors in modulating MSNA (50).

Furthermore, as the highest modulation of sympathetic outflow in the study by Grewal et al. (48) occurred at 0.2 Hz, we explored whether lower frequencies of stimulation (0.08–0.18 Hz) produce higher or lower modulation. These are frequencies specifically associated with very slow postural displacements (i.e., such as those experienced during tall building sway, evoking motion sickness) (51, 52). Analysis of the sympathetic discharge revealed that such low-frequency GVS induces two peaks of modulation of MSNA per cycle of stimulation—one associated with the positive peak and the other with the negative peak (Figure 4) (51). This observation also held true when recording sympathetic activity to the skin (52).

While very few subjects reported nausea at the high frequencies of sGVS, half of the subjects experienced nausea at frequencies of sGVS < 0.2 Hz. Moreover, those subjects who did report nausea displayed a greater vestibular modulation of SSNA, as shown in Figure 5 (52). It is interesting that this augmented vestibular modulation of sympathetic outflow to skin was not generalized to the sympathetic outflow to muscle (53). However, perhaps this is not surprising, given that increases in SSNA explain two of the features of nausea—pallor and sweating.

In order to explain the two-peak response, it is noteworthy that in all experiments we recorded sympathetic nerve activity from the left side (51, 52). In addition, the anode was always located over the right mastoid process, making it more straightforward in interpreting the results. The larger (primary) peak (see Figure 4A) was related to the positive phase of the sinusoid (i.e., 0 to 2 mA), while the smaller (secondary) peak was related to the negative phase. Given that hyperpolarization of the vestibular nerves occurs at the anode and depolarization at the cathode (37), we can see that the positive phase of stimulation corresponds to hyperpolarization on the right side. Naturally, because we are applying current bilaterally (across both mastoid processes) hyperpolarization on the right side means that the left side is being depolarized. As the current slowly shifts toward the left side, it causes hyperpolarization on this side but depolarization on the right. We suggest that this secondary depolarization is responsible for the secondary burst of modulation. This pattern of modulation—a primary peak corresponding to the positive phase of sGVS and a smaller secondary peak corresponding to the negative phase—matched the stimulus frequency but was never observed at the higher frequencies of stimulation used previously (46, 48, 49), presumably because at frequencies >0.2 Hz there is not enough time for a second peak to be seen.

These series of studies showed that cyclically changing vestibular nerve input could generate a marked modulation of

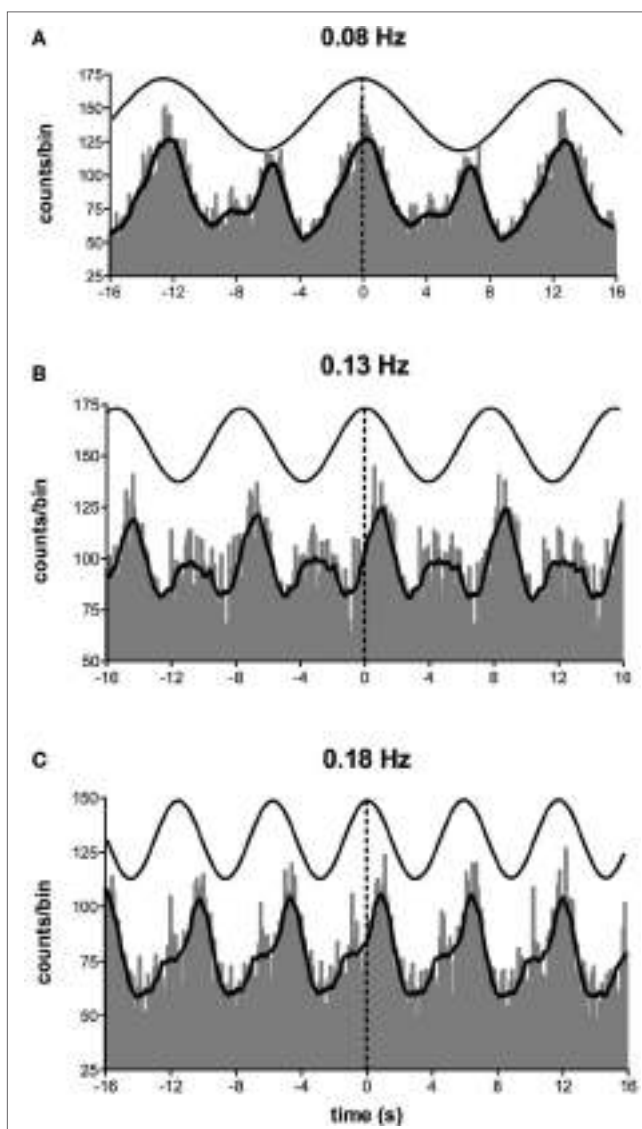


FIGURE 4 | Cross-correlation histograms between muscle sympathetic nerve activity and sinusoidal GVS in one subject. The thick curve superimposed on the histograms is the smoothed polynomial that was fitted to the data. The sinusoid above represents the galvanic stimulus, delivered at (A) 0.08, (B) 0.13, and (C) 0.18 Hz. Each cross-correlation histogram shows a large peak of modulation (primary peak), associated with the positive peak of the sinusoid, and a smaller peak (secondary peak). The secondary peak was largest at 0.08 Hz and smallest at 0.18 Hz. Reproduced with permission from Hammam et al. (51).

muscle vasoconstrictor activity (46, 48, 49, 51). This most likely acts through the rostral ventrolateral medulla (RVLM), which is the primary output nucleus for muscle vasoconstrictor neurones (54, 55) and receives direct excitatory inputs from the otoliths (56, 57). So, the frequency-dependant modulation of MSNA may reflect vestibular inputs arriving from both sides projecting onto RVLM. This was later confirmed during experiments involving bilateral recordings of MSNA, where cross-correlation analysis did indeed reveal a reversal of modulation in the primary and secondary peaks recorded from the left and right sides: a

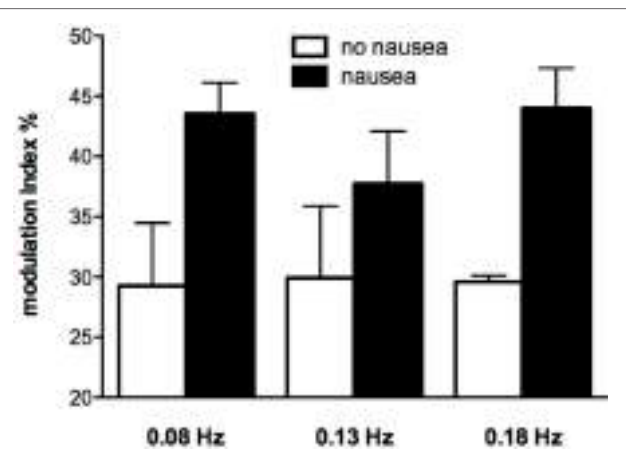


FIGURE 5 | Modulation indices of primary peak of skin sympathetic nerve activity during sinusoidal GVS at different frequencies as a function of whether or not subjects reported nausea. It can be seen that modulation indices were higher in those subjects who reported nausea. Reproduced with permission from Hammam et al. (52).

primary peak on the left was associated with a secondary peak on the right and a secondary peak on the left was associated with a primary peak on the right (**Figures 6** and **7**). This is probably of greater interest physiologically, given that it supports the idea that sympathetic control of blood pressure and blood flow is lateralized, at least with respect to the vestibulosympathetic reflexes studied.

It is generally assumed that sympathetic nerve activity is symmetrical: burst rates and burst amplitude distributions of MSNA have been shown to be similar on the two sides (59, 60); the same has been shown for SSNA (61). However, apart from our own observations (58), only one other study has demonstrated lateralization of sympathetic outflow. Diedrich et al. (62) found differential expression of MSNA on the left and right sides during sinusoidal neck suction, abolishing the normally right-sided dominance of carotid sinus baroreceptors on MSNA.

As noted above, the otoliths, rather than the semicircular canals, are believed to be primarily responsible for vestibulosympathetic reflexes (6, 10). And while GVS affects the firing of vestibular afferents originating in all parts of the vestibular apparatus (35, 36), recent evidence supports the idea that sGVS acts only *via* the otolith organs (38, 40). However, what we do not know is whether it is the utricular or saccular components of the otolith organs that are mediating the vestibulosympathetic reflexes. This requires a different means of vestibular afferent stimulation, one that can eliminate the semicircular canals and differentiate between the otolith organs.

LINEAR ACCELERATION

Linear acceleration is a natural means of activating the vestibular apparatus. Yates et al. (63) had demonstrated increases in blood pressure and heart rate during linear acceleration (200 mG), and that these cardiovascular responses were absent in patients with bilateral loss of vestibular function. Jauregui-Renaud et al. (64)

found similar results, control subjects exhibiting a sustained increase in heart rate and transient increase in breathing during linear acceleration (260 mG) that were absent in patients with vestibular dysfunction. These and other studies (63, 65–68) provide good evidence supporting the contribution of the otoliths to cardiovascular control. Direct recordings of MSNA during sinusoidal linear acceleration were first reported by Cui et al. (69), who found that MSNA decreased in subjects exposed to five cycles acceleration (100, 150, and 200 mG) in both the antero-posterior and medio-lateral directions (69, 70). However, all of these studies used fairly high accelerations (100–260 mG), which in addition to activating the vestibular organs will also activate extra-cranial receptors, such as those responsive to fluid shifts.

To circumvent this problem, we recently undertook a series of experiments that used low-amplitude (4 mG), low-frequency (0.08 Hz), sinusoidal linear acceleration of the body, seated on a motorized platform. By positioning the head vertically linear acceleration in the horizontal plane targets the utricular component of the vestibular apparatus (71, 72). These studies demonstrated a robust modulation of MSNA (32 ± 3 and $29 \pm 3\%$ for the X and Y axes), which was even higher for SSNA (97 ± 3 and $91 \pm 5\%$, for the X and Y axes). Although there were no significant differences in amplitude of the modulation when delivered in the X or Y axes, the magnitude of modulation was markedly different between the two systems of sympathetic outflow. This can be simply due to the fact that the predominant influence on muscle vasoconstrictor drive is the arterial baroreceptors—cardiac modulation of MSNA is much greater than vestibular modulation of MSNA. Cardiac modulation is also higher than respiratory modulation of MSNA, which is of comparable amplitude to the respiratory and cardiac modulation of SSNA (73). In addition, while individual utricular afferents exhibit directional sensitivity, as a population there is no directional preference for evoking vestibulosympathetic reflexes. A noteworthy observation from these studies is that while the mean modulation indices produced by sinusoidal linear acceleration in the X and Y axes showed similar distributions across subjects, individual subjects could exhibit larger changes in sympathetic modulation in one axis than another. Indeed, it has been suggested that individual experiences may modulate the responses of vestibular hair cells responses and, hence, the magnitude of vestibulosympathetic responses (63).

In another series of experiments, subjects were supine with the neck aligned with the spine: sinusoidal linear acceleration, at the same amplitude and frequency, in the rostro-caudal (X) direction (longitudinal axis of the body) excites the saccular hair cells (although not exclusively). Cross-correlation analysis revealed modulation of MSNA (29% in the X-axis) that was no different to that produced by selective stimulation of the utricle (32% in the X-axis, 29% in the Y-axis), nor was it significantly different from that produced by acceleration of the supine body in the medio-lateral (Y) axis (32%), in which both the saccule and utricle are involved (72). This shows that both saccular and utricular organs contribute to the generation of vestibulosympathetic reflexes. This is also evident in the results from the composite sequences, reported by Grewal and colleagues, in which sinusoidal displacements of seated subjects were delivered in the X and Y axes (71).

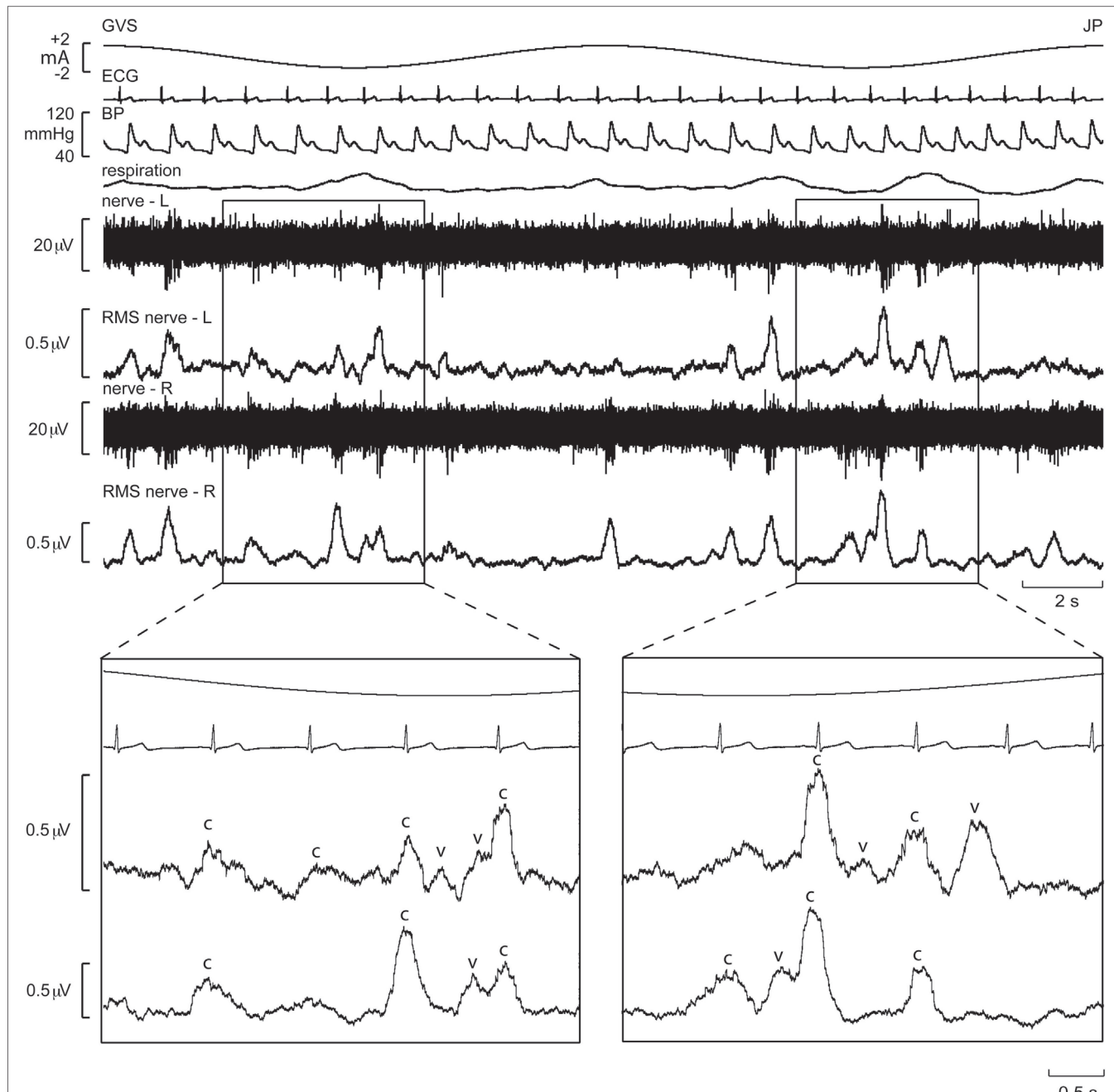


FIGURE 6 | Bilateral recordings of muscle sympathetic nerve activity, together with ECG, blood pressure, and respiration, during sinusoidal GVS (galvanic vestibular stimulation) at 0.08 Hz in one subject. Overall, sympathetic outflow was similar between the two sides, but close inspection revealed subtle differences. In the expanded sections, the sympathetic bursts have been shifted back 1.25 s in time to account for peripheral conduction delays, allowing those bursts aligned with the cardiac cycle (“c”) or vestibular stimulus (“v”) to be identified. Reproduced with permission from El Sayed et al. (58).

Importantly, most subjects noted that they could not feel any motion, and if they did they could not tell in which direction they were moving (71, 72). To further quantify the capacity for subjects to perceive motion and accurately detect the direction of displacement during sinusoidal linear acceleration, we exposed participants to a range of acceleration amplitudes, extending from 1.25 to 30 mG at 0.2 Hz. As illustrated in Figure 8, the average threshold required to be able to detect the motion is

6.5 mG, while the acceleration required to accurately determine the direction of motion is 10.2 mG (74). Despite the fact that subjects could not perceive motion <6 mG, vestibular modulation of MSNA was apparent even at the lowest acceleration tested—1.25 mG (74). Modulation of MSNA at 1.25 mG and 30 mG is shown for one subject in Figure 9.

Figure 10 shows mean data from all subjects: there was a positive slope of the magnitude of modulation as a function of

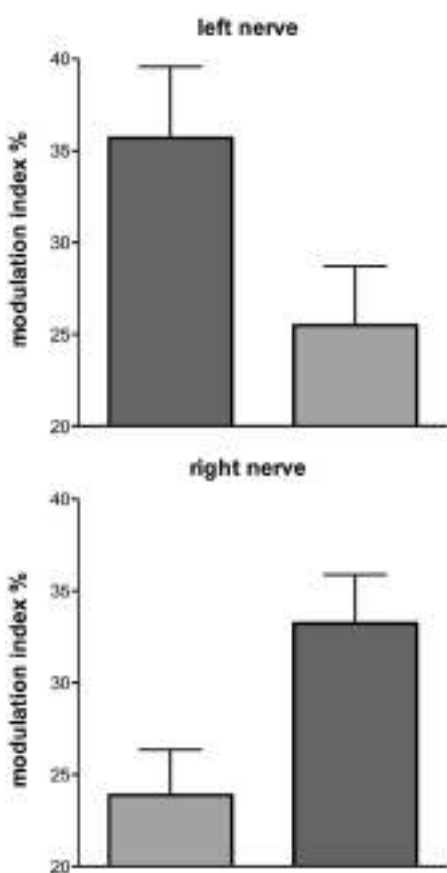


FIGURE 7 | Mean \pm SE modulation indices for the primary (dark gray) and secondary (light gray) peaks of modulation of muscle sympathetic nerve activity. Data obtained from 10 subjects. Reproduced with permission from El Sayed et al. (58).

acceleration amplitude. Based on studies in the monkey higher acceleration amplitudes would be expected to generate a greater vestibular input and thereby a greater modulation of sympathetic nerve activity Fernández and Goldberg (75). These authors used accelerations up to 5 G—*two orders of magnitude higher than that discussed here*. The outcome of this study highlights that the vestibular afferents certainly do respond to the higher accelerations (30 mG), but more importantly, they also respond during acceleration of the lowest magnitude (1.25 mG). That we observed robust modulation of MSNA during very low amplitude, sub-perceptual sinusoidal motion, indicates that the modulation of MSNA was not due to any conscious awareness or arousal-related component and purely reflects the expression of a vestibulosympathetic reflex. Indeed, detection of motion did not occur until accelerations of \sim 6.5 mG, with knowledge of the direction of movement not being apparent until \sim 10 mG. However, while these reflexes are robust, it is worth pointing out that they are certainly smaller than the baroreceptor-mediated reflexes: as seen in **Figure 10**, cardiac modulation was much higher than the vestibular modulation and was not affected by the amplitude of acceleration. Overall, this highlights the exquisitely rapid detection of acceleration by the vestibular hair cells; however, this seems to only be of importance at larger postural changes when immediate blood pooling is compromised, until the relatively slower unmyelinated baroreceptor fibers unload (76–78).

CONTRIBUTIONS OF NECK AFFERENTS

Interestingly, there are some circumstances when the head moves (and, hence, the vestibular system is engaged) but the body does not move—such as lifting the head while lying supine. In these circumstances, there is no need to increase vasomotor tone to the lower limbs. So the question arises, how does

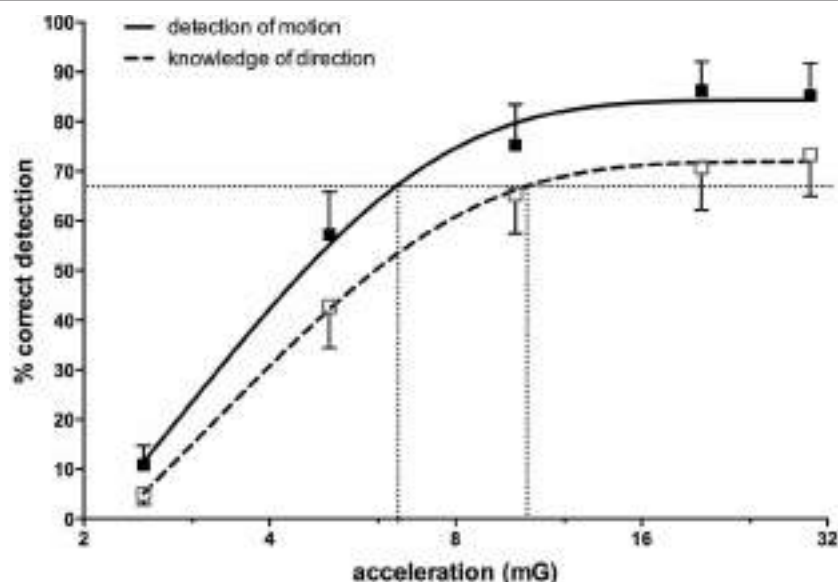


FIGURE 8 | Percentage correct (mean \pm SE) detection of motion, and correct detection of the direction of motion, for 16 subjects exposed to sinusoidal linear acceleration at a constant rate of 0.2 Hz but at accelerations ranging from 1.25 to 30 mG. Semi-logarithmic plot of data from 2.5 to 30 mG, with fitted sigmoidal curves shown superimposed. Reproduced with permission from Hammam et al. (74).

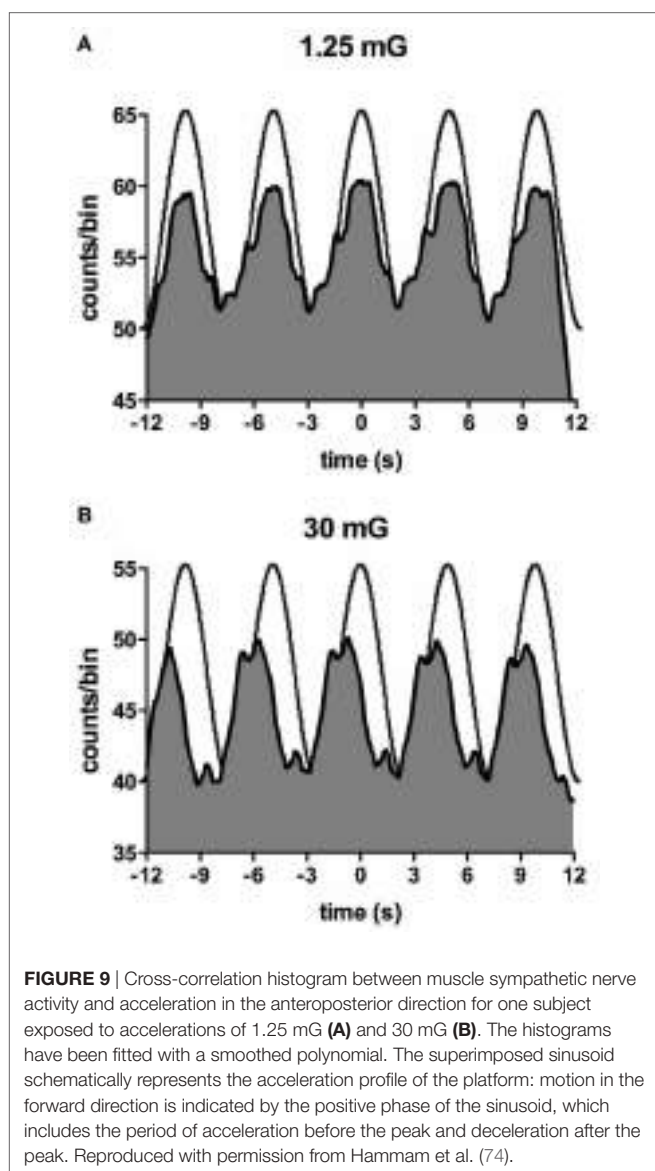


FIGURE 9 | Cross-correlation histogram between muscle sympathetic nerve activity and acceleration in the anteroposterior direction for one subject exposed to accelerations of 1.25 mG (**A**) and 30 mG (**B**). The histograms have been fitted with a smoothed polynomial. The superimposed sinusoid schematically represents the acceleration profile of the platform; motion in the forward direction is indicated by the positive phase of the sinusoid, which includes the period of acceleration before the peak and deceleration after the peak. Reproduced with permission from Hammam et al. (74).

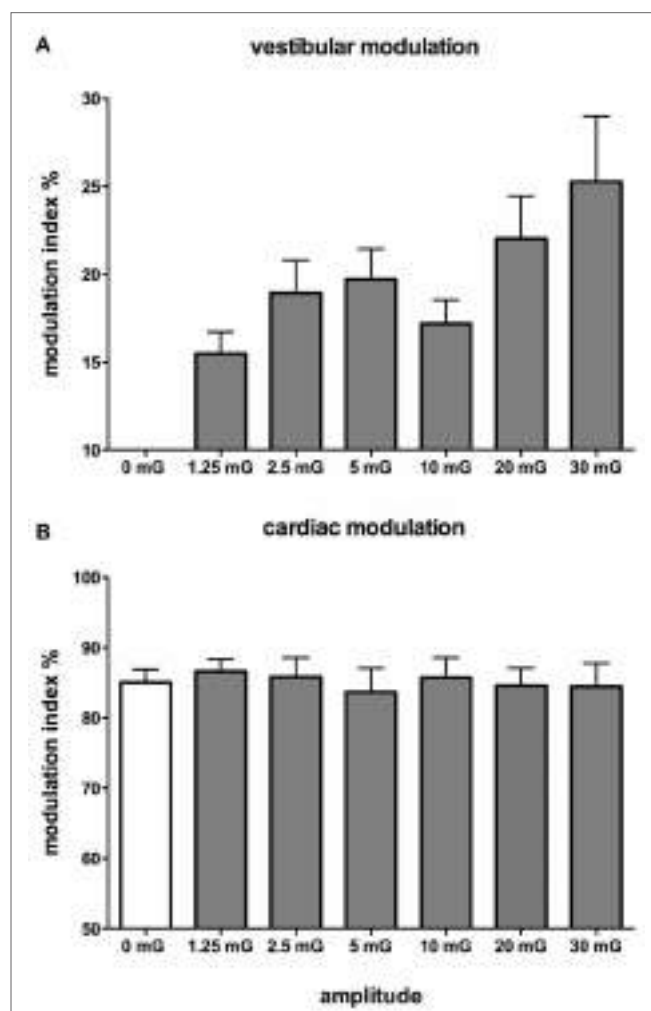


FIGURE 10 | Mean vestibular (**A**) and cardiac (**B**) modulation indices of muscle sympathetic nerve activity as a function of acceleration amplitude; 0 mG = static condition (vestibular modulation = 0 in the absence of a sinusoidal vestibular input). Mean \pm SE data from 13 subjects. Reproduced with permission from Hammam et al. (74).

the brain know when it is appropriate to modulate vasomotor tone to the lower limbs of the habitually upright human? We recently examined the influence of neck afferents on MSNA by employing sinusoidal displacement of the body about the neck—and reported two new findings. First, neck proprioceptors can modulate MSNA in the lower limbs of awake humans and, second, the cardiac modulation of MSNA is reduced in the presence of neck modulation of MSNA [Figure 11 (79)]. While a previous study had examined the influence of neck afferent input on MSNA, they found that neck afferents did not modulate lower limb MSNA (80). However, a significant difference is that the Ray and Hume studies analyzed the MSNA of subjects during *static* flexion or extension of the head and neck while subjects were in the lateral decubitus or supine position, respectively. By contrast, Bolton et al. (79) recorded MSNA during *dynamic* stretching of the neck. That the stimulus may need to be dynamic in order to have an effect on MSNA has been observed with

respect to vestibular modulation of MSNA in humans. *Dynamic* (sinusoidal or trains of pulses) GVS modulates MSNA in the human (46, 81) but *static* (1 s step) stimuli fail to do so (41). This makes teleological sense since *dynamic* changes in posture (body position) are more likely to require modulation of vascular tone than during static states. However, further research is required to determine if the magnitude of neck modulation of MSNA in postures that are likely to induce an orthostatic challenge is sufficient to increase vasomotor tone in the lower limbs and thereby reduce the likelihood of orthostatic hypotension.

Moreover, cardiac modulation of MSNA was reduced in the presence of *dynamic* neck stretch. Animal studies suggest that the vestibular nuclei and regions of the brainstem are involved in integrating information from both somatic and visceral sources and higher centers in order to regulate blood pressure in different body positions and contexts (82–84). The cross-correlation analysis in Bolton et al. (79) showed cyclical modulation of MSNA in

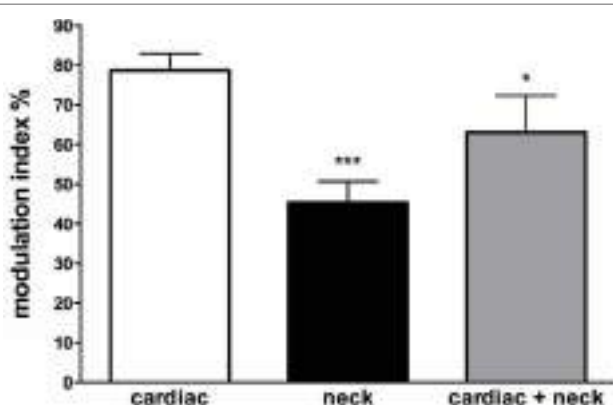


FIGURE 11 | Mean modulation indices (see Methods) calculated from the cross-correlation histograms between muscle sympathetic nerve activity (MSNA) and ECG at rest (*cardiac*), MSNA and neck angle during sinusoidal neck displacement (*neck*) and between MSNA and ECG during sinusoidal neck displacement (*cardiac + neck*). Neck modulation of MSNA was significantly lower than cardiac modulation at rest and cardiac modulation was significantly lower during neck stimulation. $*P < 0.05$; $***P < 0.001$. Reproduced with permission from Bolton et al. (79).

all subjects during neck muscle stretching induced by sinusoidal body displacement about the fixed head. This most likely involved the pathways that mediate vestibulosympathetic reflexes (85). Experimental evidence from animal studies have shown that neck muscle spindle afferents, which are exquisitely sensitive length sensors (86), project to the medial and descending vestibular nuclei and can modulate vestibular neuronal activity (87, 88). Electrical stimulation of nerves innervating muscles of the neck at currents just sufficient to stimulate muscle spindle (and Golgi tendon organ) afferents has been shown to change activity in respiratory and sympathetic nerves in the cat (89). Moreover, it has been shown that the presence of intact neck afferents inhibits the influence of the vestibular system on sympathetic outflow during natural stimulation of the labyrinths (89).

It should be pointed out, however, that sinusoidal displacement of the body about the neck might change transmural pressures at the carotid sinus and, hence, change the input from the arterial baroreceptors. Notwithstanding the fact that the phasic cardiac modulation of MSNA was much greater than that produced by sinusoidal neck movements in the study by Bolton et al. (79), or by electrical or physiological activation of the otolithic organs in previous studies, Shortt and Ray (15) discounted changes in carotid baroreceptor input in their experiments by arguing that there were no changes in blood pressure and, because there were no changes in thoracic volume, discounted any contribution from the low-pressure baroreceptors.

CLINICAL CONSIDERATIONS

The physiological adjustments to a hydrostatic challenge imposed during postural changes is predominantly a function of the baroreflex mechanism, with afferent contributions from the vestibular system (defining head acceleration) and the neck afferents (defining the position of the body in space). Clinical

studies are limited, and while a lot of work has been conducted in quadrupedal mammals, its translation to bipedal humans is somewhat limited.

Nevertheless, we know that acute vestibular lesions produce distressing symptoms of nausea, vomiting, tachycardia, and palpitations—all of which are autonomic markers (29). A study that examined patients with acute vertigo due to unilateral vestibular neuritis (48 h from onset) showed a depression in sympathetic reactivity to orthostatic challenges—a dysfunction that resolved in 2 weeks (65). Similarly, patients with bilateral loss of vestibular function, when exposed to linear motorized accelerations, exhibit an inadequacy in cardiovascular control when compared with healthy controls (64). Moreover, on their return from space, astronauts face the challenge of deconditioned gravitational accelerometers—the otolith organs—resulting in orthostatic intolerance, though resolving 10 days after return (31). The short-lasting dysfunction is echoed and well described in the animal literature, but little is known about the replacement or recovery mechanism following vestibular damage in humans (3).

However, aging-related orthostatic hypotension is a chronic condition and is commonly found in the elderly (90). It is derived from multiple etiologies, including sympatholytic drugs associated with comorbidities, but it has been documented that vestibulosympathetic reflexes depresses with increase in aging (18, 19), suggesting a co-contribution to the debilitating effects of orthostatic intolerance in the elderly. It is, however, an understudied area and requires further investigations to establish a better understanding of the relationship of vestibulospinal reflexes and aging-related orthostatic intolerance.

CONCLUSION

It is now abundantly clear that the vestibular system can modulate sympathetic outflow to both muscle and skin. While our use of low-frequency sGVS has shown that sympathetic outflow can be strongly entrained to vestibular inputs, it is our use of low-frequency sinusoidal linear acceleration that has revealed that both the utricular and saccular components of the vestibular apparatus are responsible for the generation of vestibulosympathetic reflexes. Given that the otolithic organs encode both static position and linear acceleration of the head in space, these findings emphasize that the vestibular apparatus contributes to the control not just of motoneurones involved in posture and locomotion but also sympathetic neurones involved in the control of blood pressure. However, why it should also influence sympathetic outflow to the skin is more difficult to understand. It may well be that vestibular modulation of SSNA has no physiological significance, and may simply reflect coupling of control mechanisms between thermoregulation and blood pressure regulation. Indeed, given that vestibular modulation of muscle sympathetic outflow clearly does play a role in the regulation of blood pressure, and that the distribution of cardiac output to skeletal muscle and skin needs to be controlled with the opposing regulatory demands of blood pressure and body temperature, it makes physiological sense for there to be some common mechanisms for controlling blood flow in muscle and skin when these two demands compete, such as in exercise.

AUTHOR CONTRIBUTIONS

EH drafted the manuscript. VM contributed to the writing. Both authors approved the final manuscript.

REFERENCES

- Cannon WB. *The Wisdom of the Body*. New York: W. W. Norton (1963).
- Jänig W, McLachlan EM. Neurobiology of the autonomic nervous system. In: Mathias CJ, Bannister SR, editors. *Autonomic Failure: A Textbook of Clinical Disorders of the Autonomic Nervous System*. Oxford: Oxford University Press (2013). p. 21–34.
- Yates BJ, Bolton PS, Macefield VG. Vestibulo-sympathetic responses. *Comp Physiol* (2014) 4:851–87. doi:10.1002/cphy.c130041
- Wallin BG, Charkoudian N. Sympathetic neural control of integrated cardiovascular function: insights from measurement of human sympathetic nerve activity. *Muscle Nerve* (2007) 36:595–614. doi:10.1002/mus.20831
- Wallin BG. Regulation of sympathetic nerve traffic to skeletal muscle in resting humans. *Clin Auton Res* (2006) 16:262–9. doi:10.1007/s10286-006-0357-0
- Costa F, Lavin P, Robertson D, Biaggioni I. Effect of neurovestibular stimulation on autonomic regulation. *Clin Auton Res* (1995) 5:289–93. doi:10.1007/BF01818894
- Cui J, Iwase S, Mano T, Kitazawa H. Responses of sympathetic outflow to skin during caloric stimulation in humans. *Am J Physiol Regul Integr Comp Physiol* (1999) 276:738–44.
- Cui J, Mukai C, Iwase S, Sawasaki N, Kitazawa H, Mano T, et al. Response to vestibular stimulation of sympathetic outflow to muscle in humans. *J Auton Nerv Syst* (1997) 66:154–62. doi:10.1016/S0165-1838(97)00077-5
- Carter JR, Ray CA. Sympathetic responses to vestibular activation in humans. *Am J Physiol Regul Integr Comp Physiol* (2008) 294:681–8. doi:10.1152/ajpregu.00896.2007
- Ray CA, Hume KM, Steele SL. Sympathetic nerve activity during natural stimulation of horizontal semicircular canals in humans. *Am J Physiol Regul Integr Comp Physiol* (1998) 275:1274–8.
- Wilson TE, Kuipers NT, McHugh EA, Ray CA. Vestibular activation does not influence skin sympathetic nerve responses during whole body heating. *J Appl Physiol* (2004) 97:540–4. doi:10.1152/japplphysiol.00174.2004
- Yates BJ, Miller AD. Properties of sympathetic reflexes elicited by natural vestibular stimulation: implications for cardiovascular control. *J Neurophysiol* (1994) 71:2087–92.
- Essandoh LK, Duprez DA, Shepherd JT. Reflex constriction of human resistance vessels to head-down neck flexion. *Am J Physiol* (1988) 64:767–70.
- Normand H, Etard O, Denise P. Otolithic and tonic neck receptors control of limb blood flow in humans. *J Appl Physiol* (1997) 82:1734–8.
- Shortt TL, Ray CA. Sympathetic and vascular responses to head-down neck flexion in humans. *Am J Physiol Heart Circ Physiol* (1997) 272:1780–4.
- Ray CA, Hume KM, Shortt TL. Skin sympathetic outflow during head-down neck flexion in humans. *Am J Physiol Regul Integr Comp Physiol* (1997) 273:1142–6. doi:10.1113/jphysiol.2011.214528
- Hume KM, Ray CA. Sympathetic responses to head-down rotations in humans. *J Appl Physiol* (1999) 86:1971–6.
- Monahan KD, Ray CA. Limb neurovascular control during altered otolithic input in humans. *J Physiol* (2002) 538:303–8. doi:10.1113/jphysiol.2001.013131
- Monahan KD, Ray CA. Vestibulosympathetic reflex during orthostatic challenge in aging humans. *Am J Physiol Regul Integr Comp Physiol* (2002) 283:R1027–32. doi:10.1152/ajpregu.00298.2002
- Kerman IA, Yates BJ, McAllen RM. Anatomic patterning in the expression of vestibulosympathetic reflexes. *Am J Physiol Regul Integr Comp Physiol* (2000) 279:109–17.
- Wilson TD, Cotter LA, Draper JA, Misra SP, Rice CD, Cass SP, et al. Vestibular inputs elicit patterned changes in limb blood flow in conscious cats. *J Physiol* (2006) 575:671–84. doi:10.1113/jphysiol.2006.112904
- Yavorcik KJ, Reighard DA, Misra SP, Cotter LA, Cass SP, Wilson TD, et al. Effects of postural changes and removal of vestibular inputs on blood flow to and from the hindlimb of conscious felines. *Am J Physiol Regul Integr Comp Physiol* (2009) 297:R1777–84. doi:10.1152/ajpregu.00551.2009
- Bolton PS, Ray CA. Neck afferent involvement in cardiovascular control during movement. *Brain Res Bull* (2000) 53:45–9. doi:10.1016/S0361-9230(00)00307-5
- Benson AJ, Bodin MA. Interaction of linear and angular accelerations on vestibular receptors in man. *Aerospace Med* (1966) 37:144–54.
- Guedry FE Jr. Orientation of the rotation-axis relative to gravity: its influence on nystagmus and the sensation of rotation. *Acta Otolaryngol* (1965) 60:30–48. doi:10.3109/00016486509126986
- Angelaki DE, Hess BJ. Three-dimensional organization of otolith-ocular reflexes in rhesus monkeys. I. Linear acceleration responses during off-vertical axis rotation. *J Neurophysiol* (1996) 75:2405–24.
- Clement G, Wood SJ. Translational otolith-ocular reflex during off-vertical axis rotation in humans. *Neurosci Lett* (2016) 616:65–9. doi:10.1016/j.neulet.2016.01.049
- Barmack NH. Central vestibular system: vestibular nuclei and posterior cerebellum. *Brain Res Bull* (2003) 60:511–41. doi:10.1016/S0361-9230(03)00055-8
- Yates BJ, Bronstein AM. The effects of vestibular system lesions on autonomic regulation: observations, mechanisms and clinical implications. *J Vestib Res* (2005) 15:119–29.
- Fagioli J, Wallin BG. Sympathetic reflex latencies and conduction velocities in normal man. *J Neurosci* (1980) 47:433–48. doi:10.1016/0022-510X(80)90099-4
- Hallgren E, Migeotte PF, Kornilova L, Delière Q, Fransen E, Glukhikh D, et al. Dysfunctional vestibular system causes a blood pressure drop on astronauts returning from space. *Sci Rep* (2015) 5:17627. doi:10.1038/srep17627
- Kaufmann H, Biaggioni I, Voustianiouk A, Diedrich A, Costa F, Clarke R, et al. Vestibular control of sympathetic activity. An otolith-sympathetic reflex in humans. *Exp Brain Res* (2002) 143:463–9. doi:10.1007/s00221-002-1002-3
- Cathers I, Day BL, Fitzpatrick RC. Otolith and canal reflexes in human standing. *J Physiol* (2005) 563:229–34. doi:10.1113/jphysiol.2004.079525
- Fitzpatrick RC, Butler JE, Day BL. Resolving head rotation for human bipedalism. *Curr Biol* (2006) 16:1509–14. doi:10.1016/j.cub.2006.05.063
- Goldberg JM, Smith CE, Fernandez C. Relation between discharge regularity and responses to externally applied galvanic currents in vestibular nerve afferents of the squirrel monkey. *J Neurophysiol* (1984) 51:1236–56.
- Minor LB, Goldberg JM. Vestibular-nerve inputs to the vestibulo-ocular reflex: a functional-ablation study in the squirrel monkey. *J Neurosci* (1991) 11:1636–48.
- Fitzpatrick RC, Day BL. Probing the human vestibular system with galvanic stimulation. *J Appl Physiol* (2004) 96:2301–16. doi:10.1152/japplphysiol.00008.2004
- Cohen B, Yakushin SB, Holstein GR. What does galvanic vestibular stimulation actually activate: response. *Front Neurol* (2012) 3:148. doi:10.3389/fneur.2012.000148
- Cohen B, Martinelli GP, Raphan T, Schaffner A, Xiang Y, Holstein GR, et al. The vasovagal response of the rat: its relation to the vestibulosympathetic reflex and to Mayer waves. *FASEB J* (2013) 27:2564–72. doi:10.1096/fj.12-226381
- Holstein GR, Friedrich VL Jr, Martinelli GP, Ogorodnikov D, Yakushin SB, Cohen B. Fos expression in neurons of the rat vestibulo-autonomic pathway activated by sinusoidal galvanic vestibular stimulation. *Front Neurol* (2012) 3:4. doi:10.3389/fneur.2012.00004
- Bolton PS, Wardman DL, Macefield VG. Absence of short-term vestibular modulation of muscle sympathetic outflow, assessed by brief galvanic vestibular stimulation in awake human subjects. *Exp Brain Res* (2004) 154:39–43. doi:10.1007/s00221-003-1631-1
- Voustianiouk A, Kaufmann H, Diedrich A, Raphan T, Biaggioni I, Macdougall H, et al. Electrical activation of the human vestibulo-sympathetic reflex. *Exp Brain Res* (2006) 171:251–61. doi:10.1007/s00221-005-0266-9
- Ishikawa T, Miyazawa T. Sympathetic responses evoked by vestibular stimulation and their interactions with somato-sympathetic reflexes. *J Auton Nerv Syst* (1980) 1:243–54. doi:10.1016/0165-1838(80)90020-X
- Kerman IA, Emanuel BA, Yates BJ. Vestibular stimulation leads to distinct hemodynamic patterning. *Am J Physiol Regul Integr Comp Physiol* (2000) 279:R118–25.

FUNDING

This work was supported by the Australian Research Council (DP 1096179).

45. Uchino Y, Kudo N, Tsuda K, Iwamura Y. Vestibular inhibition of sympathetic nerve activities. *Brain Res* (1970) 22:195–206. doi:10.1016/0006-8993(70)90004-1
46. Bent L, Bolton PS, Macefield VG. Modulation of muscle sympathetic bursts by sinusoidal galvanic vestibular stimulation in human subjects. *Exp Brain Res* (2006) 174:701–11. doi:10.1007/s00221-006-0515-6
47. Macefield VG, James C. Super entrainment of muscle sympathetic nerve activity during sinusoidal galvanic vestibular stimulation. *J Neurophysiol* (2016) 116:2689–94. doi:10.1152/jn.00036.2016
48. Grewal T, James C, Macefield VG. Frequency-dependent modulation of muscle sympathetic nerve activity by sinusoidal galvanic vestibular stimulation in human subjects. *Exp Brain Res* (2009) 197:379–86. doi:10.1007/s00221-009-1926-y
49. James C, Stathis A, Macefield VG. Vestibular and pulse-related modulation of skin sympathetic nerve activity during sinusoidal galvanic vestibular stimulation in human subjects. *Exp Brain Res* (2010) 202:291–8. doi:10.1007/s00221-009-2131-8
50. James C, Macefield VG. Competitive interactions between vestibular and cardiac rhythms in the modulation of muscle sympathetic nerve activity. *Auton Neurosci* (2010) 158:127–31. doi:10.1016/j.autneu.2010.07.005
51. Hammam E, James C, Dawood T, Macefield VG. Low-frequency sinusoidal galvanic stimulation of the left and right vestibular nerves reveals two peaks of modulation in muscle sympathetic nerve activity. *Exp Brain Res* (2011) 213:507–14. doi:10.1007/s00221-011-2800-2
52. Hammam E, Dawood T, Macefield VG. Low-frequency galvanic vestibular stimulation evokes two peaks of modulation in skin sympathetic nerve activity. *Exp Brain Res* (2012) 219:441–6. doi:10.1007/s00221-012-3090-z
53. Klingberg D, Hammam E, Macefield VG. Motion sickness is associated with an increase in vestibular modulation of skin but not muscle sympathetic nerve activity. *Exp Brain Res* (2015) 233:2433–40. doi:10.1007/s00221-015-4313-x
54. Dampney RAL, Polson JW, Potts PD, Hirooka Y, Horiuchi J. Functional organization of brain pathways subserving the baroreceptor reflex: studies in conscious animals using immediate early gene expression. *Cell Mol Neurobiol* (2003) 23:597–616. doi:10.1023/A:1025080314925
55. Dampney RAL, Horiuchi J, Tagawa T, Fontes MAP, Potts PD, Polson JW. Medullary and supramedullary mechanisms regulating sympathetic vasomotor tone. *Acta Physiol Scand* (2003) 177:209–18. doi:10.1046/j.1365-201X.2003.01070.x
56. Yates BJ, Goto T, Bolton PS. Responses of neurons in the rostral ventrolateral medulla of the cat to natural vestibular stimulation. *Brain Res* (1993) 601:255–64. doi:10.1016/0006-8993(93)91718-8
57. Yates BJ, Yamagata Y, Bolton PS. The ventrolateral medulla of the cat mediates vestibulosympathetic reflexes. *Brain Res* (1991) 552:265–72. doi:10.1016/0006-8993(91)90091-9
58. El Sayed K, Dawood T, Hammam E, Macefield VG. Evidence from bilateral recordings of sympathetic nerve activity for lateralisation of vestibular contributions to cardiovascular control. *Exp Brain Res* (2012) 221:427–36. doi:10.1007/s00221-012-3185-6
59. Sundlof G, Wallin BG. The variability of muscle nerve sympathetic activity in resting recumbent man. *J Physiol* (1977) 272:383–97. doi:10.1113/jphysiol.1977.sp012050
60. Svarteborg YB, Rundqvist B, Elam M. Relative burst amplitude in human muscle sympathetic nerve activity: a sensitive indicator of altered sympathetic traffic. *Clin Auton Res* (1998) 8:95–100. doi:10.1007/BF02267819
61. Bini G, Hagbarth KE, Wallin BG. Cardiac rhythmicity of skin sympathetic activity recorded from peripheral nerves in man. *J Auton Nerv Syst* (1981) 4:17–24. doi:10.1016/0165-1838(81)90003-5
62. Diedrich A, Porta A, Baribe F, Brychta RJ, Bonizzi P, Diedrich L, et al. Lateralization of expression of neural sympathetic activity to the vessels and effects of carotid baroreceptor stimulation. *Am J Physiol Heart Circ Physiol* (2009) 296:H1758–65. doi:10.1152/ajpheart.01045.2008
63. Yates BJ, Aoki M, Burchill P, Bronstein AM, Gresty MA. Cardiovascular responses elicited by linear acceleration in humans. *Exp Brain Res* (1999) 125:476–84. doi:10.1007/s002210050705
64. Jauregui-Renaud K, Reynolds R, Bronstein AM, Gresty MA. Cardiorespiratory responses evoked by transient linear acceleration. *Aviat Space Environ Med* (2006) 77:114–20.
65. Jauregui-Renaud K, Hermosillo AG, Gomez A, Marquez MF, Cardenas M, Bronstein AM. Vestibular function interferes in cardiovascular reflexes. *Arch Med Res* (2003) 34:200–4. doi:10.1016/S0188-4409(03)00023-7
66. Jauregui-Renaud K, Aw ST, Todd MJ, McGarvie LA, Halmagyi GM. Benign paroxysmal positional vertigo can interfere with the cardiac response to head-down tilt. *Otol Neurotol* (2005) 26:484–8. doi:10.1097/01.mao.0000169783.76964.f6
67. Radtke A, Popov K, Bronstein AM, Gresty MA. Evidence for a vestibulo-cardiac reflex in man. *Lancet* (2000) 356:736–7. doi:10.1016/S0140-6736(00)02635-0
68. Radtke A, Popov K, Bronstein AM, Gresty MA. Vestibulo-autonomic control in man: short and long-latency vestibular effects on cardiovascular function. *J Vestib Res* (2003) 13:25–37.
69. Cui J, Iwase S, Mano T, Katayama N, Mori S. Muscle sympathetic outflow during horizontal linear acceleration in humans. *Am J Physiol Regul Integr Comp Physiol* (2001) 281:R625–34.
70. Cui J, Iwase S, Mano T, Katayama N, Mori S. Sympathetic nerve response to muscle during anteroposterior acceleration in humans. *Environ Med* (1998) 42:71–5.
71. Grewal T, Dawood T, Hammam E, Kwok K, Macefield VG. Low-frequency physiological activation of the vestibular utricle causes biphasic modulation of skin sympathetic nerve activity in humans. *Exp Brain Res* (2012) 220:101–8. doi:10.1007/s00221-012-3118-4
72. Hammam E, Kwok K, Macefield VG. Modulation of muscle sympathetic nerve activity by low-frequency physiological activation of the vestibular utricle in awake humans. *Exp Brain Res* (2013) 230:137–42. doi:10.1007/s00221-013-3637-7
73. Fatouleh R, Macefield VG. Cardiorespiratory coupling of sympathetic outflow in humans: a comparison of respiratory and cardiac modulation of sympathetic nerve activity to skin and muscle. *Exp Physiol* (2013) 98:1327–36. doi:10.1113/expphysiol.2013.072421
74. Hammam E, Chui LVH, Wong KS, Kwok K, Macefield VG. Vestibular modulation of muscle sympathetic nerve activity by the utricle during sub-perceptual sinusoidal linear acceleration in humans. *Exp Brain Res* (2014) 232:1379–88. doi:10.1007/s00221-014-3856-6
75. Fernández C, Goldberg JM. Physiology of peripheral neurons innervating otolith organs of the squirrel monkey. II. Directional selectivity and force-response relations. *J Neurophysiol* (1976) 39:985–95.
76. Wang W, Han HY, Zucker IH. Depressed baroreflex in heart failure is not due to structural change in carotid sinus nerve fibers. *J Auton Nerv Syst* (1996) 57:101–8. doi:10.1016/0165-1838(95)00107-7
77. Hargens AR, Richardson S. Cardiovascular adaptions, fluid shifts and countermeasures related to space flight. *Respir Physiol Neurobiol* (2009) 169:S30–3. doi:10.1016/j.resp.2009.07.005
78. Hinghofer-Szalkay H. Gravity, the hydrostatic indifference concept and the cardiovascular system. *Eur J Appl Physiol* (2011) 111:163–74. doi:10.1007/s00421-010-1646-9
79. Bolton PS, Hammam E, Macefield VG. Neck proprioceptors contribute to the modulation of muscle sympathetic nerve activity to the lower limbs of humans. *Exp Brain Res* (2014) 232(7):2263–71. doi:10.1007/s00221-014-3917-x
80. Ray CA, Hume KM. Neck afferents and muscle sympathetic activity in humans: implications for the vestibulosympathetic reflex. *J Appl Physiol* (1998) 84:450–3.
81. Voustianiouk A, Diedrich A, Ogorodnikou D, MacDougall H, Raphan T, Biaggioni I, et al. Vestibular activation of human sympathetic activity: the Vestibulo-Sympathetic reflex (VSR). *Neurology* (2005) 64(6):168–168.
82. Yates BJ, Stocker SD. Integration of somatic and visceral inputs by the brainstem: functional considerations. *Exp Brain Res* (1998) 119:269–75. doi:10.1007/s002210050342
83. Yates BJ, Miller DM. Integration of nonlabyrinthine inputs by the vestibular system: role in compensation following bilateral damage to the inner ear. *J Vestib Res* (2009) 19:183–9.
84. DeStefino VJ, Reighard DA, Sugiyama Y, Suzuki T, Cotter LA, Larson MG, et al. Response of neurons in the rostral ventrolateral medulla to whole body rotations: comparisons in decerebrate and conscious cats. *J Appl Physiol* (2011) 110:1699–707. doi:10.1152/japplphysiol.00180.2011

85. Yates BJ. Vestibular influences on the autonomic nervous system. *Ann N Y Acad Sci* (1996) 781:458–73. doi:10.1111/j.1749-6632.1996.tb15720.x
86. Richmond FJ, Abrahams VC. Physiological properties of muscle spindles in dorsal neck muscles of the cat. *J Neurophysiol* (1979) 42:604–17.
87. Kasper J, Schor RH, Wilson VJ. Response of vestibular neurons to head rotations in vertical planes. II. Response to neck stimulation and vestibular-neck interaction. *J Neurophysiol* (1988) 60:1765–78.
88. Neuhuber WL, Zenker W. Central distribution of cervical primary afferents in the rat, with emphasis on proprioceptive projections to vestibular, perihypoglossal, and upper thoracic spinal nuclei. *J Comp Neurol* (1989) 280:231–53. doi:10.1002/cne.902800206
89. Bolton PS, Kerman IA, Woodring SF, Yates BJ. Influences of neck afferents on sympathetic and respiratory nerve activity. *Brain Res Bull* (1998) 47:413–9. doi:10.1016/S0361-9230(98)00094-X
90. Krecinic T, Mattace-Raso F, Van Der Velde N, Pereira G, Van Der Cammen T. Orthostatic hypotension in older persons: a diagnostic algorithm. *J Nutr Health Aging* (2009) 13:572–5. doi:10.1007/s12603-009-0109-7

Conflict of Interest Statement: The authors declare that the research was conducted in the absence of any commercial or financial relationships that could be construed as a potential conflict of interest.

Copyright © 2017 Hammam and Macefield. This is an open-access article distributed under the terms of the Creative Commons Attribution License (CC BY). The use, distribution or reproduction in other forums is permitted, provided the original author(s) or licensor are credited and that the original publication in this journal is cited, in accordance with accepted academic practice. No use, distribution or reproduction is permitted which does not comply with these terms.



Vestibular Activation Habituates the Vasovagal Response in the Rat

Bernard Cohen^{1*}, Giorgio P. Martinelli¹, Yongqing Xiang², Theodore Raphan² and Sergei B. Yakushin¹

¹Department of Neurology, Icahn School of Medicine at Mount Sinai, New York, NY, USA, ²Department of Computer and Information Science, Brooklyn College, City University of New York, New York, NY, USA

OPEN ACCESS

Edited by:

Michael Strupp,
Ludwig-Maximilians-Universität
München, Germany

Reviewed by:

Seong-Hae Jeong,
Chungnam National University,
South Korea
Yi-Ho Young,
National Taiwan University, Taiwan

***Correspondence:**

Bernard Cohen
bernard.cohen@mssm.edu

Specialty section:

This article was submitted to
Neuro-otology,
a section of the journal
Frontiers in Neurology

Received: 02 November 2016

Accepted: 24 February 2017

Published: 15 March 2017

Citation:

Cohen B, Martinelli GP, Xiang Y, Raphan T and Yakushin SB (2017)

Vestibular Activation Habituates the
Vasovagal Response in the Rat.

Front. Neurol. 8:83.

doi: 10.3389/fneur.2017.00083

Vasovagal syncope is a significant medical problem without effective therapy, postulated to be related to a collapse of baroreflex function. While some studies have shown that repeated static tilts can block vasovagal syncope, this was not found in other studies. Using anesthetized, male Long-Evans rats that were highly susceptible to generation of vasovagal responses, we found that repeated activation of the vestibulosympathetic reflex (VSR) with ± 2 and ± 3 mA, 0.025 Hz sinusoidal galvanic vestibular stimulation (sGVS) caused incremental changes in blood pressure (BP) and heart rate (HR) that blocked further generation of vasovagal responses. Initially, BP and HR fell \approx 20–50 mmHg and \approx 20–50 beats/min (bpm) into a vasovagal response when stimulated with SgVS in susceptible rats. As the rats were continually stimulated, HR initially rose to counteract the fall in BP; then the increase in HR became more substantial and long lasting, effectively opposing the fall in BP. Finally, the vestibular stimuli simply caused an increase in BP, the normal sequence following activation of the VSR. Concurrently, habituation caused disappearance of the low-frequency (0.025 and 0.05 Hz) oscillations in BP and HR that must be present when vasovagal responses are induced. Habituation also produced significant increases in baroreflex sensitivity ($p < 0.001$). Thus, repeated low-frequency activation of the VSR resulted in a reduction and loss of susceptibility to development of vasovagal responses in rats that were previously highly susceptible. We posit that reactivation of the baroreflex, which is depressed by anesthesia and the disappearance of low-frequency oscillations in BP and HR are likely to be critically involved in producing resistance to the development of vasovagal responses. SGVS has been widely used to activate muscle sympathetic nerve activity in humans and is safe and well tolerated. Potentially, it could be used to produce similar habituation of vasovagal syncope in humans.

Keywords: baroreflex sensitivity, head-up tilt, sinusoidal galvanic vestibular stimulation, vestibulosympathetic reflex, vasovagal syncope

Abbreviations: BP, arterial blood pressure; bpm, heart in beats per minute; CVLM, caudal ventral lateral medulla; g, imputed acceleration of gravity; HR, heart rate; MSNA, muscle sympathetic nerve activity; NTS, nucleus tractus solitarius; RVLM, rostral ventral lateral medulla; sGVS, sinusoidal Galvanic Vestibular Stimulation; VSR, vestibulosympathetic reflex; \approx , approximate; $^\circ$, degrees.

DEFINITIONS

Habituation: “A behavioral response decrement that results from repeated stimulation and that does not involve sensory adaptation/sensory fatigue or motor fatigue” (1, 2). **Susceptible Rats:** rats that readily had vasovagal responses from vestibular (otolith) stimulation. **Vasovagal Response:** a combined fall in blood pressure (BP) of $\approx 20\text{--}50$ mmHg and $\approx 20\text{--}50$ bpm that takes seconds to develop and is followed by a slower return to baseline levels over the course of minutes. **Vasovagal Syncope:** a loss of consciousness due to a decrease in BP and heart rate (HR) causing a loss of blood flow to the brain. **Syncope:** fainting, loss of consciousness—old English, without cause.

INTRODUCTION

Vasovagal syncope is a significant medical problem (3–6). The symptoms that lead to vasovagal syncope and the preceding vasovagal response that underlies syncope have been well described (5, 7, 8), and the reductions in blood pressure (BP), heart rate (HR), and baroreflex sensitivity associated with syncope are also known (7, 9–11). Using combined tilt and lower body negative pressure, as BP fell, HR transiently increased but then also collapsed in the pre-syncopal state (7). A critical observation was that the vasovagal response and vasovagal syncope involved a reduction in baroreflex sensitivity (7, 10, 12, 13). As yet, neither is it known why this occurs nor is it apparent where and what the signal might be that initiates the combined fall in BP and HR. A model of the vasovagal response has suggested, however, that a fall in desired BP could be the critical signal that initiates the combined fall in BP and HR (14). Where such a signal would arise and how it is transmitted is still unknown. Consequently, there has been no effective therapy for vasovagal syncope.

Therapeutic measures for unexpected syncope have included beta blockers, corticosteroids, and pacemakers (5, 8, 15), but none of these has been generally more effective than placebo (8, 16). An apparently promising therapy in which “syncope-sensitive” patients were repetitively tilted 60° for prolonged periods was originally shown to habituate the vestibulosympathetic reflex (VSR) and to reduce or abolish syncope (17–21). These studies used repeated episodes of 60° static head-up tilt or standing against a wall for substantial periods of time that activated otolith and body tilt receptors (22–24), both of which play a role in producing cardiovascular changes through the VSR in humans (25–29). In fact, 60° head-up tilt is widely used to determine if humans suspected of having vasovagal syncope become faint during the tilt-test. Sustained habituation of syncope was not found in other studies that utilized tilt training (30, 31). Foglia-Manzillo speculated that while it was probably possible to habituate some subjects with prolonged bouts of static head-up tilt, the habituation techniques were too tedious to be effective in the general population (30). If a less tedious procedure that activated the vestibular system were to be devised, it could be used to habituate syncope through the VSR.

Recently, we developed a small animal model of the cardiovascular changes during vasovagal responses in the anesthetized rat

(14, 32–35). In these studies, susceptible rats readily developed synchronous $\approx 20\text{--}50$ mmHg decreases in BP and $\approx 20\text{--}50$ bpm decreases in HR over seconds that recovered slowly over minutes in response to repeated vestibular (otolith) stimulation, i.e., to sGVS and 70° nose-up tilt. The sudden decreases in BP and HR and the slower return to pre-stimulus values are the essential components of the vasovagal response that underlie and generate vasovagal syncope (7, 9–11, 36). A wide range of vestibular stimuli that activate the otolith system are capable of inducing vasovagal responses (32–34). These include ± 2 and ± 3 mA, 0.025 and 0.05 Hz sinusoidal galvanic vestibular stimulation (sGVS), translation while rotating, $\pm 70^\circ$ oscillation in pitch, and 70° head-up tilt (32–34). Specific frequencies were critical for the generation of vasovagal responses, namely, vasovagal responses were only induced with low-frequency stimulations (0.025 and 0.05 Hz sGVS) and stimulus currents of ± 2 and ± 3 mA (33, 34). Moreover, vasovagal responses were only induced when there were 0.025 and 0.05 Hz oscillations in BP and HR (33, 34).

A striking finding in the previous experiments was that rats that were initially susceptible to the induction of vasovagal responses progressively lost their susceptibility as testing continued in the experiments that formed the basis for three papers that were previously reported (32–34). None of these rats had an increase in susceptibility when tested regularly; although, cessation of testing for prolonged periods could result in transient increases in susceptibility. However, when these animals were stimulated again, such increased sensitivity quickly disappeared. This loss of susceptibility to vasovagal responses suggests that the rats were becoming progressively habituated by the recurrent stimulation of the vestibular (otolith) system through activation of the VSR, i.e., they had met the classic criteria for habituation as defined by Rankin and Thompson: “Habituation is defined as a behavioral response decrement that results from repeated stimulation and that does not involve sensory adaptation/sensory fatigue or motor fatigue” (1, 2).

Thus, the first objective of the present study was to document the loss of sensitivity through a more detailed study of animals that were initially susceptible to the induction of vasovagal responses but became habituated when repeatedly given stimuli that excited the VSR. Additionally, we intended to show the various stages that were involved in the habituation, i.e., the specific changes in BP and HR that occurred as the rats became insensitive to development of vasovagal responses, since, to our knowledge, this has not been described before.

A second goal was to determine whether both ± 2 and ± 3 mA sGVS produced habituation of vasovagal responses. The ± 2 mA sGVS has been widely used to study muscle sympathetic nerve activity (MSNA) in humans. The sGVS used to generate MSNA is safe and does not have significant side effects other than mild nausea in some subjects (37–40). Thus, if effective, ± 2 mA sGVS could potentially be used to induce habituation and reduce susceptibility to vasovagal syncope in humans.

Since vasovagal responses and vasovagal syncope are associated with a reduction in baroreflex sensitivity (7, 10), the third goal of this study was to determine whether the habituation that had been observed as a result of vestibular stimulation was also associated with a change in baroreflex

sensitivity. Finally, we intended to determine whether the low-frequency activity, which is critically associated with production of vasovagal responses, would be affected by the habituation process (33, 34, 36).

MATERIALS AND METHODS

Animals

Eleven adult, male, Long-Evans rats (Harlan Laboratories, MA, USA) weighing between 400 and 500 g were used in this study. These rats were selected for their susceptibility to the development of vasovagal responses when stimulated with ± 2 and ± 3 mA, 0.025 Hz sGVS; 70° nose-up tilts (0.91 g); and $\pm 70^\circ$ oscillation in pitch (± 0.91 g). Results of experiments in seven of these rats have been reported in previous publications (14, 32–35). However, in these studies, we did not address the change in susceptibility produced by repeated vestibular stimulation. Four other rats (R009, R011, R012, and R020), that were also highly susceptible to the generation of vasovagal responses, were used in this study to characterize the changes in BP and HR associated with habituation of vasovagal responses. All experiments were approved by the Institutional Animal Care and Use Committee of the Icahn School of Medicine at Mount Sinai.

Surgical Procedures, Implantation of a DSI Telemetric Sensor (St. Paul, MN, USA)

Surgery and testing were conducted under isoflurane anesthesia (4% induction, 2% maintenance with oxygen). Rats were prepared for aseptic surgery, and normothermia was maintained during and after surgery by keeping the animals on an Isotherm heating pad regulated by the feedback from a rectal thermometer. A telemetric BP sensor (DSI, St. Paul, MN, USA) was implanted in the abdominal aorta during aseptic surgery. The femoral artery, which was exposed through a small incision in the inguinal area, was dissected from the surrounding tissue, mobilized, and temporarily occluded. After dilating the vessel with a drop of lidocaine, the transmitter catheter was inserted into the vessel *via* a partial transverse arteriotomy. After releasing the occluding ligature, the catheter was gently threaded into the abdominal aorta and secured in place with two ligatures around the femoral artery. The body of the transmitter was placed in the flank of the rat in a subcutaneous pocket sealed with a purse-string suture. The skin was closed with surgical clips. Surgical pain was managed with pre-emptive and post-operative administration of Buprenorphine (0.05 mg/kg, SQ BID for 72 h). The animals were allowed a 7- to 10-day recovery period before being used in experiments.

During experiments, the animals were anesthetized with isoflurane (4% induction, and 2% maintenance with oxygen) and kept on a heating pad (27, 28, 32–34). The sinusoidal galvanic vestibular stimulation (sGVS) was generated by a computer-controlled stimulator (32–34, 41, 42). Currents were delivered *via* sub-dermal needle electrodes placed in the skin over the mastoids. Rats were also subjected to a tilt-test, i.e., a 70° nose-up (0.91 g) change in position using a computer-controlled tilt table.

Habituation Protocol

Four susceptible rats (R009, R011, R012, and R020) were studied intensively. After initial testing, they were trained for 5 days with recurrent sGVS over 2 weeks with three, 30 min epochs of ± 2 mA, 0.025 Hz sGVS (R009) or ± 3 mA, 0.025 Hz sGVS (R011, R012, and R020) on each day. The rats were in the prone position under anesthesia while they were receiving the sGVS. HR and BP were recorded, and the rats were tested with 70° head-up tilt before and after each period of habituation. Each of the four susceptible animals that were habituated had a vasovagal response to each stimulus when initially tested. Each experimental session began with a 45-min test period, followed by three alternating habituation and test periods. If there was no response to the head-up tilt, 15 min were allowed to elapse before the next habituation sequence began. If a vasovagal response was induced, 30 min were allowed to elapse before the next habituation sequence.

Measurement of BP and HR

Intra-aortic BP telemetric data were continuously captured by a wand receiver (DSI, St. Paul, MN, USA) placed in close proximity to the animals, and BP and HR were recorded. The BP and HR, as well as the position of the tilt table and the current levels of sGVS were sampled at 1 kHz with 12 bit resolution (Data Translation, Inc., Marlborough, MA, USA). HR was computed offline from the systolic peaks in the BP. It was converted to an analog signal in beats per minute (bpm). BP was derived from systoles and diastoles, and mean BP was also calculated. When they were compared, there was no substantial difference between them. Therefore, the BP in this report is an estimate of averaged systolic BP, but reflects both mean and diastolic BP. Because measurements of BP were dependent on the occurrence of systoles, which occurred on average at about 300–330 bpm, the effective sampling rate for the BP derived from the systoles was limited to ≈ 1 sample/200 ms, i.e., 5 samples/s. Low-frequency oscillations in BP and HR (0.025 and 0.05 Hz), which are active during vasovagal responses (34) were also monitored (see Wavelet Analysis).

Measurement of Baroreflex Sensitivity

Twenty seconds of BP signal before the onset of the sGVS were used to calculate the baroreflex sensitivity. A peak finding algorithm identified each systolic/diastolic cycle. The time durations between two systolic peaks ($systBP_i$ and $systBP_{i+1}$) or the RR-interval, were plotted against the first systolic peak ($systBP_i$). The slope of the linear regression was defined as the baroreflex sensitivity, i.e., the ratio between the change of the RR-interval and the change of systolic BP.

Phase Plots

The temporal sequence of the changes in BP and HR induced by sGVS from the beginning of the habituation process to its end were determined in a typical rat (R009). This animal, which was initially susceptible to generation of vasovagal responses, became progressively resistant as it became habituated. BP was plotted against HR in response to single trains of sGVS from the end of the train until the resting BP was reached. From this, it was

possible to determine how the direction and magnitude of the modulations in BP and HR were altered during the habituation process. The data were fitted with a least squares regression, and the slopes were plotted sequentially from the beginning of testing until the end of habituation. This involved 33 tests over the 10 habituation sessions in this rat. These data are presented in Figures 5 and 6.

Wavelet Analysis

The time-frequency characteristics of BP and HR functions were studied using a discrete wavelet analysis. This identified the contribution of particular bands of frequencies as a function of the time domain. The 0.025 Hz sGVS stimulus was confined to single bands of frequencies in the wavelet decompositions that were verified in previous studies (26, 33, 34). The signal was resampled so that its frequency was in the center of a band whose upper frequency limit was $\sqrt{2} * \text{stim_freq}$ and the lower frequency limit was $\text{stim_freq}/\sqrt{2}$. Because the vagovagal oscillation range was 0–0.2 Hz (34), only four low-frequency bands were analyzed in this study. Activity in Band 12, i.e., in an approximation band at 0–0.018 Hz, indicated that a transient response was induced, i.e., the low-frequency combined fall and return of BP and HR that constitute a vagovagal response (32). The other three bands were Band 11 (0.018–0.035 Hz), Band 10 (0.035–0.071 Hz), and Band 9 (0.071–0.141 Hz). Activity in Band 8 (0.141–0.282 Hz) and Band 7 (0.282–0.564 Hz) was minimal in previous experiments (26, 33, 34). In the experiments in this paper, the stimulus frequency was confined to Band 11, while adjacent bands (Bands 10 and 9) incorporated the second and fourth harmonics of stimulation, centered at twice and four times the stimulus frequency. The distribution of power in each frequency band comprising the signal was used as a metric for determining how the stimulus had generated the harmonics, and was used as a basis for comparing the response to different stimuli and to the same stimuli at different points in the experimental protocol. The power of each frequency band was computed as the average energy of the signal when it was reconstructed from frequency components in the band, calculated by $(\text{signal}^2/\text{time})$. Each sample lasted 400 s and the original sampling interval was 16 ms to remove frequencies above 36.2 Hz, which were outside the range of interest. Using resampling and the db12 wavelet, the leakage from the band associated with the stimulus frequency to other bands was less than 5%, and a sinusoid at a single frequency had all of its energy in a single band of frequencies. The analysis was performed using Matlab (Mathworks, Inc., Natick, MA, USA). Standard deviations of wavelet-filtered responses for each frequency band were computed in order to compare results of wavelet decomposition of different data sets.

Statistical Analysis

Changes in BP or HR were considered to be significant if they exceeded 2 SD of the pre-stimulus data. The dominant peaks at the frequency of stimulation and twice the frequency of stimulation were compared statistically using a Student's paired *t*-test or a one way ANOVA with repeated measures applying a post Bonferroni adjustment. Changes in BP and HR were deemed significant when $p < 0.05$.

RESULTS

Habituation from Repeated Testing (Unreported Data from Previous Experiments)

Our earlier studies employed single sinusoids, sGVS at different frequencies, $\pm 70^\circ$ oscillation in pitch, trains of sGVS at different frequencies from 0.2–0.25 Hz, 15–70° nose-up tilts, and translation while rotating (32). The results of these studies clearly indicated that ± 2 and ± 3 mA, 0.025 Hz sGVS and 70° nose-up tilts were potent stimuli for induction of vagovagal responses.

The rats from these studies were selected for their initial susceptibility to the development of vagovagal responses using these stimuli and for their subsequent development of resistance to such vagovagal responses or vagovagal oscillations. Because the changes in behavior were maintained between stimulation sessions, despite irregular intervals between them, we considered the stimulus sessions to be sequential and disregarded the inter-stimulus intervals in order to compare stimulation results in the individual rats. The combined results from these seven rats are described in the text (below) and included in the results shown in Figure 1C.

Results of testing in seven rats and their progressive loss of susceptibility will be considered first.

These animals were repeatedly given the various forms of vestibular stimulation outlined above, and there was a continual loss of susceptibility to the induction of vagovagal responses as testing progressed. Tests included single and multiple sinusoids, pulses, oscillations in pitch, and tilts of various amplitudes. The most productive stimuli for inducing vagovagal responses were ± 2 and ± 3 mA, 0.025 Hz sGVS; 70° head-up tilt; or $\pm 70^\circ$ oscillation in pitch (26, 33, 34).

Testing of the animals occurred between 30 and 300 days. The number of tests varied from day to day and from animal to animal in these seven initial rats. To normalize the test results, the data were labeled as being from sequential test days, regardless of the time interval between them. The total number of tests for vagovagal responses each day was calculated, and the number of positive vagovagal responses was expressed as a percentage of the number of tests. The criterion for the loss of susceptibility was a failure to generate a vagovagal response on three consecutive days despite repeated testing. When this occurred, the animal was removed from the sample and no longer tested for induction of a vagovagal response. The total number of tests for vagovagal responses for each day and the total number of positive tests in which vagovagal responses were induced were registered. Based on these criteria, the frequency of occurrence for induction of vagovagal responses on each day was calculated, and plotted as a function of testing day. With the removal of unresponsive rats, seven animals were tested on days 1–4, six on days 5–7, five on day 8, two on days 9 and 10, and only one animal on day 11. Tests for vagovagal responses were performed approximately 30 times each day on days 1–7, except for day 6 when the animals were only tested 19 times. On days 8–11 the animals were tested 16, 9, 18, and 5 times, respectively. Vagovagal responses occurred during approximately 60% of tests on days 1 and 2, 40% on days 3–5, 21% on day 6, and 40% on days 7 and 8. Only one vagovagal response

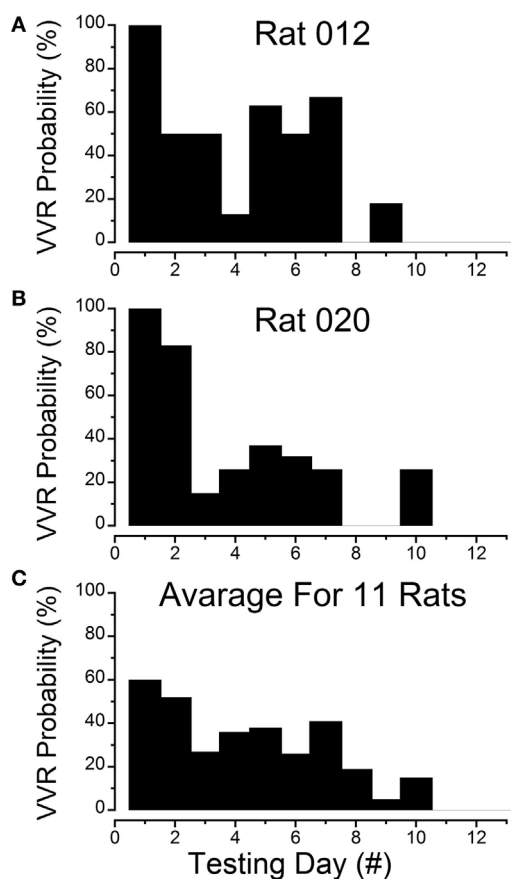


FIGURE 1 | Progressive loss of susceptibility to generation of vasovagal responses. **(A)** Incidence of generation of vasovagal responses on repeated tests for R012 with ± 3 mA, 0.025 Hz sinusoidal galvanic vestibular stimulation (sGVS) on the ordinate and sequential test days on the abscissa. The rat progressively lost its susceptibility until vasovagal responses were no longer induced by repeated testing on days 8, 10, 11, and 12. **(B)** Similar loss of susceptibility to generation of vasovagal responses for R020 induced by repeated stimulation with ± 3 mA, 0.025 Hz sGVS. The incidence of vasovagal responses fell rapidly after day 2 and they could not be induced, despite repeated testing on days 8, 9, 11, and 12. **(C)** Loss of susceptibility in the 11 rats that form the basis of this report. Of the 11, 7 rats were repeatedly stimulated with the various forms of vestibular (otolith) stimulation over extended periods in previous studies. These seven rats lost their susceptibility progressively (see text for description). Also included are four rats (R009, R011, R012, and R020) that were habituated with ± 2 and ± 3 mA, 0.025 Hz sGVS over a 2-week period. The percentage of positive responses to the multiple test stimuli of the rats in the tested sample for each day of testing is shown on the ordinate and sequential test days on the abscissa. If the original group of rats did not respond to the multiple tests for 3 consecutive test days, they were removed from the sample after the third day. Despite the different time sequences in the original and later habituation procedures, the rats successively lost their susceptibility to the generation of vasovagal responses after approximately the same number of test sessions. As in **(A,B)**, the number of susceptible rats declined steadily until none were left by the 11th day.

was induced out of 18 tests on day 10 (6%), and no vasovagal responses were induced on days 9 or 11. Thus, there was a continual loss of susceptibility to induction of vasovagal responses as testing progressed in these rats. Moreover, when a reduction in

susceptibility occurred, it was maintained until the next test date, despite differences in the intervals between tests. This implies that changes in susceptibility were held for significant periods of time.

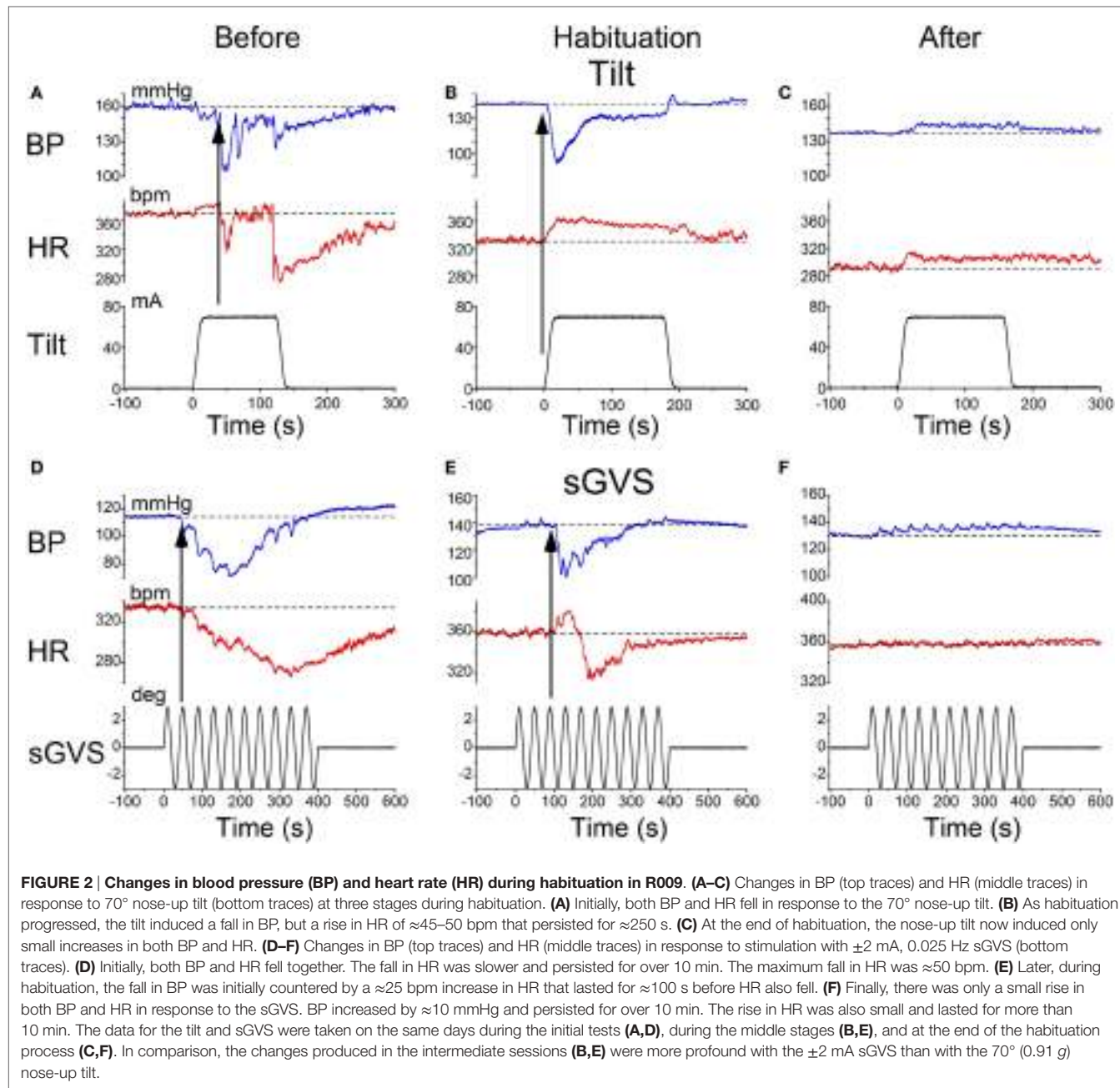
Habituation with ± 2 and ± 3 mA sGVS

Four susceptible animals were used to determine the responses to intensive stimulation with sGVS, Rats R009, R011, R012, and R020. The sequence of loss of susceptibility in R012 and R020 are shown in **Figures 1A,B**. R012 had 15 tests each day and R020 had 10 tests each day, both with ± 3 mA, 0.025 Hz sGVS. Initially, each rat had a vasovagal response to every ± 3 mA, 0.025 Hz sGVS and/or every 70° nose-up tilt on the first day that they were tested. The response to these stimuli fell rapidly, and they became unresponsive by the third day of testing. Their responsiveness increased slightly over the next 3 days, but they were unresponsive on the seventh day. They responded to $\approx 10\%$ of trials on the 8th day, and then became completely unresponsive and no longer responded from the 9th to 12th day of testing. Thus, there was a steady loss of susceptibility in these animals in response to repeated testing with sGVS and/or nose-up tilt.

The steady progression of the loss of susceptibility in R012, R020, R009, and R011 is plotted in **Figures 1A,B**, 3, 4A, 5, and 6A, and the cumulative loss of susceptibility in all 11 rats, disregarding intervals between training sessions, is plotted in **Figure 1C**. The steady decline in susceptibility was present in the whole group of 11 rats, despite the fact that the time between stimulations was different for the group of seven initial animals, and for the four rats that were more intensively stimulated. Every animal in the first group had at least one vasovagal oscillation or vasovagal response on the first day. The overall response on this day was 60%, and this responsiveness progressively fell so that there were no responders after day 10. The combined data confirm the loss of susceptibility in R009, R011, R012, and R020, but they have an additional implication. Since there were short and long periods between stimulations in the original group of seven rats, there must have been some storage of the habituation that had been attained by activation of the VSR in the original group. These data also indicate that habituation can be induced with shorter, intense periods of vestibular stimulation.

Modification of BP and HR during Habituation

Characteristic changes in BP and HR were produced by habituation in each of these rats. Here, two examples are shown. In the first, before conditioning, R009 developed a vasovagal response on each of nine tests. About 50 s after a 70° nose-up tilt, there was a drop in BP of ≈ 50 mmHg followed by a reduction in HR of ≈ 35 bpm (**Figure 2A**). The animal developed a second drop in BP and HR when it was tilted back to the nose-up position, demonstrating its susceptibility to development of vasovagal responses. In this instance, the decline in HR only slightly outlasted the decline in BP. On the same day, activation with ± 2 mA, 0.025 Hz sGVS (**Figure 2D**) also induced typical vasovagal responses ≈ 45 s after the onset of the stimulus (Upward arrow). There was a drop in BP of ≈ 50 mmHg and in HR of ≈ 50 bpm. The decline in BP lasted ≈ 300 s, and the decline in HR continued past the end of



the trace beyond 600 s (10 min). During the course of habituation, the 70° nose-up tilt again caused a \approx 35 mmHg drop in BP (**Figure 2B**), but now this was countered by an increase in HR (from 285 to 295 bpm) that lasted beyond 300 s (**Figure 2B**). The \pm 2 mA, 0.025 Hz sGVS appeared to be somewhat stronger in generating a vasovagal response and it produced a drop in BP of \approx 50 mmHg, and a drop in HR of \approx 50 bpm (**Figure 2E**). Now, however, there was an initial increase in HR of \approx 30 bpm. The HR rose to \approx 360 bpm followed by a \approx 40 bpm decline to \approx 320 bpm, which lasted \approx 1 min (**Figure 2E**). The vasovagal response in this instance was similar to the Phase 2 response in the development of vasovagal responses described by Julu et al. in humans; i.e., in

which HR initially countered the drop in BP but was only partially successful (7). Finally, at the end of the habituation process, both the 70° nose-up tilt (**Figure 2C**) and the \pm 2 mA, 0.025 Hz sGVS (**Figure 2F**) only produced small increases in BP and HR that lasted for the duration of the stimulus.

Similar results were obtained in R011, the susceptible rat from this group stimulated with \pm 3 mA, 0.025 Hz sGVS. Initially, the sGVS caused a drop in BP of \approx 20 mmHg and a fall in HR of \approx 100 bpm that outlasted the drop in BP (**Figure 3A**). During habituation, the same stimulus caused a more profound drop in BP. This was partially countered by an initial \approx 50 bpm rise in HR over the first \approx 100 s, before HR fell for more than 600 s (10 min)

(Figure 3B). A similar rise in HR was induced that countered a brief fall in BP produced by a 70° nose-up tilt at the same time in the habituation process in this rat (Figure 3C). Thus, there was a consistent increase in HR during habituation that countered the falls in BP, until there was only a small rise in both BP and HR in response to the vestibular stimuli (Figure 3C). These examples demonstrate that the habituation was induced in both of these rats by an activation of the heart, which opposed the falls in BP.

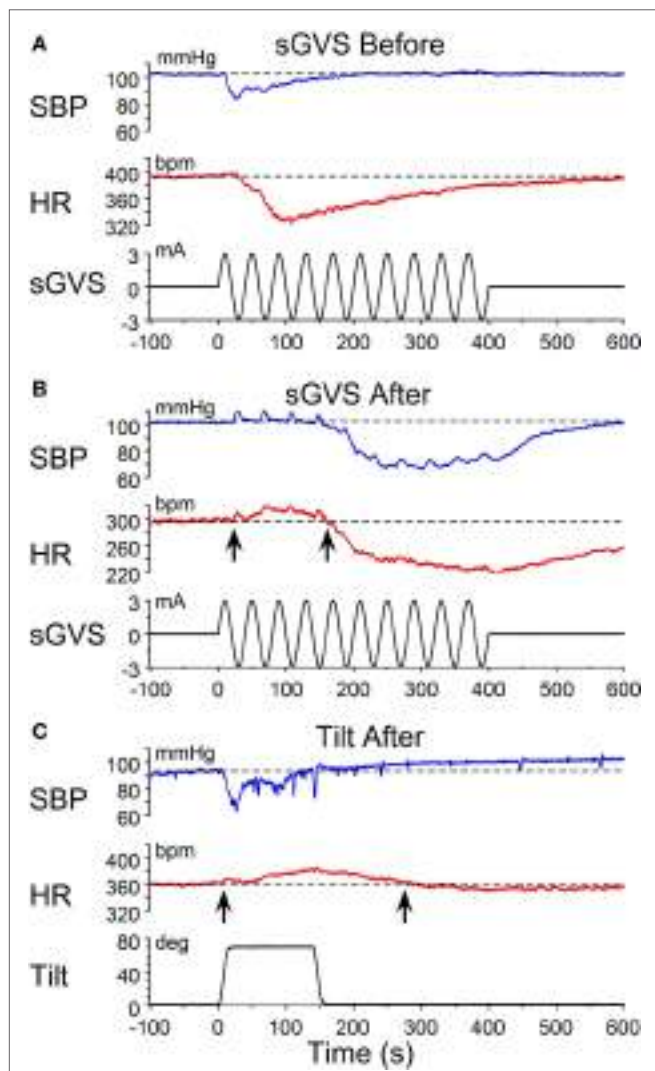


FIGURE 3 | Changes in blood pressure (BP) and heart rate (HR) during habituation in R011. Changes in BP (top traces) and HR (middle traces) in response to ± 3 mA, 0.025 Hz sGVS (bottom traces). **(A)** There was an initial fall in both BP and HR that was larger and lasted longer for the HR. **(B)** During the habituation process, initially, there were several, small transient increases in BP before BP fell in response to the sGVS. There was also a ≈ 20 bpm initial increase in HR (first upwards arrow) that persisted for ≈ 150 s before HR also fell (second upwards arrow). **(C)** At the same time as in B, nose-up tilt caused a drop in BP, but a concomitant rise in HR of ≈ 30 bpm (first upwards arrow) that persisted for nearly 300 s (second upwards arrow). The difference in the response of the HR to ± 3 mA sGVS and the 70° nose-up tilt suggests that the sGVS was a more powerful stimulus to the otolith system than the 70° nose-up tilt.

Such activation of HR strongly suggests an increase in baroreflex sensitivity.

Progressive Changes in Susceptibility and HR during Habituation

The changes in susceptibility and HR in R009 demonstrate the progressive fall in susceptibility and the rise in HR as a function of the habituation process. The animal was habituated with ± 2 mA, 0.025 Hz sGVS. The ± 2 mA sGVS was used to determine whether this stimulus, which has been widely used in studies of MSNA, would also produce habituation. Initially, R009 had a vasovagal response every time it was tested (Figure 4A, day 1), but it shortly developed resistance, and only responded to $\approx 30\%$ of the tests on day 2. Beginning on day 4 (Figure 4B), there was a dramatic 80% rise in HR that was also present on day 6, and then fell to 10% above resting level by day 10. Concurrently, the sGVS only caused a minimal decrease in BP. These data and those in Figures 2–4 also raise the possibility that it was activation of the heart through the baroreflex, in response to the fall in BP and HR that countered the drop in BP and brought the rat back to normality.

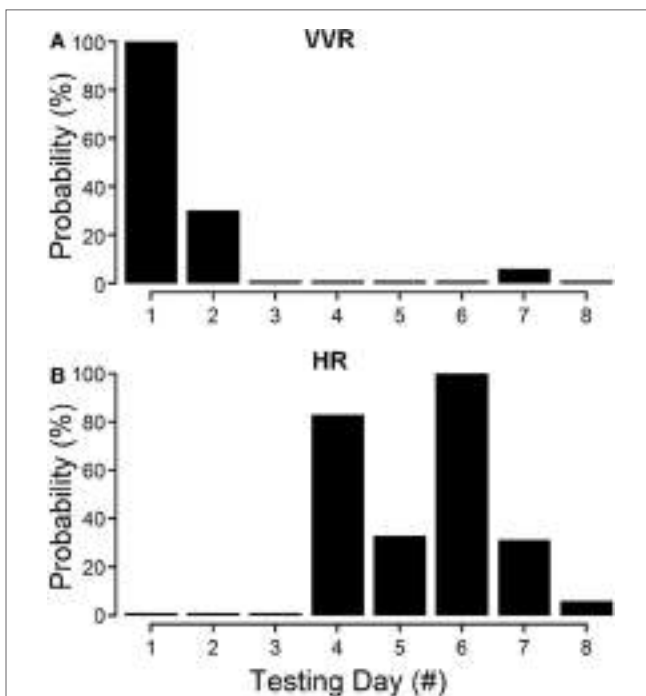


FIGURE 4 | Progressive decline in susceptibility to generation of vasovagal responses and coincident increase in heart rate (HR) during habituation in R009. The days of habituation are represented sequentially on the abscissae (see Materials and Methods). **(A)** Susceptibility fell rapidly over the first 2 days. **(B)** HR increased dramatically on the fourth day of testing, peaked on the sixth test day, and then fell rapidly over the next 2 test days. Finally, there was only a minimal response in blood pressure and HR by the eighth day, when the animal had become habituated. These data demonstrate that the fall in susceptibility was associated with a transient increase in HR that then fell back as the habituation proceeded.

Temporal Progression of Habituation

The moment-to-moment changes in BP and HR were characterized further during the various phases of habituation in R009 to demonstrate the continuous progression of BP and HR more completely as R009 became habituated. The changes in BP and HR during habituation were initially characterized at three stages in the process, using the coincidence that the changes in both parameters were of similar magnitudes. That is, both BP and HR fell by $\approx 20\text{--}50 \text{ mmHg}$ or $\approx 20\text{--}50 \text{ bpm}$ at the onset of a vasovagal response and then slowly recovered toward their original values. The recovery of the responses were fitted with a least square linear regression starting from the largest changes in BP and HR, and extending toward the origin, which contained the original values of BP and HR before stimulation (Figures 5A,C). The

direction of the recovery toward the pre-stimulus values is shown by the adjacent arrows (Figures 5D,F). These vectors are shown in a polar representation (Figure 6A). Initially, the direction of recovery toward the origin (0°) was similar in both BP and HR, i.e., in the $180\text{--}240^\circ$ quadrant (Figures 5B and 6A). Later during the habituation process, HR opposed the drop in BP. Although BP started from a depressed level, the fall in BP was opposed by an increase in HR (Figure 5D), so that the combined curve fell toward the origin in the $240\text{--}360^\circ$ quadrant (Figure 6A). Later, both BP and HR rose and then fell together toward their original values in the $0\text{--}90^\circ$ quadrant (Figures 5F and 6A).

Similar plots were made for BP and HR in each of the 30 tests during the habituation of R009 and for three tests made on the day after the end of habituation (Figure 6B). They demonstrate

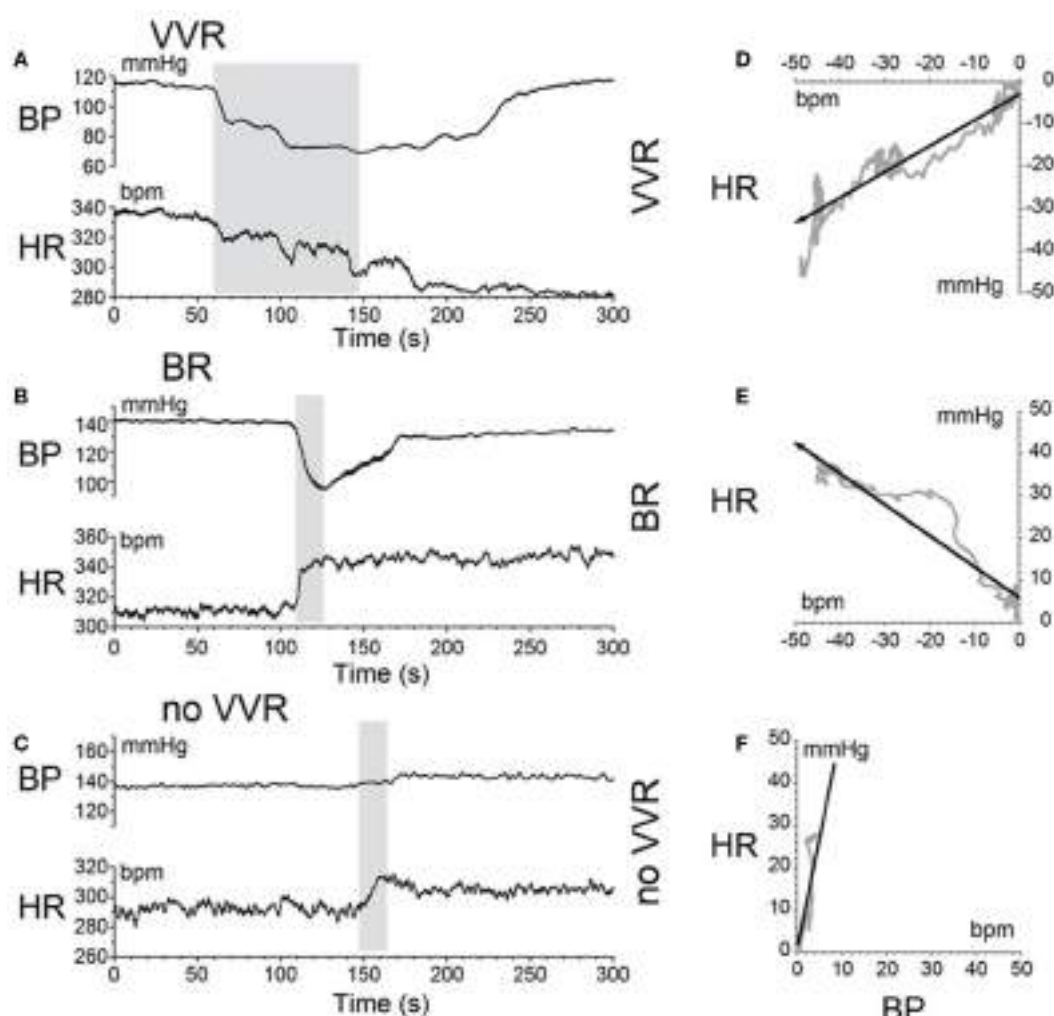


FIGURE 5 | Sequential changes in blood pressure (BP) and heart rate (HR) during habituation in R009. (A–C) Graphs of changes in BP (top traces) and HR (bottom traces) induced by activation of the vestibulosympathetic reflex with 400 ms trains of $\pm 2 \text{ mA}$, 0.025 Hz sGVS at the beginning, during, and at the end of habituation. The trains of sGVS caused different slopes of the combined responses in BP and HR at the different times during the habituation process. **(A)** At the beginning of habituation, both BP and HR fell together. The decline in HR persisted for more than 100 s. **(B)** During habituation, BP fell, but there was an increase in HR that persisted for >100 s. **(C)** At the end of habituation, BP was essentially unaffected, but there was a small rise in HR. **(D–F)** The slopes of the combined changes in BP and HR from **(A–C)** were derived from a least squares regression of these recordings. The vectors were originally in the $180\text{--}240^\circ$ quadrant (**D**), then in the $240\text{--}360^\circ$ quadrant during habituation (**E**), and finally in the $0\text{--}90^\circ$ quadrant after habituation had taken place (**F**).

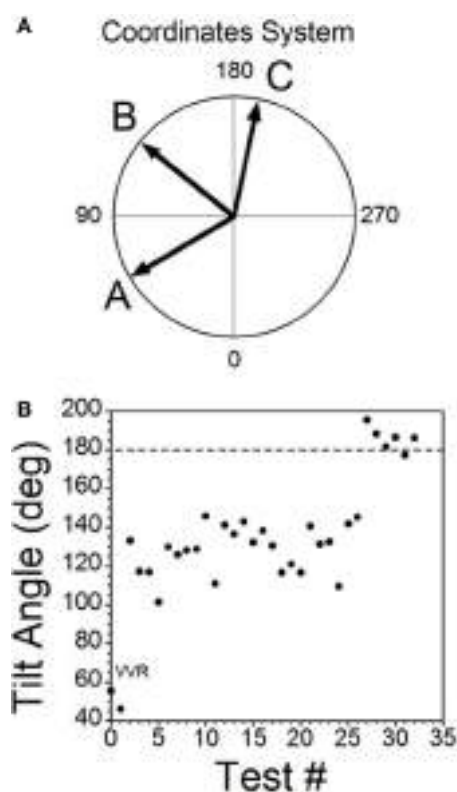


FIGURE 6 | Consecutive changes in blood pressure (BP) and heart rate (HR) during habituation in R009. **(A)** Plots of the vectors from Figures 5D–F are given in polar coordinates. This graph demonstrates the progressive changes in BP and HR during habituation. **(B)** Changes in the slopes of the BP/HR relationship as R009 became habituated plotted from the first to the last tests (bottom to top). The angle of tilt of the vector formed from BP and HR is shown on the ordinate, and the sequential test numbers are shown on the abscissa. There were 30 tests during the habituation procedure and 3 tests after the animal was habituated. The relationship between BP and HR systematically and gradually changed during habituation. There was a continual increase in the angle of the vector formed from BP and HR. The dashed line at 180° was achieved by the 27th test and was maintained through the 33rd test. Thus, there was a steady change in BP and HR from the beginning to the end of habituation.

a continuous modification of the relationship between BP and HR over the process of habituation. The values progressed at an increased tilt angle until they finally reached the values shown by the tilt angles in Figure 6B. Thus, the simultaneous drops in BP and HR had been continuously modified by the ± 2 mA, 0.025 Hz sGVS so that increases in HR initially countered subsequent drops in BP for several trials, after which HR rose above its resting level to counter the drop in BP. Finally, both BP and HR became much less responsive to further stimulation, and this condition was maintained for three additional tests given over the next several weeks.

Activation of the VSR

The habituating stimulus, sGVS, primarily activates the vestibular (otolith) system and the VSR. We questioned whether

the repetitive stimuli to the vestibular nerves induced by sGVS had made the VSR unresponsive. Further experiments demonstrated that this was not the case. Normally, current pulses and sinusoids of sGVS induce increases in BP, similar to the increases that occur in humans in changes of posture relative to gravity (orthostasis) (29), and HR is not generally activated by these stimuli unless the stimulus currents are large (34). To study whether the responsiveness of the vestibular nerve had been altered by the habituation process, a rat that was habituated with ± 3 mA, 0.025 Hz sGVS (R012, Figure 1A), was given 1 s ± 3 mA pulses of sGVS before, during, and after habituation (Figure 7).

Activation of the VSR with $+ 3$ mA sGVS continued to induce increases in BP before (≈ 150 – 162 mmHg lasting for 8 s), during (≈ 120 – 132 mmHg lasting for 10 s), and after habituation (≈ 130 – 152 mmHg lasting for 10 s; Figures 7A–C). Results were similar for -3 mA pulses of sGVS before (≈ 140 – 155 mmHg lasting for 10 s), during (≈ 115 – 123 mmHg lasting for 3 s), and after habituation (≈ 110 – 125 mmHg lasting for 10 s; Figures 7D–F). There were no changes in HR with these stimuli. Thus, habituation had not altered the response of the VSR to vestibular (otolith) stimulation, although such stimulation no longer induced vasovagal oscillations or vasovagal responses.

Low-Frequency Activity in BP and HR

In previous wavelet analyses, we demonstrated that vasovagal oscillations and vasovagal responses could only be induced when there was significant 0.025 and 0.05 Hz low-frequency activity in both BP and HR, and that this activity disappeared when rats were no longer susceptible to the generation of vasovagal oscillations or vasovagal responses (33, 34). Such low-frequency activity has also been demonstrated in a human fainter associated with a faint (36) and in alert dogs after withdrawal of blood, presumably when the dogs were in a pre-syncopal state (43, 44). We questioned whether there would be increased activity in the Bands that contain the 0.025 and 0.05 Hz oscillations in BP and HR when the rats were susceptible to the generation of vasovagal responses and during the active phases of habituation, and we predicted that these low-frequency oscillations would disappear as a consequence of the habituation.

The changes in Band 11 (0.025 Hz) and Band 10 (0.05 Hz) in BP and HR in R009 during a several month pretest period (3/5/14–6/4/14) and the condensed 2-week period of habituation, are shown in Figure 8. The horizontal dashed lines in the BP and HR traces indicate the upper limit of the low-frequency oscillations in Bands 11 and 10 for both BP and HR, and were determined using rats that had not been stimulated. The presence and amplitude of these frequencies are shown on the ordinate, with each circle representing the result of a separate determination, listed sequentially. However, the intervals between individual tests varied according to the demands of the experiment. There was a substantial amount of low-frequency activity present in both BP and HR until shortly after the habituation procedure began.

Then, both low frequencies of BP and HR fell toward normal levels. The fall was more substantial in BP than in HR but even HR was maintained close to normal levels. Thus, there was substantial

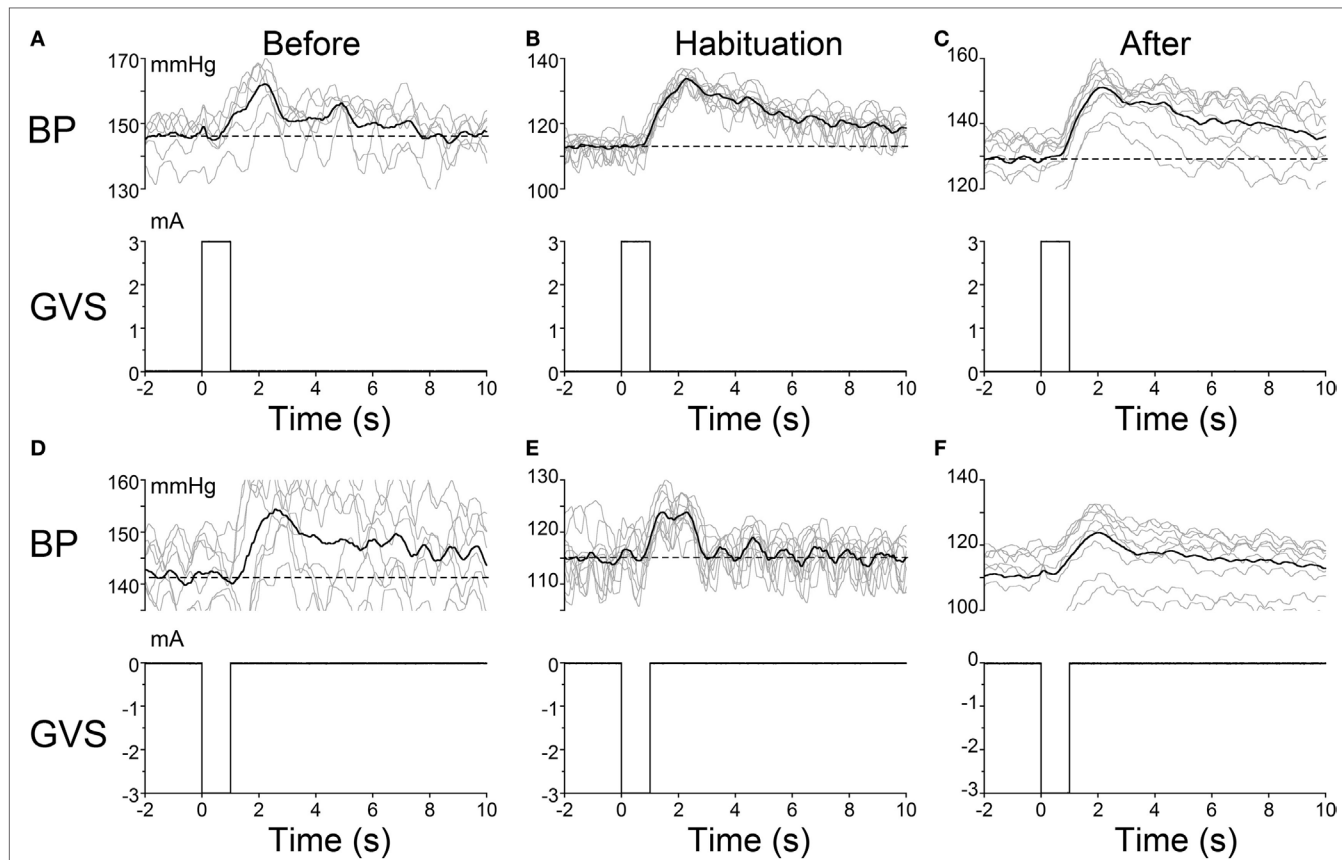


FIGURE 7 | Pulse stimulation of the vestibulosympathetic reflex before, during, and after habituation in R012. Increases in blood pressure (BP) (top traces) from +3 mA (A–C) and -3 mA (D–F) 1 s pulses of Galvanic Vestibular Stimulation. The stimuli induced increases in BP of \approx 10–25 mmHg and were somewhat larger when the initial BP was lower. The BP rose rapidly at the onset of stimulation before, during and after habituation. These data demonstrate that the response of the cardiovascular system to vestibular stimulation was not significantly affected by the habituation process. There were no changes in HR (not shown).

low-frequency activity in both BP and HR during the prolonged pretest period that promptly disappeared after the onset of the vestibular stimulation at the time when vasovagal responses could no longer be induced in this rat.

The sequence of the changes in BP and HR produced by the habituation procedure in R011 from 6/6/14 to 6/20/14 was similar to those in R009, but the pretest procedures were done rapidly, over a several day period, and it took longer for the low-frequency activity (0.025 and 0.05 Hz) in both BP and HR to fall below or close to normal levels (Figure 9). Nevertheless, it was not possible to induce vasovagal responses or vasovagal oscillations in either rat by the end of habituation as shown in Figures 2C,F and 3C. Therefore, we can conclude that habituation had been successful in reducing the susceptibility to generation of vasovagal responses by blocking occurrence of low-frequency oscillations in BP and HR in these rats.

Baroreflex Sensitivity

There is a reduction in baroreflex sensitivity in the anesthetized state (45–48). Presumably, this reduction contributed to the loss of susceptibility of the generation of vasovagal responses. As shown in Figures 2A,D and 3A, both BP and HR fell together, and the baroreflex did not counter the combined fall in BP

and HR until habituation began (Figures 2B,E and 3B). We questioned whether baroreflex sensitivity was altered during the progressive habituation induced by the consistent use of sGVS. As shown in Figure 10 (first and third traces), there was a steady increase in baroreflex sensitivity in the two susceptible rats that lost their susceptibility during the habituation process ($p < 0.01$ for both rats). Each circle in Figures 9A,D represents a separate determination, listed sequentially. Although sequential, the intervals between individual tests varied according to the demands of the experiment. The increase in baroreflex sensitivity began during the preliminary testing, in R009, and continued through the habituation period in both rats. Traces of the low-frequency (0.025 Hz) activity are repeated to demonstrate that there was no inflection in the rise in baroreflex sensitivity during habituation (second and fourth traces). This is particularly notable for R011, which was habituated intensively from its susceptibility state.

These data are compatible with the postulate that an increase in baroreflex sensitivity plays a role in the habituation of vasovagal responses, and there was no similar increase in baroreflex sensitivity in several rats that failed to become habituated with $\pm 70^\circ$ oscillation in pitch (not shown). Nevertheless, these data imply that an increase in baroreflex sensitivity was not solely

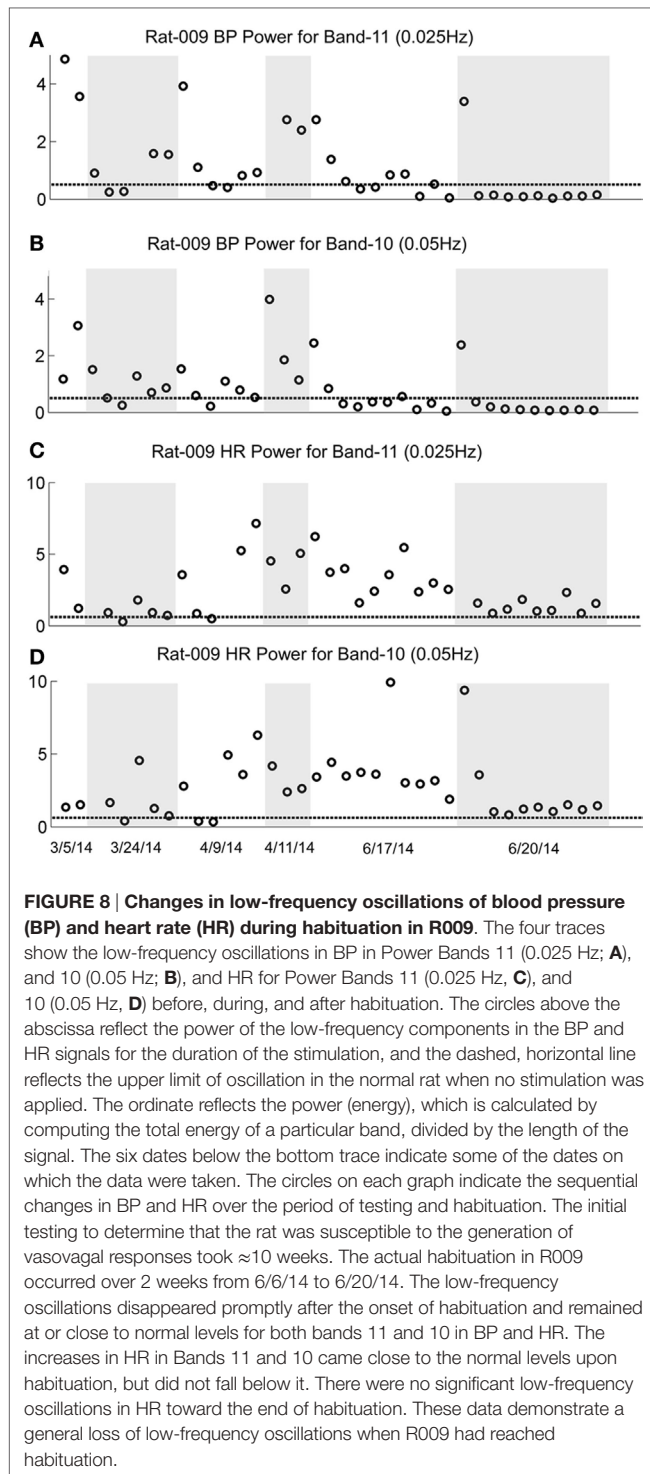


FIGURE 8 | Changes in low-frequency oscillations of blood pressure (BP) and heart rate (HR) during habituation in R009. The four traces show the low-frequency oscillations in BP in Power Bands 11 (0.025 Hz; **A**), and 10 (0.05 Hz; **B**), and HR for Power Bands 11 (0.025 Hz; **C**), and 10 (0.05 Hz; **D**) before, during, and after habituation. The circles above the abscissa reflect the power of the low-frequency components in the BP and HR signals for the duration of the stimulation, and the dashed, horizontal line reflects the upper limit of oscillation in the normal rat when no stimulation was applied. The ordinate reflects the power (energy), which is calculated by computing the total energy of a particular band, divided by the length of the signal. The six dates below the bottom trace indicate some of the dates on which the data were taken. The circles on each graph indicate the sequential changes in BP and HR over the period of testing and habituation. The initial testing to determine that the rat was susceptible to the generation of vasovagal responses took \approx 10 weeks. The actual habituation in R009 occurred over 2 weeks from 6/6/14 to 6/20/14. The low-frequency oscillations disappeared promptly after the onset of habituation and remained at or close to normal levels for both bands 11 and 10 in BP and HR. The increases in HR in Bands 11 and 10 came close to the normal levels upon habituation, but did not fall below it. There were no significant low-frequency oscillations in HR toward the end of habituation. These data demonstrate a general loss of low-frequency oscillations when R009 had reached habituation.

responsible for the reduction in susceptibility to the generation of vasovagal responses. That is, the sequence of changes in baroreflex sensitivity is not in close accord with the sequence of development of habituation. Baroreflex sensitivity increased steadily in R009, but it was possible to induce vasovagal responses at the onset of habituation (**Figures 2A,D**) almost three months after testing had begun.

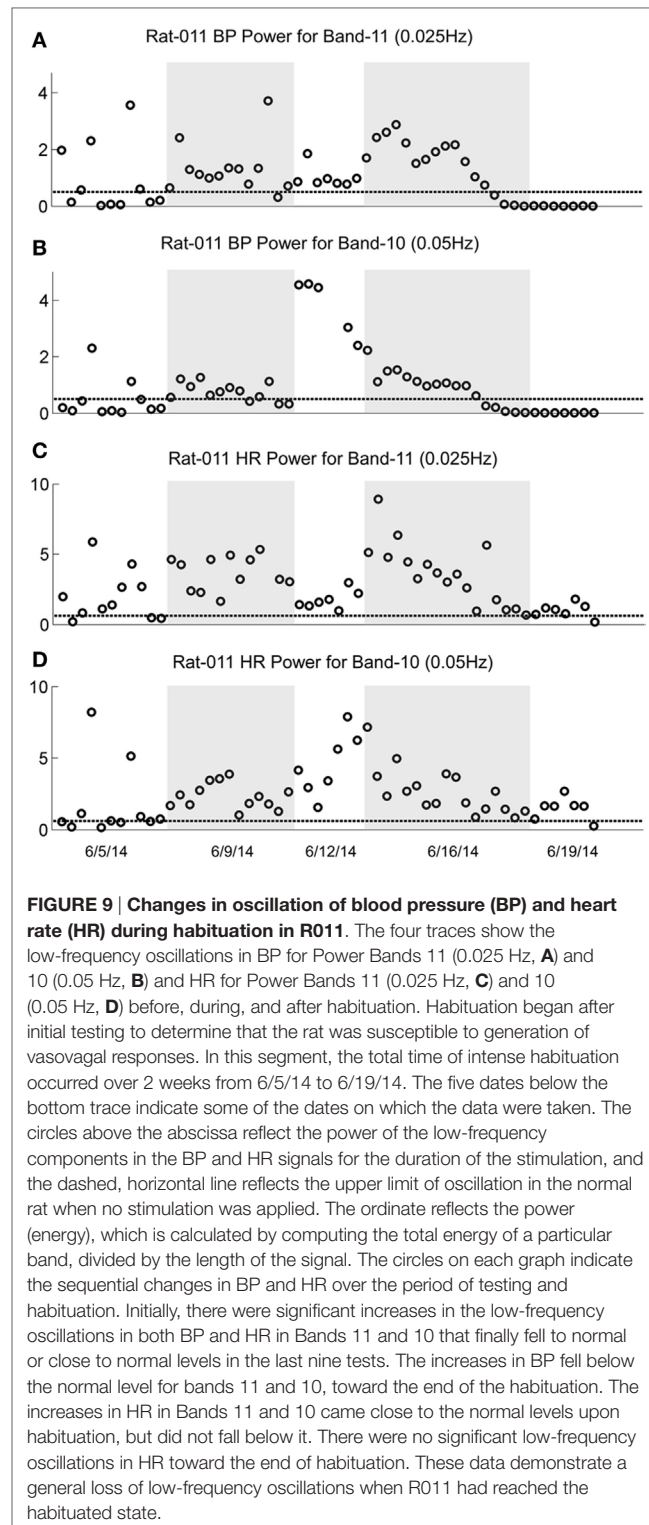


FIGURE 9 | Changes in oscillation of blood pressure (BP) and heart rate (HR) during habituation in R011. The four traces show the low-frequency oscillations in BP for Power Bands 11 (0.025 Hz, **A**) and 10 (0.05 Hz, **B**) and HR for Power Bands 11 (0.025 Hz, **C**) and 10 (0.05 Hz, **D**) before, during, and after habituation. Habituation began after initial testing to determine that the rat was susceptible to generation of vasovagal responses. In this segment, the total time of intense habituation occurred over 2 weeks from 6/5/14 to 6/19/14. The five dates below the bottom trace indicate some of the dates on which the data were taken. The circles above the abscissa reflect the power of the low-frequency components in the BP and HR signals for the duration of the stimulation, and the dashed, horizontal line reflects the upper limit of oscillation in the normal rat when no stimulation was applied. The ordinate reflects the power (energy), which is calculated by computing the total energy of a particular band, divided by the length of the signal. The circles on each graph indicate the sequential changes in BP and HR over the period of testing and habituation. Initially, there were significant increases in the low-frequency oscillations in both BP and HR in Bands 11 and 10 that finally fell to normal or close to normal levels in the last nine tests. The increases in BP fell below the normal level for bands 11 and 10, toward the end of the habituation. The increases in HR in Bands 11 and 10 came close to the normal levels upon habituation, but did not fall below it. There were no significant low-frequency oscillations in HR toward the end of habituation. These data demonstrate a general loss of low-frequency oscillations when R011 had reached the habituated state.

DISCUSSION

This study shows that the susceptibility of anesthetized rats to the induction of vasovagal responses can be effectively reversed by activation of the VSR. This was demonstrated in two sets of

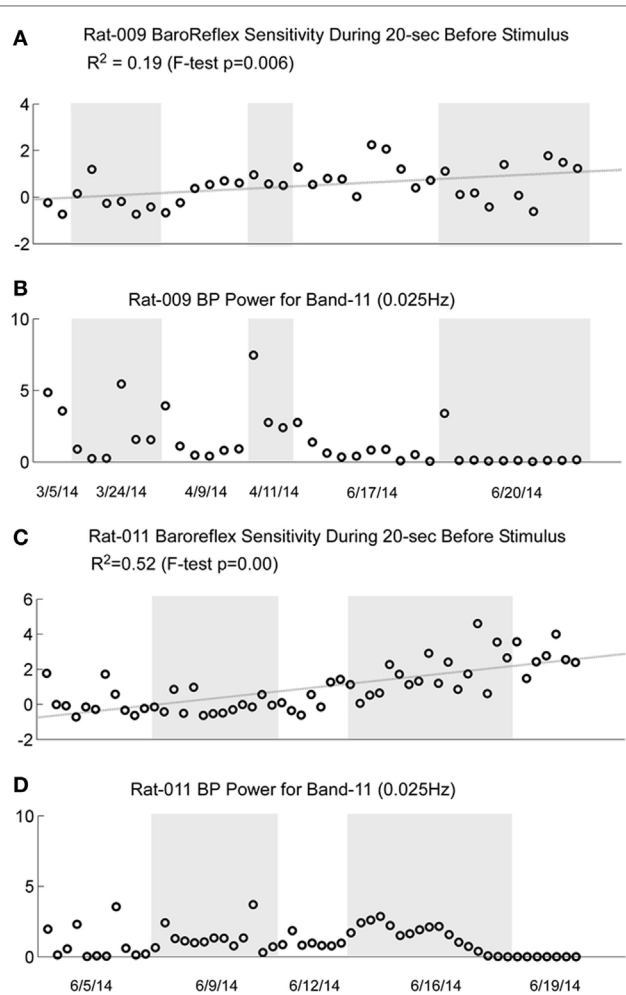


FIGURE 10 | Comparison of the increase in baroreflex sensitivity and blood pressure (BP) Power Band 11 responses (0.025 Hz) for R009 and R011. The four traces show the increase in baroreflex sensitivity (A and C) and low-frequency oscillations in BP for Power Band 11 (B and D) for R009 and R011. The increases in baroreflex sensitivity were significant in both animals (R009: $p = 0.006$, R011: $p < 0.001$). The R^2 value was higher in R011 than in R009, indicating that there was a higher linear correlation for R011. There was no dramatic change in baroreflex sensitivity that was associated with the loss of low-frequency oscillations in BP and HR in both animals. The traces of the low-frequency oscillations in BP were repeated to demonstrate that changes in these oscillations were not reflected specifically in the changes in baroreflex sensitivity. Regardless, these data demonstrate that baroreflex sensitivity could significantly increase as a result of the vestibular stimulation and the habituation process.

study was to uncover the actual changes in BP and HR that had been responsible for the habituation. This was shown by the close study of four rats that were susceptible to the generation of vasovagal responses and lost that susceptibility when the VSR was repeatedly stimulated with ± 2 and ± 3 mA, 0.025 Hz sGVS. The loss of susceptibility was associated with an initial and then a more substantial rise in HR to oppose the fall in BP. Finally, the same stimuli only caused a slight increase in BP and HR. After habituation, vasovagal responses could no longer be induced by any of the vestibular (otolith) stimuli including 70° nose-up tilt and ± 3 mA sGVS. These findings were supported by the loss of low-frequency oscillations (0.025 and 0.05 Hz) in BP and HR (**Figures 8 and 9**) that have been shown to be essential for activation of vasovagal oscillations and vasovagal responses in anesthetized rats, dogs, and humans (33, 34, 36, 43, 44). The habituation was also associated with a significant rise in baroreflex sensitivity (**Figure 10**). To our knowledge, this is the first demonstration of the processes that are likely to underlie the habituation of syncope, as well as the changes in HR and BP that resulted in the loss of susceptibility to the induction of vasovagal oscillations and vasovagal responses. Here, we consider the characteristics of BP and HR that were produced by repeated activation of the VSR, speculate on the central mechanisms that could have been involved in producing the loss of susceptibility, and propose potential clinical implications of these findings.

Development of habituation took a characteristic, continuous course, shown by the modifications in BP and HR that occurred in each of the rats during habituation. These changes were demonstrated in a typical rat (R009), using the coincidence of similar numerical values for BP and HR at the onset of habituation to compare the relative changes in each parameter. This comparison provided insight into the nature of the process that alters BP and HR during habituation, namely, a significant but limited rise in HR rather than the combined fall in BP and HR (**Figure 4**) that are the essential components of the vasovagal response. Thus, although the rats were under anesthesia where baroreflex sensitivity is low (49–51), a significant increase in baroreflex sensitivity was associated with the habituation during which the rat cardiovascular system became impervious to strong activation of the VSR. However, the slope of the restoration in baroreflex function consistently increased as habituation proceeded, and during the time it took to determine if R009 was suitable, there was a continuous rise in baroreflex sensitivity at a time when it was still possible to drive the rat into vasovagal responses. This is shown quite clearly in **Figures 2–4** that demonstrate that both of the rats were susceptible to the generation of vasovagal responses on 6/5/14 and 6/6/14 when the habituation procedures began, and when vasovagal responses could be induced (**Figures 2A,D and 3A**). A comparison of the rise in baroreflex sensitivity, in both rats (**Figure 10**, first and third traces) demonstrates that the rise in sensitivity was smooth and showed no inflection on or about 6/5/14 and 6/6/14 when there was a dramatic turnaround in the low-frequency oscillations (**Figure 10**, second and fourth traces) that were associated with the loss of the ability to generate vasovagal responses. Thus, although baroreflex sensitivity may have a critical role in

rats: seven rats that were initially susceptible to the generation of vasovagal responses and were utilized in other experiments lost their susceptibility when they were stimulated at different intervals with various forms of vestibular stimulation (**Figure 1C**). These studies were directed to other ends, and it was not possible to isolate the specific stimuli that had caused the loss of susceptibility to the generation of vasovagal responses nor to determine the specific changes in BP and HR that accompanied the habituation process. Thus, the prime goal of the present

reactivating HR to oppose drops in BP, events around the production of low-frequency oscillations (i.e., 0.025 and 0.05 Hz) are likely to be critical elements in initiating vasovagal responses and vasovagal syncope (33, 34, 36), and their disappearance is a critical part of the habituation process.

Also lacking from this formulation are the specific trigger for the combined drop in BP and HR during the vasovagal responses as well as the source of the signal that reverses the reduction in function of the baroreflex. A model showing how the baroreflex and VSR impinge on the cardiovascular system suggests that there is a critical variable that governs the onset of the vasovagal response (14), namely an element labeled desired BP (Desired BP), which is comprised of the diastolic/systolic amplitudes. When the amplitude of the Desired BP fell in the simulations, there was an initiation of a reduction in both BP and HR, leading to a simulated vasovagal response by the model. Where such a signal arises is unknown, but it could come from the interaction of the uvula with the VSR and the cardiovascular system (52). Direct projections extend from the uvula to the otolithic portions of the Vestibular Nuclei to the parabrachial nuclei and the Nucleus Tractus Solitarius (NTS) that receive the input from the baroreflex receptors (53–57). There is also a disynaptic projection from the uvula to NTS that could control baroreflex sensitivity (29, 52, 58–61). If this is correct, then projections from the uvula could be the critical input to control susceptibility to sympathetic activation of syncope, regardless of whether it arises from direct activation of the VSR or from one of the many other causes of vasovagal syncope that project through the parabrachial nuclei. It is also possible that among the inhibitory processes generated onto the baroreflex is a clamp on the low-frequency activity from inhibitory input that arises in the uvula. If this speculation is correct, then the increased low-frequency activity in BP and HR could be a reflection of cerebellar-generated activity that controls baroreflex sensitivity that inhibits production of syncope and promotes generation of MSNA (62).

Clinical Implications

Our findings support the studies of Ector, Kinay, Reybrouck, and Di Girolamo (17, 18, 20, 21, 63), which habituated vasovagal syncope with static head-up tilt that would have activated otolith and body tilt receptors (23, 64). Habituation with head-up tilt takes significant time in the upright position and, therefore, would not involve the vertical semicircular canals. Whether this would make their habituating stimulus less powerful than sGVS, which activates the combined input from the vertical semicircular canals and the otolith organs to the vestibular nuclei (27, 28) is not known. Why these findings were not supported by the studies of Foglia-Manzillo (30) and Duygu (31) is also not clear. Perhaps as suggested by Foglia-Manzillo, the use of the boring bouts of static head-up tilt that formed the basis of the static tilt treatment was responsible for non-compliance among the subjects.

Sinusoidal galvanic vestibular stimulation (sGVS) has more potential for use in this regard. It has been widely used to activate MSNA without serious consequences other than production of motion sickness in some of the test subjects (37–40, 65–67).

The apparatus to deliver sGVS is small, electrically safe, and the electrodes are easy to apply over the mastoids. During such habituation, moreover, it would be possible for subjects to read, listen to music, and/or watch TV or a movie during the habituation periods.

Although relatively few rats were intensively studied, it was also possible to gain a preliminary estimate of the relative strength of the various stimuli on the otolithic system from a comparison of the effects of the nose-up tilts and sGVS on the changes in BP and HR during development of habituation (Figures 2 and 3). The ± 2 and ± 3 mA sGVS were more potent in causing continued dissociation of BP and HR than the nose-up tilts that imposed a known load of ≈ 0.91 g on the head and body (Figures 2 and 3). This implies that the sGVS was perceived by the vestibular system as somewhat more potent than the nose-up tilts that were equivalent to 0.91 g. We can estimate, therefore, that the sGVS was probably perceived as being equivalent to about 1 g, which is a similar estimate of the strength of the sGVS that we previously derived from a comparison of its effect on the low-frequency activity in BP and HR (33).

Limits of the Study

Although the results were clear cut in the four rats that were intensively studied in this report and in the seven rats used in previous studies, additional rats must be used to determine how long habituation is maintained, and whether, in accordance with the definition of Rankin et al. (1) and Thompson (2), reactivation of the habituated state would be considerably faster than the original habituation process. More rats are also needed to determine whether ± 2 mA sGVS is as effective in producing habituation as ± 3 mA sGVS, since there have been a wide range of studies using ± 2 mA sGVS, which is safe and without significant side effects in humans. Nevertheless, despite the limited number of animals, the results were deemed to be of potential value in directing habituation of syncope in humans.

A critical question is what is stimulated by the sGVS. Galvanic stimuli activate all axons in the vestibular nerves (68, 69). This causes excitation of canal and otolith neurons in the Vestibular Nuclei related to rotation and tilt. The lateral canal-related neurons are rapidly inhibited, however, leaving the otolith-related input intact (26, 70). The sGVS causes generation of cfos in otolithic portions of the vestibular nuclei and in the superior vestibular nuclei (27), suggesting that the vertical canal input may also be maintained. Neurons in these nuclei project monosynaptically through the inferior vestibular nuclei to the rostral ventral lateral medulla bilaterally. Utilizing glutamatergic transmission (27–29, 71), they excite paraspinal neurons in the sympathetic chain in the thoracic spinal cord (72) to produce the VSR, probably through constriction of peripheral vessels because the VSR does not cause significant changes in HR (35).

An alternate pathway could also have been activated by the sGVS, namely a branch of the vagus nerve that originates in the tragus of the external ear and projects to the NTS and the dorsal motor nucleus of the vagus (73). Therefore stimulation of the tragal branch of the vagus could have affected the function of the NTS, namely its control of the baroreflex, possibly causing modification of the baroreflex sensitivity that was observed

with continued stimulation. However, there was also a response to 70° nose-up tilt that would not have activated the vagus nerve endings in the tragus. In fact, 60° and 70° Head-up tilts are widely used to determine if humans suspected of having vasovagal syncope become faint during the tilt-test, and small currents of galvanic vestibular stimulation also maintain BP during head-up tilts (74). Moreover, the sequence of habituation was characterized by an increase in HR to counter the drop in BP, and activation of the vagus would cause a reduction in HR, not an increase. Therefore, it is not likely that vagus activation from the tragus had significantly affected the results shown in this study.

Before such use in humans can be considered, however, it is essential to determine that the bouts of habituation do not cause serious side effects, and to determine how long the habituation produced by such an apparatus persists, and how often the treatments have to be repeated to maintain the habituation. It would also be critical to know the origin or the nature of the signal that causes the baroreflex to come alive in the anesthetized rat. Neither do we know the duration of the habituation process that is generated by activation of the VSR. Nevertheless, this work provides support for studies that suggest that vasovagal syncope can be habituated. For the first time, it demonstrates that habituation of vasovagal oscillations and vasovagal responses, the underlying processes that lead to vasovagal or neurogenic syncope, can be blocked by repetitive activation of the VSR. Furthermore, it

indicates that sGVS with ± 2 or ± 3 mA, 0.025 Hz is likely to be a strong habituating stimulus in humans as in rats.

AUTHOR CONTRIBUTIONS

BC conceived the study, monitored its progress, and wrote the paper. GM helped to plan the study, did the surgery, monitored care of the animals, and made critical suggestions to improve the manuscript. SY helped to plan the study, performed the experiments, analyzed the data, made the figures, and helped with the manuscript. YX analyzed the data and did the analysis of low-frequency activity and baroreflex sensitivity. TR initiated and supervised the wavelet analyses and the results of baroreflex sensitivity.

ACKNOWLEDGMENTS

The authors thank Dmitri Ogorodnikov for the technical assistance with equipment maintenance and for developing algorithms to determine systolic, diastolic, and mean BP. They also thank Mark Hajjar, Shruti Shenbagam, and Rupa Mirmira for editorial assistance.

FUNDING

This study was supported by NIH Grants: DC012573, DC05204.

REFERENCES

- Rankin CH, Abrams T, Barry RJ, Bhatnagar S, Clayton DF, Colombo J, et al. Habituation revisited: an updated and revised description of the behavioral characteristics of habituation. *Neurobiol Learn Mem* (2009) 92(2):135–8. doi:10.1016/j.nlm.2008.09.012
- Thompson RF. Habituation: a history. *Neurobiol Learn Mem* (2009) 92(2):127–34. doi:10.1016/j.nlm.2008.07.011
- Gendelman HE, Linzer M, Gabelman M, Smoller S, Scheuer J. Syncope in a general hospital patient population. Usefulness of the radionuclide brain scan, electroencephalogram, and 24-hour Holter monitor. *N Y State J Med* (1983) 83(11–12):1161–5.
- Soteriades ES, Evans JC, Larson MG, Chen MH, Chen L, Benjamin EJ, et al. Incidence and prognosis of syncope. *N Engl J Med* (2002) 347(12):878–85. doi:10.1056/NEJMoa012407
- Grubb BP. Clinical practice. Neurocardiogenic syncope. *N Engl J Med* (2005) 352(10):1004–10. doi:10.1056/NEJMcp042601
- Schroeder C, Tank J, Heusser K, Diedrich A, Luft FC, Jordan J. Physiological phenomenology of neurally-mediated syncope with management implications. *PLoS One* (2011) 6(10):e26489. doi:10.1371/journal.pone.0026489
- Julu POO, Cooper VL, Hansen S, Hainsworth R. Cardiovascular regulation in the period preceding vasovagal syncope in conscious humans. *J Physiol* (2003) 549(1):299–311. doi:10.1113/jphysiol.2002.036715
- Moya A, Sutton R, Ammirati F, Blanc JJ, Brignole M, Dahm JB, et al. Guidelines for the diagnosis and management of syncope (version 2009). *Eur Heart J* (2009) 30(21):2631–71. doi:10.1093/eurheartj/ehp298
- Lewis T. A lecture on vasovagal syncope and the carotid sinus mechanism. *Br Med J* (1932) 1(3723):873–6. doi:10.1136/bmj.1.3723.873
- Thomson HL, Wright K, Frenneaux M. Baroreflex sensitivity in patients with vasovagal syncope. *Circulation* (1997) 95(2):395–400. doi:10.1161/01.CIR.95.2.395
- Kaufmann H, Hainsworth R. Why do we faint? *Muscle Nerve* (2001) 24(8):981–3. doi:10.1002/mus.1102
- Morillo CA, Eckberg DL, Ellenbogen KA, Beightol LA, Hoag JB, Tahvanainen KU, et al. Vagal and sympathetic mechanisms in patients with orthostatic
- vasovagal syncope. *Circulation* (1997) 96(8):2509–13. doi:10.1161/01.CIR.96.8.2509
- Mosqueda-Garcia R, Furlan R, Fernandez-Violante R, Desai T, Snell M, Jarai Z, et al. Sympathetic and baroreceptor reflex function in neurally mediated syncope evoked by tilt. *J Clin Invest* (1997) 99(11):2736–44. doi:10.1172/JCI119463
- Raphan T, Cohen B, Xiang Y, Yakushin SB. A model of blood pressure, heart rate, and vaso-vagal responses produced by vestibulo-sympathetic activation. *Front Neurosci* (2016) 10:96. doi:10.3389/fnins.2016.00096
- Calkins H. Pharmacologic approaches to therapy for vasovagal syncope. *Am J Cardiol* (1999) 84(8A):20Q–5Q. doi:10.1016/S0002-9149(99)00626-8
- Sheldon R, Connolly S; Vasovagal Pacemaker Study II. Second Vasovagal Pacemaker Study (VPS II): rationale, design, results, and implications for practice and future clinical trials. *Card Electrophysiol Rev* (2003) 7(4):411–5. doi:10.1023/b:cepr.0000023157.37745.76
- Ector H, Reybrouck T, Heidbuchel H, Gewillig M, Van de Werf F. Tilt training: a new treatment for recurrent neurocardiogenic syncope and severe orthostatic intolerance. *Pacing Clin Electrophysiol* (1998) 21(1 Pt 2):193–6. doi:10.1111/j.1540-8159.1998.tb01087.x
- Ector H. Neurocardiogenic, vasovagal syncope. *Eur Heart J* (1999) 20(23):1686–7. doi:10.1053/euhj.1999.1827
- Reybrouck T, Heidbuchel H, Werf F, Ector H. Tilt training: a treatment for malignant and recurrent neurocardiogenic syncope. *Pacing Clin Electrophysiol* (2000) 23(4):493–8. doi:10.1111/j.1540-8159.2000.tb00833.x
- Reybrouck T, Heidbuchel H, Van De Werf F, Ector H. Long-term follow-up results of tilt training therapy in patients with recurrent neurocardiogenic syncope. *Pacing Clin Electrophysiol* (2002) 25(10):1441–6. doi:10.1046/j.1460-9592.2002.01441.x
- Kinay O, Yazici M, Nazli C, Acar G, Gedikli O, Altinbas A, et al. Tilt training for recurrent neurocardiogenic syncope: effectiveness, patient compliance, and scheduling the frequency of training sessions. *Jpn Heart J* (2004) 45(5):833–43. doi:10.1536/jhh.45.833
- Yates BJ, Holmes MJ, Jian BJ. Adaptive plasticity in vestibular influences on cardiovascular control. *Brain Res Bull* (2000) 53(1):3–9. doi:10.1016/S0361-9230(00)00302-6

23. Mittelstaedt H. Somatic graviception. *Biol Psychol* (1996) 42(1–2):53–74. doi:10.1016/0301-0511(95)05146-5
24. Mittelstaedt H. Origin and processing of postural information. *Neurosci Biobehav Rev* (1998) 22(4):473–8. doi:10.1016/S0149-7634(97)00032-8
25. Yates BJ, Miller AD. Properties of sympathetic reflexes elicited by natural vestibular stimulation: implications for cardiovascular control. *J Neurophysiol* (1994) 71(6):2087–92.
26. Cohen B, Yakushin SB, Holstein GR. What does galvanic vestibular stimulation actually activate: response. *Front Neurol* (2012) 3:148. doi:10.3389/fneur.2012.00148
27. Holstein GR, Friedrich VL Jr, Martinelli GP, Ogorodnikov D, Yakushin SB, Cohen B. Fos expression in neurons of the rat vestibulo-autonomic pathway activated by sinusoidal galvanic vestibular stimulation. *Front Neurol* (2012) 3:4. doi:10.3389/fneur.2012.00004
28. Holstein GR, Friedrich VL Jr, Martinelli GP. Projection neurons of the vestibulo-sympathetic reflex pathway. *J Comp Neurol* (2014) 522(9):2053–74. doi:10.1002/cne.23517
29. Yates BJ, Bolton PS, Macefield VG. Vestibulo-sympathetic responses. *Compr Physiol* (2014) 4(2):851–87. doi:10.1002/cphy.c130041
30. Foglia-Manzillo G, Giada F, Gaggioli G, Bartoletti A, Lolli G, Dinelli M, et al. Efficacy of tilt training in the treatment of neurally mediated syncope. A randomized study. *Europace* (2004) 6(3):199–204. doi:10.1016/j.eupc.2004.01.002
31. Duygu H, Zoghi M, Turk U, Akyuz S, Ozerkan F, Akilli A, et al. The role of tilt training in preventing recurrent syncope in patients with vasovagal syncope: a prospective and randomized study. *Pacing Clin Electrophysiol* (2008) 31(5):592–6. doi:10.1111/j.1540-8159.2008.01046.x
32. Cohen B, Dai M, Ogorodnikov D, Laurens J, Raphan T, Muller P, et al. Motion sickness on tilting trains. *FASEB J* (2011) 25(11):3765–74. doi:10.1096/fj.11-184887
33. Cohen B, Martinelli GP, Raphan T, Schaffner A, Xiang Y, Holstein GR, et al. The vasovagal response of the rat: its relation to the vestibulosympathetic reflex and to Mayer waves. *FASEB J* (2013) 27(7):2564–72. doi:10.1096/fj.12-226381
34. Yakushin SB, Martinelli GP, Raphan T, Xiang Y, Holstein GR, Cohen B. Vasovagal oscillations and vasovagal responses produced by the vestibulo-sympathetic reflex in the rat. *Front Neurol* (2014) 5:37. doi:10.3389/fneur.2014.00037
35. Yakushin SB, Martinelli GP, Raphan T, Cohen B. The response of the vestibulosympathetic reflex to linear acceleration in the rat. *J Neurophysiol* (2016) 116(6):2752–64. doi:10.1152/jn.00217.2016
36. Nowak JA, Ocon A, Taneja I, Medow MS, Steward JM. Multiresolution wavelet analysis of time dependent physiological response in syncopal youths. *Am J Physiol Heart Circ Physiol* (2009) 296:H171–9. doi:10.1152/ajpheart.00963.2008
37. Klingberg D, Hammam E, Macefield VG. Motion sickness is associated with an increase in vestibular modulation of skin but not muscle sympathetic nerve activity. *Exp Brain Res* (2015) 233(8):2433–40. doi:10.1007/s00221-015-4313-x
38. Bent LR, Bolton PS, Macefield VG. Modulation of muscle sympathetic bursts by sinusoidal galvanic vestibular stimulation in human subjects. *Exp Brain Res* (2006) 174(4):701–11. doi:10.1007/s00221-006-0515-6
39. Grewal T, James C, Macefield VG. Frequency-dependent modulation of muscle sympathetic nerve activity by sinusoidal galvanic vestibular stimulation in human subjects. *Exp Brain Res* (2009) 197(4):379–86. doi:10.1007/s00221-009-1926-y
40. Hammam E, James C, Dawood T, Macefield VG. Low-frequency sinusoidal galvanic stimulation of the left and right vestibular nerves reveals two peaks of modulation in muscle sympathetic nerve activity. *Exp Brain Res* (2011) 213(4):507–14. doi:10.1007/s00221-011-2800-2
41. Kaufmann H, Biaggioni I, Voustianiouk A, Diedrich A, Costa F, Clarke R, et al. Vestibular control of sympathetic activity. An otolith-sympathetic reflex in humans. *Exp Brain Res* (2002) 143(4):463–9. doi:10.1007/s00221-002-1002-3
42. Voustianiouk A, Kaufmann H, Diedrich A, Raphan T, Biaggioni I, Macdougall H, et al. Electrical activation of the human vestibulo-sympathetic reflex. *Exp Brain Res* (2006) 171(2):251–61. doi:10.1007/s00221-005-0266-9
43. Akselrod S, Gordon D, Ubel FA, Shannon DC, Berger A, Cohen RJ. Power spectrum analysis of heart rate fluctuation: a quantitative probe of beat-to-beat cardiovascular control. *Science* (1981) 213(4504):220–2. doi:10.1126/science.6166045
44. Akselrod S, Gordon D, Madwed JB, Snidman N, Shannon D, Cohen R. Hemodynamic regulation: investigation by spectral analysis. *Am J Physiol* (1985) 249(4 Pt 2):H867–75.
45. Yamamoto H, Kawada T, Shimizu S, Kamiya A, Turner MJ, Miyazaki S, et al. Acute effects of intravenous nifedipine or azelnidipine on open-loop baroreflex static characteristics in rats. *Life Sci* (2015) 126:37–41. doi:10.1016/j.lfs.2015.01.024
46. Mužík M, Ebert TJ. A comparison of baroreflex sensitivity during isoflurane and desflurane anesthesia in humans. *Anesthesiology* (1995) 82(4):919–25. doi:10.1097/00000542-199504000-00015
47. Mendez GD, Aletti F, Toschi N, Canichella A, Coniglione F, Sabato E, et al. Estimation of baroreflex sensitivity during anesthesia induction with propofol. *Conf Proc IEEE Eng Med Biol Soc* (2011) 2011:3788–91. doi:10.1109/emb.2011.609076
48. Yi-Ming W, Shu H, Miao CY, Shen FM, Jiang YY, Su DF. Asynchronism of the recovery of baroreflex sensitivity, blood pressure, and consciousness from anesthesia in rats. *J Cardiovasc Pharmacol* (2004) 43(1):1–7. doi:10.1097/00005344-200401000-00001
49. Kotrly K, Ebert T, Vucins E, Igler F, Barney J, Kampine J. Baroreceptor reflex control of heart rate during isoflurane anesthesia in humans. *Anesthesiology* (1984) 60(3):173–9. doi:10.1097/00000542-198403000-00001
50. Conzen PF, Vollmar B, Habazettl H, Frink EJ, Peter K, Messmer K. Systemic and regional hemodynamics of isoflurane and sevoflurane in rats. *Anesth Analg* (1992) 74(1):79–88. doi:10.1213/00000539-199201000-00014
51. Lee JS, Morrow D, Andresen MC, Chang K. Isoflurane depresses baroreflex control of heart rate in decerebrate rats. *Anesthesiology* (2002) 96(5):1214–22. doi:10.1097/00000542-200205000-00026
52. Tsubota T, Ohashi Y, Tamura K, Miyashita Y. Optogenetic inhibition of Purkinje cell activity reveals cerebellar control of blood pressure during postural alterations in anesthetized rats. *Neuroscience* (2012) 210:137–44. doi:10.1016/j.neuroscience.2012.03.014
53. Paton JF, La Noce A, Sykes RM, Sebastiani L, Bagnoli P, Ghelarducci B, et al. Efferent connections of lobule IX of the posterior cerebellar cortex in the rabbit – some functional considerations. *J Auton Nerv Syst* (1991) 36(3):209–24. doi:10.1016/0165-1838(91)90045-5
54. Paton JF, Rogers WT, Schwaber JS. The ventrolateral medulla as a source of synaptic drive to rhythmically firing neurons in the cardiovascular nucleus tractus solitarius of the rat. *Brain Res* (1991) 561(2):217–29. doi:10.1016/0006-8993(91)91598-U
55. Holmes MJ, Cotter LA, Arendt HE, Cass SP, Yates BJ. Effects of lesions of the caudal cerebellar vermis on cardiovascular regulation in awake cats. *Brain Res Bull* (2002) 938(1–2):62–72. doi:10.1016/S0006-8993(02)02495-2
56. Bradley DJ, Ghelarducci B, Paton JF, Spyer KM. The cardiovascular responses elicited from the posterior cerebellar cortex in the anaesthetized and decerebrate rabbit. *J Physiol* (1987) 383:537–50. doi:10.1113/jphysiol.1987.sp016427
57. Bradley DJ, Ghelarducci B, Spyer KM. The role of the posterior cerebellar vermis in cardiovascular control. *Neurosci Res* (1991) 12(1):45–56. doi:10.1016/0168-0102(91)90099-K
58. Balaban CD, Beryozkin G. Vestibular nucleus projections to nucleus tractus solitarius and the dorsal motor nucleus of the vagus nerve: potential substrates for vestibulo-autonomic interactions. *Exp Brain Res* (1994) 98(2):200–12. doi:10.1007/BF00228409
59. Guyenet PG. The sympathetic control of blood pressure. *Nat Rev Neurosci* (2006) 7(5):335–46. doi:10.1038/nrn1902
60. Guyenet PG, Koshiya N, Huangfu D, Baraban SC, Stornetta RL, Li YW. Role of medulla oblongata in generation of sympathetic and vagal outflows. *Prog Brain Res* (1996) 107:127–44. doi:10.1016/S0079-6123(08)61862-2
61. Guyenet PG, Stornetta RL, Schreihofen AM, Pelaez NM, Hayar A, Aicher S, et al. Opioid signalling in the rat rostral ventrolateral medulla. *Clin Exp Pharmacol Physiol* (2002) 29(3):238–42. doi:10.1046/j.1440-1681.2002.03636.x
62. Henderson LA, James C, Macefield VG. Identification of sites of sympathetic outflow during concurrent recordings of sympathetic nerve activity and fMRI. *Anat Rec (Hoboken)* (2012) 295(9):1396–403. doi:10.1002/ar.22513
63. Di Girolamo E, Di Iorio C, Leonzio L, Sabatini P, Barsotti A. Usefulness of a tilt training program for the prevention of refractory neurocardiogenic syncope in adolescents: a controlled study. *Circulation* (1999) 100(17):1798–801. doi:10.1161/01.CIR.100.17.1798

64. Yates BJ, Jian BJ, Cotter LA, Cass SP. Responses of vestibular nucleus neurons to tilt following chronic bilateral removal of vestibular inputs. *Exp Brain Res* (2000) 130(2):151–8. doi:10.1007/s002219900238
65. James C, Stathis A, Macefield VG. Vestibular and pulse-related modulation of skin sympathetic nerve activity during sinusoidal galvanic vestibular stimulation in human subjects. *Exp Brain Res* (2010) 202(2):291–8. doi:10.1007/s00221-009-2131-8
66. Hammam E, Dawood T, Macefield VG. Low-frequency galvanic vestibular stimulation evokes two peaks of modulation in skin sympathetic nerve activity. *Exp Brain Res* (2012) 219(4):441–6. doi:10.1007/s00221-012-3090-z
67. El Sayed K, Dawood T, Hammam E, Macefield VG. Evidence from bilateral recordings of sympathetic nerve activity for lateralisation of vestibular contributions to cardiovascular control. *Exp Brain Res* (2012) 221(4):427–36. doi:10.1007/s00221-012-3185-6
68. Goldberg JM, Fernandez C, Smith CE. Responses of vestibular-nerve afferents in the squirrel monkey to externally applied galvanic currents. *Brain Res* (1982) 252(1):156–60. doi:10.1016/0006-8993(82)90990-8
69. Goldberg JM, Smith CE, Fernández C. Relation between discharge regularity and responses to externally applied galvanic currents in vestibular nerve afferents of the squirrel monkey. *J Neurophysiol* (1984) 51(6):1236–56.
70. Courjon J, Precht W, Sirkin D. Vestibular nerve and nuclei unit responses and eye movement responses to repetitive galvanic stimulation of the labyrinth in the rat. *Exp Brain Res* (1987) 66(1):41–8. doi:10.1007/BF00236200
71. Yates B, Goto T, Bolton P. Responses of neurons in the rostral ventrolateral medulla of the cat to natural vestibular stimulation. *Brain Res* (1993) 601(1):255–64. doi:10.1016/0006-8993(93)91718-8
72. DeStefino VJ, Reighard DA, Sugiyama Y, Suzuki T, Cotter LA, Larson MG, et al. Responses of neurons in the rostral ventrolateral medulla to whole body rotations: comparisons in decerebrate and conscious cats. *J Appl Physiol* (2011) 110(6):1699–707. doi:10.1152/japplphysiol.00180.2011
73. Murray AR, Atkinson L, Mahadi MK, Deuchars SA, Deuchars J. The strange case of the ear and the heart: the auricular vagus nerve and its influence on cardiac control. *Auton Neurosci* (2016) 199:48–53. doi:10.1016/j.autneu.2016.06.004
74. Tanaka K, Abe C, Sakaida Y, Aoki M, Iwata C, Morita H. Subsensory galvanic vestibular stimulation augments arterial pressure control upon head-up tilt in human subjects. *Auton Neurosci* (2012) 166(1–2):66–71. doi:10.1016/j.autneu.2011.10.003

Conflict of Interest Statement: The authors declare that the research was conducted in the absence of any commercial or financial relationships that could be construed as a potential conflict of interest.

Copyright © 2017 Cohen, Martinelli, Xiang, Raphan and Yakushin. This is an open-access article distributed under the terms of the Creative Commons Attribution License (CC BY). The use, distribution or reproduction in other forums is permitted, provided the original author(s) or licensor are credited and that the original publication in this journal is cited, in accordance with accepted academic practice. No use, distribution or reproduction is permitted which does not comply with these terms.



A Historical View of Motion Sickness—A Plague at Sea and on Land, Also with Military Impact

Doreen Huppert^{1*}, Judy Benson² and Thomas Brandt¹

¹ Institute for Clinical Neurosciences, German Center for Vertigo and Balance Disorders, Ludwig-Maximilians University, Munich, Germany, ² Institute for Clinical Neurosciences, Ludwig-Maximilians University, Munich, Germany

OPEN ACCESS

Edited by:

Bernard Cohen,
Icahn School of Medicine at Mount
Sinai, USA

Reviewed by:

Catherine Cho,
New York University, USA
Michael Schubert,
Johns Hopkins University, USA

***Correspondence:**

Doreen Huppert
doreen.huppert@med.
uni-muenchen.de

Specialty section:

This article was submitted
to Neuro-otology,
a section of the journal
Frontiers in Neurology

Received: 19 December 2016

Accepted: 13 March 2017

Published: 04 April 2017

Citation:

Huppert D, Benson J and Brandt T (2017) A Historical View of Motion Sickness—A Plague at Sea and on Land, Also with Military Impact.
Front. Neurol. 8:114.
doi: 10.3389/fneur.2017.00114

Seasickness and its triggers, symptoms, and preventive measures were well known in antiquity. This chapter is based on an analysis of descriptions of motion sickness, in particular seasickness, in ancient Greek, Roman, and Chinese literature. A systematic search was made from the Greek period beginning with Homer in 800 BC to the late Roman period and ending with Aetios Amidenos in 600 AD, as well as in the Chinese medical classics dating from around 300 AD. Major aspects are the following: body movements caused by waves were identified in all cultures as the critical stimuli. The ancient Greeks and Romans knew that other illnesses and the mental state could precipitate seasickness and that experienced sailors were highly resistant to it (habituation). The Chinese observed that children were particularly susceptible to motion sickness; they first described the type of motion sickness induced by traveling in carts (cart-sickness) or being transported on a litter or in a sedan chair (litter-sickness). The western classics recommended therapeutic measures like fasting or specific diets, pleasant fragrances, medicinal plants like white hellebore (containing various alkaloids), or a mixture of wine and wormwood. The East knew more unusual measures, such as drinking the urine of young boys, swallowing white sand-syrup, collecting water drops from a bamboo stick, or hiding earth from the kitchen hearth under the hair. The Greek view of the pathophysiology of seasickness was based on the humoral theory of Empedokles and Aristoteles and differed from the Chinese medicine of correspondences, which attributed malfunctions to certain body substances and the life force Qi. Many sources emphasized the impact of seasickness on military actions and famous naval battles such as the Battle of the Red Cliff, which marked the end of the Han dynasty in China, or the defeat of the Spanish Armada by the English in 1588. A peculiar form of motion sickness is associated with Napoleon's camel corps during the Egyptian campaign of 1798/1799, a sickness induced by riding on a camel. Thus, motion sickness in antiquity was known as a physiological response to unadapted body motions during passive transportation as well as a plague at sea.

Keywords: seasickness, cart-sickness, litter-sickness, camel-sickness, Chinese antiquity, Greek antiquity, Roman antiquity, Red Cliff Battle

INTRODUCTION¹

Travel by sea was an important development in the history of mankind, for with it trade began on an even wider scale than was possible on land. Professional sailors were in demand; however, as the classical authors East and West inform us, not everyone was suited. Ruler and ruled alike could suffer from the so-called “plague at sea,” i.e., seasickness. The clinically most relevant facts about seasickness were already described in the Greek and Roman classics: triggers and susceptibility, symptoms, preventive measures, and therapy (1). The Chinese medical classics distinguished several forms of travel sickness, and each form had its own written character (2).

Medical knowledge of the times was initially limited and typically dominated by fears and superstitions. In the West, the Greek *Empedokles* was the first to propose a theory to explain human nature and illnesses: the four humors or body fluids (yellow bile, phlegm, black bile, and blood) had to be in equilibrium for a harmonious personality and health. Any imbalance led to deviation from normal and to illness. The theory continued to be influential into medieval times. In particular, it was the primary source for Greek, Roman, and medieval explanations of seasickness. In the East, belief in magic and charms lasted longer, perhaps because of the dominating quasi scientific theory of the medicine of correspondences. This theory connected climatic phenomena, cardinal directions, and calendric constellations with the actions of specific forces in the world and with the supply of the life force (Qi) and blood (xue) in the human body.

HISTORICAL TEXT SOURCES

Beginning with the works of *Homer* (ca. 800 BC) and ending with the work of *Aetios Amidenos*, we searched Greek and Roman texts up to 600 AD (Table 1). This search focused on terms like “ναυτία, ναυσία, ναῦς, nausea, navis” and their linguistic derivatives such as “ναυτιάω, ναυσιάω, ναυσιάσις, ναυτιῶντι, nauseare, nautea” (see Etymology and Terminology) in the dictionaries *Totius Latinitatis lexicon* (3), *Georges* (4), and *Thesaurus Linguae Latinae* (5) as well as in the commentaries on the citations and cross-references. The most important original sources included texts by *Hippokrates*, *Aristoteles*, *Plautus*, *Cicero*, *Celsus*, *Seneca Pater* and *Seneca Minor*, *Plinius*, *Plutarchos*, *Ovid*, *Juvenal*, *Lucian*, *Philostratos*, *Gellius*, and *Galenos* (see Table 1 in which all classical sources cited are listed in alphabetical order by author). Furthermore, secondary literature on the history of seasickness (6–10) and a comprehensive doctoral dissertation on seasickness in antiquity (11) were searched.

To analyze the Chinese historical texts, we first searched primarily for specific terms for seasickness in the Internet and in modern dictionaries (12). The dictionaries indicate which Chinese characters are used and cite classical works in which they appear. There have always been attempts throughout the

Chinese tradition to record and summarize large encyclopedic works, the last and most important of which is the *Siku quanshu* (Encyclopedia in four parts) from 1782. In a second step, the different words used for seasickness were entered into the most important databases of full texts, allowing selection of relevant text passages. The immense written tradition of Chinese culture is, nowadays, readily accessible in databases like *Scripta Sinica*, *The Complete Classics Collection of Ancient China*, *The Treasure of National Culture*, the *Siku quanshu*, *The Chinese Text Project*, and *Dissertations of China* (Table 2). We concentrated on the characters for the different types of dizziness: ship-influence, cart-influence, and wave-influence. Search words included the various concepts of dizziness: (1) 注船 zhuchuan, ship-influence, (2) 注車 zhuche, cart-influence, (3) 痘船 zhuchuan, ship-influence (different character), (4) 注浪 zhuliang, waves-influence, (5) 量車 yunche, cart-dizziness, (6) 量船 yunchuan, ship-dizziness, (7) 苦船 kuchuan, ship-illness, (8) 苦车 kuche, cart-illness, and (9) 船疰 chuanzhu, ship-influence (different character). The third part of the search involved the analysis of relevant text passages, in particular the sea battle of Chibi, during which seasickness evidently played a decisive role. See Table 3 for a chronological list of citations from the original Chinese works.

HISTORICAL THEORIES OF THE MECHANISMS UNDERLYING SEASICKNESS

Humoral Theory—From Greek and Roman to Medieval Times

The classical authors tried to explain disorders in general within the framework of the humoral theory of *Empedokles*, which was valid at that time: the four body fluids (“χολή” = yellow bile, “φλέγμα” = phlegm, “μέλαινα χολή” = black bile, “αἷμα” = blood) were said to be at such times out of balance (13). *Aristotle* was the first to explain seasickness on the basis of the humoral theory. One of his students and eventual successor, the philosopher *Theophrastus* also used the humoral theory to analyze seasickness. Later, the Roman stoic philosopher *Seneca the Younger*, a medical layman, delved deeper. He localized seasickness in the stomach. The Latin “stomachus” or the Greek “στόμαχος” at that time referred not only to the anatomic organ of the stomach but also to the esophagus. For *Seneca*, an important feature of seasickness was the bile vomited by the seasick. He graphically described a bout of seasickness as “a convulsion of the bile.”

Medieval European medicine observed correspondences between the heavenly bodies, the fluids in the human body, the temperaments, and illnesses by means of which the phenomena of the macrocosm (world) and the microcosm (man) were ordered and divined.

Chinese Medicine of Correspondences and Ancient Magic

A passage from the book *Chi shui yuan zhu* (Pearls of wisdom lifted out of the purple sea) by *Sun Yikui* from 1596 shows a similar interest in bile (14):

¹The names of the ancient authors are written in italics; their writings and citations from them are written in bold. All other authors and titles appear in a normal font. Throughout the text, we have either quoted directly the original sources and their translations (quotation marks) or we have paraphrased them for more immediacy.

TABLE 1 | Classical Roman and Greek sources describing seasickness, alphabetized by author [mod. after Huppert et al. (1)].

Author	Biographical data	Opus	Text source/	Publisher
Aetios Amidenos Aëtios of Amida	6th c. AD Medical books	Logon iatrikon biblioi	Corpus Medicorum Graecorum, Vol VIII, 1. Oliveri A. (ed.)	Leipzig, Berlin, 1935
Aretaeus Cappadocus	81–138 AD The extant works	Opera quae supersunt	Therapeutics of chronic affections. Book II. Adams F. (ed., trans.)	Printed for the Sydenham Society, London, 1956
Ariston Chiou Ariston of Chios	2nd c. BC Ancient stoicism: the editions of fragments and <i>testimonia</i>	Stoicorum veterum fragmenta	Bd. I, Zeno et Zenonis discipuli. V. Arnim H. F. (ed)	Leipzig, 1905
Aristoteles Aristotle	384–322 BC Problems	Problemata physika	Flashar H. (ed., trans.)	Wissenschaftliche Buchgesellschaft, Darmstadt, 1962
Athenaios Athenaios of Naukratis	Late 2nd c. AD Banquet of the learned	Deipnosophistai	Book XV, Garlands (Loeb Classical Library 519) Olson S. D. (ed., trans.)	Harvard University Press, Cambridge, London, 2012
Caesar (Caius Julius)	100–44 BC The civil war	Bellum civile	Book III (Loeb Classical Library Vol 39). Peskett A. G. (ed., trans.)	Heinemann, London, The Macmillan Co., New York, 1914
Celsus (Aulus Cornelius)	25 BC–50 AD On medicine	De Medicina	Vol. I (Loeb Classical Library 292). Spencer W. G. (ed., trans.)	Heinemann, London, Harvard University Press, Cambridge, 1935
Cicero	106–43 BC Letters to his friends	Epistulae ad familiares	Vol. III, Epistulae ad familiares, XVI.XI. (Loeb Classical Library Vol 230N). Williams W. G. (ed., trans.)	Heinemann, London, Harvard University Press, Cambridge, 1940
Galenos	129–199 AD Aphorisms of Hippocrates and Galen with commentaries	Hippokratou aphorismoi kai Galenou eis autous hypomnemata	Vol XVII, 1,2; XVIII, 1. Claudi Galeni opera omnia. Kühn C. G. (ed)	Leipzig, 1829
Gellius Aulus	125–180 AD Attic nights	Noctes Atticae	Auli Gelli Noctes Atticae cum indicibus locupletissimis	Tauchnitz, Lipsiae, 1835
Hesychios Alexandrinos Hesychios of Alexandria	5th/6th c. AD Alphabetical collection of all words	Synagogae pason Lexeon kata Stoicheion	Hesychii Alexandrini Lexicon, Schmidt M. (ed.)	Jena, 1867
Hippokrates	460–370 BC Aphorisms	Aphorismoi	IV.VIII.-XV. (Loeb Classical Library Vol 150) Jones W. H. S. (ed., trans.)	Heinemann, London, Harvard University Press, Cambridge, 1959
Homer	8th c. BC The Odyssey	Odysseias	Vol. I, V.304–330; Vol I, V. 442–466 (Loeb Classical Library Vol 104) Murray AT (ed., trans.)	Harvard University Press, Cambridge, Heinemann, London, 1945
		Odysseias The Odyssee	Schadewaldt W. (ed., trans.)	Artemis Verlag, Zürich, 1966
Horatius Horace	65–8 BC Epistles	Epistulae	I.I.62–85 (Loeb Classical Library Vol 194). Rushton Fairclough H. (ed., trans.)	Heinemann, London, Harvard University Press, New York, 1942
Juvenal	60–130 AD Satires	Saturae	Satire VI (Loeb Classical Library Vol 91N). Ramsay GG (ed., trans.)	Heinemann, London, Putnam's Sons, New York, 1928
Livius Titus	59 BC–17 AD Hannibal's War	Ab urbe condita	Lat.: Book XXI, 25 Engl.: Book 21, chapters 25–27	Oxford University Press, 1929 (lat.), 2006 (engl.)
Lucian	120–180 AD Charon	Charon	Vol. II (Loeb Classical Library Vol 54). Harmon AM (ed., trans.)	Heinemann, London, Putnam's Sons, New York, 1919
		Toxaris	Vol. V (Loeb Classical Library Vol 302). Harmon AM (ed., trans.)	Heinemann, London, Harvard University Press, New York, 1962
		Hermotimus or the rival philosophies	Vol. VI (Loeb Classical Library Vol 430). Kilburn K (ed., trans.)	Heinemann, London, Harvard University Press, Cambridge, 1949

(Continued)

TABLE 1 | Continued

Author	Biographical data	Opus	Text source/	Publisher
Macer, Aemilius (Pseud.)		De viribus herbarum About Herbal Plants	Choulant L (ed., trans.)	Leopoldi Vosii, Leipzig, 1932
Martial	40–104 AD	Martialis Epigrammata Epigrams	Book IV.XXXVII (Loeb Classical Library Vol 94). Ker WCA (ed., trans.)	Heinemann, London, Putnam's Sons, New York, 1919
Oreibasios	325–403 AD	Oreibasiou iatrikai synagogai Collection of medical relics	Corpus Medicorum Graecorum, Vol VI.1.1. Raeder I (ed.)	Leipzig, Berlin, 1928
		Oreibasiou synopsis pros Eustathion ton huion Synopsis to Eustathium	Corpus Medicorum Graecorum, Vol VI.3. Raeder I (ed.)	Leipzig, Berlin, 1926
Ovid	43–18 AD	Amores The Art of Love, and Other Poems	The remedies of love (Loeb Classical Library Vol 232). Mozley J. H. (ed., trans.)	Heinemann, London, Harvard University Press, Cambridge, 1957
Petronius	14–66 AD	Satyricon	(Loeb Classical Library Vol 15). Peskett M. (ed., trans.)	Heinemann, London, The Macmillan Co., New York, 1913
Philostratos	170–247 AD	Ta es ton Tyanea Apollonion The life of Apollonius of Tyana	Vol. I, book IV (Loeb Classical Library Vol 16N). Conybeare F. C. (ed., trans.)	Heinemann, London, The Macmillan Co., New York, 1912
Plato	428/7–348/7 BC	Nomoi Laws	Vol. I, Laws, book I (Loeb Classical Library Vol 187). Bury R. G. (ed., trans.)	Harvard University Press, Cambridge, Heinemann, London, 1940
Plautus	255–184 BC	Amphytrion	Vol I (Loeb Classical Library Vol 60). Nixon N. (ed., trans.)	Heinemann, London, Putnam's Sons, New York, 1916
Plinius (the Elder)	23–79 AD	Historiae naturales Natural History	Vol VI, libri XX, XXI and Vol VII, liber XXVII (Loeb Classical Library Vols 392, 393). Jones W. H. S. (ed., trans.)	Harvard University Press, Cambridge, Heinemann, London, 1951, 1956
Plutarchos Plutarch	40–120 AD	Moralia. Aitiae physikai Natural phenomena	Vol XI (Loeb Classical Library Vol 322). Pearson L, Sandbach F. H. (trans.), Capps E. (ed.)	Heinemann, London, Harvard University Press, Cambridge, 1965
		Moralia. Hygieina parangelmata Advice about keeping well	Vol. II, 86B–171F., 126 (Loeb Classical Library Vol 222). Babbitt FC (ed., trad.)	Harvard University Press, Cambridge, Heinemann, London, 1962
		Politika parangelmata Precepts of statecraft	Vol X, 798 (Loeb Classical Library Vol 321). Fowler H. N. (trad.), Warmington E. (ed.)	Heinemann, London, Harvard University Press, Cambridge, 1969
Pseudo-Apuleius Platonicus	4th c. AD	Herbarius Herbarium	Corpus Medicorum Latinorum, Vol IV. Howald E, Sigerist H. E. (eds.)	Leipzig, Berlin, 1927
Semonides	7th/6th c. BC	Iamboi	Anthologia lyrica Graeca 3: Iamborum scriptores. Diehl E. (ed.)	Teubner, Leipzig, 1952
Seneca Pater Seneca the Elder	54 BC–39 AD	Suasoriae The Suasoriae of Seneca the Elder	(Loeb Classical Library Vol 464). Edward W. A. (ed., trans.)	Harvard University Press, Cambridge, New York, 1928
Seneca Minor Seneca the Younger	4 BC–65 AD	Ad Lucilium Epistulae Morales The Epistles of Seneca	Vol. I, Epistle LIII (Loeb Classical Library Vol 77). Gummere R. M. (ed., trans.)	Harvard University Press, Cambridge, Heinemann, London, 1979
Soranos	2nd c. AD	Peri gynaikēion On Midwifery and the Diseases of Women	Lüneburg H. (ed., trans.), Huber J. C. (ed.)	Lehmann, München, 1842
Theophrastus Theophrast	371–287 BC	Peri phyton historias Enquiry into plants	Wimmer F. (ed.)	Paris, 1866

"Later due to seasickness she vomited up a number of bowls of saliva, her condition did not improve, it originated in her observation of [her own] vomited blood and in her condition

of liver stagnation." However, the dominating feature of Chinese medicine is Qi, the body's life force. If it flows incorrectly or is agitated by emotions, problems arise. For example, liver stagnation

TABLE 2 | Important databases of the written tradition of ancient Chinese culture [mod. after Brandt et al. (2)].

Scripta Sinica: the largest Chinese full-text database with an enormous breadth of historical materials. More than 460 titles and 402,000,000 characters of materials pertaining to the traditional Chinese classics are categorized. It contains almost all of the important Chinese classics, especially those related to Chinese history

The Complete Classics Collection of Ancient China: The Gujin tushu jicheng 古今圖書集成, compiled by Chen Menglei and co-workers. It was published with movable copper type in 1726–1728 AD and is the largest reference book historically compiled in China (*leishu*) to have been printed (6,109 subsections; 852,408 pages). Each subsection contains excerpts from sources dating from the beginnings of writing to the 17th century AD. All were selected from an eighteenth-century standpoint

The Treasure of National Culture: The Guoxue baodian 国学宝典 is the largest volume in Chinese classical literature and covers most varieties of subjects in Chinese classical literature. It contains a database of more than 50,000 poems from all epochs, a number of notebooks 笔记, theater pieces, and novels (白话 and 文言). By 2012 AD, the database contained more than 4,000 titles

The encyclopedia **Siku quanshu:** it provides an electronic database published by the Chinese University of Hong Kong and Digital Heritage Publishing Ltd., consisting of the complete contents, in full text and images, of the 3,460+ titles of the Wenyuange edition of the **Siku quanshu** (1,782) plus a few other useful tools. The staggering 800 million characters are arranged by almost 2 million titles

The Chinese Text Project: an ancient text database containing the full text of various Chinese texts of philosophical, historical, or linguistic interest from the pre-Qin era through to the Han dynasty and beyond. <http://ctext.org/>

Dissertations of China: it collects dissertations, master theses, and post-doc papers from PRC universities, graduate schools, and research institutes. Starting with the year 1980 and as of the year 2012, about 2.3 million qualification works had been provided in searchable full text

is said to occur due to an incorrect flow of Qi—the life force in the body which is generally triggered by such internal factors as emotional agitation.

In contrast to the Greeks and Romans who focused on the stomach as the site of the causes of dizziness, the Chinese emphasized the liver and the eyes. They drew attention to the interconnection between the liver and eyes already in the 4th century BC, but interpreted dizziness to be an optical phenomenon and thus a malfunction of the eyes. The most important Chinese character for dizziness was 眩 xuan, which consists of the phonetic character xuan on the right and a semantic indicator “eye” on the left. This character stands for the semantic field of darkness, black, unsureness, but also suggests the pronunciation of the character. Thus an image is evoked of how it becomes dark before the eyes during dizziness. The dictionaries indicate that the character refers to different types of dizziness which were never really differentiated from each other. The early dictionaries [Shuowen Jiezi, ca. 1st century (15)] use the character xuan to refer to visual malfunction or movement and chaos.

Based on the systematic correspondences of specific forces in the macro- and microcosm, the quasi-scientific Chinese medical theory is called a medicine of correspondences. Dizziness is a good example of how the Chinese understood this term: certain elements in the macrocosm like wood and wind were connected with the organs of the liver and the eyes of the microcosm. The following often repeated citation comes from **Huangdi Neijing**

Suwen (15): “[diseases with] wind [that causes] tumbling and dizziness belong without exception to the liver.” Thus, in the case of optical phenomenon, the liver is immediately considered the cause.

Another organ (in our modern meaning) that was associated with the phenomenon of dizziness is the brain. Although the brain plays no role in Chinese medicine, belonging neither to the yin organs (heart, spleen, lungs, kidneys, liver) nor the yang organs (small intestine, stomach, large intestine, bladder, gallbladder), it was apparently considered an organ in which the substance “marrow” was stored. Marrow is another word for the spinal cord. Thus, in one of the oldest and most fundamental texts of Chinese medical theory, the Yellow Emperor’s Inner Canon—Axis of the forces (Huangdi Neijing Lingshu (15)), there is a description of height intolerance: a pathogen is said to enter through the neck, make the brain roll around, and as a result the interconnection to the eyes becomes taught, causing dizziness. This suggests there was anatomical knowledge of a connection between the brain and the eyes. It is interesting that this very clear and mechanistic description of the cause of dizziness was taken over also in later works. It apparently was based on a theory of anatomy, which was not thematized thereafter. In general, the ancient Chinese with very rare exceptions never investigated the anatomy of the human body.

Different scholars and physicians have made various subdivisions, for example, essences (jing) and blood (xue) were conceived as implementations or various aggregate conditions of the same life force Qi. Assertions about the significance of these substances in connection with dizziness appear in the earliest sources:

If Qi is insufficient above, the brain is not sufficiently filled by it, the ears suffer a ringing noise, the head is bent low by it, the eyes [experience] dizziness.

Here the brain is to be understood as the “sea of marrow,” i.e., the storage site of the marrow—a body substance. Thus, dizziness occurs in connection with tinnitus and an imbalance of the head due to deficient Qi in the head (16). The following citation from the chapter “Discussion of the sea” refers to the same subject matter: “Is the sea of marrow not sufficiently filled, the brain begins rotating around, the ears ring, the calves/shins suffer from sour pains and the veil-dizziness (xuannao) appears, the eyes can see nothing and passivity and hypersomnia occur.” Besides a deficit of Qi in the head, numerous other sick conditions of dizziness, which can be ascribed to a lack or surplus of substances or “energies” in the body, are described: “dizziness due to increasing fire,” due to phlegm, to a deficit in yin, a deficit in yang, a surplus of yang, and a blood deficit.

ETYMOLOGY AND TERMINOLOGY

Greek and Roman Times

In Greek antiquity, the term used to express the experience of seasickness (nausea) was based on the word for ship: “ναῦς” [naus]. The corresponding verb meaning “I am seasick” was “ναυτιάω” [nautiao] or “ναυσίω” [nausiao]. The Latin words “nausea” and “nauseare” were derived from the Greek. The meaning of these

TABLE 3 | Chronological overview of relevant text passages in the original Chinese works on cart-sickness and seasickness [mod. after Brandt et al. (2)].

Time	Concept	Works	Author
ca. 300 AD	Cart-influence and ship-influence (注車注船, zhuche zhuchuan, literally, influence-cart, influence-ship)	Zhou hou bei ji fang 肘后备急方 (emergency remedies/formulae to carry behind the elbows)	Ge Hong (281–341) 葛洪;
610 AD	Cart-influence and ship-influence	Zhu bing yuan hou lun 诸病源侯论 (discussion about signs and causes of all illnesses)	Chao Yuanfang 巢元方 (ca.550–630)
725~777 AD	苦车 Cart-illness (literally, bitterness-cart)	Poem: 《癸卯岁赴南丰道中闻京师失守寄权士繇韩幼深》	Du Guji 独孤及 (725~777)
983 AD	苦车 Cart-illness (literally, bitterness-cart)	Taiping yulan 太平御覽, (imperial notes from the Taiping era); <i>juan</i> 918 卷九百一十八.羽族部五 (found in Gujin tushu jicheng)	
12th century AD	Ship-illness, cart-illness (苦船 kuchuan 苦车 kuche; literally, illness-ship and illness-cart)	Xi xi cong yu 西溪叢語 (collection of talks about the Western stream)	Yao Kuan 姚寬 (1105–1162)
14th century AD	注船 Ship-influence	Danxi Xinfǎ 丹溪心法 (core of the teachings of [Zhu] Danxi)	Zhu Danxi 朱丹溪 (1281–1358)
1578 AD	注車注船 Cart-influence and ship-influence	Ben cao gang mu 本草綱目 (Compiled medical material); Section Herbs 草部, 10th <i>juan</i> 凡十卷/第十三卷/草之二山草類下三十九種/徐長卿 (p 822) refers to the entry for the herbal substance Xú Zhǎng Qīng 徐長卿 RADIX CYNANCHI PANICULATI, Panicle Swallowwort Root	Li Shizhen 李時珍 (1518–1593)
1596 AD	注船 Ship-influence	Chi shui yuan zhu 赤水元珠 (Pearls of wisdom lifted out of the purple sea); Cited in Siku quanshu , Section on Medicine, 9th <i>juan</i> , 子部/醫家類/赤水元珠/卷九	Sun Yikui 孙一奎 (1538–1600)
17th/18th century AD	Ship-dizziness and cart-dizziness (晕船晕车 yunchuan yunche, literally, dizziness-ship and dizziness-cart)	Yan fang xin pian 驗方新編 (New collection of proven remedies); <i>juan</i> 16, various treatments [卷十六\杂治], ship-dizziness-cart-dizziness晕船晕车	Bao Xiang'ao 鮑相璈
18th century AD	注船注轿 Ship-influence and litter-influence	Tong su bian 通俗編 (Notebooks on miscellaneous things); <i>juan</i> 26. (Zhai Hao 翟灏, Tong su pian 《通俗編》-卷二十六) (in Guoxue Baodian)	Zhai Hao 翟灏 (?–1788)

words had been amplified already in antiquity: besides seasickness they also stood for a general sick feeling and vomiting as well as disgust and tedium (11). Examples of such amplification and diversification of the original meaning can be found in early texts of the Greek poet *Semonides*, who in the 7th/6th century BC already used “*vavτία*” to describe such a sick feeling. In the 5th/6th century AD *Hesychios Alexandrinos* presented an alphabetical dictionary on these different meanings of “*vavτία*” and “*vavσία*” and their derivatives. The connotation of seasickness in the word for sea travel was subsumed by the term “*vavτίωντι*” [nautionti], which he paraphrased with the words “κλύδωνι περιφερομένῳ” [klydoni peripheromeno]. The latter means “he whom the waves of the sea make dizzy.” Like many things in Greek culture, the Romans took over these multiple meanings. For example, the poet *Ovid* used “nausea” when describing a revolting meal and later *Martial* also used it to suggest disgust. Such multiplicity recalls the results of our search for the first descriptions of fear of heights in Greek and Roman antiquity. The Latin word “*caligo*” had multiple meanings: vertigo as a symptom occurring in the context of heights, but also metaphorically, as evoking feelings of exultation (17).

Despite all of these multiple meanings for antiquity, motion sickness was mainly connected with the sea and ships. Beginning

with the First Punic War in the second century BC (18), marine navigation became more important in classical antiquity. Many different sizes of boats were used (Figure 1), not only for trade but particularly for warfare.

Ancient China

Whereas the Greeks had observed the effect of the stimulus marine travel on individuals (cause and effect thinking), the ancient Chinese focused on the type of transport: ship, cart, etc. Only in modern times did this focus change. In ancient Chinese literature, for example in **Zhou hou bei ji fang** (emergency prescriptions/remedies to carry behind the elbow, around ca. 300 AD), the terms cart-influence (注车, zhu che) and ship-influence (注船, zhu chuan) are found. This first reference to illnesses due to motion is discussed by the author, a famous physician and alchemist, in a chapter on remedies to protect someone from evil forces, i.e., the influence of demons and corpses.

The poet *Du Guji* 独孤及 (725~777 AD) wrote a poem in which he uses the term cart-sickness (literally cart-bitterness). This poem can only be understood in the historical context of the collapse of the kingdom a few centuries earlier into a northern and a southern realm. In the early 3rd and 4th centuries AD,



FIGURE 1 | Roman rowing boat. Fragment of a wall painting of marine life from the Museo Nazionale Romano, Palazzo Massimo alle Terme, Rome (Dalla località Pietra Papa presso il Porto Fluviale di San Paolo lungo la via Portuense. 125–150 AD; private photograph Doreen Huppert).

many aristocrats fled from the northern barbarians, traveling south into the inaccessible mountainous regions in the province of Jiangzi.

长叹指故山，三奏归来词。不逢眼中人，
调苦车逶迤。

With a profound sigh they point to the unexpected mountains, already having thrice sung the Gulai Song. One will not see again those close to us, we move on, travel sick and weak

The work **Taiping yulan**, imperial records from the Taiping Era, an encyclopedia from the year 983 AD, refers to an alleged story from the records of Jin (Jin shu). The story is about an official named Chi Shen whose mother had a cart-illness. After she dies, he decides not to return her to her village with the cart, out of filial respect, and works for three years, sowing and reaping grain and raising chickens to earn enough money to transport the coffin home in style with eight horses and finally bury his mother. With slight variations, this story is found on Chinese internet sites as a copy of Jin (Jin shu, 九家舊晉書輯本).

The non-medical work **Xi xi cong yu** (notebooks) from the 12th century has an entry mentioning that people in the south use the term ship illness (苦船kuchuan), while people in the north say cart illness (/苦车 kuche).

今人不善乘船，谓之苦船；北人谓之苦车。

If people are not good at traveling by ship, it is called ship illness. People in the north call it cart illness.

The terms dizziness ship yunchuan (for seasickness) and dizziness cart yunche (for travel illness with the cart) (晕船晕车 yun chuan yun che) are common usage in **Yan fang xin pian** from the 17th/18th centuries and are still standard today. This alteration of the terminology is also seen in the fact that old citations continued to be used with the additional clarification “Today one



FIGURE 2 | An ancient form of human transportation. A litter was a vehicle without wheels which porters carried by means of wooden rails (see photograph). The cabin of such a litter, also called a sedan chair, could be enclosed for protection from the elements. According to our current understanding of the pathomechanism of motion sickness, this means that while the vestibular system sensed the movements during transportation, the visual system received no information about motion. Such a sensory mismatch is known to facilitate the occurrence of motion sickness. The Chinese called this “litter sickness” or “litter influence” (photograph: sedan chair, China, 1874/75; https://commons.wikimedia.org/wiki/File:Sedan_Chair_Carried_by_Four_Men._China,_1874-75_WDL1930.png).

calls this dizziness ship (yunchuan).” In the notebooks of *Zhai Hao* entitled **Tong su bian** (notebooks on miscellaneous things) there is in juan 14 in the chapter “Collection of the nunnery Pin Lu” an explanation of the word ship-influence-litter-influence. This is the sole proof for the concept litter-influence, but it is clear that the swaying movements can lead to a travel illness similar to that of seasickness. A litter is a conveyance for transporting persons who sit on a bed or couch suspended between two long poles and are thus carried (Figure 2). Such vehicles were not only used in China (jiao or wo) but also in ancient Rome (lectica or sella), pharaonic Egypt, and various other countries throughout the centuries (it was called a sedan chair in Britain). As the nascent investigation of Chinese medical manuscripts shows, the less-educated social classes resorted more often to therapeutic concepts from the realm of demons and other magic and religious beliefs, as was seen in the concepts of cart-influence and ship-influence (see above). These manuscripts, however, are not available in printed form and could not be evaluated for our study. The entry in **Xi xi cong yu** was quoted in numerous later works and continued to be handed down. In many versions, the quote reads “persons from the south do not travel well by ship, they have ship-illness, persons from the north call the illness cart-illness.” This may actually be related to the fact that the rivers in southern China play a much more significant role in transport and travel than in the more arid north.

The modern term for motion sickness in China is 运动病 (yundong bing). It can be subdivided into car sickness, train sickness, or also travel illness 晕车 (yunche, literally dizziness-car) and seasickness 晕船 (yunchuan, literally dizziness-ship) (19).

Various terms have been used in the Chinese written tradition to describe this phenomenon. The current term “yunche yunchuan,” i.e., travel illness and seasickness, first appeared in the 17th/18th centuries.

HISTORICAL KNOWLEDGE OF TRIGGERS, SYMPTOMS, SUSCEPTIBILITY, AND MENTAL STATE

Precipitating Stimuli

Several ancient Roman and Greek authors reported how wave-induced body motion was a predominant trigger and provoking factor of seasickness. According to *Horatius (Epistulae)*, the ship size appeared to be of no importance for the development of seasickness. The medical layman *Caius J. Caesar* referred to a causal connection between the high undulations of the open sea and seasickness in his *De bellum civile*. This was later emphasized by the Greek physician *Galenos* in his *Hippokratou aphorismoi*. *Oreibasios (Oreibasiou iatrikai synagogai)* cited *Antyllos* from the first century AD, who claimed that particularly pitching and tossing are triggers at sea. They occur less often near the shore where also seasickness is less frequent. This was confirmed by *Plutarchos* in his *Aitiae physikai*: seasickness is reported less often on rivers than on the open sea. The latter also mentioned unpleasant odors as provocative stimuli for seasickness in susceptible persons:

ἐν δὲ τῇ θαλάτῃ τήν τ' ὀσμὴν ἀηθείᾳ δυσχεραίνουσι καὶ φοβοῦνται, μὴ πιστεύοντες τῷ παρόντι, περὶ τοῦ μέλλοντος.

At sea, on the other hand, men find the smell disagreeable because of its strangeness, and not trusting the present weather to last, are anxious about what the future holds.

This was supported by *Caesar* and *Juvenal*, who also mentioned the “sickening smell” of bilgewater as a provocative factor.

While the Greeks primarily focused on the external world as the source of triggers, the Chinese, in accordance with their medical theory, basically emphasized internal imbalances or deficits of vital substances in the body. The external world, however, was also influential as the source of pathogens that could upset the body's harmonious balance. The search for the causes of symptoms like dizziness, height intolerance, or motion sickness took place in ancient China within the prevailing view of the body. In the case of dizziness, the external pathogen was primarily the wind, which was generally associated with movement. It was assumed that the wind could penetrate a weakened body and induce symptoms and cause illness. This was then reflected in the body by disordered movements and sudden appearances. The wind was described as an especially aggressive force that gets everything moving (tumbling and falling) and can lead to chaotic conditions in the world and to illness in the human body. It is also instrumental in promoting the entry of other factors such as heat, moisture, and cold. Its connection

with the liver, which was considered to play an important role in the storage of blood, could play havoc with the body. Blood is basically a material, and if there is a deficit of blood, the more mutable features of Qi cannot connect with it, thus leading to symptoms of an internal wind, which expresses itself in dizziness, tics, and twitches.

Symptoms

Several classical authors describe the various symptoms of a manifest seasickness. In his biography (*Ta es ton Tyanea Apollonion*), *Philostratos* mentioned the prodromal symptoms of seasickness: these included the inability to maintain a conversation, the absence of concentration, and a certain indifference.

...οὐ γάρ ναυτιῶν γε, ἢ ὑπὸ τοῦ πλοῦ πονηρῶς ἔχων ἀποστρέψῃ τοὺς λόγους, ἡ γὰρ θάλαττα, ὁρᾶς, ὡς ὑποτέθεικεν ἐαυτὴν τῇ νηὶ καὶ πέμπει.

For I am sure that it is not because you are seasick or in any way inconvenienced by the voyage, that you object to our conversation; for you see how smoothly our ship is wafted over her bosom by the submissive sea.

Bodily symptoms like nausea and vomiting are reported by, among others, *Petronius* and *Aretaeus*. The desiccative effects of vomiting were interpreted also in terms of a possible therapeutic effect for conditions like cephalgia, renal diseases, or elephantiasis. *Juvenal* vividly described how vertigo is sometimes manifested:

... tunc sentina gravis, tunc summus vertitur aer.

... the bilge-water then sickens her, the heavens go round and round.

Due to nausea, seasick persons are anorectic, have no desire for cooked, boiled, or fried food according to *Plutarchos* in his *Hygieina parangelmata*. Instead, they crave salty food, even if they later have to disgorge it. In modern medical terms, this suggests an electrolyte imbalance. Other authors, such as *Homer* and *Gellius*, stress the occurrence of faintness, apathy, and abulia during seasickness. A passage in *Homer's Odysseias* evokes the physical state of Ulysses, washed up on the beach:

...ό δ' ἄρ' ἀπνευστος καὶ ἀνανδος κεῖτ' ὀλιγηπελέων, κάματος δέ μιν αἰανὸς ἵκανεν.

...So he lay breathless and speechless, with scarce strength to move; for terrible weariness had come upon him.

Further, the association of anxiety and seasickness was recognized quite early. *Plato* was the first to emphasize this:

...καν δειλὸς ὁν ἐν τοῖς δεινοῖς ὑπὸ μέθης τὸν φόβου ναυτιᾶ;

... even though he be a coward and sea-sick with a kind of tipsy terror when danger comes?

In addition, *Gellius* mentions paleness of the face as a symptom arising together with anxiety. *Lucian* in *Hermotimus* adds headache:

ἀλλὰ ἀνάγκη ἐν τῷ πελάγει διαφέρεσθαι ναυτιῶντα
ώς τὸ πολὺ καὶ δεδιότα καὶ καρηβαροῦντα ὑπὸ τοῦ
σάου,...

... he must be tossed about the sea, usually sick and frightened and with a bad head from the swell, ...

In other classical texts, such as *Satyricon* by *Petronius*, symptoms of seasickness were considered relatively harmless, whereas *Plutarchos* in *Politika parangelmata* regarded them as a most distressing condition, in which one loses all self-control. *Plautus* stressed that seasickness may persist after sea travel, when leaving the ship and walking on stable land.

In ancient China, the source *Zhou hou bei ji fang* (300 AD) describes similar symptoms elicited as well during ship- or cart-travel ("Cart- and ship-influences"). Thus, afflicted individuals were described as suffering from agitation and pressure on the breast, headaches, and the urge to vomit.

Susceptibility

The Greek classical authors observed that professional sailors reacted differently to the sea than did novices to sea travel. For example, *Ariston Chiou* notes in a passage of *Stoicorum veterum fragmenta*:

Κυβερνήτης μὲν οὕτε ἐν μεγάλῳ πλοίῳ οὕτε ἐν μικρῷ
ναυτιάσει, οἱ δὲ ἄπειροι ἐν ἀμφοῖν.

Whereas a helmsman does not become seasick on a large ship or on a small boat, the inexperienced become seasick on both.

This description of unsusceptibility to seasickness, i.e., the result of repeated exposure to the stimulus, is now called habituation. Also *Livius* reported in his *Ab urbe condita* how many of Scipio's soldiers, especially those who were not accustomed to the sea, had to spend some time recuperating after travel before entering battle:

...necdum satis refectis ab iactatione maritima
militibus,...

... as his men were not yet fully recovered from the rigours of their sea voyage.

General illness was also regarded as a factor that augments susceptibility. *Cicero*, who suffered from seasickness as several passages in his *Epistulae* suggest, mentioned in the *Epistulae ad familiares* that it is not advisable to start a sea voyage when sick:

Festinare te nolo, ne nauseae molestiam suspicias
aeger et periculose hieme naves.

I would not have you to hurry yourself, lest you should have to suffer the agonies of sea-sickness in your feeble state, and lest a winter voyage should prove dangerous.

Lucian agreed in *Toxaris* that the ill will become seasick before anyone who is healthy and strong.

Ancient Chinese texts noted that children were particularly affected by cart travel and ship travel: they develop disorders of the heart, have headaches, and have to vomit. Susceptibility in children is described in *Zhou hou bei ji fang*:

(...)女子小兒多注车、注船、心闷乱、头痛吐(...)

many of the girls and boys [suffer] from cart-influence, ship-influence, pressure and disorder of the heart, headaches, and vomiting ...

A similar concept is found in *Zhu bing yuan hou lun*:

嬖子小兒注車船候 signs of cart- and ship-influence in small spoiled children, or 無間男子女人, 乘車船則心悶亂, 頭痛吐逆, 謂之注車、注船。特由質性自然, 非關宿挾病也。

It makes no difference whether boy or girl, if they travel with the cart or the ship and this leads to pressure and chaotic feelings in the heart, if they have headaches and vomit, then this is called motion sickness. It is due to the actual nature of the individual and is not related to any past or other disease still present.

We did not find any hint in the classical Greek and Roman texts that infants were particularly susceptible to seasickness. Today, it is well known that infants below the age of 1–2 years usually do not become seasick, whereas their susceptibility increases significantly with age and reaches a peak between the ages of 7–12 years, before it declines to the susceptibility of adulthood (20, 21).

Mental State/Psychological Predisposition

Caesar is one of several ancient Roman authors who emphasized that the prevailing mental state plays a role in developing seasickness. The satirical poet *Decimus Iunius Juvenal* also captures this aspect in a vivid and drastic scene in *Saturae* which evokes the suffering caused by seasickness without mentioning the word "nausea". In his Sixth Satire, the well-meant advice of a friend is given to a groom: "Don't get married." All the vices of women are described, even a piece of scandal from the times of Emperor Domitian (51–96 AD): Eppia the wife of a senator has set off for Egypt with her lover, a gladiator. Although she was always seasick when traveling by water with her husband, her inner feelings will protect her during this sea crossing with her lover. Psychological factors made the crossing possible at all.

...tunc sentina gravis, tunc summus vertitur aer.
Quae moechum sequitur, stomach valet. Illa mari-
tum convomit, haec inter nautas et prandet et errat
per puppem et duros gaudet tractare rudentis.

... the bilge-water then sickens her, the heavens go round and round. When she is following her lover, her stomach is robust; but as wife, she pukes all over her husband.

After the death of Caesar in 44 BC, the men of the second triumvirate (Octavian, Antonius, and Lepidus) took power. For Cicero, this meant that he was now considered an enemy of the state and had to flee the country. Traveling by ship as it was the fastest means of travel, Cicero suffered repeated bouts of seasickness until weary of life, he felt his will power broken. He could no longer flee, returned home, and took to his bed where he was assassinated by Anthony's soldiers (43 BC). The Roman writer and rhetorician *Seneca Pater* describes Cicero's fate in his *Suasoriae* from the first century AD, in which his aversion to the sea played a major role: forced to rest, he was assassinated,

...unde aliquotiens in altum provectum cum modo venti adversi rettulissent, modo ipse iactationem navis caecovolente fluctu pati non-posset, taedium tandem eum et fugae et vitae cepit, regressusque ad superiorem villam, quae Paulo post plus mille passibus a mari abest, 'moriar' inquit 'in patria saepe servata'.

... From there he traveled several times on the sea. However, soon the opposing winds forced him back; he could no longer bear the movements of the ship in the blindly whirling flood. Suddenly a great weariness to flee and even to live seized him. He turned back to his higher-lying villa, only about 1000 steps from the sea, saying "I will die in my fatherland, which I have often saved from annihilation."

Plutarch too was aware of the influence of an individual's emotions on his reaction to sea travel. Having extensively examined the various aspects of seasickness in *Aitiai physikai*, he was of the opinion that the psyche played a decisive role:

ουδὲν οὐν ὅφελος τῆς ἔξω γαλήνης, ἀλλὰ ἡ ψυχὴ σάλον ἔχουσα καὶ θορυβομένη συγκινεῖ καὶ ἀναπίμπλησι τὸ σῶμα τῆς ταραχῆς.

Thus the calm in their surroundings does them no good: their psychological tossing and being upset cause an accompanying disturbance in the body and infect it with their disorder.

Even quite bizarre behavior is said to result from seasickness. For example, *Lucian* in his description of Homer being transported by the ferryman Charon on a stormy river Styx in the Underworld has Charon witness Homer's bout of seasickness. He is said to vomit some passages from *The Odyssey*.

In Medieval England, William Shakespeare (1564–1616) evokes the psychological effects of seasickness. Three years before the defeat of the Spanish Armada, Shakespeare settled in London. A writer famous for his awareness of the interests of his rulers

and compatriots, he makes an unusual reference to seasickness in a rather surprising context in one of his most famous plays, *Romeo and Juliet*, finished in 1594. As Shakespeare is believed not to have traveled outside England, it is highly doubtful that he had first-hand experience of seasickness. Perhaps, he overheard descriptions of it in the pubs where the sailors of the main sea-faring country after Spain gathered or recycled them from another literary source. In the last act, last scene of the play before swallowing poison, Romeo takes leave of Juliet, who he mistakenly believes is dead, by saying

Come, bitter conduct, come, unsavoury guide!
Thou desperate pilot, now at once run on
The dashing rocks thy sea-sick weary barque!
Here's to my love!
[He drinks] (22)

In his despair, Romeo identifies with the "weary barque" that itself is seasick. Its pilot (the poison) crashes it onto the rocks, destroying it and extinguishing his anguish at the loss of Juliet.

THERAPY

Greek and Roman Approaches

Prevention

Some ancient authors reflected on how to prevent seasickness, most often emphasizing the importance of becoming accustomed to sea travels. The Greek author *Dieuches* who is cited by *Oreibasios* (*Oreibasiou iatrikai synagogai*) emphasized this as early as in the fourth century BC. Later, *Ariston* in the second century BC and *Aetios* in the 6th century AD in his *Logon iatrimon biblio* also stressed the role of what one would today call habituation. *Juvenal*, however, disagreed. He believed that the psyche was the most important factor in the development of seasickness and thus did not think that habituation was possible—either one got seasick or did not. Other prophylactic advice given by classical authors were to fixate the shore (*Athenaios*) and avoid looking at the rough, open sea. Further, it was recommended to smell pleasantly fragrant plants like thyme, mint, or quince (*Dieuches*—cited by *Oreibasios* in *Oreibasiou synopsis pros Eustathion ton huion*). A passage from a herbal book from the fifth century AD, which is based on Greek sources (*Herbarius, Pseudo-Apuleius Platonicus*), recommends grinding up wormwood and mint, mixing it with olive oil and wine vinegar, and then frequently rubbing the mixture into the nostrils. The remedy "wormwood" for preventing seasickness was also recommended in a pharmaceutical didactic poem found in the *Macer floridus*, a work from the Middle Ages which is based on classical sources:

Nausea non-poterit quemquam vexare marina,
Antea commixtam vino qui sumpserit illam
[absinthium].

Seasickness will not be able to torment him who drinks vermouth mixed with wine before setting off.

Lucian offered some advice in his **Hermotimus**, for example, to carefully observe the weather conditions and choose a reliable helmsman who is able to reduce upsetting ship motion by skillful steering maneuvers. Finally, *Soranos* at the beginning of the second century AD refers to nutrition, recommending fasting for 1 day before setting off on a sea voyage:

...διόπερ ἀνατάσει χρηστέον. Καὶ γὰρ οἱ πλέοντες συστολῇ χρησάμενοι πρὸ μᾶς ἡμέρας τὴν ναυτίαν οὐχ ὑπομένουσιν ἢ οὐκ ἐπὶ τοσοῦτον.

... Thus fasting is the proper thing to do. In this way the sailors who fast one day before the voyage do not get seasick at all or only slightly so.

Therapeutic Recommendations

The above-mentioned preventive measures such as pleasant fragrances or wormwood are also used as therapy for acute seasickness; *Plinius*, for example, described in his **Historiae naturales** certain aromatic plants and herbs that can be taken to control nausea. Among these were mallow, fennel, wild cumin, rose petals boiled in wine, mint, or wormwood. Many of these plants can be found in other ancient sources like the **Macer floridus** (see above). *Athenaios* reports on divine help from the goddess Aphrodite who was believed to send pleasing aromas:

'Η δὲ θεὸς (προσφιλῆς γὰρ τοῖς Ναυκρατίαταις ἦν) αἰφνίδιον ἐποίησε πάντα τὰ παρακείμενα αὐτῇ μυρρίνης χλωρᾶς πλήρη ὄδμῆς τε ἡδίστης ἐπλήρωσεν τὴν ναῦν ἥδη ἀπειρηκόσι τοῖς ἐμπλέουσιν τὴν σωτηρίαν διὰ τὴν πολλὴν ναυτίαν γενομένου τε ἐμέτου πολλοῦ':

The goddess – who was well-disposed to the inhabitants of Naucratis – immediately filled all the vessels that had been set before her with fresh myrtle, and the entire ship with a delicious scent, even though everyone on board had given up any hope of surviving, because they were so seasick, and there was a great deal of vomiting.

Dietary measures were also reported to be therapeutic by *Celsus*, a famous classical writer on medicine:

Is vero, qui navigavit et nausea pressus est, si multam bilem emovuit, vel abstinere a cibo debet vel paulum aliquid adsumere. Si pituitam acidam effudit, utique sumere cibum, sed adsueto leviorem: si sine vomitu nausea fuerit, vel abstinere vel post cibum vomere.

He too who on a voyage is troubled by seasickness, if he has vomited out a quantity of bile, should fast or take very little food. If he has spewed out sour phlegm, he may take food notwithstanding, but lighter than usual; if he has nausea without vomiting, he should either fast, or after food excite a vomit.

Similarly *Oreibasios* reports that fasting or restricting oneself to a certain diet, namely dry or boiled lentils with mint or bread,

pulverized in fragrant wine, can help. In case of continuous vomiting, sour honey was recommended. *Hippocrates*, who reported on seasickness in his **Aphorismoi**, recommended using the medicinal plant *Veratrum album* (white hellebore, “έλλεβόρος λευκός”), a violent gastrointestinal poison. The effective alkaloid-based emetic was widely used in antiquity, but therapeutic dosages differed from those currently used. *V. album* (white hellebore, Figure 3) contains five different alkaloids (rubijervine, pseudojervine, jervine, protoveratrine, and protoveratridine), which were first isolated by Salzberger (23). The habilitation thesis of Hahnemann (24) mentions that the contemporary white hellebore is thought to be identical to the plant referred to in classical texts. Its area of distribution includes the Alps, the Apennine mountains, and Eastern Europe. Several species of this genus also originated in Asia. The concentration of the alkaloid in the plant decreases with the increasing altitude of its habitat.



FIGURE 3 | *Veratrum album* (white hellebore, έλλεβόρος λευκός) contains five alkaloids (rubijervine, pseudojervine, jervine, protoveratrine, and protoveratridine), all of which are poisonous.

Frequently used in antiquity as an emetic. *Hippocrates* (460–370 BC) already recommended it for seasickness in his **Aphorismoi**. The plant originated in the moderate climate zones of Asia and Europe, where it is still found in the Alps at heights of 700–2,000 m and more. It grows best on meadows and pastures, preferably in moist, nitrogen-rich soil, and reaches a height of 160 cm (https://de.wikipedia.org/wiki/Wei%C3%9Fer_Germer) (25).

Chinese Recommendations

The physician and author *Zhu Danxi* (1281–1358) is considered one of the most important physicians of his time. The following entry appears in paragraph 29, in the third chapter of *Danxi Xinfa*, his book on vomiting;

注船大吐,渴飲水者即死,童便飲之最妙。(26)

Ship-influence with pronounced vomiting; those who have thirst and drink water will die, whereas it is very helpful to drink the urine of young boys.

A specific substance is discussed in *Ben cao gang mu* (Medical material organized by categories) from 1578. Its efficacy for cart- and ship-influence 注车注船 zhuche zhuchuan is also assessed as part of a definite remedy.

Reference is made here to the source *Zhou hou bei ji fang*.

注车注船:凡人登车船烦闷,头痛欲吐者。

Cart- and ship-influence describes the phenomenon of suffering from agitation and pressure on the breast, headaches and the urge to vomit when traveling on a cart or a ship.

An entry in *Yan fang xin pian* (New collection of tested remedies) from the 17th/18th century discusses the same phenomenon under the concept of ship-dizziness and cart-dizziness 1 晕船晕车 yun chuan yun che: “As regards head-dizziness (tou-yun) and vomiting caused by sitting on a ship, earnestly pray at the start of the trip to the palace of the goddess of sailors or to the place of the river and water spirits; this will bring peace. Or drink the urine of young boys, this has a wondrous effect, or take white sand-sirup, that's also effective. Another remedy is to collect water that drops from a long bamboo stick into a bowl, add this to boiling water, and drink the mixture; this too is effective. Another remedy: If you go on a ship, take some earth from the middle of the kitchen hearth and hide a piece under your hair; don't tell anyone, this gives peace. Or write the character for dirt/earth on your palms. If you then go on a ship, you will have nothing to fear. Earth can protect you from the meaning (threat) of water.”

HISTORICAL EVIDENCE OF MILITARY IMPACT

Roman Period

Titus Livius (59 BC–17 AD), a historian from Patavium (today known as Padua), spent a large part of his life in Rome. In his historical opus *Ab urbe condita* (Buch XXI, 26), it is obvious that the troops of Scipio who were unaccustomed to sea travel became seasick and needed time to recover. This is described in an episode from The Punic War (218–201 BC). Hannibal was marching with his troops in the direction of the estuary of the Rhone. To oppose him, Publius Cornelius Scipio Africanus Maior was moving 60 of his warships along the coast of Etruria and Liguria and along the regions of the Saluer toward Massilia,

modern-day Marseille. Unfortunately Scipio's soldiers, unaccustomed to sea travel, had become seasick. It was feared that Hannibal could begin crossing the Rhone at any moment. Fortunately, in the end, however, Scipio was able to allow his soldiers to take a rest to sufficiently recover: they did not have to immediately engage in a great battle with Hannibal upon landing.

...necdum satis refectis ab iactatione maritima militibus,...

... as his men were not yet fully recovered from the rigours of their sea voyage.

In the commentaries to his book *De bellum civile*, *Gaius Julius Caesar* (100–44 BC) reports how his troops crossed over from Brandisium (48 BC) (contemporary Brindisi) to the Greek mainland. The stormy weather swept some of the soldiers onto the shores, which were patrolled by the enemy. Exhausted by seasickness, they surrendered and were put to death. Others were nevertheless able to mobilize energy for the ensuing battle.

...tirones enim multitudine navium perterriti et salo nausiaque confecti iureiurando accepto nihil iis nocituros hostes se Otacilio dediderunt; qui omnes ad eum producti contra religionem iusurandi in eius conspectu crudelissime interficiuntur. at veteranae legionis milites, item conflictati et tempestatis et sentinae vitiis, neque ex pristina virtute remittendum aliquid putaverunt,...

... For the recruits, terrified by the number of ships and exhausted by the rough water and seasickness, after receiving a solemn pledge that the enemy would do them no harm, surrendered themselves to Otacilius; and all of them, when brought to him, were most cruelly massacred before his eyes in violation of the sanctity of his oath. But the men of the veteran legion, though equally distressed by the discomforts of the storm and the bilge-water, considered it their duty to relax nothing of their pristine valour, ...

In this context, it is interesting that another medical condition, namely the fear of heights, also influenced historical warfare, for example, the conquest of Carthago Nova reported by *Titus Livius* in his History of Rome (*Ab urbe condita*, libri CXLII).: “But neither the men nor the projectiles nor anything else defended itself as well as the city wall. The few scaling ladders that were as high as the wall were flawed, and the taller the ladder was, the more flawed it was. For this reason they broke under the weight of the soldiers. Those who had just reached the highest point were not able to escape, while others pressed up from below. Several plunged down to the ground, while the ladders were still standing, since the heights (altitudo) had veiled their eyes with dizziness (caligo).” Ultimately, the high walls did not prevent the conquest of Carthago Nova (17).

Chinese Antiquity and the Battle of Red Cliff

Chinese society has long valued the past, especially ancient history and stories of former times. The Battle of Red Cliff (also known as the Battle of Chibi) took place in 207 AD. It is the subject of poems and films about the heroic battle to unify the empire. The narrative describing the battle suggests that the swaying motion of the ships was perceived as causing illness and an absence of well-being; however, none of the known terms indicating seasickness appear. Two works contain information about the story and the battle. The first report, "Records of the Three Kingdoms" (*San guo zhi*) from the 3rd century, is the officially authorized history book, covering the years 184–280. The second book, "Romance of the Three Kingdoms" (*San guo yan yi*), is a popular novel about ancient history (27). Dating from the 14th century, it is considered one of the four classical novels of ancient China, and thus the crowning achievement of Chinese narrative art.

The novel gives a more fictionalized and dramatized report on the famous battle, hinting that health problems arose from the continuous swaying of the ships. Commander Cao Cao and his soldiers are northerners and unfamiliar with warring on ships. The enemy exploits this by having an alleged friend of Cao Cao suggest an apparent solution: to increase the stability of the ships by tying and nailing them together, and thus prevent the soldiers from becoming sick. Cao Cao follows the advice and acts accordingly, with the result that the enemy successfully sets fire to the entire fleet, in the ensuing battle. The following fateful dialog takes place:

While conversing with commander Cao Cao an officer named Tong asks: "May I inquire whether there are any good physicians among the soldiers (liang yi)?" Cao responds' "Why is that important?" Tong replies: "Many of the soldiers are sick, and good physicians are needed to treat them." It was actually true that Cao's troops were not accustomed to the local climate and began vomiting; many died. After Cao had thoroughly considered the situation, he suddenly asks Tong how to avoid this? Tong replies: "In the middle of the Great River (Jiangzi) the water rises and falls, the wind continually creates waves, the soldiers from the north are not used to traveling by ship. This rolling and lurching causes illness. It would help to connect the large and the small boats together, 30 or 50 per row, prow to stern, with iron hoops or to put broad planks on them so that men and horses can cross over them. Then regardless of how the wind, waves, and tides danced, what would there be to still fear?" It is clear that the motion of the river is considered to be the cause of the soldiers' weakness and sickness.

Medieval England and Defeat of the Spanish Armada in 1588

A naval battle probably equal in importance and heroic qualities to the Battle of Red Cliff for the Chinese was for the English the battle against the Spanish Armada off the shore of England in 1588 (Figure 4). A lot was at stake—the rule of Spain over England and the reversal of the reformation that had been bought at such high costs. The English saw the defeat of the Spanish as a



FIGURE 4 | Spanish Armada. Unknown contemporary artist painting before 1700 AD. The defeat of the Spanish Armada in 1588 was the beginning of English dominance of the sea. In foreground English ships are shown surrounding and attacking Spanish galleons. Painting in National Maritime Museum, London (https://de.wikipedia.org/wiki/Spanische_Armada#/media/File:Invincible_Armada.jpg) (28).

turning point in their history. Not only were Spain's plans to conquer England dashed but it also lost its reputation as the world's main naval force. Afterward, naval power was concentrated in the north Atlantic and was primarily in the hands of the English and the Dutch fleets.

Many factors played a role in the defeat of the Spanish. A major one was that King Philipp II of Spain failed to consult his naval experts and had proposed a plan that at the time was considered unpromising if not disastrous. He assumed his naval forces were sufficient and sent around 160 Spanish galleons, mostly massive and old ships. These proved too unwieldy to counter the smaller, faster ships of the English. While the English had advanced, very effective long-range cannons, the Spanish had nothing comparable and were poorly armed. Their battle strategy also differed. The English specialized in fireships, setting afire old galleons loaded down with gun powder and wood that were then directed toward the Spanish. The slow movement of the Spanish ships often meant they could not escape, falling victim to the conflagration. The strategy of the Spanish had relied on forces from Parma, which did not arrive in time due to Dutch interference. No other alternative plan had been made. Luck also played a role. A storm arose, and the choppy waters of the channel and the open sea to which the Spanish were unaccustomed, became even more threatening. Trying to flee, they crashed upon the shore.

Incredibly, Spanish manpower consisted of three times as many foot soldiers as sailors, for the plan had been to fight mainly on land, not on water. The man in charge of these forces, Don Alonzo Perez de Guzman el Bueno, the Seventh Duke of Medina Sidonia, had no experience with naval battles and was often seasick. He had tried to refuse the appointment by openly stressing his lack of experience to Phillip II, but he was not heard (29). Many of his soldiers likewise had never fought on water

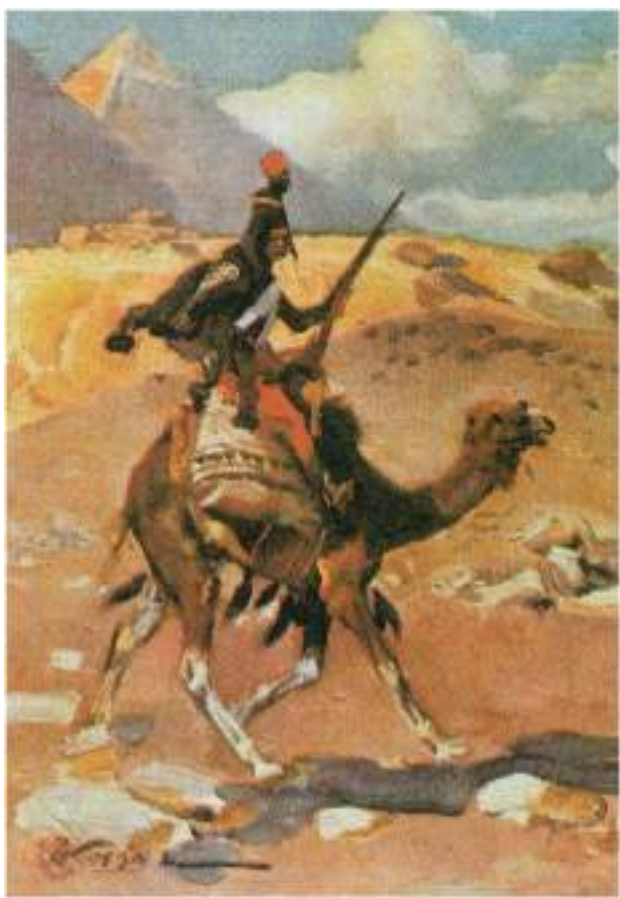


FIGURE 5 | Napoleon and camel-sickness. A soldier of Napoleon's camel (dromedary) regiment, initiated by Napoleon in 1799. Interestingly, the soldiers were considered infantry, because they dismounted to fight. Those who couldn't adapt to the movements of the "ship of the desert" became seasick, proving rather ineffective combattants (*Un soldat du régiment dromédaires*, par Wojciech Kossak, 1912; [https://fr.wikipedia.org/wiki/Régiment_des_dromedaires#/media/File:WKossak028.jpg](https://fr.wikipedia.org/wiki/R%C3%A9giment_des_dromedaires#/media/File:WKossak028.jpg)).

before and were not only seasick but also afflicted with typhus. In contrast, the English had very experienced commanders, Lord Howard of Effingham and his second-in-command Sir Francis Drake. The Spanish especially feared Francis Drake, who was known as "the Dragon," an erroneous translation of his name. While many considered him a pirate, he proved his sailing and

REFERENCES

1. Huppert D, Oldelehr H, Krammling B, Benson J, Brandt T. What the ancient Greeks and Romans knew (and did not know) about seasickness. *Neurology* (2016) 86:560–5. doi:10.1212/WNL.0000000000002355
2. Brandt T, Bauer M, Benson J, Huppert D. Motion sickness in ancient China: seasickness and cart-sickness. *Neurology* (2016) 87:331–5. doi:10.1212/WNL.0000000000002871
3. Forcellini E, Faccioli J. *Totius Latinitatis lexicon, consilio et cura Jacobi Faccioli opera et studio Aegidii Forcellini, lubucratum.* (Vol. 4). Padua: Typis Seminarii (1771).

commanding skills (30). Only half of the original Spanish forces made it back home alive (31).

Napoleon and His “Camel-Sick Corps”

A curious footnote to the history of war and "seasickness" is connected with Napoleon. While the military significance was not considered important, the appearance of seasickness in the desert was unusual. In his first military campaign against Egypt (1798–1799), General Napoleon conceived the idea of creating a camel corps. He supposedly had become aware of the camel's suitability for transportation quite early. Although riding a camel did cause him some nausea, it was not so considerable as to prevent him from using one himself. Indeed his special camel was embalmed when it died of natural causes and is said to still be on exhibit in the African museum in Paris. In January 1799, Napoleon instituted the dromedary regiment which saw action after an attack of the Beduins (Figure 5).

Camels had several advantages over horses, namely, they did not have to drink so often and were adapted to the harsh conditions of the desert. They could easily travel for hours and outrun as well as outlast enemies on horses. One major drawback, however, was that soldiers who were susceptible to motion sickness could become "seasick" on this "ship of the desert" and not be able to engage in battle (32). The corps saw action for a period of three years (1798–1801). It was disbanded after France withdrew from Egypt following losses to the British.

AUTHOR CONTRIBUTIONS

DH and TB conceived and designed the study, analyzed and interpreted the classical texts, and wrote the paper. JB analyzed and interpreted the classical texts, and edited the manuscript.

ACKNOWLEDGMENTS

The authors would like to thank Matthias Bauer from the Horst-Görtz-Institute for Theory, History, and Ethics of Chinese Life Sciences, Berlin, Germany, and Hermann Oldelehr for their thorough search in the ancient texts.

FUNDING

This work was supported by funds from the German Federal Ministry of Education and Research (BMBF grant code 01 EO 0901) and the Hertie Foundation.

4. Georges KE. *Ausführliches Lateinisch-Deutsches Handwörterbuch*. Hannover: Hahnsche Buchhandlung (2010).
5. Thesaurus. (2016). Available from: <http://www.thesaurus.badw.de>
6. Rolfe JC. Some references to seasickness in the Greek and Latin writers. *Am J Philol* (1904) 2:192–200. doi:10.2307/288418
7. Cury H, Bohec J. La mal de mer dans le passé. *Aesculape* (1927) 17:67–75.
8. Pezzi G. La cura del mar di mare attraverso I tempi. *Ann Med Nav (Roma)* (1951) 5:630–8.
9. Schadewaldt H. Seekrankheit in der Antike. *Ärzt Praxis* (1956) 8:30.
10. Schadewaldt H. Zur Geschichte der Seekrankheit. *Med Welt* (1967) 38: 2258–65.

11. Oldelehr H. *Seekrankheit in der Antike* [Doctoral dissertation]. Düsseldorf (1977).
12. Zhufeng L, editor. *Hanyu da cidian* (Comprehensive Dictionary of Chinese). (Vol. 1-13). Shanghai: Cishu chubanshe (1986–1993).
13. Schöner E. *Das Viererschema in der antiken Humoralpathologie*. Wiesbaden: Steiner (1964).
14. Zeitlin JT. The literary fashioning of authority – a study of Sun Yikui's case histories. In: Furth C, Zeitlin JT, Hsiung P-C, editors. *Thinking with Cases: Specialist Knowledge in Chinese Cultural History*. Honolulu: University of Hawai'i Press (2007). p. 169.
15. Wang H, editor. *Huangdi neijing yanjiu dacheng* (The Great Compendium of the Research on the Huangdi Neijing). Beijing: Beijing chubanshe (1997).
16. Huppert D, Brandt T. Descriptions of vestibular migraine and Menière's disease in Greek and Chinese antiquity. *Cephalgia* (2016). doi:10.1177/0333102416646755
17. Huppert D, Benson J, Krammling B, Brandt T. Fear of heights in Roman antiquity and mythology. *J Neurol* (2013) 260:2430–2. doi:10.1007/s00415-013-7073-1
18. Köster A. *Das antike Seewesen*. Berlin: Schoetz & Parrhysius Verlag (1923).
19. NewChinese-German Dictionary. (*Das neue Chinesisch-Deutsche Wörterbuch*) (*xin han de cidian*). Beijing: New Chinese-German Dictionary (1996). 1009 p.
20. Brandt T, Wenzel D, Dichgans J. Visual stabilization of free stance in infants: a sign of maturity (article in German). *Arch Psychiat Nervenkr* (1976) 223:1–13. doi:10.1007/BF00367449
21. Henriques IF, de Oliveira DWD, Oliveira-Ferreira F, Andrade PMO. Motion sickness prevalence in school children. *Eur J Pediatr* (2014) 173:1473–82. doi:10.1007/s00431-014-2351-1
22. Shakespeare W. Romeo and Juliet. 2nd ed. In: Wells S, Taylor G, Jowett J, editors. *The Oxford Shakespeare*. Oxford: Oxford University Press (2005). Act 5, Scene 3, Lines 117-120.
23. Salzberger G. Über die Alkaloide der weißen Nieswurz (Veratrum album). *Arch Pharm* (1890) 228:462–83. doi:10.1002/ardp.18902280906
24. Hahnemann S. *De helleborismo veterum*. Habilitation thesis, Leipzig (1812).
25. Thomé OW. *Flora von Deutschland, Österreich und der Schweiz*. Gera: Unterthaus (1885).
26. Zhenheng Z. *Dan xi yi ji* (Collected Medical Works of [Zhu] Danxi). Beijing (1993).
27. Guanzhong L. *San guo yan yi* 三國演義 (The three kingdoms). Beijing (1991).
28. Trevelyan GM. *History of England. New Illustrated Edition*. London: Longman Group Limited (1973) p. 416.
29. Pierson P. *Commander of the Armada: The Seventh Duke of Medina Sidonia*. New Haven, CT: Yale University Press (1989).
30. Harris N. *The Armada: The Decisive Battle*. London: Dryad Press Limited (1987).
31. Harbottle TB. *Dictionary of Battles: From the Earliest Date to the Present Time*. New York, NY: E.P. Dutton and Co. (1905). (1966; reprint, Detroit: Gale Research Company).
32. Thibaudeau AC. *Histoire générale de Napoléon Bonaparte*. (Vol. 4-5). Paris: Ponthieu et Comp (1827-1828).

Conflict of Interest Statement: The authors declare that there are no conflicts of interest and that there exist no financial or other relationships that have influenced the work.

Copyright © 2017 Huppert, Benson and Brandt. This is an open-access article distributed under the terms of the Creative Commons Attribution License (CC BY). The use, distribution or reproduction in other forums is permitted, provided the original author(s) or licensor are credited and that the original publication in this journal is cited, in accordance with accepted academic practice. No use, distribution or reproduction is permitted which does not comply with these terms.



Determinants of Motion Sickness in Tilting Trains: Coriolis/Cross-Coupling Stimuli and Tilt Delay

Giovanni Bertolini^{1*}, Meek Angela Durmaz¹, Kim Ferrari^{2,3}, Alexander Küffer⁴, Charlotte Lambert¹ and Dominik Straumann¹

¹Department of Neurology, Zurich University Hospital, Zurich, Switzerland, ²Institute of Pharmacology and Toxicology, University of Zurich, Zurich, Switzerland, ³Neuroscience Center, University and ETH Zurich, Zurich, Switzerland

⁴Department of Neurosurgery, Zurich University Hospital, Zurich, Switzerland

OPEN ACCESS

Edited by:

Bernard Cohen,
Icahn School of Medicine at
Mount Sinai, USA

Reviewed by:

Sergei B. Yakushin,
Icahn School of Medicine at
Mount Sinai, USA

Dan M. Merfeld,
Massachusetts Eye and Ear
Infirmary, USA

Marianne Dieterich,
Ludwig-Maximilians-Universität
München, Germany

*Correspondence:

Giovanni Bertolini
giovanni.bertolini@usz.ch

Specialty section:

This article was submitted to
Neuro-otology,
a section of the journal
Frontiers in Neurology

Received: 19 November 2016

Accepted: 21 April 2017

Published: 15 May 2017

Citation:

Bertolini G, Durmaz MA, Ferrari K, Küffer A, Lambert C and Straumann D (2017) Determinants of Motion Sickness in Tilting Trains: Coriolis/Cross-Coupling Stimuli and Tilt Delay. *Front. Neurol.* 8:195.

doi: 10.3389/fneur.2017.00195

Faster trains require tilting of the cars to counterbalance the centrifugal forces during curves. Motion sensitive passengers, however, complain of discomfort and overt motion sickness. A recent study comparing different control systems in a tilting train, suggested that the delay of car tilts relative to the curve of the track contributes to motion sickness. Other aspects of the motion stimuli, like the lateral accelerations and the car jitters, differed between the tested conditions and prevented a final conclusion on the role of tilt delay. Nineteen subjects were tested on a motorized 3D turntable that simulated the roll tilts during yaw rotations experienced on a tilting train, isolating them from other motion components. Each session was composed of two consecutive series of 12 ideal curves that were defined on the bases of recordings during an actual train ride. The simulated car tilts started either at the beginning of the curve acceleration phase (no-delay condition) or with 3 s of delay (delay condition). Motion sickness was self-assessed by each subject at the end of each series using an analog motion sickness scale. All subjects were tested in both conditions. Significant increases of motion sickness occurred after the first sequence of 12 curves in the delay condition, but not in the no-delay condition. This increase correlated with the sensitivity of motion sickness, which was self-assessed by each subject before the experiment. The second sequence of curve did not lead to a significant further increase of motion sickness in any condition. Our results demonstrate that, even if the speed and amplitude are as low as those experienced on tilting trains, a series of roll tilts with a delay relative to the horizontal rotations, isolated from other motion stimuli occurring during a travel, generate Coriolis/cross-coupling stimulations sufficient to rapidly induce motion sickness in sensitive individuals. The strength and the rapid onset of the motion sickness reported confirm that, even if the angular velocity involved are low, the Coriolis/cross-coupling resulting from the delay is a major factor in causing sickness that can be resolved by improving the tilt timing relative to the horizontal rotation originating from the curve.

Keywords: motion sickness, tilting trains, cross-coupling, otolith, semicircular canal, self-motion perception

INTRODUCTION

The growing demand of high-speed land transport of goods and passengers in the last 30 years led to reinforcing the offer of fast trains, capable of maintaining high speed in curves by tilting the car bodies. The tilting mechanism compensates for the centripetal acceleration during turns by bringing the vertical axes of the cars closer to the gravito-inertial force vector. As a result, the trains can run faster, and the lateral thrusts of centrifugal force on the passengers during turns are decreased. Although, at first glance, this can be expected to increase comfort, many passengers in tilting trains develop symptoms of motion sickness (1, 2). Motion sickness (3–7) is a syndrome elicited in otherwise healthy subjects, whenever they are exposed to combination of motion stimuli at variance with those expected by the brain during our natural self-propelled motion. Its symptoms vary from simple stomach awareness to severe nausea and vomiting, but include also drowsiness, apathy, and irritability (3, 4, 8). These symptoms, besides decreasing the comfort, can also have consequences on the performance of workers exposed to passive motion (e.g., co-drivers, navigators, service personnel, and others), possibly affecting them without their awareness (sopite syndrome) (9, 10). Several years of research highlighted many combinations of motion stimuli that can induce motion sickness (3–5). In everyday life, these motion stimuli occur mainly, but not exclusively, when an individual is subject to a motion that he or she does not actively control (passive motion). For this reason, motion sickness is often associated with transport systems (car, boat, planes) as any of them induces unnatural motion stimuli (5, 11, 12).

Traveling on a tilting train provides a complex combination of passive motion stimulation. A detailed understanding of the mechanism underlying motion sickness in tilting trains is essential because only such knowledge allows developing technical solutions for the problem (13). Previous research, following accurate recording of the linear and angular motion of the cars, suggested that three components of train motion can possibly cause motion sickness: the jitters of the car, the centrifugal acceleration during the curves, and the tilt of train itself. The jitters show peaks at 0.5 and 1.7 Hz both in roll rotation and lateral linear accelerations (14). The latest are often pointed out as the main cause of motion sickness evoked by road transport, but the critical frequencies for these stimuli to evoke motion sickness was found to be around 0.16–0.2 Hz (15–18), suggesting a relative minor role of these stimuli in the train. The centrifugal forces also generate lateral accelerations. These accelerations are present in any train entering a curve. In the tilting trains, the magnitude of centrifugal acceleration is larger due to the higher velocity allowed by the tilt of the cars, but the actual amount of lateral acceleration on the passenger is also decreased on the tilts as they align the body vertical axis to the gravito-inertial vector. Various studies showed the nauseogenic role of the lateral linear acceleration in actual and simulated conditions, in particular if combined with roll tilts (1, 13, 19–22). Accordingly, motion sickness of passengers in tilting trains can be reduced by decreasing the angle of the compensatory roll tilt (2, 14, 23). The usefulness of this approach is limited because the velocity of trains on curves has to decrease, which negates the purpose of the tilt. The tilt of the train

while in curves, finally, provides a typical nauseogenic stimulus, known as Coriolis/cross-coupling. Such stimulus occurs when, during an ongoing rotation around a space fixed Earth-vertical axis, a person suddenly tilts the head around an Earth-horizontal axis (24). In the head reference frame the change direction of the gravity vector describing the re-orientation with respect to gravity from the subject point of view is not accompanied by the correct re-orientation of the sensed rotation axis that will keep it aligned to gravity as it actually is (remember that the ongoing rotation is around a space fixed Earth-vertical axis). This occurs because the semicircular canals behave like a high-pass filter of the input velocity and the sensed velocity of the ongoing rotation decay according to an approximately exponential function determined by the property of the semicircular canals, the neural transduction, and the different step of central processing (25–27). If there is a delay between the onset of the first rotation and the tilt, the velocity sensed along the Earth-vertical axis is less than the actual one. As a consequence, after the tilt, the component of the sensed velocity along the head-axis that was previously aligned with Earth-vertical is wrongly computed and the subject senses an overall rotation around an off-vertical axis that is not aligned with the axis of the actual rotation. It is important to remark that, although the tilt around the Earth-horizontal axis implies a re-orientation with respect to gravity, the axis of the ongoing rotation remains Earth-vertical in Coriolis/Cross-coupling. Therefore, no actual off-vertical axis rotation occurs and the orientation of the subject respect to gravity is fixed after the tilt, but the perceived rotation is equivalent to an off-vertical axis rotation not accompanied by the expected re-orientation with respect to gravity. In the train, a Coriolis/cross-coupling stimulus occurs due to the roll movements during both the acceleration and deceleration phases of yaw rotation (14). Cross-coupling occurring during high angular velocity rotations is one of the most powerful nauseogenic stimuli; whether the relatively low yaw velocities typical on curved train tracks (around 4°/s) are, however, adequate to cause motion sickness is not known.

It has been observed that if subjects' heads were tilted during lateral acceleration, subjects had strong motion sickness, but if the head roll was initiated before the lateral acceleration, there was no motion sickness (28). By comparing different tilting systems in trains, it has been recently shown that an adequate synchronization of roll tilt with changes of yaw velocity on curves eliminates motion sickness during a 25-min travel on a curvy track (14). This could be expected if the sickness derives from the Coriolis/cross-coupling stimulus because the delay increases the drop in the sensed velocity caused by the high-pass filter behaviors of the semicircular canals. A larger drop of the sensed velocity before the tilt corresponds to a stronger miscalculation of the velocity component along the head-axis after the tilt (that was previously aligned with the Earth-vertical). This would imply a stronger Coriolis/cross-coupling, possibly causing more sickness. Nonetheless, other aspects of the stimulus in the study by Cohen et al. (14) changed concurrently with the change in tilt delay. This, together with the uncertainty on the strength of the Coriolis/cross-coupling stimulus at the low angular velocity involved prevented a definite conclusion on the cause of the sickness reduction. Moreover, the actual relevance of a delay in the

tilt for such slow rotation is also unclear. The aim of this paper is to study the cross-coupling stimuli occurring in tilting train, isolating them from other motion stimuli to determine whether the phasing between the change of yaw velocity and the change of roll position is a decisive factor for tilting train motion sickness.

MATERIALS AND METHODS

Study Cohort

Nineteen healthy subjects (nine females; mean age \pm SD: 31 \pm 9 years, range 22–66 years) participated in the study. Informed consent was obtained from all participants after full explanation of the experimental procedure. The protocol was approved by the Ethic committee of the Canton Zurich. In the recruiting phase, the subjects were requested to fill a questionnaire describing their previous experience on tilting train (Questionnaire Q0 in Supplementary Material). All included subjects had previous experience of traveling on tilting trains and declared to travel on a tilting train at least once per year. All subjects were naïve with respect to the apparatus used in the experiment.

Experimental Setup

Subjects were seated upright on a turntable with three servo-controlled motor-driven axes (prototype built by Acutronic, Switzerland). The head was restrained with an individually molded thermoplastic mask (Sinmed BV, Reeuwijk, the Netherlands) to ensure that the movements matched those of the turntable. Subjects were positioned so that the intersection of the inter-aural and naso-occipital axes was at the intersection of the three axes of the turntable. A four-point safety harness secured the subjects. All experiments were performed in complete darkness.

Experimental Protocol

Motion Stimuli

For each subject, the experiment was split in two separate experimental sessions. Each experimental session consisted of two subsequent sequences of 12 simulated, ideal train curves each, reproduced using a 3D turntable (**Figure 1C**). The motion profile of the ideal curve was based on the data recorded from gyroscopes and accelerometers mounted on an actual train car during the experiment of the study by Cohen et al. (14). Since kinematics varied between the different curves recorded, parameters were adjusted to obtain an ideal curve based on the average values extrapolated from examples and graphs of Cohen et al. (14). Each simulated curve in our experiment consisted of a 30-s constant velocity yaw rotation with peak angular velocity of 4°/s and accelerations of 2°/s². At the beginning of the curve, the subject was tilted 8° around the naso-occipital axis toward the inner part of the curve (i.e., toward right during rightward yaw rotation and left during leftward yaw rotation) and brought back upright at the end of the simulated curve (**Figure 1B**). The tilt profile had a peak velocity of 4°/s and acceleration of 10°/s². This motion reproduced the misalignment between the body yaw axis and the rotation yaw axis occurring on tilting train. Different from the stimulus induced by a real train curve, the ideal curve did not reproduce the centrifugal acceleration

(i.e., the gravito-inertial vector was not aligned with the body axis after the tilt, but remained aligned with the yaw axis of rotation). Moreover, the roll tilt axis of the simulated curve coincided with the naso-occipital axis of the subject, while in the tilting train is roughly 2 m below it (**Figures 1A,B**). After each curve, the subject was stationary for 20 s before a new curve was initiated. Each sequence contained six curves in clockwise direction and six in counterclockwise direction in randomized order. One entire session included, therefore, 24 simulated curves in 22–25 min, i.e., less than in the track described in Cohen et al. (14). All simulated rides were performed in total darkness.

After at least 2 h from the completion of the two sequences forming the first session, a second session was performed (**Figure 2A**). The two sessions were identical except for the timing of the tilt with respect to the onset of the curve. In one session, named “no-delay session,” the first tilt (at the beginning of the simulated curve) began at the same time of the yaw rotation and the second tilt, bringing the subject upright at the end of the curve, was initiated together with the deceleration of the yaw rotation. In the other session, named “delay session,” a delay of 3 s was added to the tilt with respect to the “no-delay” session (**Figure 2B**). The order of the two sessions was randomized across subjects and they were always performed within the same day.

Motion Sickness Evaluation

Before the experiment, subjects were instructed how to report motion sickness scores with a modified version of the simplified Pensacola motion sickness rating scale. This scale has been previously used in a number of studies and was proved effective for rapid reports of motion sickness score during the experiments (29–34). It requires the subject to rate the current feeling on a 0–20 scale, where 0 corresponds to “no reaction,” 5 to “starting to feel warm or have slight malaise,” 10 to “moderate gastrointestinal distress and/or dizziness with or without sweating,” 15 to “strong feeling of nausea or dizziness, but the test could still be continued,” and 20 to “nausea/dizziness too strong to continue, vomiting.” In our modified version, we substituted the digital scale with analog scale (Questionnaire Q1–3 in Supplementary Material). The subjects were asked to rate their current feeling by marking a position along a 100-mm long vertical line, where the top of the line correspond to the 0 of the simplified Pensacola scale (i.e., no discomfort) and the bottom to the 20 (i.e., unable to continue the experiment). The position corresponding to 5, 10, and 15 of the simplified Pensacola scale were marked on the vertical line with short horizontal lines every 25 mm. The descriptions corresponding to the 0, 5, 10, 15, and 20 were provided in written form next to the line as a reference for the subject. The choice of the analog scale was motivated by the need to identify small variation of motion sickness scores and reduce the memory effects between subsequent reports, which we observed in pilot tests of the experimental protocol. The analog scale allows measuring variation of motion sickness score smaller than 1/20 (maximal sensitivity of the classical simplified Pensacola scale) without requiring the subject to use large numbers.

A questionnaire presenting the analog scale was provided to the subjects three times in each experimental session (Questionnaire Q1–3 in Supplementary Material): Q1—before the first 12-curves

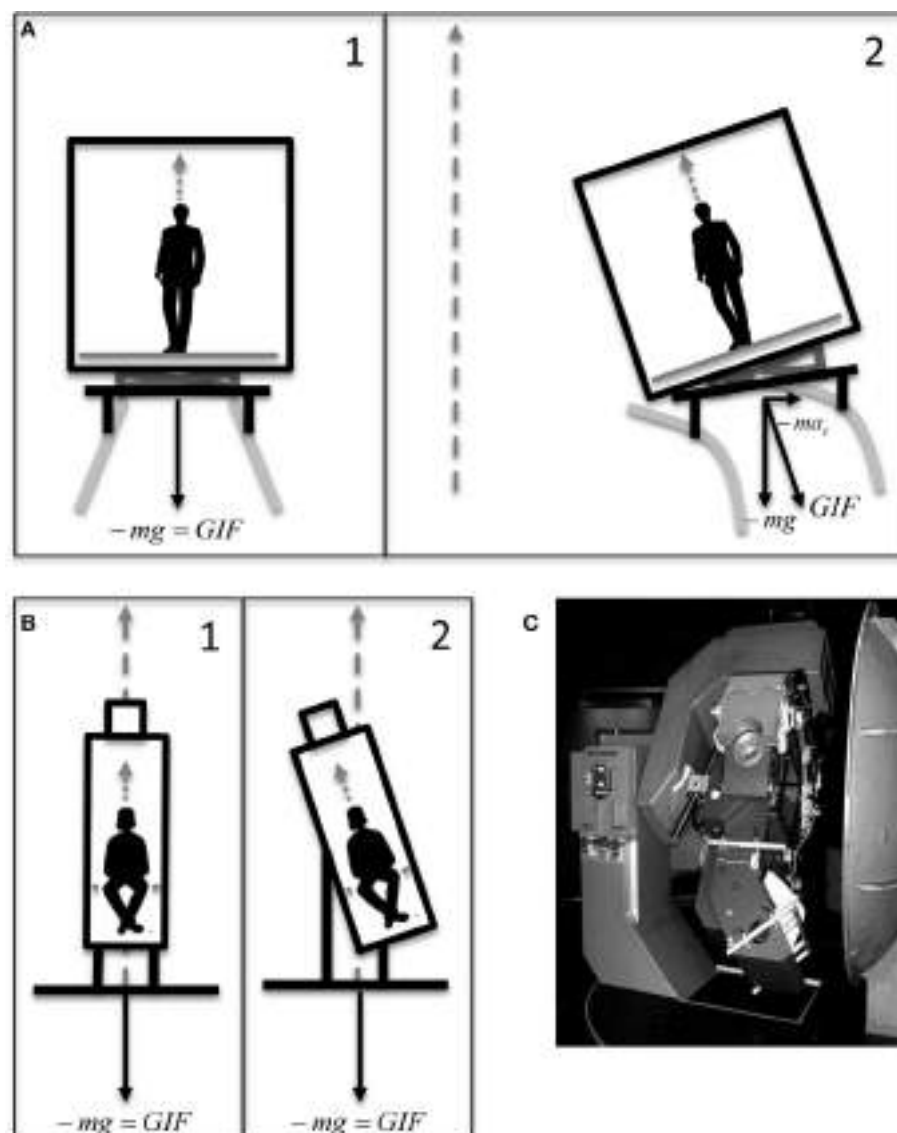


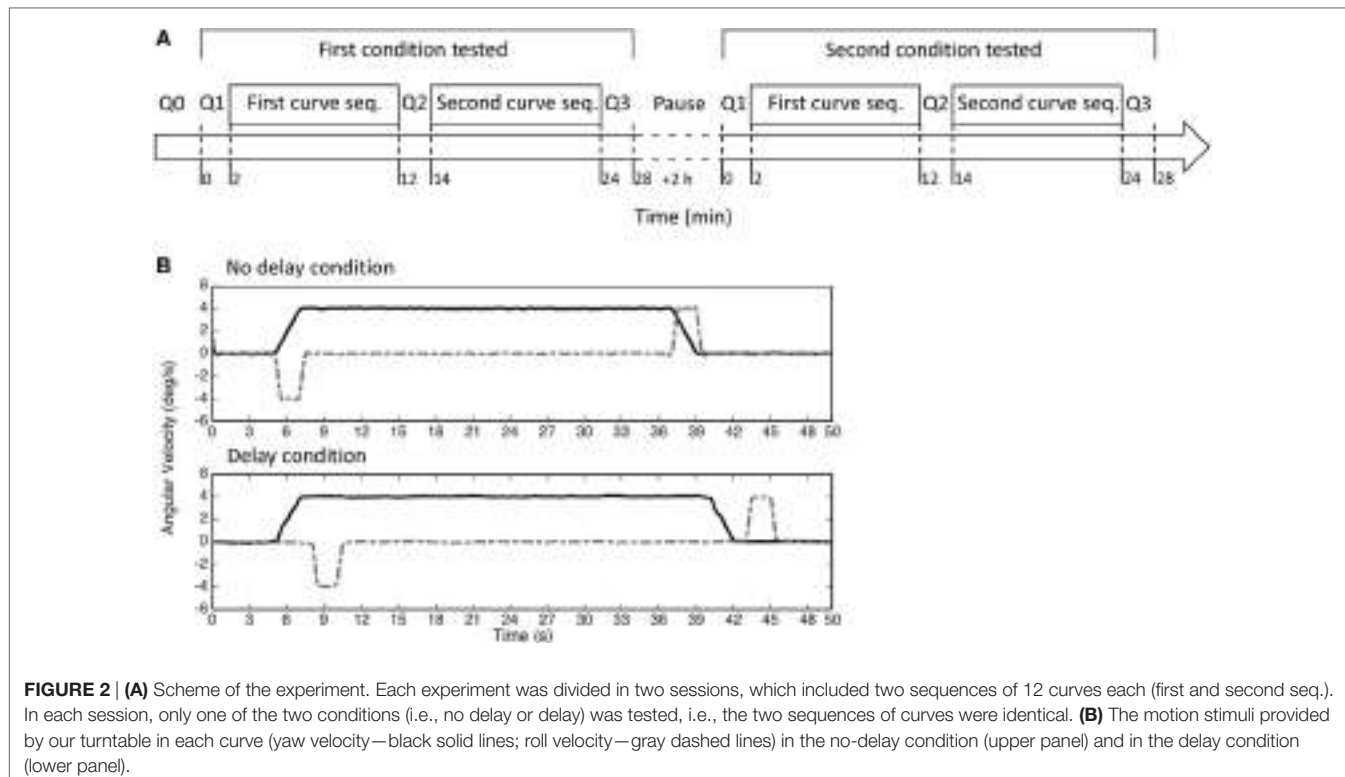
FIGURE 1 | (A) Graphical representation of the motion of a car of a tilting train before (A1) and during (A2) a curve. The yaw axis of the curve (gray dashed arrow) does not coincide with the subject yaw axis before the tilt, since it passes through the center of the curve. This generates a centrifugal acceleration (\vec{a}_c) tilting the gravito-inertial vector (\overrightarrow{GIF}). The roll axis is below the car. **(B)** Graphical representation of the motion of the 3D turntable during our simulation of tilting trains before (B1) and during (B2) a simulated curve. The yaw axis of the turntable (gray dashed arrow) is aligned with the subject yaw axis before the tilt, and no tilt of the gravito-inertial vector (\overrightarrow{GIF}) occurs. The roll axis is through the center of the head. Dotted gray arrows represent the yaw axis of the subject. **(C)** The 3D turntable.

sequence; Q2—between the first and the second sequence; Q3—after the second sequence. A different questionnaire (Questionnaire Q0 in Supplementary Material) was provided to the subject in the recruiting phase, asking to report the frequency of their travel on tilting trains (from never to daily) and to rate the feeling induced by a typical ride on a tilting train using the same analog scale used in the experiment.

Data Analysis

Questionnaires were analyzed by measuring the distance (millimeters) between the top of the line of the analog scale and the point marked by the subject. The number was rounded to

the lower integer. This procedure transformed the 100-mm long line of the analog scale in a 0–100 simplified Pensacola scale. The values were imported into Matlab R2014b (Mathworks, USA) for further processing and statistical analysis. The differences $D1 = Q2 - Q1$ and $D2 = Q3 - Q2$ were calculated on a subject by subject basis to assess the variation of motion sickness due to the first and second sequence of curves separately. The resulting values were first grouped according to the order of session, obtaining $D1_{\text{first_session}}$, $D1_{\text{second_session}}$ and a $D2_{\text{first_session}}$, $D2_{\text{second_session}}$, and then according to the stimulus condition (no-delay condition and delay condition) obtaining $D1_{\text{no-delay}}$, $D1_{\text{delay}}$ and $D2_{\text{no-delay}}$, $D2_{\text{delay}}$, respectively. Due to the crossover study design, all subjects



were represented in all groups. Additionally, we calculated the values $R1 = D1_{\text{delay}} - D1_{\text{no-delay}}$ and $R2 = D2_{\text{delay}} - D2_{\text{no-delay}}$. These values express, for each subject, the differential increase of motion sickness score between the two conditions observed after the first (R1) and the second (R2) sequence, separately.

Statistical Analysis

Lilliefors test was used to assess the normality of the distribution of the difference vectors D1 and D2 for both data grouping strategies (no-delay/delay condition and first/second session). As the null hypothesis of normality was rejected, we presented the results using median and median absolute deviation [using the format: median (median absolute deviation)]. A Wilcoxon paired signed rank test was used to compare the values of D1 and D2 within and between the two conditions and the two sessions, separately. The Spearman correlation coefficient (ρ) was calculated between R1 and the results of the questionnaire Q0 and R2 and the results of the questionnaire Q0, computing the p -values for the estimated coefficients. To further verify whether the relative increase R1 of motion sickness due to the delay grows linearly with the sensitivity in tilting train Q0, a linear regression was calculated computing the p -values for the estimated coefficients and the R^2 for the regression fits.

RESULTS

All subjects were able to complete the experiment in both conditions. Pooling data from both conditions, motion sickness scores recorded either after the first 12 curves of either condition (i.e., after the first sequence—Questionnaire B2) or at the

end of each session (total of 24 curves, i.e., after the second sequence—Questionnaire B3) varied considerably ranging from 0/100 to 47/100. Similarly, the scores before starting the first sequence also showed considerable variations (0/100–39/100); in fact, some subjects were already feeling some unease before starting the experiment, but only one of them exceeded the score of 25/100, i.e., the first marked level on the analog scale (Questionnaire Q1–3 in Supplementary Material). The overall median (MAD = Median absolute deviation) motion sickness score recorded pooling all questionnaires of the three conditions were B1 = 0 [0], B2 = 4 [4] and B3 = 4 [4].

Effect of the Order of the Sessions

Pooling the data of all subjects, we did not observe a significant difference of motion sickness scores (B Questionnaires) between the values reported before the first ($B1_{\text{first_session}} = 0.5$ [0.5]) and the before the second session ($B1_{\text{second_session}} = 0$ [0]) on the same day. By subtracting the motion sickness scores after each sequence from the one obtained before it, we computed the changes (D1, D2) in the score resulting from each of the two sequences of each session. Pooling the values based on the session order, no significant difference was found in the score change due to the first ($D1_{\text{first_session}} = 1$ [3]; $D1_{\text{second_session}} = 0$ [0.5]) or the second sequence ($D2_{\text{first_session}} = 0$ [2]; $D2_{\text{second_session}} = 0$ [1]) of the two sessions.

Effect of the Simulation Condition

Different subjects reacted differently to the various sequence of curves, showing increases, decreases, or no variations of motion sickness scores in both conditions (Table 1). The median increase

in motion sickness score during the first sequence in the delay condition was significantly higher ($p = 0.04$) than in the no-delay condition both in the pooled data of all subjects ($D1_{\text{delay}} = 1$ [4]; $D1_{\text{no-delay}} = 0$ [1]) and in the data of only the 12 subjects showing a variation in at least one of the two conditions ($D1_{\text{delay}} = 8$ [8]; $D1_{\text{no-delay}} = 1.5$ [4]). Moreover, $D1_{\text{delay}}$ was found to have a median significantly different from 0 ($p = 0.03$), while it was not the case for $D1_{\text{no-delay}}$.

The second sequence did not lead to increases with a median different from 0 ($D2_{\text{delay}} = 0$ [4]; $D2_{\text{no-delay}} = 0$ [2.5]) in any conditions, and no significant difference was found between the increases due to the second sequence when comparing the two conditions. These results were confirmed even when considering only the 14 subjects changing their motion sickness score during to the second sequence in at least one condition ($D2_{\text{delay}} = 4$ [4]; $D2_{\text{no-delay}} = 1$ [2.5]).

Correlation with Motion Sickness Experienced in Tilting Train

A significant ($p = 0.003$, $\rho = 0.65$) correlation was found between the variation $D1_{\text{delay}}$ due to the first sequence of curves in the delay condition and the motion sickness score reported

to describe the previous experience on tilting trains (Q0). This was, however, not the case for the variation $D1_{\text{no-delay}}$ resulting from the first sequence of curves in the no-delay condition. The relative increase $R1$ of motion sickness score as a result of the delay (Figure 3) also significantly correlate with Q0 ($p = 0.01$, $\rho = 0.58$). As $R1$ was obtained by subtracting the increases in the no-delay condition from those in the delay condition within each subject, this results further evidence that the delay in the tilt is the factor leading to a correlation of the recorded score with Q0. A linear regression of $D1_{\text{delay}}$ and $R1$ with respect to the score experienced on tilting trains (Q0) confirmed the above correlations ($p = 0.004$, $R^2 = 0.40$ and $p = 0.008$, $R^2 = 0.35$ for $D1_{\text{delay}}$ and $R1$, respectively), supporting the hypothesis of a linear relation between the variables. No correlation was observed between the further increases caused by the second sequence of curves neither considering the two conditions alone, or the relative increase $R2$.

DISCUSSION

Our results demonstrate that the Coriolis/cross-coupling stimuli can induce motion sickness even when the velocity of the yaw rotation is relatively low, as it occurs during train travels (14).

TABLE 1 | Number of subjects showing either a decrease or an increase in motion sickness score after each sequence of 12 simulated curves.

Sequence of curves	No delay		Delay		Pooled conditions		
	Condition	First sequence	Second sequence	First sequence	Second sequence	First sequence	Second sequence
Increase in MS		6	9	10	8	12	14
Decrease in MS		3	3	2	2		
No change in MS		10	7	7	9	7	5

Values are shown both divided by condition and pooled.

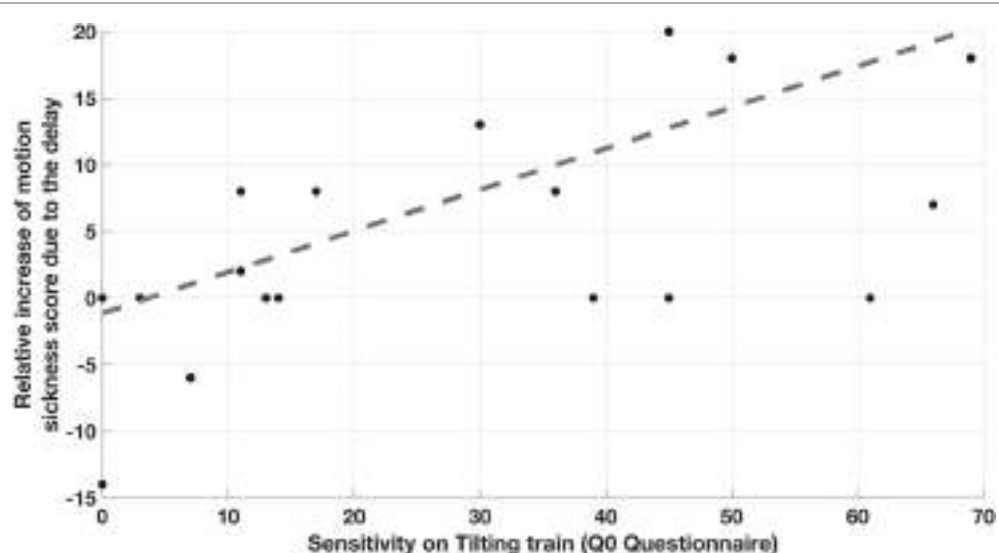


FIGURE 3 | Correlation between the relative increase of motion sickness score caused by the delay and the motion sickness sensitivity experienced on previous tilting train rides. Each point correspond to one subject and report on the y-axis the difference between the increases in motion sickness score caused by the first sequence of curves with 3 s of delay ($D1_{\text{delay}}$) and the one caused by the sequence with 0 s delay ($D1_{\text{no-delay}}$).

This confirms the hypothesis of the previous study performed during an actual train ride (14), which suggested that Coriolis/cross-coupling caused by the delay in the tilt of the train cars was one of the key causes of motion sickness in tilting trains. In that experiment, however, jitters of the cars, as well as lateral accelerations due to centripetal forces, could have played a role in determining the subjects' responses. In our experiment, no additional linear translation due to the centrifugal force were present (the turntable yaw axis was aligned with the subject midline), and the conflict between motion stimuli only depended on the misalignment between the perceived direction of gravity and the perceived rotation axis, i.e., we tested the effect of a pure Coriolis/cross-coupling stimuli induced by the angular rotation motion profile typical of tilting train during a very short ride (24 curves).

The Coriolis/cross-coupling stimulus was only nauseogenic when the tilt of the chair was delayed with respect to the beginning of the constant velocity rotation (i.e., the simulated curve). The 3-s used in this simulation exaggerated the delay observed in the tilting train (14). This difference, however, allowed to clearly discriminate between the two conditions tested and to evidence that the delay is the relevant variable causing Coriolis/cross-coupling dependent motion sickness in tilting train. The no-delay condition, indeed, did not induce any change in the median motion sickness in our tested subject.

Motion sickness was significantly stronger in the most sensitive subjects. Instead of assessing general sensitivity to motion sickness (35), we decided to collect information specifically oriented on the recent experience on tilting train, with the aim of understanding the contribution of tilt delay to the specific motion stimulus. The self-assessed sensitivity to tilting trains did correlate significantly with the motion sickness observed in the delay condition but not in the no-delay condition. The lack of correlation found in the no-delay condition implies that even those of our subjects showing the highest train-specific sensitivity did not suffer from significant increases of symptoms when no delay was present. Although with a lower correlation coefficient than the non-parametric correlation, the significant correlation found with the linear regression (**Figure 3**) between the relative increase of motion sickness due to the delay and the self-assessed sensitivity supports the hypothesis that our simulation reproduces a portion of the sickness experienced in the train, i.e., tilt delay is a specific trait of the motion stimulus causing disturbances to the subjects complaining for motion sickness on tilting trains.

The present experiment, by isolating the Coriolis/cross-coupling stimuli occurring in the train from all others stimuli present in the study of Cohen et al. (14), clearly demonstrates that, even at angular velocity as low as $4^{\circ}/s$, a small tilt (i.e., the cause of the Coriolis/cross-coupling stimulus) is nauseogenic if it is delayed with respect to the rotation onset. It can be argued, however, that our study does not prove that the cross-coupling stimulation with delay is the major factor causing sickness during actual rides. Only a concurrent series of test, isolating each stimulus present in the actual rides, could indeed provide the exact

weight of each component. With respect to this, it is interesting to consider that, when the delay was present, motion sickness rose rapidly in our subjects, reaching a stable level within the first 12 curves (10 min) and did not increase further. The nauseogenic effect that we observed is, therefore, unlikely to be preceded by that of other motion stimuli caused by the train. The high motion sickness scores reported in such short time by the subjects with the highest train-specific susceptibility suggest that the delay in the tilt of the car provide a relevant contribution to the overall motion sickness experienced by passengers. For a thorough comparison, however, two aspects of our simulation need to be considered. First, the simulated curves of the delay condition exaggerated the tilt delay to magnify the difference between the conditions and were likely more provoking than the curve of the train. Second, our simulation included less curves than the train ride tested by Cohen and colleagues (14), but the overall duration was similar, i.e., the frequency of nauseogenic stimuli was lower than on the train, and therefore possibly less nauseogenic. Combining these two differences between our simulation and an actual train ride (14), it is difficult to draw a conclusion on the relative role of the tilt based on the intensity of the nauseogenica, and we cannot exclude that the other nauseogenic stimuli still contribute to the motion sickness and, if tested in isolation, could generate high level of motion sickness in a similarly short time.

Although only additional experiments testing the linear stimulations in isolation could provide a definitive answer on the relative role of each component, we can conclude that even the low angular velocities of the tilting train generate cross-coupling stimuli capable of causing high motion sickness. Cross-coupling is, therefore, a relevant contributor to motion sickness in tilting train. More interesting, we further evidence that the effect of cross-coupling is almost nulled by reducing the delay, as suggested by Cohen et al. (14).

ETHICS STATEMENT

This study was carried out in accordance with the recommendations of Ethic Committee of the Canton Zurich with written informed consent from all subjects. All subjects gave written informed consent in accordance with the Declaration of Helsinki.

AUTHOR CONTRIBUTIONS

GB and DS conceived the study, designed the experiment, critically contributed to interpretation of the results and draw the conclusions, and wrote the manuscript. GB analyzed the data and performed the statistic. MD, KF, CL, and AK refined the experimental design, performed the experiment, acquired and analyzed the data, and interpreted the results.

ACKNOWLEDGMENTS

The authors thank M. Penner for technical assistance.

FUNDING

Swiss National Science Foundation; Betty and David Koetser Foundation for Brain Research; Baasch Medicus Foundation; Zurich Center for Integrative Human Physiology.

REFERENCES

- Ueno M, Ogawa T, Nakagiri S, Arisawa T, Mino Y, Oyama K, et al. Studies on motion sickness caused by high curve speed railway vehicles. Evaluation of the swing and its effects on passengers and conductors. *Sangyo Igaku* (1986) 28(4):266–74. doi:10.1539/joh1959.28.266
- Forstberg J, Andersson E, Ledin T. Influence of different conditions for tilt compensation on symptoms of motion sickness in tilting trains. *Brain Res Bull* (1998) 47(5):525–35. doi:10.1016/S0361-9230(98)00097-5
- Reason JT, Brand JJ. *Motion Sickness*. London: Academic Press (1975).
- Money KE. Motion sickness. *Physiol Rev* (1970) 50(1):1–39.
- Bertolini G, Straumann D. Moving in a moving world: a review on vestibular motion sickness. *Front Neurol* (2016) 7:14. doi:10.3389/fneur.2016.00014
- Oman CM. Motion sickness: a synthesis and evaluation of the sensory conflict theory. *Can J Physiol Pharmacol* (1990) 68(2):294–303. doi:10.1139/y90-044
- Oman CM. A heuristic mathematical model for the dynamics of sensory conflict and motion sickness. *Acta Otolaryngol Suppl* (1982) 392:1–44.
- Sheehan SE, Oman CM, Duda KR. Motion sickness: a cholinomimetic agent hypothesis. *J Vestib Res* (2011) 21(4):209–17. doi:10.3233/VES-2011-0417
- Matsangas P, McCauley ME. Sopite syndrome: a revised definition. *Aviat Space Environ Med* (2014) 85(6):672–3. doi:10.3357/ASEM.3891.2014
- Graybiel A, Knepton J. Sopite syndrome: a sometimes sole manifestation of motion sickness. *Aviat Space Environ Med* (1976) 47(8):873–82.
- Oman CM. Are evolutionary hypotheses for motion sickness “just-so” stories? *J Vestib Res* (2012) 22(2):117–27. doi:10.3233/VES-2011-0432
- Oman CM, Cullen KE. Brainstem processing of vestibular sensory exafference: implications for motion sickness etiology. *Exp Brain Res* (2014) 232(8):2483–92. doi:10.1007/s00221-014-3973-2
- Beard GF, Griffin MJ. Discomfort caused by low-frequency lateral oscillation, roll oscillation and roll-compensated lateral oscillation. *Ergonomics* (2013) 56(1):103–14. doi:10.1080/00140139.2012.729613
- Cohen B, Dai M, Ogorodnikov D, Laurens J, Raphan T, Muller P, et al. Motion sickness on tilting trains. *FASEB J* (2011) 25(11):3765–74. doi:10.1096/fj.11-184887
- Griffin MJ. *Handbook of Human Vibration*. London: Academic Press (1990).
- McCauley ME, Royal JW, Wylie CD, O’Hanlon JF, Mackie RR. *Motion Sickness Incidence: Exploratory Studies of Habituation, Pitch and Roll and the Refinement of a Mathematical Model*. Contract No.: Technical Report 1733-2. Goleta, CA: Human Factor Research Inc. (1976).
- Lawther A, Griffin MJ. Prediction of the incidence of motion sickness from the magnitude, frequency, and duration of vertical oscillation. *J Acoust Soc Am* (1987) 82(3):957–66. doi:10.1121/1.395295
- O’Hanlon JF, McCauley ME. Motion sickness incidence as a function of the frequency and acceleration of vertical sinusoidal motion. *Aerospace Med* (1974) 45(4):366–9.
- Donohew BE, Griffin MJ. Motion sickness with fully roll-compensated lateral oscillation: effect of oscillation frequency. *Aviat Space Environ Med* (2009) 80(2):94–101. doi:10.3357/ASEM.2345.2009
- Donohew BE, Griffin MJ. Motion sickness with combined lateral and roll oscillation: effect of percentage compensation. *Aviat Space Environ Med* (2010) 81(1):22–9. doi:10.3357/ASEM.2555.2010
- Golding JF, Markey HM. Effect of frequency of horizontal linear oscillation on motion sickness and somatogravic illusion. *Aviat Space Environ Med* (1996) 67(2):121–6.
- Golding JF, Markey HM, Stott JR. The effects of motion direction, body axis, and posture on motion sickness induced by low frequency linear oscillation. *Aviat Space Environ Med* (1995) 66(11):1046–51.
- Persson R. *Motion Sickness in Tilting Trains. Description and Analysis of Present Knowledge*. Contract No.: VTI Report 614A. Linkoping: VTI (2008).
- Sanderson J, Oman CM, Harris LR. Measurement of oscillillopsia induced by vestibular Coriolis stimulation. *J Vestib Res* (2007) 17(5–6):289–99.
- Ramat S, Bertolini G. Estimating the time constants of the rVOR. A model-based study. *Ann N Y Acad Sci* (2009) 1164:140–6. doi:10.1111/j.1749-6632.2009.03855.x
- Bertolini G, Ramat S, Laurens J, Bockisch CJ, Marti S, Straumann D, et al. Velocity storage contribution to vestibular self-motion perception in healthy human subjects. *J Neurophysiol* (2011) 105(1):209–23. doi:10.1152/jn.00154.2010
- Dai M, Klein A, Cohen B, Raphan T. Model-based study of the human cupular time constant. *J Vestib Res* (1999) 9(4):293–301.
- Joseph JA, Griffin MJ. Motion sickness from combined lateral and roll oscillation: effect of varying phase relationships. *Aviat Space Environ Med* (2007) 78(10):944–50. doi:10.3357/ASEM.2043.2007
- Hecht H, Kavelaars J, Cheung CC, Young LR. Orientation illusions and heart-rate changes during short-radius centrifugation. *J Vestib Res* (2001) 11(2):115–27.
- Young LR, Hecht H, Lyne LE, Sienko KH, Cheung CC, Kavelaars J. Artificial gravity: head movements during short-radius centrifugation. *Acta Astronaut* (2001) 49(3–10):215–26. doi:10.1016/S0094-5765(01)00100-X
- Young LR, Sienko KH, Lyne LE, Hecht H, Natapoff A. Adaptation of the vestibulo-ocular reflex, subjective tilt, and motion sickness to head movements during short-radius centrifugation. *J Vestib Res* (2003) 13(2–3):65–77.
- Garrick-Bethell I, Jarchow T, Hecht H, Young LR. Vestibular adaptation to centrifugation does not transfer across planes of head rotation. *J Vestib Res* (2008) 18(1):25–37.
- Dai M, Kunin M, Raphan T, Cohen B. The relation of motion sickness to the spatial-temporal properties of velocity storage. *Exp Brain Res* (2003) 151(2):173–89. doi:10.1007/s00221-003-1479-4
- Dai M, Sofroniou S, Kunin M, Raphan T, Cohen B. Motion sickness induced by off-vertical axis rotation (OVAR). *Exp Brain Res* (2010) 204(2):207–22. doi:10.1007/s00221-010-2305-4
- Golding JF. Motion sickness susceptibility questionnaire revised and its relationship to other forms of sickness. *Brain Res Bull* (1998) 47(5):507–16. doi:10.1016/S0361-9230(98)00091-4

SUPPLEMENTARY MATERIAL

The Supplementary Material for this article can be found online at <http://journal.frontiersin.org/article/10.3389/fneur.2017.00195/full#supplementary-material>.

22. Golding JF, Markey HM, Stott JR. The effects of motion direction, body axis, and posture on motion sickness induced by low frequency linear oscillation. *Aviat Space Environ Med* (1995) 66(11):1046–51.
23. Persson R. *Motion Sickness in Tilting Trains. Description and Analysis of Present Knowledge*. Contract No.: VTI Report 614A. Linkoping: VTI (2008).
24. Sanderson J, Oman CM, Harris LR. Measurement of oscillillopsia induced by vestibular Coriolis stimulation. *J Vestib Res* (2007) 17(5–6):289–99.
25. Ramat S, Bertolini G. Estimating the time constants of the rVOR. A model-based study. *Ann N Y Acad Sci* (2009) 1164:140–6. doi:10.1111/j.1749-6632.2009.03855.x
26. Bertolini G, Ramat S, Laurens J, Bockisch CJ, Marti S, Straumann D, et al. Velocity storage contribution to vestibular self-motion perception in healthy human subjects. *J Neurophysiol* (2011) 105(1):209–23. doi:10.1152/jn.00154.2010
27. Dai M, Klein A, Cohen B, Raphan T. Model-based study of the human cupular time constant. *J Vestib Res* (1999) 9(4):293–301.
28. Joseph JA, Griffin MJ. Motion sickness from combined lateral and roll oscillation: effect of varying phase relationships. *Aviat Space Environ Med* (2007) 78(10):944–50. doi:10.3357/ASEM.2043.2007
29. Hecht H, Kavelaars J, Cheung CC, Young LR. Orientation illusions and heart-rate changes during short-radius centrifugation. *J Vestib Res* (2001) 11(2):115–27.
30. Young LR, Hecht H, Lyne LE, Sienko KH, Cheung CC, Kavelaars J. Artificial gravity: head movements during short-radius centrifugation. *Acta Astronaut* (2001) 49(3–10):215–26. doi:10.1016/S0094-5765(01)00100-X
31. Young LR, Sienko KH, Lyne LE, Hecht H, Natapoff A. Adaptation of the vestibulo-ocular reflex, subjective tilt, and motion sickness to head movements during short-radius centrifugation. *J Vestib Res* (2003) 13(2–3):65–77.
32. Garrick-Bethell I, Jarchow T, Hecht H, Young LR. Vestibular adaptation to centrifugation does not transfer across planes of head rotation. *J Vestib Res* (2008) 18(1):25–37.
33. Dai M, Kunin M, Raphan T, Cohen B. The relation of motion sickness to the spatial-temporal properties of velocity storage. *Exp Brain Res* (2003) 151(2):173–89. doi:10.1007/s00221-003-1479-4
34. Dai M, Sofroniou S, Kunin M, Raphan T, Cohen B. Motion sickness induced by off-vertical axis rotation (OVAR). *Exp Brain Res* (2010) 204(2):207–22. doi:10.1007/s00221-010-2305-4
35. Golding JF. Motion sickness susceptibility questionnaire revised and its relationship to other forms of sickness. *Brain Res Bull* (1998) 47(5):507–16. doi:10.1016/S0361-9230(98)00091-4

Conflict of Interest Statement: The authors declare that the research was conducted in the absence of any commercial or financial relationships that could be construed as a potential conflict of interest.

The reviewer, SY, and handling editor declared their shared affiliation, and the handling editor states that the process nevertheless met the standards of a fair and objective review.

Copyright © 2017 Bertolini, Durmaz, Ferrari, Küffer, Lambert and Straumann. This is an open-access article distributed under the terms of the Creative Commons Attribution License (CC BY). The use, distribution or reproduction in other forums is permitted, provided the original author(s) or licensor are credited and that the original publication in this journal is cited, in accordance with accepted academic practice. No use, distribution or reproduction is permitted which does not comply with these terms.

Advantages of publishing in Frontiers



OPEN ACCESS

Articles are free to read for greatest visibility and readership



FAST PUBLICATION

Around 90 days from submission to decision



HIGH QUALITY PEER-REVIEW

Rigorous, collaborative, and constructive peer-review



TRANSPARENT PEER-REVIEW

Editors and reviewers acknowledged by name on published articles



REPRODUCIBILITY OF RESEARCH

Support open data and methods to enhance research reproducibility



DIGITAL PUBLISHING

Articles designed for optimal readership across devices



FOLLOW US
@frontiersin



IMPACT METRICS

Advanced article metrics track visibility across digital media



EXTENSIVE PROMOTION

Marketing and promotion of impactful research



LOOP RESEARCH NETWORK

Our network increases your article's readership